
CHEMICAL CONCEPTS IN POLLUTANT BEHAVIOR

SECOND EDITION

Ian J. Tinsley
Oregon State University

 **WILEY-
INTERSCIENCE**

A JOHN WILEY & SONS, INC., PUBLICATION

Copyright © 2004 by John Wiley & Sons, Inc. All rights reserved.

Published by John Wiley & Sons, Inc., Hoboken, New Jersey.
Published simultaneously in Canada.

No part of this publication may be reproduced, stored in a retrieval system, or transmitted in any form or by any means, electronic, mechanical, photocopying, recording, scanning, or otherwise, except as permitted under Section 107 or 108 of the 1976 United States Copyright Act, without either the prior written permission of the Publisher, or authorization through payment of the appropriate per-copy fee to the Copyright Clearance Center, Inc., 222 Rosewood Drive, Danvers, MA 01923, 978-750-8400, fax 978-646-8600, or on the web at www.copyright.com. Requests to the Publisher for permission should be addressed to the Permissions Department, John Wiley & Sons, Inc., 111 River Street, Hoboken, NJ 07030, (201) 748-6011, fax (201) 748-6008.

Limit of Liability/Disclaimer of Warranty: While the publisher and author have used their best efforts in preparing this book, they make no representations or warranties with respect to the accuracy or completeness of the contents of this book and specifically disclaim any implied warranties of merchantability or fitness for a particular purpose. No warranty may be created or extended by sales representatives or written sales materials. The advice and strategies contained herein may not be suitable for your situation. You should consult with a professional where appropriate. Neither the publisher nor author shall be liable for any loss of profit or any other commercial damages, including but not limited to special, incidental, consequential, or other damages.

For general information on our other products and services please contact our Customer Care Department within the U.S. at 877-762-2974, outside the U.S. at 317-572-3993 or fax 317-572-4002.

Wiley also publishes its books in a variety of electronic formats. Some content that appears in print, however, may not be available in electronic format.

Library of Congress Cataloging-in-Publication Data:

Tinsley, Ian J., 1929–

Chemical concepts in pollutant behavior/Ian J. Tinsley.—2nd ed.
p. cm.

“A Wiley-Interscience publication.”

Includes bibliographical references.

ISBN 0-471-09525-7 (cloth)

1. Agricultural chemicals—Environmental aspects. 2.

Pollution—Environmental aspects. I. Title.

QH545.A25 T56 2004

577.27- -dc22

2003025152

Printed in the United States of America

10 9 8 7 6 5 4 3 2 1

CONTENTS

<i>Preface</i>	vii
1. Introduction	1
2. Physical Chemical Parameters	5
3. Sorption	75
4. Evaporation	123
5. Absorption and Bioconcentration	149
6. Photochemical Processes	193
7. Redox Processes	261
8. Hydrolysis	285
9. Metabolic Transformation	311
10. Synthesis	359
Appendix	387
Index	393

■ PREFACE

Two developments in the early 1960s were major factors in the development of the field of environmental chemistry. The first was the introduction of the electron capture detector for the gas chromatograph (GC). This development provided a dramatic improvement in the level of sensitivity (several orders of magnitude) along with some improvement in selectivity. A direct consequence of the introduction of this technology was the demonstration of the widespread distribution of the polychlorinated biphenyls (PCBs) and organochlorine insecticides such as DDT and its metabolites. In her book, *Silent Spring*, Rachel Carson dramatized the potential biological consequences of chemicals in the environment and it was recognized that dilution could no longer be considered the answer to pollution. Research workers and government agencies realized that a systematic approach would be required to anticipate and manage the impact of compounds released into the environment.

Colleagues in my department were involved in the analytical area while others such as the late Dr. Virgil Freed were focusing on research that would improve the understanding of the environmental behavior of agricultural chemicals. At the same time, Dr. Cary Chiou was making significant contributions to our understanding of sorption in soil and evaporation processes. The department decided to develop a course that would focus on those chemical concepts that influence the environmental behavior of organic compounds. This area became very important to the Civil Engineer who was responsible for water quality issues and solid waste management. Those in agriculture and forestry needed to improve their understanding of the chemicals used in pest management to maximize efficacy and minimize adverse effects. The curriculum for students in these fields provided a limited background in chemistry—freshman chemistry and perhaps a term of organic chemistry. I had been teaching freshman chemistry for a number of years and realized that although students were introduced to many of the needed concepts they were only interested in accumulating sufficient information to pass the course and really were in no position to understand how these concepts could be applied.

I have offered a one-term course every year for about 27 years that has become the basis for this text, a complete rewrite of my first effort published almost 25 years ago. The content of the course has changed dramatically over this time as the field matured, however, the objective to demonstrate chemical factors determining environmental behavior has remained the same. The student response has been gratifying. Students with limited background in chemistry were at times threatened by

the subject matter but developed a better understanding of the basic concepts as they were able to apply them to the definition of environmental behavior. Chemistry majors on the other hand were encouraged to find how much of the material they had studied was so directly applicable in the environmental area.

Introduction

When a chemical is introduced into the environment, there is a certain probability that it can move from the point where it was released. The distribution of some compounds has been shown to be global in scope having been detected on mountain peaks and in polar regions. This discovery could involve their use over a broad geographical area or their ability to be transported over large distances. It is possible that problems associated with the widespread distribution of chemicals could have been avoided or at least reduced if the properties of the chemicals influencing their movement had been understood when they were first introduced. However, the recognition of these problems has provided the incentive to define the processes and outline the chemical concepts involved resulting in the development of a new focus of “environmental chemistry”. This field has matured over the past 25 years to the point where predictions can be made concerning the fate and distribution of organic compounds.

Distribution pathways are summarized in Figure 1.1. First of all, there can be movement within a compartment; for example, any chemical introduced into an aquatic compartment can move to the extent that the water moves, whether or not the chemical is in solution or sorbed on a particle. This movement would be defined by the appropriate hydrological parameters. A chemical may find its way into the atmosphere where it may be transported in atmospheric currents: In this situation the appropriate meteorological phenomena will determine the rate and direction of movement. Distribution in a plant or animal will be controlled by the transport mechanisms in that organism; either the vascular system in an animal or the phloem in a plant. In a much broader context, the transport of a chemical in an ecosystem must have some relation to the overall mass flow in the system since the chemical moves with the food constituents of the various components in the ecosystem.

Soil particles may carry chemicals in the air or water, however, movement through the soil compartment is accomplished primarily through diffusion or mass transport in water that seeps through the soil. In the situation where chemicals move within a compartment, the transport processes of that compartment are controlling and the effects of the properties of the chemical are minimal.

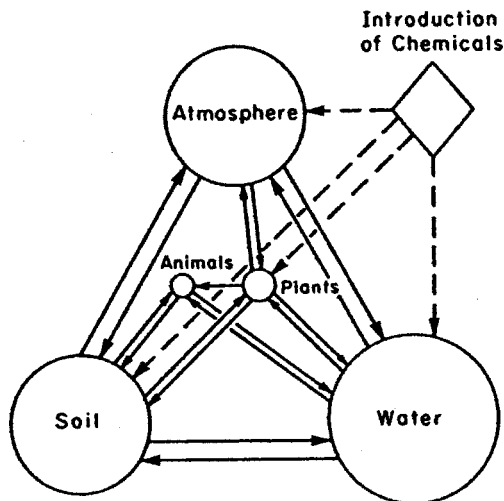


Figure 1.1 Processes by which chemicals distribute in the environment.

By contrast, the properties of the chemical become most significant in determining its tendency to move between compartments. Thermodynamic and kinetic factors influence distribution and although natural systems are rarely reversible, such an assumption can provide an indication of the trend for movement between compartments. The primary objective, then, will be to predict the environmental distribution of an organic compound as a function of its physical chemical properties using the following approach:

1. Define the process as concisely as possible: for example, what mechanisms may account for binding in soil, or how do compounds move through a biological membrane?
2. Demonstrate which properties of the chemical are controlling in each situation.
3. Develop quantitative treatment when possible.

This analysis will be applied to the following distribution processes:

1. Distribution between soil and water.
2. Evaporation from water and soil.
3. Absorption across a biological membrane into animals and plants.
4. Bioconcentration, a biological distribution process.

Having defined how an organic compound might distribute in the environment, the next question to address is, What is the potential for that compound to be transformed? This answer will involve the identification of processes that would

be of significance. For any compound of interest, it will be necessary to identify which of these processes might be active, what products may be produced, and if possible assess the rate at which the transformations might occur under ambient conditions. In this analysis, the functional characteristics of the molecule, rather than the physical chemical parameters, will be determining.

Solar radiation represents a ubiquitous source of energy that can drive chemical reactions and, consequently, photochemical processes must be considered. Many oxidative processes are also photochemically induced. At low-oxygen tension, reductive reactions become important. The potential for organic compounds to react with water must be considered given the general distribution of this reactant in all compartments of the environment. Biochemical degradation processes in biota represent the most versatile since most are enzyme catalyzed and the organism can provide energy through cellular respiratory processes.

An understanding of transformation pathways will establish whether the compound is broken down to simple derivatives, such as carbon dioxide and water, and be incorporated into natural cycles or results in products that may be more toxic than the parent. A good example of the latter situation is photochemical smog. Automobile emissions, particularly the hydrocarbons and nitrogen oxides, are themselves undesirable; however, when these are acted upon by solar radiation a number of components are produced that are much more active and produce direct effects upon populace and plant life.

Reaction rates can be critical in determining the environmental impact of a compound. Those that are transformed at slower rates will be persistent and consequently result in more significant effects. Transformation rates will be influenced by distribution and site specific characteristics. For example, a compound that may be transformed by photochemical processes will persist if it is distributed primarily in the soil, and soil pH, which can vary with location, may have a marked influence on reactions with water.

In an environmental context, these processes are all occurring simultaneously, and it is not always apparent how they might interact. It is beyond the scope of this publication to provide a comprehensive analysis of this area, however, some discussion is given of how laboratory systems and mathematical models are being used to provide a more holistic analysis. These approaches are being used to predict levels of organics in different environmental compartments, which facilitate exposure assessment, one of the factors in defining the toxicological risk associated with a given site.

Physical Chemical Parameters

The potential for an organic compound to distribute among environmental compartments is determined by its physical chemical properties. Thus it is necessary to review these parameters in this context. For example, environmental conditions impose temperature constraints of 10–40°C, which are often considerably lower than those used under laboratory conditions or in other processes. Observations at 20–25°C are usually acceptable. The only solvent of consequence is water; not a very effective solvent for many nonpolar organic compounds and determining aqueous solubilities at ambient temperatures can present significant experimental challenges. This chapter will address equilibrium vapor pressure, aqueous solubility, Henry's law constant, octanol–water partition coefficient, and acid–base dissociation constants (pK_a). The objective will be to develop a theoretical background, provide some perspective on how these quantities are determined, and if possible some basis for determining their validity—in some cases values reported in the literature for a given compound can vary by orders of magnitude. Useful data references will be summarized along with procedures for predicting values that may not have been reported.

2.1 EQUILIBRIUM VAPOR PRESSURE

When a pure liquid or solid is held at a constant temperature in a closed system some molecules at the surface will achieve sufficient energy to escape to the gas phase. In time, molecules in the gas phase will begin to return to the solid or liquid ultimately achieving a steady state with the evaporation rate balancing the condensation rate. The equilibrium vapor pressure, P^0 , is thus defined as the pressure of the vapor that is in equilibrium with its pure condensed phase.

Pressure is force per unit area and although the Pascal, Pa ($\text{N} \cdot \text{m}^{-2}$ or $\text{kg} \cdot \text{m}^{-1} \text{s}^{-2}$) is the accepted SI unit, older terms found in the literature are listed in Table 2.1. Equilibrium vapor pressures for selected compounds of environmental interest are tabulated in Table 2.2. Equilibrium vapor pressure is considered to be an index of volatility, but this refers only to the pure compound. It will be seen that

TABLE 2.1 Units of Pressure

Unit	Symbol	SI Equivalent
Pascal	Pa	
Atmosphere	atm	101,325 Pa
Torr	Torr	101,325/760 = 133.32 Pa
mm Mercury	mmHg	101,325/760 = 133.32 Pa

some of the more highly chlorinated PCBs can evaporate from water at significant rates despite having low vapor pressures. This process is defined by the Henry's law constant, which involves water solubility as well as vapor pressure.

2.1.1 Vapor Density and Concentration Terms

It is often useful to convert equilibrium vapor pressures to vapor densities using the ideal gas law

$$PV = nRT \quad PV = \frac{m}{MW}RT$$

where MW = molecular weight and the vapor density in $\text{g} \cdot \text{L}^{-1}$ would be given by

$$\frac{m}{V} = \frac{P \cdot MW}{RT}$$

where P is expressed in atmospheres (atm), V in liters (L), MW is in $\text{g} \cdot \text{mol}^{-1}$, and the gas constant $R = 0.082 \text{ L} \cdot \text{atm} \cdot \text{mol}^{-1} \cdot \text{K}^{-1}$. For example, P^0 (25°C) for 4,4'-(DCB) is 0.0050 Pa and

$$\begin{aligned} \text{vap density} &= \frac{0.0050/101325(\text{atm}) \times 223(\text{g} \cdot \text{mol}^{-1})}{0.082(\text{L} \cdot \text{atm} \cdot \text{mol}^{-1} \cdot \text{K}^{-1}) \times 298 \text{ K}} \\ &= 0.451 \mu\text{g} \cdot \text{L}^{-1} = 451 \mu\text{g} \cdot \text{m}^{-3} \end{aligned}$$

In the vapor phase, the concentration term, parts per million, (ppm), is defined as molecules per million molecules of air, and since the gas laws tell us that equal volumes of gases at the same temperature and pressure contain equal numbers of molecules, this is a volume-to-volume relation. The number of moles in a liter of air at 25°C and 1 atm would be

$$n/V(\text{air}) = 1 \text{ atm}/[0.082(\text{L} \cdot \text{atm} \cdot \text{mol}^{-1} \cdot \text{K}^{-1}) \times 298 \text{ K}] = 0.0409 \text{ mol} \cdot \text{L}^{-1}$$

Under equilibrium conditions at 25 K the number of mol of 4,4'-DCB per liter would be

$$\begin{aligned} n/V(4,4\text{-DCB}) &= [0.0050/101325](\text{atm})/[0.082(\text{L} \cdot \text{atm} \cdot \text{mol}^{-1} \cdot \text{K}^{-1}) \times 298 \text{ K}] \\ &= 2.019 \times 10^{-9} \text{ mol} \cdot \text{L}^{-1} \end{aligned}$$

TABLE 2.2 Equilibrium Vapor Pressures

Compound	$P^\circ, 25^\circ\text{C}$ (Pa)	$\text{Log } P(\text{Pa}) = f(1/T) 5-50^\circ\text{C}$	Compound	$P^\circ, 25^\circ\text{C}$ (Pa)	$\text{Log } P(\text{Pa}) = f(1/T) 5-50^\circ\text{C}$
<i>Chlorobenzenes</i> ^a					
1,2-DCB ^b	170	$\log P^c = 19.40 - 6013/T$	2,8-	3.9×10^{-4}	$\log P = 14.30669 - 5281.67/T$
1,4-DCB ^b	130	$\log P = 1.63209 - 2829.32/T$	Octo-	5.0×10^{-10}	$\log P = 16.88937 - 7808.74/T$
1,3,5-TCB ^d	25	$\log P^c = 8.301 - 2956/T$	<i>Aromatic Hydrocarbons</i> ^e		
PentaCB	0.22	$\log P = 15.6174 - 4138.4/T$	Benzene	12,700	$\log P^c = 6.02994 - 1211.003/(T - 52.)$
HCB	0.0023	$\log P = 10.83 - 4044/T$	Toluene	3800	$\log P^c = 6.16273 - 1391.005/(T - 48.97)$
<i>Chlorinated Biphenyls</i> ^b					
3-	1.0	$\log P = 11.64178 - 3515.0/T$	1,2,4-	270	$\log P^c = 6.16866 - 1573.267/(T - 64.586)$
4,4'-	0.0050	$\log P = 14.10 - 4977/T$	Trimethylbenzene	880	$\log P^c = 7.3945 - 2221.3/T$
2,4,5-	0.132	NA ^b	Styrene	10.4	$\log P = 13.59 - 3742/T$
2,2',5,5'-	0.0049	NA ^b	Naphthalene	1.30	$\log P^c = 14.840 - 4402.1/T$
2,3,4,5-	0.00037	$\log P = 12.10 - 4632/T$	Biphenyl	0.30	$\log P^c = 10.883 - 4290.5/T$
2,2',4,4',6,6'	0.0005	$\log P = 14.84 - 5399/T$	Acenaphthene	0.09	$\log P = 14.385 - 4616.07/T$
2,2',3,3',5,5',6,6'	2.7×10^{-5}	$\log P = 14.84 - 5399/T$	Fluorene	0.001	$\log P = 12.977 - 4791.89/T$
<i>Chlorinated Dibenzodioxins</i> ^b					
1-	0.012	$\log P = 15.35327 - 5150.4/T$	Anthracene	0.020	$\log P = 14.852 - 4962.77/T$
2,7-	1.2×10^{-4}	$\log P = 14.6083 - 5523.34/T$	Phenanthrene	6.0×10^{-4}	$\log P = 12.748 - 4760.73/T$
2,3,7,8-	2.0×10^{-7}	$\log P = 15.0391 - 6482.7/T$	Pyrene	5.7×10^{-7}	$\log P = 14.848 - 6189/T$
1,2,3,4,7-	8.8×10^{-8}	$\log P = 17.0221 - 7179.05/T$	Chrysene	7.0×10^{-7}	$\log P = 11.6067 - 6181/T$
			Benzoflpyrene	0.055	$\log P = 14.91018 - 4820.43/T$
			Dibenzodioxin	0.30	$\log P = 13.17192 - 4083/T$
			Dibenzofuran		

^aFrom Ref. 1.

^bDichlorobiphenyl = PCB

^c $P = kPa.$

^dTrichlorobiphenyl = TCB

^eFrom Ref. 2.

^fNot available = NA.

Thus, the vapor density of this biphenyl can be expressed in ppm

$$\begin{aligned}\text{vap density} &= (2.019 \times 10^{-9} \times N \times 1 \times 10^6)/(0.0409 \times N) \\ &= 0.0494 \text{ ppm} = 49.4 \text{ ppb (parts per billion)}\end{aligned}$$

$$N \text{ is Avogadro's number, } 6.022 \times 10^{23} \text{ molecules} \cdot \text{mol}^{-1}$$

Air quality standards are often expressed in ppm and it can be useful to convert these values to mass per unit volume, usually $\mu\text{g} \cdot \text{m}^{-3}$. If a liter of air contains 0.0409 mol, a concentration of 1 ppm of say ozone, would thus contain $4.09 \times 10^{-8} \text{ mol} \cdot \text{L}^{-1}$ which would convert to $4.09 \times 10^{-5} \text{ mol}$ per cubic metre or $4.09 \times 10^{-5}(\text{mol} \cdot \text{m}^{-3}) \times \text{MW}(\text{g} \cdot \text{mol}^{-1}) \times 1 \times 10^6 (\mu\text{g} \cdot \text{g}^{-1})$. Thus

$$\mu\text{g} \cdot \text{m}^{-3} = \text{ppm} \times 40.9 \times \text{MW}$$

A background concentration of 0.03 ppm of ozone would correspond to

$$\mu\text{g} \cdot \text{m}^{-3} = 0.03 \times 40.9 \times 48 = 59 \mu\text{g} \cdot \text{m}^{-3}$$

2.1.2 Procedures for Measuring Vapor Pressure

Different procedures can be used to determine equilibrium vapor pressure.³ When a compound is sufficiently volatile, one can simply use head-space analysis of a closed system. Boiling points can be measured as a function of pressure down to ~ 10 mmHg, defining the liquid–vapor equilibrium of the phase diagram (Fig. 2.1). The Knudson effusion method⁴ measures the rate of loss of vapor through a small aperture into a vacuum, which is accomplished using a Knudsen cell and monitoring, over time, the weight loss of the container or trapping and measuring the mass of vapor effusing. The weight loss, W , over time, t , is defined by the Knudsen equation developed from the kinetic theory of gases

$$W = PA(\text{MW}/[2\pi RT])^{1/2}t$$

where P is the vapor pressure, A is the area of the orifice, and MW is the molecular weight. This procedure can provide accurate data but is very sensitive to the presence of impurities, particularly those more volatile than the compound under investigation.

The gas saturation or transpiration method³ can measure vapor pressures as low as 10^{-8} mmHg and involves the saturation of a slowly moving stream of carrier gas with the chemical and trapping and analysis of the chemical in the vapor phase. The vapor pressure is derived from the concentration of the vapor in the carrier gas. The accuracy of this method is predicated on achieving equilibrium between the liquid or solid and the vapor phase. This accuracy is accomplished by passing the carrier gas through a column containing quartz sand coated with the compound under study (Fig. 2.2) and providing sufficient residence time in the column (30–40 min) either

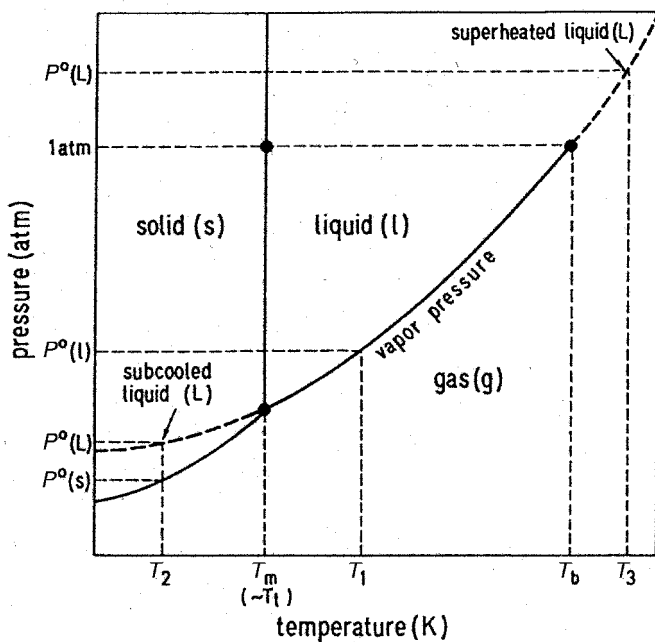


Figure 2.1 Phase diagram for an organic compound indicating temperature–pressure relations between the phases.

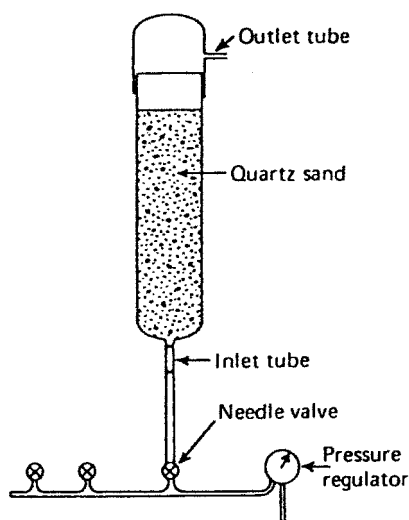


Figure 2.2 A vapor saturator.

by using low flow rates or a large column. If the analytical method is specific, this method is not affected by impurities and, in fact, the vapor pressures of several compounds can be determined simultaneously providing there are no interactions between compounds in the vapor phase (Table 2.3). These data illustrate the effect of impurities on vapor composition. The technical product contains <1% of the *o,p'*-DDE, which contributes 27% of the vapor density.

2.1.3 Temperature Relations

Many organic compounds of environmental interest are solids at ambient temperatures and have low vapor pressures. Consequently, it has been expedient to measure vapor pressures at elevated temperatures to provide a response that is easier to detect. These data may be useful to a process engineer who might be managing these compounds at elevated temperatures, but the environmental chemist is put in the position of extrapolating from these observations to ambient conditions.

Phase diagrams (Fig. 2.1) summarize the pressure and temperature relations defining the equilibria between different phases. From an environmental perspective, the more important processes are the solid–vapor and liquid–vapor equilibria. The effect of temperature on the vapor pressure of the solid and the liquid are defined by the lines separating the two phases and, of course, the boiling point is the temperature at which the vapor pressure is 1 atm. Also note that a liquid can be cooled below its melting point providing a super-cooled liquid and in this state the vapor pressure is higher than the solid at the same temperature. It will be demonstrated that, in some situations there are advantages in considering the response of compounds in this state.

Thermodynamic analysis of the equilibrium between a condensed phase (solid or liquid) and the vapor is summarized by the Clausius–Clapeyron equation:

$$\frac{dP}{dT} = \frac{\Delta H}{T\Delta V}$$

TABLE 2.3 Composition at 30°C of 1–2% Technical DDT on Silica Sand

Compound	Vapor Density		P^0 (Pa)	Conc. in Tech. DDT (%)
	(ng · L ⁻¹)	% of Total		
<i>p,p'</i> -DDT	13.6	8.0	9.66×10^{-5}	74.6
<i>o,p'</i> -DDT	104	61.7	7.39×10^{-4}	21.1
<i>p,p'</i> -DDE	24.1	14.3	1.91×10^{-4}	0.81
<i>o,p'</i> -DDE	26.9	16.0	2.13×10^{-4}	0.07

with ΔH the enthalpy change and ΔV the change in molar volume. For liquid–gas (evaporation) or solid–gas (sublimation) transformations, ΔV is essentially the molar volume of the gas, RT/P^0 , for an ideal gas and thus

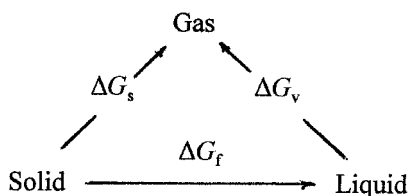
$$\frac{dP^0}{dT} = \frac{P^0 \Delta H}{RT^2} \quad \text{or} \quad \frac{d \ln P^0}{dT} = \frac{\Delta H}{RT^2}$$

where ΔH would be the molar heat of vaporization or sublimation. Most vapor pressure–temperature relations are represented by an integrated form of the equation

$$\ln P^0 = -B/T + A$$

where $B = \Delta H/R$. The heat of vaporization is relatively constant at temperatures well below the boiling point, however, over extended temperature ranges the data may give a better fit to the Antoine equation; $\ln P^0 = -B/(T + C) + A$. A number of these $\ln P^0/1/T$ relations are listed in Table 2.2, and note that those cited for benzene, toluene, and trimethylbenzene are of the latter form. These data have been compiled from several sources for some chlorinated aromatic compounds¹ and $\ln P^0$ versus $1/T$ relations for 1,2-dichlorobenzene and pentachlorobenzene are given in Figure 2.3. Note the discontinuity in the pentachlorobenzene relation at the melting point, 86°C, $1/T = 0.00279$. For values of $1/T < 0.00279$, P^0 would give the vapor pressure of the liquid and with $1/T > 0.00279$, the vapor pressure of the solid. The vapor pressure of the super-cooled liquid would be represented by an extrapolation of the liquid–vapor relation giving values of P^0 higher than those observed with the solid at the same temperature.

2.1.3.1 Vapor Pressure of Super-Cooled Liquid, P_{scf}^0 A thermodynamic cycle relating transitions between the three phases and the related free energies can be defined.



It follows that

$$\Delta G_s = \Delta G_f + \Delta G_v$$

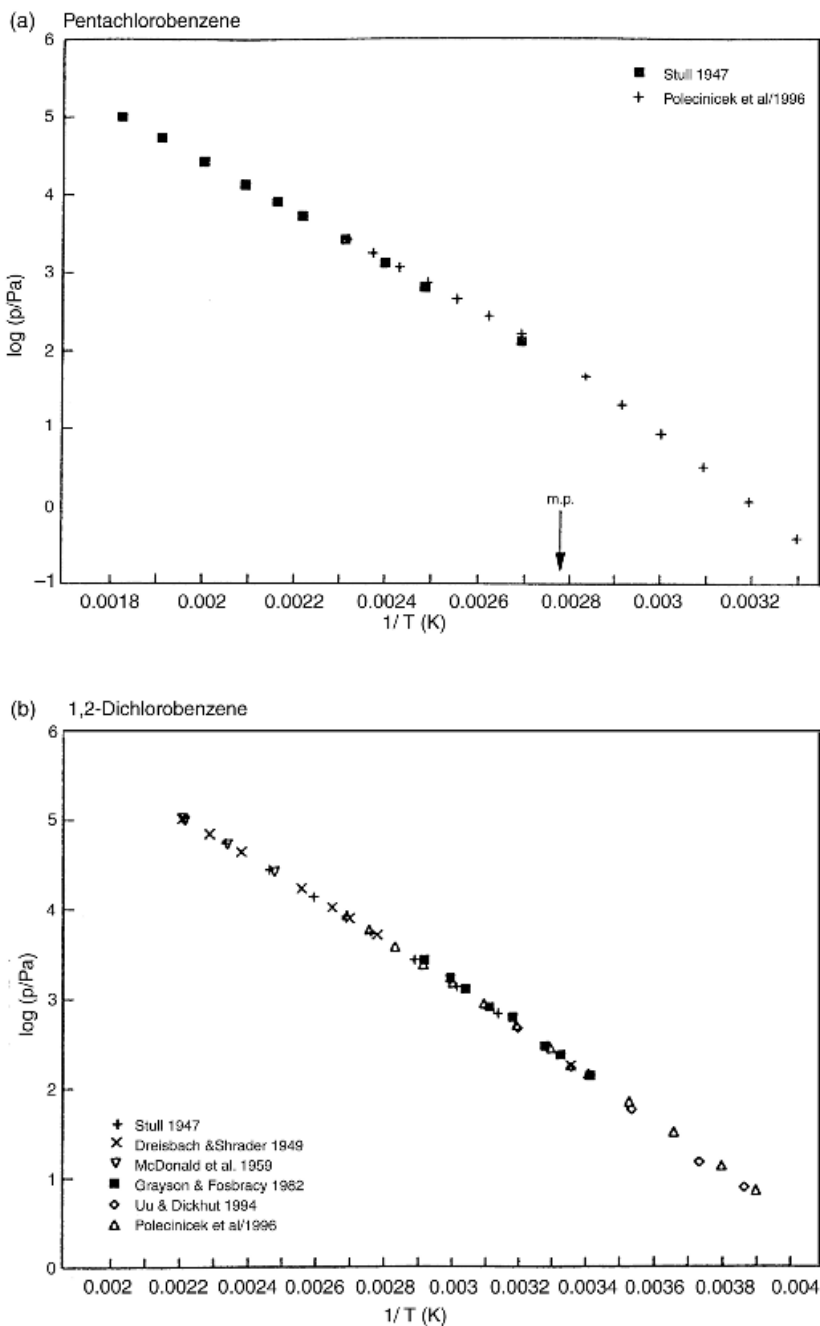


Figure 2.3 Temperature–vapor pressure relations compiled from different studies for (a) pentachlorobenzene and (b) 1,2-dichlorobenzene. Note the discontinuity at the melting point for the pentachlorobenzene. [Reproduced with permission from, W. Shiu and K. Ma. *J. Phys. Chem. Ref. Data* **29**, 387 (2000). Copyright © 2000, American Chemical Society.]

From thermodynamic concepts,

$$\begin{aligned}\Delta G_s &= -RT \ln P_s & \text{and} \\ \Delta G_v &= -RT \ln P_l\end{aligned}$$

and

$$\Delta G_f \approx \Delta S_f(T_m - T) \quad (\text{recalling that } \Delta H_f = T_m \Delta S_f)$$

where ΔS_f is the entropy of fusion and T_m is the melting point. Substituting for the free energy terms one obtains a relation relating P_s^0 and P_{scl}^0

$$\ln P_{\text{scl}} = \ln P_s + \Delta S_f(T_m - T)/RT = \ln P_s + \Delta S_f/R(T_m/T - 1)$$

For example, for hexachlorobenzene¹:

$$\begin{aligned}P_s^0 &= 0.0023 \text{ Pa}(25^\circ\text{C}) \\ \text{mp} &= 230^\circ\text{C} \\ \Delta H_f &= 23.849 \text{ kJ} \cdot \text{mol}^{-1}\end{aligned}$$

Since

$$\begin{aligned}\Delta S_f &= \Delta H_f/T_m = 23,849/(273 + 230) = 47.3 \text{ J} \cdot \text{mol}^{-1} \cdot \text{K}^{-1} \\ \ln P_{\text{scl}} &= \ln P_s + 47.3/8.3145[(230 + 273)/(25 + 273) - 1] \\ &= -6.075 + 5.69(1.688 - 1) \\ &= -2.16 \\ P_{\text{scl}} &= 0.115 \text{ Pa}\end{aligned}$$

The vapor pressure of the super-cooled liquid is shown to be significantly higher than that of the solid, which would be expected. Melting points are usually available in the literature, however, values for the entropy of fusion, ΔS_f are not as common. Molar heats of vaporization, ΔH_v are more likely to be listed, for example, values for this parameter have been compiled for a number of chlorinated aromatic compounds¹ and for aromatic hydrocarbons.² For many compounds it has been shown that the entropy of fusion approximates $56 \text{ J} \cdot \text{mol}^{-1} \cdot \text{K}^{-1}$, and $\Delta S/R = 6.79$.⁵

2.1.4 Estimating Vapor Pressures

The magnitude of boiling points, vapor pressures, and heats of vaporization all reflect the strength of forces that hold molecules in the condensed phases. With the nonpolar molecules, van der Waal's forces are involved and bonding strength is a function of size. Consequently, one observes consistent decreases in vapor pres-

sure with increase in molecular weight of nonpolar homologous series. Dipole interactions of polar molecules are stronger than van der Waal's forces resulting in higher vapor pressures. The influence of hydrogen bonding is illustrated by water that shows an unusually high boiling point for such a small molecule.

Many procedures have been developed to predict vapor pressure, and the predictive error of eleven different methods have been evaluated using a series of PCBs.⁶ A number of approaches use a set of known vapor pressures to develop a correlation with molecular properties that can be used for predictions of unknowns. For example, the free energy of vaporization has been correlated with molecular surface area to predict vapor pressures of PCB congeners.⁷ More direct approaches are based on the Clausius–Clapeyron equation, and vapor pressures can be predicted quite effectively for some series of compounds using only boiling points along with melting points for compounds that are solids at ambient temperatures.

One such method uses a linear relation between temperature and the molar heat of vaporization which is estimated using the Kistiakowsky Constant.⁸ The integrated form of the Clausius–Clapeyron equation may be expressed

$$\ln(P_1/P_2) = -\Delta H/R(1/T_1 - 1/T_2)$$

When T_2 is the boiling point, T_B , P_2 is 1 atm and

$$\ln P_1 = -\Delta H/R(1/T_1 - 1/T_B)$$

and it would be possible to calculate P_1 at say, 25°C knowing T_B and the molar heat of vaporization, ΔH . It was noted above that enthalpies of vaporization are available for some compounds, however, Trouton's rule states that the entropy of vaporization at the boiling point is essentially constant at $86.4 \text{ J} \cdot \text{mol}^{-1} \cdot \text{K}^{-1}$ and consequently, $\Delta H_B = 86.4 \cdot T_B \text{ J} \cdot \text{mol}^{-1}$, and thus

$$\ln P_1 = -(86.4 \cdot T_B/R)(1/T_1 - 1/T_B) = -10.6(T_B/T_1 - 1)$$

This relation will overestimate the vapor pressure because ΔH_v varies with temperature, however, it can be used as a first-level approximation. To account for the temperature effect, a constant K was defined by the following relation:

$$\Delta H = \Delta H_B(1 + K)(1 - T/T_B)$$

and using regression analysis with the 72 compounds studied, was found to be 0.803. This gives the following relation for $\ln P$

$$\ln P = -10.6[(1 + K)(T_B/T_1 - 1) - K \ln T_B/T_1]$$

An additional refinement can be used for estimating ΔH_B

$$\Delta H_B/T_B = 36.6 + R \ln T_B$$

provides the final relation for estimating vapor pressure in atmospheres

$$\ln P = -(4.40 + \ln T_B) \times [1.803(T_B/T - 1) - 0.803 \ln T_B/T] - 6.8(T_M/T - 1)$$

The last term is only used for calculating the vapor pressure of compounds that are solids and would be neglected with compounds that are liquids at ambient temperature. Vapor pressures calculated at 25°C for some compounds listed in Table 2.2 are compiled in Table 2.4. The calculated values are well within the range of the recommended experimental values. It should be emphasized that this relation was developed for relatively nonpolar compounds and is not suited to more polar compounds such as phenols. Other procedures for predicting vapor pressure have been outlined.^{6,9} In addition, procedures are available for calculating boiling points from molecular properties.

2.1.5 Vapor Pressure of Solutions

The vapor pressure of a simple two-component solution would be the sum of the partial pressures that would be defined by Raoult's law

$$P_A = P_A^0 \cdot x_A$$

$$P_B = P_B^0 \cdot x_B$$

where P^0 is the vapor pressure of the pure compound and x , the mole fraction. There is nothing mysterious about this relation since the mole fraction simply estimates the relative number of molecules of each component at the surface that would be available to move into the vapor phase. Solutions that conform to this relation such as a benzene–toluene system are said to be ideal in that A—A, B—B, and A—B interactions are equivalent. Aqueous solutions of organic compounds usually show positive deviations from Raoult's law ($P_A > P_A^0$), which reflect the fact that the organic molecule is not “comfortable” being associated with water molecules and would prefer to escape to the vapor phase. The degree of incompatibility is indicated by the activity coefficient, γ :

$$P_A = P_A^0 \cdot x_A \cdot \gamma_A$$

Activity coefficients for some organic compounds in aqueous solution are compiled in Table 2.5. It is customary to cite these values at “infinite dilution” when the organic molecule only “sees” water molecules. Note the wide range and that the more nonpolar compounds show higher values while the more polar alcohols,

TABLE 2.4 Comparison of Calculated and Experimental Vapor Pressures 25°C

Compound	T_B (K)	T_M (K)	P calculated			P Exptl. ^a (Pa)
			atm	Pa	Pa	
1,2-Dichlorobenzene	453.5	256.0	1.75×10^{-3}	177	170 ± 20	
1,4-Dichlorobenzene(s)	447.0	326.1	1.24×10^{-3}	125.6	130 ± 20	
1,3,5-Trichlorobenzene(s)	481.0	336.0	2.01×10^{-4}	20.4	25 ± 6	
2,7-Dichlorodibenzodioxin(s)	646.5	482	1.32×10^{-9}	1.34×10^{-4}	1.2×10^{-4}	
2,3,7,8-Tetrachlorodibenzodioxin(s)	719.5	578	2.66×10^{-12}	2.70×10^{-7}	2.0×10^{-7}	
Toluene	383.6	178.0	3.83×10^{-2}	3881	3800 ± 200	
Naphthalene(s)	491.0	353.2	8.40×10^{-5}	8.51	10.4 ± 1.0	
Biphenyl(s)	528.9	344.0	1.60×10^{-4}	1.62	1.30	
Acenaphthene(s)	550.5	369.2	3.02×10^{-6}	0.306	0.30 ± 0.03	
Fluorene	568.0	389.0	7.82×10^{-7}	0.079	0.09 ± 0.01	
Dibenzo- <i>p</i> -dioxin	556.5	395	1.37×10^{-6}	0.139	0.055	

^aRecommended values (Ref. 1,2).

TABLE 2.5 Activity Coefficients in Water at Infinite Dilution at 25°C^a

Compound	γ^∞	Compound	γ^∞
2-Butanol	54.2	1,3-Dichlorobenzene	1.73×10^5
Hexanol	473	Hexachlorobenzene	9.78×10^8
Octanol	3.69×10^3	Biphenyl	1.06×10^6
Diethyl ether	162	2,4'-Dichlorobiphenyl	5.83×10^7
Chloroform	864	2,2',5,5'-Tetrachlorobiphenyl	4.16×10^9
Carbon tetrachloride	1.04×10^4	2,2',4,4',5,5'-Hexachlorobiphenyl	2.91×10^{11}
Benzene	2.42×10^3	Naphthalene	1.39×10^5
Toluene	1.21×10^4	Phenanthrene	7.41×10^6
Chlorobenzene	1.92×10^4	Benzo[<i>a</i>]pyrene	2.80×10^9

^aSee Ref. 10.

which would associate with water, show the lower values. Activity coefficients will be useful in the discussion of solubilities and partition coefficients.

2.2 AQUEOUS SOLUBILITY

The tendency of a compound to distribute into the water compartment, indicated by its solubility, is an important factor in determining its environmental distribution. The solubility of a compound at a specified temperature is defined by the concentration of a saturated solution where the molecules dispersed in the solvent are at equilibrium with those in the pure solid or liquid, present in excess. Note that water is unique in many ways. For such a small molecule it has a very high boiling point, which can be explained by its ability to form hydrogen bonds. It has a high heat capacity and floats when it freezes, properties important to our general well being. It is not surprising, then, that the solvent properties of water are also unique.

Solubility data for organic compounds, many of which are not very soluble in water, are quite variable (orders of magnitude) and an understanding of the experimental approaches used to measure this parameter will provide a basis for identifying the best value. An understanding of factors controlling the solution process will explain how solubility relates to molecular properties. Water in the environment is far from the distilled product used in laboratory studies so it will be useful to consider how such variables as DOM, salts, and temperature affect the solubility.

2.2.1 The Solution Process

Introductory approaches to solubility always emphasize that “like dissolves like”. That is polar solvents will dissolve polar solutes and nonpolar solvents nonpolar solutes. Polarity depends on the presence of polar bonds formed between atoms that differ in electronegativity. For example, a C—H bond will be relatively nonpolar with a difference in electronegativity of 0.4 in contrast to an O—H bond with a

difference of 1.4. The charge distribution in a polar molecule produces a dipole that results in stronger intermolecular forces than the van der Waal's forces holding non-polar molecules together. Water is a polar molecule with a small negative charge associated with the oxygen and a comparable positive charge with the hydrogens. Methanol is miscible with water because the —OH group essentially overrides the effect of replacing the —H of water with a more nonpolar —CH₃. However, as the length of the carbon chain increases the molecule assumes a more nonpolar character and, for example, 1-octanol shows a solubility at 25°C of only $4.5 \times 10^{-3} M$ and gives two phases when mixed with water. Water is able to dissolve salts because of its ability to associate with both anions and cations. This property is important in evaluating the environmental behavior of organic acids and bases that form anions or cations as a function of the environmental pH which, in turn, results in increases in aqueous solubility.

When an organic compound dissolves in water the transition results in the distribution of the dissolved molecules in the water environment with the following energy transactions:

1. The organic molecule is first dissociated from like molecules and for a liquid, the energy cost would be proportional to ΔH_{vap} . If the compound dissolves as the solid, the breakdown of the solid structure would involve an additional energy cost proportional to ΔH_{fus} .
2. It would require energy to rearrange the water molecules to produce a “cavity” to accommodate the organic molecule.
3. Forces resulting from the interaction of the organic molecule in the cavity with surrounding water molecules would release energy.

The overall enthalpy of solution is usually positive (requires energy), however, with some smaller alcohols it is negative, reflecting the more favorable interaction of these molecules with water.

One would anticipate a positive entropy change with the solution process in moving to a more random system. However, it appears that the organization of the water (formation of the cavity and arranging the water molecules around the cavity) to accept the organic molecule counteracts this tendency resulting in an overall negative entropy change. Both the enthalpy and entropy changes vary with the size of the molecule and, consequently, it is not surprising that solubilities of some series of organic compounds can be correlated with molecular volume or surface area. This discussion provides a simple overview of the process and more comprehensive treatments are provided in physical chemistry texts.

The thermodynamics of solution evaluate the overall energetics of the process. What is the driving force that results in a compound dissolving? This question can be approached by considering the chemical potential of a compound in solution, μ , which is defined as a function of the chemical potential of that compound in some standard state, μ^0 (in this case, the pure liquid), its mole fraction, x , and its activity

coefficient, γ . So in the aqueous phase

$$\mu_w = \mu^0 + RT \ln x_w \gamma_w$$

Chemical potential is an index of the “activity” of a compound that could reflect its tendency to move in or out of a phase or to react with some other compound. It is clear that this potential will involve both the amount of compound in the system, x , and the extent to which it is “comfortable” in that environment. The higher the values of γ , the less “comfortable” the molecule in that particular environment. The tendency of a compound to dissolve in water will then depend on its chemical potential in the pure liquid, $\mu_{\text{pure liq}}$:

$$\mu_{(\text{pure liq})} = \mu^0 + RT \ln x_{(\text{pure liq})} \gamma_{(\text{pure liq})}$$

as it relates to μ_w , its potential in solution and the free energy change, ΔG_{soln} is defined

$$\Delta G_{\text{soln}} = \mu_w - \mu_{(\text{pure liq})} = RT \ln x_w \gamma_w - RT \ln x_{(\text{pure liq})} \gamma_{(\text{pure liq})}$$

Both x and γ will be essentially one in the pure liquid, since the amount of water dissolving in the liquid organic compound will be very small and, consequently,

$$\Delta G_{\text{soln}} = RT \ln x_w + RT \ln \gamma_w$$

At equilibrium the solution will be saturated and $\Delta G = 0$, so

$$RT \ln x_w(\text{sat}) = -RT \ln \gamma_w(\text{sat}) \quad \text{or} \quad x_w(\text{sat}) = 1/\gamma_w(\text{sat})$$

It is useful to be aware of these relations since both mole fraction and activity coefficients are used both to define solubility and to explore the relation of solubility to the physical properties of molecules.

2.2.2 Determining Aqueous Solubility

Determining the aqueous solubility of organic compounds would seem to be a straightforward experiment; measure the concentration of a saturated solution, and this is true for soluble compounds. However, determining the solubility of compounds in the low ppm and ppb range is another matter and data cited in the literature may show considerable variation. An extensive analysis of publications that cite the solubility of DDT and DDE is critical of the lack of experimental detail provided, and reports variation of two-to-four orders of magnitude.¹⁰ Aqueous solubility data cited for PCB congeners also vary by orders of magnitude.¹¹ Since aqueous solubility is a critical factor in defining environmental distribution, it is necessary

to provide some basis for discriminating among values cited in the literature and the experimental methodology is one such key.

2.2.2.1 Shake Flask Method This straightforward approach simply involves shaking or stirring the compound, in excess, with water at a defined temperature and measuring the concentration of the saturated solution produced. Unfortunately, the shaking action disperses small aggregates through the system and solubility will be overestimated unless these are first removed. For example, the amount of hydrocarbon detected in water after shaking can be affected by the pore size of filters used. A similar response is observed when the "solution" is centrifuged to remove the aggregates. The magnitude of this effect is illustrated in Figure 2.4 where the compound was shaken with water for 16 h and the "solution" concentration monitored.¹² A constant value was achieved after standing for 90 days indicating a solubility of $3.3 \times 10^{-4} \mu\text{g} \cdot \text{mL}^{-1}$ (0.33 ppb). What is important to note, however, is that the amount of compound detected decreased by four orders of magnitude over that period. It is clear that, for compounds with very low aqueous solubility, this technique can result in an overestimate if the generation of aggregates is not addressed.

2.2.2.2 Generator Column This method is the same as that used to measure vapor pressure with the exception that water rather than air is passed through the column containing inert support material coated with the compound in question. This procedure avoids the mechanical action that generates the dispersed aggregates, however, if insufficient contact time is provided to establish equilibrium an underestimate of the solubility would result. Solubility data reported for some polynuclear

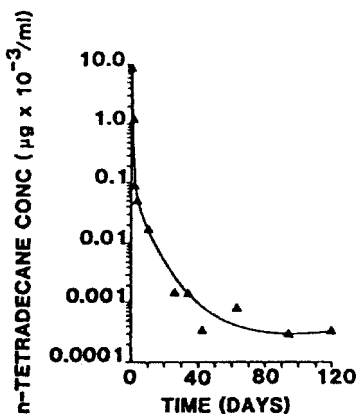


Figure 2.4 Change in concentration of *n*-tetradecane upon standing after shaking to stimulate solution in water. [Reproduced with permission from M. Coates, D. W. Connel, and D. M. Barron, *Environ. Sci. Technol.* **19**, 628 (1985). Copyright © 1985, American Chemical Society.]

aromatic hydrocarbons¹³ and chlorinated hydrocarbons¹ provide an opportunity to compare these two procedures (Table 2.6). With the most soluble compound, naphthalene, no difference in solubility is observed between the two methods. This could be explained by the fact that the amount in solution would be greater than that due to any dispersed aggregates. Larger values are observed with the shake flask method with four of the other polynuclear aromatic hydrocarbons (PAHs) with a more pronounced effect observed in the less soluble compounds. This difference is also observed with the two least soluble chlorinated hydrocarbons, but these data also show that it is possible to obtain comparable results with both methods.

The following criteria have been used to evaluate solubility data¹⁴:

1. Purity of the solute and solvent.
2. Date of the experiment—more recent studies would have the advantage of improved analytical technology, etc.
3. Accuracy of the method—one would be more likely to suspect a shake flask study.
4. Reproducibility.
5. Experience of the investigators—Have they extensive experience in the area?
6. Are the data consistent with relations relating solubility to properties such as molecular surface area, and do they correspond with related properties such as K_{ow} , etc.?

2.2.3 Concentration Units

The units used to define concentration depend on whether one is interested in the properties of the solution or using the solution as a convenient vehicle to transfer specified quantities of solute, or compare solute levels in different solutions. In the former case, equivalent concentrations imply like solute/solvent ratios while in the latter case equivalent concentrations specify identical amounts of solute per

TABLE 2.6 Reported Aqueous Solubilities ($\mu\text{g} \cdot \text{mL}^{-1}$) at 25°C

Compound	Shake Flask	Generator Column
Naphthalene	$32,100 \pm 1,500$ ($n = 8$)	$31,500 \pm 800$ ($n = 7$)
Phenanthrene	$1,170 \pm 90$ ($n = 4$)	$1,050 \pm 120$ ($n = 6$)
Anthracene	66 ± 17 ($n = 4$)	46 ± 13 ($n = 8$)
Fluoranthene	262 ± 4 ($n = 2$)	201 ± 17 ($n = 5$)
Benzo[<i>a</i>]anthracene	12 ± 3 ($n = 2$)	11 ± 4 ($n = 4$)
Chrysene	4 ± 3 ($n = 2$)	1.9 ± 0.8 ($n = 5$)
1,2,3,5-Trichlorobenzene	3.79 ± 0.93 ($n = 7$)	3.55 ± 0.72 ($n = 3$)
Hexachlorobenzene	0.085 ± 0.15 ($n = 6$)	0.019 ± 0.024 ($n = 3$)
4-Chlorobiphenyl	1.25 ± 0.125 ($n = 3$)	1.36 ± 0.039 ($n = 6$)
2,2',4,4,5,5'-PentaCB	0.016 ± 0.010 ($n = 4$)	0.011 ± 0.0070 ($n = 4$)

unit volume of solution. Mole fraction (x_i or sometimes, X_i) and molality (m) are used to define solute/solvent ratios:

$$x_i = \frac{n_1}{\Sigma(n_1, n_2, n_3, \dots)} \quad \text{where "n" represents the number of moles}$$

of a given component

$$m = \text{moles solute}/1000 \text{ g solvent}$$

In the field of environmental chemistry, molality is rarely used, however, mole fraction can be used in relating solubility to molecular properties.

A Mass fraction, (w_i), can be defined that is a counterpart to and directly related to mole fraction¹⁴:

$$w_i = \frac{g_1}{\Sigma(g_1, g_2, g_3, \dots)} \quad \text{where "g" represents the mass of each component}$$

To date, this term is not commonly observed in texts, however, $100w_i$ would be what is commonly referred to as "weight percent". Strictly speaking ppm is a weight/weight term being 1 mg in a 999.999 g of H_2O .

Molarity (M) is defined as moles of solute per liter of solution and is usually represented by [formula]. SI units would require that this concentration term be expressed as $\text{mol} \cdot \text{m}^3$, but this unit has not found common use to date. Millimolar (mM), 1×10^{-3} mol, and micromolar (μM), 1×10^{-6} mol/L of solution are often used.

Research workers are not consistent in the use of concentration units, and solubility relations, for example, may be based on mole fraction. Therefore it often becomes necessary to interconvert concentration units. To convert weight/weight values to molar concentration one must know the density of the solution. For example, what would be the molar concentration of a 2% aqueous solution of glycerol (MW, $92 \text{ g} \cdot \text{mol}^{-1}$) whose density at 25°C is $1.0030 \text{ g} \cdot \text{mL}^{-1}$?

A 2% solution would comprise 20 g of glycerol and 980 g H_2O .

The volume of this solution would be $1000 \text{ g}/1.0030 \text{ g} \cdot \text{mL}^{-1} = 997.009 \text{ mL}$.

This would correspond to $(20 \times 1000)/997.009 = 20.06\text{-g glycerol/L solution}; 0.218 M$.

Note, if one assumed that the density of the solution was one, the molar concentration would be $20/92 = 0.217 M$, a very small error. This observation illustrates the fact that for dilute solutions where the density of the solution would be effectively that of the water, this approximation results in a very small error. Con-

sequently, it is acceptable to consider 1 ppm as 1 mg of solute per liter of solution, and thus

$$1 \text{ ppm} = 1 \text{ mg} \cdot \text{L}^{-1} \text{ or } 1 \mu\text{g} \cdot \text{mL}^{-1} \text{ of solution or } 1 \text{ g} \cdot \text{m}^{-3}$$

$$1 \text{ ppb} = 1 \mu\text{g} \cdot \text{L}^{-1} \text{ or } 1 \text{ ng} \cdot \text{mL}^{-1} \text{ of solution}$$

$$1 \text{ ppt} = 1 \text{ ng} \cdot \text{L}^{-1} \text{ or } 1 \text{ pg} \cdot \text{mL}^{-1} \text{ of solution}$$

Expressions relating aqueous solubility and temperature involve mole fraction, x (Table 2.5) and for 1,4-dichlorobenzene:

$$\ln x = -4.178 - 2186.7/T \quad \text{and at } 25^\circ\text{C}, x = 9.97 \times 10^{-6}$$

How does this calculated value convert to, say, ppm, a more useful term for comparing solubility?

$$x_{\text{su}} = \frac{x_{\text{su}}}{x_{\text{su}} + x_{\text{sv}}} \approx x_{\text{su}}/x_{\text{sv}} \quad \text{since} \quad x_{\text{su}} \ll x_{\text{sv}}$$

where su = solute and sv = solvent

Assuming a liter of aqueous solution, $x_{\text{sv}} = 1000/18 = 55.56$ mol, and moles of solute per liter of solution would be given by

$$9.97 \times 10^{-6} = x_{\text{su}}/55.56 \quad \text{and}$$

$$x_{\text{su}} = 5.539 \times 10^{-4} \text{ mol} \times 147 \text{ g/mol} = 0.0814 \text{ g}$$

Thus the solubility of this dichlorobenzene at 25°C would be 81.4 ppm.

An alternative approach to this calculation depends on the fact that in dilute solutions:

$$x_{\text{su}} = C_{\text{su}}V_{\text{sv}}$$

with V , the molar volume, in this case, of water, $0.018 \text{ L} \cdot \text{mol}^{-1}$.

The aqueous solubilities of some chlorinated aromatic hydrocarbons and mono-nuclear and polynuclear aromatic hydrocarbons are compiled in Table 2.7. Values cited are taken from comprehensive reviews^{1,2} in which the experimental observations have been evaluated and recommended values listed.

TABLE 2.7 Aqueous Solubility at 25°C

Compound	S_w (ppm)	$\ln x = f(1/T)$ 5–50°C	Compound	S_w (ppm)	$\ln x = f(1/T)$ 5–50°C
<i>Chlorobenzenes</i>					
1,2-DCB	140	$-31.529 + 3834/T + 8.72 \times 10^{-5}T^2$	2,8-	0.0145	$2.515 - 5398.4/T$
1,4-DCB	80	$-4.178 - 2186.7/T$	Octo	1.16×10^{-6}	$-5.0496 - 7455.1/T$
1,3,5-TCB	8	$-5.083768 - 2650.68/T$	<i>Aromatic Hydrocarbons</i>		
PentaCB	0.50	$-3.61482 - 4093.10/T$	Benzene	1780	$-15.5446 + 1442.4/T + 3.283 \times 10^5 T^2$
HCB	0.005	$-8.22956 - 4037.26/T$	Toluene	530	$-46.1 + 7259/T + 1.411 \times 10^{-4}T^2$
<i>Chlorinated Biphenyls</i>					
3-	2.5	NA ^a	1,2,4-Trimethylbenzene	57	$-8760 - 868.70/T$
4,4'-	0.06	$-2.8677 - 4839.46/T$	Styrene	320	$-19.471 + 1655.9/T + 4.6224 \times 10^{-5}T^2$
2,4,5-	0.14	$-3.06175 - 4633.86/T$	Naphthalene	31.5	$-1.54117 - 3193.9/T$
2,2',5',5'-	0.03	NA ^a	Biphenyl	7.2	$1.5792 - 3669.26/T$
2,3,4,5-	0.0177	$-3.967 - 4970.5/T$	Acenaphthene	3.80	$-3.51593 - 3297.48/T$
2,2',4',6',6'-	0.002	$-8.9206 - 4122.07/T$	Fluorene	1.90	$0.82861 - 4824/T$
2,2',3',5',5',6',6'-	0.0003	$-5.34 - 6100/T$	Anthracene	0.045	$-1.43611 - 5307.35/T$
<i>Chlorinated-Dibenzodioxins</i>					
1-	0.417	$-0.68385 - 4912.75/T$	Phenanthrene	0.132	$-4.007476 - 4252.03/T$
2,7-	0.00375	$-3.48833 - 5543.9/T$	Pyrene	0.0020	$-7.94471 - 4396.26/T$
2,3,7,8-	1.9×10^{-5}	NA ^a	Chrysene	0.003	$-2.59638 - 6046.87/T$
1,2,3,4,7-	1.2×10^{-4}	NA ^a	Benzol[<i>a</i>]pyrene	0.865	$4.1680 - 6087.88/T$
			Dibenzodioxin	4.75	$-1.6385 - 3842.2/T$
			Dibenzofuran		

^aNot available = NA.

2.2.4 Solubility of Super-Cooled Liquids

An approach similar to that used for vapor pressure provides a relation for estimating the solubility of the super-cooled liquid, S_{scl}

$$\ln S_{\text{scl}} = \ln S_s + \frac{\Delta S_{\text{fus}}}{R} \left(\frac{T_m}{T} - 1 \right)$$

The entropy change, can be derived from the enthalpy change ($\Delta S_{\text{fus}} = \Delta H_{\text{fus}}/T$), however, a value of $56 \text{ J} \cdot \text{mol}^{-1} \cdot \text{K}^{-1}$ can be used as a reasonable approximation if necessary.⁵ Examples of the solubilities of super-cooled liquids are summarized in Table 2.8 and as might be expected these values are higher than those of the corresponding solid. It will be seen that expressing solubility as the super-cooled liquid is useful when considering the relation of solubility to related physical chemical parameters.

2.2.5 Factors Influencing Solubility

Laboratory data is generated at specific temperatures using distilled water that is not representative of conditions occurring in the environment. To understand the behavior of organic compounds in the aquatic compartment, it is necessary to consider variables such as temperature since surface waters will be higher than those observed in groundwater, and salinity because a large proportion of the environmental water compartment is indeed seawater. Natural waters also contain varying amounts of dissolved organic matter (DOM) that can influence the amount of compound that can be “dissolved”.

2.2.5.1 Temperature The relation between aqueous solubility and temperature can be defined by a relation analogous to the Clausius–Clapeyron relation derived for vapor pressure

$$\frac{d \ln x}{dT} = \frac{\Delta H_{\text{sol}}}{RT^2}$$

and in an integrated form

$$\ln x = \frac{-\Delta H_{\text{sol}}}{RT} + A$$

where ΔH_{sol} is the enthalpy of solution and A , an integration constant. Examples of these relations are given in Table 2.7. In contrast to vapor pressure, changes in aqueous solubility are not large over the environmental temperature range. Solids will show an increase in solubility with increase in temperature reflecting the need to overcome the enthalpy of fusion. For example, the solubility of anthracene at 15°C is calculated to be 0.0234 ppm, which increases by a factor of 2 when the

TABLE 2.8 Solubility of Super-Cooled Liquids at 25°C

Compound	S_s (ppm)	ΔH_{fus} (kJ · mol ⁻¹)	T_m (°C)	ΔS_{fus} (J · mol ⁻¹ · K ⁻¹)	S_{scf} (ppm)
1,4-Dichlorobenzene	80	18.2	53.1	55.8	150
Hexachlorobenzene	0.005	23.8	230	47.3	0.251
2,3,4,5-Tetrachlorobiphenyl	0.0177	25.2	92	69.0	0.114
2,3,7,8-Tetrachlorodibenzodioxin	1.93×10^{-5}	39.9	305	69.0	3.11×10^{-4}
Naphthalene	31.5	18.0	80.2	51.0	98.1
Anthracene	0.045	29.0	216.2	59.3	4.37
Phenanthrene	1.10	18.6	101	49.7	5.05

temperature is increased to 25°C (Table 2.5). By contrast, the solubility of toluene, a liquid at ambient temperatures, only increases from 521 to 530 ppm over the same temperature range.

2.2.5.2 Salinity When salts dissolve, the ions produced associate strongly with the water molecules to form hydration shells. This “bound” water is not available to dissolve organic compounds reducing solubility and producing what is termed a “salting out” effect defined by the Setschenow or salting out constant (K^s) with units, M^{-1}

$$\log\left(\frac{S_w}{S_{\text{salt}}}\right) = K^s[\text{salt}]$$

This constant varies with both the compound and the salt since ions differ in the extent to which they hydrate. An alternative approach has used ionic strength rather than molar concentration,¹⁵ with ionic strength, I , defined

$$I = \frac{1}{2}\sum m_i(z_i)^2$$

where m is the molal concentration of the ion and z is the charge, giving a salting out constant K^i with units m^{-1} . The effect of increasing the concentration of sodium chloride to 1 m on the solubility of *m*-nitrophenol is illustrated in Figure 2.5 yielding $K = 0.147$.

Salting out constants, K , for a series of compounds are compiled in Table 2.9. It is apparent that this effect is more pronounced in compounds of lower aqueous solubility with K inversely related to $\log S_w$ (Fig. 2.6). It was observed that solubilities determined in sea water corresponded with those determined in sodium chloride solution (35 g · kg⁻¹ H₂O; $I = 0.60$) whose concentration approximated the total salt concentration of sea water. It was concluded that the salting-out constants derived from observations in sodium chloride solutions could be used to predict solubilities in sea water. Using the regression equation relating K and $\log S_w$:

$$K = -0.0298 \log S_w + 0.114$$

solubility in sea water, S_{sw} , can be expressed as a function of S_w (M) and I :

$$\log S_{sw} = (0.0298 + 1) \log S_w - 0.114 I$$

This approach is validated by the correspondence between calculated and experimental values.

2.2.5.3 Dissolved Organic Matter—Solubility Enhancement The amount of organic matter in natural waters will vary (Fig. 2.7) depending on the

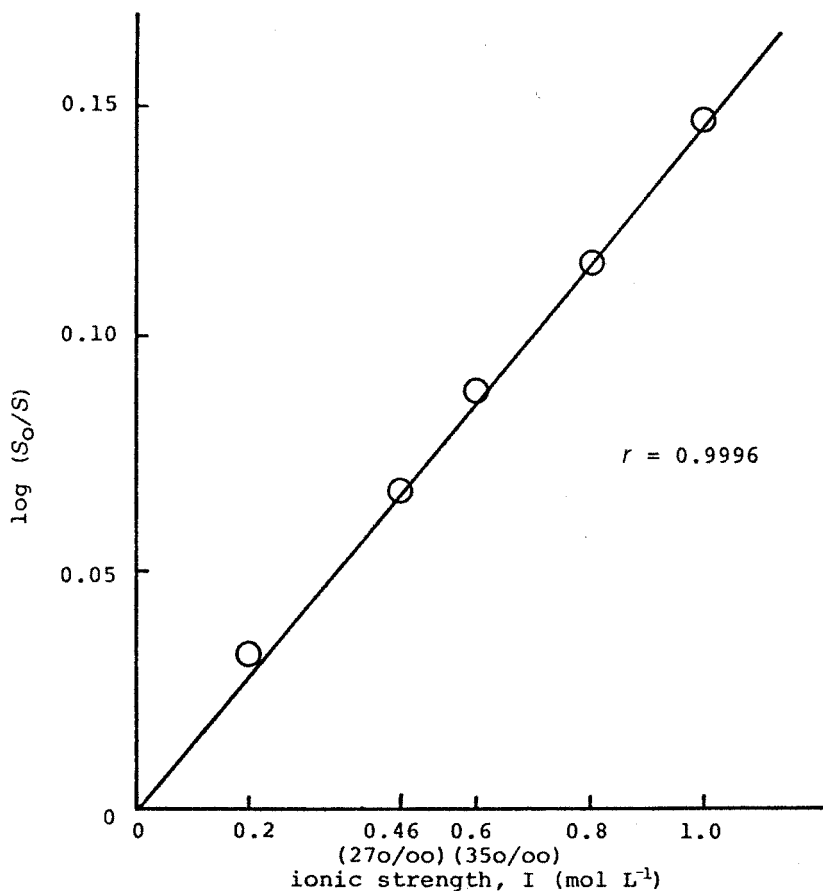


Figure 2.5 The ratio of the solubility of *m*-nitrophenol in water (S_0) and sodium chloride solution (S) as a function of ionic strength. [Reprinted from *Chemosphere* **13**, 881, Y. Hashimoto, K. Tokura, and W. M. J. Strachan, "Prediction of seawater solubility of aromatic compounds". Copyright 1984, with permission from Elsevier.]

source (organic matter content is $2 \times$ organic carbon).¹⁶ This constituent is derived from plant material and other organisms and one observes a continuum ranging from a dissolved fraction that is fully hydrated through a colloidal fraction of high molecular weight species or aggregates of smaller molecules to suspended particulates. The soluble constituents would be represented by fulvic and humic acids whose chemistry is quite complex, but for the purposes of this discussion these molecules can be perceived as having hydrophobic regions associated with aliphatic and aromatic skeletons and phenolic and carboxylic acid functional groups that account for their aqueous solubility. Additional information on this topic is provided in Chapter 3 (Sorption).

TABLE 2.9 Salting-Out Constants and Solubility in Sea Water

Compound	K (m^{-1})	S_w (M) ($20^\circ C$)	S_{sw} (M) ($20^\circ C$)	
			Exptl.	Calc.
Anthracene	0.326	1.8×10^{-7}	1.18×10^{-7}	1.18×10^{-7}
Pyrene	0.294	4.7×10^{-7}	3.22×10^{-7}	3.08×10^{-7}
Phenanthrene	0.272	6.2×10^{-6}	4.15×10^{-6}	4.25×10^{-6}
Biphenyl	0.259	3.8×10^{-5}	2.39×10^{-5}	2.71×10^{-5}
Naphthalene	0.230	1.9×10^{-4}	1.34×10^{-4}	1.40×10^{-4}
<i>p</i> -Nitrotoluene	0.163	2.1×10^{-3}	1.83×10^{-3}	1.60×10^{-3}
<i>p</i> -Toluidine	0.170	6.2×10^{-2}	4.89×10^{-2}	5.01×10^{-2}
<i>o</i> -Nitrophenol	0.136	1.0×10^{-2}	8.34×10^{-3}	7.87×10^{-3}
<i>m</i> -Nitrophenol	0.147	8.3×10^{-2}	6.49×10^{-2}	6.80×10^{-2}
<i>p</i> -Nitrophenol	0.165	9.7×10^{-2}	7.76×10^{-2}	8.01×10^{-2}
Phenol	0.111	1.6	1.35	1.35

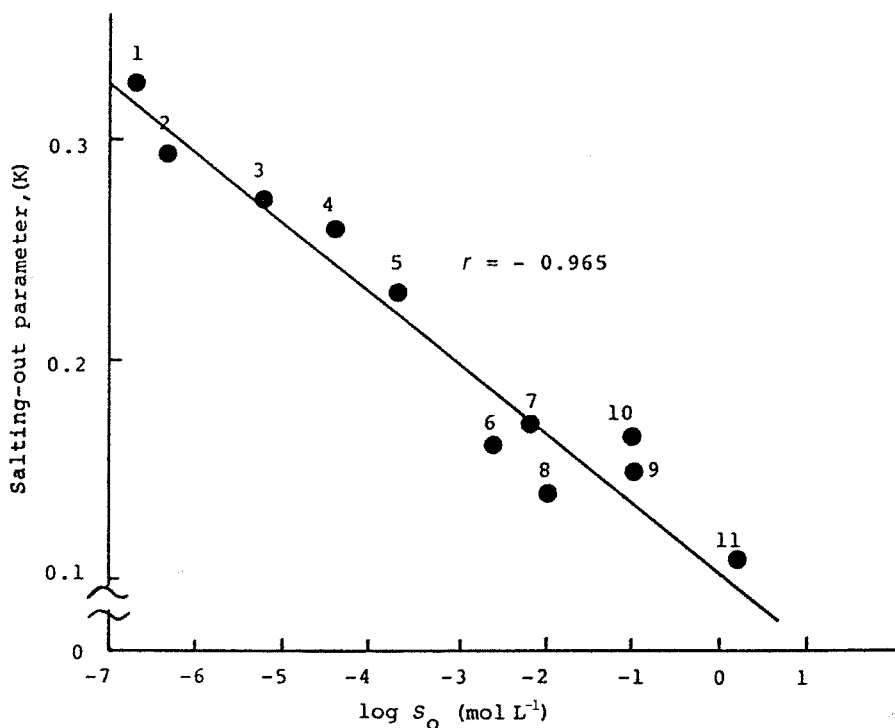


Figure 2.6 Relation of the salting out parameter, K , with aqueous solubility. [Reprinted from *Chemosphere* **13**, 881, Y. Hashimoto, K. Tokura, and W. M. J. Strachan, "Prediction of seawater solubility of aromatic compounds". Copyright 1984, with permission from Elsevier.]

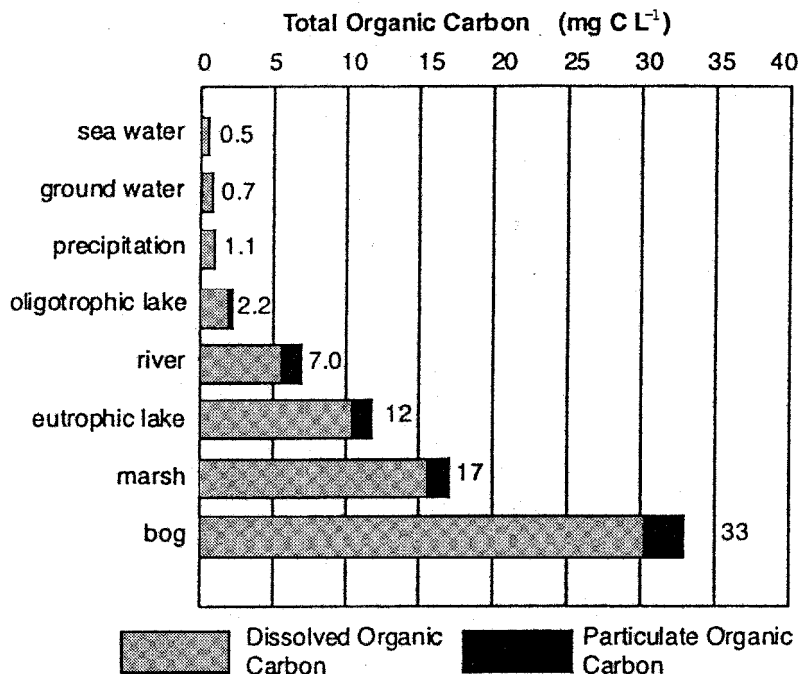


Figure 2.7 Dissolved and particulate organic carbon in natural waters. [Reproduced from E. M. Thurman, *Organic Geochemistry of Natural Waters*, p. 8, Martinus Nijhoff/Dr. W. Junk Publishers, Kluwer Academic Publishers Group, 1985, with kind permission of Kluwer Academic Publishers.]

The effect of dissolved organic matter on the solubility of DDT and two PCB congeners is illustrated in Figure 2.8. This study demonstrates that the “solubility” of the chlorinated hydrocarbon was increased with the amount of soil humic acid added.¹⁷ It must be emphasized that this increase does not result from an effect on the solvent but it is due to the association of the solute with the dissolved humic acid. With these hydrophobic compounds it would appear that the association is due to their partitioning into rather than adsorption onto the humic acid since the two PCB congeners do not compete, that is, the trichlorobiphenyl does not reduce the association of the pentachlorobiphenyl. (The partitioning process is discussed in more detail in the analysis of the sorption in soil.)

The “dissolved” solute would then exist in two compartments whose distinction is important in determining a compound’s environmental behavior. Only the fraction in “true” solution is directly available for evaporation or absorption by organisms, for example. The total amount of solute dissolved, S_{tot} , is thus the sum of the amount in each compartment.

$$S_{\text{tot}} = S_w + S_{\text{dom}}$$

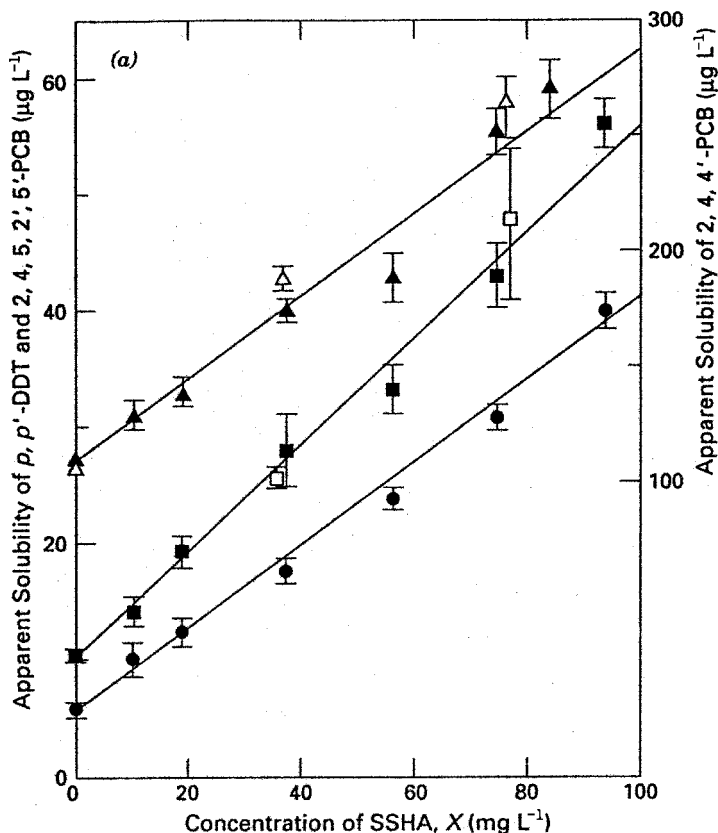


Figure 2.8 Apparent water solubility of *p,p'*-DDT (●), 2,4,5,2',5'-PCB (■,□), and 2,4,4'-PCB (▲,△). [Reproduced with permission from Chiou et al. *Environ. Sci. Technol.* **20**, 502 (1986). Copyright © 1986, American Chemical Society.]

The amount of solute associated with the DOM would depend on the concentration of the DOM, X ($\text{g} \cdot \text{mL}^{-1}$) and the concentration of the solute in the DOM, C_{dom} .

$$S_{\text{tot}} = S_w + X \cdot C_{\text{dom}}$$

Introducing a distribution ratio, $K_{\text{dom}} (\text{mL} \cdot \text{g}^{-1}) = C_{\text{dom}}/S_w$,

$$S_{\text{tot}} = S_w + X(K_{\text{dom}} \cdot S_w)$$

The linear relation between S_{tot} and X gives an intercept, S_w , and slope, $K_{\text{dom}} \cdot S_w$. The K_{dom} values determined for these three organochlorine compounds using two humic acid (HA) and two fulvic acid (FA) samples are summarized in Table 2.10.

TABLE 2.10 The K_{dom} Values with Different Samples of Dissolved Organic Matter

Compound	S_w (25°C) (mg · L ⁻¹)	log K_{ow}	log K_{dom}			
			SSHA ^a (58.03) ^b	SSFA (48.71)	SRHA (54.22)	SRFA (53.78)
<i>p,p'</i> -DDT	5.4×10^{-3}	6.36	4.82	4.27	4.12	4.13
2,4,5,2',5'-PCB	1.1×10^{-2}	6.11	4.63	3.81	3.80	3.83
2,4,4'-PCB	0.116	5.62	4.16	3.58	3.27	3.30

^aSS = Sanhedron soil, SR = Suwannee river.

^b% OC.

These data indicate that the tendency to distribute into the DOM varies both with the nature of the compound and the DOM. The soil humic acid was a more effective receptor and the magnitude of the K_{dom} was directly related to the octanol–water partition coefficient, K_{ow} , which is also an index of a compound's tendency to distribute into a hydrophobic environment. Experiments with 1,2,3-trichlorobenzene (log $K_{\text{ow}} = 4.14$) and lindane (log $K_{\text{ow}} = 3.70$) did not give the same degree of solubility enhancement. Note that the distribution constant for DDT based on organic carbon, K_{doc} would be given by

$$K_{\text{doc}} = \frac{66,069}{0.5803} = 113,854 \quad \log K_{\text{doc}} = 5.06$$

This distinction between organic matter and organic carbon is also a factor in the discussion of the sorption by the soil organic fraction (see Chapter 3, Sorption). A comprehensive analysis of this phenomenon including an extensive compilation of experimental K_{dom} and K_{doc} values is available.¹⁸

When a natural body of water is sampled and filtered or centrifuged to remove particulates, an analysis for a specific organic compound would provide an estimate of C_{tot} . Given the fact that these samples will contain DOM, it is important to be able to discriminate between the amount of chemical associated with the DOM and that in free solution since the latter will define the proportion that is "available". One could determine the amount of DOM in the sample, X , and if a value for K_{dom} was available, C_w could be calculated

$$C_w = \frac{C_{\text{tot}}}{1 + X \cdot K_{\text{dom}}}$$

One might use a gas–purge method, bubbling air or some inert gas through the sample and measuring the concentration in the air, C_{air} using procedures similar to that used to determine vapor pressures. The concentration in water, C_w would then be defined by the Henry's law constant as discussed in Section 2.3. Other experimental approaches to this problem have been outlined.¹⁸

2.3 HENRY'S LAW CONSTANT

Henry's law, stated in 1803, addressed the effect of pressure on the solubility of gases and noted that the mass of gas, m , dissolved by a given volume of solvent

at constant temperature is proportional to the pressure of the gas with which it is in equilibrium.

$$m = kP$$

The mass of gas, m , dissolved in unit volume of solvent is defined by a concentration term and with aqueous systems would be the concentration in water, C_w . Vapor pressure, P , is dependent on the number of molecules per unit volume and can be expressed as vapor density (see section on vap. press.) or the concentration in the air, C_{air} . Thus Henry's law would predict that

$$\frac{C_{\text{air}}}{C_w} = H'$$

a dimensionless constant defining the distribution of a compound between aqueous solution and the vapor phase. It was originally observed that Henry's law applied to gases of low solubility that did not interact with the solvent, that is, the compound exists in the same form in both phases. For example, ammonia would deviate from this law because it reacts with water.

It can be demonstrated that for compounds that are slightly or even moderately soluble in water such that there is minimal solute-solute interaction in solution, a Henry's law constant can be approximated by the ratio of the compound's vapor pressure and its aqueous solubility at a specified temperature.

$$H = \frac{P^0}{S_w}$$

An unfortunate consequence of this approach is that there are as many units for the Henry's law constant as there are units for expressing vapor pressure and solubility!

2.3.1 Units for the Henry's Law Constant

This state of confusion can be illustrated using vapor pressure and solubility data for carbon tetrachloride at 25°C as an example:

$$\begin{aligned} S_w &= 800 \text{ ppm} = 0.800 \text{ g} \cdot \text{L}^{-1} = 0.800 \text{ g} \cdot \text{L}^{-1} / 154 \text{ g} \cdot \text{mol}^{-1} \\ &= 0.00519 \text{ mol} \cdot \text{L}^{-1} = 0.00519 \text{ mol} \cdot \text{L}^{-1} \times 1000 \text{ L} \cdot \text{m}^{-3} = 5.19 \text{ mol} \cdot \text{m}^{-3} \\ P^0 &= 113 \text{ Torr} = 113 \text{ Torr} \cdot 1 \text{ atm} / 760 \text{ Torr} \\ &= 0.149 \text{ atm} = 0.149 \text{ atm} \times 101,325 \text{ Pa} / 1 \text{ atm} = 15,097 \text{ Pa} \\ H &= P^0 / S_w \\ &= (0.149 \text{ atm}) / (0.00519 \text{ mol} \cdot \text{L}^{-1}) = 28.7 \text{ L} \cdot \text{atm} \cdot \text{mol}^{-1} \\ &= (0.149 \text{ atm}) / (5.19 \text{ mol} \cdot \text{m}^{-3}) = 0.0287 \text{ atm} \cdot \text{m}^3 \cdot \text{mol}^{-1} \\ &= (15,097 \text{ Pa}) / (5.19 \text{ mol} \cdot \text{m}^{-3}) = 2.91 \times 10^3 \text{ Pa} \cdot \text{m}^3 \cdot \text{mol}^{-1} \end{aligned}$$

The dimensionless constant, H' , can be determined by first converting the vapor pressure to vapor density using the equation of state:

$$\begin{aligned} C_{\text{air}} &= n/V = P^0/RT \\ &= 0.149 \text{ atm}/(0.082 \text{ L} \cdot \text{atm} \cdot \text{mol}^{-1} \cdot \text{K}^{-1} \times 298 \text{ K}) = 0.00610 \text{ mol} \cdot \text{L}^{-1} \\ H' &= C_{\text{air}}/S_w = 0.00610 \text{ mol} \cdot \text{L}^{-1}/0.00519 \text{ mol} \cdot \text{L}^{-1} = 1.18 \end{aligned}$$

The dimensionless constant, H' , provides a definite advantage in that, in comparison with the other units, it provides a clear indication of how a compound distributes between the two phases.

The relation between H and H' is as follows:

$$H' = \frac{C_{\text{air}}}{S_w} = \frac{P^0/RT}{S_w} = \frac{P^0}{S_w RT} = \frac{H}{RT}$$

It is not always apparent to a student just what value should be used for the gas constant, R , but one can always calculate the appropriate value using the units used for H and remembering that 1 mol of gas occupies 22.4 L at standard temperature and pressure. For example, given that $H = 2910 \text{ Pa} \cdot \text{m}^3 \cdot \text{mol}^{-1}$ at 25°C,

$$R = \frac{101,325 \text{ Pa} \times 22.4 \text{ L}/1000 \text{ m}^3 \cdot \text{L}^{-1}}{273} = 8.314 \text{ J} \cdot \text{mol}^{-1} \cdot \text{K}^{-1}$$

and

$$H' = \frac{2910}{8.314 \times 298} = 1.17$$

2.3.2 Determining Henry's Law Constant

Experiments to measure the Henry's law constant use either a direct approach of measuring C_{air} and C_w in a system at equilibrium or a kinetic approach that monitors the rate of evaporative loss from an aqueous solution, which depends on this parameter (see Evaporation, Chapter 4).

2.3.2.1 Head-Space Analysis An aqueous solution of the compound(s) under study is allowed to come to equilibrium with the air in a closed system and both phases are sampled and analyzed. This approach has been used to determine H' values for a PCB mixture.¹⁹ This technique is not well adapted to compounds of low solubility because the low concentrations in both phases become limiting.

2.3.2.2 Gas Purging This technique uses the same experimental approach used to determine vapor pressure except that the gas stream is passed through an

aqueous solution rather than the pure compound. When equilibrium is established (determined by the length of the purging path) between the gas bubbles and the solution, the concentration in the gas phase is determined by H' . Trapping the compound evaporating in the gas phase provides an estimate of C_{air} , which, with the original C_w , gives a direct estimate of H' similar to the analysis of the head space. The advantage being that it is possible to trap sufficient compound to analyze in the gas phase with only a small decrease in C_w that is well within experimental error.²⁰ A more sophisticated procedure utilizes concurrent flow of the solution and purging gas through a glass helix mounted in a thermostatted tube to give effective interaction between the two phases.²¹

This same experimental protocol provides data that can be used in a kinetic approach to determining H' . The rate of evaporation of the compound from solution is defined by the purge gas-flow rate, F in $\text{L} \cdot \text{min}^{-1}$ and C_{air} and the change in solution concentration is thus

$$dC_w/dt = -F/VC_{\text{air}}$$

where V is the volume of the solution. Integrating this relation and substituting $H'C_w$ for C_{air} :

$$[\ln C_w]_t = [\ln C_w]_0 - (F \cdot H')/V \cdot t$$

a first-order rate expression defining loss from the purging with the first-order constant, k_1 , given by

$$k_1 = F \cdot H'/V$$

Thus k_1 can be obtained by monitoring C_w as a function of time giving $\ln C_w$ as a linear function of t with an intercept of $\ln [C_w]_0$ and slope $-k_1$. The change in C_w may be determined directly by analyzing the solution or indirectly by trapping the compound in the gas phase.²² Since F and V are known, H' can then be determined.

It is useful to compare experimental values of H' with those derived from vapor pressure and solubility data. Two methods^{21,22} have been used to determine Henry's law constants for some PCB congeners and these values are compiled along with solubility and vapor pressures in Table 2.11. Although it is not possible to carry out a comprehensive analysis with the limited number of observations it appears that the kinetic technique has a tendency to produce higher values than the direct measurement of C_{air} and C_w . The use of P^0 and S_w provide estimates of H' that are reasonably consistent with experimental values with the exception of a hexa- and octachloro congener. Considerable experimental error could be anticipated with these compounds because of their very low solubilities and vapor pressures. Some confusion can arise with solids in the use of P^0 and S_w if one does not clarify if the values cited are for the solid or the super-cooled liquid. For example, the more recent observations of S_w are based on generator columns that would give a solubility value for the solid. Vapor pressure values derived from gas chromatographic

TABLE 2.11 Henry's Law Constants for PCB Congeners at 25°C

PCB Congener	S_w^a (ppm)	P^{0b} (Pa)	$H = P^0/S_w$ (Pa · m ³ · mol ⁻¹)	$H' = H/RT$ (× 10 ⁻³)	$H'_{\text{Exptl}} = (\times 10^{-3})$	
					C_{air}/C_w^c (k ₁ V)/F ^d	
4,4-	0.06	0.005	18.6	7.50		8.14
2,4,5-	0.14	0.132	24.3	9.81	7.9	
2,2',3,3'-	0.016	0.00109	20.5	8.3	4.1	8.26
2,2',5,5'-	0.03	0.0049	47.7	19.3	8.0	14.0
2,2',6,6'-	0.012	0.0383	18.2	7.35	8.1	22.5
2,2',3,3', 4,4'-	0.001	1.96×10^{-5}	7.08	2.09	0.53	1.24
2,2',4,4',5,5'-	0.001	1.2×10^{-4}	43.3	17.4	0.93	5.40
2,2',3,3',5,5',6,6'-	0.0003	2.7×10^{-5}	38.7	15.6	0.74	

^aFrom Refs. 1 and 23.^bFrom Refs. 1 and 24.^cFrom Ref. 21.^dFrom Ref. 22.

(GC) data, on the other hand give values for the super-cooled liquid. Either the solid or the super-cooled liquid values are valid providing one uses the same form for each parameter.

Henry's law constants derived from data compiled in Tables 2.2 and 7 are compiled in Table 2.12.

2.3.3 Factors Influencing Henry's Law Constant

One could predict that the same variables affecting vapor pressure and solubility would also have an effect on Henry's law constant and, consequently, temperature, salinity, and DOM will be addressed.

TABLE 2.12 Henry's Law Constants at 25°C

Compound	H (Pa · m ³ · mol ⁻¹)	H'	Compound	H (Pa · m ³ · mol ⁻¹)	H'
<i>Chlorobenzenes</i>			<i>Aromatic Hydrocarbons</i>		
1,2-DCB	178	0.071	Benzene	557	0.225
1,4-DCB	239	0.096	Toluene	660	0.266
1,3,5-TCB	567	0.228	Naphthalene	43	0.0174
PentaCB	110	0.0444	Biphenyl	28	0.0113
HCB	131	0.0529	Fluorene	7.87	3.18×10^{-3}
<i>Chlorinated dibenzodioxins</i>			Anthracene	3.96	1.60×10^{-3}
1-	7.28	2.94×10^{-3}	Phenanthrene	3.24	1.31×10^{-3}
2,7-	8.1	3.27×10^{-3}	Pyrene	0.92	3.7×10^{-4}
2,3,7,8-	3.34	1.35×10^{-3}	Chrysene	0.065	2.6×10^{-5}
1,2,3,4,7-	0.45	1.82×10^{-4}	Dibenzodioxin	11.7	4.72×10^{-3}

2.3.3.1 Temperature Aqueous solubility and vapor pressure can be expressed as a function of the respective enthalpy change and absolute temperature, A and B being integration constants.

$$\begin{aligned}\ln P^0 &= -\Delta H_{\text{vap}}/RT + A \\ \ln x &= -\Delta H_{\text{sol}}/RT + B\end{aligned}$$

and since the mole fraction, x , is directly related to mass fraction and molar terms used to express solubility

$$\ln P^0 - \ln S_w = \ln P^0/S_w = \ln H = -(\Delta H_{\text{vap}} - \Delta H_{\text{sol}})/RT + (A - B)$$

For organic compounds, solution enthalpies are positive and relatively small so the change in H with temperature would be primarily due to the enthalpy of vaporization. The Henry's law constant would then increase with temperature but not to the same degree as vapor pressure giving a linear relation between $\ln H$ and $1/T$ (Fig. 2.9).

2.3.3.2 Salinity It has been shown above that the solubility of organic compounds is decreased as the ionic strength of the solution increases and, consequently, one would anticipate a corresponding increase in the Henry's law constant. This effect is illustrated by a comparison of dimensionless constants, H' , determined by the kinetic approach in distilled water and sea water²⁵ (Table 2.13). These observations were made at room temperature, $\sim 23^\circ\text{C}$. Values observed in sea water are higher than those in distilled water by a factor of 2–6.

2.3.3.3 Dissolved Organic Matter The effect of DOM on H' is illustrated by experiments that studied the effect of humic acid on the air–water distribution of the organochlorine insecticide, mirex (Fig. 2.10).²⁶ The concentration of mirex in air in equilibrium with an aqueous solution was determined using a gas-purge procedure. A linear relation was observed between C_{air} and C_w in distilled water over a concentration range of three orders of magnitude. The parameter H' was 0.0213 at 22°C . The addition of only $1.1 \text{ mg} \cdot \text{L}^{-1}$ of humic acid produced a large decrease in C_{air} compared to that observed over distilled water. For example, with $C_w = 6 \text{ ng} \cdot \text{L}^{-1}$, over distilled water, $C_{\text{air}} = 0.127 \text{ ng} \cdot \text{L}^{-1}$, but in the presence of the humic acid C_{air} was reduced to $0.031 \text{ ng} \cdot \text{L}^{-1}$, giving an apparent H' of 0.0052. Note that DOM can enhance the solubility of hydrophobic compounds such as mirex ($S_w = 0.07 \text{ ppb}$) who partition into these complex polymers. It is clear from these observations that the fraction of the mirex associated with the humic acid is not in equilibrium with mirex in the vapor phase. In the presence of the humic acid, the actual concentration in solution in equilibrium with the $0.031 \text{ ng} \cdot \text{L}^{-1}$ observed with $C_{\text{tot}} = 6 \text{ ng} \cdot \text{L}^{-1}$ would be $1.46 \text{ ng} \cdot \text{L}^{-1}$ ($0.031/0.0213$).

Providing a large enough sample is available, purging and determining C_{air} gives an estimate of C_w , the proportion of the compound in true solution that would be

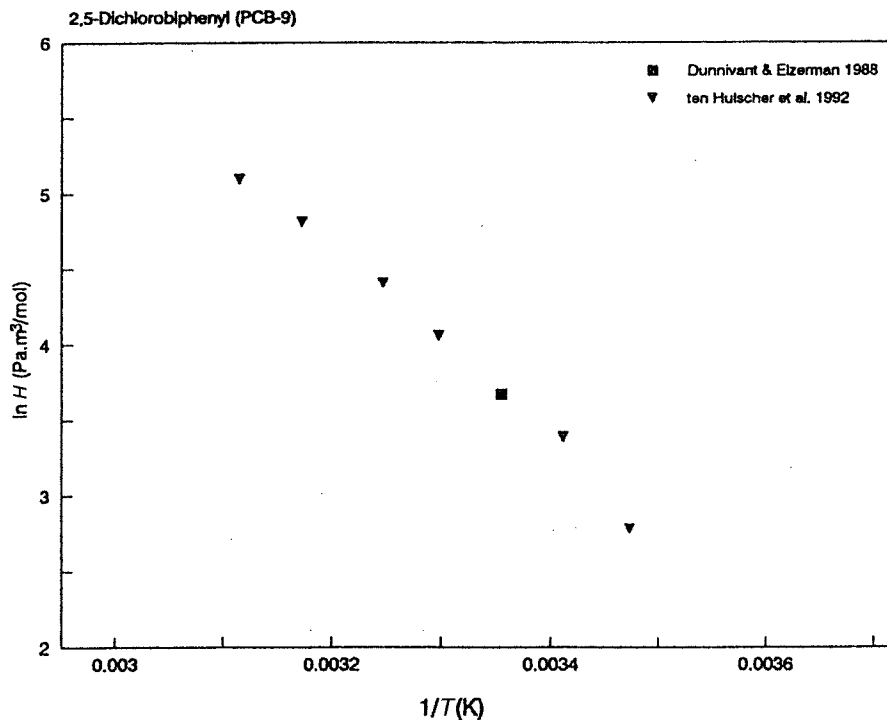


Figure 2.9 Effect of temperature on the Henry's law constant of 2,5-dichlorobiphenyl. [Reproduced with permission from W. Shiu and K. Ma. *J. Phys. Chem. Ref. Data* **29**, 387 (2000). Copyright © 2000, American Chemical Society.]

available to evaporate or be taken up by an organism. It has also been shown that C_{tot} , the total amount of compound in solution, is defined by the amount in true solution C_w and that associated with the DOM.

$$C_{\text{tot}} = C_w + X(K_{\text{dom}} \cdot C_w)$$

TABLE 2.13 Dimensionless Henry's Law Constant in Sea Water

Compound	H'		Compound	H'	
	Dist. Water	Sea Water		Dist. Water	Sea Water
HCB ^a	0.054	0.07	2,5,4'-CB	0.038	0.15
<i>p,p'</i> -DDE	0.050	0.15	3,4,4'-CB	0.034	0.19
2,4-CB ^b	0.039	0.079	2,2',4,6'-CB	0.031	0.20
2,2',3-CB	0.033	0.13	2,3,4,4'-CB	0.034	0.19

^aHexachlorobenzene.

^bCB = chlorobiphenyl.

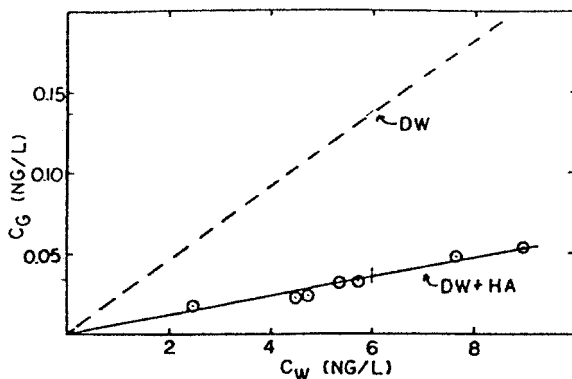


Figure 2.10 Concentration of mirex in the gas phase (C_g) in equilibrium with concentration in distilled water (C_w) and in distilled water (DW) plus 1.1-mg/L humic acid (HA). [Reproduced with permission from C. Yin and J. P. Hassett, *Environ. Sci. Technol.* **12**, 1213 (1986). Copyright © 1986, American Chemical Society.]

with X ($\text{g} \cdot \text{mL}^{-1}$) the concentration of the DOM, and K_{DOM} ($\text{mL} \cdot \text{g}^{-1}$) a partition coefficient defining the distribution between C_w and that associated with the humic acid. In this study, C_{tot} , and X are known and C_w can be derived (C_{air}/H') and it is thus possible to calculate K_{DOM} , which in this case is $2.8 \times 10^6 \text{ mL} \cdot \text{g}^{-1}$. It would also be possible to derive a value for X if a value for K_{DOM} was available.

2.4 OCTANOL-WATER PARTITION COEFFICIENT

The Henry's law constant is an important criteria in determining the extent to which an organic compound will distribute into the atmosphere from water and vice versa. Another important environmental process is the extent to which a compound will distribute into a hydrophobic region. It will be shown that soil organic matter controls sorption of organic compounds in soil, while movement into an organism involves passage across the hydrophobic barrier of the membrane. This tendency is indicated by the octanol-water partition coefficient, K_{ow} .

A partition coefficient is defined by the ratio of the concentrations of a compound in two immiscible phases that are at equilibrium. It is common, though not necessary, for one phase to be water and the second an organic solvent, such as hexane, benzene, ether, and so on. It is important to emphasize that K_{ow} is not the ratio of the solubilities of the compound in octanol and water, because, since the two liquids are at equilibrium, the octanol phase will be saturated with water and the water with octanol. The use of *n*-octanol dates from the late nineteenth century when water-octanol was chosen as a surrogate to reflect uptake of pharmaceuticals into organisms.²⁷ In retrospect, this turned out to be a wise choice and over the past 30 years there has been a continuing interest in the study of K_{ow} , initially stimulated

by pharmacological interests²⁸ and augmented by environmental applications. This discussion will develop an understanding of this parameter, review experimental procedures for its measurement and how it relates to other quantities such as aqueous solubility.

2.4.1 Some Thermodynamics

The K_{ow} for toluene is 490, which shows that this compound favors the environment of the octanol phase. What characteristics of toluene account for this equilibrium distribution? When a compound partitions in an octanol–water system, the equilibrium depends on the fact that the chemical potential of the compound must be the same in both phases and there will be no residual “potential” to drive the compound into one phase or the other.

At equilibrium, then

$$\begin{aligned} \mu_w &= \mu_{oct}, & \text{and} \\ \mu_{(\text{pure liq.})} + RT \ln x_{oct} \gamma_{oct} &= \mu_{(\text{pure liq.})} + RT \ln x_w \gamma_w & \text{and, consequently,} \\ x_{oct} \gamma_{oct} &= x_w \gamma_w \end{aligned}$$

In dilute solution, x is a function of the molar concentration, M , and the molar volume of the solvent, V ($\text{L} \cdot \text{mol}^{-1}$):

$$x = M \cdot V \quad \text{and so}$$

$$M_{oct} V_{oct} \gamma_{oct} = M_w V_w \gamma_w$$

and since K_{ow} is defined as the ratio of the concentrations at equilibrium

$$K_{ow} = M_{oct}/M_w = (\gamma_w/\gamma_{oct})(V_w/V_{oct})$$

Values for K_{ow} can range over eight to nine orders of magnitude and, consequently, are usually cited as $\log K_{ow}$, and so

$$\log K_{ow} = \log \gamma_w - \log \gamma_{oct} + \log \left(\frac{V_w}{V_{oct}} \right)$$

Since the ratio of the molar volumes is constant K_{ow} simply reflects the deviation from ideal behavior of the compound in the two solvent systems. It is also apparent that, for organic compounds, γ_w is the major factor contributing to K_{ow} . Organic compounds would approach ideal behavior ($\gamma \sim 1$) in the octanol phase while in water nonpolar organics, γ_w can be as high as 10^8 (Table 2.5).

By applying this relation to toluene

V_w , the molar volume of water saturated with octanol is essentially $0.018 \text{ L} \cdot \text{mol}^{-1}$, since the solubility of octanol in water is negligible ($4.5 \times 10^{-3} \text{ mol} \cdot \text{L}^{-1}$)

V_{oct} , the molar volume of octanol saturated with water is $0.12 \text{ L} \cdot \text{mol}^{-1}$. The molar volume of pure octanol is $0.157 \text{ L} \cdot \text{mol}^{-1}$ and the solubility of water in octanol is $2.3 \text{ mol} \cdot \text{L}^{-1}$ ($x = 0.27$). Thus, assuming molar volumes are additive

$$\begin{aligned} V_{\text{oct}} &= 0.27 \times 0.018 \text{ L} \cdot \text{mol}^{-1} + 0.73 \times 0.157 \text{ L} \cdot \text{mol}^{-1} \\ &= 0.12 \text{ L} \cdot \text{mol}^{-1} \quad \text{and} \end{aligned}$$

$$\log\left(\frac{V_w}{V_{\text{oct}}}\right) = -0.82$$

Assuming that the octanol has a small effect on γ_w , and that concentration has little effect on γ at the levels involved

$$\log K_{\text{ow}}(\text{toluene}) = \log(1.2 \times 10^4) - \log 3.02 - 0.82 = 2.78$$

(see Tables 2.5 and 2.18)

which is comparable with the experimental value of 2.69.

This analysis illustrates the major role of γ_w in determining K_{ow} and the fact that toluene shows close to ideal behavior in the octanol phase.

2.4.2 Determination of K_{ow}

Experimental values can be obtained directly by determining the concentration of the compound in the two phases at equilibrium using a “shake flask” or equilibrator column methods. An indirect approach compares the partitioning behavior of compounds with unknown K_{ow} with those with known K_{ow} in a reverse-phase liquid chromatography system.

2.4.2.1 Direct Measurement The compound is usually dissolved in octanol, water added, and the system shaken for sufficient time to achieve equilibrium after which the concentration is determined in both phases. Vigorous shaking can introduce errors due to the contamination of the aqueous phase with emulsions and the variation observed with compounds of high K_{ow} is attributed to this variable. This interference has been minimized using a “slow-stirring” approach.²⁹

An alternative approach to direct measurement involves the use of a generator column.³⁰ The compound is dissolved in octanol and the solution equilibrated with water before adding to a column filled with inert solid support. Water saturated with octanol is then passed through the column allowing the compound to equilibrate between the two phases. The concentration in the octanol phase is determined prior to adding to the column and that of the aqueous phase after passage through the column. This technique also reduces the potential for producing emulsions,

however, longer columns are needed for compounds of higher K_{ow} ($\log K_{ow} > 6$) to ensure that equilibrium is achieved.

2.4.2.2 Indirect Measurement by Liquid Chromatography This technique separates compounds on the basis of the difference in their partitioning behavior between a nonpolar stationary phase (reverse phase) and a polar mobile phase. Compounds that partition to a greater extent into the stationary phase will take longer to move through the system and give a higher retention time or retention volume. Providing the partitioning between the two phases in the chromatography system is comparable to that of octanol–water, K_{ow} values can be determined by comparing retention times of unknowns with a retention time/ K_{ow} relation based on compounds with known K_{ow} 's (Fig. 2.11). Note that this study³¹ relates experimental K_{ow} values with k' , a relative retention time or “capacity factor” that is the retention time of the compound, t_r , relative to that of some compound not retained by the reverse phase column, t_o .

$$k' = \frac{(t_r - t_o)}{t_o}$$

This approach has the advantage that a detection system is an integral part of the chromatograph and several compounds can be evaluated in the same run. Also the same precision needed for determining concentration in the shake flask procedure is not required since it is only necessary to establish the retention time of

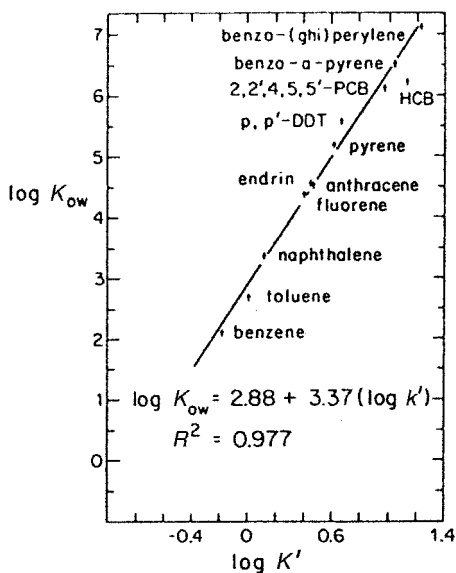


Figure 2.11 The $\log K_{ow}$ versus k' . Chromatographic approach to determining K_{ow} . [Reproduced with permission from R. A. Rapaport and S. J. Eisenreich, *Environ. Sci. Technol.* **18**, 163 (1984). Copyright © 1984, American Chemical Society.]

the compounds under investigation. This procedure has given low values for compounds showing high K_{ow} values ($\log K_{ow} > 6$) by the shake flask method and it has been suggested that this could result from equilibrium not being achieved. Steric effects can also be a factor.³¹ The high-performance liquid chromatography (HPLC) procedure has given K_{ow} values for ortho-substituted (2,2',6,6'-) PCB congeners that are lower than those determined using a generator column (Table 2.14).

This difference could be due to the fact that the interaction of the PCB congeners in the reverse-phase HPLC system could involve surface adsorption rather than partitioning that would be affected by the nonplanar configuration induced by ortho substitution. Correction factors have been derived to account for this anomaly.

2.4.2.3 π Values and Fragment Constants The influence of different substituents on K_{ow} are given by a π value defined as follows:³²

$$\pi_X = \log [K_{ow}]_X - \log [K_{ow}]_H$$

For example, the effect of a chlorine substituent π_{Cl} , can be derived from K_{ow} for chlorobenzene and the unsubstituted benzene,

$$\begin{aligned}\pi_{Cl} &= \log [K_{ow}]_{\text{chlorobenzene}} - \log [K_{ow}]_{\text{benzene}} \\ &= 2.84 - 2.13 \\ &= 0.71\end{aligned}$$

It can be seen that π values depend on the substituent and vary slightly among different series of compounds (Table 2.15).³² Substituents such as $-\text{Cl}$ and $-\text{CH}_3$ have positive π values and will increase K_{ow} while $-\text{OH}$ and $-\text{COOH}$ negative values making the compound more polar. The variation for a specific π value is attributed to changes in its electronic environment. For example, the presence of $-\text{OH}$ in the phenols has a larger influence on the values of halogen substituents than the effect of the carboxylic acids of the other series.

TABLE 2.14 Steric Effects in Determining K_{ow}

PCB Congener	$\log K_{ow}$	
	HPLC ^a	Gen. Column ^b
2-Chloro-	3.90	4.38
3-Chloro-	4.42	4.58
4-Chloro-	4.40	4.49
2,2'-Dichloro-	3.63	4.90
4,4'-Dichloro-	4.82	5.33
2,2',5-Trichloro-	4.39	5.60
2,4',5-Trichloro-	5.11	5.79

^aSee Ref. 31.

^bSee Ref. 30.

TABLE 2.15 Values of π Derived from Different Series of Compounds

Substituent	Phenoxyacetic Acids	Phenylacetic Acids	Benzoic Acids	Phenols
3-Cl	0.76	0.68	0.83	1.04
3-Br	0.94	0.91	0.99	1.17
3-CH ₃	0.51	0.49	0.52	0.56
3-COOH	-0.15	-0.32	-0.19	0.04
3-OH	-0.49	-0.52	-0.38	-0.66
3-OCH ₃	0.12	0.04	0.14	0.12
3-NO ₂	0.11	-0.01	-0.05	0.54

One can thus use π values (Table 2.16)³³ to estimate K_{ow} for a compound when an experimental value is not available providing K_{ow} is known for a related compound that differs from the unknown by one or at the most two substituents. For example, if $\log K_{ow}$ for anisole (methoxybenzene) is known to be 2.11, one would predict that $\log K_{ow}$ for 3-chloroanisole would be $2.11 + 0.77 = 2.88$. This procedure illustrates the concept of linear free energy relations (LFERs) that depends on the fact that the different components of an organic molecule interact both with one another and their environment in a consistent manner and the behavior of the molecule can be defined as the sum of its components.

An extension of this approach can be illustrated by considering a simple aromatic compound such as *p*-chlorophenol.

*p*-Chlorophenol**TABLE 2.16** π Values^a

Substituent	ortho		meta		para	
	π	π^b	π	π_-	π	π_-
-CH ₃	0.84	0.49	0.52	0.50	0.60	0.48
-C ₂ H ₅	1.39	0.99	0.99	0.94	1.10	0.98
-C ₆ H ₅			1.92	1.77	1.74	1.74
-OH	-0.41	-0.58	-0.50	-0.66	-0.61	-0.87
-OCH ₃	-0.33	-0.13	0.12	0.12	-0.03	-0.12
-OCOCH ₃	-0.58	-1.02	-0.60	-0.23	-0.58	-1.06
-NO ₂			0.11	0.54	0.22	0.45
-COOCH ₃			-0.04	0.43	-0.04	0.50
-Cl	0.76	0.69	0.77	1.04	0.73	0.93
-Br	0.84	0.89	0.96	1.17	1.19	1.13

^aSee Ref. 33.

^b π_- Used with compounds having electron-donating substituents such as -OH and -NH₂.

One could calculate a value for K_{ow} using either $\pi(Cl)$ if a K_{ow} value was available for phenol or $\pi(OH)$ if a K_{ow} value was available for chlorobenzene and this would be the preferred approach. However, were this option not available, it is possible to calculate a value for K_{ow} using “fragment constants” such that

$$\log K_{ow} = \sum a_i f_i$$

where “ a ” is the number of fragment “ i ” with fragment constant “ f ” which in this case would be given by

$$\log K_{ow} = f_{Cl} + f_{OH} + f_{C_6H_4} \quad \text{or} \quad = f_{Cl} + f_{OH} + 4f_{CH} + 2f_C$$

Fragment constants have been derived by a statistical approach³⁴ or by considering the volumes of cavities involved in dissolving.³⁵ Calculation of a given K_{ow} must take into account molecular flexibility, unsaturation, multiple halogen substituents, branching, and polar interactions using a series of correction factors. The details involved have been outlined³⁶ and will not be summarized in this discussion. For the most part, calculated K_{ow} values compare favorably with experimental observations.^{29,37}

Different procedures provide comparable values for K_{ow} with $\log K_{ow} < 5$. However, there is some indication that lower values can result from the shake flask procedure probably resulting from higher concentrations in the aqueous phase due to the formation of emulsions.²⁹ Some octanol-water partition coefficients are compiled in Tables 2.17 and 2.18.

TABLE 2.17 Octanol-Water Partition Coefficients for PCBs and Dioxins

PCBs ^a		Dibenzo- <i>p</i> -dioxins ^b	
Compound	$\log K_{ow}$	Compound	$\log K_{ow}$
Biphenyl	4.01	Dibenzo- <i>p</i> -dioxin	4.3
2,6-Dichloro-	4.98	1-Chloro-	4.75
2,4,5-Trichloro-	5.90	2,3-Dichloro-	5.60
2,4,6-Trichloro-	5.71	2,8-Dichloro-	5.60
2,2',6,6'-Tetrachloro-	5.94	1,2,4-Trichloro-	6.35
2,3,4,5-Tetrachloro-	6.41	1,2,3,4-Tetra-chloro-	6.60
3,3',4,4'-Tetrachloro-	6.63	1,3,6,8-Tetrachloro-	7.10
2,3,4,5,6-Pentachloro-	6.75	2,3,7,8-Tetrachloro-	6.80
2,2',3,3',6,6'-Hexachloro-	7.12	1,2,3,4,7-Pentachloro-	7.49
3,3',4,4',5,5'-Hexachloro-	7.41	Octachloro-	8.20

^aSee Ref. 29.

^bSee Ref. 37.

TABLE 2.18 Octanol–Water Partition Coefficients and Water Solubilities

Compound	$\log S_w^a$	$\log K_{ow}$	$\log \gamma_o^b$	Compound	$\log S_w$	$\log K_{ow}$	$\log \gamma_o$
Aniline	-0.405	0.90	0.43	<i>o</i> -Xylene	-2.72	3.64	0.87
<i>o</i> -Toluidine	-0.817	1.29	0.45	<i>m</i> -Xylene	-2.73	3.65	0.45
<i>m</i> -Toluidine	-0.853	1.40	0.37	<i>p</i> -Xylene	-2.73	3.65	0.50
<i>N</i> -Methylaniline	-1.28	1.66	0.54	<i>o</i> -Dichlorobenzene	-2.98	3.90	0.52
<i>N,N'</i> -Dimethylaniline	-2.04	2.31	0.65	<i>m</i> -Dichlorobenzene	-3.04	3.96	0.58
<i>o</i> -Chloroaniline	-1.53	1.90	0.55	<i>p</i> -Dichlorobenzene	-3.31 (-3.03) ^c	3.95	0.56
<i>m</i> -Chloroaniline	-1.37	1.88	0.41	1,2,4-Trichlorobenzene	-3.57	4.02	0.47
Benzene	-1.64	2.13	0.43	Biphenyl	-4.31 (-3.88)	4.09	0.71
Toluene	-2.25	2.69	0.48	2-Chlorobiphenyl	4.54		
Ethylbenzene	-2.84	3.76	0.61	3-Chlorobiphenyl	-5.16	6.08	1.13
Propylbenzene	-3.30	3.68	0.54	Diphenylmethane	-4.07	4.95	0.85
Isopropylbenzene	-3.38	3.66	0.64	Naphthalene	-3.61 (-3.08)	4.00	0.64
1,3,5-Trimethylbenzene	-3.09	3.42	0.59	2-Methylnaphthalene	-3.75 (-3.69)	4.11	0.50
<i>tert</i> -Butylbenzene	-3.60	4.11	0.41	Phenanthrene	-5.14 (4.48)	4.57	0.83
Fluorobenzene	-1.80	2.27	0.45	Anthracene	-6.38 (-4.41)	4.54	0.79
Chlorobenzene	-2.36	3.28	0.44	Pyrene	-6.18 (-5.24)	5.18	0.98
Bromobenzene	-2.55	3.47	0.48	Hexachlorobenzene	-7.76 (-5.57)	5.50	0.99
Iodobenzene	-2.78	3.70	0.45	<i>p,p'</i> -DDT	-7.81 (-6.74)	6.36	1.30

^a S_w at 25°C.^b $\log \gamma_o = \log K_{ow}^0 - \log K_{ow}$, where K_{ow}^0 is calculated from the ideal line using $[S_w]_{liquid}$.^cValue in parenthesis is solubility of the super-cooled liquid.

2.4.3 Factors Influencing Octanol–Water Partition Coefficients

The effect of temperature on K_{ow} is a function of the enthalpies of solution

$$dK_{ow}/dt = f(\Delta H_{oct} - \Delta H_w)$$

and since this difference is not large, variation in temperature within the ambient range would result in only small changes in K_{ow} .

Since $K_{ow} = (\gamma_w/\gamma_{oct})(V_w/V_{oct})$, the effect of concentration would reflect changes in the activity coefficient, γ , and molar volume, V . At low concentrations these parameters would be relatively constant and one would not anticipate K_{ow} to vary to any degree with concentration. The activity coefficient decreases with increasing concentration and K_{ow} could increase with increasing concentration with a compound that is very soluble in octanol. In this case γ_{oct} would decrease more rapidly with an increase in concentration than γ_w . However, under environmental conditions one is not usually dealing with high concentrations and K_{ow} is considered to be constant; certainly within the range of experimental error involved in its determination.

2.4.4 Octanol–Water Partition Coefficient and Aqueous Solubility

An inverse relation between the octanol–water partition coefficient, K_{ow} , and aqueous solubility, S_w , is intuitive, since compounds that are soluble in water are usually less soluble in solvents like octanol and vice versa. A systematic evaluation of this relation³⁸ is based on the expression defining K_{ow} as a function of activity coefficients and molar volumes

$$K_{ow} = (\gamma_w/\gamma_{oct})(V_w/V_{oct})$$

It has also been noted (p. 19) that the solubility of a compound expressed as mole fraction, $x_{sat} = 1/\gamma_{sat}$, and since $x_{sat} = C_{sat} \cdot V_w$, $C_{sat} = 1/(\gamma_{sat} \cdot V_w)$. The relation between K_{ow} and S_w would thus be, since $S_w = C_{sat}$.

$$K_{ow} = (1/S_w)1/(\gamma_{oct} \cdot V_{oct})$$

expressed logarithmically

$$\log K_{ow} = -\log S_w - \log \gamma_{oct} - \log V_{oct}$$

Assuming that compounds show ideal behavior in octanol, $\gamma_{oct} = 1$, one obtains an ideal line

$$\log K_{ow}^0 = -\log S_w + 0.92$$

since V_{oct} , the molar volume of octanol saturated with water is $0.12 \text{ L} \cdot \text{mol}^{-1}$ (p. 41). The parameter S_w would be expressed in $\text{mol} \cdot \text{L}^{-1}$. This relation also assumes

that γ_w is not affected by the small amount of octanol dissolved in the water and that activity coefficients in both phases are essentially constant over the concentration ranges involved. Thus the ideal line would show a slope of -1 and an intercept of 0.92 .

If $\log K_{ow}$ is plotted as a function of $\log S_w$ (Fig. 2.12) a good correlation is observed with compounds that are liquids at 25°C .³⁹ However, solids deviate from this regression line showing lower aqueous solubility than would be predicted from their K_{ow} values. This reflects the melting effect on solubility that is not a factor in the partition coefficient since it cancels out being involved in the solubility of the

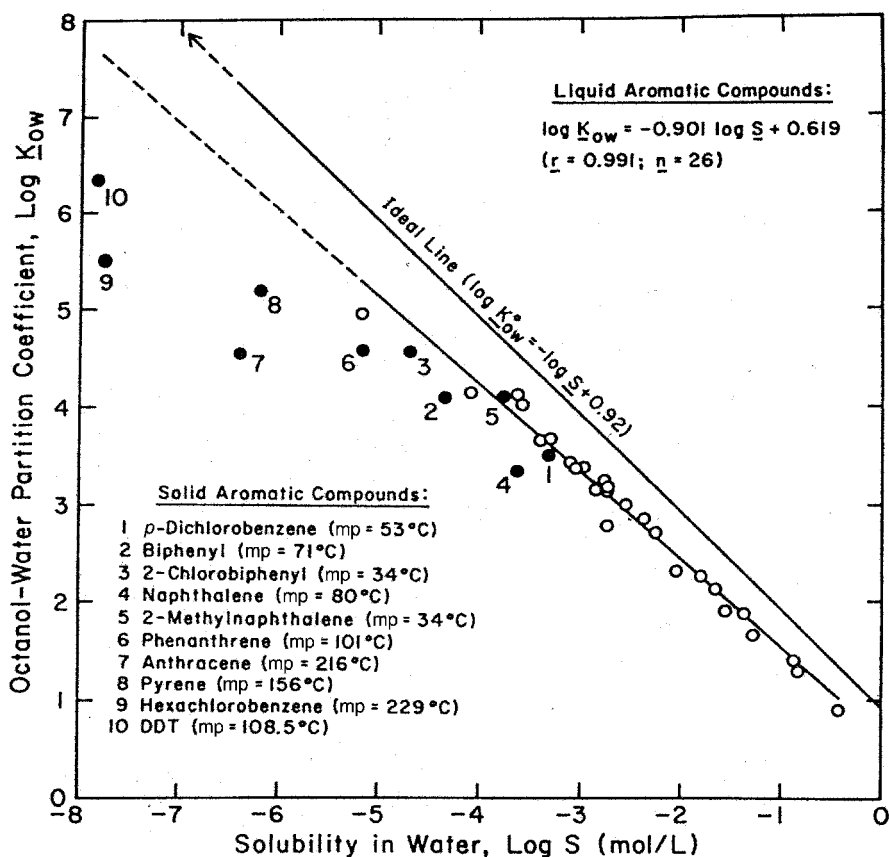


Figure 2.12 Correlation of K_{ow} with S_w at 25°C (Table 2.18) illustrating the deviation due to using solubility of the solid. [Reproduced with permission of the authors from C. T. Chiou and D. W. Schmedding, "Measurement and Interrelation of Octanol-Water Partition Coefficient and Water Solubility of Organic Chemicals", in *Test Protocols for Environmental Fate & Movement of Toxicants*, Proceedings of a Symposium, Association of Official Analytical Chemists, 94th Annual Meeting, Arlington, VA, pp. 28-42, 1981.]

compound in both phases. This discontinuity is eliminated by using the solubility of the super-cooled liquid (Fig. 2.13) giving a significant correlation with K_{ow} varying over five orders of magnitude and aqueous solubility over six. The following relation;

$$\log K_{ow} = -0.862 \log S_w + 0.710$$

with S_w expressed as a molar concentration will allow the calculation of K_{ow} from S_w and vice versa provided the super-cooled liquid solubility is used for solids.

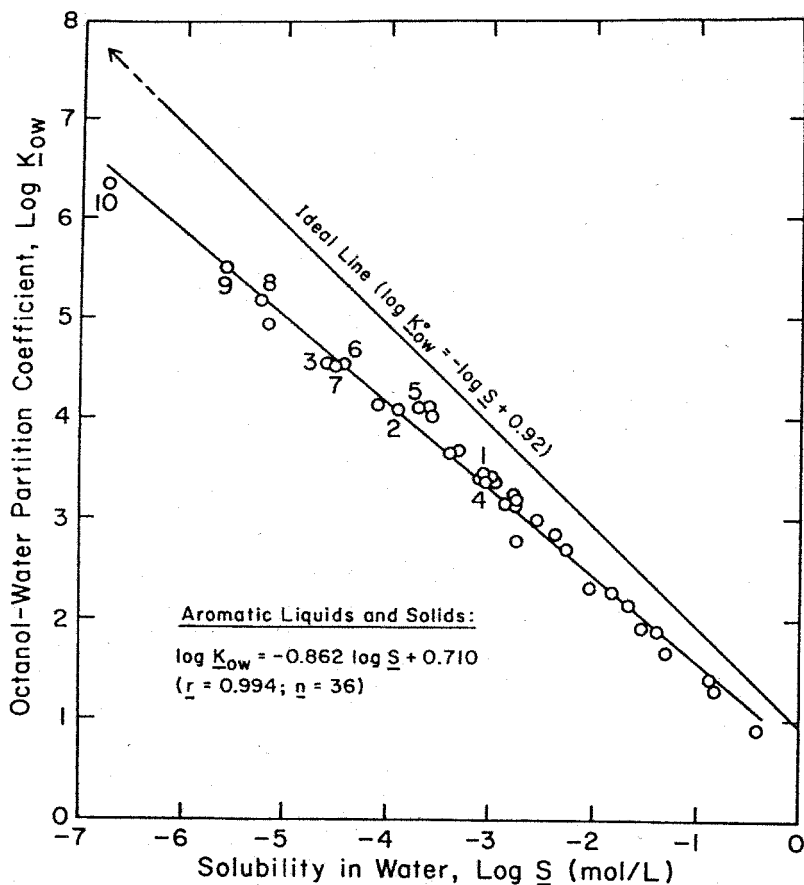


Figure 2.13 Correlation of K_{ow} with S_w at 25°C (Table 2.18) using solubility of the super-cooled liquid for solids. [Reproduced with permission of the authors from C. T. Chiou and D. W. Schmedding, "Measurement and Interrelation of Octanol-Water Partition Coefficient and Water Solubility of Organic Chemicals" in *Test Protocols for Environmental Fate & Movement of Toxicants*, Proceedings of a Symposium, Association of Official Analytical Chemists, 94th Annual Meeting, Arlington, VA, pp. 28–42, 1981.]

The regression line relating K_{ow} and S_w is displaced from the ideal line due primarily to the non-ideal behavior in the octanol phase. What is of interest, however, is the relatively constant value for $\log \gamma_0$ with compounds that vary in polarity. The hydrophobic aliphatic chain of octanol associates with nonpolar compounds, while the hydroxyl group would associate with more polar species. The assumption that γ_w for DDT and hexachlorobenzene is not affected by octanol is not valid and corrected values for $\log \gamma_0$ of 0.89 and 0.73, respectively, incorporate an adjustment for this effect.³⁸ Thus solubility and/or K_{ow} data that plot above the ideal line would be suspect as would any regression relation.

2.4.5 Octanol–Air Partition Coefficient

This quantity is finding use in predicting the distribution between air and a hydrophobic compartment such as the waxy surface of a leaf and can be estimated from the dimensionless Henry's law constant, H' , and the octanol–water partition coefficient:

$$K_{oa} = K_{ow}/H' = (C_{oct}/C_w)/(C_w/C_{air}) = C_{oct}/C_{air}$$

Keep in mind that with K_{ow} , C_{oct} is the concentration in octanol saturated with water not the concentration in the pure octanol and, hence, using the above ratio would be an approximation. The error involved in using this approach to estimate K_{oa} has been evaluated by comparing estimated with experimental values derived by passing air saturated with octanol through a generator column containing glass wool saturated with an octanol solution of the compound in question.⁴⁰ A summary of the data from this study (Table 2.19) shows that the calculated values tend to underestimate the experimental values, although, for the most part, the difference is probably within

TABLE 2.19 Comparison of Calculated and Experimental Values for K_{oa} at 25°C

	$H' = P^0/S_w$	$\log K_{ow}$	$\log K_{oa}$	
			K_{ow}/H'	Exptl
Chlorobenzenes				
1,2-Dichloro-	0.0986	3.4	4.41	4.36
1,2,3-Trichloro-	0.0977	4.1	5.11	5.19
1,2,3,4-Tetrachloro-	0.0581	4.5	5.74	5.64
1,2,4,5-Tetrachloro-	0.0494	4.5	5.81	5.63
Penta-	0.0342	5.0	6.46	6.27
Hexa-	0.0529	5.5	6.78	6.90
PCBs				
4-Chloro-	0.0172	4.5	6.27	6.78
4,4-Dichloro-	0.00721	5.3	7.46	7.67
2,4,5-Trichloro-	0.00981	5.6	7.61	7.96
2,2',4,4',6,6'-Hexachloro-	0.0350	7.0	8.46	8.99
<i>p,p'</i> -DDT	0.000955	6.2	9.22	10.1

experimental error. This is fortunate since an extensive data base exists for H' and K_{ow} , but at the present, not for K_{oa} .

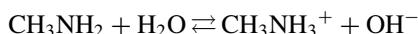
The octanol–air partition coefficient will increase with temperature similar to the Henry's law constant and data is available to demonstrate this response.⁴⁰

2.5 ACIDS AND BASES: DISSOCIATION CONSTANTS, pK_a

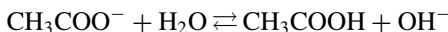
According to the Brönsted–Lowry convention, acids are defined as proton donors and bases as proton acceptors. In aqueous solution, then, acetic acid donates a proton to water producing the negatively charged acetate anion:



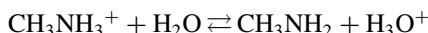
In this dissociation process, water acts as the base, accepting the proton. Methyl amine is an example of an organic base and in aqueous solution reacts:



producing the positively charged methyl ammonium cation with water acting as the acid. The acetate anion is the conjugate base of acetic acid since it can react with water, accepting a proton:



Conversely, the methyl ammonium ion is the conjugate acid of methyl amine and donates a proton to water



These equilibria are important in an environmental context because organic compounds that have acid or base functional groups may exist in either neutral or charged forms that can have a significant effect on their environmental behavior.

2.5.1 Dissociation Constant and pK_a

The mass action expression defining the dissociation equilibrium of acetic acid (abbreviated HAC) can be represented

$$K_{eq} = \frac{[\text{Ac}^-][\text{H}_3\text{O}^+]}{[\text{HAc}][\text{H}_2\text{O}]}$$

Introductory discussions of this relation note that $[\text{H}_2\text{O}]$ is constant and the dissociation constant for acetic acid can be represented

$$K_a = K_{eq}[\text{H}_2\text{O}] = \frac{[\text{Ac}^-][\text{H}_3\text{O}^+]}{[\text{HAc}]}$$

Strictly speaking this equilibrium relation should be expressed in terms of activities, $\gamma[\text{HAc}]$, for example, involving activity coefficients but the simple relation involving molar units is usually considered acceptable for low concentrations. A comparable K_b expression can be written for methylamine

$$K_b = \frac{[\text{CH}_3\text{NH}_3^+][\text{OH}^-]}{[\text{CH}_3\text{NH}_2]}$$

and for the conjugate base of acetic acid, Ac^-

$$K_b = \frac{[\text{HAc}][\text{OH}^-]}{[\text{Ac}^-]}$$

Similarly, an expression can be written for the K_a of the methylammonium ion, the conjugate acid of methyl amine

$$K_a = \frac{[\text{CH}_3\text{NH}_2][\text{H}_3\text{O}^+]}{[\text{CH}_3\text{NH}_3^+]}$$

Comparable to the pH convention, acid dissociation constants are usually represented by $\text{p}K_a$:

$$\text{p}K_a = -\log K_a$$

and taking negative logarithms, the expression for the dissociation of acetic acid can be written

$$\begin{aligned} -\log K_a &= -\log ([\text{Ac}^-]/[\text{HAc}]) - \log[\text{H}_3\text{O}^+] \quad \text{or} \\ \text{p}K_a &= \text{pH} - \log[\text{Ac}^-]/[\text{HAc}] \end{aligned}$$

This relation is often expressed for the generic acid, HA as the Henderson–Hasselbach equation with pH as the dependent variable

$$\text{pH} = \text{p}K_a + \log[\text{A}^-]/[\text{HA}]$$

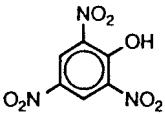
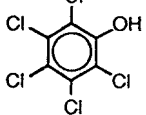
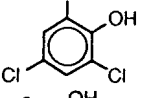
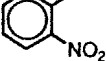
and is used to calculate the pH of buffer solutions consisting of a weak acid (or base) and its conjugate base (or acid).

For any weak acid–conjugate base or weak base–conjugate acid pair $K_a \cdot K_b = [\text{H}^+][\text{OH}^-] = K_w$ the ion product of water that is 1.01×10^{-14} at 25°C , and so

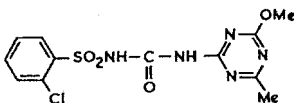
$$\text{p}K_a + \text{p}K_b = 14$$

Some $\text{p}K_a$ values for organic acids are listed in Table 2.20. The carboxyl group $-\text{COOH}$ and aromatic or phenolic $-\text{OH}$ are primarily responsible for acidic func-

TABLE 2.20 Some Organic Acids (Reproduced from R. P. Schwarzenbach, P. M. Gschwend and D.M. Imboden, *Environmental Organic Chemistry*, p 160. Copyright 1993. This material is used by permission of John Wiley & Sons Inc.)

Name	Structure of Acid	pK_a (at 20–25°C)
2,4,6-Trinitrophenol		0.38
Trichloroacetic acid		0.70
Chloroacetic acid		2.85
Acetic acid		4.75
Pentachlorophenol		4.75
2,4,6-Trichlorophenol		6.13
2-Nitrophenol		7.17
4-Chlorophenol		9.18
β -Naphthol		9.51
Phenol		9.82
Methyl mercaptan	CH_3SH	10.7
Aliphatic alcohols	$R-CH_2OH$	> 14.0

tion in organic compounds, although other functional groups can be active. For example, chlorsulfuron is representative of



Chlorsulfuron

the sulfonurea herbicides and the NH of the sulfonamide group shows a pK_a of 3.6. The lower the pK_a the stronger the acid; that is, it can donate a proton at low pH or in the presence of a relatively high concentration of H^+ . Within the ambient temperature range there is little change in pK_a value.

Organic bases are primarily nitrogen-containing compounds (Table 2.21). Since one usually deals with pH it is convenient to consider pK_a values of the base's conjugate acid and stronger bases with higher affinity for accepting protons, will show higher pK_a values.

It is not unusual for organic compounds to contain more than one acid and/or base functional group with each showing a characteristic pK_a . For example, succinic acid, an aliphatic dicarboxylic acid, $HOOCCH_2CH_2COOH$, shows $pK_{a1} = 4.2$ and $pK_{a2} = 5.6$. For the amino acid glycine, $_2HNCH_2COOH$, pK_a for the carboxyl group is 2.4 while the pK_a for the conjugate acid of the amine is 9.6.

2.5.2 pH as the Independent Variable and Charged/Neutral Ratio

The pH of natural waters is determined by the presence of inorganic acids and bases, such as HCO_3^- and CO_3^{2-} , which would be present in higher concentrations than any organic contaminant. A similar situation prevails in soils where the pH results from the interaction of soil minerals with ions in the soil solution. Under these conditions an organic acid or base would not have any significant effect on the pH of its environment, however, conversely the environmental pH will determine the ratio of the neutral and charged species

$$\log[A^-]/[HA] = pH - pK_a$$

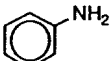
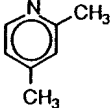
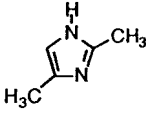
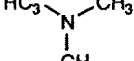
For example, at an environmental pH of 4 an organic acid of $pK_a = 6$

$$\log[A^-]/[HA] = 4 - 6 = -2 \quad \text{or} \quad [A^-]/[HA] = 0.01 \quad \text{or} \quad [A^-] = 0.01[HA]$$

This might be predicted from the application of Le Chatelier's principle where increasing concentrations of H^+ would tend to reverse the dissociation process and increase the proportion of the undissociated or neutral species. Conversely, with the same compound at pH 8,

$$\log[A^-]/[HA] = 8 - 6 = 2 \quad \text{and} \quad [A^-] = 100[HA]$$

TABLE 2.21 Some Organic Bases (Reproduced from R. P. Schwarzenbach, P. M. Gschwend and D. M. Imboden, Environmental Organic Chemistry, p 160. Copyright 1993. This material is used by permission of John Wiley & Sons Inc.)

Name	Structure of Base	$pK_a (=pK_{BH^+})$ (at 20–25°C)
Acetamide		0.63
4-Nitroaniline		1.00
3-Chloropyridine		2.84
4-Chloroaniline		4.15
Aniline		4.63
Isoquinoline		5.25
Pyridine		5.42
2,4-Dimethylpyridine		6.95
Imidazol		6.95
2,4-Dimethylimidazol		8.36
Trimethylamine		9.81
Methylamine		10.66
Pyrrolidine		11.27

Thus over a pH range of 4–8, which would correspond to what might be observed in the environment, the form in which an acid of $pK_a = 6$ would exist would range from almost 100% HA, a neutral species to almost 100% A^- , the anion as illustrated in Figure 2.14. At $pH = pK_a$ it is obvious that $[A^-] = [HA]$. Compounds of differing pK_a would all show the same relation over an equivalent pH range with the curve shifting up or down the pH scale depending on the pK_a . A similar treatment can be applied to bases and the general relations are summarized

Compound	Predominant Form	
	$pH < pK_a$	$pH > pK_a$
Acid	Neutral	Anion
Base	Cation	Neutral

If the total concentration of the A containing species is, $C_T = [A^-] + [HA]$ one can express the concentration of each species at that concentration

$$[HA] = \frac{C_T[H^+]}{K_a + [H^+]} \quad \text{and} \quad [A^-] = \frac{C_T K_a}{K_a + [H^+]}$$

which is illustrated in Figure 2.14.

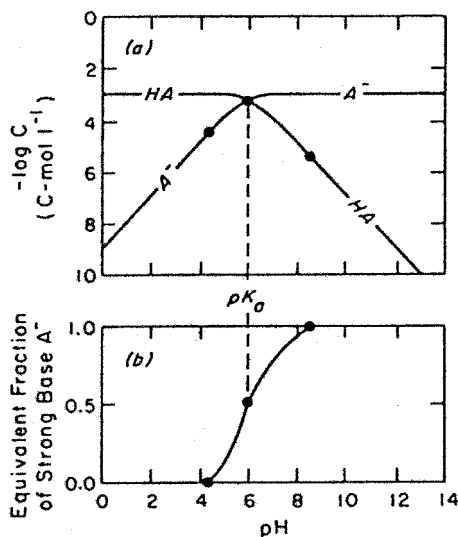


Figure 2.14 Effect of pH on the concentration (a) and the proportion (b) of the undissociated acid (HA) and its conjugate base (A^-) in a $1 \times 10^{-3} M$ solution, $pK_a = 6$.

The herbicide glyphosate, usually referred to as “Roundup” is a relatively simple molecule but its response to changes in environmental pH is complex because it contains two acid functional groups (carboxylic and phosphonic acids) and one basic group. The forms in which it exists as a function of varying environmental pH (e.g., plant vs. soil vs. surface water) will be determined by the pK_a values and from Figure 2.15 it can be seen that the mono- and dianions are the predominant species at environmental and physiological pH values reflecting $pK_{a1} = 2.27$ ($-\text{COOH}$); $pK_{a2} = 5.58$ (phosphonic acid) and $pK_{a3} = 10.25$ due to the base.⁴¹

Whether an acid or base exists as the neutral or complementary ionic species will have a profound influence on its environmental behavior. First, the ionic species will be much more water soluble than its neutral counterpart and consequently would not distribute as readily into a hydrophobic compartment, neither would it have a tendency to evaporate. Second, the charge can directly affect behavior. For example, soils have cation exchange sites that can bind the conjugate acid of a base.

2.5.3 Effect of pH on the Partitioning of Acids and Bases in Octanol–Water

One would predict that increasing the proportion of the ionic species by appropriate changes in pH in the aqueous phase would reduce the tendency of an acid or base to distribute into the octanol phase. This effect is illustrated by studies with the base, 2,4,5-trimethylaniline (TMA).⁴² A distribution ratio, D , can be defined to take into account both the charged and neutral species

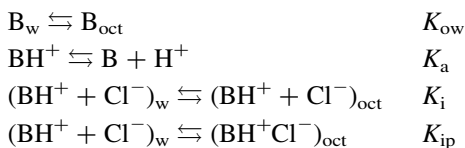
$$D = ([B] + [BH^+])_{\text{oct}} / ([B] + [BH^+])_{\text{w}}$$

and this parameter decreases as $[H^+]$ increases consistent with the expected increase in the proportion of the conjugate acid, BH^+ (Fig. 2.16). Acids show a comparable response with a decrease in D with decreasing $[H^+]$.⁴³

At high pH values, the base, B , is the predominant species in both phases and the distribution constant, D , does not vary with pH and is the same as K_{ow} . The conjugate base, BH^+ , is the predominant form in the aqueous phase at intermediate pH values with the neutral species, B , predominating in the octanol phase. At low pH values, the cation, BH^+ , becomes the predominant species in both phases and the value of D decreases and becomes independent of pH. However, increasing the concentration of potassium chloride in the aqueous phase at low pH results in an increase in D . This effect is attributed to the formation of an ion pair (BH^+Cl^-) resulting from the association of the two ions to produce a neutral species. Consequently, D would be more accurately defined

$$D = ([B] + [BH^+] + [BH^+Cl^-])_{\text{oct}} / ([B] + [BH^+])_{\text{w}}$$

and this distribution would depend on the following equilibria:



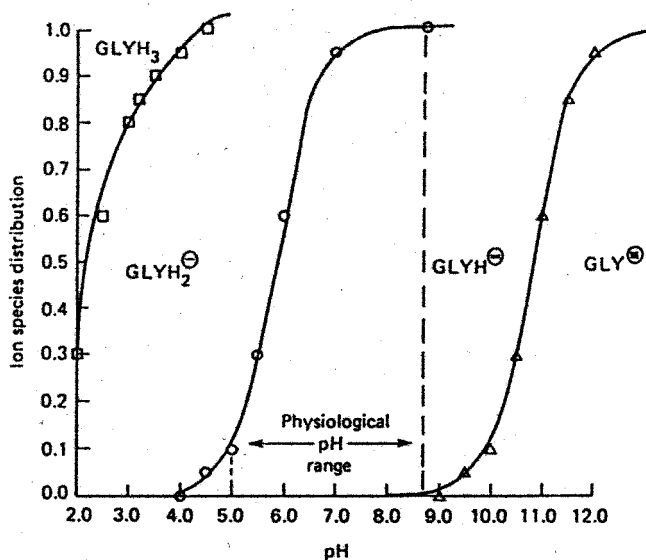
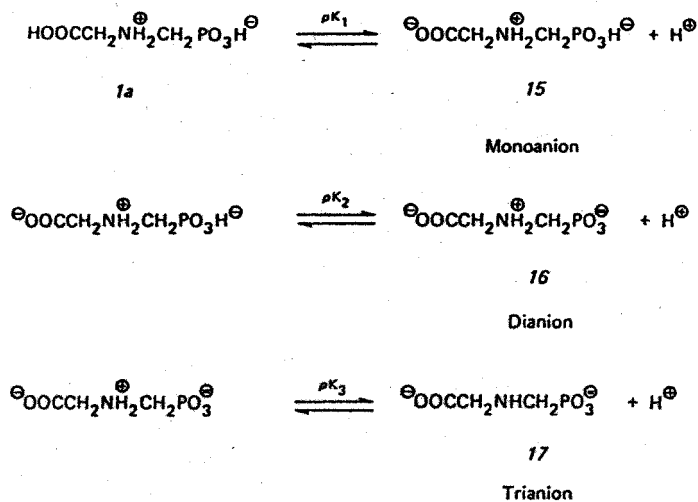


Figure 2.15 Ion species distribution of the herbicide, Glyphosate, as a function of pH. [Reproduced with permission from D. Wauchope, *J. Agric. Food Chem.* **24**, 717 (1976). Copyright © 1976, American Chemical Society.]

where, K_i and K_{ip} define the distribution of the ions and ion pair between the two phases. Values calculated for K_i and K_{ip} along with pK_a and $\log K_{ow}$ for the neutral species for several acids and bases^{42,43} have been tabulated in Table 2.22. The low values for K_i illustrate the limited tendency for ions compared to the neutral species

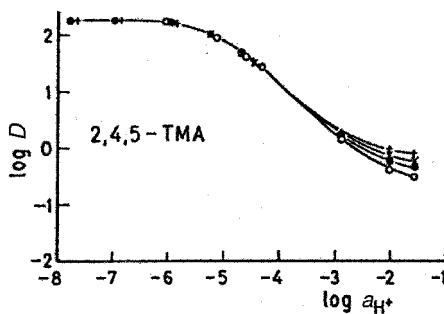


Figure 2.16 Distribution ratios (D) of 2,4,5-trimethylaniline between octanol and water as a function of pH at $I = 0.05$ (○), 0.10 (●), 0.15 (×), and 0.20 (+) M KCl. [Reproduced with permission from C. A. Johnson and J. C. Westall, *Env. Sci. Technol.* **24**, 1869 (1990). Copyright © 1990, American Chemical Society.]

to distribute into the octanol phase (compare K_{ow} and K_i). Ion pairs, as might be expected, show a higher tendency than the ion to distribute into the octanol phase and K_{ip} correlates with K_{ow} .⁴³ The ionic strength of the aqueous phase can have a significant effect on both the amount of compound that distributes into the octanol phase as well as the species distribution (Fig. 2.17). There is not much information available regarding the effect of this variable in environmental systems.

2.5.4 Determining pK_a Values

Experimental values are derived by defining the ratio of $[A^-]/[HA]$ (or $[B]/[BH^+]$ for the base) as a function of pH. For example, this can be accomplished in a titration when pH is monitored as a specified amount of acid is titrated with a solution of base of known concentration providing curves comparable to those shown in Figure 2.14. Stoichiometric relations provide the required estimates of $[A^-]/[HA]$. With many aromatic and heterocyclic compounds it is possible to use a spectrophotometric

TABLE 2.22 Octanol–Water Equilibria for Acids and Bases

Compound	pK_a	$\log K_{ow}$	$\log K_i^a$	$\log K_{ip}^a$
Pentachlorophenol	4.83	5.09	-1.95	2.64
2,3,4,5-Tetrachlorophenol	6.35	3.31	-3.69	1.81
2-Methyl-4,6-dinitrophenol	4.46	2.14	-3.88	0.016
2,4-Dichlorophenoxyacetic acid	2.90	2.83	-4.16	-0.042
3,6-Dichloro-2-methoxybenzoic acid	1.90	2.49	-5.95	-0.654
4-Methylaniline	5.17	1.40	-4.84	-0.22
2,4,5-Trimethylaniline	5.09	2.27	-3.88	0.69

^aIn the presence of KCl.

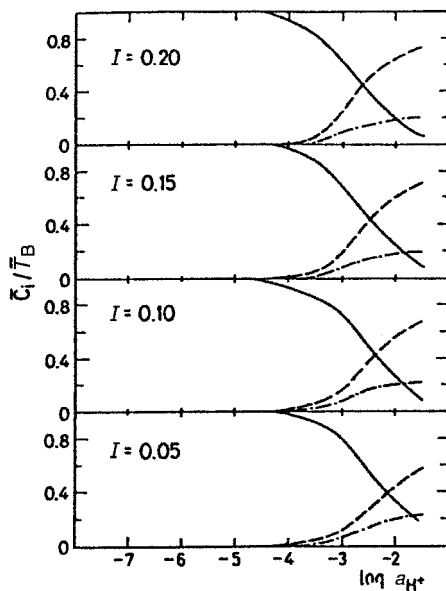


Figure 2.17 Calculated distribution of the 2,4,5-trimethylaniline (initial conc in water 1.00 mM) species in the octanol phase as a function of pH and KCl concentration using equal volumes of octanol and water; neutral compound (—), free ion (- · -) and the ion pair (- · -). [Reproduced with permission from C. A. Johnson and J. C. Westall, *Env. Sci. Technol.* **24**, 1869 (1990). Copyright © 1990, American Chemical Society.]

approach since there can be significant differences in the spectra of the neutral and charged species. Determining dissociation constants for acids and bases has been of interest to the organic chemist for many years and other procedures used have been reviewed.⁴⁴

2.5.5.1 Hammett Equations: Predicting pK_a Values If one substitutes a chlorine for hydrogen in the $-\text{CH}_3$ group of acetic acid, the pK_a decreases by almost two units (Table 2.20). Substituting all the methyl hydrogens with chlorine gives trichloroacetic acid, a strong acid with $pK_a = 0.70$. Chlorine is considerably more electronegative than hydrogen and, consequently, electrons in the C—Cl bond tend to be displaced toward the chlorine, inducing an electron deficiency in the carbon and the carboxyl oxygens. As a consequence of this “inductive effect”, it becomes easier to lose the H^+ and the pK_a decreases.

The pronounced effect of nitro- and chloro- substituents on the pK_a of phenol (Table 2.20) are due to the fact that the influence of these groups is transmitted through the delocalized π electrons of the benzene ring. This response is often referred to as a resonance effect and is associated with ortho and para but not meta substituents that show primarily an inductive effect. A systematic treatment of these effects is given by Hammett equations, another example of linear free

TABLE 2.23 Hammett σ Values for Common Substituents^a

Substituent	σ_{meta}	σ_{para}	σ_{ortho}		
			—COOH	—OH	—NH ₂
—Br	0.39	0.22	1.35	0.70	0.71
—Cl	0.37	0.24	1.28	0.68	0.67
—I	0.35	0.21	1.34	0.63	0.70
—OH	0.13	—0.38	1.22	0.04	—0.09
—NH ₂	0.00	—0.57		0.03	0.00
—NO ₂	0.74	0.78	1.99	1.40	1.72
—N(CH ₃) ₂	—0.15	—0.83		—0.36	
—CH ₃	—0.06	—0.14	0.29	—0.13	0.10
—C ₂ H ₅	—0.07	—0.15	0.41	—0.09	0.05
—CH(CH ₃) ₂	—0.07	—0.15	0.56	—0.23	0.03
—C ₆ H ₅	0.05	—0.01	0.74	0.00	
—COOH	0.35	0.44	0.95		
—CONH ₂	0.28	0.31	0.45	0.72	
—COOCH ₃	0.32	0.39	0.63		
—OCH ₃	0.11	—0.28	0.12	0.00	0.00
—CN	0.62	0.70	1.06	1.32	

^aTaken from Ref. 45.

energy relations introduced in the discussion of π values and octanol–water partition coefficients. In a Hammett equation, the pK_a of a substituted acid, pK_X is expressed as a function of the pK_a of the unsubstituted reference acid, pK_H and the sum of the σ constants for the different substituents:

$$pK_X = pK_H - \rho(\sum\sigma)$$

The σ value for a meta and para substituent (Table 2.23) indicates its tendency to withdraw (positive) or donate electrons (negative). Experimental pK_a values of substituted benzoic acids are used to estimate σ . The influence of substituents in the ortho positions is more complex and can involve steric effects and, on occasion, hydrogen bonding with the acidic functional group along with the inductive and resonance effects. “Apparent” σ_{ortho} values, specific for phenols, benzoic acids, and anilines are listed (Table 2.24) that can be used with σ_{meta} and σ_{para} in predicting pK_a . Specific values are necessary because the interactions of the ortho substituents will vary among these three functional groups. Hammett equations for different series of aromatic compounds are compiled in Table 2.24. The magnitude of ρ is an index of the sensitivity of the particular functional group to the substituent effects and is assigned a value of one for benzoic acids. Predicting the pK_a of 2,4-dichloro-3,5-dimethylphenol illustrates the use of these relations.

TABLE 2.24 Examples of Hammett Equations^a

Acid Series	pK_H	σ
Benzoic acid C_6H_5COOH	4.20	1
2-Methylbenzoic acid $2-CH_3C_6H_4COOH$	3.90	1.22
Phenoxyacetic acid $C_6H_5OCH_2COOH$	3.18	0.23
Phenylacetic acid $C_6H_5CH_2COOH$	4.30	0.49
Phenylpropanoic acid $C_6H_5CH_2CH_2COOH$	4.55	0.21
Phenol C_6H_5OH	9.92	2.23
Anilinium ion $C_6H_5NH_3^+$	4.58	2.88
<i>N,N'</i> -Dimethylanilinium ion $C_6H_5N(CH_3)_2H^+$	5.06	3.46
Benzylaminium ion $C_6H_5CH_2NH_3^+$	9.39	1.05

^aTaken from Ref. 45.

2-Cl	σ_{ortho} 0.68
4-Cl	σ_{para} 0.24
3-CH ₃	σ_{meta} -0.06
5-CH ₃	σ_{meta} -0.06
$\Sigma\sigma = 0.80$	

For phenol $pK_a = 9.92 - 2.23(0.80) = 8.14$, which is in agreement with an experimental value of 8.28, where the uncertainty lies between 1 and 10%.⁴⁶

Values for many more substituents are available along with Hammett equations for many additional acids along with Taft equations and substituent constants for aliphatic compounds.^{45,47} So this approach is quite versatile and it is possible to predict pK_a values for molecules with rather complex structures. This procedure provides a system for evaluating how substituents influence the distribution of charge in a molecule.

2.6 SOURCES FOR PHYSICAL CHEMICAL CONSTANTS

To be able to assess the distribution of organic compounds among the different compartments in the environment one must have access to the solubility, vapor pressure, Henry's law constant, octanol-water partition coefficient, and pK_a for an acid or base. In many cases, these values may be available in the literature and some of these sources will be cited. Government agencies often require that these physical chemical quantities be measured for compounds in commercial use. For example, pesticides cannot be registered for use without this information. So this data will be available. However, it is not unusual to find that compounds that are of interest are not the parent compound but a product contaminant or derivative. The most noted example of this situation would be the chlorinated dibenzodioxins originally

detected as contaminants of products produced from chlorinated phenols. Combustion products and natural constituents such as the terpenes released from plants would be other examples of compounds of environmental interest for which physical parameters might not be available. Until experimental values are derived, the only recourse is to utilize the procedures that predict on the basis of structure, examples of which have been discussed.

The next challenge is to assess the validity of the information since, with some compounds, there can be a large variation in experimental values. Some criteria that can be used have been noted (p. 21). In addition, some correlations such as that between aqueous solubility and octanol–water partition coefficient can provide a reference. Another quantity that can be useful in this regard is molecular size.

2.6.1 Correlation of Physical Chemical Properties with Molecular Size

Forces holding molecules together in a condensed phase will increase with the size of the molecule and, consequently, more energy will be needed to overcome these forces in phase transitions. Thus, as the size of the molecule increases, boiling point will increase and the vapor pressure will decrease at ambient temperatures. These forces are also a factor when a solute dissolves in a solvent and in addition, energy is required to generate the space in the solvent that accommodates the solute molecule. So one might predict that both vapor pressure and solubility could correlate with the size of the molecule. The question then becomes, What parameters can be used as an index of molecular size? The most useful have been molecular surface area and volume as well as molar volume.

It is possible to compute the molecular surface area and volume using the van der Waal's radii of the atoms and the appropriate interatomic distances. Each atom is assumed to be a sphere of designated radius located at the equilibrium position of the nucleus. The van der Waal's surface is then that surface defined by the intersection of the spheres and the volume contained, the van der Waal's volume. Programs have been developed to carry out these calculations and the different approaches used have been reviewed.⁴⁸ Molar volume can be calculated by an empirical approach using volume increments for each atom.⁴⁹ Another procedure derives molar volume from the density of the liquid at the boiling point where the intermolecular forces have been overcome. The Grain equation⁵⁰ is used to estimate density at the boiling point and for alkanes the molar volume at the boiling point, V_b , is given by

$$V_b = \frac{MW(3 - 2T/T_b)^{0.29}}{\rho_L}$$

where ρ_L is the density, $\text{g} \cdot \text{mL}^{-1}$, at temperature T (K), T_b (K) is the boiling point, MW is the molecular weight, and the exponent 0.29 specific for hydrocarbons.⁵¹

The relation between the logarithm of the vapor pressure at 25°C and molar volume for alkanes is illustrated in Figure 2.18.⁵¹ Small but consistent variation is

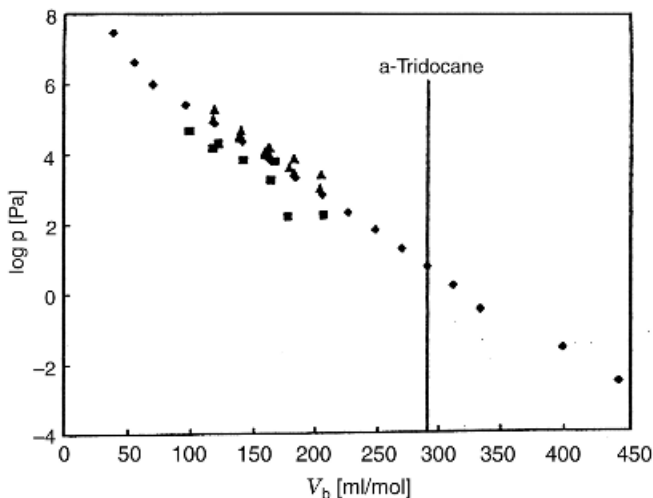


Figure 2.18 Literature data for vapor pressure for linear (◆), branched (▲), and cycloalkanes (■) as a function of molar volume. [Reproduced with permission from E. M. J. Verbruggen, J. L. M. Hermens, and J. Tolls, *J. Phys. Chem. Ref. Data* **29**, 1435 (2000). Copyright © 2000, American Chemical Society.]

observed between the normal and branched chain and cycloalkanes. The correlation obtained with C_5 – C_{13} alkanes was

$$\log P(\text{Pa}) = 7.521 - 0.023 V_b \quad r^2 = 0.9978$$

The vapor pressure (of the super-cooled liquid) of chlorinated dibenzodioxins also correlates with molar volume ($\text{cm}^3 \cdot \text{mol}^{-1}$)³⁷

$$\log P(\text{Pa}) = 7.97 - 0.0431 V$$

The aqueous solubility of n -alkanes is an inverse function of molar volume from C_5 – C_{13} (Fig. 2.19)⁵¹:

$$\log S_w(\text{mol} \cdot \text{L}^{-1}) = 0.518 - 0.032 V(\text{ml} \cdot \text{mol}^{-1}) \quad r^2 = 0.9935 \quad (n = 9)$$

These data illustrate the utility of these relations in that observations deviating from the relation would be suspect. In fact, the solubility data used for the higher homologues ($>C_{13}$) is older data obtained by the “shake flask” procedure that is known to overestimate solubility because of the colloidal dispersions that form during shaking.

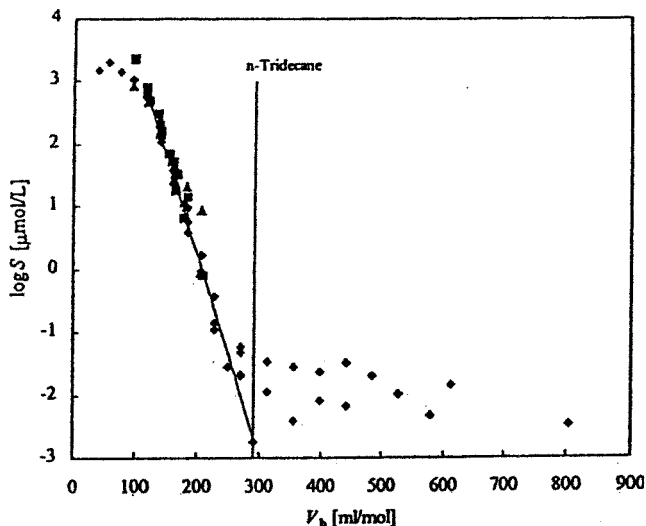


Figure 2.19 Literature data for aqueous solubility as a function of molar volume for linear (◆), branched (▲) and cycloalkanes (■). [Reproduced with permission from E. M. J. Verbruggen, J. L. M. Hermens and J. Tolls, *J. Phys. Chem. Ref. Data* **29**, 1435 (2000). Copyright © 2000, American Chemical Society.]

The solubility ($\text{mol} \cdot \text{m}^{-3}$) of chlorinated dioxins as super-cooled liquids can be related to molecular volume ($\text{cm}^3 \cdot \text{mol}^{-1}$) by the expression³⁷:

$$\log S_{\text{scf}} = 5.03 - 0.0334 V$$

A comprehensive study of the relation between molecular structure and aqueous solubility of some 117 PCB congeners,¹¹ has shown that solubility (as the mole fraction, x) can be expressed as a function of the van der Waal's surface, \AA^2

$$-\ln x = 0.108A - 6.976T_m + 30.281$$

This relation provides a satisfactory correlation between experimental and predicted values and can be applied to both solids and liquids. We recall that

$$-\ln x = \ln \gamma$$

and keeping in mind that $x = C \cdot V_{(\text{H}_2\text{O})}$, where C is concentration in $\text{mol} \cdot \text{L}^{-1}$ and V the molar volume of water, the solubility of a solid can be expressed in terms of mole fraction

$$-\ln x = \ln \gamma + \Delta S_{\text{fus}}/R(T_m/T - 1)$$

A significant correlation between $\ln \gamma$ and the reported van der Waal's molecular surface has been reported⁵² and with the PCB data:

$$\ln \gamma = 0.106A + 9.095 \quad r = 0.967 \quad (n = 45)$$

Substituting for $\ln \gamma$ and using a value of $58 \text{ J} \cdot \text{mol}^{-1} \cdot \text{K}^{-1}$ and $T = 295 \text{ K}$ gives the relation above. It is suggested that a reasonable estimate of the solubility of all 209 PCB congeners could be derived from this relation.

A comparable study with 32 polynuclear aromatic hydrocarbons⁵³ has also demonstrated a significant correlation between aqueous solubility ($\text{mol} \cdot \text{L}^{-1}$) and the van der Waal's surface, \AA^2

$$\ln S_w = -0.0282A - 0.0095T_m(^{\circ}\text{C}) + 1.42 \quad r = 0.9877 \quad (n = 32)$$

and the correspondence between predicted and experimental values is summarized in Table 2.25.

In addition, it has been shown that the aqueous solubility of both PCB congeners¹¹ and polynuclear aromatic hydrocarbons⁵⁴ can be correlated with molecular volume that is not surprising since one would anticipate a relation between volume and surface area.

Since the attractive forces between molecules will vary greatly with the nature of the functional groups on the molecule the correlations are valid only within specific classes of molecules. However, if the appropriate relations have been established they can be used to both predict and validate solubility and vapor pressures.

TABLE 2.25 Prediction of Solubility of PAHs from Molecular Surface

Compound	T_m ($^{\circ}\text{C}$)	Surface (\AA^2)	Log S_w ($\text{mol} \cdot \text{L}^{-1}$)	
			Exp.	Pred.
Naphthalene	80.2	155.8	-3.606	-3.735
2-Methylnaphthalene	34.6	176.3	-3.748	-3.830
1,3-Dimethylnaphthalene	25.0	192.9	-4.292	-4.257
Biphenyl	71.0	182.0	-4.345	-4.386
Acenaphthene	96.2	175.0	-4.594	-4.429
Phenanthrene	101.0	198.0	-5.150	-5.123
Anthracene	216.2	202.2	-6.377	-6.336
Pyrene	156.0	213.0	-6.176	-6.069
Chrysene	255.0	241.0	-8.057	-7.799
Naphthacene	357.0	248.0	-8.687	-8.965
Perylene	277.0	251.5	-8.804	-8.304

2.6.2 Literature and On-Line Data Sources

The physical chemical parameters of organic compounds are presently available in a variety of sources. They include comprehensive publications and on-line web sites that compile data for thousands of compounds. Other papers in the literature are restricted to either specific physical chemical parameters and/or chemical classes. Some of these data bases are peer reviewed and one can depend on the values cited while others may cite references and the investigator has to draw his/her own conclusions. Some recent publications have chosen to summarize all the data reported for say, the solubility of a compound, and critique values cited before indicating a preferred value. This approach is most useful to those interested in assessing the environmental behavior of compounds. Examples of these different data sources are given, but this list is by no means complete.

2.6.2.1 General Sources The following publications and web sites summarize data on many organic compounds:

*Chemical Properties Handbook*⁵⁵ Vapor pressure, aqueous solubility, Henry's law constant, and the octanol-water partition coefficient are listed for over 1300 compounds along with other quantities such as enthalpies of vaporization and fusion, van der Waal's surface and volume. Compounds are indexed by CAS No. and formula.

*Physical and Thermodynamic Properties of Pure Chemicals: Data Compilation*⁵⁶ This comprehensive data base is designed primarily for the chemical engineer and, consequently, includes many thermodynamic quantities such as enthalpies and free energies of formation, standard entropies, and so on. Molar volume calculated from density, and van der Waal's surface, and volume are also cited. Supplementary updates are published periodically.

Illustrated Handbook of Physical-Chemical Properties and Environmental Fate for Chemicals,⁵⁷

Vol. I Monoaromatic hydrocarbons, chlorobenzenes, and PCBs,

Vol. II Polynuclear aromatic hydrocarbons, polychlorinated dioxins, and dibenzofurans.

Vol. III Volatile organic chemicals.

Vol. IV Oxygen, nitrogen and sulfur-containing compounds.

Vol. V Pesticide chemicals.

The data sets compiled in this series provide the most comprehensive information for assessing the overall behavior of a compound in the environment. For each compound the following physical chemical quantities are listed:

Melting and boiling points.

Density at 20°C.

Molar volume.

Molecular volume and surface area.
 Heat of fusion.
 Aqueous solubility.
 Vapor pressure at 25°C.
 Henry's law constant.
 Octanol–water partition coefficient.

When available, a series of experimental values are listed and referenced and the most reliable value selected. Graphs are included for each series of compounds illustrating the relation between the physical chemical parameters and molar volume. Soil–water distribution values and bioconcentration ratios are included along with data summarizing the rates of different transformation processes. In addition, the distribution and fate of many of the compounds listed is defined and illustrated using fugacity models (see Chapter 10).

Syracuse Research Corporation Environmental Science Databases (<http://esc.syrres.com/>) The subscription series includes
 Environmental fate data base.
 The physical properties database (25,070 compounds).
 Solvents database.

A free K_{ow} section contains experimental values for 13,000 compounds and will also provide a value calculated from fragment constants. This web site is probably the most comprehensive in regard to chemicals of environmental significance.

Hazardous Substance Data Bank (HSDB) (<http://toxnet.nlm.nih.gov/>) Although this database compiles information on only 4500 chemicals, it has the advantage of being peer-reviewed and focusing on compounds with environmental impacts. This system is maintained by the National Library of Medicine and although the focus is primarily on toxicological properties, exposure is determined by environmental behavior and consequently the physical chemical properties of the compounds are included.

2.6.2.2 Specific Physical Chemical Parameters Some examples of useful sources would include

Ionisation Constants of Organic Acids in Aqueous Solution^{45,46} pK_a values for 4500 compounds are compiled and an indication of the reliability is provided for the values cited.

AQUASOL dATABASE of Aqueous Solubility. This on-line subscription service provides solubility data for 4000 compounds. A “recommended” value is provided when possible and the references are cited. (<http://chin.icm.ac.cn/database/aquasol.htm>).

*The Vapor Pressure of Environmentally Significant Organic Chemicals*⁵⁸ Vapor pressures are provided for polynuclear aromatic hydrocarbons, PCBs, chlorinated dioxins and furans, and some pesticides. Values for each compound are compiled and referenced.

2.6.2.3 Chemical Classes Either because of their persistence and/or the manner and extent to which they are produced and released, different series of compounds tend to be of more significance in the environment. Consequently, it is not unusual to find their properties compiled by chemical class similar to the illustrated handbook mentioned above.⁵⁷

2.6.2.4 Pesticides *Pesticide Properties in the Environment*⁵⁹ The efficacy and environmental impact of these compounds depends on their distribution and persistence. This monograph contains data on >340 active ingredients including, aqueous solubility, vapor pressure, and pK_a . Soil behavior is defined by sorption coefficients and degradation half-lives. In most cases a range of referenced values is cited along with selected values.

2.6.2.5 Chlorinated Hydrocarbons Short-chain alkyl halides find extensive use as solvents and are common contaminants of ground water. Polychlorinated biphenyls are global contaminants as a consequence of their extensive use and persistence. Chlorinated dioxins and furans are produced as combustion by products or contaminants in reactions with chlorophenols. Consequently, there has been considerable interest in defining the physical chemical properties that determine their environmental behavior.

*Halogenated Hydrocarbons, Solubility-Miscibility with Water*⁶⁰ In addition to a comprehensive discussion of solution theory, this publication contains solubility data on C_1 – C_6 halogenated compounds including both benzene and cyclohexane derivatives. Thermodynamic information is also compiled.

*Aqueous Solubility of Polychlorinated Biphenyls Related to Molecular Structure*¹¹ This paper contains solubility data for 44 PCB congeners and outlines correlations with molecular volume and surface area. Several values are listed and referenced for most congeners.

*Physical-Chemical Properties of Chlorinated Dibenzo-p-dioxins*³⁷ Reported and experimental data for aqueous solubility, octanol–water partition coefficient, vapor pressure, and Henry's law constant are compiled and correlated with molar volumes and chlorine number.

*Environmental Chemistry and Toxicology of Polychlorinated n-Alkanes*⁶¹ This series of compounds are produced from C_{10} to C_{30} with chlorine levels ranging from 30 to 70%. The C_{10} – C_{13} series are the more important from the environmental perspective. Aqueous solubility, vapor pressure, Henry's law constant, and octanol–water partition coefficient are provided along with information on degradation processes.

*IUPAC–NIST Solubility Data Series 67. Halogenated Ethanes and Ethenes with Water*¹⁴ This series is sponsored by The International Union for Pure & Applied Chemistry & The National Institute of Standard & Technology. Literature data is compiled, examined critically and recommended values given. The effect of temperature is noted and the solubility of water in the halogenated compound is also noted.

*Temperature Dependence of Physical-Chemical Properties of Selected Chemicals of Environmental Interest. II Chlorobenzenes, Polychlorinated Biphenyls, Polychlorinated Dibenzo-p-dioxins, and Dibenzofurans*¹ This comprehensive data set compiles aqueous solubility, vapor pressure and Henry's law constant for temperatures in the environmental range. Recommended values are given along with equations for estimating values as a function of temperature. Phase change enthalpies are also included.

2.6.2.6 Hydrocarbons Global dependence on carbonaceous material, primarily coal, and petroleum accounts for the wide distribution of aliphatic and aromatic hydrocarbons. These compounds are often released during combustion or simply through a spill.

*Water Solubilities of Polynuclear Aromatic and Heteroaromatic Compounds*⁶² Water solubilities of polynuclear aromatic and heteroaromatic (oxygen, sulfur, and nitrogen) hydrocarbons have been compiled and evaluated and correlated with molecular volume, and surface area.

Critical Properties and Vapor pressure Equation for Alkanes C_nH_{2n+2} : Normal Alkanes with $n \leq 36$ and Isomers for $n = 4-11$ ⁶³ Literature values have been compiled and reviewed and predicting equations evaluated.

*Physicochemical Properties of Higher Nonaromatic Hydrocarbons: A Literature Study*⁶⁴ Aqueous solubility, vapor pressure, Henry' law constant, and octanol–water coefficients are compiled and related to molar volume. Data is included for normal, cyclo- and branched-chain alkanes, alkenes, and alkynes.

2.6.2.7 World Health Organization (WHO) Monographs The Environmental Health Criteria (EHC) documents published by WHO focus on toxicological effects of a wide range of chemicals, and since risk depends also on exposure, environmental behavior is addressed. Consequently, these publications usually contain information on the physical chemical properties and discuss degradation processes as well as sources and the extent to which these compounds are found in the environment. Over 220 of these monographs have been published and many focus on organic compounds. A current listing of these publications can be found at <http://www.who.int/dsa/cat98/zehc.htm> while the IPCS INCHEM web site provides access to the full text of many of the monographs, <http://www.inchem.org/pages/ehc.html/>. An example of some of the important compounds or series of compounds includes

- EHC No. 93 Chlorophenols, 1989
 EHC No. 131 Diethylhexylphthalate, 1992
 EHC No. 140 Polychlorinatedbiphenyls and Terphenyls, 1992
 EHC No. 171 Diesel fuel and exhaust emissions, 1996
 EHC No. 181 Chlorinated paraffins, 1996
 EHC No. 218 Flame retardants, 2000



REFERENCES

1. W. Shiu and K. Ma, *J. Phys. Chem. Ref. Data* **29**, 387 (2000).
2. W. Shiu and K. Ma, *J. Phys. Chem. Ref. Data* **29**, 41 (2000).
3. W. F. Spencer and M. M. Cliath, *Residue Rev.* **85**, 57 (1983).
4. J. W. Hamaker and H. O. Kerlinger, "Vapor Pressure of Pesticides", in R. F. Gould's, Ed., *Pesticidal Formulations Research, Physical and Colloidal Chemical Aspects*, ACS Advances in Chemistry Series No. 86, American Chemical Society, Washington D.C., 1969, pp. 39–54.
5. S. H. Yalkowsky, *Ind. Eng. Chem. Fundam.* **18**, 108 (1979).
6. L. P. Burkhard, A. W. Andron, and D. E. Armstrong, *Environ. Sci. Technol.* **19**, 500 (1985).
7. G. L. Amidon and S. T. Anik, *J. Chem. Eng. Data* **26**, 28 (1981).
8. D. Mackay, A. Bobra, D. W. Chan, and W. Y. Shiu, *Environ. Sci. Technol.* **16**, 645 (1982).
9. C. F. Grain, "Vapor Pressure", in W. J. Lyman, W. F. Reehl, and D. H. Rosenblatt's, Eds., *Handbook of Chemical Property Estimation Methods*, McGraw-Hill, New York, 1982, pp. 14-1–14-20.
10. S. Banerjee, *Env. Sci. Technol.* **19**, 369 (1985).
- 10a. J. Pontolillo and R. P. Eganhouse, "The Search for Reliable Aqueous Solubility(S_w) and Octanol–Water Partition Coefficient (K_{ow}) Data for Hydrophobic Organic Compounds: DDT and DDE as a Case Study" USGS Water-Resources Investigations Report 011-4201, Reston (<http://pubs.water.usgs.gov/wri01-4201>) 2002.
11. A. Opperhuizen, F. A. P. C. Gobas, and J. M. D. Van der Steen, *Environ. Sci. Technol.* **22**, 638 (1988).
12. M. Coates, D. W. Connel, and D. M. Barron, *Environ. Sci. Technol.* **19**, 628, (1985).
13. P. G. de Maagd, D. Th. E. M. ten Hulsher, H. van den Heuvel, A. Opperhuizen, and D. T. H. M. Sijm, *Environ. Toxicol. Chem.* **17**, 251 (1998).
14. A. L. Horvath, F. W. Getzen, and Z. Maczynska, *J. Phys. Chem. Ref. Data* **28**, 395 (1999).
15. Y. Hashimoto, K. Tokura, and W. M. J. Strachan, *Chemosphere* **13**, 881 (1984).
16. E. M. Thurman, *Organic Geochemistry of Natural Waters*, Martinus Nijhoff/Dr. W. Junk Publishers, Kluwer Academic Publishers Group, Dordrecht, 1985, 497 pp, p. 8.
17. C. T. Chiou, R. L. Malcom, T. I. Brinton, and D. E. Kile, *Environ. Sci. Technol.* **20**, 502 (1986).

18. H. B. Krop, P. C. M. van Noort, and H. A. J. Govers, *Rev. Env. Contam. Toxicol.* **169**, 1 (2001).
19. T. J. Murphy, M. D. Mullin, and J. A. Meyer, *Environ. Sci. Technol.* **21**, 155 (1987).
20. C. Yin and J. P. Hassett, *Environ. Sci. Technol.* **12**, 1213, (1986).
21. S. Brunner, E. Hornung, H. Santl, E. Wolff, O. G. Piringer, J. Altschuh, and R. Brüggemann, *Environ. Sci. Technol.* **24**, 1751 (1990).
22. F. M. Dunnivant, J. T. Coates, and A. W. Elzerman, *Environ. Sci. Technol.* **22**, 448 (1988).
23. F. M. Dunnivant and A. W. Elzerman, *Chemosphere* **17**, 525 (1988).
24. R. L. Falconer and T. F. Bidleman, *Atmos. Environ.* **28**, 547 (1994).
25. E. Atlas, R. Fostern, and C. S. Giam, *Environ. Sci. Technol.* **16**, 283 (1982).
26. C. Yin and J. P. Hassett, *Environ. Sci. Technol.* **12**, 1213 (1986).
27. H. Meyer, *Arch. Exp. Pathol. Pharmacol.* **42**, 109 (1899).
28. A. Leo, C. Hansch, and D. Elkins, *Chem. Rev.* **71**, 525 (1971).
29. J. de Bruijn, F. Busser, W. Seinen, and J. Hermens, *Eviron. Toxicol. Chem.* **8**, 499 (1989).
30. K. B. Woodburn, W. J. Doucette, and A. W. Andren, *Environ. Sci. Technol.* **18**, 457 (1984).
31. R. A. Rapaport and S. J. Eisenreich, *Environ. Sci. Technol.* **18**, 163 (1984).
32. T. Fujita, J. Iwasa, and C. Hansch, *J. Am. Chem. Soc.* **86**, 5175 (1964).
33. F. E. Norrington, R. M. Hyde, S. G. Williams, and R. Wootton, *J. Med. Chem.*, **18**, 604 (1975).
34. R. F. Rekker and H. M. de Kort, *Eur. J. Med. Chem.* **14**, 479 (1979).
35. C. Hansch and A. J. Leo, *Substituent Constants for Correlation Analysis in Chemistry and Biology*, John Wiley & Sons, New York, 1979.
36. W. J. Lyman, "Octanol/Water Partition Coefficient", in W. J. Lyman, W. F. Reehl, and D. H. Rosenblatt's, Eds., *Handbook of Chemical Property Estimation Methods*, McGraw-Hill, New York, 1982, pp. 1-10–1-38.
37. W. Y. Shiu, W. Doucette, F. A. P. C. Gobas, A. Andren, and D. Mackay, *Environ. Sci. Technol.* **22**, 651 (1988).
38. C. T. Chiou, D. W. Schmedding, and M. Manes, *Environ. Sci. Technol.* **16**, 4 (1982).
39. C. T. Chiou and D. W. Schmedding, "Measurement and Interrelation of Octanol–Water Partition Coefficient and Water Solubility of Organic Chemicals", in *Test Protocols for Environmental Fate & Movement of Toxicants*, Proceedings of a Symposium, Association of Official Analytical Chemists, 94th Annual Meeting, Arlington, VA, 1981, pp. 28–42.
40. T. Harner and D. Mackay, *Environ. Sci. Technol.* **29**, 1599 (1995).
41. D. Wauchope, *J. Agric. Food Chem.* **24**, 717 (1976).
42. C. A. Johnson and J. C. Westall, *Env. Sci. Technol.* **24**, 1869 (1990).
43. C. T. Jafvert, J. C. Westall, E. Grieder, and R. P. Schwarzenbach, *Env. Sci. Technol.* **24**, 1795 (1990).
44. G. Kortum, W. Vogel, and K. Andrussov, *Dissociation Constants of Organic Acids in Aqueous Solution*, Butterworths, London, 1961.
45. D. D. Perrin, B. Dempsey, and E. P. Serjeant, *pK_a Prediction for Organic Acids and Bases*, Chapman and Hall, London, 1981.

46. E. P. Serjeant and B. Dempsey, *Ionisation Constants of Organic Acids in Aqueous Solution*, Pergamon Press, Oxford, 1979.
47. J. C. Harris and M. J. Hayes, "Acid Dissociation Constants", in W. J. Lyman, W. F. Reehl, and D. H. Rosenblatt's, Eds., *Handbook of Chemical Property Estimation Methods*, McGraw-Hill, New York, 1982, pp. 6-1–6-28.
48. R. S. Pearlman, "Molecular Surface Areas and Volumes and their Use in Structure/Activity Relationships", in S. H. Yalkowsky, A. A. Sinkula, and S. C. Valvani's, Eds., *Physical Chemical Properties of Drugs*, Medicinal Research Series, Vol. 10, Marcel Dekker, New York, 1980, pp. 321–347.
49. B. E. Poling, J. M. Prausnitz, and J. P. O'Connell, *The Properties of Gases and Liquids*, 5th Ed. McGraw-Hill, New York, 2000, pp. 4.33–35.
50. L. H. Nelken, "Density of Vapors, Liquids and Solids", in W. J. Lyman, W.F. Reehl, and D. H. Rosenblatt's, Eds., *Handbook of Chemical Property Estimation Methods*, McGraw-Hill, New York, 1982, pp. 19-1–19-24.
51. E. M. J. Verbruggen, J. L. M. Hermens, and J. Tolls, *J. Phys. Chem. Ref. Data* **29**, 1435 (2000).
52. D. Mackay, R. Mascarenhas, W. Y. Shiu, S. C. Valvani, and S. H. Yalkowsky, *Chemosphere* **9**, 257 (1980).
53. S. H. Yalkowsky and S. C. Valvani, *J. Chem. Eng. Data* **24**, 127 (1979).
54. R. S. Pearlman, S. W. Yalkowsky, and S. Banerjee, *J. Phys. Chem. Ref. Data* **13**, 555 (1984).
55. C. L. Yaws, *Chemical Properties Handbook*, McGraw-Hill, New York 1999.
56. T. E. Daubert and R. P. Danner, *Physical and Thermodynamic Properties of Pure Chemicals: Data Compilations*. Design Institute for Physical Property Data, Project 801. Taylor and Francis, Philadelphia, 1999.
57. D. Mackay, W.Y. Shiu and K. C. Ma, *Illustrated Handbook of Physical-Chemical Properties and Environmental Fate for Chemicals*, Lewis Publishers, Boca Raton, FL. Vol. I, Monoaromatic Hydrocarbons, Chlorobenzenes and PCBs, 1992. Vol. II, Polynuclear Aromatic Hydrocarbons, Polychlorinated Dioxins, Bibenzofurans, 1993. Vol. III, Volatile Organic Chemicals. Vol. IV Oxygen, Nitrogen and Sulfur Containing Compounds. Vol. V Pesticide Chemicals 1997.
58. A. D. Site, *J. Phys. Chem. Ref. Data* **26**, 157 (1997).
59. A. G. Hornsby, R. D. Wauchope, and A. E. Herner, *Pesticide Properties in the Environment*, Springer, New York, 1996.
60. A. L. Horvath, *Halogenated Hydrocarbons, Solubility-Miscibility with Water*, Marcel Dekker, Inc. New York, 1982.
61. G. T. Tomy, A. T. Fisk, J. B. Westmore, and D. C. G. Muir, *Rev. Env. Chem. and Toxicol.* **158**, 53, (1998).
62. R. S. Pearlman, S. H. Yalkowsky, and S. Banerjee, *J. Phys. Chem. Ref. Data* **13**, 555 (1984).
63. E. W. Lemmon and A. R. H. Goodwin, *J. Phys. Chem. Ref. Data* **29**, 1 (2000).
64. E. M. J. Verbruggen, J. L. M. Hermens, and J. Tolls, *J. Phys. Chem. Ref. Data* **29**, 1435 (2000).

Sorption

A major sink for compounds released into the environment is the soil or sediment in aquatic systems. Some compounds (e.g., a herbicide) may be applied directly to the soil, other compounds applied to plants may reach the soil as leaves fall. Compounds in the atmosphere may be deposited in “rain-out” or as particulates settle. Waste material will ultimately be consigned to a landfill. Consequently, the processes by which compounds distribute into and are bound in soil or sediment will influence their environmental distribution.

This topic will be developed by first considering the nature of the major components in soil, particularly in relation to their potential to be involved in the binding of organic compounds. Experimental approaches used to define this process will be outlined along with options to analyze this information and generate quantitative descriptors. The mechanisms by which organics distribute into soil will then provide a basis for identifying how the properties of the compound can predict its response. While the most important system is soil–water, some observations will be presented regarding nonaqueous situations, the distribution from the vapor phase into soil, and onto plant foliage. Kinetics of the sorption process will also be considered.

3.1 SOIL COMPONENTS

Soil scientists divide the mineral components into size groups called “soil separates”, sand, silt and clay, and the texture of soils is defined by the proportions of these components.

Sand, the larger particles in soil, is composed primarily of weathered grains of quartz, which is a covalent solid of silicon dioxide. This constituent will have a relatively small surface area because of the large particle size and would not provide any significant binding sites for organic compounds.

Silt constitutes the medium sized particles that are essentially broken down fragments of such minerals as quartz, feldspars, and so on. Like sand, silt is relatively inert and would not be involved to any significant extent in the binding of organic compounds.

Clays are the smallest particles, comprised of layer silicates that are formed from two basic units: a tetrahedron of four oxygen atoms surrounding a central cation, which is usually Si^{4+} , but is occasionally Al^{3+} , and an octahedron of six oxygens (or hydroxyls) around a large cation that is commonly Al^{3+} . Layers of the silicon tetrahedra and the aluminum octahedryl systems interact in various combinations to give the layered structures (Fig. 3.1). If ions of lower valence and similar radii substitute for Si^{4+} or Al^{3+} , a residual negative charge results that can be balanced by a cation external to the layered structure. Clay surfaces can assume a negative charge that is pH dependent, resulting from the dissociation of the hydroxyl hydrogens.

Thus the layer silicates have a planar geometry, a very large surface area and can achieve a high residual negative charge that accounts for their cation exchange capability illustrated in Figure 3.2. Clays are obviously hydrophylic and may absorb

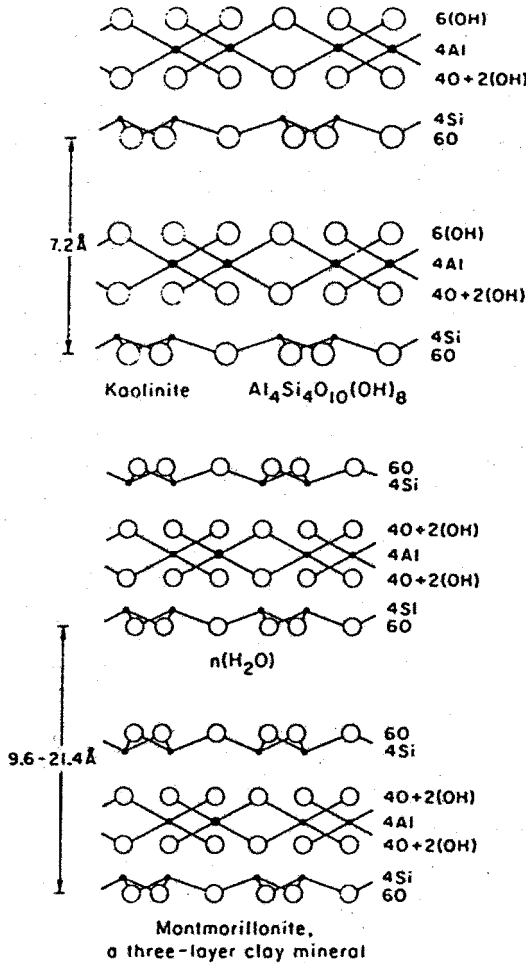


Figure 3.1 Layer structure of clay minerals.

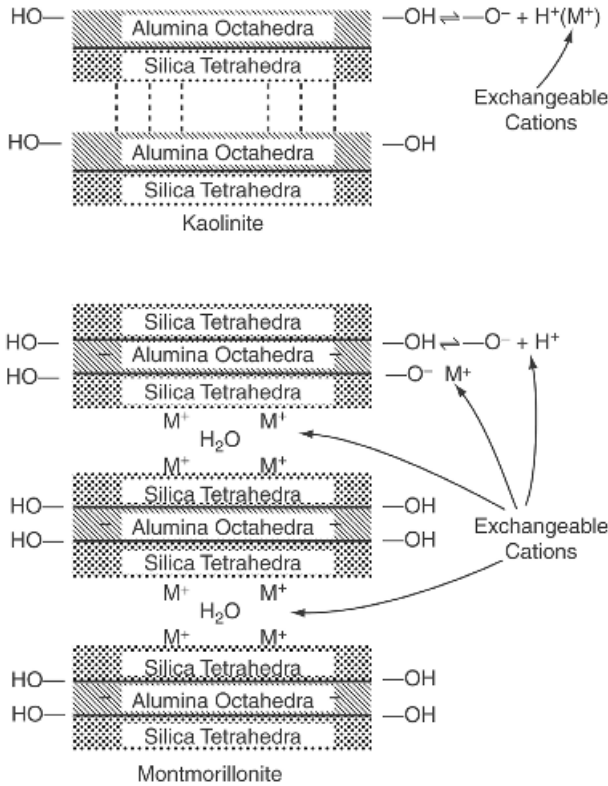


Figure 3.2 Distribution of charge and cation exchange potential of a clay.

considerable quantities of water and swell and shrink as they gain and lose water. Clays could be expected to adsorb hydrophilic compounds and cationic species with the process being enhanced by the large surface.

3.1.1 Soil Organic Matter

Soil organic matter (SOM) is often referred to as **humus** and is derived primarily from the degradation of plant material; lignin, carbohydrates, protein, fats, and waxes. Mineral soils may contain 0.5–3.0% of soil organic matter while muck soils and peat contain 50% and higher. Operationally, the material that cannot be extracted by alkaline agents is called **humic**. The material that precipitates from the alkaline extract on acidification is called **humic acid**, and what remains in solution **fulvic acid**. Felback¹ summarized some of the properties of these complex polymeric materials as follows:

1. The molecular weights range from ~3000 for fulvic acids to >300,000.

2. A dark brown or black color is characteristic of higher molecular weight species, whereas the lower molecular weight components tend to be light brown or yellow.
3. A high degree of unsaturation is indicated.
4. Acidity is due primarily to phenolic or carboxylic functional groups.
5. Almost 50% of the oxygen exists in nonreactive structural units, possibly as ether bonds or heterocyclic oxygen.
6. Amino groups are commonly observed, and the nitrogen is resistant to hydrolysis.
7. Humic substances are quite sensitive to oxidation.
8. The carbon skeleton is resistant to both chemical and microbial attack.

The complex nature of these materials is illustrated by the structure (Fig. 3.3) recently proposed for fulvic acid,² the simplest of these polymeric materials.

Hydrophobic regions are indicated by the distribution of hydrocarbon chains and aromatic rings. Carboxylic acid and phenolic functional groups would confer polar characteristics and would account for the fact that SOM can retain a considerable

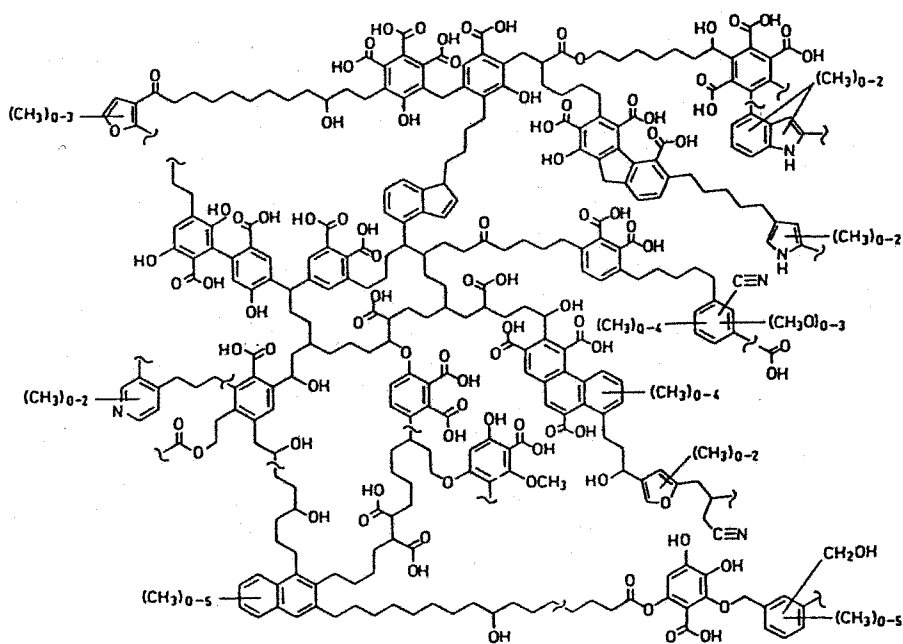


Figure 3.3 A structure proposed for fulvic acid. [Reproduced with permission from J. Buffle et al., *Environ. Sci. and Technol.* **32**, 2887 (1998). Copyright © 1998, American Chemical Society.]

amount of water. Humus may retain up to six times its weight of water.³ In fact, the polarity of samples of soil organic matter can be important in differentiating their behavior and the weight ratio of O + N to C has been used to approximate the polar–nonpolar balance.⁴ Another approach has been to use nuclear magnetic resonance (NMR) techniques to establish the “polar organic carbon” content as the portion of carbon associated with oxygen and nitrogen functional groups.⁵ This value ranged from 36.5 to 60% in a selection of 30 soils and sediments. These same functional groups could also account for the cation exchange capacity of this soil component. Soil organic matter has been found to have a surface area of $\sim 1 \text{ m}^2 \cdot \text{g}^{-1}$.⁶

The use of these soil components are illustrated in Table 3.1 for several subsoils used in a study of the distribution of an organic base into soils.⁷ Note first that the organic matter content is expressed as “organic carbon” and it is usually assumed that 1 g of organic carbon is equivalent to 1.72 g of organic matter. Literature will use either percent organic matter or percent organic carbon. Also note that a low surface area is associated with a high sand content and cation exchange capacity is more closely associated with clay and organic carbon content. It is also important to note that the pH of these samples ranges from 4.23 to 8.17. Soils may show extreme pH values of 3.5 on the acid side and 10.5 on the basic side, however, the normal soil pH range is from 5 to 8. Soil pH is an important variable in determining the behavior of weak acids and bases since it determines whether these compounds exist as neutral or charged species.

3.2 ADSORPTION, PARTITIONING, SORPTION

Soil is a very complex system and the different constituents provide a variety of options for chemicals to bind. To be able to assess how the properties of a chemical influence its behavior in soil it is necessary to develop an understanding of the mechanisms that could be involved.

TABLE 3.1 Illustrative Soil Properties

Subsoil	Per. Org. C	Particle Distribution (%)			Surface area ($\text{m}^2 \cdot \text{g}^{-1}$)	CEC ($\text{mequiv} \cdot 100 \text{ g}^{-1}$)	pH
		Sand	Silt	Clay			
Elk	0.22	11	57	32	27.2	6.7	4.23
Loring	0.24	2	70	28	30.5	8.4	4.85
Vernita	0.02	66	33	1	2.64	1.7	7.16
Vebar	0.35	75	11	14	9.20	11.23	8.00
Anvil points	0.58	28	44	28	23.4	12.45	8.15
Zahl	1.21	26	50	24	15.0	14.15	8.17

3.2.1 Adsorption

A substance is said to be adsorbed if the concentration in a boundary region is higher than in the interior of a contiguous phase. Different types of adsorption equilibria may be defined such as the adsorption of gas on a solid or a liquid on a solid; however, the most significant process in this environmental context is the adsorption of a solute onto a solid. A number of factors will determine the extent to which such a process will proceed. Both the physical and chemical characteristics of the **adsorbent** (adsorbing surface) will be factors. The availability of adsorption sites will be a function of surface area. The nature of adsorption sites and their distribution will determine the nature of the adsorption process. The **adsorbate** (molecule adsorbed) that adsorbs from solution, does so against a force that would retain it in solution. Solubility would provide an indication of this tendency. This principle finds use in column chromatography where a mixture of compounds may be adsorbed on an adsorbent and solvents of increasing polarity are used to remove compounds as a function of their solubilities. In the adsorption of a solute, it is assumed that the surface will be modified since the solvent will saturate that surface. In most environmental processes, the solvent is water and the solvent effect is consistent. However, adsorption on a dry soil, say from the vapor phase, will be quite distinct from the solution process.

A thermodynamically spontaneous process will involve a decrease in free energy. Since the entropy change is negative, the system becomes more ordered with surface binding and the enthalpy change (heat of adsorption) must be negative. Heats of adsorption provide an index of the strength of binding, with smaller values ($< 10 \text{ kcal} \cdot \text{mol}^{-1}$) being due to physical adsorption resulting from London van der Waal's forces usually involving neutral molecules. If the values approach those observed in a chemical reaction, chemical bonding could be involved and the process would be classified as **chemisorption**. The distinction between these two mechanisms is not always clear cut since the adsorption of a polar molecule onto polar surfaces could indicate either mechanism.

As a chemical adsorbs on a surface, the characteristics of the surface will change and ultimately approach that of the adsorbate. This will occur with a nonselective process and once a monolayer is formed, the heat of adsorption will approximate the heat of solution since the surface of the adsorbent almost represents the surface of the solid form of the adsorbate. The heat of adsorption in this situation will vary with the amount of compound adsorbed. A negative heat of adsorption also indicates that an increase in temperature will result in a decrease in adsorption.

3.2.2 Partitioning

Partitioning involves a process in which the compound dissolves in an organic phase similar to the situation where an organic solute might be extracted from water by an organic solvent. When the organic phase is a solid (as will be illustrated for soil organic matter) partitioning is differentiated from adsorption by the fact that the compound is distributed homogeneously through the solid rather than being

bound on the surface. The partition coefficient defining the distribution of a compound between the two phases depends on its solubilities in those two phases. Solubilities in the two phases will depend on polarity of the solute; that is, like dissolves like. In contrast to adsorption, surface area of the solid is not a factor in the equilibrium distribution. The enthalpy change for such a process will depend on the difference in the heats of solution of the compound in the two phases and will be smaller in magnitude and less negative than a heat of adsorption.

3.2.3 Sorption

This term denotes distribution of a compound into/onto a soil or sediment without considering a specific mechanism. Soils are so complex that in some situations several mechanisms could be active and in an experimental context, on occasion, one could simply be observing inclusion in some pore in the soil structure distinct from any of the processes discussed. Thus sorption is a more inclusive and less definitive term and would be a more appropriate designator for the distribution of chemicals between soil and water.

3.3 EXPERIMENTAL APPROACH: SORPTION ISOTHERMS

Most of the data cited in the literature defining the sorption of organic compounds in soil has been derived from “batch” experiments. The soil is added to an aqueous solution, allowed to equilibrate, and the equilibrium concentration (C_e) is determined along with the amount sorbed on or into the soil (x/m). The experiment is usually carried out as a sorption study; starting out with chemical-free soil, although it is theoretically possible to use a desorption approach, starting with the chemical sorbed in the soil. A sorption study can be set up using a constant amount of soil and varying the initial concentration of the chemical or as is illustrated by the data in Table 3.2, the initial chemical concentration can be held constant and the amount of soil varied. The objective is to observe how the extent of sorption varies over a range of equilibrium concentrations of the chemical in solution. The data sets given for the sorption of 2,2',5,5'-tetrachlorobiphenyl and 2,4'-dichlorobiphenyl on a Woodburn soil (3.1% SOM) involved the addition of specified quantities of soil to 30 mL of PCB solution, and equilibration on a shaker overnight (found to be sufficient time to attain equilibrium). The equilibrium concentration in solution was determined after centrifuging and the amount sorbed was determined by difference.⁸

3.3.1 Sorption Isotherms

An **isotherm** describes the relationship of the concentrations of a solute between two separate phases at equilibrium at a constant temperature. An **adsorption isotherm**, then would express the relation between the amount of vapor or solute adsorbed as a function of the equilibrium concentration of the vapor or solute in solution. A **sorption isotherm** describes the process without reference to the mechanism.

TABLE 3.2 Sorption Experiment Data for PCB Congeners

Soil (g)	2,2',5,5'-Tetrachlorobiphenyl				2,4'-Dichlorobiphenyl			
	C_e , (ng · mL ⁻¹)	ng PCB (in soln)	Sorbed (ng)	x/m (ng · g ⁻¹)	C_e , (μg · mL ⁻¹)	μg PCB (in soln)	Sorbed (μg)	x/m (μg · g ⁻¹)
0	24.9	747			0.600	18.0		
0.010	17.4	522	225	22,500	0.525	15.75	2.25	225
0.025	11.2	336	411	16,440	0.454	13.62	4.38	175
0.050	5.62	168.6	578	1,157	0.383	11.49	6.51	130
0.100	4.13	123.9	623	6,231	0.301	9.03	8.97	89.7
0.250	2.10	63.0	684	2,736	0.211	6.33	11.67	46.7
0.500	0.934	28.0	719	1,438	0.126	3.78	14.22	28.4
0.750	0.615	18.5	729	971.3	0.094	2.82	15.18	20.2
1.00	0.469	14.1	733	732.9	0.058	1.74	16.26	16.3
1.25	0.474	14.2	733	586.2	0.049	1.47	16.53	13.2

3.3.1.1 Langmuir Isotherm This relationship has a sound conceptual base and was originally developed for defining the adsorption of gases on solids. The following assumptions are made.

1. The energy of adsorption is constant and independent of the extent of surface coverage.
2. The adsorption is on localized sites and there is no interaction between the adsorbed molecules.
3. The maximum adsorption possible is that of a complete monolayer.

The moles of solute adsorbed per gram of adsorbent (X) are expressed as a function of the equilibrium concentration of solute in solution (C):

$$X = \frac{X_m \cdot b \cdot C}{1 + bC}$$

- X_m Number of moles adsorbed per gram of adsorbent to give a complete monolayer.
- b Constant related to the energy of adsorption (when $C = 1/b$, $X = X_m/2$)

At low concentrations of solute the relation is approximately linear ($X \simeq X_m b C$), but the extent of adsorption is limited at high concentration due to the limited number of sites (Fig. 3.4). This isotherm has found use in the study of the adsorption of gases on solids; however, it is not as useful in defining the adsorption of compounds from solution, particularly onto soils. The heterogeneous nature of a soil would obviously invalidate the first assumption.

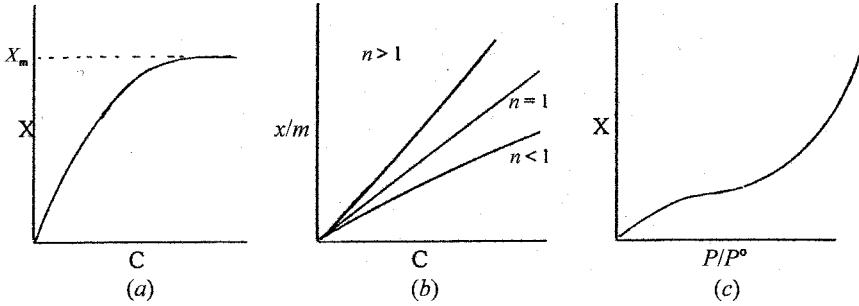


Figure 3.4 Langmuir (a), Freundlich (b), and BET (c) isotherms.

The Langmuir isotherm can be expressed in a linear form:

$$1/X = 1/X_m + (1/[b \cdot X_m])1/C$$

which can be used to evaluate experimental data. A linear relation would result from plotting $1/X$ as a function of $1/C$ with an intercept of $1/X_m$ and slope of $1/bX_m$.

3.3.1.2 Brunauer–Emmet–Teller (BET) Isotherm If a gas continues to adsorb on a surface after a monolayer is achieved, the process essentially represents a condensation and the overall process is represented by this isotherm (Fig. 3.4).⁹ The mass of gas adsorbed per unit mass of adsorbent (X) is expressed as follows:

$$X = \frac{B \cdot X_m \cdot x}{(1 - x)(1 + [B - 1]x)}$$

where

- X_m is the monolayer capacity in $\text{mg} \cdot \text{g}^{-1}$ of adsorbent.
- $x = P/P^0$ (experimental vap. pressure)/sat. vapor pressure.
- B is a dimensionless constant defined as a function of the molar heats of adsorption (ΔH_X) and vaporization (ΔH_v).

$$-\ln B \simeq (\Delta H_X + \Delta H_v)/(RT)$$

A linear form of the relation is given by

$$\frac{x}{X(1 - x)} = \frac{1}{B \cdot X_m} + \frac{(B - 1) \cdot x}{B \cdot X_m}$$

Values for X_m and B can be derived from the slope, $(B - 1)/BX_m$, and intercept, $1/BX_m$, when $x/[X(1 - x)]$ is plotted as a function of x . The relation may also define adsorption from solution replacing concentration for vapor pressure.

3.3.1.3 Freundlich Isotherm An empirical relation expresses the relation between the amount of compound sorbed (x/m) and the equilibrium concentration, C_e :

$$x/m = K \cdot C_e^n$$

A logarithmic form of this expression gives a linear relation from which values for the Freundlich constant, K , and the exponent, n , can be derived:

$$\log x/m = \log K + n \log C_e$$

The use of this relation to evaluate experimental data is essentially “curve fitting” since it has no mechanistic base. Values of K provide an index of the extent of sorption and often are listed without units. However, if sorption (x/m) is expressed as $\mu\text{mol/g}$ and equilibrium concentration (C_e) in $\mu\text{mol/mL}$, K would have units $(\mu\text{mol})^{1-n} \cdot \text{mL}^n \cdot \text{g}^{-1}$. The exponent, n , simply indicates whether the relation between x/m and C_e is linear ($n = 1$), concave down ($n < 1$) or concave up ($n > 1$), Figure 3.4. Values for the Freundlich K and exponent “ n ” derived by a simple regression from the experimental data summarized in Table 3.2 are given in Table 3.3.

3.3.1.4 Other Isotherms Most of the sorption–adsorption data in the literature has been evaluated using either the Langmuir or Freundlich isotherms along with the special case of the latter represented by the direct distribution ratios ($n = 1$). The mathematics is simple and most data fits these relations. These relations are probably oversimplifications given the complexity of the soil systems and more comprehensive approaches that take advantage of improved computing capabilities have been reviewed.¹⁰ For example, a two-site Freundlich expression has been used in the study of the sorption of pesticides,¹¹ and a double Langmuir expression has been used to interpret the sorption of a quaternary ammonium compound¹² assuming that two different adsorption sites are active with differing capacities and binding affinities.

TABLE 3.3 Sorption Indices for PCB Congeners

Compound	Freundlich			Distribution Ratio	
	K	n	r	K_D	r
2,4-Dichloro-	165	1.19	0.924	427	0.981
2,5,2',5'-Tetrachloro-	1,481	1.01	0.994	1,342	0.984

3.3.1.5 Soil Distribution Ratios, K_d , K_{om} , K_{oc} The sorption of nonpolar organic compounds on soil usually approximates a linear relation as illustrated in Figure 3.5¹³ The slope of these lines defines a soil–water distribution ratio, K_d , which is expressed

$$K_d(\text{mL} \cdot \text{g}^{-1}) = (x/m)/C_e \quad (\mu\text{g} \cdot \text{g}^{-1}\text{soil})/(\mu\text{g} \cdot \text{mL}^{-1}\text{water})$$

Values for K_d are usually obtained from batch experiments and for a given compound will vary depending on the soil or sediment as is illustrated in Table 3.4 for a polynuclear aromatic hydrocarbon, pyrene;¹⁴ a 15-fold difference. Consideration of the sorbent characteristics, it is clear that, for pyrene, there is no relation between sorption and pH or the amount of clay, however, the association between K_d and the SOM, expressed as soil organic carbon (SOC) in this case, is obvious (Fig. 3.7).

Numerous observations have confirmed that the extent of sorption of non-polar adsorbates in soil is dependent on the amount of SOM and two quantities, K_{oc} and

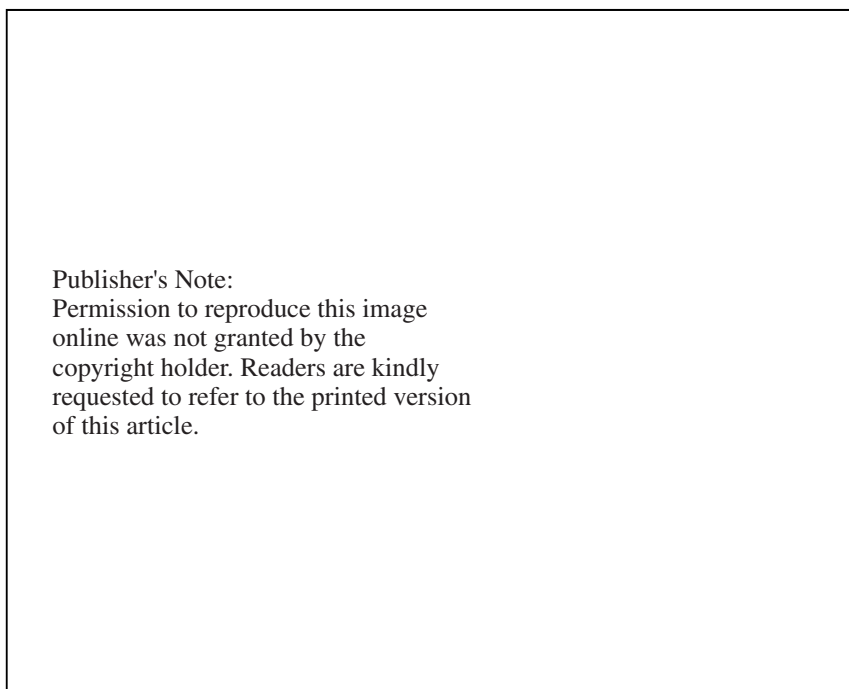


Figure 3.5 Soil–water isotherms of halogenated organic liquids on Willamette silt loam ($f_{om} = 0.016$) at 20°C. [Reproduced with permission from, C. T. Chiou, L. J. Peters, and V. H. Freed, *Science* **206**, 831. Copyright 1979 American Association for the Advancement of Science.

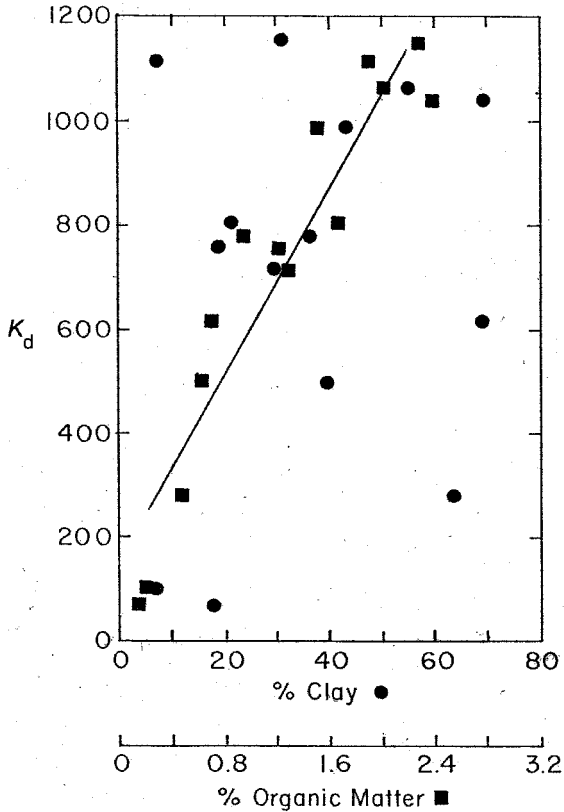


Figure 3.6 The relation of K_d to SOM content.

K_{om} , are used to express sorption in terms of the amount of SOC or SOM, respectively,

$$K_{oc}(\text{mL} \cdot \text{g}^{-1}) = (\mu\text{g sorbed} \cdot \text{g}^{-1}\text{SOC})/(\mu\text{g} \cdot \text{mL}^{-1})$$

$$K_{om}(\text{mL} \cdot \text{g}^{-1}) = (\mu\text{g sorbed} \cdot \text{g}^{-1}\text{SOM})/(\mu\text{g} \cdot \text{mL}^{-1})$$

Since SOM contains $\sim 58\%$ carbon, 1 g SOC would be equivalent to 1.72 g of SOM. Consequently,

$$K_{oc} = 1.72 K_{om} \quad \text{and} \quad K_{oc} = K_d/f_{oc}$$

where f_{oc} is the proportion of SOC in a given soil or sediment.

The K_{oc} values have been calculated from the experimental K_d values for pyrene listed in Table 3.4 and one now observes that there is only a twofold variation in the value of the former. Some of this variation may be due to differences in the nature of the organic matter from sample to sample. Also lower values for K_{om} (or K_{oc}) are

TABLE 3.4 Soil Properties and Sorption of Pyrene

Soil/Sediment	pH	% Org Carbon	% Clay	K_d	K_{oc}
EPA-B2	6.35	1.21	18.6	760	62,860
EPA-4	7.79	2.07	55.2	1065	51,470
EPA-5	7.44	2.28	31.0	1155	50,650
EPA-6	7.83	0.72	68.6	614	85,260
EPA-8	8.32	0.15	6.8	101	67,470
EPA-9	8.34	0.11	17.4	71	64,710
EPA-14	4.54	0.48	63.6	277	57,760
EPA-15	7.79	0.95	35.7	783	82,420
EPA-18	7.76	0.66	39.5	504	76,320
EPA-20	5.50	1.30	28.6	723	59,650
EPA-21	7.60	1.88	7.1	1119	59,515
EPA-22	7.55	1.67	21.2	806	48,240
EPA-23	6.70	2.38	69.1	1043	43,807
EPA-26	7.75	1.48	42.9	994	67,190

often observed with soils or sediments with higher levels of SOM. It is assumed that some of the SOM leaches into solution and the DOM results in a higher value of C_e . While the magnitude of K_d depends on the nature of the chemical and the level of SOM in the soil or sediment, K_{oc} (and K_{om}) are characteristic for the chemical

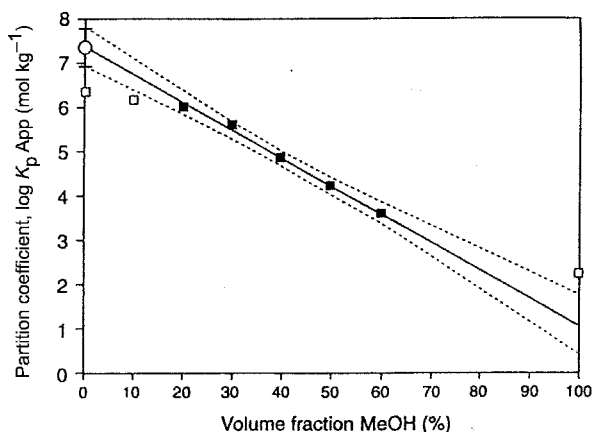


Figure 3.7 Apparent partition coefficient of benzo[a]pyrene as a function of volume fraction of methanol with 95% confidence intervals. Salinity = 35‰; suspension concentration = 10.8 g · L⁻¹. Filled squares denote apparent partition coefficients used for the regression and the intercept with the y axis (open circle) the cosolvent partition coefficient. [Reproduced with permission from W. J. M. Hegeman, C. H. van der Weijden, and J. P. G. Loch, *Environ. Sci. Technol.* **29**, 363 (1995). Copyright © 1995, American Chemical Society.]

and some illustrative values are listed in Table 3.5. A comprehensive summary of K_{oc} values has been published.¹⁵

A “cosolvent” partitioning approach¹⁶ has been developed, based on the solubility in mixed solvents, to account for the effect of DOM and colloidal material that could result in a higher value for C_e . The distribution of a compound, in this case, benzo[*a*]pyrene, is observed as a function of the volume fraction of methanol (Fig. 3.7) The influence of DOM and colloids is overcome when the volume fraction of methanol is $>20\%$ and extrapolation to the *y* axis provides a “cosolvent” distribution ratio that can be converted to a K_d by multiplying by the molar volume of water.

The question as to whether the characteristics of SOM would vary sufficiently from soil to soil to influence K_{oc} values is an important consideration that determines whether values obtained from one soil can be used to assess the behavior of a chemical in another. This issue has been addressed in a study where the sorption of carbon tetrachloride and 1,2-dichlorobenzene has been determined in 32 soils and 36 sediments (f_{oc} 0.0016 – 0.061).¹⁷ A summary of the K_{oc} data is given in Table 3.6. For each compound, the variation among K_{oc} values is only $\sim 10\%$ indicating that the composition of the organic matter is relatively consistent certainly in respect to the sorption of nonpolar compounds. Aquatic sediments show consistently higher values and it is postulated that this could result from the more polar components distributing into the aqueous phase with the sediment organic matter becoming more nonpolar. Higher K_{oc} values have also been observed with contaminated sediments.¹⁸

3.4 SORPTION MECHANISM

3.4.1 Nonpolar Organic Compounds

It has been demonstrated¹⁹ that a partitioning process from water into soil organic matter is the major mechanism by which nonpolar organic compounds sorb in soil. This conclusion is based on the observation of linear isotherms, the magnitude

TABLE 3.5 Illustrative K_{om} Values

Compound	K_{om}	Compound	K_{om}
1,2-Dichloroethane	19	Lindane	1730
Carbon tetrachloride	35	2,2'-Dichlorobiphenyl	4,800
1,2-Dibromoethane	36	2,4,4'-Trichlorobiphenyl	24,000
Benzene	18	2,5,2',5'-Tetrachlorobiphenyl	47,000
Anisole	20	Pyrene	36,500
Chlorobenzene	48	7,12-Dimethylbenzanthracene	137,000
Ethylbenzene	95	<i>p,p'</i> -DDT	140,000
Atrazine	98	3-Methylcholanthrene	1,040,000
1,3-Dichlorobenzene	170	Naphthalene	284
1,2,4-Trichlorobenzene	501	Phenanthrene	9,430

TABLE 3.6 Variation of K_{oc} in Soils and Sediments

Sorbent	K_{oc} Mean and SD	
	Carbon Tetrachloride	Dichlorobenzene
Soils	60 ± 7	290 ± 42
Sediments	102 ± 11	502 ± 66

of the enthalpy changes, and noncompetitive nature of the sorption process. It is significant that the sorption isotherms are linear at equilibrium concentrations approaching the solubilities of the compound in question. For example, 1,2-dichlorobenzene has an aqueous solubility at 20°C of 148 mg · L⁻¹ and the isotherm is linear up to $C_e/S_w = 0.95$ (Fig. 3.6), which is not the case for the adsorption of such compounds on activated charcoal (Fig. 3.8). In this case, the isotherm would approximate a linear relation at low values of C_e/S_w . One consequence of this linearity is that the molar heat of sorption will be constant and independent of the loading.

For a partitioning process, the molar heat of sorption ΔH_{sorp} ; that is, transfer of the solute from water to the partitioning phase, in this case SOM, would be expressed

$$\Delta H_{sorp} = \Delta H_{som} - \Delta H_w$$

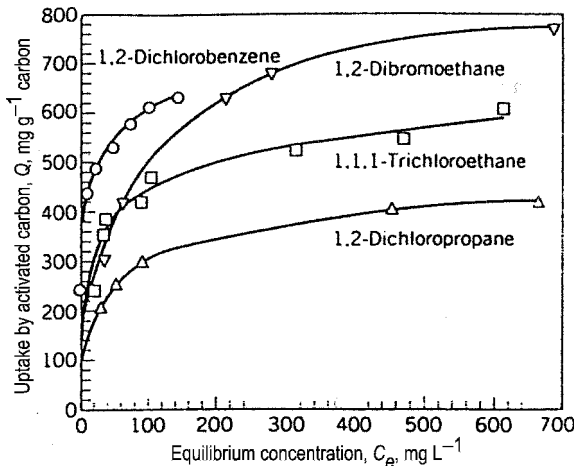


Figure 3.8 Adsorption isotherms of selected halogenated organic liquids from water on Pittsburgh CAL (12 × 40) activated carbon at 20°C. [Reproduced from C. T. Chiou, "Partition coefficients and water solubility in environmental chemistry", in J. Saxena and F. Fisher, Eds., *Hazard Assessment of Chemicals: Current Developments*, Vol. I, Academic Press, New York, 1981, p. 115, with permission from Elsevier.]

Since, both ΔH_{som} and ΔH_{w} are usually positive, $\Delta H_{\text{sorp}} > -\Delta H_{\text{w}}$ because the enthalpy change in water is larger. Consequently, in contrast to a true adsorption process, temperature would not be expected to have a large influence on the sorption process since the enthalpy change would not be large. Note that a change in temperature from 3.5 to 20°C has virtually no effect on the sorption of 1,2-dichlorobenzene (Fig. 3.6) and 1,1,1-trichloroethane shows higher sorption at 20°C than at 3.5°C indicating a negative ΔH_{w} for this compound.

Another characteristic of a partitioning process in contrast to a true surface adsorption is that for multiple solutes there is no competitive interaction. This is illustrated in Figure 3.9, where the sorption of parathion, an organophosphate, on soil is not affected by the presence of lindane and vice versa.²⁰

3.4.2 Nonlinear Isotherms

Nonlinear isotherms have been reported^{21,22} particularly at low C_e values (Fig. 3.10a). The sorption of both dibromoethane (EDB) and the herbicide diuron (DUN) on a peat soil (49.3%OC) both show this response, which is more pronounced with the latter. A similar type of response is also observed in soils of lower organic carbon content. A competitive effect is also demonstrated with trichloroethylene and phenol suppressing the sorption of EDB and EDB (at a sufficient concentration), monuron and dichlorophenol affecting the sorption of diuron. The

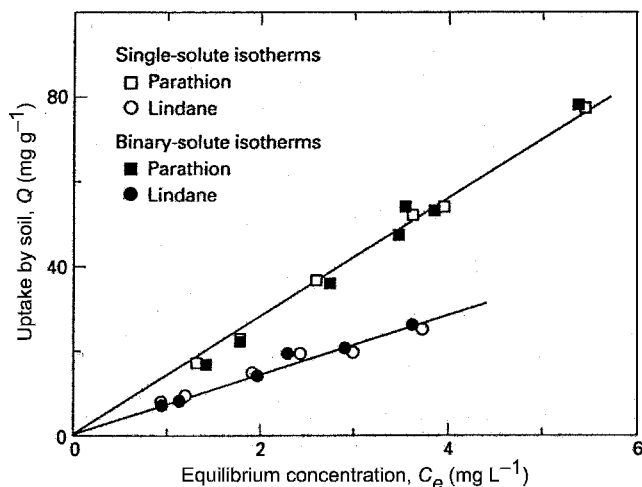


Figure 3.9 Sorption isotherms of parathion (squares) and lindane (circles) as single and binary solutes from water on Woodburn soil ($f_{\text{om}} = 0.019$) at 20°C. Open symbols are for single solute data and solid symbols for binary-solute data. [Reproduced from C. T. Chiou, T. D. Shoup, and P. E. Porter, "Mechanistic roles of soil humus and minerals in the sorption of nonionic compounds from aqueous and organic solutions", *Org. Geochem.*, **8**, 9, Copyright © 1985, with permission from Elsevier.]

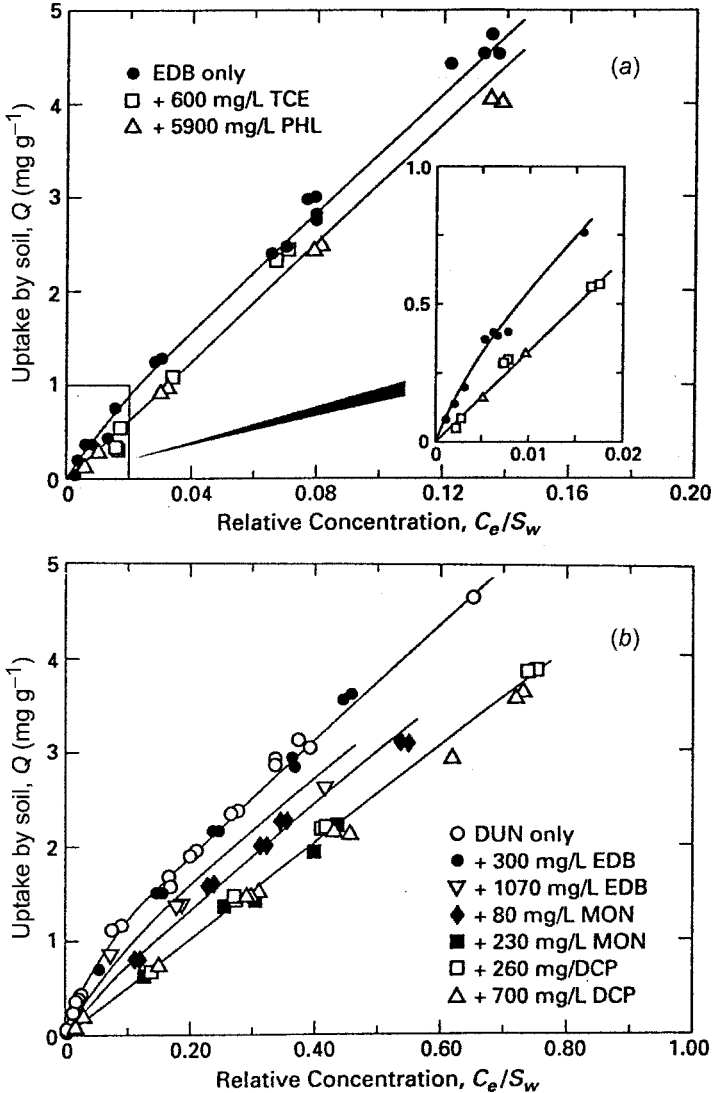


Figure 3.10 (a) Sorption of EDB alone on peat soil and with trichloroethylene (TCE) and phenol (PHL) as cosolutes. (b) Sorption of diuron (DUN) alone on peat soil and with EDB, monuron (MON), and dichlorophenol (DCP) as cosolutes. [Reproduced with permission from C. T. Chiou and D. E. Kile, *Environ. Sci. Technol.* **32**, 338 (1998). Copyright © 1998 American Chemical Society.]

data suggest that a different mechanism must account for the nonlinear phase, which can be saturated with subsequent sorption being consistent with the partitioning model.

The intercept obtained from extrapolation of the linear phase provides an estimate of the nonlinear sorption capacity that varies with the adsorbate and the soil

(Table 3.7). The concentration needed to saturate is also listed. In postulating a mechanism for this effect, one must account both for the nonlinear effect and the difference in response of compounds such as diuron and EDB. Several hypotheses have been proposed such as the availability of different sets of internal pores in SOM with differing affinities for molecules of different polarities. It has also been suggested that organic matter can exist in either a glassy or rubber-like form accounting for different sorption behavior. Perhaps the most viable hypothesis at present accounts for the nonlinear sorption of molecules such as EDB by the presence of small amounts of high surface area carbonaceous material (charcoal-like) in the organic matter. This would provide a true adsorption surface and account for the competition and it is not difficult to explain how such material might be produced. This phenomenon would not explain the high nonlinear capacity of a compound such as diuron. It is suggested that highly active sites exist in soil organic matter that can interact through other bonding mechanisms with molecules having appropriate functional groups. For example, EDB might bond to charcoal through van der Waal's forces, but the urea functional group in diuron presents a possibility for hydrogen bonding. At this point, the nature of these sites has not been established.

With a nonlinear isotherm, K_{oc} values will vary with C_e and the interpretation of soil–water distribution processes will be more complex. For example, from Figure 3.10 with diuron alone in the system, one can calculate K_{oc} values of 670 and 448 at C_e/S_w of 0.10 and 0.30, respectively, in contrast to a value of 270 for the linear partition process. However, under field conditions one is not usually dealing with a single adsorbate and any competitive process would result in a distribution closer to linear partitioning.

3.5 SORPTION AND PROPERTIES OF THE SORBATE

3.5.1 Aqueous Solubility–Partition Coefficient

The distribution of a solute from water into SOM can be represented by a modification of the Flory–Huggins theory, which describes solubility in amorphous

TABLE 3.7 Nonlinear Sorption Capacities and Saturation Concentrations

Sorption System	Capacity (mg · g)	Conc. C_e/S_w
TCE/peat	0.15	0.012
EDB/peat	0.18	0.010
DUN/peat	0.60	0.10
MON/peat	0.82	0.13
DCP/peat	25	0.12
EDB/Woodburn ^a	<0.008	0.015
DCP/Woodburn	0.38	0.080

^aWoodburn soil 1.26%OC.

polymers:²³

$$\log K_{\text{om}} = \log S_w V - \log \rho - (1 + \chi)/2.303 - \log (\gamma_w / \gamma_w^*)$$

where

V is the molar volume of the sorbate in $\text{L} \cdot \text{mol}^{-1}$.

ρ is the density of the SOM, assumed to be 1.2 and allows expression of conc. in the organic phase on a mass–mass basis.

χ , the Flory–Huggins interaction parameter to represent accessibility and flexibility of the polymer; assumed to be ~ 0.25 for SOM.

γ ratio reflects solubility enhancement from SOM distributing into water. This factor will be negligible for compounds with $\log K_{\text{om}} < 3$ providing the SOM level in water is small; $< 100 \text{ mg L}^{-1}$.

Good correlations of $\log K_{\text{om}}$ with $\log S_w V$ have been reported,²³ however, since the variation in V is small compared with the variation in S_w the correlation of K_{om} is usually reported as a function of S_w . Since aqueous solubility is the major factor determining distribution into SOM it follows that there should be a direct relation between K_{om} and K_{ow} . The relations between K_{om} and S_w (expressed as the supercooled liquid for solids) or K_{ow} have been compiled for several series of neutral organic compounds¹⁹ and are summarized in Tables 3.8 and 3.9. To illustrate the differences among these relations a K_{om} and an S_{om} has been calculated assuming S_w of $1 \times 10^{-4} \text{ mol} \cdot \text{L}$. Given the linear sorption relation it is assumed that solubility in SOM (S_{om}) is approximately given by $K_{\text{om}} \cdot S_w$.

For the relations in Table 3.8 the slope “ a ” reflects the change in $\log S_{\text{om}}$ with the change in $\log S_w$ and the intercept, “ b ” represents the $\log K_{\text{om}}$ of a compound with S_w of 1. It is also clear that the solubility of different series of compounds in SOM varies considerably reflecting its polar features. Unlike the $\log K_{\text{ow}}/\log S_w$ the $\log K_{\text{om}}/\log K_{\text{ow}}$ is sensitive to solute polarity and octanol is not a good surrogate

TABLE 3.8 Relations between K_{om} and Aqueous Solubility

Compound Class	$\log K_{\text{om}}(\text{ml g}^{-1}) =$ $a \log S_w(\text{mol L}^{-1}) + b$		Calc. for $S_w = 1 \times 10^{-4}$	
	a	b	$\log K_{\text{om}}$	$S_{\text{om}}(\text{mol kg}^{-1})$
Aromatic hydrocarbons	−0.93	−0.17	3.55	0.355
Chlorinated hydrocarbons	−0.70	0.35	3.15	0.142
Chlorinated hydrocarbons ^a	−0.729	0.001	2.92	0.0832
Chloro- <i>s</i> -triazines	−0.41	1.20	2.84	0.0692
Phenyl ureas	−0.56	0.97	3.21	0.162

^aTaken from Ref. 18.

TABLE 3.9 Relations between K_{om} and K_{ow}

Compound Class	$\log K_{om} (\text{ml g}^{-1}) = a \log K_{ow} + b$		Calc for $\log K_{ow} = 3.5$
	<i>a</i>	<i>b</i>	K_{om}
Aromatic hydrocarbons	1.01	-0.72	2.82
Chlorinated hydrocarbons	0.88	-0.27	2.81
Chlorinated hydrocarbons ^a	0.94	-0.78	2.51
Chloro- <i>s</i> -triazines	0.37	1.15	2.45
Phenyl ureas	1.10	0.15	4.00
Chlorophenols	0.81	-0.25	2.59

^aTaken from Ref. 18.

for SOM (variation in “*a*”). The following relation (p. 274)²⁴ was derived from observations on a range of compounds and can provide an estimate of K_{om}

$$\log K_{om} = 0.82 \log K_{ow} + 0.14$$

however, a more precise estimate would be derived if a relation defining K_{om}/K_{ow} were available for that particular class of compounds.

3.5.2 Weak Acids and Bases

The pH of soils may vary, in extreme cases, from 3.5 to 10.5, with a range of 4.0 to 8.0 representing a more common situation. The soil pH will determine whether a weak acid or base will exist as a charged or neutral species if their pK_a is in this range (see Physical Chemical Properties, Chapter 2). This differentiation will affect sorption since the charged species will be more water soluble. The conjugate base (CH_3COO^-) of acetic acid (CH_3COOH) will be an anion carrying a negative charge while the conjugate acid (NH_4^+) of the weak base ammonia (NH_3) will be a cation with a positive charge. This distinction will also influence sorption since it will determine the mechanism.

3.5.2.1 Weak Acids A comprehensive analysis of the sorption behavior of pentachlorophenol ($pK_a = 4.75$) provides a good example of how environmental pH influences sorption in soils.²⁵ The fraction (Φ_n) of the neutral pentachlorophenol (PCP) present can be expressed

$$\Phi_n = [\text{PCP}]/([\text{PCP}] + [\text{PCP}^-]) = (1 + 10^{\text{pH} - pK_a})^{-1}$$

At $\text{pH} < 3$ PCP is essentially 100% neutral, while at $\text{pH} > 7$ the compound will exist as the anion. An expression for the overall sorption of PCP would be expressed

$$K_d = ([\text{PCP}]_s + [\text{PCP}^-]_s)/([\text{PCP}]_w + [\text{PCP}^-]_w)$$

considering the concentrations of both forms of PCP in the sorbed ($[]_s$) and the equilibrium aqueous concentration ($[]_w$). Soil/water distribution ratios ($K_{d(n)}$ and $K_{d(i)}$) for the neutral anionic species would be given by

$$K_{d(n)} = [\text{PCP}]_s / [\text{PCP}]_w \quad \text{and} \quad K_{d(i)} = [\text{PCP}^-]_s / [\text{PCP}^-]_w$$

The corresponding K_{oc} values could be derived from K_d/f_{oc} assuming that this soil constituent is the primary sorbent for both species. If the sorption is due primarily to the neutral PCP, the K_{oc} for a given pH would depend on the proportion of the PCP in that form and would be expressed

$$K_{oc}(\text{given pH}) = K_{oc(n)}\Phi_n$$

For pH values <7 the experimental K_{oc} values would fit this expression (Fig. 3.11) with a $\log K_{oc(n)}$ of 4.5.²⁶ However, it has been observed that sorption is observed at $\text{pH} >7$ and the sorption of the PCP^- must be considered in a more inclusive expression

$$K_{oc}(\text{given pH}) = K_{oc(n)}\Phi_n + K_{oc(i)}(1 - \Phi_n)$$

which does fit the observed data over a wider pH range with $\log K_{oc(i)}$ of 2.7.

The fact that the anion sorbs raises the question as to what mechanism could be involved. It has been suggested that the hydrophobic component of the molecule might associate with hydrophobic regions of SOM while the charged area associates with the water. In addition, it has been observed that sorption of the anion but not the neutral species is increased as the ionic strength of solution increases.²⁵ Although increasing ionic strength can reduce the $\text{p}K_a$ the magnitude of this response is not sufficient to account for the effect. It is suggested that the sorption is best explained by the formation of neutral ion pairs (M^+PCP^-) that can distribute into the SOM.

3.5.2.2 Weak Bases In the discussion of dissociation constants of weak acids and bases (see Physical Chemical Properties, Chapter 2) it was shown that the $\text{p}K_a$ of the conjugate acid of a base defined the following equilibrium:



If the $\text{p}K_a$ of the base is in the range of soil pH values (say 5–8) then the soil pH will determine the extent to which the base will exist as a neutral or positively charged species. Sorption of the charged species will involve a cation-exchange process.

The negative sites on the soil surface (primarily clays and OM) are balanced by inorganic cations in a very thin layer (0.3–10 nm) associated with the surface—the “diffuse double layer”. These cations can exchange with ions in the bulk solution.

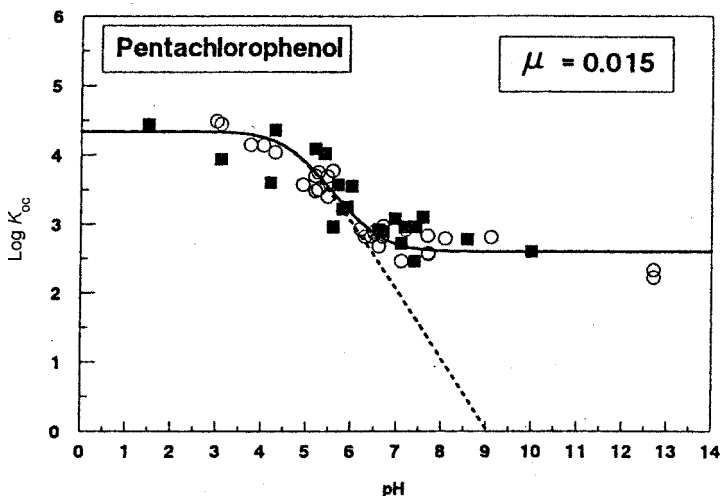


Figure 3.11 Sorption of pentachlorophenol as a function of pH on clays and soil; experimental (○) and literature (■) values. Sorption predicted assuming (1) that only the neutral species (---) or (2) the neutral species plus ion pairs (—) sorb in organic matter. [Reproduced with permission from L. S. Lee, P. S. C. Rao, P. Nikedi-Kizza, and J. J. Delfino, *Environ. Sci. Technol.* **24**, 654 (1990). Copyright © 1990 American Chemical Society.]

Sorption of an organic cation by ion exchange would be represented by



with the exchanged organic cation neutralizing a surface charge and releasing an inorganic cation to the bulk solution. The equilibrium expression for this ion exchange process would be

$$K_{\text{ie}} = \frac{[\text{RNH}_3\text{-Sur}][\text{X}^+]}{[\text{RNH}_3^+][\text{X-Sur}]}$$

To preserve the electroneutrality of the system, the quantity of cations associated with the surface must be constant to balance the negative charge of the surface ($\sigma_{\text{ie}} \cdot A$) defined by surface area, A ($\text{m}^2 \text{kg}^{-1}$) and the charge density σ_{ie} (mol m^{-2}). Consequently,

$$\sigma_{\text{ie}} \cdot A = [\text{RNH}_3\text{-Sur}] + [\text{X-Sur}]$$

and substituting for $[\text{X-Sur}]$

$$K_{\text{ie}} = \frac{[\text{RNH}_3\text{-Sur}][\text{X}^+]}{[\text{RNH}_3^+]\{\sigma_{\text{ie}} \cdot A - [\text{RNH}_3\text{-Sur}]\}}$$

The amount of organic cation sorbed can be expressed

$$[\text{RNH}_3\text{—Sur}] = \{\sigma_{\text{ie}} \cdot A \cdot (K_{\text{ie}}/[\text{X}^+])[\text{RNH}_3^+]\} / \{1 + (K_{\text{ie}}/[\text{X}^+])[\text{RNH}_3^+]\}$$

which corresponds to a Langmuir isotherm (p. 80) with X_m corresponding to the cation exchange capacity ($\sigma_{\text{ie}} \cdot A$) and “ b ” defined by $K_{\text{ie}}/[\text{X}^+]$.

The effect of soil pH on the sorption of organic bases is well illustrated by observations with pyridine, quinoline, and acridine,^{27,28} three heterocyclic nitrogen compounds, using subsurface materials whose properties are listed in Table 3.1. The Freundlich K values and exponents are summarized for two subsoils in Table 3.10.

Note that the pH of the acid subsoil is lower than the $\text{p}K_a$'s of the three bases and that the Freundlich K values for pyridine and quinoline are much higher than observed in the basic subsoil. The “ n ” values are <1 as one would expect from a Langmuir-type relation that would define the cation exchange process primarily responsible for sorption. Both the K and n values are abnormally high for acridine illustrating that in some situations, with molecules containing larger hydrophobic components, the sorption observed can far exceed the cation exchange capacity.²⁴ By contrast, in the alkaline soil the n values are ~ 1 and the Freundlich K values show an inverse relation to aqueous solubility that would be expected from a partitioning of the neutral species into the SOM. Pyridine competes with the sorption of quinoline in the acid, but not the alkaline soil (Fig. 3.12) as one might anticipate based on the two sorption mechanisms. A higher heat of sorption (more exothermic) was observed in the acid soil than the alkaline soil ($\Delta H^0 = -7.10$ vs. -2.89 kcal mol⁻¹) and the entropy change indicated a more ordered system resulting from the cation exchange process ($\Delta S^0 = -2.45$ vs. -0.83 cal mol⁻¹ K⁻¹). These observations emphasize the distinctions between these two sorption mechanisms.

In contrast to the observations with pentachlorophenol (Fig. 3.11) the sorption of quinoline on these soils did not correspond to the cation/neutral ratio (Fig. 3.13). The actual sorption did not show an inflection until one pH unit above the $\text{p}K_a$ of the quinoline. This may reflect the possibility of enhanced protonation of the quinoline at the surface and it has also been suggested that the apparent “surface acidity” of clay minerals may be 2–4 pH units lower than the bulk solution.

TABLE 3.10 Freundlich Constants for Sorption of Quinoline and Acridine

Subsoil	Quinoline S_w , 6,000 ppm; $\text{p}K_a$, 4.92		Acridine S_w , 38.4 ppm; $\text{p}K_a$, 5.68		Pyridine S_w misc; $\text{p}K_a$, 5.23	
	K^a	n	K	n	K	n
Loring (pH 4.18)	5.17	0.567	75,000	1.31	5.56	0.720
Anvil Points (pH 8.15)	0.480	0.868	23.5	1.02	0.231	1.04

^aUnits $\mu\text{mol}^{1-n} \text{g}^{-1} \text{mL}^n$

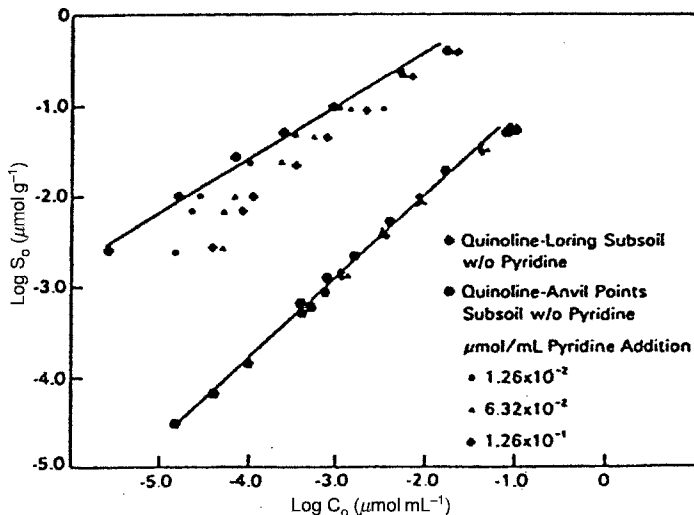


Figure 3.12 Sorption of quinoline at 1:5 solid-to-solution ratio with and without pyridine. [Reproduced with permission from J. M. Zachara, C. C. Ainsworth, C. C. Cowan, and B. L. Thomas, *Environ. Sci. Technol.* **21**, 397 (1987). Copyright © 1987, American Chemical Society.]

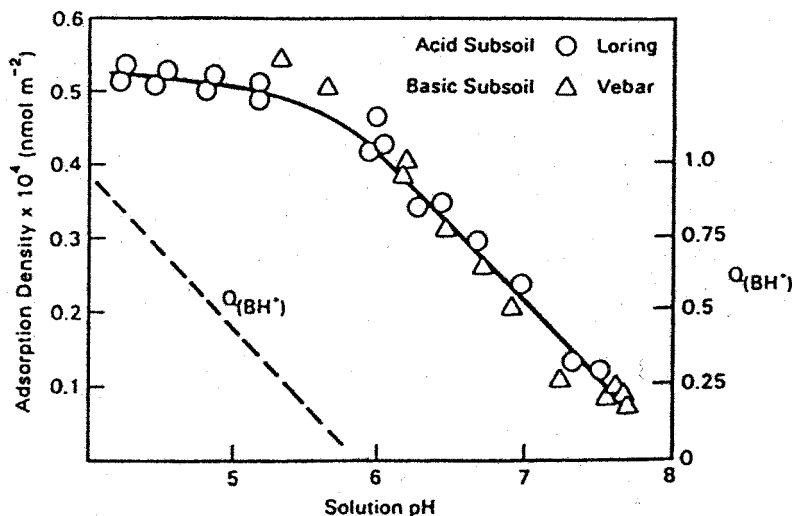
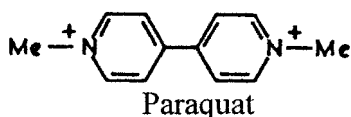


Figure 3.13 Influence of pH on adsorption density of quinoline ($9.8 \times 10^{-6} M$) on acidic and basic subsoils. [Reproduced with permission from J. M. Zachara, C. C. Ainsworth, L. J. Felice, and C. T. Resch, *Environ. Sci. Technol.* **20**, 620 (1986). Copyright © 1986, American Chemical Society.]

This discussion emphasizes the need to understand the nature of the compound to interpret its sorption behavior. Many compounds of environmental significance are nonpolar and one tends to relate sorption to aqueous solubility. The herbicide, Paraquat, by contrast shows a K_{oc} of 1×10^6 despite having a high aqueous solubility ($>600 \text{ g L}^{-1}$). This compound is a bipyridinium salt and the high tendency to sorb would be due to cation exchange not partitioning. A comparable response would be expected with quaternary ammonium detergents.



3.5.3 Molecular Structure

Sorption can be influenced by the physical chemical properties of the compound as well as by functional groups that determine charge on the molecule. It has recently been reported²⁹ that structural characteristics of the molecule may also be a factor in the sorption process. Planar molecules, such as polynuclear aromatic hydrocarbons, and planar PCBs (no ortho substituents) show higher K_{oc} values than nonplanar counterparts, that is, PCBs with ortho substituents. Further refinements in this area can be expected.

3.6 SORPTION ON SOIL IN NONAQUEOUS SYSTEMS

The sorption of parathion and Lindane from a hexane solution has been studied using a Woodburn soil ($f_{om} = 0.019$; 68% silt; 21% clay).²⁰ An oven-dried soil gives a nonlinear isotherm (Fig. 3.14) that shows a much higher sorption capacity than that observed using water as solvent (Fig. 3.9). It is preferable to make this comparison on a relative basis since parathion, at 20°C, has a higher solubility in hexane (57 g L^{-1}) than water (12 mg L^{-1}). Thus $C_e = 4 \text{ ppm}$ ($C_e/S_w = 0.33$) in an aqueous system corresponds to a sorption of $55 \mu\text{g g}^{-1}$ of soil. In a hexane system with $C_e = 100 \text{ ppm}$ ($C_e/S_h = 0.002$) a sorption of $\sim 4000 \mu\text{g g}^{-1}$ of soil is observed. Sorption is decreased by water (compare the air- and oven-dried soils), and essentially no sorption is observed if the soil water content is increased to 5%. Decreased sorption at higher temperature would suggest an exothermic adsorption process. Parathion did not sorb to any extent from hexane onto a peat soil ($f_{om} = 0.51$). The effect of water on the sorption of Lindane on the Woodburn soil from hexane (Fig. 3.15) was more pronounced and it was also demonstrated that parathion could compete with and reduce the sorption of Lindane.

These responses are best explained by adsorption on the mineral surfaces where water can displace the adsorbed compounds. Parathion is a more polar molecule than hexane and is more readily sorbed on these soil constituents. The larger capacity would also be explained by the extensive surface available in the absence of

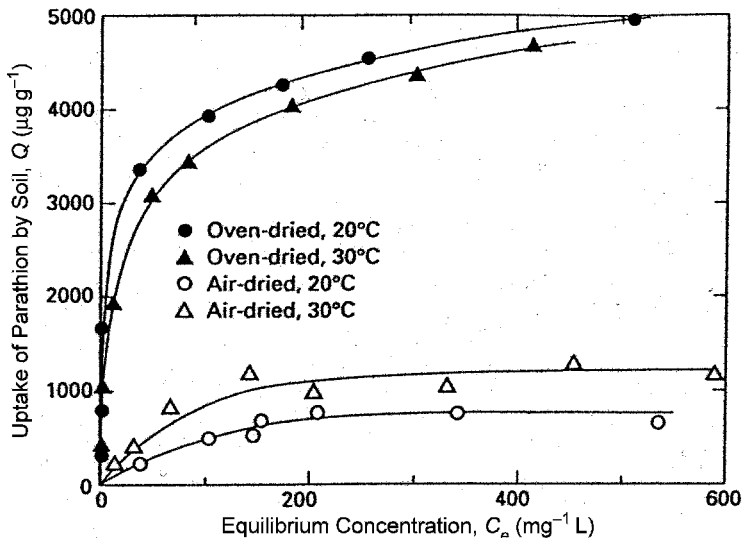


Figure 3.14 Sorption isotherms of parathion from hexane on oven-dried (solid symbols) and air dried (open symbols) Woodburn soil at 20 and 30°C. The air-dried soil contained $\sim 2.5\%$ moisture. [Reproduced from C. T. Chiou, T. D. Shoup, and P. E. Porter, "Mechanistic roles of soil humus and minerals in the sorption of nonionic compounds from aqueous and organic solutions", *Org. Geochem.* 8, 9, Copyright © 1985, with permission from Elsevier.]

water. Parenthetically, it should be noted that these data explain why analysts routinely moisten a dry soil sample with water before extracting with a nonpolar solvent.

Vapor-phase sorption onto the same dry Woodburn soil is illustrated in Figure 3.16 where soil uptake is expressed as a function of the relative pressure–equilibrium partial pressure/saturated vapor pressure.³⁰ The data indicate a BET adsorption process. Increasing relative humidity decreases the adsorption (Fig. 3.17) of dichlorobenzene ultimately resulting in a linear isotherm. It is concluded that at low humidities adsorption on the mineral surfaces is involved. Increasing availability of water reduces the availability of these sites until sorption is due to partitioning into the SOM. It will be demonstrated that the converse of this relation is important in assessing the potential for evaporative loss from soils.

Vapor-phase sorption of carbon tetrachloride and benzene onto a peat soil ($f_{\text{om}} = 0.864$) give linear isotherms indicating partitioning into the organic matter (Fig. 3.18).³¹ The sorption of these two compounds on the same soil from water is only 40–50% less than that observed from the vapor phase. This effect is much less than that observed when the mineral fraction is the primary absorbent.

It is thus apparent that the distribution of organic compounds into soil is a complex process involving the interplay of the soil constituents, properties of the adsorbate and environmental factors relative humidity and temperature. Mechanisms can range from cation exchange to partitioning and a true adsorptive

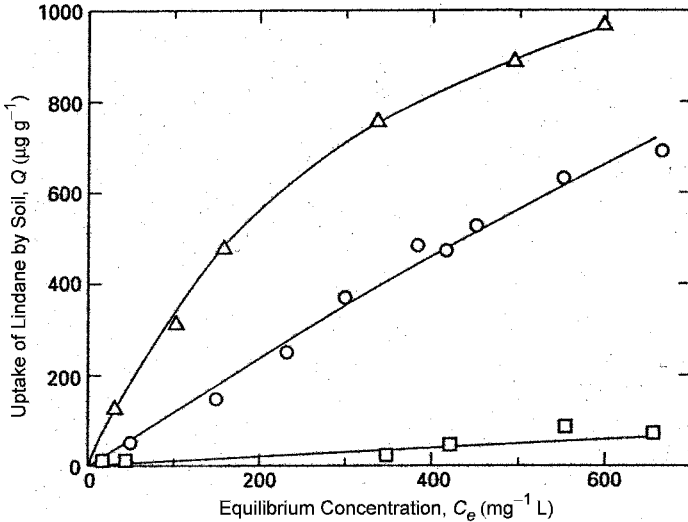


Figure 3.15 Sorption isotherms of lindane from hexane on oven-dried and partially hydrated Woodburn soil at 20°C: (Δ) oven dried soil; (\circ) 5-mg water per g soil; (\square) 25-mg water per g soil. [Reproduced from C. T. Chiou, T. D. Shoup, and P. E. Porter, "Mechanistic roles of soil humus and minerals in the sorption of nonionic compounds from aqueous and organic solutions", *Org. Geochem.* **8**, 9, Copyright © 1985, with permission from Elsevier.]

process with the data approximating a Langmuir isotherm in some cases and a linear relation with partitioning in others. A BET isotherm is observed in vapor-phase systems.

3.7 SORPTION KINETICS

3.7.1 Column Studies

To this point, the distribution of compounds into soil has been defined by a sorption rather than a desorption process studied in batch experiments. It has been customary to run these experiments for ~ 24 h assuming that equilibrium had been attained between the sorption and desorption processes. Sorption is indeed quite rapid in a batch study where small amounts of soil are dispersed in water while shaking continually. Up to 90% of the sorption can occur in the first 5–10 min and 99% of the 24-h equilibrium value is achieved in 2–3 h.³² However, a true equilibrium is not attained since subsequent observations of desorption do not provide sorption–solution concentration values comparable to those observed during sorption.³³

The sorption process can also be studied in column experiments where the movement of the chemical through the soil can be monitored as a function of soil type, column dimensions, and flow rates of water acting as the eluant. Application of the principles of chromatography, in particular the transport equations for the

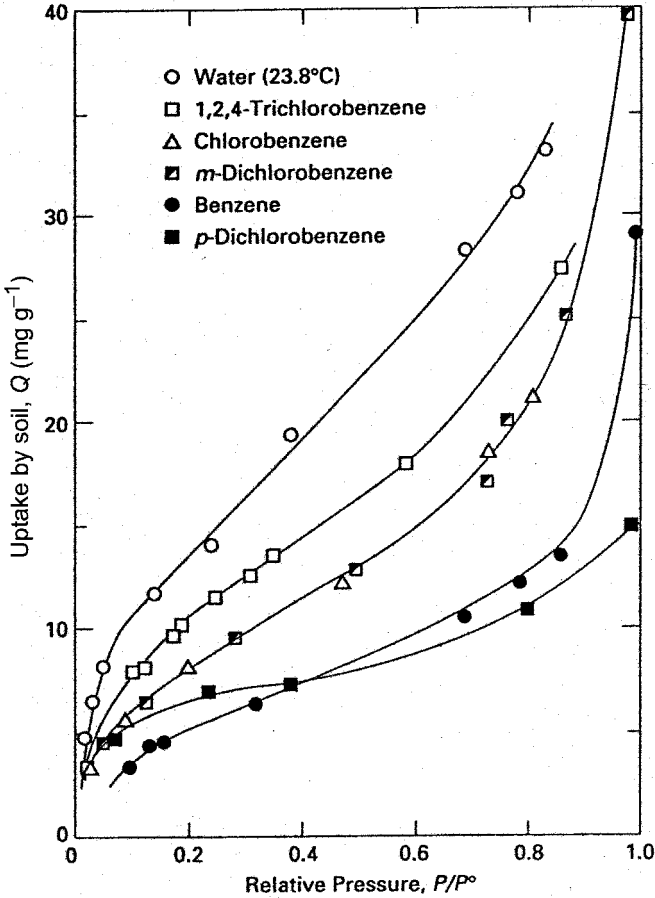


Figure 3.16 Uptake of organic vapors on dry Woodburn soil at 20°C as a function of relative vapor pressure. [Reproduced with permission from C. T. Chiou, and T. D. Shoup, *Environ. Sci. Technol.* **19**, 1196 (1985). Copyright © 1985, American Chemical Society.]

nonlinear distribution of a solute can define sorption as a function of time.³⁴ These data have been used to analyze sorption kinetics using a two-site Freundlich relation³² where the rate of sorption at the two sites can be expressed

$$\begin{aligned}
 dS_1/dt &= k_1(K_1 C^n - S_1) & \text{and} \\
 dS_2/dt &= k_2(K_2 C^n - S_2)
 \end{aligned}$$

where

S is the amount sorbed at the respective site.

C is the concentration in solution.

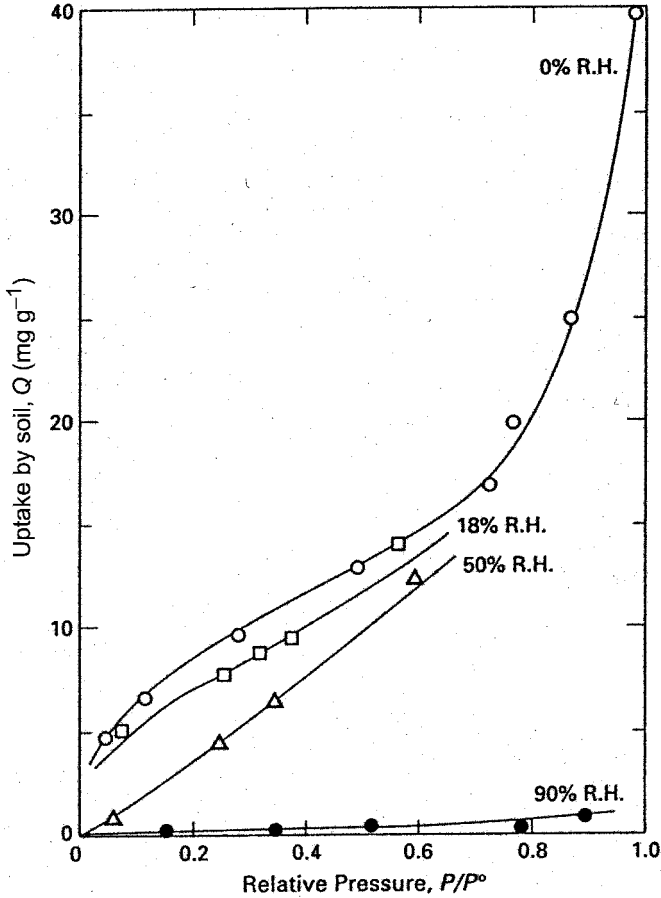


Figure 3.17 Uptake of *m*-dichlorobenzene vapor on Woodburn soil at 20°C as a function of relative humidity. [Reproduced with permission from C. T. Chiou, and T. D. Shoup, *Environ. Sci. Technol.* **19**, 1196 (1985). Copyright © 1985, American Chemical Society.]

f is the fraction of type-1 sites.

K and n are the Freundlich parameters derived in batch experiments.

k is the respective rate constant.

$$K_1 = Kf$$

$$K_2 = K(1 - f)$$

Numerical solutions of these relations have been obtained using the data from column studies and the estimates of “ f ” and k_2 have been derived, making the assumption that sorption at site-1 is very rapid with $k_1 = 1000 \text{ day}^{-1}$. Results with a common triazine herbicide, Simazine, in different soils are summarized in

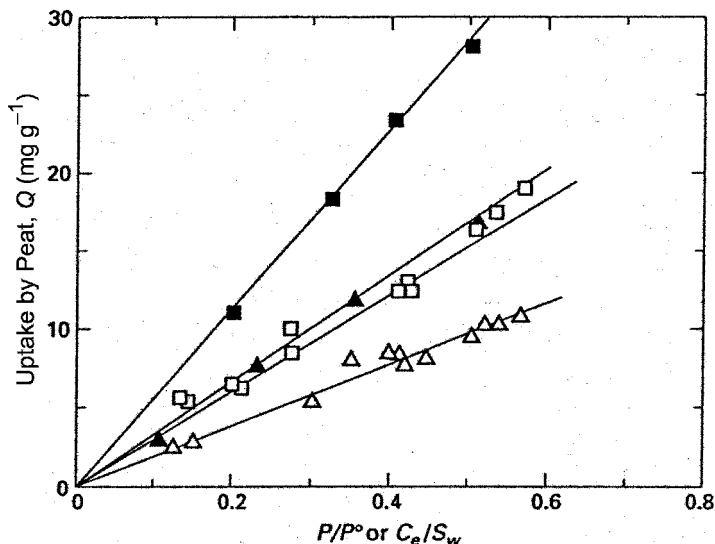


Figure 3.18 Comparison of uptake capacities of carbon tetrachloride (squares) and benzene (triangles) from the vapor phase (solid symbols) and aqueous solution (open symbols). [Reproduced with permission from D. W. Rutherford, and C. T. Chiou, *Environ Sci. Technol.* **26**, 965 (1992). Copyright © 1992, American Chemical Society.]

Table 3.11. The simulation assumes that both sorption sites have the same characteristic (equivalent Freundlich values) however they are not equally accessible. The analysis illustrates differences among soils, particularly with respect to the availability of the type-1 sites that can sorb rapidly. The sorption rate at the type-2 site is orders of magnitude slower than the type-1 site and it is proposed that this reflects the time needed to diffuse to that site. It also demonstrates that it is not appropriate to use batch studies to reflect sorption rates under field conditions.

3.7.2 “Aged Residues”

Another observation involving longer term kinetics is illustrated by the sorption behavior of a relatively soluble insecticide, Imidacloprid (S_w $0.61 \text{ g} \cdot \text{L}^{-1}$ at 20°C).³⁵ The compound was allowed to incubate with soil for up to 100 days and at intervals, a desorption experiment was run to derive a K_d value. From Figure 3.19 it is seen that the K_{oc} value increases over threefold during this incubation period. So what is being termed “aged residue” is less readily desorbed the longer the compound is in contact with the soil. Other examples of this response have been tabulated³⁶ and mechanisms based on limiting diffusion and heterogeneous sorption proposed. Chemisorption is not involved, since the compound can be recovered by appropriate extraction procedures.

This phenomenon has been studied using a series of sorption and desorption steps.³⁷ For example, in Figure 3.20a, a sequence of four sorption steps were carried

TABLE 3.11 Sorption Kinetics for Simazine from Column Studies

Soil	Soil Properties		Freundlich Values		Sorption Kinetics	
	% OM	% Clay	K^a	n	K_2, d^{-1}	% type-1 sites
Sand	1.2	1.3	1.23	0.90	0.15	1.3
Sandy loam	1.7	15.3	0.93	0.97	4.60	11.0
Loamy sand	0.6	13.6	0.53	1.00	0.15	3.8
Clay	4.6	63.7	13.9	0.70	0.15	0.40

^a $\mu\text{mol}^{1-n} \text{g}^{-1} \text{mL}^n$

out where the soil was allowed to equilibrate with an aqueous solution of phenanthrene for 1–4 days before replacing the supernatant with fresh solution. A linear relation was observed between the amount sorbed and the equilibrium concentration in solution. A sequence of 49 desorption steps followed with equilibration times ranging up to 59 days. The solution-phase concentration tended to a constant value of $0.001 \mu\text{g mL}^{-1}$ (Fig. 3.20*b*) while the amount retained in the soil stabilized at $7.9 \mu\text{g g}^{-1}$ soil. This quantity corresponded to the maximum capacity, $q_{\text{max}}(\text{irr})$, in the “irreversible” compartment of this soil for phenanthrene. From the linear sorption relation of Figure 3.20, $\log K_{\text{oc}}$ of 4.06 can be calculated (given %OC = 0.27) defining the distribution between soil organic carbon and water. A comparable value of $\log K_{\text{oc}}(\text{irr})$ defining the distribution between water and the irreversible compartment

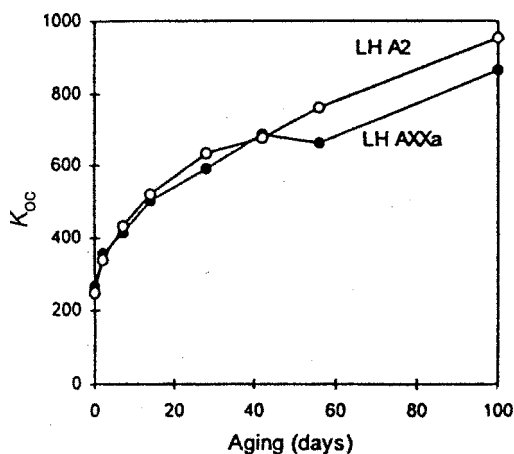


Figure 3.19 Increase with incubation time, in the K_{oc} of imidacloprid in a sandy loam (LH AXXa) and a silt loam (LH A2) as defined by desorption batch experiments. [Reproduced with permission from M. Oi, *J. Agr. Food Chem.* **47**, 327 (1999). Copyright © 1999, American Chemical Society.]

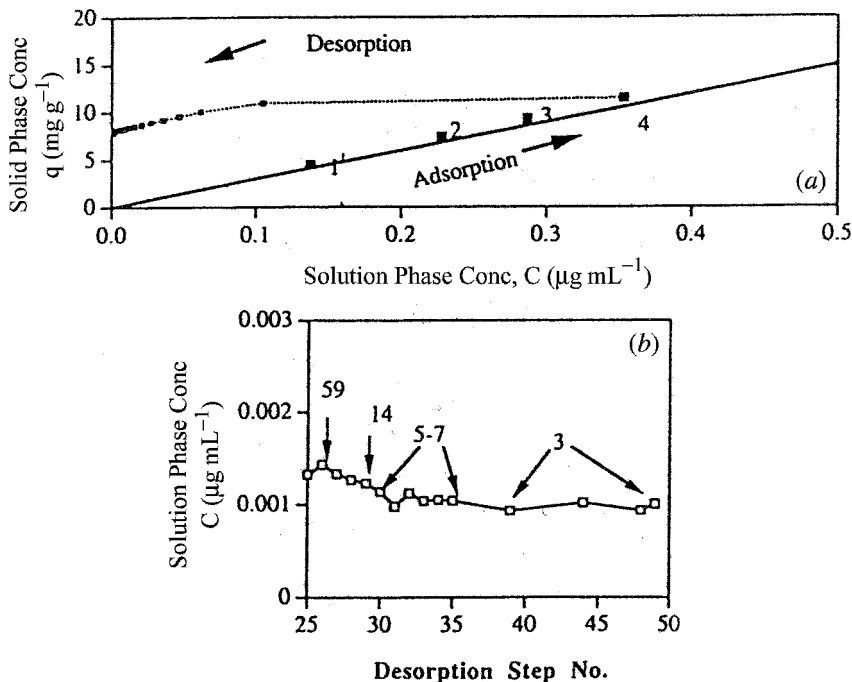


Figure 3.20 Sorption and desorption of phenanthrene from sediment. (a) Concentration in sediment as a function of equilibrium concentration in solution after 4 sorption steps followed by 49 repetitive desorption steps. (b) Concentration in solution after desorption. Numbers denote equilibrium time (days) for desorption steps. [Reproduced with permission from A. T. Kan, G. Fu, M. Hunter, W. Chen, C. H. Ward, and M. B. Thomson, *Environ. Sci. Technol.* **32**, 892 (1998). Copyright © 1998, American Chemical Society.]

is 6.40. A summary of observations on a series of compounds using a Lula sediment³⁴ that contained 0.027% OC is given in Table 3.12.

The variation in the distribution between the irreversible compartment and aqueous solution observed with these compounds is not very large, however, the capacity of this compartment varies with the chemical. The K_{oc} values observed for the reversible process are consistent with what might be predicted.

It has been concluded from these sorption–desorption studies that the “irreversible” compartment can be filled stepwise in a series of sorption–desorption steps. Once the maximum capacity of the “irreversible” compartment is attained subsequent sorption steps are completely reversible. It has been suggested that the irreversibility results from some conformational change or physical rearrangement of the organic matter during sorption that changes the environment of the sorbed compound and restricts its desorption. However, the nature of these changes are not known. A sorption isotherm has been proposed to account for both the reversible and

TABLE 3.12 Distribution into the Soil “Irreversible” Compartment

Compound	$\log K_{ow}$	$\log K_{oc}$ mL g ⁻¹ (exptl.)	C_e $\mu\text{g mL}^{-1}$ with $q_{max}(\text{irr})$	$q_{max}(\text{irr})$ ($\mu\text{g g}^{-1}$)	$\log K_{oc}(\text{irr})$
Toluene	2.69	2.17	0.138	125	5.31
Naphthalene	3.36	2.91	0.0035	11.0	6.05
1,2-Dichlorobenzene	3.38	3.13	0.0204	44	5.50
Phenanthrene	4.57	4.08	0.0011	7.9	6.38
4,4'-Dichlorobiphenyl	5.33	4.71	0.0095	5.9	5.38
2,2',5,5'-Tetrachlorobiphenyl	6.18	4.34	0.00064	0.36	5.50

“irreversible” components

$$x/m(\text{total}) = x/m(\text{reversible}) + x/m(\text{irr})$$

$$x/m(\text{total}) = (K_{oc} \cdot f_{oc} \cdot C_e) + ([K_{oc}(\text{irr}) \cdot f_{oc} \cdot q_{max} \cdot f_{irr}]/[q_{max} \cdot f_{irr} + \{K_{oc}(\text{irr}) \cdot f_{oc} \cdot C_e\}])$$

The first term defines the simple linear partitioning process while the second term is a Langmuir expression defining distribution into the “irreversible” compartment as a function of compartment capacity, the fraction of this compartment (f_{irr}) filled at the time of exposure and the distribution factor $K_{oc}(\text{irr})$, which appears to be relatively constant. The capacity of the “irreversible” compartment, expressed per unit of SOC, shows an inverse relation to K_{ow} , however, the utility of this relation will depend on further evaluation of how widely it can be applied.

Another approach to this issue has been to investigate the status of residues in soil and sediments that have been contaminated for many years with PCBs.³⁸ The question would be whether residues move slowly into and saturate an irreversible compartment or whether there is some equilibrium distribution among the different binding “sites”. Carbon dioxide has proved to be an efficient extraction medium that appears to have little effect on the integrity of the sorbent. Since the triple point of this compound is -56.6°C and 5.11 atm it will exist as a liquid only at high pressures. This technology, “supercritical fluid extraction” (SFE) is being used extensively in analytical laboratories and with these samples, the rate of extraction of PCB congeners was monitored as a function of the extraction conditions. Each sample was extracted in sequence for 1 h at

120 bar and 40°C	Fast
400 bar and 40°C	Moderate
400 bar and 100°C	Slow
400 bar and 150°C	Very slow

Increasing temperature increases solubility and also can overcome the energy barrier to desorption.

The rate of extraction of PCB congeners (note numbers indicate specific congeners according to the IUPAC convention) for two of the sediments are reproduced in

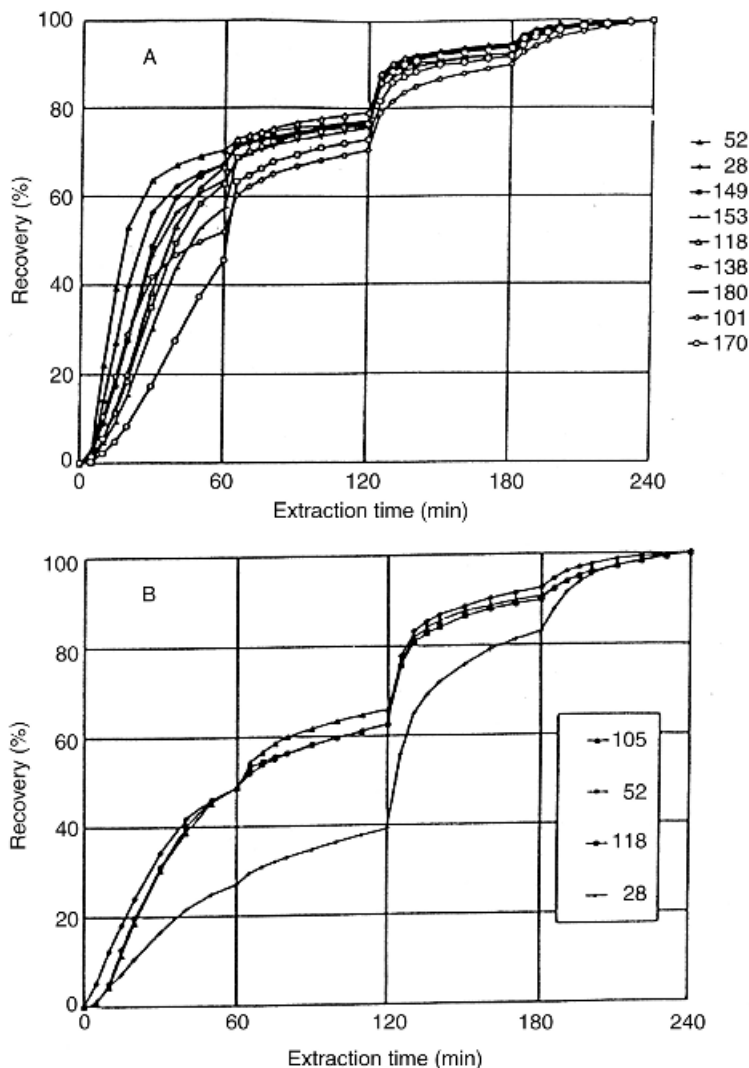


Figure 3.21 Selective desorption behavior of PCB congeners from historically contaminated sediment. (a) Harbor sediment; 15% SOM and PCB concentration of 13–50 $\text{ng} \cdot \text{g}^{-1}$. (b) Freshwater lake sediment: 3.3% SOM, 2–50 $\text{ng} \cdot \text{g}^{-1}$ PCB. [Reproduced with permission from E. Björklund, S. Bøwadt, L. Mathiasson, and S. B. Hawthorne, *Environ. Sci. Technol.* **33**, 2193 (1999). Copyright © 1999, American Chemical Society.]

Figure 3.21 and the overall recoveries in the four fractions are summarized in Table 3.13 along with some properties of the sediment samples.

The rate at which PCB congeners are extracted from sediments is influenced by extraction conditions that would indicate the presence of different binding environments that determine either the strength with which a compound is bound and/or the rate at which it moves out of that environment. It is also apparent that there are large differences in extraction patterns among the sediment samples. There are no simple relations between extraction efficiency and organic matter content or PCB concentration, although the number of samples analyzed is too small to draw any clear conclusions. One might predict that the less chlorinated congeners might extract more readily since they would be more soluble in the solvent and would diffuse more rapidly should this process be limiting. The extraction pattern for the harbor sediment would be consistent with this hypothesis. Note that 46–70% of the nine congeners is extracted in the first 60 min under mild conditions (Fig. 3.21a). Higher proportions of congeners 52 and 28, trichloro-PCBs are extracted than 170, a heptachloro-PCB. By contrast, only 40% of the congener 28 is extracted from the lake sediment under comparable conditions. It was concluded that strength of association of the congeners with sediment is more dependent on the matrix than the congener, which is comparable to the conclusion drawn from laboratory sorption–desorption studies. The fact that the PCBs are distributed among different sorption environments in these “historical” samples indicates that distribution among these sites is based on partitioning among the sites rather than saturation of the “slowest” sites. In other words, it does not appear that, with time, all the residues distribute into and saturate the “slowest” sites.

More studies will be needed to clarify the nature of this process, however, it is quite clear that “aged” residues behave quite differently than their recently applied counterparts. The rate at which residues are desorbed from these environments will control the biological activity of an herbicide and the rate of microbial degradation in soil. It will also influence availability for both leaching and evaporation and will be an important consideration in remediation procedures. For example, in “pump and purge” procedures for treating contaminated groundwater, pumping periodically

TABLE 3.13 Recovery of PCB Congeners from Aged Sediments

Sediment	%OM	PCB Conc ^a (ng g ⁻¹)	Percent recovered in fraction ^b			
			Fast	Moderate	Slow	Very Slow
River	12	100–4000	43–48	10–14	24–30	13–17
Marine	9.2	25–80	72–89	3–10	4–16	3–7
Harbor	15	13–50	46–70	7–26	15–19	5–10
Industrial soil	12.5	3–137 × 10 ³	68–81	5–18	8–11	5–7
Lake	3.3	2–50	27–49	12–17	25–44	7–17

^aConcentration range of individual PCB congeners.

^bRange of recovery for the individual congeners.

is preferable to continuous pumping since the chemical has time to be released from the substrate. This phenomenon can also account for the detection of a soil fumigant, 1,2-dibromoethane in soil some 19 years after application despite the fact that this material is highly volatile and degrades rapidly in soil,³⁹ and the detection of the parent *p,p'*-DDT in soils many years after its use was discontinued when one would only expect to detect the persistent metabolite, DDE.

3.8 FOLIAR SORPTION

It has been estimated⁴⁰ that the global vegetation surface is of the order of 7×10^8 km² and that the distribution of compounds from the atmosphere onto the leaf surface can be significant in reducing levels of atmospheric contaminants as well as providing a pathway for human exposure through the ingestion of plants or herbivorous animals. Vegetation may also provide an index of atmospheric contaminants. In understanding the environmental behavior of chemicals it is thus important to define those factors that will control this process, which involves the interaction of a chemical with the plant cuticle.

The aerial surfaces of plants are covered by a thin film, the cuticle, which acts as a barrier against the uncontrolled loss of water and soluble solutes from leaves. The cuticle also can influence the extent of the damage caused by insects and fungal pathogens. Extraction with solvents yields two primary fractions: the soluble waxes and an amorphous polymer fraction. Cutin has been considered the primary component of the latter fraction although more recently an additional component, cutan, has been described. Cutin is a high molecular weight, crossed-linked polymer, based on interesterified C₁₆ to C₁₈ aliphatic acids and is susceptible to alkaline hydrolysis. Cutan, on the other hand, is resistant to alkaline hydrolysis and it is proposed to be a polymethylene polymer. The proportions of these two constituents varies among species. The waxes, 1–10% of the mass of the cuticle, represent the main transport barrier, and are deposited as solid aggregates in the outer regions of the cutin polymer and, in some cases, on the outer surface of the cuticle. The composition of the wax fraction is very complex and a sample may contain >100 components that can include waxes (esters of long-chain alcohols and acids) long-chain alcohols and acids, alkanes, aldehydes, and so on.⁴¹ The lipophylic character of the cuticle will thus affect the sorption process with the hydrophobic compounds being favored.

The distribution of chemicals onto the foliar surface can occur by vapor-phase transfer, particle deposition (wet or dry), or from aqueous solution, which would be negligible for most organic compounds. It has been established that dry gaseous uptake is the predominant pathway for the foliar uptake of relatively nonvolatile compounds such as the chlorinated dibenzo-dioxins and -furans.⁴² The distribution of compounds between air and the cuticular polymer matrix follows Henry's law (Fig. 3.22).⁴³ This conclusion was drawn from observation of how a series of 50 low molecular weight (<175) compounds distributed between the vapor phase

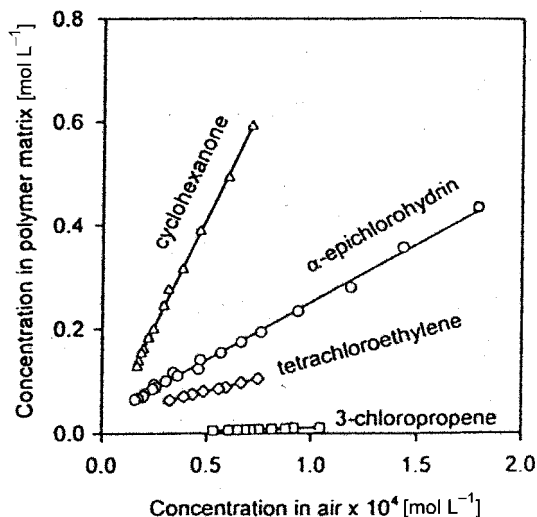


Figure 3.22 Representative isotherms for the sorption of volatile organic compounds in plant cuticular matrix at 25°C. Plant matrix–air partition coefficients derived from slopes of the isotherms. [Reproduced with permission from B. Welke, K. Ettlinger, and M. Riederer, *Environ. Sci. Technol.* **32**, 1099 (1998). Copyright © 1998, American Chemical Society.]

and a polymer matrix (assumed to be primarily cutin-like material) that was prepared from the cuticular membrane of tomatoes by extracting the wax fraction with chloroform. A matrix/air distribution ratio, $K_{MX/a}$ was defined as the ratio of the concentrations in the two phases.

$$K_{MX/a} = C_{MX}/C_a$$

Experimental values of $K_{MX/a}$ ranged from 33,000 for 1-hexanol to 39 for isoprene indicating the tendency for compounds to distribute onto plants from air. A significant correlation was observed between $K_{MX/a}$ and the octanol/air distribution ratio K_{oa}

$$\log K_{MX/a} = 0.820(\pm 0.375) + 0.668(\pm 0.106)K_{oa}$$

which can be derived from K_{ow} and H' .

$$K_{oa} = K_{ow}/H'$$

Studies with different plants and a range of compounds have provided estimates of plant–air distribution constants, K_{pa} , which are usually cited as dimensionless values based on volume (mass per unit volume) or mass (mass per unit mass) in

contrast to the practice with soils for K_d . Illustrative values on a volume basis for K_{pa} in azalea leaves⁴⁴ are summarized in Table 3.14. It is apparent that leaves are able to accumulate significant concentrations of compounds from air. Despite several outliers, the octanol/air distribution coefficient is a reasonable predictor of K_{pa} (Fig. 3.23). The reference line, $K_{pa} = 0.05K_{oa}$, assumes that K_{oa} is a good surrogate for K_{pa} and the 0.05 modifier indicates that 5% of the leaf acts as a reservoir for the chemical. Parenthetically, it is of interest to note that this relation represents the relation between bioconcentration in fish from aqueous solution (Chapter 5).

The variation in the K_{pa}/K_{oa} relation among plants is illustrated in Figure 3.24. Values for K_{pa} were observed for PCB congeners in five grass and herb species common to agricultural grassland in Central Europe.⁴⁵ These species were selected to reflect diversity in leaf shape and surface morphology. Plants were "loaded" with PCBs by exposing in a chamber containing high concentrations of PCBs in the vapor phase. The atmospheric concentration of PCB congener in equilibrium with that in the plant was determined by passing air over the contaminated plant material, trapping and analysis. Up to 15 PCB congeners were monitored and highly significant correlations were obtained between $\log K_{pa}$ and $\log K_{oa}$ (Table 3.15) although these relations differed among the five species. Note that experimental values rather than H'/K_{ow} , were used for K_{oa} . If the regression coefficient, B , is one, there would be a linear relation between K_{pa} and K_{oa} . Since this observation was not made, we conclude that octanol is not a good surrogate for the leaf compartment into which the chemical distributes. The reasons for the different responses is not apparent, however, it was concluded that the composition of the leaf storage compartment was probably more important than its size. Further research will be needed to explain these differences.

Experimental values for K_{oa} have been determined for some chlorobenzenes and PCBs⁴⁶ and it was observed that values derived from K_{ow} and H' tend to be

TABLE 3.14 Plant–Air Distribution Constants Observed in Azalea Leaves

Compound	H'	$\log K_{ow}$	K_{oa}	K_{pa} (vol)
Trifluralin	0.00165	3	6.06×10^5	1.04×10^5
Hexachlorobenzene	0.0540	6	1.85×10^7	4.18×10^5
Mirex	0.0215	6.9	3.70×10^8	1.18×10^7
Thionazin	3.5×10^{-5}	1.2	4.44×10^5	2.71×10^4
Sulfotep	1.19×10^{-4}	3	8.40×10^6	2.24×10^4
DDT	0.00247	6	4.05×10^8	4.32×10^7
DDE	0.00326	5.7	1.5×10^8	3.03×10^7
α -Hexachlorocyclohexane	3.57×10^{-4}	3.8	1.77×10^7	1.03×10^6
γ -Hexachlorocyclohexane	5.34×10^{-5}	3.8	1.18×10^8	7.63×10^5
Alachlor	2.55×10^{-6}	2.8	2.48×10^8	2.82×10^5
Dieldrin	4.60×10^{-4}	3.7	1.09×10^7	1.08×10^6
3,3',4,4'-Tetrachlorobiphenyl	3.92×10^{-3}	6.1	1.19×10^9	8.44×10^7
1,2,3,4-Tetrachlorobenzodioxin	1.55×10^{-3}	6.6	2.57×10^9	9.11×10^7

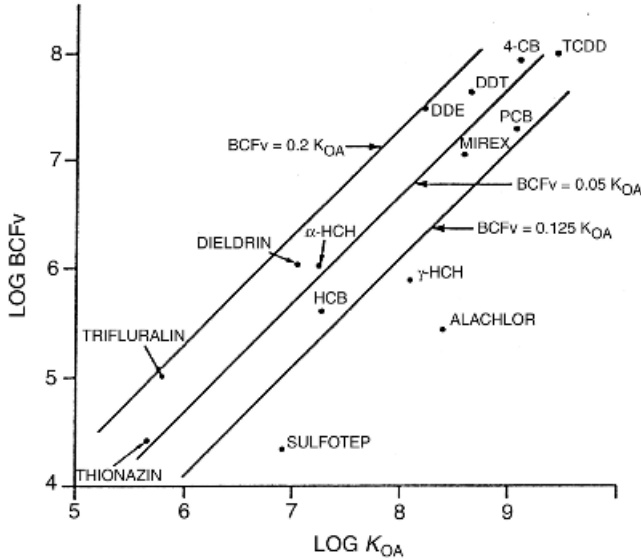


Figure 3.23 Relation between a volumetric bioconcentration factor, BCF_v , (K_{pa}) and K_{oa} for observations with azalea leaves. [Reproduced with permission from S. Paterson, D. Mackay, E. Bacci, and D. Calamari, *Environ. Sci. Technol.* **25**, 866 (1991). Copyright © 1991, American Chemical Society.]

underestimated with more hydrophobic compounds. This probably reflects the fact that K_{ow} defines the distribution between water saturated octanol and octanol saturated water while H' defines the distribution between pure water and air. A linear relation was observed between $\log K_{oa}$ and $1/T$ (Arrhenius relation) with K_{oa}

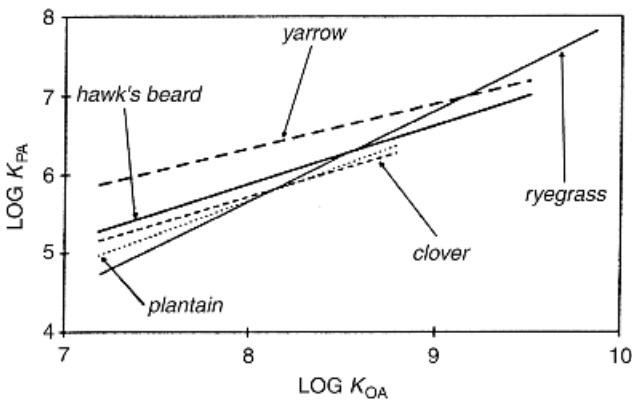


Figure 3.24 $\log K_{pa}$ (25°C) as a function of $\log K_{oa}$ (25°C) for a range of PCB congeners for five plant species. [Reproduced with permission from P. Komp and M. S. McLachlan, *Environ. Sci. Technol.* **31**, 2944 (1997). Copyright © 1997, American Chemical Society.]

TABLE 3.15 Regression Equations for $\log K_{pa}$ versus $\log K_{oa}$ for Five Plants

Plant	A^a	B^a	r^2
Ryegrass	-3.56	1.15	0.98
Clover	0.15	0.70	0.86
Plantain	-1.30	0.87	0.98
Hawk's beard	-0.07	0.74	0.97
Yarrow	1.80	0.57	0.93

^aFor the equation: $\log K_{pa} = A + B \log K_{oa}$

decreasing with increasing temperature. For example, with hexachlorobenzene, a 30°C drop in temperature resulted in a 30-fold increase in K_{oa} . One would thus expect temperature to have a significant effect on the distribution from air onto foliage.

Kinetic studies have demonstrated that uptake of compounds into leaves is best represented by a two-compartment process; a rapid distribution into the outer leaf surface, followed by a slower diffusion into the interior of the leaf. This is illustrated by studies of the uptake of DDE in spruce needles.⁴⁷ A 10-year old spruce tree was placed in a chamber and exposed to air containing 50 ng · m⁻³ of DDE. It can be seen from Figure 3.25 that DDE concentration increased more rapidly in a soluble cuticular lipid fraction than in the needle remaining after extraction. The former was obtained by extraction with dichloromethane and was considered to be representative of the lipophylic needle surface. Note that introducing the tree into the exposure chamber reduced the concentration of the DDE in the air. When the tree was transferred to a "clearance chamber", DDE was lost rapidly from the extracted lipid fraction and only slowly from the remaining needle. A two-compartment model has been developed to simulate DDE uptake and release. Based on this response, if needles were to be used for monitoring, it is important to recognize that one portion of the needle reacts within hours to atmospheric concentrations, whereas the needle as a whole could take months to achieve some steady state.

The uptake of compounds from the atmosphere by plants involves primarily direct partitioning of the compound into the leaf matrix or the deposition of contaminated particles on the leaf surface. In the former, one must consider both an equilibrium process and a kinetically limited transition where the concentration gradient limits diffusion into the leaf that has a high capacity to accept the compound. These three processes have been considered in a recent analysis⁴⁸ of the distribution of compounds from the atmosphere into plants. The rate of change in the amount of chemical in a plant resulting from gaseous uptake is expressed

$$d(VC_{Vg})dt = Av_G(C_G - C_{Vg}/K_{pa})$$

where V is the volume of the plant, C_G , the atmospheric gaseous concentration, and C_{Vg} is the concentration in the plant due to gaseous deposition. The parameter A is the vegetation surface area and v_G is the mass transfer coefficient in air. This

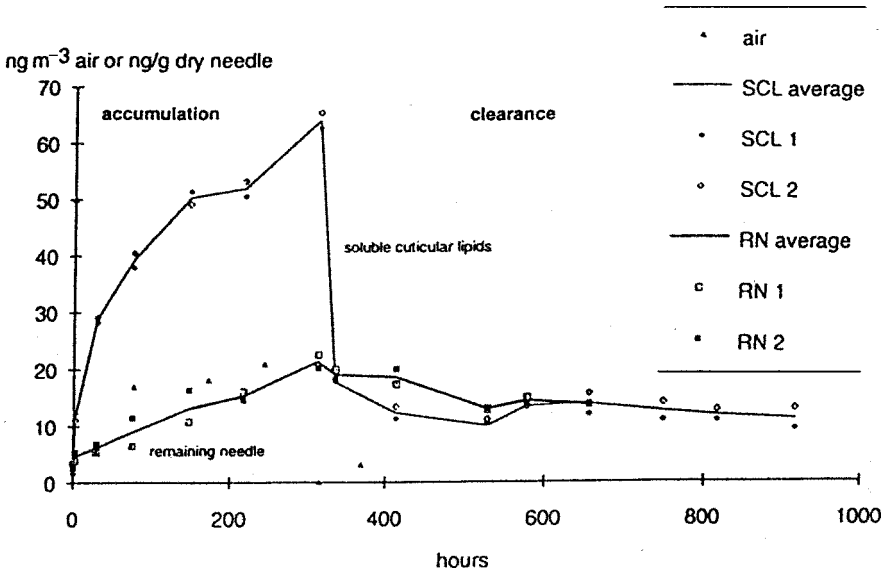


Figure 3.25 Concentrations of *p,p'*-DDE (parallel samples 1 and 2) in air, soluble cuticular lipids (SCL), and remaining needle (RN) of spruce, *P. omorika* during exposure to DDE vapor and subsequent clearance. [Reproduced with permission from H. Hauk, G. Umlauf, and M. S. McLachlan, *Environ. Sci. Technol.* **28**, 2372 (1994). Copyright © 1994, American Chemical Society.]

parameter is defined in more detail in the discussion of the two-layer model of the evaporation of a compound from water (see evaporation, Chapter 4). To be exact, one should consider both transport from the vapor phase to the leaf surface as well as movement from the surface into the leaf, however, the former is usually considered limiting in overall uptake. The concentration gradient is defined by $(C_G - C_{Vg}/K_{pa})$ with C_{Vg}/K_{pa} defining the concentration at the surface of the leaf. Given that K_{pa} can be expressed as a function of K_{oa} ($K_{pa} = mK_{oa}^n$). The parameter C_{Vg} can be expressed

$$C_{Vg} = mK_{oa}^n \cdot C_G(1 - \exp[-Av_Gt/(VmK_{oa}^n)])$$

A comparable approach can define change in concentration resulting from particle deposition as a balance between uptake and loss:

$$d(VC_{Vp})/dt = Av_p C_p - k_E C_{Vp}$$

where C_{Vp} is the concentration due to particle deposition, v_p is the particle deposition velocity, C_p is the concentration of compound in the particles, and k_E is a first-order rate constant defining loss of particles from the plant surface.

The concentration in the vegetation due to particle deposition can then be expressed as

$$C_{Vp} = (v_p A C_p) / (V k_E) [1 - e^{-k_E t}]$$

C_p can be expressed as a function of the gas-phase concentration, C_G , and the concentration of suspended particles, TSP:

$$C_p = B \cdot \text{TSP} \cdot K_{oa}$$

with B being a proportionality constant. Thus uptake by direct gaseous partitioning and particle deposition can be expressed as a function of the gaseous concentration, K_{oa} , and a complex algebraic expression for overall uptake can be derived by combining these two functions.

Three mechanisms of uptake from the atmosphere can be defined as a function of K_{oa} (Fig. 3.26). For low values of K_{oa} the distribution between the two compartments is defined by the equilibrium

$$C_V / C_G = m K_{oa}^n$$

giving a linear logarithmic relation with slope “ n ”, which would be expected to vary with the plant species (Table 3.15). With a low K_{oa} , vegetation would have a lower capacity for the compound and the concentration gradient between the bulk vapor phase and the leaf surface ($C_G - C_{Vg}/K_{pa}$) would be small. Consequently, kinetics would not limit uptake. With medium values of K_{oa} ($\log K_{oa} = 9 - 11$) gaseous uptake is limited by diffusion to the leaf surface since the concentration gradient would become greater and

$$C_V / C_G = A \cdot v_{Gt} / V$$

Vegetation would have a higher capacity for the compound but an equilibrium condition may not be established. In this case distribution between the vapor phase and plant is independent of K_{oa} .

With high values of K_{oa} , particle deposition would predominate reflecting the preferred atmospheric distribution of the chemical and

$$C_V / C_G = v_p \cdot A \cdot B \cdot (\text{TSP}) \cdot K_{oa} / V k_E$$

giving a logarithmic relation with slope of 1.

The validity of this analysis is illustrated by $(\log C_V / C_G) / (\log K_{oa})$ relations observed in two plant species (Fig. 3.27). These data were generated in a field study⁴⁹ where the air-vegetation distribution was determined for 40 compounds in ambient air (10 chlorobidenzodioxins and furans, 12 polynuclearhydrocarbons, 16 PCBs, penta- and hexachlorobenzenes). Air samples were taken over a

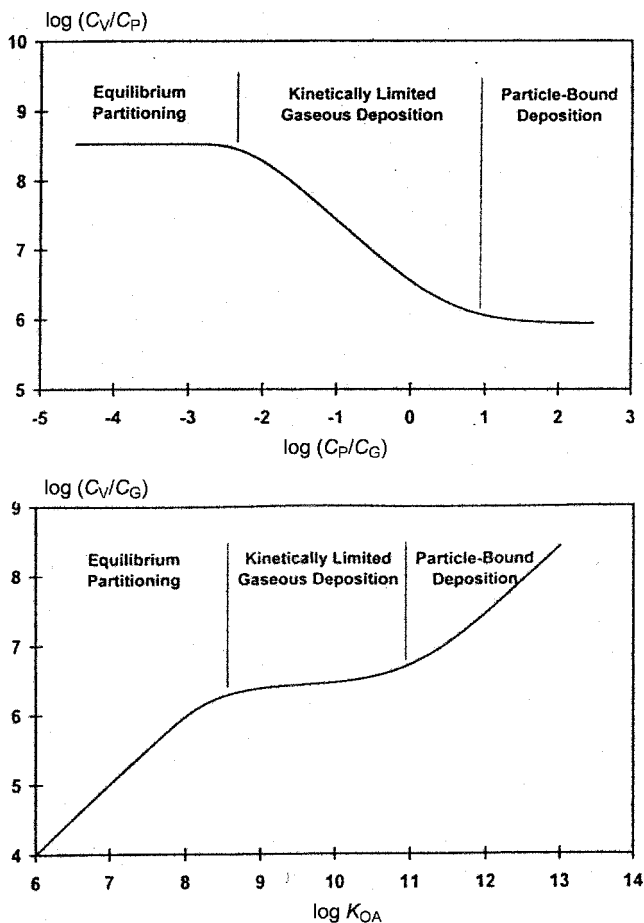


Figure 3.26 Schematic representation of the ratio of the total amount of compound in vegetation, C_V and concentration in the vapor phase, C_G as a function of K_{oa} and the C_V/C_G ratio as a function of C_P/C_G , which illustrate the processes involved in chemical uptake by plant vegetation. [Reproduced with permission from M. S. McLachlan, *Environ. Sci. Technol.* **33**, 1799 (1999). Copyright © 1999, American Chemical Society.]

5-month period prior to sampling 10 different plant species. Compounds with high K_{oa} are excluded from this analysis because C_V/C_G cannot be determined due to the very low values of C_G . This situation can be remedied by considering the relation between C_V/C_P as a function of C_P/C_G (Fig. 3.26). In this case, compounds with low K_{oa} are excluded since C_P would be very low. For the low K_{oa} , equilibrium situation, multiplying by C_G/C_P gives

$$C_V/C_P = mK_{oa}^n C_G/C_P$$

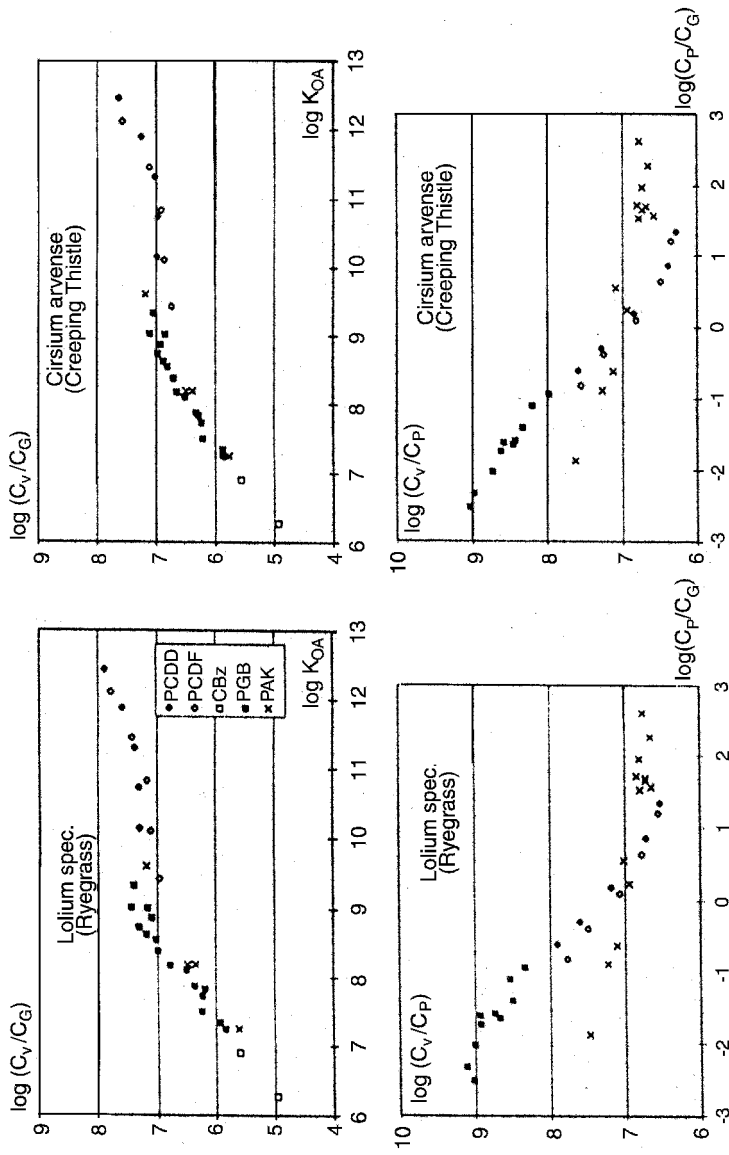


Figure 3.27 Field observations on the uptake of organic compounds in the ambient air by ryegrass and creeping thistle that illustrate the variation in uptake mechanism. [Reproduced with permission from F. Böhme, K. Welsch-Pausch, and M. McLachlan, *Env. Sci. Technol.* **33**, 1805 (1999). Copyright © 1999, American Chemical Society.]

The logarithmic relation should be relatively flat since C_G/C_p is also a function of K_{oa} . The same approach can be used with the kinetically limited phase giving

$$C_V/C_p = (A v_G t / V) \cdot (C_G / C_p)$$

which would give the logarithmic expression

$$\log(C_V/C_p) = \log(A v_G t / V) - \log(C_p/C_G)$$

which would show a slope of -1 .

For particle deposition, substituting for C_G , $C_p/(B \cdot TSP \cdot K_{oa})$ gives

$$C_V/C_p = v_p A / V k_E$$

which would be independent of C_p/C_G . It can be seen that this treatment does include many of those compounds that would have high K_{oa} values (Fig. 3.27).

Equilibrium partitioning was observed with trichlorobiphenyls and the chlorobenzenes, while the tetra- and pentachloro dioxins and furans, and heptachlorobiphenyls distributed into the vegetation by kinetically limited gaseous uptake. Octochloro dioxins and furans along with the higher molecular weight PAHs distributed onto plants by particle deposition. This would be consistent with the known propensity of the latter to distribute onto particles. These data also provide an opportunity to evaluate differences among plant species and the ratio of surface to volume accounted for much of the variation observed.

REFERENCES

1. G. T. Felback, Jr., "Structural Chemistry of Soil Humic Substances", in A. G. Norman, Ed., *Advances in Agronomy*, Vol. 17, Academic, New York, 1965, pp. 328–368.
2. J. Buffle et al., *Environ. Sci. Technol.* **32**, 2887 (1998).
3. E. J. Plaster, *Soil Science and Management*, 3rd ed., Delmar, Albany NY, 1996, p. 133.
4. D. W. Rutherford, C. T. Chiou, and D. E. Kile, *Environ. Sci. Technol.* **26**, 336 (1992).
5. D. E. Kile, R. L. Wershaw, and C. T. Chiou, *Environ. Sci. Technol.* **33**, 2053 (1999).
6. C. T. Chiou, J. Lee, and S. A. Boyd, *Environ. Sci. Technol.* **24**, 1164 (1990).
7. J. M. Zachara, C. A. Ainsworth, L. J. Felice, and C. T. Resch, *Environ. Sci. Technol.* **20**, 620 (1986).
8. C. T. Chiou and D. Schmedding, personal communication.
9. A. W. Adamson, *Physical Chemistry of Surfaces*, 5th ed., Wiley-Interscience, New York, 1990, pp. 609–614.
10. D. G. Kinniburgh, *Environ. Sci. Technol.* **20**, 895 (1986).
11. R. S. Kookana, L. A. G. Aylmore, and R. G. Gerritse, *Soil Sci.* **154**, 214 (1992).
12. B. J. Brownawell, H. Chen, J. M. Collier, and J. C. Westall, *Environ. Sci. Technol.*, **24**, 1234 (1990).

13. C. T. Chiou, L. J. Peters, and V. H. Freed, *Science* **206**, 831 (1979).
14. J. C. Means, S. G. Wood, J. J. Hassett, and W. L. Banwart, *Environ. Sci. Technol.* **14**, 1524 (1980).
15. A. D. Site, *J. Phys. Chem. Ref. Data* **30**, 187 (2001).
16. W. J. M. Hegeman, C. H. van der Weijden, and J. P. G. Loch, *Environ. Sci. Technol.* **29**, 363 (1995).
17. D. E. Kile, C. T. Chiou, H. Zhou, and O. Xu, *Environ. Sci. Technol.* **29**, 1401 (1995).
18. C. T. Chiou, S. E. McGroddy, and D. E. Kile, *Environ. Sci. Technol.* **32**, 264 (1998).
19. C. T. Chiou, *Partition and Adsorption of Organic Contaminants in Environmental Systems*, John Wiley & Sons Inc., New York, 2002.
20. C. T. Chiou, T. D. Shoup, and P. E. Porter, *Org. Geochem.* **8**, 9 (1985).
21. C. T. Chiou and D. E. Kile, *Environ. Sci. Technol.* **32**, 338 (1998).
22. C. T. Chiou, D. E. Kile, D. W. Rutherford, G. Sheng, and S. A. Boyd, *Environ. Sci. Technol.* **34**, 1254 (2000).
23. C. T. Chiou, P. E. Porter, and D. W. Schmedding, *Environ. Sci. Technol.* **17**, 227 (1983).
24. R. P. Schwarzenbach, P. M. Gschwend, and D. M. Imboden, *Environmental Organic Chemistry*, John Wiley & Sons Inc., New York, 1993, p. 274.
25. L. S. Lee, P. S. C. Rao, P. Nikedi-Kizza, and J. J. Delfino, *Environ. Sci. Technol.* **24**, 654 (1990).
26. K. Schellenberg, C. Leuenberger, and R. P. Schwarzenbach, *Environ. Sci. Technol.* **18**, 652 (1984).
27. J. M. Zachara, C. C. Ainsworth, L. J. Felice, and C. T. Resch, *Environ. Sci. Technol.* **20**, 620 (1986).
28. J. M. Zachara, C. C. Ainsworth, C. C. Cowan, and B. L. Thomas, *Environ. Sci. Technol.* **21**, 397 (1987).
29. M. T. O. Jonker and F. Smedes, *Environ. Sci. Technol.* **34**, 1620 (2000).
30. C. T. Chiou and T. D. Shoup, *Environ. Sci. Technol.* **19**, 1196 (1985).
31. D. W. Rutherford and C. T. Chiou, *Environ. Sci. Technol.* **26**, 965 (1992).
32. R. S. Kookana, L. A. G. Aylmore, and R. G. Gerritse, *Soil Sci.* **154**, 214 (1992).
33. A. T. Kan, G. Fu, M. A. Hunter, and M. B. Tomson, *Environ. Sci. Technol.* **31**, 2176 (1997).
34. R. S. Kookana, R. G. Gerritse, and L. A. G. Aylmore, *Soil Sci.* **154**, 344 (1992).
35. M. Oi, *J. Agr. Food Chem.* **47**, 327 (1999).
36. J. J. Pignatello and B. Xing, *Environ. Sci. Technol.* **30**, 1 (1996).
37. A. T. Kan, G. Fu, M. Hunter, W. Chen, C. H. Ward, and M. B. Thomson, *Environ. Sci. Technol.* **32**, 892 (1998).
38. E. Björklund, S. Bøwadt, L. Mathiasson, and S. B. Hawthorne, *Environ. Sci. Technol.* **33**, 2193 (1999).
39. S. M. Steinberg, J. J. Pignatello, and B. L. Sawhney, *Environ. Sci. Technol.* **21**, 1201 (1987).
40. S. L. Simonich, and R. A. Hites, *Environ. Sci. Technol.* **29**, 2905 (1995).
41. C. E. Jeffree "Structure and Ontogeny of Plant Cuticles", in G. Kersteins, Ed., *Plant Cuticles: an Integrated Functional Approach*, Bios Scientific Publishers, Oxford, UK, 1996, p. 33.

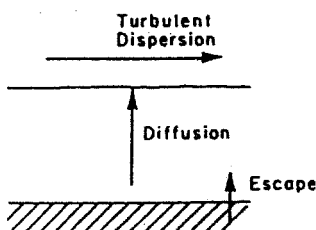
42. K. Welsch-Pausch, M. S. McLachlan, and G. Umlauf, *Environ. Sci. Technol.* **29**, 1090 (1995).
43. B. Welke, K. Ettliger, and M. Riederer, *Environ. Sci. Technol.* **32**, 1099 (1998).
44. S. Paterson, D. Mackay, E. Bacci, and D. Calamari, *Environ. Sci. Technol.* **25**, 866 (1991).
45. P. Komp and M. S. McLachlan, *Environ. Sci. Technol.* **31**, 2944 (1997).
46. T. Harner and D. Mackay, *Environ. Sci. Technol.* **29**, 1599 (1995).
47. H. Hauk, G. Umlauf, and M. S. McLachlan, *Environ. Sci. Technol.* **28**, 2372 (1994).
48. M. S. McLachlan, *Environ. Sci. Technol.* **33**, 1799 (1999).
49. F. Böhme, K. Welsch-Pausch, and M. McLachlan, *Env. Sci. Technol.* **33**, 1805 (1999).
50. C. Chiou, "Partition Coefficient and Water Solubility in Environmental Chemistry", in J. Saxena and F. Fisher, Eds., *Hazard Assessment of Chemicals Vol. I*, Academic Press, Inc., New York, 1981, pp. 117–153.

Evaporation

Recent observations of the global distribution of persistent contaminants such as PCBs and some organochlorine pesticides¹ emphasize the importance of defining the tendency of compounds to move into the vapor phase. This transition not only provides access to active degradation processes (see Photochemical Processes, Chapter 6), but it also results in a broader distribution through the influence of atmospheric processes. The PCBs and related compounds would not be considered volatile by usual criteria, however, it will be demonstrated that evaporation of a compound is influenced by its environment; that is, compounds that might have little tendency to evaporate as the pure compound may be lost rapidly from water. Also, the magnitude of the response may reflect the area over which the compound is distributed.

Chemistry texts usually focus on closed-system equilibriums, however, evaporation is a kinetic process and involves

1. The **escaping tendency** that defines the distribution between the solid or liquid and vapor phases. The physical chemical properties of a compound will be the major determinants and will depend on the environment from which the compound evaporates.



2. **Diffusion** away from the surface. The rate of evaporation is determined in large part by the rate of diffusion through the thin stagnant layer, usually referred to as the boundary layer, of air at the surface. The thickness of this layer is determined by the turbulence while diffusion rate depends on the diffusion coefficient in air and the concentration gradient.

3. **Dispersion.** Atmospheric currents will then move the compound away from the site of evaporation.

Evaporation is an endothermic process. Temperature will obviously affect evaporation rate, however, thermal conductivity is not often a limiting factor given the heat capacities of the environments from which compounds are lost. An exception would be the evaporation of a small drop in air where thermal conductivity through the air could be limiting.

4.1 EVAPORATION OF THE PURE COMPOUND

For a pure compound, the escaping tendency at a given temperature will be defined by its equilibrium vapor pressure and the vapor density, or concentration at the vapor-phase interface. Diffusion across the stagnant air layer will be determined by the concentration differential and diffusion coefficient that is inversely proportional to \sqrt{M} . So given constant environmental conditions, temperature, and air movement the rate of evaporation (Q) would be a function of P^0 and M

$$Q \propto P\sqrt{M}$$

The validity of this relation is illustrated by the data summarized in Table 4.1 where the ratio $W/(P\sqrt{M})$ is essentially constant for a given temperature and wind speed.² The data also illustrate the effect of wind speed on evaporation rate.

The rate of evaporation of pure compounds can be derived by simply observing the weight loss with time under controlled conditions as illustrated in Figure 4.1.³

TABLE 4.1 Rate of Loss from Petri Dishes at 20°C

Ventilation	Substance	P at 20°C (Torr)	Rate of Loss (W)		
			MW	$g \cdot \text{min}^{-1}$	$\frac{W}{P\sqrt{MW}}$
Still	2,2,4-Trimethylpentane	37	114	540	1.37
	<i>m</i> -Xylene	6.2	106	76	1.19
	Anisole	2.8	108	30	1.03
Strong wind ^a	2,2,4-Trimethylpentane	37	114	1186	3.01
	<i>m</i> -Xylene	6.2	106	267	4.18
	Anisole	2.8	108	158	5.04
	<i>p</i> -Dichlorobenzene	0.8	147	54	5.6
	<i>N,N</i> -Dimethylaniline	0.66	121	41	5.6
	<i>n</i> -Octanol	0.073	130	4.1	4.9

Source: Reprinted from *Advances in Chemistry Series*, No. 86, Pesticidal Formulations Research—Physics and Colloidal Chemical Aspects, J. W. Van Valkenburg, Editor. Copyright © 1969 by the American Chemical Society. Reprinted by permission of the copyright owner.

^aWinds ~10 mph at the surface.

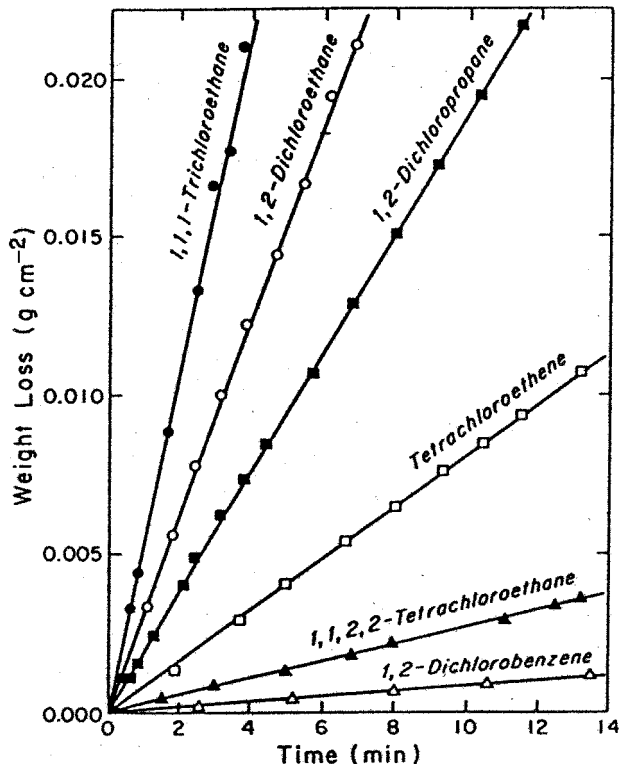


Figure 4.1 Evaporation of chlorinated hydrocarbons into still air at ambient temperatures (23–25°C).

These data can be evaluated using a modified Knudsen equation where the evaporative flux Q is expressed by

$$Q = \beta P^0 (M/2\pi RT)^{1/2}$$

with P^0 being the equilibrium vapor pressure at the temperature in question and M the molecular weight. The evaporation coefficient, β (equal to 1 for evaporation into a vacuum) depends on atmospheric pressure and turbulence and can be derived from the experimental data as outlined in Table 4.2. Under the conditions of this study the variation in the calculated values for the nondimensional constant, β , is relatively small and using a larger number of compounds a value of $1.98 \times 10^{-5} \pm 0.18$ was reported.³ There has been no systematic evaluation of the effect of air movement on this constant although a 1% increase per degree Celsius increase in temperature has been reported.⁴ Since these data were obtained in still air, this relation can provide a minimum estimate of evaporative loss under ambient conditions.

Note that in this study, since the evaporative flux is expressed in $\text{g} \cdot \text{cm}^{-2} \cdot \text{s}^{-1}$, the equivalent c.g.s. unit, $\text{dyn} \cdot \text{cm}^{-2}$ is used for pressure and the universal gas constant, R , would have units of $8.314 \times 10^7 \text{ erg} \cdot \text{mol}^{-1} \cdot \text{K}^{-1}$. A dyne is the force exerted by 1 g and pressure in mm of mercury is converted to dynes cm^{-2} by calculating

TABLE 4.2 Evaporation of Organic Chemicals at Ambient Conditions

Compound	M	t ($^{\circ}\text{C}$)	P^0 (mm)	$Q^a \times 10^5$	F^b	$\beta \times 10^5$
1,1,1-Trichloroethane	133.5	23.7	120	9.04	4.68	1.93
1,2-Dichloroethane	99.0	23.7	78.0	5.20	2.63	1.98
1,2-Dichloropropane	113	23.6	48.4	3.15	1.74	1.81
Tetrachloroethene	166	23.2	16.7	1.36	0.727	1.87
1,1,2,2-Tetrachloroethane	168	23.4	4.70	0.448	0.206	2.17
1,2-Dichlorobenzene	147	23.2	1.25	0.118	0.0510	2.31

^a Experimental flux in $\text{g} \cdot \text{cm}^{-2} \cdot \text{s}^{-1}$.

^b $F = P(M/2\pi RT)^{1/2}$ and $\beta = Q/F$.

the mass of the column of mercury (density of $13.6 \text{ g} \cdot \text{mL}^{-1}$) and multiplying by acceleration due to gravity, $980 \text{ cm} \cdot \text{s}^{-2}$. Units in this expression can be reconciled as follows:

$$\text{Flux } M \cdot \text{L}^{-2} \cdot \text{T}^{-1}$$

$$\text{Pressure force per unit area } (M \cdot \text{L} \cdot \text{T}^{-2})\text{L}^{-2} = M \cdot \text{L}^{-1} \cdot \text{T}^{-2}$$

$$\text{Erg} = \text{dyne cm } M \cdot \text{L}^2 \cdot \text{T}^2$$

$$M/RT (M \cdot \text{mol}^{-1}) / (M \cdot \text{L}^2 \cdot \text{T}^{-2} \cdot \text{mol}^{-1} \cdot \text{temp}^{-1} \cdot \text{temp}) = \text{L}^{-2} \cdot \text{T}^2$$

$$(M/RT)^{1/2} = \text{L}^{-1} \cdot \text{T}$$

$$\text{Pressure} \times (M/RT)^{1/2} = (M \cdot \text{L}^{-1} \cdot \text{T}^{-2})(\text{L}^{-1} \cdot \text{T}) = M \cdot \text{L}^{-2} \cdot \text{T}^{-1} = \text{Flux}$$

Flux expressed in $\text{kg} \cdot \text{m}^{-2} \cdot \text{s}^{-1}$ can be obtained from the same relation using Pascals for pressure, and a value of $8.314 \text{ J} \cdot \text{mol}^{-1} \cdot \text{K}^{-1}$ for R and expressing M in kg. It is of interest to note that $1 \text{ Pas} = 10 \text{ dyn} \cdot \text{cm}^{-2}$.

4.2 EVAPORATION FROM WATER

Maintaining water quality is a major environmental priority and it has been demonstrated that evaporation from water can be a significant process in the dynamics determining levels of contaminants. When dealing with compounds that are completely miscible with water, the rate of evaporation can be defined by the same relation used with pure compounds. Partial pressures derived from Raoult's law would be used and the total rate of evaporation would be the sum of the losses of the individual constituents. This approach cannot be used with slightly soluble compounds since their solution behavior is quite different. Two models will be introduced to define the evaporation of the latter and illustrate how their properties influence the process.

4.2.1 Surface Depletion Model

The relation used to define the evaporation of a pure compound can be adapted to represent the evaporation of a solute³

$$Q_i = dm_i / Adt = \beta \alpha_i P_i (M_i / 2\pi RT)^{1/2}$$

with P_i being the partial pressure of the solute corresponding to the bulk concentration of the solute, C_i . If the solute evaporates at a faster rate than water, the concentration of the solute at the water–air interface will be depleted and the vapor pressure of the solute at the interface P_i^* will be expressed as $\alpha_i P_i$, where $\alpha = (C^*/C)_i$ with C^* being the concentration of the solute at the interface. For solutes in dilute aqueous solution, $P_i = H_i C_i$ and the flux will be expressed

$$Q_i = \beta \alpha_i H_i (M_i / 2\pi RT)^{1/2} C_i = k_i C_i$$

which is a first-order process with k_i being a transfer coefficient with units of velocity.

It is often more important to define change in concentration rather than the evaporative flux and, since the actual mass of solute evaporating can be expressed

$$\Delta m_i = \Delta C_i V$$

with V being the volume of the system,

$$Q_i = (\Delta C_i \cdot V) / (\Delta t \cdot A) = k C_i \quad \text{and} \quad \Delta C_i / \Delta t = k_i \cdot (A/V) C_i = (k_i/L) C_i$$

Since this is a first-order process, evaporative half-life can be expressed

$$t^{1/2} = \ln 2 / (k_i/L) = 0.693L/k_i$$

where L is the depth of the water column.

To use this relation to predict the rate of evaporation of a solute from water, it is necessary to derive values for α and β . Values for the latter can be derived experimentally from observations on the evaporation of pure compounds under comparable conditions. Estimates of α can also be derived by comparing experimental values with calculated values assuming $\alpha = 1$ as illustrated in Table 4.3. These laboratory studies³ were carried out under ambient conditions ($\sim 24^\circ\text{C}$). Compounds with higher Henry's law constants show lower α values than one would anticipate given the tendency of the compound to distribute into the vapor phase, and stirring increased the value of α reducing the concentration gradient. These effects are illustrated in Figure 4.2. With higher concentrations lower α values are observed only with compounds of higher Henry's law constants. These concentrations were 75% or greater of the aqueous solubility of the compounds and would not be of environmental significance. Compounds with low Henry's law constants, such as chlorophenols, show α values of ~ 1 and, in addition, stirring the liquid phase increases evaporation only by increasing the β value (Table 4.4). In this case, the evaporation rate is controlled in the vapor phase while with compounds with high Henry's law constants the evaporation rate would be controlled primarily in the liquid phase.

It is possible to use this relation to predict the rate of evaporation from water under static conditions given the Henry's law constant. A value for α can be

TABLE 4.3 Evaporation Half-Lives from Water ($L = 1.6$ cm)

Compound	H ($\text{dyn} \cdot \text{cm} \cdot \text{g}^{-1}$)	C° (ppm) ^a	Stirred	Half-life (min)		
				Calc. ($\alpha = 1$)	Obs.	α
Carbon tetrachloride	5.9×10^7	742	Y ^c	0.40	2.8	0.143
	(0.366) ^b	~ 1	Y	0.40	8.0	0.050
		~ 1	N ^d	0.51	81	0.0062
1,1,1-Trichloroethane	4.8×10^7	1350	Y	0.52	2.0	0.260
	(0.259)	~ 0.1	Y	0.52	7.2	0.0722
		~ 0.1	N	0.66	78	0.0084
Tetrachloroethene	2.1×10^7	180	Y	1.1	3.2	0.344
	(0.141)	~ 0.1	Y	1.1	7.0	0.157
		~ 0.1	N	1.39	69	0.020
1,2-Dichlorobenzene	1.1×10^7	137	Y	2.3	4.8	0.479
	(0.0653)	~ 2	Y	2.3	8.1	0.284
1,2-Dibromoethane	3.0×10^6	2750	Y	7.1	6.4	1.11
	(0.0228)	~ 0.1	Y	7.1	6.8	1.04
1,1,2,2-Tetra- chloroethane	2.0×10^6	2270	Y	11	9.2	1.20
	(0.0136)	~ 0.1	Y	11	8.6	1.28
		~ 0.1	N	13.9	78	0.18

^aInitial concentration.^bCorresponding dimensionless HLC.^c $\beta = 2.5 \times 10^{-5}$.^d $\beta = 1.98 \times 10^{-5}$.

estimated from the $\alpha - H$ relation (Fig. 4.2). For example, a transfer coefficient, k_i , can be calculated for DDT, at 25°C given

$$\begin{aligned}
 M &= 354.5 \text{ g} \cdot \text{mol}^{-1} \\
 S_w &= 4 \text{ ppb} = 4 \times 10^{-9} \text{ g} \cdot \text{cm}^{-3} \\
 P^0 &= 3.2 \times 10^{-7} \text{ mmHg} = 4.265 \times 10^{-3} \text{ dyn} \cdot \text{cm}^{-2} \\
 \text{HLC} &= 4.265 \times 10^{-3} / 4.0 \times 10^{-9} = 1.07 \times 10^5 \text{ dyn} \cdot \text{cm} \cdot \text{g}^{-1} \\
 &\quad (0.0015 \text{ dimensionless}) \\
 \alpha &\sim 0.90 \text{ from Figure 3.2} \\
 \beta &= 1.98 \times 10^{-5} \text{ in still air}
 \end{aligned}$$

$$k_i = \alpha\beta H(M/2\pi RT)^{1/2} = 9.09 \times 10^{-5} \text{ cm} \cdot \text{s}^{-1}$$

For a depth of 4.5 cm, the half-life is

$$t_{1/2} = (0.693 \times 4.5) / 9.09 \times 10^{-5} = 9.5 \text{ h}$$

which corresponds to an experimental value of 8.8 h (Fig. 4.3). The rapid loss of DDT from water (the flux is not high, however, given the low solubility) was a surprise for those who traditionally equated volatility with vapor pressure and

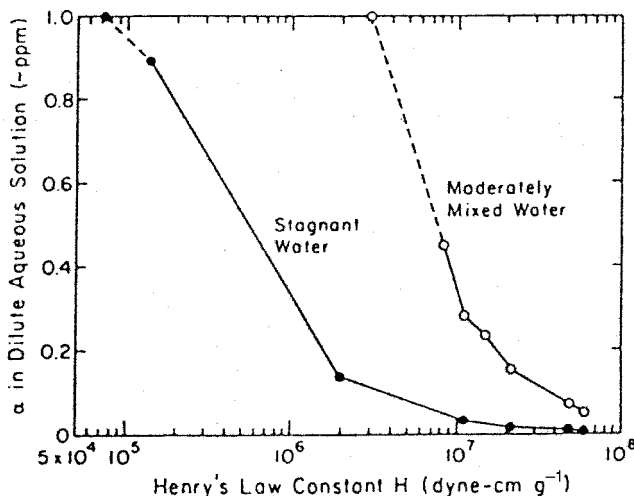


Figure 4.2 The relation between α and H for solutes evaporating from dilute aqueous solution at ambient temperature ($\sim 24^\circ\text{C}$) and 40% relative humidity. [Reproduced from C. T. Chiou, V. H. Freed, L. J. Peters, and R. L. Kohnert. "Evaporation of Solutes from Water"; *Environ. Internat.* **3**, 231. Copyright © 1980, with permission from Elsevier.]

early literature⁵ suggested that the DDT was swept away as water evaporated, that is, a codistillation effect. It has been demonstrated that DDT will evaporate from water even as water is moving in the opposite direction, condensing.⁶

Additional examples of how experimental observations coincide with calculated values are provided in Table 4.5. The agreement between calculated and experimental values is quite good and indicates that this model could provide reliable estimates of evaporation from water under static conditions. Laboratory studies can evaluate the effect of water and air movement on α and β , however, it would be difficult to use this data to assess evaporation rates under more complex conditions that might exist in the environment.

TABLE 4.4 Evaporation of Chlorophenols from Water^a ($L = 0.38$ cm)

Compound	HLC		Stirred	Half-life (hr)		
	$\text{dyn} \cdot \text{cm} \cdot \text{g}^{-1}$	Dimensionless		Est. ($\alpha = 1$)	Exptl.	α
2-Chlorophenol	7.54×10^4	3.92×10^{-4}	N ^b	1.70	1.60	1.06
			Y ^c	1.36	1.35	1.01
4-Chlorophenol	7.07×10^3	3.68×10^{-5}	N	18.2	17.4	1.05
			Y	14.5	12.8	0.88

^aInitial concentration of 2 ppm at 24°C .

^b $\beta = 1.98 \times 10^{-5}$.

^c $\beta = 2.50 \times 10^{-5}$.

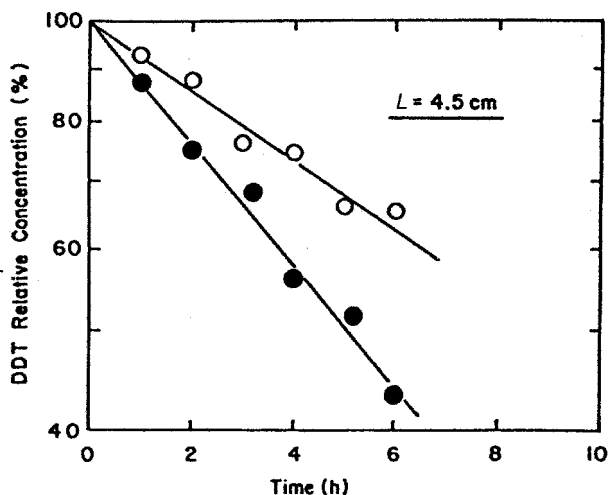


Figure 4.3 The evaporative loss of DDT from water with stirring (●) and without stirring (○). [Reproduced from C. T. Chiou, V. H. Freed, L. J. Peters, and R. L. Kohnert. "Evaporation of Solutes from Water"; *Environ. Internat.* **3**, 231. Copyright © 1980, with permission from Elsevier.]

4.2.2 Two-Film Model

Another approach^{8,9} used to define evaporation from water assumes that the rate is controlled by diffusion through stagnant layers at the interface with the Henry's law constant determining the distribution at the interface (Fig. 4.4). The flux

TABLE 4.5 Comparison of Estimated and Observed Evaporation Rates at 24°C ($L = 4.5 \text{ cm}$)^a

Compound	MW ($\text{g} \cdot \text{mol}^{-1}$)	C° (ppm)	H ($\text{dyne} \cdot \text{cm} \cdot \text{g}^{-1}$)	α^b	Half-life	
					Calc.	Obs.
2,2'-Dichlorobiphenyl	223.1	0.1	1.7×10^6 (0.015)	0.22	3.1 h	3.9 h
4,4'-Dichlorobiphenyl	223.1	0.03	4.5×10^5 (0.0041)	0.57	4.5 h	4.0 h
2,2',5,5'-Tetrachloro- biphenyl	292	0.005	1.04×10^6 (0.012) ^c	0.35	2.8 h	2.8 h
Lindane	291	5	1.1×10^4 (1.3×10^{-4})	1	3.4 h	3.2 h
Parathion	291	2	3.3×10^3 (3.9×10^{-5})	1	13 day	14 day

^aTaken from Ref. 3.

^bEstimated from Figure 3.2.

^cHLC for 2,2',5,5'-tetrachlorobiphenyl from Ref. 7.

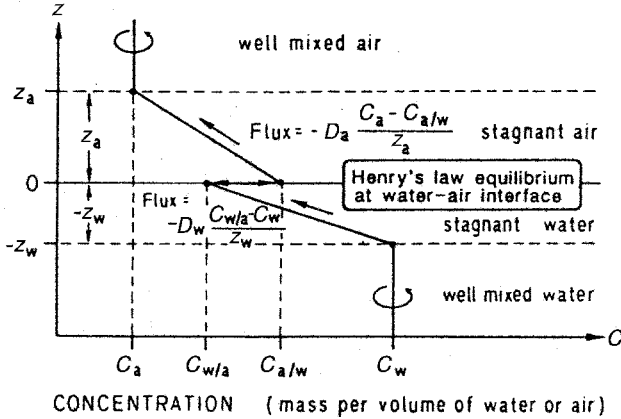


Figure 4.4 Schematic representation of the two-film model for the distribution of organic compounds between air and water.

($M \cdot L^{-2} \cdot T^{-1}$) across the stagnant air layer according to Fick's law would be defined by the molecular diffusion coefficient in air, D_a , the concentration gradient and the thickness of the film, z_a :

$$Q_a = -D_a(C_a - C_{aw})/z_a \tag{1}$$

With this sign convention the flux is positive for movement from water to air with $C_a < C_{aw}$. In this regard, note that the model could also account for condensation from air into water when $C_a > C_{aw}$. It is assumed that the compound is not reacting to any significant extent during this transition and that concentrations defining the gradient are constant for a sufficient time to attain a steady state. The flux Q_w through the water film is defined by a comparable relation

$$Q_w = -D_w(C_{wa} - C_w)/z_w \tag{2}$$

At steady state the flux through the two interfacial layers must be equal and, hence, the overall flux, Q , would be expressed

$$\begin{aligned} Q &= Q_w = Q_a \\ Q &= -D_w(C_{wa} - C_w)/z_w = -D_a(C_a - C_{aw})/z_a \end{aligned} \tag{3}$$

It is clear that values for the interfacial surface concentrations, C_{as} and C_{ws} , could not be obtained, neither could estimates of the thickness of the films, z_a and z_w . The dimensionless Henry's law constant H' defines the distribution across the water air interface and,

$$H' = C_{aw}/C_{wa}$$

and substituting for $C_{aw} = H' \cdot C_{wa}$ in Eq. (3), C_{wa} can be expressed as a function of C_w and C_a . This expression for C_{wa} is then substituted in Eq. (2) and performing the necessary algebra,⁹ a relation for flux can be obtained

$$Q = \left(\frac{1}{(z_w/D_w) + (z_a/D_a H')} \right) \left(C_w - \frac{C_a}{H'} \right) \quad (4)$$

$$= k_{tot}(C_w - C_a/H) \quad (5)$$

With k_{tot} having units $\text{cm} \cdot \text{s}^{-1}$ and concentration in g or $\text{mol} \cdot \text{cm}^{-3}$, the flux would be expressed in g or $\text{mol} \cdot \text{cm}^{-2} \cdot \text{s}^{-1}$. In many cases, C_a is essentially zero and the evaporative flux would be a first order function of the bulk water concentration, C_w . The overall mass transfer velocity, k_{tot} , can be perceived as the mean velocity with which the molecules cross the boundary and as demonstrated earlier, the evaporative half-life would be given by

$$t_{1/2} = \frac{0.693 \times L}{k_{tot}}$$

where L would be depth in centimeters.

Since

$$k_{tot} = \frac{1}{(z_w/D_w) + (z_a/D_a H')} \quad (6)$$

$$\frac{1}{k_{tot}} = \frac{1}{k_w} + \frac{1}{k_a H'} \quad (7)$$

with k_w and k_a , the partial-transfer velocities through the water and air layers, respectively, with

$$k_a = D_a/z_a \quad \text{and} \quad k_w = D_w/z_w$$

The resistance to evaporation, $1/k_{tot}$ can be conceived as the sum of the resistance in the aqueous phase, $1/k_w$ and the vapor phase, $1/k_a H'$. When

$$k_w \ll k_a H' \quad 1/k_w \gg 1/k_a H' \quad \text{and} \quad k_{tot} \sim k_w$$

and the rate of evaporation would be controlled primarily in the liquid phase. When the reverse is true ($k_w \gg k_a H'$), then the rate is controlled by the vapor phase. A resistance ratio $R_{a/w}$ can be defined

$$R_{a/w} = \frac{(1/k_a H')}{(1/k_w)} = k_w/k_a H'$$

When $R_{a/w} < 0.1$, the overall transfer rate is controlled in the water layer and when $R_{a/w} > 10$ the air layer is controlling. Intermediate values indicate that both layers contribute significantly.

It has been demonstrated that the partial-transfer velocities, k_a and k_b , can be estimated in terms of reference values obtained by experiment. Extensive studies of the evaporation of water have shown that, under static conditions, $k_a = 0.3 \text{ cm} \cdot \text{s}^{-1}$, which would give a value of $\sim 0.9 \text{ cm}$ for z_a , given D_a for water in air is $0.26 \text{ cm}^2 \cdot \text{s}^{-1}$. Investigation of gas exchange with water have provided estimates of k_w and it has been shown that for O_2 , $k_w = 4 \times 10^{-4} \text{ cm} \cdot \text{s}^{-1}$. Under static conditions, giving a value of $\sim 0.05 \text{ cm}$ for z_w with D_w for O_2 in water of $2.1 \times 10^{-5} \text{ cm}^2 \cdot \text{s}^{-1}$. For a given compound, then, values for k_a and k_w can be derived from the reference values for water in air and oxygen in water as follows:

$$k_a(\text{compound}) = k_a(\text{H}_2\text{O}) \left[\frac{D_a(\text{compound})}{D_a(\text{H}_2\text{O})} \right]^{0.67} = 0.30 \left[\frac{D_a(\text{compound})}{0.26} \right]^{0.67}$$

$$k_w(\text{compound}) = k_w(\text{O}_2) \left[\frac{D_w(\text{compound})}{D_w(\text{O}_2)} \right]^{0.57} = 4 \times 10^{-4} \left[\frac{D_w(\text{compound})}{2.1 \times 10^{-5}} \right]^{0.57}$$

Values for D_a and D_w can also be estimated in terms of reference values for water in air and oxygen in water ($D_x = D_{\text{ref}}[\text{MW}_{\text{ref}}/\text{MW}_x]^{1/2}$). The exponents have been estimated from experimental observations.⁹ It is now possible to estimate evaporation rates under static conditions by first estimating molecular diffusion coefficients, deriving values for the partial transfer velocities and calculating k_{tot} . The data summarized in Table 4.6 use some laboratory observations listed in Tables 4.3–4.5 to evaluate this model. Reasonable agreement is observed between the calculated and observed values, considering possibilities for experimental error and uncertainties in the values for Henry's law constant, and so on.

These two models illustrate how the properties of the compound influence the rate of evaporation from water under static conditions. Environmental conditions such as wind speed and turbulence in the water phase will have a marked influence on rates of evaporation that would reduce gradients and also reduce the width of the interfacial diffusion layers and systematic analysis of these effects have been discussed.⁹ Other variables will affect evaporation rates by controlling the actual concentration of the compound in solution. Suspended sediments and/or DOM would act in this manner. Weak acids and bases would only evaporate as the neutral species since the complementary anions or cations would be more water soluble and essentially have no vapor pressure. Consequently, environmental pH relative to pK_a values will be a consideration. It should be mentioned that compounds may distribute into the vapor phase by other processes than evaporation. Formation of aerosols, for example, can be a factor.

TABLE 4.6 Evaporation Half-lives Calculated Using the Two-Film Model

Compound	MW	H'	L (cm)	Trans. Velocity ($\text{cm} \cdot \text{s}^{-1}$)			$t_{1/2}$		R_a/w
				k_a	k_w	k_{tot}	Calc.	Obs.	
1,1,1-Trichloroethane	133.5	0.259	1.6	0.153	2.67×10^{-4}	2.66×10^{-4}	70 min	78 min	0.0067
Tetrachloroethene	166	0.141	1.6	0.143	2.50×10^{-4}	2.46×10^{-4}	75 min	69 min	0.012
DDT	354.4	0.0015	4.5	0.111	2.01×10^{-4}	9.1×10^{-5}	9.5 h	8.8 h	1.21
4,4-Dichlorobiphenyl	223.1	0.0041	4.5	0.129	2.31×10^{-4}	1.6×10^{-4}	5.4 h	4.0 h	0.44
Lindane	291	1.3×10^{-4}	4.5	0.119	2.13×10^{-4}	1.43×10^{-5}	60 h	3.2 h	13.8
Parathion	291	3.9×10^{-5}	4.5	0.119	2.13×10^{-4}	4.54×10^{-6}	7.9 day	14 day	46
2-Chlorophenol	128.5	3.9×10^{-4}	0.38	0.155	2.65×10^{-4}	4.95×10^{-5}	1.5 h	1.6 h	4.4

4.3 EVAPORATION FROM SOIL

This process is more complex than evaporation from water since there are many variables that influence the distribution between soil and the vapor phase. This discussion will first illustrate how different soil parameters can influence vapor density, an index of “escaping tendency”, then outline the factors that control evaporation from the surface of the soil. The analysis will then address the process by which compounds evaporate from a soil column.

4.3.1 Factors Influencing Vapor Density over Soil

The vapor density of dieldrin over a Gila silt loam (0.6% om) increases with the concentration in the soil (Fig. 4.5) and at soil concentrations of only 100 ppm gives a vapor density essentially equal to that of the pure compound.¹⁰ As would be expected, vapor density over the soil increases with temperature. The effect of soil water content on the vapor density of dieldrin over the same soil has been reported¹⁰ and from Figure 4.6 it is clear that a dry soil results in a dramatic reduction in vapor density. In discussing sorption of gases on soil (see Physical chemical properties, Chapter 2) it was suggested that this effect resulted from water displacing the compound from the more polar sorption surfaces (e.g., clays) and it can be seen that this transition occurs quite abruptly. The effect of composition on the vapor density of dieldrin over soil is illustrated by the data in Table 4.7.¹⁰

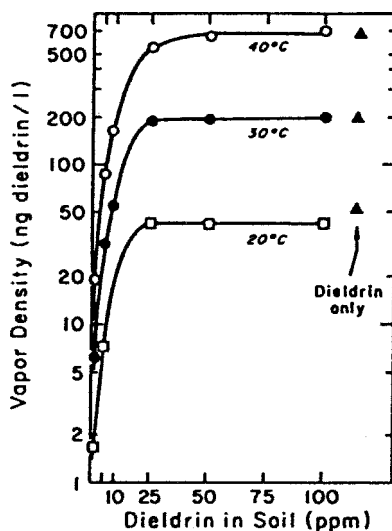


Figure 4.5 Vapor density of dieldrin over loam with a water content of 10%—effect of temperature and dieldrin concentration. [Reproduced with permission from W. F. Spencer et al., *Residue Rev.* **49**, 17, (1973).]

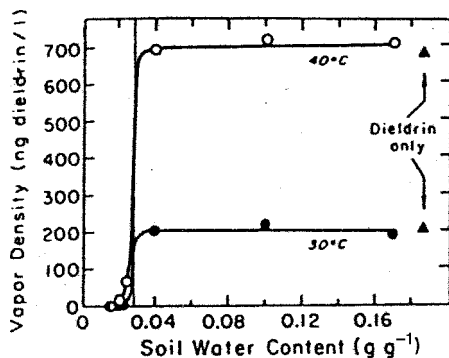


Figure 4.6 Effect of soil water content on vapor density of dieldrin over a Gila silt loam with 100 ppm dieldrin in the soil. [Reproduced with permission from W. F. Spencer et al., *Residue Rev.* **49**, 17 (1973).]

Organic matter level, but not clay, clearly influences vapor density in a wet soil, but the overriding influence of soil moisture is obvious. In a wet soil vapor density would be a function of the HLC and concentration of the compound in the soil moisture that in turn is determined by the K_d and soil concentration:

$$C_{\text{air}} = H' \cdot C_w = (H'/K_d)x/m \quad \text{since } C_w = (x/m)/K_d$$

Calculated values correspond reasonably well with observed values considering experimental errors and uncertainties in H' and K_d estimates.

4.3.2 Evaporation from the Soil Surface

Experimental approaches have been developed to measure the rate of evaporation from the soil surface in the laboratory or under field conditions. Laboratory studies

TABLE 4.7 Soil Composition and Vapor Density of Dieldrin ($10 \mu\text{g} \cdot \text{g}^{-1}$)

Soil	% Clay	% OM	Dieldrin K_d ($\text{mL} \cdot \text{g}^{-1}$) ^a	Vapor density ($\text{ng} \cdot \text{L}^{-1}$)		
				Dry	Wet	
					obs.	calc. ^{a,b}
Rosita vf. sa. loam	16.3	0.19	72.2	1.7	175	249
Imperial clay	67.6	0.20	76.0	0.9	200	236
Gila si. loam	18.4	0.58	220	0.7	52	81
Kentwood sa. loam	10.0	1.62	616	0.4	32	29
Linn clay loam	33.4	2.41	916	0.6	32	20

^aBased on a K_{om} of 38,000.

^bCalculated using K_d and $H' = 0.0018$.

are usually carried out under controlled conditions using small amounts of soil in a confined system. Under field conditions, the rate of evaporation can be calculated by measuring the concentration gradient with height above the site in question along with appropriate meteorological parameters. These procedures have been outlined elsewhere.¹¹

The effect of flow rate over the soil surface and concentration of dieldrin is illustrated in Figure 4.7, where evaporation of dieldrin from a moist soil (Gila silt loam, Table 4.7) was monitored by passing air (RH 100%) over a 10 g soil sample contained in a 29 × 95 mm pan.¹² The evaporation rate decreases with time as the initial surface deposit is lost and the rate becomes dependent on diffusion to the surface. An initial rate of evaporation can be derived by extrapolation to zero time, which for a 2 mL · s⁻¹ flow rate and 10 μg · g⁻¹ would be ~300 ng · cm⁻² · day⁻¹ °C. For a moist soil one can express the rate of evaporation as

$$Q = kC_s/K_d$$

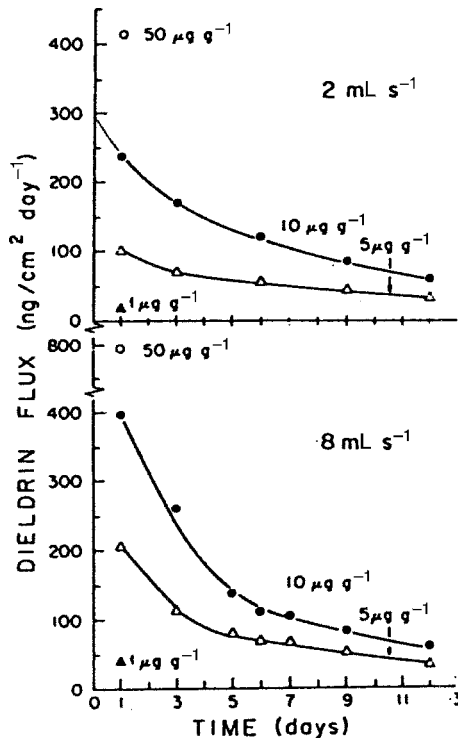


Figure 4.7 Rate of dieldrin volatilization from Gila silt loam as a function of time, concentration, and air flow rates at 10% soil water content, 100% relative humidity and 30°C. [Reproduced with permission from W. J. Farmer, K. Igue, W. F. Spencer, and J. P. Martin. *Soil Sci. Soc. Amer. Proc.* 36, 443, Copyright © Soil Science Society of America 1972.]

where k is the overall mass transfer coefficient from water to air and one would assume that initially the rate of movement from soil to water would not be limiting. Based on the following values for dieldrin

MW	381
HLC	$1.17 \times 10^5 \text{ dyn} \cdot \text{cm} \cdot \text{g}^{-1}$ ($H' = 1.8 \times 10^{-3}$)
K_{oc}	65,000 calculated from $S_w = 0.20$ ppm (see p. 93)
α	0.78 from Figure 3.2
D_a	$0.057 \text{ cm}^2 \cdot \text{s}^{-1}$
D_w	$6.09 \times 10^{-6} \text{ cm}^2 \cdot \text{s}^{-1}$

from the surface depletion model

$$\begin{aligned} k &= \beta \cdot \alpha \cdot H(M/2\pi RT)^{1/2} = 1.98 \times 10^{-5} \times 0.78 \times 1.17 \times 10^5 \\ &\quad \times [381/(2\pi \cdot 8.314 \times 10^7 \times 303)]^{1/2} \\ &= 8.87 \times 10^{-5} \text{ cm} \cdot \text{s}^{-1} \end{aligned}$$

which would give an evaporative flux

$$\begin{aligned} Q &= 8.87 \times 10^{-5} \times \left[\frac{10 \mu\text{g} \cdot \text{g}^{-1}}{234 \text{ cm}^3 \cdot \text{g}^{-1}} \right] = 3.79 \times 10^{-6} \mu\text{g} \cdot \text{cm}^{-2} \cdot \text{s}^{-1} \\ &\equiv 327 \text{ ng} \cdot \text{cm}^2 \cdot \text{day}^{-1} \end{aligned}$$

From the two-film model

$$\begin{aligned} 1/k_{\text{tot}} &= 1/(k_a H) + 1/k_w \\ k_a &= 0.30(0.057/0.26)^{0.67} = 0.108 \text{ cm} \cdot \text{s}^{-1} \\ k_w &= 4 \times 10^{-4}(6.09 \times 10^{-6}/2.1 \times 10^{-5})^{0.57} = 1.98 \times 10^{-4} \text{ cm} \cdot \text{s}^{-1} \\ k_{\text{tot}} &= 9.81 \times 10^{-5} \text{ cm} \cdot \text{s}^{-1} \end{aligned}$$

which would give an evaporative flux

$$\begin{aligned} Q &= 9.81 \times 10^{-5} \left[\frac{10 \mu\text{g} \cdot \text{g}^{-1}}{234 \text{ cm}^3 \cdot \text{g}^{-1}} \right] = 4.19 \times 10^{-6} \mu\text{g} \cdot \text{cm}^{-2} \cdot \text{s}^{-1} \\ &\equiv 362 \text{ ng} \cdot \text{cm}^{-2} \cdot \text{s}^{-1} \end{aligned}$$

This analysis assumes that the low rate of air movement across the soil surface ($2 \text{ mL} \cdot \text{min}^{-1} \sim 0.005 \text{ mph}$) approximates static conditions and the fact that the calculated flux overestimates the observed value would suggest that a wet soil sur-

face provides a more complex situation than a water–air interface. However, it does appear that this approach can provide a reasonable estimate of the initial rate of evaporation from a wet soil.

4.3.3 Evaporation from a Soil Column

When dealing with a chemical distributed through the soil, the initial loss would come from the surface. Once this was depleted, further evaporation would depend on movement of the chemical to the surface. The apparatus illustrated in Figure 4.8 has been used to evaluate the processes involved.¹³ Lindane was incorporated in the Gila silt loam to give a concentration of $10 \mu\text{g} \cdot \text{g}^{-1}$ and the humidity of the nitrogen passing over the surface of the column was varied. The lindane evaporating was trapped in the ethylene glycol and analyzed. Water evaporating from the surface was replenished from the base of the column. The Lindane flux decreased over the first 28 days when the relative humidity was maintained at 100% (Fig. 4.9). Under these conditions there would be no water lost from the column and consequently no water movement through the soil so the only way that Lindane could reach the surface was by diffusion. When the relative humidity was reduced to 50% the Lindane flux increased to a maximum at 42 days of $575 \text{ ng} \cdot \text{cm}^{-2} \cdot \text{day}^{-1} (B_2)$. The increased flux reflects the mass transport of Lindane through the soil due to water loss from the surface and consequent capillary movement up through the column. At 42 days, the relative humidity was increased to 100%, the Lindane flux decreased to A_2 . The flux resulting from diffusion is represented by the line $A_1 - A_2$ and at 42 days would be $234 \text{ ng} \cdot \text{cm}^{-2} \cdot \text{day}^{-1}$. Mass transport through the soil would then account for $341 \text{ ng} \cdot \text{cm}^{-2} \cdot \text{day}^{-1}$.

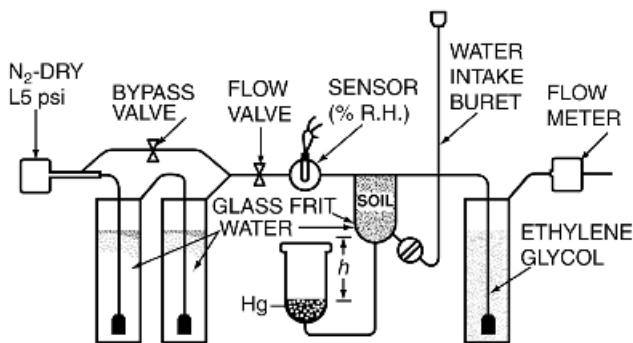


Figure 4.8 Schematic diagram of the apparatus used to measure the rate of pesticide evaporation from soil as influenced by relative humidity of gas moving across the surface of the soil column. The soil column was 5.8 cm in diameter and 10 cm deep. [Reproduced from W. F. Spencer and M. M. Cliath, *J. Environ Qual.* **2**, 285 (1973) by permission of the American Society of Agronomy, Crop Science Society of American and Soil Science Society of America.]

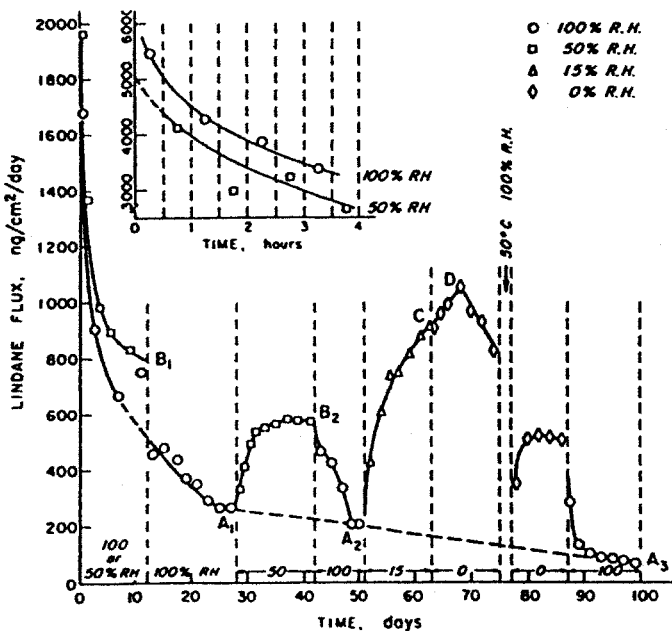


Figure 4.9 Rate of evaporation of lindane from soil at 30°C as a function of relative humidity of nitrogen passing over the soil surface—lindane concentration in the soil, 10 ppm. [Reproduced from W. F. Spencer and M. M. Cliath *J. Environ. Qual.* 2, 285 (1973) by permission of the American Society of Agronomy, Crop Science Society of America and Soil Science Society of America.]

This conclusion is confirmed by the fact that the calculated flux would be $356 \text{ ng} \cdot \text{cm}^{-2} \cdot \text{day}^{-1}$ based on water movement through the soil at 50% RH of $0.274 \text{ mL} \cdot \text{cm}^{-2} \cdot \text{day}^{-1}$ and a C_e of $1300 \text{ ng} \cdot \text{mL}^{-1}$ in equilibrium with a soil concentration of $10 \mu\text{g} \cdot \text{g}^{-1}$. Reducing the relative humidity to 15% increased the water movement to $0.501 \text{ mL} \cdot \text{cm}^{-2} \cdot \text{day}^{-1}$ and the mass transport of Lindane to $651 \text{ ng} \cdot \text{cm}^{-2} \cdot \text{day}^{-1}$. Note that with dry nitrogen the flux increased to a point, *D*, and then decreased, which was doubtless due to the soil surface drying out increasing the sorption. Thus evaporation of a compound incorporated in soil will depend first on diffusion through the soil and mass transport to the surface in the soil water when the water is evaporating. Both processes are influenced by properties of the soil and the chemical.

Evaporation of a compound from a moist soil is dependent on sorption as defined by K_d and distribution between water and air defined by H' . How these parameters can influence evaporation of compounds incorporated in soil is demonstrated by the comparison of the response of Lindane and a triazine herbicide, prometone.¹⁴ These two compounds were incorporated in a sandy loam (0.72%OC) at concentrations of 3.0 and $10.3 \mu\text{g} \cdot \text{g}^{-1}$, respectively and the rate of evaporation monitored in a system comparable to that illustrated in Figure 4.8. A comparison was made between

TABLE 4.8 Properties of Prometone and Lindane

Property	Prometone	Lindane
$S_w \text{ g} \cdot \text{L}^{-1}$	7.5	0.075
H'	1.0×10^{-7}	1.33×10^{-4}
$K_{oc} \text{ (mL} \cdot \text{g}^{-1}\text{)}$	305	1300
$K_d \text{ (0.72\%OC)}$	2.2	9.36
$C_s \text{ } \mu\text{g} \cdot \text{g}^{-1}$	10.3	3.0
$C_e \text{ } \mu\text{g} \cdot \text{mL}^{-1}$	4.68	0.32
Vap. Dens. ($T = 0$) $\mu\text{g} \cdot \text{L}^{-1}$	4.5×10^{-4}	0.0426

no water evaporating, $-E$ (RH, 100%) and water evaporating, $+E$ (RH, 42.5%). Properties of these two compounds along with related experimental values are summarized in Table 4.8. With both Lindane and prometone, the rate of evaporation is higher when water is evaporating and mass transport is involved in moving the

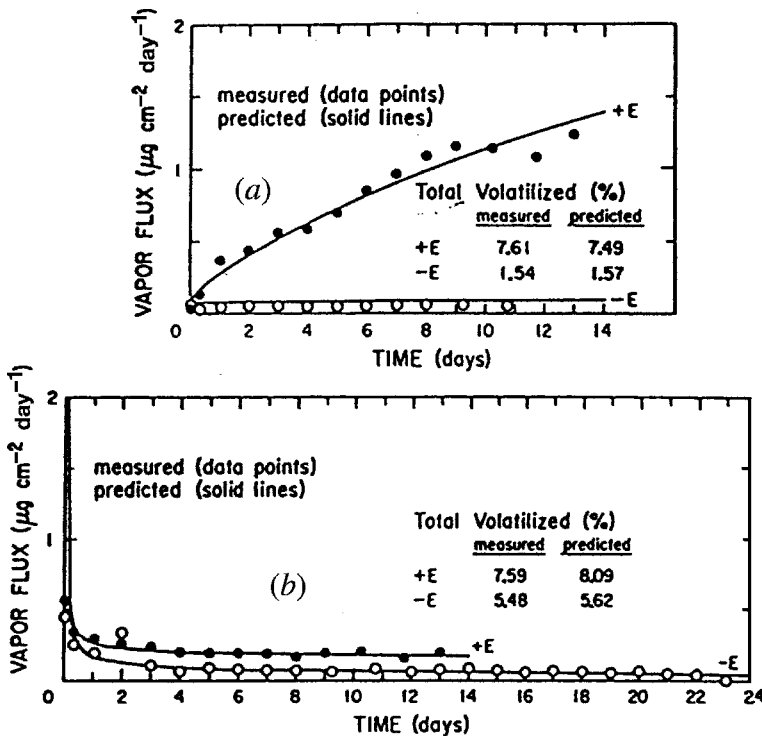


Figure 4.10 Evaporation of prometone (a) and lindane (b) from San Joaquin sandy loam with ($+E$) and without ($-E$) water evaporation. [Reproduced from W. F. Spencer, M. M. Cliath, W. A. Jury, and L. Zhang, *J. Environ. Quality* 17, 504 (1988) by permission of the American Society of Agronomy, Crop Science Society of America and Soil Science Society of America.]

compound to the surface (Fig. 4.10), however, the rate of evaporation of prometone increases with time in direct contrast to Lindane. The reason for this difference can be seen in Figure 4.11 where the distribution in the soil column after 14 days is given.

The concentration of prometone at the surface has increased eightfold over the initial concentration, which would result in a commensurate increase in the vapor density over the soil. This increase in the concentration at the soil surface results from limited evaporation from the surface (low H' and low K_d), while the rate of mass transport to the surface is higher (low K_d and a higher C_e). By contrast, with lindane mass transport to the surface is limiting relative to evaporation from the surface (higher H' and higher K_d). Mathematical models have been developed to simulate this process (represented by lines in the figures) but will not be discussed in this analysis where the focus is on the properties of the chemical in relation to its environmental behavior.

4.3.4 Field Studies

It can be seen that the rate of evaporation from soil under field conditions would be a complex process being influenced by the properties and location of the chemical, the

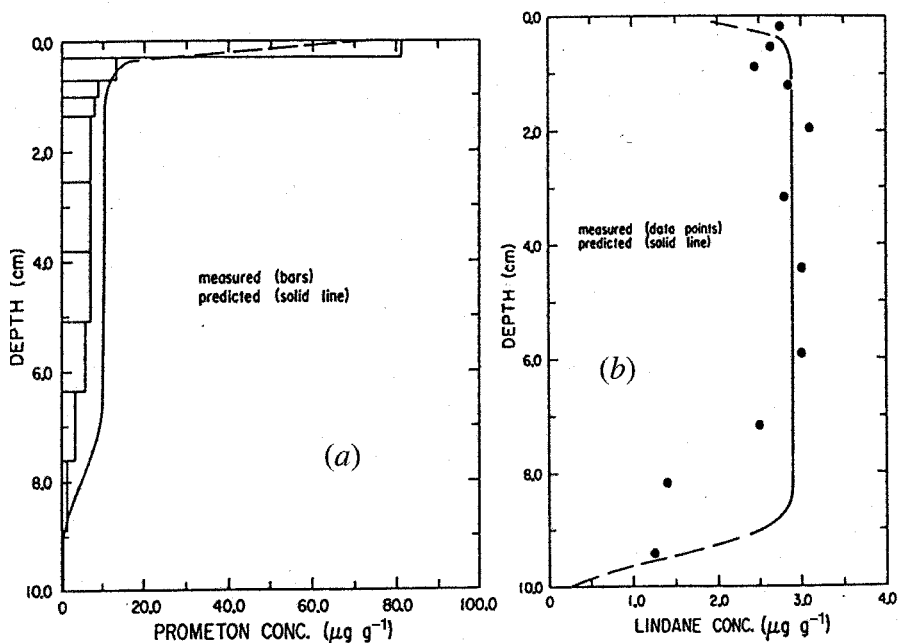


Figure 4.11 Distribution of prometone (a) and lindane (b) in soil after 14 days with water evaporating at $0.55 \text{ cm} \cdot \text{day}^{-1}$. [Reproduced from W. F. Spencer, M. M. Cliath, W. A. Jury, and L. Zhang, *J. Environ. Quality* **17**, 504 (1988) by permission of the American Society of Agronomy, Crop Science Society of America and Soil Science Society of America.]

structure, and composition of the soil and meteorological variables such as temperature, wind speed, and moisture. The evaporation of pesticides, particularly herbicides, has been studied because movement from site of application could result in damage to sensitive plants. A study of the atmospheric movement of the herbicide dimethyl, 2,3,5,6-tetrachloroterephthalate, commonly known as Dacthal or DCPA has provided quantitative information under field conditions.¹¹ The aqueous solubility of DCPA is 0.5 ppm and the Henry' law constant, $2.2 \text{ atm} \cdot \text{m}^3 \cdot \text{mol}^{-1}$. The herbicide was applied to an experimental plot of onions at the rate of 7.08 kg/acre and air samples taken downwind up to 21 days after application. The air first passed through a fiberglass filter to remove particles, then through a resin to trap chemical in the vapor phase.

Under dry conditions a higher proportion of the DCPA was detected in the particles, however, after irrigation the total amount detected in the sampler increased as did the proportion in the vapor phase (Table 4.9). This observation is consistent with laboratory studies of the effect of soil moisture on evaporation from the soil surface. It was estimated that over the 21-day experimental period, evaporative flux from the treated area accounted for $\sim 10\%$ of the herbicide applied.

TABLE 4.9 Concentration of DCPA in Air 30 m Downwind of the Experimental Plot

Day ^b	Hour ^c	Irrigation ^d	Concentration (ng m ⁻³) ^a			F/T ^e Ratio
			Resin	Filter	Total	
0	0835–1000		290	420	710	0.59
0	1030–1300		35	150	185	0.81
0	1315–1630		71	48	119	0.40
1	1230–1530	X	910	100	1010	0.10
1	1720–1920	X	260	41	301	0.14
2	1000–1300		150	52	202	0.26
2	1400–1730		22	18	40	0.45
3	1350–1700		47	210	257	0.82
4	1510–1840	X	200	120	320	0.38
8	1035–1535	X	320	24	344	0.07
11	1235–1635	X	61	6	67	0.09
14	1110–1530	X	270	49	319	0.15
21	1014–1415		33	15	48	0.31

Source: Reproduced from *J. Environ Qual.* **19**, 715 (1990) by permission of the American Society of Agronomy, Crop Science Society of America and Soil Science Society of America.

^aConcentrations are an average of two replicate samples except for the sample taken on Day 1 at 1230, which is a single measurement.

^bDays after application.

^cAir sampling interval.

^dAn "X" indicates irrigation occurred just prior to air sampling.

^eRatio of filter to total concentration.

Evaporative losses from the soil surface can be quite large. For example, 50% of the heptachlor applied to a moist silt loam evaporated in only 6 h,¹⁵ whereas on the dry soil the loss was reduced to 40% in 50 h. However, if the compound is incorporated to 7.5 cm in the soil, only 7% was lost in 170 days.¹⁶

4.4 EVAPORATION AND ATMOSPHERIC DISTRIBUTION

Compounds that evaporate into the atmosphere are subject to atmospheric processes, which may result in deposition through rain-out or gaseous exchange or distribution through the movement of air masses. It is appropriate to provide some illustration of these phenomena to emphasize the importance of understanding the significance of the evaporation transition. An example at a regional level is provided by the study of the extent to which agricultural chemicals used in the Central Valley of California move east into the Sierra Nevada mountains.¹⁷ This study was carried out during the summer when chemical use is high and when the atmospheric conditions favored movement to the east. Gas-phase samples were taken at higher elevations and atmospheric concentrations observed for several compounds are summarized in Table 4.10. For the most part, the levels detected corresponded to the use patterns and decrease with distance from site of application. Note that chlorpyrifos is oxidized to the oxon in the atmosphere and this derivative predominates in air samples. The lowest sampling site was adjacent to citrus groves, however, the Ash Mtn. site was 18 km to the east and the highest sampling site a further 7–8-km east. The tendency of compounds to evaporate and move to higher altitudes is demonstrated by this study. Note that although the concentrations detected were low, they were well above the detection limits that

TABLE 4.10 Pesticide Concentrations (ng · m⁻³) in Air

Location	Date	Trifluralin	Chlorpyrifos	Chlorpyrifos oxon
Kaweah Reservoir—200 m	5/30	0.27	n.d. ^a	30.4
	6/25	0.18	17.5	4.89
	7/10	0.13	2.1	11.7
	8/16	0.13	1.08	6.04
	9/21	0.64	2.14	18.8
Ash Mountain—533 m	5/30	0.17	1.71	2.86
	6/25	0.03	0.9	0.94
	7/10	0.07	0.05	0.52
	9/21	0.27	0.22	1.74
Lower Kaweah—1920 m	7/10	0.13	0.35	1.17
	8/16	0.28	0.16	0.19
	9/21	0.25	0.2	0.1
Detection limits, ng · m ⁻³		0.0016	0.0005	0.0008

^anot detected

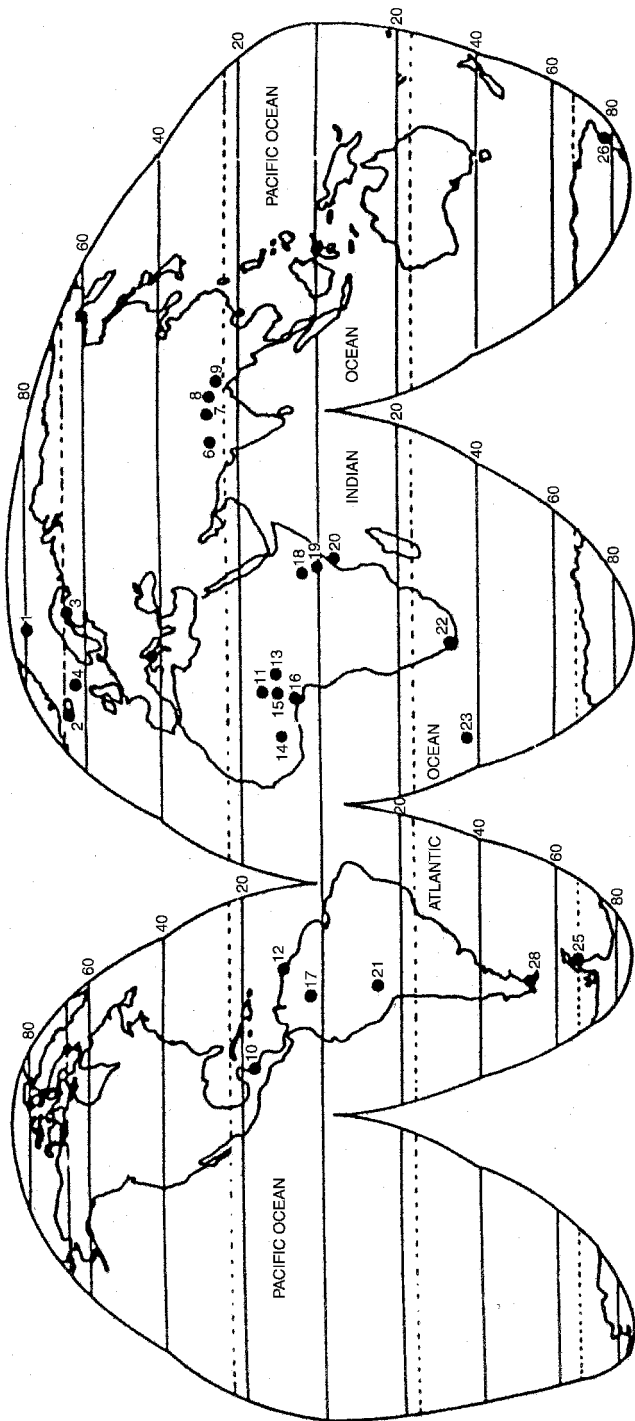


Figure 4.12 Geographical distribution of the 26 sampling sites. [Reproduced with permission from D. Calamari, et al., *Environ. Sci. Technol.* **25**, 1489 (1991). Copyright © 1991, American Chemical Society.]

emphasizes the need for sensitive analytical technology to produce reliable data. These compounds could also be detected at the ppt level in surface waters, in some cases, to an elevation of 3322 m.

The PCB levels have become a concern¹⁸ in the Great Lakes, the largest fresh water body in the world, and the management of these levels depends on the development of an understanding of the environmental dynamics of these compounds. A large surface is involved and removal processes in the lakes are minimal. Determination of the concentration of these contaminants in air and water and estimates of input rates by different processes have provided the data for the development of mass balance models.¹⁹ This analysis indicates that atmospheric deposition, both rain-out and direct gaseous exchange account for 58–91% of the input in the three upper lakes (Superior, Huron, and Michigan). It is also projected that evaporation is the primary loss process from the lakes. Evaporation and regional transport is thus taken to a much larger scale.

Distribution of persistent compounds on a global scale has been evaluated in a study¹⁹ of 306 foliage samples taken from 26 locations ranging from latitude 78°N to 74°S (Fig. 4.12). Chlorinated hydrocarbons, hexachlorobenzene, DDT and metabolites, and hexachlorocyclohexanes, were analyzed in mango leaves from tropical locations and lichens and mosses at higher latitudes. Different distribution patterns were observed for each series depending on transport characteristics in relation to geographical use patterns. The distribution of hexachlorobenzene with latitude (Fig. 4.13) was most striking with little being detected in the tropics and higher levels observed in polar regions. This compound would evaporate at a higher

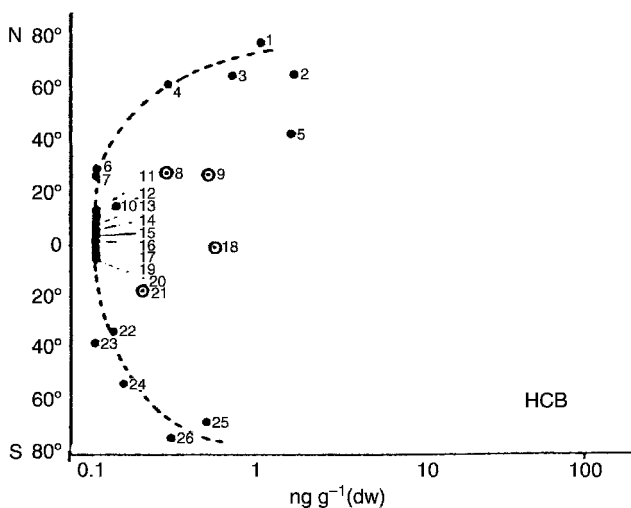


Figure 4.13 Distribution of hexachlorobenzene (HCB) in the 26 sampling sites as a function of latitude. Circled points represent mountain sites. [Reproduced with permission from D. Calamari et al., *Environ. Sci. Technol.* **25**, 1489 (1991). Copyright © 1991, American Chemical Society.]

TABLE 4.11 Mobility of Persistent Organic Pollutants

Transport behavior	Immobile Retained close to the source	Low mobility Condense at mod. temp.; mid-latitudes	Mod. mobility Condense at low temp. (polar)	Mobile General atmos. distribution
log K_{oa}	>10	8–10	6–8	<6
P_{scl} (Pa)	<0.00001	0.0001–0.01	0.01–1	>1
Chlorobenzenes			5–6 Cl	0–4 Cl
PCBs	8–9 Cl	4–8 Cl	1–4 Cl	0–1 Cl
Organochlorine pesticides	Mirex	DDT, toxaphene, chlordan	HCB, hexachlor cyclohexane	

rate in warmer locations and would tend to condense, or more correctly distribute from air to water or foliage at lower temperatures. In fact the outliers from sampling sites 8, 9, 18, and 21 were from Nepal mountains, Everest, Mount Kenya, and Bolivia at elevations of 3000 m and higher. Deposition could be correlated with temperatures of the sampling sites. In fact one can observe “global fractionation” of persistent organic pollutants (POPS) based on their tendency to distribute into the atmosphere (K_{OA} and vap pressure and H) and condensation temperature (Table 4.11).²⁰ Compounds with high K_{oa} would have a low tendency to distribute into the atmosphere and would be essentially immobile by this mechanism. By contrast compounds of higher vapor pressure and lower K_{oa} would have little tendency to condense and would persist in the atmosphere providing they were resistant to degradation like the freons. Compounds with vapor pressures and K_{oas} between these extremes can distribute into the atmosphere and the distance they move would be determined by their stability and the temperature required for condensation. A good illustration of this phenomenon is the observation that in polar regions, trichlorobiphenyls consist of better than 40% of the PCBs detected in air samples.²¹

REFERENCES

1. F. Wania and D. Mackay, *Environ. Sci. Technol.* **30**, 390A (1996).
2. G. S. Hartley, “Evaporation of Pesticides”, in *Pesticidal Formulation Research—Physical and colloidal Aspects*, Advances in Chemistry Series, 86, American Chemical Society, Washington, D.C., 1969, pp. 115–134.
3. C. T. Chiou, V. H. Freed, L. J. Peters, and R. L. Kohnert. *Environ. Internat.* **3**, 231 (1980).
4. R. E. Rathbun and D. Y. Tai, *Water Res.* **15**, 243 (1981).
5. F. Acree, M. Beroza, and M. C. Bowman. *J. Agric. Food Chem.* **11**, 278 (1963).
6. C. T. Chiou and M. Manes. *Environ. Sci. Technol.* **14**, 1253 (1980).
7. F. M. Dunnivant and A. W. Elzerman. *Chemosphere* **17**, 525 (1988).

8. P. S. Liss and P. G. Slater. *Nature* (London) **247**, 181 (1974).
9. R. P. Schwarzenbach, P. M. Gschwend, and D. M. Imboden, *Environmental Organic Chemistry*, John Wiley & Sons Inc., New York, 1993, p. 220.
10. W. F. Spencer, W. F. Farmer, and M. M. Cliath. *Residue Rev.* **49**, 1 (1973).
11. L. J. Ross, S. Nicosia, M. M. McChesney, K. L. Hefner, D. A. Gonzalez, and J. N. Seiber, *J. Environ. Quality* **19**, 715 (1990).
12. W. J. Farmer, K. Igue, W. F. Spencer, and J. P. Martin. *Soil Sci. Soc. Amer. Proc.* **36**, 443 (1972).
13. W. F. Spencer and M. M. Cliath. *J. Environ. Quality* **2**, 284 (1973).
14. W. F. Spencer, M. M. Cliath, W. A. Jury and L. Zhang, *J. Environ. Quality*, **17**, 504 (1988).
15. D. E. Glotfelty, A. W. Taylor, B. C. Turner, and W. C. Zoller. *J. Agr. Food Chem.* **32**, 638 (1984).
16. A. W. Taylor, D. E. Glotfelty, B. L. Glass, H. P. Freeman, and W. M. Edwards. *J. Ag. Food Chem.* **24**, 625 (1976).
17. J. S. LeNoir, L. L. McConnell, G. M. Fellers, T. M. Cahill, J. N. Seiber, *Environ. Toxicol. Chem.* **18**, 2715 (1999).
18. S. J. Eisenreich, B. B. Looney, and J. D. Thornton, *Environ. Sci. Technol.* **15**, 30 (1981).
19. D. Calamari, E. Bacci, S. Focardi, C. Gaggi, M. Morosini, and M. Vighi, *Environ. Sci. Technol.* **25**, 1489 (1991).
20. F. Wania and D. Mackay, *Environ. Sci. Technol.* **30**, 390A (1996).
21. G. A. Stern, C. J. Halsall, L. A. Barrie, D. C. G. Muir, P. Fellin, B. Rosenberg, F. Y. Rovinsky, E. Y. Kononov, and B. Pastuhov, *Environ. Sci. Technol.* **31**, 3619 (1997).

Absorption and Bioconcentration

Physical chemical properties control the distribution of an organic chemical between environmental compartments; air, water, and soil. This analysis must also address the factors that determine the extent to which a compound can move into biota since this process can also influence distribution. For example, human exposure to dioxins results primarily from deposition of these compounds on plants that are consumed by animals that in turn provide milk or meat for human consumption. The key step is defining the extent to which a compound moves across a biological membrane that constitutes the boundary between the organism and its environment. For example, uptake of compounds by plants through the foliage or root system is of significance both to those interested in using plants to clean up contaminated soils and those interested in using chemicals to control undesirable plants. The pharmacologist and toxicologist must also consider absorption since the uptake through skin, intestine, or lungs determines both the therapeutic response to a drug or the toxicological effect of some compound in the environment. Consequently, the fundamentals of absorption are both developed and applied in these different fields.

This topic will be developed by first outlining the structural features of a biological membrane and discussing the different mechanisms involved in transporting compounds across this barrier. The extent to which absorption is influenced by the properties of the compound will be illustrated by considering both animal and plant systems. Some compounds can absorb and accumulate, particularly in aquatic organisms, and the requirements for this to occur will be considered.

5.1 ABSORPTION

5.1.1 Membranes

5.1.1.1 Structure Our understanding of the composition, structure, and function of biological membranes has developed rapidly in recent years. Not only do these cellular components influence uptake of nutrients, but they also play significant roles in communication between cells. In this discussion, however, the focus will be on the involvement of the membrane in the uptake of xenobiotics. The

primary transport barrier of a biological membrane is the phospholipid bilayer (Fig. 5.1).

The phosphate moiety orients toward the hydrophylic environments, while the fatty acid chains give an internal hydrophobic layer. Formation of a bilayer is favored energetically when phospholipids are dispersed in aqueous systems under appropriate conditions. Cholesterol is also a major lipid constituent of membranes that orients with its hydroxyl directed toward hydrophylic environment. The phospholipid composition will vary depending on the source of the membrane, however, the bilayer must exist in a liquid-crystal configuration for optimum biological activity. This means that the hydrophylic phosphate components provide some order to the structure while the hydrocarbon chains of the fatty acids assume a more random configuration that approaches the form of a liquid. Chain length and degree of unsaturation as well as the proportion of cholesterol are important in controlling the ability of the membranes to assume this configuration. Movement through a membrane thus involves passage across this hydrophobic barrier. Many other functions associated with the membrane involve proteins embedded in the bilayer, and other components on the membrane surface. Some of the proteins distribute across the bilayer facilitating the transfer of messages across the membrane.

5.1.1.2 Transport Processes A pure phospholipid bilayer is permeable to water and to small uncharged polar molecules such as urea and ethanol. It is not permeable to ions or large uncharged polar molecules. Nonpolar molecules of environmental significance can move down a concentration gradient across a membrane and the process is referred to as passive diffusion. By contrast, active transport, an energy requiring process, involves movement through a membrane against a concentration gradient and is observed with sodium, potassium, and calcium cations, which are important to cellular function. Some molecules have been observed to move across membranes at rates greater than might be expected for simple diffusion and it has been established that specific transport proteins are responsible for the facilitated transport. For example, uptake of glucose and bicarbonate ion by the red blood cell involves such a mechanism. This process is quite specific and shows a maximum rate when the system is saturated.

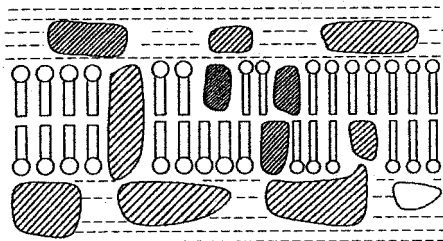
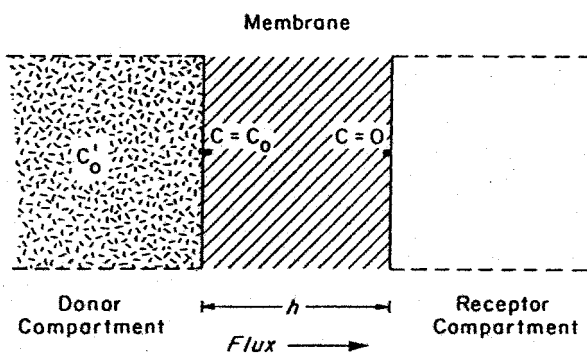


Figure 5.1 Schematic representation of a biological membrane illustrating the barrier produced by the phospholipid bilayer.

5.1.1.3 Fick's Laws and Membrane Flux Since compounds of environmental significance cross biomembranes only by passive diffusion, it is of interest to define those factors that control the flux through the membrane in order to assess which properties of the chemical may be significant. Fick's first law states that the flux, J , in mass per unit area per unit time is proportional to the concentration differential.

$$J = -D(dC/dt)$$

which according to the schematic would be $(C_o - C)$. The negative sign indicates that the mass flow is in the direction of decreasing concentration and D , the diffusivity with units of $L^2 \cdot t^{-1}$ (often $cm^2 \cdot s^{-1}$), a proportionality constant. For diffusion through a field of unit thickness, the diffusivity corresponds to the average distance the diffusing



particle travels in unit time in the direction of flow. Fick's second law states that the rate of change of concentration in a small volume within the membrane through which the compound is diffusing is proportional to the rate of change of the concentration gradient at that point:

$$dC/dt = D d^2C/dx^2$$

with D again representing the diffusivity. With a constant concentration gradient across a membrane and the concentration in the receptor compartment maintained essentially at zero, a solution of the second law provides a relation defining the cumulative mass of compound, M , diffusing through unit area as a function of time.¹ At steady state,

$$M = (DC_o/h)(t - h^2/6D)$$

where C_o would be the concentration of the compound in the donor compartment and h is the thickness of the membrane. Under these conditions, the rate of change of concentration at any point in the membrane is zero and the amount of compound moving

through the membrane is constant

$$dM/dt = DC_o/h$$

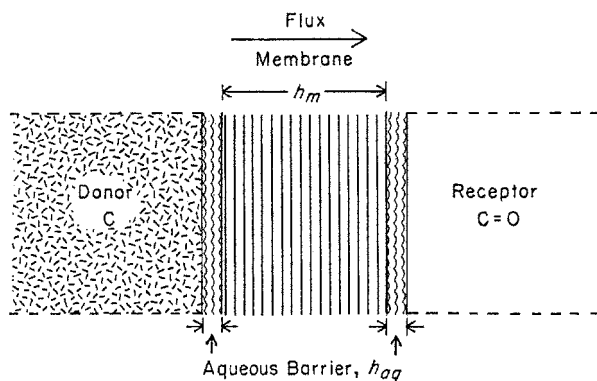
Also, when $M = 0$, the lag time, $t_L = h^2/6D$.

In membrane studies, one measures or controls the concentration, C' , in the aqueous phase adjacent to the membrane and it is assumed that a rapid partitioning determines the concentration, C_o , on the donor side of the membrane and

$$C_o = K_{mw}C'$$

with K_{mw} representing the partition coefficient between water and membrane lipid. In biological systems, it is difficult to determine either D or K_{mw} and permeability is defined as $D \cdot K_{mw}$. Diffusion is often represented as a kinetic process and when C' is maintained constant and the receptor compartment at zero concentration $K_{mw}D/h$ ($\text{cm} \cdot \text{t}^{-1}$) can be conceived as a zero-order rate constant defining the steady-state flux.

In the development of an understanding of what factors influence movement across a membrane, it has been postulated that diffusion barriers could exist on either side of the membrane as depicted in the schematic below.² The total resistance



(inverse of permeability) to movement across the membrane would then consist of three components assuming an aqueous system

$$R_{\text{tot}} = (R_{\text{aq}})_{\text{donor}} + R_m + (R_{\text{aq}})_{\text{receptor}}$$

which then can be expressed as a function of diffusivities and thickness, h , of the different layers.

$$R_{\text{tot}} = \frac{(h_{\text{aq-d}})}{D_{\text{aq}}} + \frac{h_m}{K_{mw}D_m} + \frac{(h_{\text{aq-r}})}{D_{\text{aq}}}$$

The permeability, P , or reciprocal of the resistance, of the system comprised of a membrane between two diffusion layers of equal thickness would be

$$P = \frac{1}{R_{\text{tot}}} = \frac{K_{\text{mw}}D_{\text{m}}D_{\text{aq}}}{h_{\text{m}}D_{\text{aq}} + 2h_{\text{aq}}K_{\text{mw}}D_{\text{m}}}$$

The steady-state flux would then be defined

$$F = P \cdot C = \left[\frac{K_{\text{mw}}D_{\text{m}}D_{\text{aq}}}{h_{\text{m}}D_{\text{aq}} + 2h_{\text{aq}}K_{\text{mw}}D_{\text{m}}} \right] C$$

When $h_{\text{m}}D_{\text{aq}} \gg 2h_{\text{aq}}K_{\text{mw}}D_{\text{m}}$ the flux would be

$$F = \left[\frac{D_{\text{m}}K_{\text{mw}}}{h_{\text{m}}} \right] C$$

indicating membrane control. By contrast, when the reverse is true, $2h_{\text{aq}}K_{\text{mw}}D_{\text{m}} \gg h_{\text{m}}D_{\text{aq}}$, the flux would be

$$F = \left[\frac{D_{\text{aq}}}{2h_{\text{aq}}} \right] C$$

indicating that the movement through the system is controlled in the barrier aqueous diffusion layers. It is apparent that octanol–water partition coefficients would provide reasonable indexes of the tendency to distribute into a biomembrane and compounds with high K_{ow} 's will have low aqueous solubility, and consequently the concentration gradient across the donor aqueous diffusion layer would be expected to be low, limiting diffusion. It can also be demonstrated that the lag time under the conditions of the diffusion layer control is defined

$$t_{\text{L}} = \frac{K_{\text{mw}}h_{\text{m}}h_{\text{aq}}}{2D_{\text{aq}}}$$

Experimental validation of these concepts has been provided by studies of the flux of a homologous series of esters of *p*-aminobenzoic acid through a dimethylpolysiloxane membrane.³ This polymer is a continuous, nonporous, nonpolar membrane, and provides a valid surrogate for a biomembrane in that a partitioning step is required in the permeation process. Saturated aqueous solutions of each ester were maintained in the donor compartment at 37°C and the receptor compartment flushed continuously while monitoring the amount of compound moving across the membrane. The cumulative flux through the membrane is illustrated in Figure 5.2. The steady-state flux in mass per unit time would be the slope of these lines and lag times are apparent. The properties of the *p*-aminobenzoate esters are tabulated in Table 4.1 along with steady-state fluxes and lag times using membranes 476 and 126 μm thick. The steady-state flux decreases with increasing ester chain length (C₃–C₇), however, this response reflects primarily the decrease in solubility.

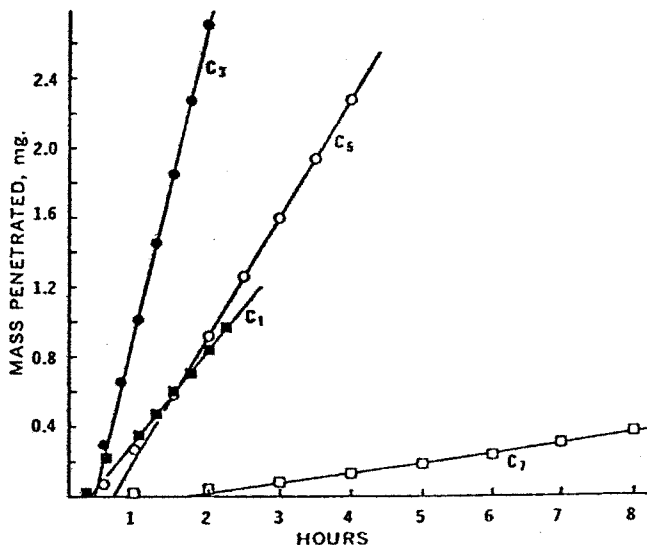


Figure 5.2 Cumulative flux of alkyl esters of *p*-aminobenzoic acid through a synthetic dimethylpolysiloxane membrane. [Reproduced from G. L. Flynn and S. H. Yalkowsky, *J. Pharm. Sci.*, **61**, 838. Copyright 1972. This material is used by permission of Wiley-Liss Inc., a subsidiary of John Wiley & Sons, Inc.]

The reverse effect is observed when a comparison is made at a constant donor concentration of 1 mM. In some cases, this value is artificial since the solubility of some esters is < 1 mM. The question to address is whether these data can provide a basis for discriminating between the membrane and diffusion layer control. With the former process one would predict a linear relation between $\log F$ and $\log K_{ow}$ (a surrogate for K_{mw}) and from Figure 5.3 it can be seen that this occurs through about

TABLE 5.1 Steady-State Flux of Esters of *p*-Aminobenzoic Acid across a Dimethylpolysiloxane Membrane

Ester	S_w (mM)	$\log K_{ow}^a$	Flux at S_w ($m \cdot mol h^{-1}$) (476 μm)	Flux at 1 mM ($m \cdot mol h^{-1}$)		t_L (min)	
				476 μm	126 μm	476 μm	126 μm
C-1	25.3	1.47	2.46×10^{-3}	0.097×10^{-3}		19.5	
C-2	10.2	2.00	6.24×10^{-3}	0.612×10^{-3}		22.5	
C-3	4.70	2.41	7.82×10^{-3}	1.66×10^{-3}		20	
C-4	1.72	2.94	7.25×10^{-3}	4.22×10^{-3}		16.5	
C-5	0.39	3.52	3.15×10^{-3}	8.08×10^{-3}	11.5×10^{-3}	41.5	6.5
C-6	0.104	3.94	1.10×10^{-3}	10.6×10^{-3}	8.75×10^{-3}	71	18
C-7	0.020	4.45	0.26×10^{-3}	13.0×10^{-3}	11.5×10^{-3}	125	33

^aCalculated from S_w .

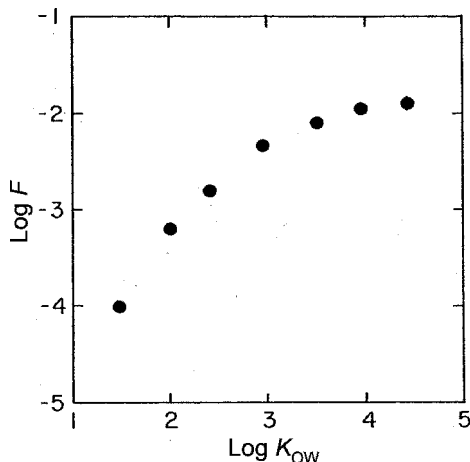


Figure 5.3 Concentration normalized flux through the 476- μm polysiloxane membrane as a function of octanol–water partition coefficient (see Table 5.1).

C-3 ($\log K_{ow} = 2.41$) after which the flux tends to level off. At this point, one would assume that diffusion through the aqueous barrier layers becomes the limiting factor. This conclusion is supported by the observation that with C-5–C-7 esters the flux is not affected to any large degree by reducing the width of the membrane by a factor of 3.8. If diffusion in the membrane were controlling, one would predict a proportionate increase in flux, however, with control in the aqueous diffusion layers, flux would be independent of the width of the membrane. With this series of compounds there will only be small differences in D_{aq} . Consequently, flux, defined by D_{aq}/h_{aq} , across the donor aqueous layer will be relatively constant (C-5–C-7). Since K_{mw} will increase with increase in ester chain length, and with membrane control, the concentration gradient across the membrane will increase resulting in an increase in flux. At some point, the flux through the donor aqueous layer will become limiting resulting in a transition from membrane control-to-barrier layer control.

Consideration of lag times also supports the conclusion of a transition from membrane to diffusion layer control. With membrane control the lag time is a function of h_m and D_m . With h_m a constant and little change in D_m expected in this series, one might expect only small changes in t_L if membrane control were in effect. This observation is made with C-1–C-4 esters. However, t_L increased consistently from C-5–C-7 consistent with the influence of K_{mw} on t_L under diffusion layer control. Also, the change in membrane thickness should also result in a proportionate change in t_L that is observed with the C-6 and C-7 esters. It would appear that with the C-5 ester some membrane involvement persists since under diffusion layer control we would predict from observations with the 126- μm membrane that t_L should be $6.5 \times 3.8 = 25$ min for the 476- μm membrane: this value is less than the observed value. On the other hand, with membrane control, the t_L predicted

is higher than that observed

$$t_L(476 \mu\text{m}) = (476)^2 / (126)^2 t_L(126 \mu\text{m}) = 14 \times 6.5 = 91 \text{ min}$$

These studies with a polymeric membrane validate this barrier model. It is clear that the tendency to partition into the membrane will influence flux through the membrane and one might anticipate that the octanol–water partition coefficients will be useful predictors of absorption. However, if this model applies in biological systems, one would not expect to observe this relation at higher values of K_{ow} . With weak acids and bases the neutral form would move across a membrane more readily than its charged counterpart, and, consequently, one would predict that variation in environmental pH will influence the uptake of these compounds. Also, if the environmental pH is relatively constant, such as is observed, say in the stomach, or small intestine, the pK_a of the acid or base will determine the proportion in the neutral form at that pH and, hence, the absorption efficiency. These relations will be illustrated with examples from studies in animals and plants.

5.1.2 Absorption in Animals

In animals, absorption is often studied *in vivo*, by exposing the animal and monitoring the levels of compound appearing in the circulatory system. On occasion *in vitro* studies are carried out using, say a small sample of excised skin. Absorption studies are important to a pharmacologist where the efficacy of a drug is dependent on its uptake and to a toxicologist where the toxic response is also dependent on how much gets into the animal.

5.1.2.1 Absorption Through the Gills of Fish The efficiency with which compounds are absorbed across the gills of fish was determined in a system that enabled the investigators to monitor the levels of compound in the inspired and expired water of exposed trout.⁴ Note that the exposure levels were well below reported solubilities and the compounds represented different chemical classes (Table 5.2). Uptake efficiency is expressed as a function of $\log K_{ow}$ in Figure 5.4. An estimate of daily gill transport was calculated using an estimate of the volume of water moving through the gills. The uptake efficiency of the three lower molecular weight compounds is not related to partition coefficient and it is proposed that these molecules are small enough and sufficiently soluble to diffuse through the aqueous pores of the membrane. As $\log K_{ow}$ increases to ~ 3 , uptake efficiency increases in a manner consistent with what might be expected with membrane control. With $\log K_{ow}$ increasing from 3 to 6, uptake efficiency remains constant suggesting a transition to aqueous diffusion layer control indicating that the barrier model can explain the responses observed. The uptake efficiency of mirex was considerably lower than that of the hexachlorobenzene although the exposure concentrations of the two compounds were comparable. The response of the pyrethroid compound, fenvalerate, was similar. It is suggested that the size of these molecules could account for the

TABLE 5.2 Compounds Used in Study of Transport across Trout Gills

Compound	MW	Log K_{ow}	S_w (M)	Exp. Conc. (M)
Ethyl formate (A) ^a	74.08	0.23	1.19	3.7×10^{-8}
Ethyl acetate (B)	88.10	0.73	0.91	3.6×10^{-8}
<i>n</i> -Butanol (C)	74.10	0.85	1.06	2.5×10^{-8}
Nitrobenzene (D)	123.1	1.85	1.7×10^{-2}	2.3×10^{-8}
<i>p</i> -Cresol (E)	108.1	2.00	1.7×10^{-2}	3.5×10^{-8}
Chlorobenzene (F)	112.6	2.84	4.3×10^{-3}	3.9×10^{-9}
2,4-Dichlorophenol (G)	163.0	2.93		5.5×10^{-8}
Decanol (H)	158.3	3.09	2×10^{-4}	3.2×10^{-8}
Pentachlorophenol (I)	266.4	3.32	6.4×10^{-5}	4.1×10^{-10}
2,4,5-Trichlorophenol (J)	197.5	3.70		2.3×10^{-8}
Dodecanol (K)	186.3	5.10	1×10^{-5}	9.3×10^{-9}
2,5,2',5'-Tetrachlorobiphenyl (L)	292.0	6.00	9×10^{-8}	9.7×10^{-10}
Hexachlorobenzene (M)	284.8	6.18	1.9×10^{-8}	4.5×10^{-11}
Fenvalerate (N)	419.9	5.01	4.76×10^{-9}	
Mirex (O)	545.6	7.50	1.3×10^{-10}	5.2×10^{-11}

^aSee Figure 5.4.

lower flux. The mechanism controlling movement through this membrane is not chemical specific given the wide range of classes studied.

5.1.2.2 Absorption Through Skin This exposure route can be important for animals and studies with this system also illustrate the relation between absorption flux and properties of the compound. The skin is a very complex system, providing a

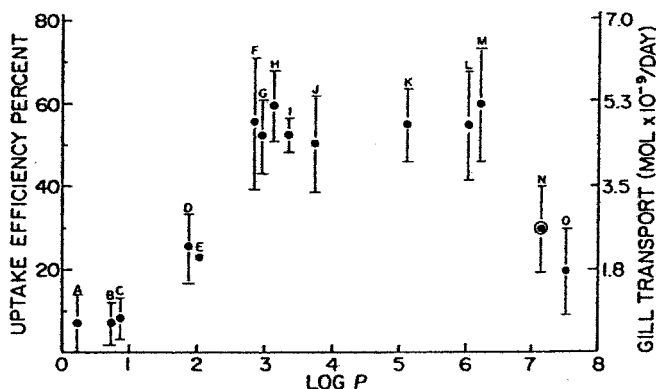


Figure 5.4 The gill uptake efficiency and 24-h gill transport of selected organic chemicals as related to their octanol–water partition coefficients. [Reprinted from *Toxicol. Appl. Pharmacol.*, 77, J. McKim, P. Schmieder, and G. Veith, “Absorption dynamics of organic chemical transport across trout gills as related to octanol–water partition coefficient” p. 1. Copyright 1985, with permission from Elsevier.]

sequence of barriers for a chemical to traverse. The chemical must first diffuse through the stratum corneum, a thin outer layer of flattened, keratinized cells, which is characterized by a lipid-rich intercellular matrix. The epidermis is composed of viable cells that provide a more hydrophylic environment. Having diffused through these two layers, a compound moves into the dermis and the circulatory system. The penetration of a series of para-substituted phenols through mouse skin has been studied *in vitro*.⁵ The compound was applied in a small volume of solution to the stratum corneum at the rate of $4 \mu\text{g} \cdot \text{cm}^{-2}$ and the appearance of the compound in the receptor compartment is monitored. The maximum flux expressed as $\% \text{ dose} \cdot \text{h}^{-1}$ is given in Figure 5.5 as a function of $\log K_{ow}$. The initial increase in flux with an increase in K_{ow} can be interpreted as membrane control. However, with increasing K_{ow} it is suggested that movement through the more hydrophylic epidermis becomes limiting as the concentration gradient across this layer decreases. Statistical analysis provides an empirical relation between maximum flux and K_{ow} for this series of compounds.

$$\log J_{\max} = -0.18 + 1.35K_{ow} - 0.30(K_{ow})^2 \quad r^2 = 0.92$$

Studies in different membrane systems thus have demonstrated that flux does increase with the potential to distribute into the membrane as indicated by K_{ow} , however, one often observes that this increase occurs over a small range because of a change in the limiting process.

5.1.2.3 Absorption Through the Gastrointestinal System The major components of this system that are of interest in the absorption of chemicals are

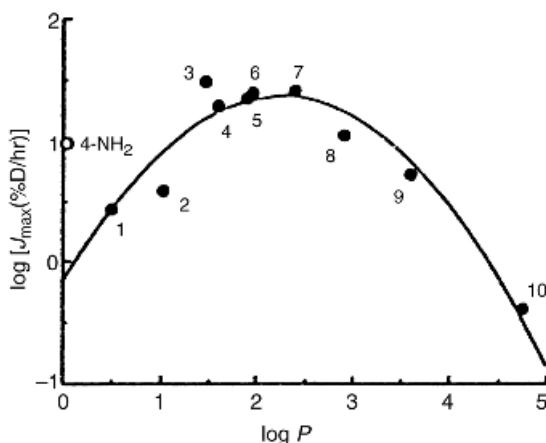


Figure 5.5 Maximum penetration rate, J , as a function of octanol–water partition coefficient, P . (1) acetamidophenol; (2) 4-propionamidophenol; (3) phenol; (4) 4-cyanophenol; (5) 4-nitrophenol; (6) 4-methylphenol; (7) 4-chlorophenol; (8) 4-iodophenol; (9) 4-pentyloxyphenol; (10) 4-heptyloxyphenol. [Reproduced with permission from R. S. Hinz, C. R. Lorence, C. D. Hodson, C. Hansch, L. L. Hall, and R. H. Guy, *Fundam. Appl. Toxicol.* **17**, 575. Copyright 1991, Society of Toxicology.]

the stomach and the small intestine, with the latter being the more important because of the large surface it provides. This absorption pathway has been studied extensively by pharmacologists since many pharmaceuticals are administered by this route. An interesting feature of this system is the large variation in pH that exists. The stomach maintains a pH of ~ 2 , while the small intestine shows a pH of ~ 6 . Uptake from the gastrointestinal (G.I.) tract is also dependent on the tendency to distribute into the membrane. With weak acids and bases the neutral species would be absorbed rather than its charged counterpart. Consequently, the pK_a will determine whether a compound might be absorbed more readily in the stomach or the intestine since it will control the neutral/ionic ratio at a given pH. Data summarized in Table 5.3 illustrates how uptake of acids and bases through the rat intestine is influenced by their pK_a 's.⁶

The response of the acids is surprising in that significant uptake is observed despite the fact that only a small proportion of the compound exists in the neutral form. This could be attributed to the fact that this is an open system and the compound is taken away by the circulation as soon as it crosses the membrane. An "ion trap" effect may be of more significance. For example, in the case of a weak acid ($pK_a = 3$), when there is a pH differential across a membrane and only the neutral species moves across that membrane, under equilibrium conditions, it can be seen that ions are "trapped" in the compartment where the pH favors the production of the anion (i.e., where the $pH > pK_a$). Since the pH of the circulating

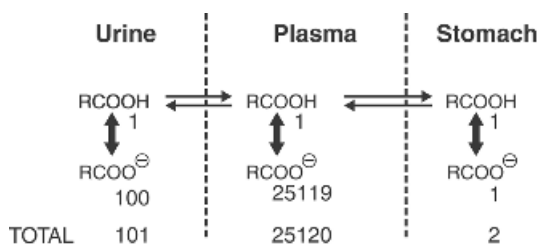


TABLE 5.3 Absorption of Acids and Bases Through the Rat Intestine

Compound	pK_a	% Absorbed	% Neutral, pH 5.3
<i>o</i> -Nitrobenzoic acid	2.2	5	~ 0.1
5-Nitrosalicylic acid	2.3	9	~ 0.1
Salicylic acid	3.0	60	~ 0.5
<i>m</i> -Nitrobenzoic acid	3.4	53	1
Benzoic acid	4.2	51	10
<i>p</i> -Nitroaniline	1.0	68	100
Aniline	4.6	54	83
Aminopyrine	5.3	33	50
Quinine	8.4	15	0.1
Ephedrine	9.6	7	0.01

system (the receptor compartment), pH 7.4, is higher than that of the stomach (the donor compartment), pH 3.0, the movement of a weak acid to the circulation would be favored. The ion-trap effect would not be as pronounced from the small intestine that has a pH \approx 6, yielding a smaller pH differential. By contrast, movement from plasma to urine (pH 5), which is important for excretion, would be less than for stomach to plasma. The uptake of bases, however, is consistent with the proportion existing as the neutral form. There is no ion-trap effect in this case since with bases this would require that the receptor pH be less than the donor pH.

5.1.3 Absorption in Plants

Chemicals are taken up by plants either from the soil environment through the roots or from the atmosphere by the foliage. In both cases, large surfaces can be available and the uptake can be from solution or the vapor phase. To understand how the properties of the chemical influence uptake it will be necessary to consider the nature of the barriers that chemicals have to traverse.

5.1.3.1 Uptake from the Roots The soil–root system, the rhizosphere, comprises a complex interaction between the plant and the soil. Roots release organic material that stimulates the growth of microorganisms that in turn may influence the overall plant status. Nutrients such as nitrogen, phosphorus, and other trace elements along with water are taken up through the roots. A schematic representation of a root is provided in Figure 5.6. Water and solutes move freely in the spaces between the cortex cells that are somewhat porous and this “apparent free space” provides an extensive surface for pollutant uptake. Movement through the cortex is restricted by the waxy material of the Casparian strip. The xylem and the phloem constitute the vascular system of the plant. Water is taken up through the roots and

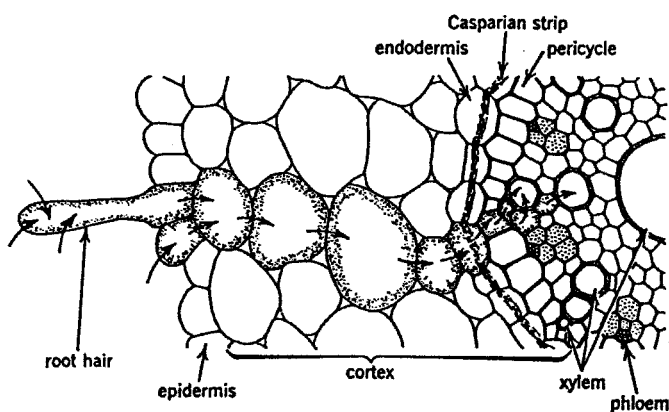
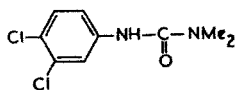


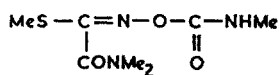
Figure 5.6 Cross-section of a root showing routes of water and solute movement into the plant. [Reproduced from K. Esau’s “Plant Anatomy”, p. 506. Copyright 1965. This material is used by permission of John Wiley & Sons Inc.]

moves in the xylem to the foliage where it evaporates. The sugar produced by photosynthesis is distributed through the plant in the phloem. Consequently, the uptake and distribution of an organic chemical from the soil would involve absorption by the roots and transport along with the water through the xylem.

1. *Influence of Compound K_{ow}* This relation has been investigated by observing the uptake from nutrient solutions of two series of compounds, *O*-methyl carbamoyloximes and phenylureas, by barley seedlings.⁷ Note that the compounds investigated are representative of pesticides that can be applied to soil. Groups of six 10-day-old plants were held individually in drilled rubber



Diuron
(phenylurea)



Oxamyl
(*O*-methylcarbamoyloxime)

stoppers with the roots immersed in a nutrient solution containing the ¹⁴C-labeled chemical under study and the amount in the roots and shoots determined at 24 and 48 h. The 24-h data for the phenylureas is compiled in Table 5.4. There was little if any difference in observations at the two exposure times. Preliminary studies had demonstrated that the tendency for compounds to distribute into dried macerated roots *in vitro* was directly related to the lipophyllicity of the compound as represented by K_{ow} . The root concentration factor, RCF, is defined

$$\text{RCF} = \frac{\text{Concentration in roots}}{\text{Concentration in external solution}}$$

TABLE 5.4 Root Concentration Factors and Transpiration Stream Concentration Factors for Phenyl Ureas in Barley Seedlings

Compound	$\log K_{ow}$	RCF	TSCF
3-Methylphenylurea	-0.12	0.69	0.048
Phenylurea	0.80	1.20	0.48
4-Fluorophenylurea	1.04	1.09	0.48
3-(Methylthio)phenylurea	1.57	0.89	0.27
4-Chlorophenylurea	1.80	2.00	0.52
4-Bromophenylurea	1.98	3.04	0.55
3,4-Dichlorophenylurea	2.64	5.50	0.39
4-Phenoxyphenylurea	2.80	6.54	0.47
4-(4-Bromophenoxy)phenylurea	3.7	35.2	0.10

and from Figure 5.7 it can be seen that this quantity increases with an increase in K_{ow} . The limiting uptake observed with the more polar compounds is attributed to rapid equilibration of the external water with the water in the "apparent free space" of the roots. It was calculated that this mechanism contributed a value of 0.82 to the RCF. It was assumed this applied to all compounds irrespective of their K_{ow} , however, this process would be more significant with polar compounds. The RCF could be expressed as a function of K_{ow} (Fig. 5.7):

$$\log(\text{RCF} - 0.82) = 0.77 \log K_{ow} - 1.52$$

The equilibrium between roots and external solution is achieved rapidly and is reversed when the roots are transferred to a nutrient solution free of the chemical.

The efficiency with which a compound moves into the shoot is defined by the transpiration stream concentration factor, TSCF

$$\text{TSCF} = \frac{\text{Concentration in xylem}}{\text{Concentration in external solution}}$$

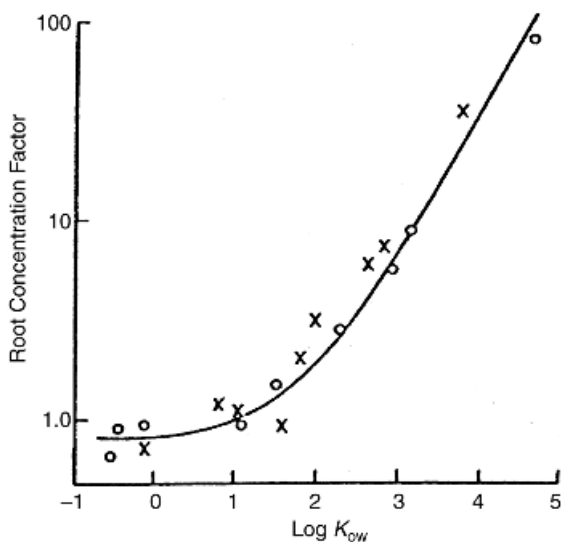


Figure 5.7 Root concentration factor (log RCF) expressed as a function of $\log K_{ow}$. O, *O*-methylcarbamoyloximes; x, substituted phenylureas. [Reproduced from G. G. Briggs, R. H. Bromilow, and A. A. Evans, "Relationships between lipophilicity and root uptake and translocation of non-ionised chemicals by barley" *Pestic. Sci.*, **13**, 495. Copyright 1982, Society of Chemical Industry. Reproduced with permission granted by John Wiley and Sons, Ltd on behalf of the S.C.I.]

An estimate of the average concentration of chemical in the xylem over a specified time interval can be obtained from the amount of chemical observed in the shoot and the volume of water moving through the plant. The chemical must move to the shoot in the water moving through the plant in the xylem. With some chemicals, it is necessary to adjust for the amount metabolized in the shoots, otherwise the concentration in the xylem could be underestimated.

Values for TSCF observed with the phenyl ureas are compiled in Table 5.4 and for both series of compounds investigated, plotted as a function of $\log K_{ow}$ in Figure 5.8. The TSCF values were all < 1 indicating simple passive diffusion into the xylem rather than any specialized overall process that would accumulate the compound against a gradient. Analysis of these data would also suggest an optimum K_{ow} for uptake into the shoots. The anomalous value observed for the thiocompound could be explained by oxidation of the thiol to produce a more water soluble derivative with a lower K_{ow} . It is of interest to note the similarity of this relation to that observed for dermal absorption and a similar process may be involved. In the latter, it was noted that an initial increase in flux with an increase of K_{ow} resulted from an increase in the tendency of the compound to distribute into the outer lipophilic layer. Higher values of K_{ow} limited the tendency to distribute into the next layer that was quite hydrophilic. Compounds with higher K_{ow} 's are more likely to distribute into the roots, however, as K_{ow} increases, the tendency to distribute

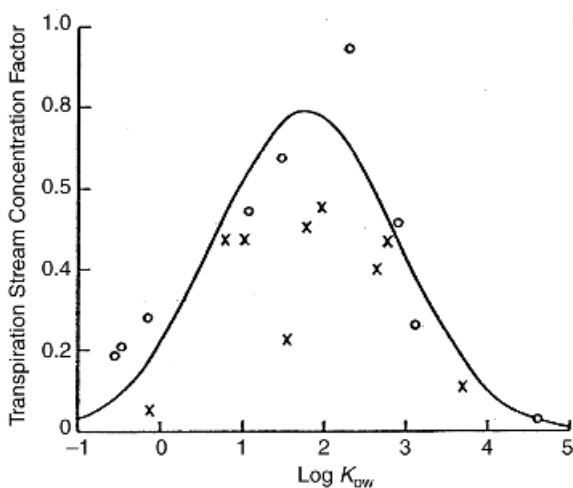


Figure 5.8 Relation between transpiration stream concentration and $\log K_{ow}$. ○, *O*-methylcarbamoyloximes; ×, substituted phenylureas. [Reproduced from G. G. Briggs, R. H. Bromilow, and A. A. Evans, "Relationship between lipophilicity and root uptake and translocation of non-ionised chemicals by barley" *Pestic. Sci.* **13**, 495. Copyright 1982, Society of Chemical Industry. Reproduced with permission granted by John Wiley and Sons, Ltd on behalf of the S.C.I.]

into water and move through the xylem would decrease. Observations with other plant systems and different classes of chemicals have confirmed this curvilinear relation.⁷

2. pK_a and Soil pH One would anticipate that the uptake from the soil of weak acids or bases would be influenced by the proportion of the compound existing in the neutral form as determined by the pK_a of the compound and the environmental pH. Both RCF and TSCF have been determined for several phenoxy acetic acids and maleic hydrazide in barley seedlings.⁸ Uptake into roots and shoots from buffered nutrient solutions was determined after 24 h. Illustrative data are summarized in Table 5.5. For all compounds tested, the RCF and TSCF values increased with decreasing pH, which would be consistent with higher proportions of the protonated neutral species at lower pH values. However, it was observed that neither the 2,4-dichloro- nor the 3,5-dichloro- derivatives distributed onto macerated roots at pH 4.0, which would be expected since at this pH only 10% of the acid would exist in the neutral form. Thus the large accumulation of these compounds in roots could not be explained by partitioning onto root solids, and thus must be due to accumulation in the cell protoplasm. This accumulation occurs against a concentration gradient and would suggest that the process would require energy. However, it has been demonstrated that this accumulation can be explained by an "ion-trap" mechanism due to the pH differential across the membrane (see p. 156). The vacuole (type of storage compartment) has a pH 5.5 and occupies 90% of the cell volume, while the cytoplasm of the cell has a pH 7.0 and represents 10% of the cell volume. Energy is required to maintain cell pH. An "ion-trap" equation has been developed to predict this distribution as a function of the pH differential, the charge on the membrane and the permeability of the neutral and charged species. This relation provides a reasonable prediction of the RCF of the two dichlorophenoxyacetic acids (Fig. 5.9).

The influence of pK_a is illustrated by maleic hydrazide, in that a significant reduction in RCF is seen when pH is >5.0 . The lower RCF observed with this

TABLE 5.5 RCF and TSCF Values in Barley Seedlings after 24 h Exposure to Weak Acids

Compound	pK_a	$\log K_{ow}^a$	RCF at pH			TSCF at pH		
			4.0	5.0	7.0	4.0	5.0	7.0
4-Chlorophenoxyacetic acid	3.1	2.25	71.6	11.6	0.58	3.70	0.91	0.05
2,4-Dichloro-	2.87	2.90	33.3	7.62	0.83	4.14	0.49	0.04
3,5-Dichloro-	2.84	2.84	24.5	6.41	0.60	4.24	0.72	0.05
4-(2,4-Dichlorophenoxy)-	3.0	4.51	55.5	26.0	4.80	0.23	0.15	0.04
Maleic hydrazide	5.65	-0.63	2.73	2.14	0.53	0.04	0.13	0.02

^aFor the neutral species.

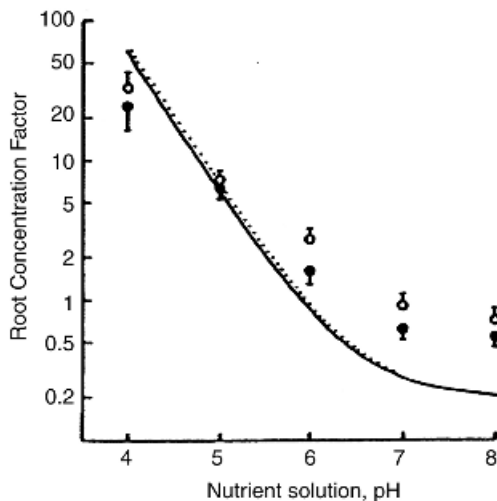


Figure 5.9 Root concentration factor in barley roots for substituted phenoxyacetic acids as a function of pH. The lines represent predictions based on the ion-trap mechanism. ○, 2,4-D; ●, 3,5-D. [Reproduced from G. G. Briggs, R. L. O. Rigitano, and R. H. Bromilow, "Physico-chemical factors affecting uptake by roots and translocation of weak acids in barley" *Pesticid. Sci.* **19**, 101. Copyright 1987, Society of Chemical Industry. Reproduced with permission granted by John Wiley and Sons, Ltd on behalf of the S.C.I.]

compound reflects the higher water solubility of the undissociated acid. Changes in TSCF with pH tend to follow changes in RCF, however, movement from the roots to the xylem is not as efficient as the movement into the roots. This type of response with weak acids will be more likely in acid soils since as soil pH increases the pH differential will decrease.

3. *Soil Organic Matter* Organic compounds may exist in soil either in solution or the vapor phase and can be absorbed through the roots in either state, absorption from solution would be the most likely process. From the discussion of the sorption process in soil (see Sorption, Chapter 3) the concentration of the compound in aqueous solution, C_{aq} , would be a function of the concentration in the soil (C_{soil}), and the soil distribution ratio, K_d , which in turn is dependent primarily on SOM content. One would predict that uptake would be inversely related to the level of SOM. Observations of the uptake of dieldrin by carrots raised in different soils⁹ provide an opportunity to evaluate this relation and demonstrate the dependence on the concentration of the compound in soil solution. If the uptake efficiency is defined by the ratio of the concentration of dieldrin in carrots to that in the soil it is clear that higher levels of soil organic matter reduce uptake by carrots (Table 5.6). The K_{om} for dieldrin is $6980 \text{ mL} \cdot \text{g}^{-1}$ from which K_d values were calculated for dieldrin in each soil. Since $K_d = C_{soil}/C_{aq}$ the concentration of dieldrin in soil solution can be determined. If uptake is defined as C_{carrot}/C_{aq} a consistent value

TABLE 5.6 Uptake of Dieldrin by Carrots Grown in Different Soils

Quantity	Soils		
	Sandy Loam	Clay	Muck
% Organic matter	1.4	3.6	66.5
Conc. in soil (ppm)	0.49	0.88	3.87
Conc. in carrot (ppm)	0.12	0.11	0.02
K_d Dieldrin	97.7	251	4640
$C_{\text{carrot}}/C_{\text{soil}}$	0.24	0.13	0.0052
Conc. soil soln. (ppm)	0.0050	0.0035	0.00083
$C_{\text{carrot}}/C_{\text{aq}}$	24	31	24

is observed in the three soils illustrating that the effect of the soil organic matter is indeed due to its effect on the distribution between soil and water.

4. *Variation with Plant Species* Recent studies have confirmed earlier observations that there are pronounced differences among plant species in their ability to absorb chemicals from soil¹⁰ and translocate these compounds in the plant. The data in Table 5.7 were derived from a study of the uptake and distribution in plants grown in soil containing residues of chlordane, a persistent chlorinated hydrocarbon. Chlordane, an insecticide, is a complex mixture that is not very water soluble ($S_w \sim 0.06$ ppm) and with $\log K_{ow}$ values in the range of 6.0. It is also of note that this site had been treated with chlordane in 1960 and the current observations were made on plants grown in 1998; obviously dealing with "aged" residues that might not be expected to be readily available (see Sorption, Chapter 3). One might predict that chlordane would absorb in roots but would be unlikely to move through the plant in the aqueous translocation system.

Levels of chlordane in soil collected from around the plant roots ranged from 2 to $5\text{-}\mu\text{g} \cdot \text{g}^{-1}$ dry weight with one sample as high as $10\text{-}\mu\text{g} \cdot \text{g}^{-1}$. High levels observed

TABLE 5.7 Chlordane in Edible Parts of Crops Grown in Contaminated Soil

Plant	$\mu \cdot \text{g}^{-1}$ dry wt.	Plant	$\mu \cdot \text{g}^{-1}$ dry wt.
White potato		Eggplant	
whole	0.199	whole	0.003
peel	0.638	peel	0.010
flesh	0.008	flesh	0.004
Carrot		Zucchini	
whole	1.684	whole	0.694
peel	5.180	peel	1.122
flesh	0.125	flesh	0.7762

in root crops would be expected, however, the levels observed in the zucchini was a surprise. Lettuce and zucchini roots were much more efficient in taking up chlordane and in the latter plant also showed high levels in both the stem and the fruit. Complementary greenhouse studies indicated that with soil concentrations of $0.320\text{--}0.330\text{-}\mu\text{g}\cdot\text{g}^{-1}$ dry weight concentrations in the fruit were $0.275\text{--}0.425\text{-}\mu\text{g}\cdot\text{g}^{-1}$ dry weight; approximately a 1:1 distribution, soil/fruit, quite different from what might have been anticipated from the relation between TSCF and $\log K_{ow}$ (Fig. 5.8). By contrast, chlordane could not be detected in tomato and pepper fruit and corn grains from plants raised in the same soil. The study also established that the chlordane was being taken up from the soil and not moving to the plant by first evaporating and then depositing on the foliage.

It has also been demonstrated that aged residues of chlorinated dibenzodioxins and dibenzo furans in soil can be taken up by zucchini plants and translocated to the fruit.¹¹ These compounds, like chlordane, would have $\log K_{ow}$ values of 6 and higher and might be expected to distribute into the roots but would have little tendency to distribute into the plant. In order to establish that the dioxins and furans detected in the plant came from the soil it was necessary to assess other pathways such as deposition from the atmosphere, direct contact of the fruit with the soil or evaporation from the soil and condensation on the foliage. These possibilities were assessed using the experimental design outlined in Figure 5.10. Zucchini plants were raised in the contaminated soil (the 148 refers to toxicological equivalents and would represent $\sim 3750\text{-ng}\cdot\text{kg}^{-1}$ dry weight ΣPCDD , PCDF) and the fruit allowed to lie on the soil (1a) or restricted from soil contact (1b). Other plants were raised on essentially contaminant-free soil where the fruit could contact the contaminated soil (II) or raised above the contaminated soil (III).

Significant amounts of the chlorinated dioxins and furans were detected in the zucchini fruit raised on the contaminated soil irrespective of whether the fruit had direct contact with the soil or not (Table 5.8). Contaminant level in the fruit was definitely associated with the plants being raised on the contaminated soil whose conclusion is also supported by the observation that the dioxin–furan composition detected in the fruit compared favorably with that observed in the soil, particularly with respect to the furans (Fig. 5.11). The octachlorodibenzodioxin (OCDD) would have a very high K_{ow} and binding in soil would limit its uptake by the roots. The dioxin–furan levels observed on leaves of plants raised on contaminant-free soil is attributed to atmospheric deposition and the composition observed is quite distinct from that of the contaminated soil.

This study also reported that pumpkins could take up these compounds from soil and distribute them to the fruit. Pumpkins and zucchini squash both belong to the genus *Cucurbita* and it would appear that these plants have an unusual ability to mobilize “aged” residues in soil, absorb these compounds through the roots, and distribute them through the plant. These plants accomplish this with hydrophobic compounds that would be expected to be absorbed by the roots but not distributed through the plant. The mechanisms involved are not known. This is a “good news/bad news” situation in that the bad news is that some plant species are particularly susceptible to accumulating persistent chemical residues that may be in the soil

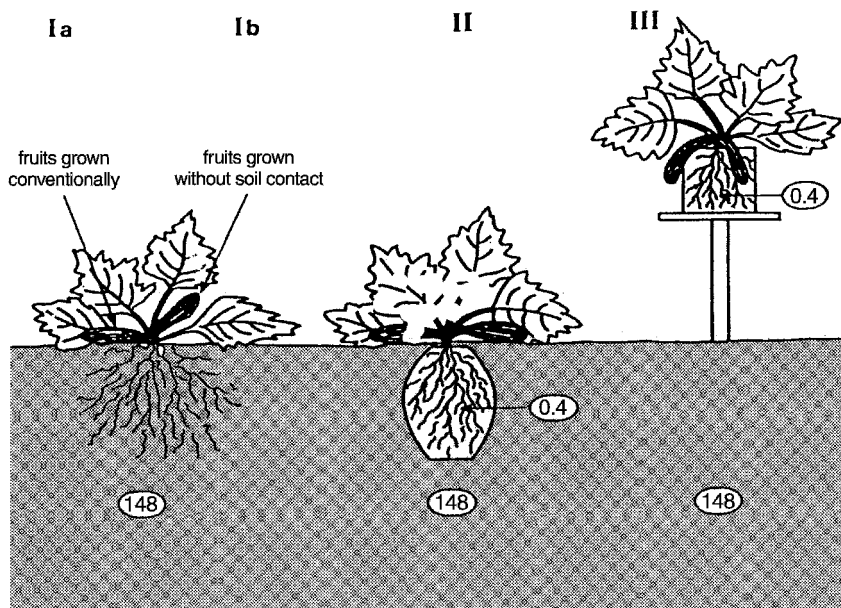


Figure 5.10 Experimental setup for evaluating uptake of chlorinated dibenzodioxins and furans into leaves and fruit of zucchini. Cumulative concentration of dioxins and furans expressed as $\text{ng} \cdot \text{kg}^{-1}$ of toxic equivalents. [Reproduced with permission from A. Hulster, J. F. Müller, and H. Marschner, *Environ. Sci. Technol.* **28**, 1110 (1994). Copyright © 1994, American Chemical Society.]

and could result in undesirable human exposure. The good news is that some plants may be quite effective in removing residues from soil and a better understanding of the processes involved may result in improved remediation options.

Plants may also play a role in the transfer of compounds to the atmosphere.¹² Eight species (soybean, barley, and lettuce; Russian olive, autumn olive, green ash, hybrid poplar, and honeysuckle) were grown hydroponically in a solution

TABLE 5.8 Uptake of Chlorinated Dibenzodioxins and Furans from Contaminated Soil by Zucchini Squash

Sample/Treatment	Soil	$\Sigma\text{PCDD} + \text{PCDF}$ ($\text{ng} \cdot \text{kg}^{-1}$ dry wt)
Fruit (Ia)	Contaminated	348.1/274.0 ^a
Fruit (Ib)	Contaminated	368.2/380.9
Leaves (I)	Contaminated	440.6/490.9
Fruit (II)	Contamination-free	31.9/34.7
Leaves (II)	Contamination-free	186.2/348.4
Fruit (III)	Contamination-free	44.2/55.8

^aValues from duplicate samples.

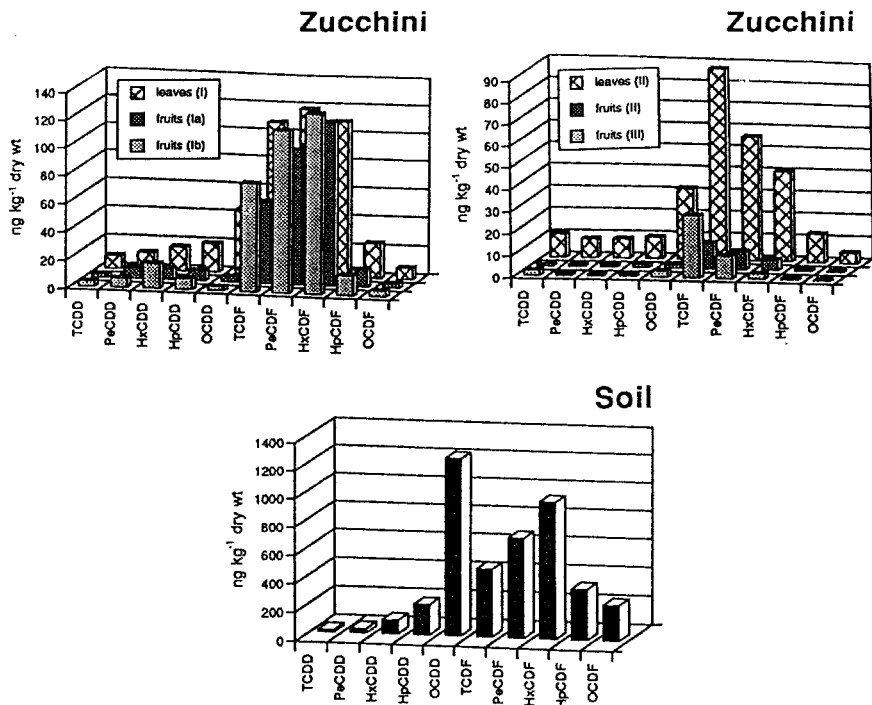


Figure 5.11 Dioxin and furan profiles in zucchini and soil. [Reproduced with permission from A. Hulster, J. F. Müller, and H. Marschner, *Environ. Sci. Technol.* **28**, 1110 (1994). Copyright © 1994, American Chemical Society.]

containing 8 ppm of nitrobenzene. After 72 h from 10 to 40% of the nitrobenzene had been lost to the air (Fig. 5.12). This transfer was correlated with the rate of water movement through the plant and only observed when the plants were present and was not due to direct evaporation from solution. Nitrobenzene has a $\log K_{ow}$ of 1.85, which would predict a $\log RCF$ of 1.62 (p. 159). Values observed ranged from 1 to 1.4 with barley giving a low of 0.5 and honeysuckle a high of 2.0. An average TSCF of 0.72 ± 0.07 was observed with no significant difference among species. This value would be consistent with that predicted for a compound with $\log K_{ow}$ of 1.85 (Fig. 4.8). At this time, there is no systematic basis either for the plant or the compound for predicting when this process may be significant.

5.1.3.2 Foliar Uptake: Adsorption and Absorption The leaf surface provides an extensive surface area that can interact with chemicals either in the vapor phase or through wet or dry deposition. The cuticle limits water loss and protects against infection by plant pathogens. Detailed descriptions of the plant cuticle are available^{13,14} and a brief synopsis has been provided in the discussion of the sorption of chemicals by foliage (see Sorption, Chapter 3). While the hydrophobic cuticle

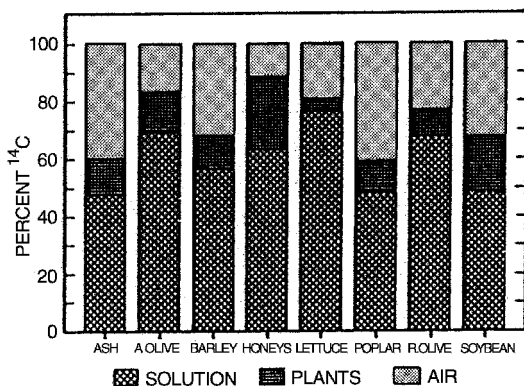


Figure 5.12 Distribution of ^{14}C by plants grown in hydroponic solution containing labeled nitrobenzene. [Reproduced with permission from C. Mc Farlane, T. Pfeleger, and J. Fletcher, *Environ. Toxicol. Chem.* **9**, 513 (1990). Copyright SETAC, Pensacola, FL, USA.]

provides a barrier for hydrophylic compounds, lipophylic compounds can distribute readily into this matrix. It is important to be able to distinguish between the extent to which compounds adsorb to the leaf surface and actually absorb into the leaf.

In a study of the uptake of pesticides (Table 5.9) from aqueous solution by needles from different conifer species, a distinct biphasic process was observed (Fig. 5.13).¹⁵ It was established that the initial rapid uptake was due to sorption on the needle surface, in that the compound would readily desorb during this phase of the study. The longer the exposure continued, the less compound was desorbed, indicating that the second phase was due to absorption into the needle. The adsorption rate would be a function of diffusion through the stirred solution to the needle surface, which would be considerably faster than diffusion through the needle cuticle that would limit absorption. An estimate of the amount of chemical sorbed on the needle surface was obtained by extrapolation of the slow uptake phase back to zero time, which for the example given would give a value of $1.6 \times 10^{-10} \text{ mol} \cdot \text{mm}^{-1}$. A sorption isotherm (Fig. 5.14) was generated by determining the amount sorbed as a function of the concentration in solution. This relation can be represented

TABLE 5.9 Compounds Used in Conifer Needle Uptake Study

Compound	MW	$\log K_{ow}$	$\log K_{cw}^a$
2,4-D	221	2.63	2.59
Triademenol	296	3.12	2.88
Lindane	291	3.80	3.73
Bitertanol	337	4.16	4.05
Pentachlorophenol	266	4.79	4.75

^aCuticle/water partition coefficient.

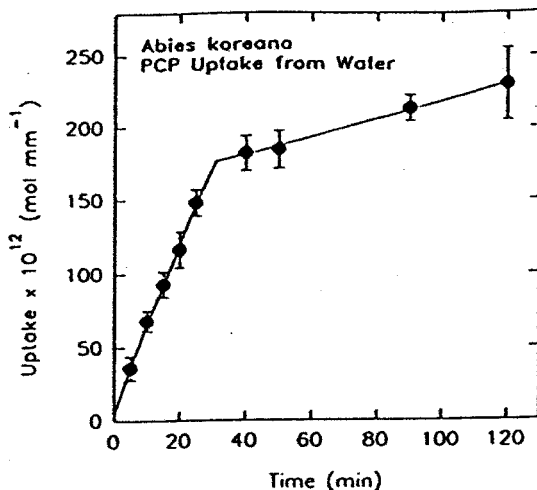


Figure 5.13 Biphasic uptake of PCP >2 by *Abies. koreana* needles. [Reproduced with permission from L. Schreiber and J. Schönherr, *Environ. Sci. Technol.* **26**, 153 (1992). Copyright © 1992, American Chemical Society.]

by the BET isotherm (see Sorption, Chapter 3) and the linear form of the relation can provide estimates of X_m , the molecules required to produce a monolayer. For PCP adsorption on *P. abies*, the BET constant B, was calculated to be 4.4 and X_m , 6.7×10^{-11} mol · mm⁻¹. For the five species of needles used, X_m ranged from

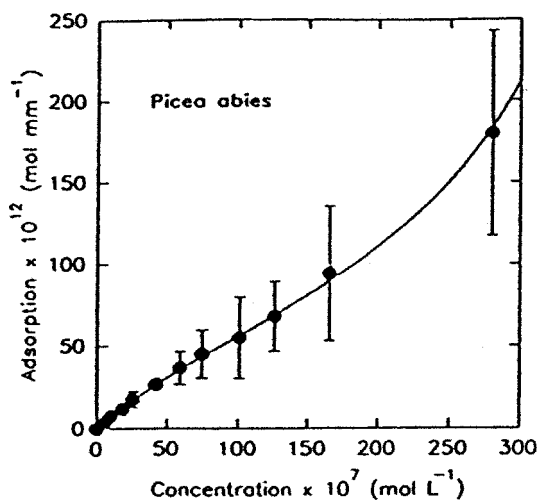


Figure 5.14 Adsorption isotherm of PCP on *Picea abies* needles. Solid lines calculated from BET isotherms. [Reproduced with permission from L. Schreiber and J. Schönherr, *Environ. Sci. Technol.* **26**, 153 (1992). Copyright © 1992, American Chemical Society.]

6.79 to $162 \times 10^{-11} \text{ mol} \cdot \text{mm}^{-1}$. Since the molecular dimensions of the pentachlorophenol can be determined, it is possible to calculate the surface area of the needles that was found to range from 29.4 to $683 \text{ mm}^2 \cdot \text{mm}^{-1}$. The absorption flux, F , in $\text{mol} \cdot \text{m}^{-2} \cdot \text{s}^{-1}$ through the cuticle would be given by

$$F = (DK_{\text{cw}}/h)C$$

where C would be the solution concentration ($\text{mol} \cdot \text{m}^3$) and D the diffusivity ($\text{m}^2 \cdot \text{s}^{-1}$) in the cuticle. The quantity (DK_{cw}/h) is defined as the permeance with units, $\text{m} \cdot \text{s}^{-1}$ and the flow, Q , through the needle per unit length would be

$$Q = F \cdot A \cdot C$$

assuming zero concentration in the cuticle. These data demonstrate that for a given compound, the rate of uptake is determined by the surface area of the needle (Fig. 5.15) and for a given species, the permeance is a function of K_{cw} (Fig. 5.16). This relation would suggest that the values of D , for the compounds evaluated, do not vary to any extent in this matrix. Note from Table 4.8 that the octanol-water partition coefficient would be a reasonable surrogate for the cuticle water partition coefficient. A more comprehensive analysis of the factors influencing the foliar uptake of organic chemicals is available.¹⁶

Studies of the absorption and translocation of ^{14}C -labeled derivatives of 2,4-dichlorophenoxy-acetic acid applied to leaves of bigleaf maple (Table 5.10) demonstrate that the more nonpolar 2-ethylhexyl ester is more readily absorbed

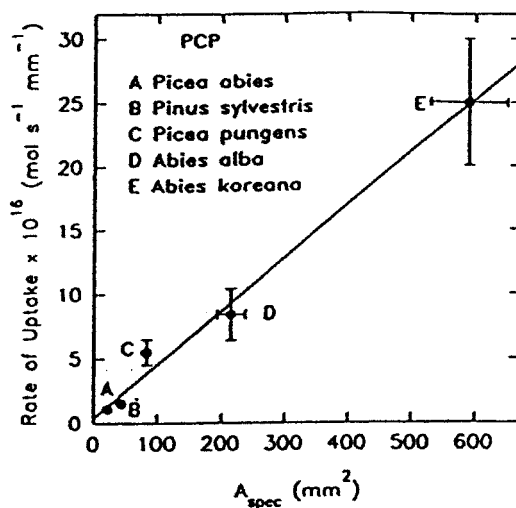


Figure 5.15 Correlation of the uptake of PCP by needles of different conifer species with the specific surface areas. [Reproduced with permission from L. Schreiber and J. Schönherr, *Environ. Sci. Technol.* **26**, 153 (1992). Copyright © 1992, American Chemical Society.]

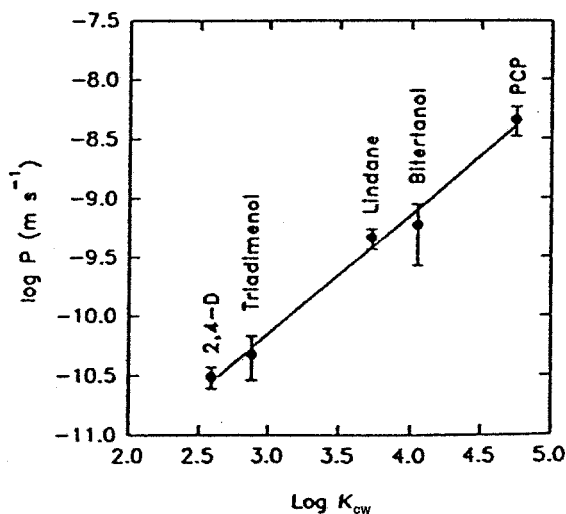


Figure 5.16 Correlation of permeance with K_{ow} . [Reproduced with permission from L. Schreiber and J. Schönherr, *Environ. Sci. Technol.* **26**, 153 (1992). Copyright ©1992, American Chemical Society.]

than either the acid or triethanolamine salt.¹⁷ However, the more polar salt and acid translocate more readily in the plant consistent with the nature of the transport processes in plants. The ester is probably hydrolysed to the acid prior to distribution.

A comprehensive summary of the studies of the uptake of chemicals by plants has been published¹⁸ classifying the information on the basis of plant and chemical studied and whether the exposure has been from soil or air.

5.2 BIOCONCENTRATION, BIOACCUMULATION, AND BIOMAGNIFICATION

The commercial use of PCBs was based on the fact that they were inert and despite the fact that these products had been in use since the early 1930s, we were unaware of the manner in which they were distributed in the environment. The advent of GC and the development of the electron-capture detector in the early 1960s provided

TABLE 5.10 Absorption and Translocation of 2,4-D and Derivatives

Treatment	Absorption (%)	Translocation: % Absorbed Activity Found in:			
		Leaves	New Growth	Stem	Roots
2,4-D acid	2.9	77.0	10.0	8.1	4.9
2,4-D salt	1.7	68.8	17.4	9.7	4.0
2,4-D ester	20.8	95.4	2.6	1.4	0.5

lower detection limits for these chlorinated compounds and soon reports of their distribution, particularly in the aquatic environment, began to appear. Observations of ppm levels in different species sparked many studies documenting the distribution of these compounds and efforts to explain the relatively high levels being detected. The concept of bioconcentration was introduced and continues to be an active area of investigation in an attempt to understand the controlling variables.

5.2.1 Definition of Terms

It is important to understand what these terms mean since they are often misused.

Bioconcentration defines the uptake by aquatic species directly from the water through the gills and/or epithelial tissue. A Bioconcentration Factor (BCF) is defined as the ratio of the concentrations of the compound in the biota (C_b) and the water (C_w) at equilibrium.

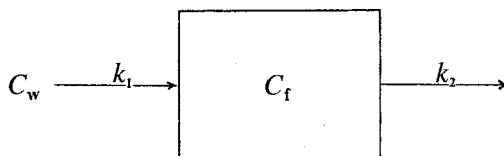
$$\text{BCF} = C_b/C_w$$

Bioaccumulation in aquatic species is essentially bioconcentration plus uptake by any other process such as ingestion of food, and usually applies to field observations where the routes of exposure are not known. The quantitative definition again is the ratio of the concentrations of the chemical in the organism and the water.

Biomagnification involves the progressive increase in tissue concentration of a chemical in successive levels of a food chain.

5.2.2 Bioconcentration Factor, K_B

The bioconcentration process is usually represented by a simple, single compartment, where the concentration in the fish, C_f (usually expressed as g/g wet wt. of tissue), is determined by the rate of uptake from the water, k_1 (or k_u), the concentration in the water, C_w , and the rate of excretion, k_2 (or k_e). The rate constants



are assumed to be first order. If, for a given compound, the rate of excretion is less than the rate of uptake, it will accumulate in the fish until a steady state is achieved with the excretion rate $k_2[C_f]_{ss} = \text{uptake rate}, k_1C_w$. It is assumed that the amount of compound in the water represents a large reservoir and its concentration is essentially constant, and so the rate of uptake would be constant. The bioconcentration factor, K_B , would be defined

$$K_B = [C_f]_{ss}/C_w$$

and would have units $\text{mL} \cdot \text{g}^{-1}$.

An experimental approach commonly used to determine K_B is summarized in Figure 5.17. Fish are exposed under controlled conditions to a constant concentration for sufficient time to establish $[C_f]_{ss}$ ($dC_f/dt = 0$) and since C_w is known, K_B can be calculated. A limitation with this approach is the problem of knowing how much time is required to achieve the steady state. During the uptake phase of the study, the rate of change in C_f is defined by both k_1 and k_2 :

$$dC_f/dt = k_1 C_w - k_2 C_f$$

and the concentration in the fish would be

$$C_f = k_1/k_2 C_w (1 - e^{-k_2 t})$$

When exposure to the compound is terminated and the fish transferred to uncontaminated water, called a depuration phase, the change in concentration in the fish will then be determined by k_2 :

$$dC_f/dt = -k_2 [C_f]_o$$

where $[C_f]_o$ is the concentration in the fish when depuration commences. The concentration in the fish during this phase would be expressed

$$C_f = [C_f]_o e^{-k_2 t}$$

and an excretion half-life would be $\ln 2/k_2$. These relations apply when there is little or no growth during the course of the study.

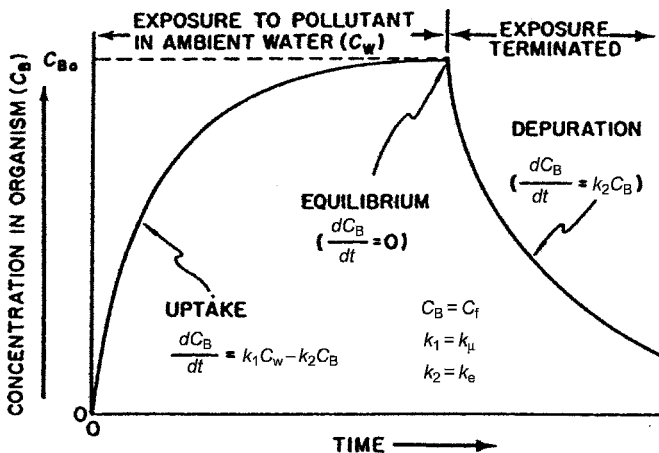


Figure 5.17 Schematic representation of an experimental design used to assess bioconcentration assuming minimal metabolism of the compound under study.

At steady state, the rate of change in C_f is 0, and hence

$$k_2[C_f]_{ss} = k_1 C_w$$

and thus

$$K_B = [C_f]_{ss}/C_w = k_1/k_2$$

The bioconcentration factor can be determined if the respective rate constants can be determined, thus avoiding the problem of demonstrating that a steady state had been achieved.

These concepts are illustrated by a study of the bioconcentration 2,3,7,8-tetrachlorobibenzo-*p*-dioxin (TCDD) in the Japanese medaka using ^3H -labeled compound.¹⁹ The study was carried out in flowing water with a unique feature being that the very insoluble TCDD was not introduced in a solvent. An aqueous solution of TCDD was prepared by passing water through a column containing beads coated with the compound and diluting the effluent to provide an exposure concentration of $101 \pm 26 \text{ pg} \cdot \text{L}^{-1}$. The fish were exposed to TCDD for 12 days followed by a 6-month depuration phase. The TCDD levels observed in the fish over the experimental period are compiled in Table 5.11. Exposure to TCDD did not result in major loss in weight. The concentration in the fish decreased by 69% during the 165-day depuration stage, however, the body burden decreased by only 47%, illustrating that a major component in the concentration change could be attributed to growth dilution. When growth is taken into account, the change in concentration would be expressed

$$dC_f/dt = k_1 C_w - (k_2 + g)C_f$$

where g is the growth rate in day^{-1} . When $g \ll k_2$, growth will not be a significant factor. Regression analysis of the tissue concentration data provided estimates of the

TABLE 5.11 TCDD Levels in Exposed Medaka

Time (day)	TCDD ($\text{pg} \cdot \text{g}^{-1}$)	Weight (g)	TCDD (pg/fish)	% Lipid
0	0	0.175		
2	572 ± 43	0.151	109 ± 7	
4	932 ± 72	0.179	167 ± 17	
6	$1,328 \pm 99$	0.200	266 ± 37	
10	$2,207 \pm 218$	0.176	389 ± 27	
12	$2,408 \pm 241$	0.213	513 ± 90	7.5
40	$1,480 \pm 175$	0.299	442 ± 133	8.9
102	$1,002 \pm 227$	0.314	315 ± 98	14.3
187	757 ± 144	0.360	272 ± 48	7.7

rate constants for uptake and excretion:

$$k_1 = 2300 \pm 110 \text{ mL} \cdot \text{g}^{-1} \cdot \text{day}^{-1}$$

$$k_2 = 0.0045 \pm 0.0006 \text{ day}^{-1}$$

Note that the units for k_1 contain a density factor ($\text{mL} \cdot \text{g}^{-1}$), since C_w is expressed as mass per unit volume while C_f is mass per unit mass. Since the density of water is essentially 1, this becomes a moot point. An estimated K_B for nongrowing fish would be

$$K_B = 2300/0.0045 = 5.1 \pm 0.5 \times 10^5 \text{ mL} \cdot \text{g}^{-1}$$

After 12 days, the medaka had shown a bioconcentration of 24,000, which is considerably less than the steady-state value predicted from kinetic parameters. It will be shown below that exposure for 1023 days would be required to achieve 99% of the steady state. A lipid-normalized bioconcentration factor, $[K_B]_{\text{lip}}$ assuming 10% lipid in the medaka would be

$$[K_B]_{\text{lip}} = K_B/f_l = 5.1 \times 10^5/0.1 = 5.1 \times 10^6$$

Because TCDD is widely distributed in the environment and because it is very toxic there have been several studies of its bioconcentration using different species of fish and different experimental approaches.¹⁰ Values of K_B from uptake and excretion rate constants ranged from 9.27×10^3 to 159×10^3 , considerably less than the value derived from the data used above. The major differences were observed in values reported for k_1 , which varied from 108 to $2300 \text{ mL} \cdot \text{g}^{-1} \cdot \text{day}^{-1}$. This discrepancy may reflect limitations of the experimental procedures used and may also be influenced by the available concentration of TCDD. If concentrations used are higher than the reported solubility or reduced by the presence of DOM, an incorrect value for the actual concentration in solution will affect the estimate of k_1 . It is clear that the determination of K_B for compounds of low S_w is a significant experimental challenge.

The bioconcentration of five PCB congeners (Table 5.12) has been studied in goldfish²¹ using a flow-through system and a 23-day exposure period followed by 116-days depuration. From this data set it is observed that $K_B = C_f/C_w$ corresponds to $K_B = k_1/k_2$, and one can conclude that for these compounds the 23-day exposure was reasonably close to the time required to achieve steady state.

5.2.2.1 Relation Between K_B and K_{ow} There have been numerous studies with different species and different classes of compounds that have reported relations of the form²¹:

$$\log K_B = a \log K_{ow} + b$$

TABLE 5.12 Bioconcentration of PCB Congeners in Goldfish

PCB Congener	K_B ($\text{mL} \cdot \text{g}^{-1}$)	k_1 ($\text{ml} \cdot \text{g}^{-1} \cdot$ day^{-1})	$k_2,$ day^{-1}	$t_{1/2},$ day	k_1/k_2 ($\text{mL} \cdot \text{g}^{-1}$)	$\log K_{ow}$	$K_B = f_1 K_{ow}^a$
2,5-Dichloro	1.54×10^4	920	0.066	10.5	1.39×10^4	5.06	3.7×10^3
2,2',5-Trichloro	2.14×10^4	950	0.048	14.4	1.98×10^4	5.24	5.6×10^3
2,4',5-Trichloro	4.48×10^4	890	0.021	33.0	4.24×10^4	5.67	1.5×10^4
2,2',5,5'-Tetra- chloro	5.26×10^4	740	0.015	46.2	4.93×10^4	5.84	2.21×10^4
2,3',4',5-Tetra- chloro	4.48×10^4	420	0.010	69.3	4.2×10^4	6.20	5.07×10^4

^a $f_1 = 0.032$.

Uncertainties in deriving K_B as well as values used for K_{ow} probably account for the range of values reported for the coefficients "a" and "b", however, many of the values for "a" are close to 1 and a generally accepted relation is

$$\log K_B = \log K_{ow} - 1.32$$

which can be expressed as

$$K_B = 0.048 K_{ow}$$

It is assumed that bioconcentration reflects the tendency for compounds to distribute into fat compartments (primarily triglyceride) in fish and since "a" ≈ 1 , one would conclude that the octanol–water partition coefficient is an acceptable surrogate for a triglyceride/water coefficient. The 0.048 modifier, then, accounts for an average level of fat observed in fish. Consequently, a more precise relation that takes into account the level of fat would be

$$K_B = f_1 K_{ow}$$

This relation predicts K_B values for the PCB congeners used in the goldfish study (Table 5.10) that are within a factor of 3 of the experimental values.

Studies of the partitioning of compounds between the triglyceride, triolein, and water have shown a linear relation between $\log K_{tg}$ and $\log K_{ow}$ with $\log K_{tg} < 5$:

$$\log K_{tw} = 1.00 \log K_{ow} + 0.105$$

validating the assumption that K_{ow} is a reasonable surrogate for the partitioning involved in estimating K_B .²² With larger molecules, however, this logarithmic relation becomes curvilinear and K_{ow} would tend to overestimate K_{tg} .

Since K_B can be expressed as a function of k_1 and k_2 it follows that

$$\log(k_1/k_2) = a \log K_{ow} + b$$

and that k_1 and k_2 should also be related to K_{ow} . A number of studies^{23–25} with different species and series of compounds have demonstrated significant inverse correlations between k_2 and K_{ow} . Data compiled from a number of studies using different halogenated hydrocarbons illustrate this relation (Fig. 5.18).²⁵ Although observations with dioxins and furans seem to be inconsistent the inverse relation is obvious. The following relation was derived from observations on several species of fish exposed to chlorobenzenes and various PCB congeners²⁴:

$$\log(1/k_2) = 0.663 \log K_{ow} - 0.947$$

There is not a comparable direct relation between k_1 and K_{ow} as illustrated in Figure 5.19 using the data from the same study although some curvilinear expressions have been reported.²⁴ This type of relation would not be unexpected given the manner that the uptake through the gills varies with K_{ow} (Fig. 5.4).

It is also apparent that the relation between $\log K_B$ and $\log K_{ow}$ becomes curvilinear for $\log K_{ow} > 6$ (Fig. 5.20). Note that the $\log K_B$ for TCDD of 5.7 (Table 5.11) is less than a predicted value of 6.2 based on $\log K_{ow}$ of 7.2 and $f_1 = 0.1$. Lower K_B

Publisher's Note:
Permission to reproduce this image
online was not granted by the
copyright holder. Readers are kindly
requested to refer to the printed version
of this article.

Figure 5.18 Relation between the excretion rate constant (k_2) and octanol–water partition coefficient ($K_{d,oct}$) for polyhalogenated hydrocarbons; chlorinated dibenzofurans; \diamond , chlorinated dibenzodioxins; \circ , brominated biphenyls; \blacktriangledown , chlorinated naphthalenes; \blacklozenge , brominated benzenes; \bullet , chlorinated biphenyls; \square , chlorinated benzenes. [Reproduced with permission from A. Opperhuizen and D. T. H. M. Sijm, *Environ. Toxicol. Chem.* **9**, 175 (1990). Copyright SETAC, Pensacola, FL, USA.]

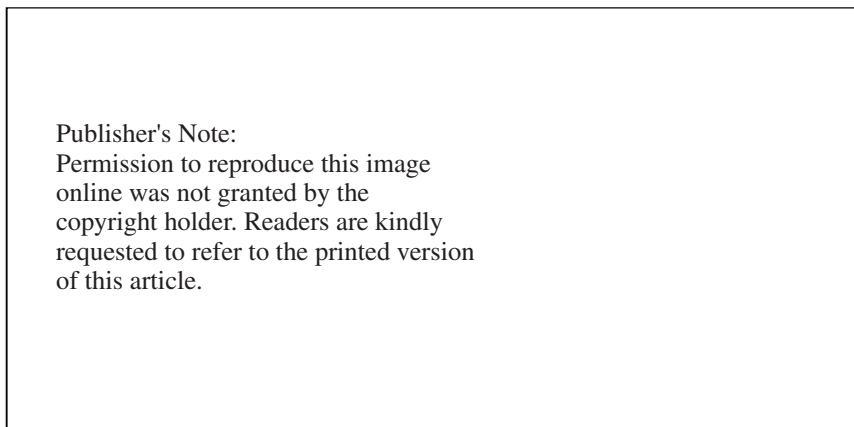


Figure 5.19 Relation between the uptake rate constant (k_1) and the octanol–water partition coefficient. Symbols defined in Figure 5.18. [Reproduced with permission from A. Opperhuizen and D. T. H. M. Sijm, *Environ. Toxicol. Chem.* **9**, 175 (1990). Copyright SETAC, Pensacola, FL, USA.]

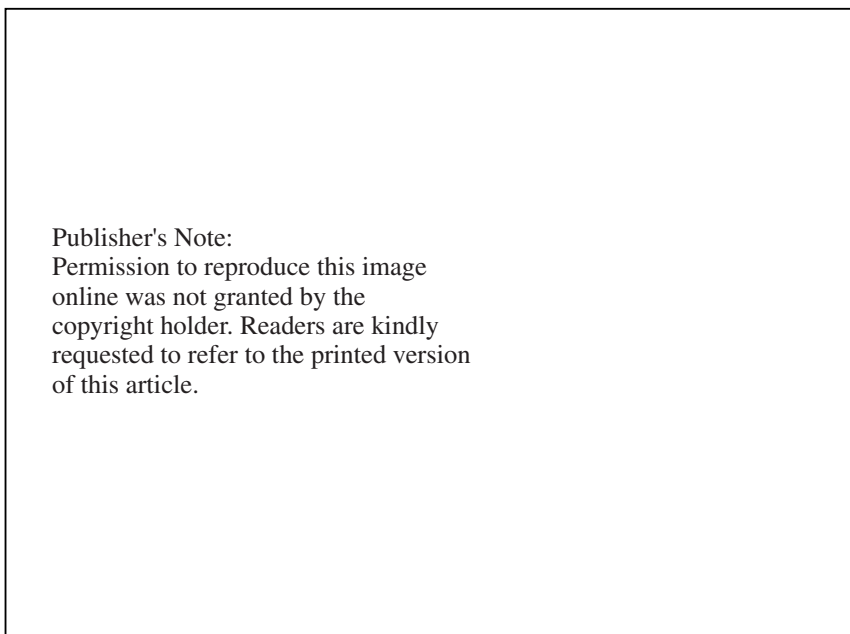


Figure 5.20 Relation between the bioconcentration factor and octanol–water partition coefficient. Symbols defined in Figure 5.18. [Reproduced with permission from A. Opperhuizen and D. T. H. M. Sijm, *Environ. Toxicol. Chem.* **9**, 175 (1990). Copyright SETAC, Pensacola, FL, USA.]

values at higher K_{ow} value may reflect both the reduced efficiency in uptake through the gills resulting in lower values of k_u and the curvilinear relation observed between K_{tg} and K_{ow} .

5.2.2.3 Factors Influencing K_B In the analysis of the environmental behavior of a compound, it is common practice to predict concentrations in aquatic organisms from observed values of C_w . Conversely, environmental levels may be extrapolated from analyses of the biota. It is thus useful to be aware of other variables that can influence bioconcentration.

1. *Time of Exposure* The concentration in the fish exposed to some compound is given by

$$C_f = (k_1/k_2)C_w(1 - e^{-k_2t})$$

at steady state

$$[C_f]_{ss} = (k_1/k_2)C_w$$

which would be attained at $t = \infty$. For $C_f = 0.99 [C_f]_{ss}$

$$C_f = 0.99[C_f]_{ss} = (k_1/k_2)C_w(1 - e^{-k_2t})$$

and thus

$$(1 - e^{-k_2t}) = 0.99$$

with $t_{0.99}$ being the time to achieve a value for C_f , which is 99% of the steady-state value. Then, $e^{-k_2t} = 0.01$, and taking natural logarithms, $-k_2 \cdot t_{0.99} = -4.605$ and

$$\log t_{0.99} = 0.663 + \log 1/k_2$$

Thus knowing k_e one can calculate $t_{0.99}$ and for TCDD, with $k_e = 0.0045 \text{ day}^{-1}$:

$$\log t_{0.99} = 0.663 + \log 1/0.0045$$

$$\log t_{0.99} = 0.663 + 2.346 = 3.01$$

and thus time to 99% of $[C_f]_{ss}$ would be 1023 days. An estimate of $t_{0.99}$ can be based on K_{ow} using the relation for k_2 above

$$\begin{aligned}\log t_{0.99} &= 0.663 + 0.663K_{ow} - 0.947 \\ &= 0.663K_{ow} - 0.284\end{aligned}$$

Those compounds that have higher K_{ow} values have a higher tendency to bioconcentrate, also have lower tendencies to be excreted, and will take longer times to achieve steady state. So, compounds that bioconcentrate will not only need to show high K_{ow} values, but will also have to persist to achieve C_f values approaching those predicted from K_B .

2. *Dissolved Organic Matter* Natural waters will always contain a certain amount of DOM. It has been demonstrated that hydrophobic compounds can partition into this compartment (Section 2.2.5.3, Chapter 2). The analysis of water samples does not usually discriminate between the amounts of compound in free solution and that associated with the DOM and, hence, the amount detected, C_{tot} would be

$$C_{tot} = C_w + C_{dom}$$

With only C_w being bioavailable, C_{tot} will overestimate the potential to bioconcentrate. The amount of compound associated with the DOM, C_{dom} , depends on the amount of organic matter [DOC], $\text{g} \cdot \text{mL}^{-1}$ (usually expressed on the basis of organic carbon) and the distribution coefficient $K_{doc} = X/C_w$, where X would be the amount of compound associated with the organic matter, $\text{g} \cdot \text{g}^{-1}$

$$C_{dom} = C_w K_{doc} [\text{DOC}]$$

The fraction of compound in solution, f_w , would then be expressed

$$f_w = \frac{C_w}{C_w + C_w K_{doc} [\text{DOC}]} = \frac{1}{1 + K_{doc} [\text{DOC}]}$$

In the presence of DOM, and observed bioconcentration factor, $[K_B]_{obs}$ would be given by

$$\begin{aligned}[K_B]_{obs} &= [K_B]_o \cdot f_w \\ &= [K_B]_o \frac{1}{1 + K_{doc} [\text{DOC}]}\end{aligned}$$

where $[K_B]_o$ would be the bioconcentration in the absence of DOM. It has been demonstrated that this relation can represent the effect of added DOM

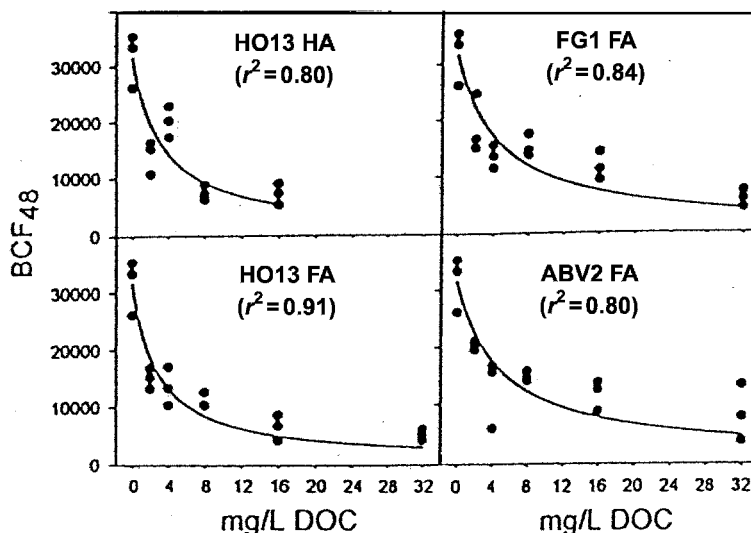


Figure 5.21 Effect of concentration of dissolved organic matter (humic acid, HA, and fulvic acid, FA) of different origin on the 48-h bioconcentration in a nematode *Caenorhabditis elegans*. [Reprinted from *Aquat. Toxicol.* **45**, M. Haitzer, S. Hoss, W. Traunspurger, and C. Steinberg, "Relationship between concentration of dissolved organic matter (DOM) and the effect of DOM on the bioconcentration of benzo[*a*]pyrene" p. 147. Copyright 1999, with permission from Elsevier.]

(humic or fulvic acids) on the observed bioconcentration factor (Fig. 5.21).^{26,27} A bioconcentration factor based on a 48-h exposure of a nematode to either pyrene or benzo[*a*]pyrene was observed in the presence of increasing amounts of the DOM. Statistical analysis of the data showed a good fit to the expression developed above and also provided an estimate of K_{doc} , Table 5.13. Values for K_{doc} vary with the compound and the nature of the DOM. Note that there have been reports that low concentrations of DOM enhance bioconcentration, that is, $[K_B]_{\text{obs}} > [K_B]_0$, however, it is not clear how consistent a response this might be nor is there any hypothesis proposed to account for such an effect.²⁸

TABLE 5.13 K_{doc} Derived from Bioconcentration Studies

DOM	$K_{\text{doc}} \text{ mL} \cdot \text{g DOC} \times 10^4$	
	Pyrene	Benzpyrene
HO13 HA	6.3 ± 1.1^a	30.2 ± 6.1
HO13 FA	3.3 ± 0.4	34.1 ± 4.7
FG1 FA	1.2 ± 0.2	20.9 ± 3.8
ABV2 FA	1.3 ± 0.2	19.8 ± 3.5

^aStandard error.

5.2.2.4 Bioaccumulation from Sediments The disposition of contaminated sediments is often a major challenge for regulating agencies. If they are left in place, what risk do they present to organisms at that site or if the site is dredged, where should the sediment be disposed? Organisms, such as clams, that reside in the sediments would be more likely to be at risk. The potential for these organisms to accumulate the chemical actually represents a competition between the sediment organic matter and the tissue lipid compartment for the chemical. The clam actually ingests the fine sediment and receives nutritive value from the organic matter. While passing through the digestive tract, the chemical would be released from the sediment organic matter to aqueous solution and subsequently be available for uptake by the organisms. So, although this would be defined as bioaccumulation—uptake from food—it would actually involve uptake from water.

A bioaccumulation factor, K_{BA} , can be defined on a dry weight basis as

$$K_{BA} = C_{org}/C_{sed}$$

If the C_{org} is expressed in terms of lipid content and C_{sed} on the basis of organic carbon a sediment bioaccumulation factor, K_{SBA} , is obtained

$$K_{SBA} = (C_{org}/f_l)/(C_{sed}/f_{oc})$$

Since the C_w , in this case the concentration in the interstitial water, is defined by both f_{oc} and K_{oc} , which in turn is expressed as a function of K_{ow} and C_{org} , depends on C_w and a K_B also related to K_{ow} , it is possible to predict K_{SBA} . The concentration in the interstitial water, C_w :

$$C_w = \mu\text{g} \cdot \text{g}^{-1} \text{org} \cdot \text{carb}/K_{oc}$$

and K_{oc} would be expressed (see Sorption, Chapter 3):

$$\log K_{oc} = 0.82 \log K_{ow} + 0.376 \quad \text{or} \quad K_{oc} = 2.38(K_{ow})^{0.82}$$

Assuming a partitioning process between C_w and the lipid phase in the organism, the steady-state concentration in the clam $[C_{org}]_{ss}$ expressed as $\mu\text{g} \cdot \text{g}^{-1}$ lipid would be expressed

$$[C_{org}]_{ss} = (K_B \cdot C_w)/f_l$$

and using the relation, $K_B = 0.048 K_{ow}$,

$$[C_{org}]_{ss} = \frac{0.048 K_{ow} C_w}{f_l}$$

Expressing C_w as a function of the sediment concentration based on organic carbon

$$[C_{\text{org}}] = \frac{0.048 K_{\text{ow}} \mu\text{g} \cdot \text{g}^{-1} \cdot \text{sed} \cdot \text{OC}}{f_1 K_{\text{oc}}} \\ = \frac{0.048 K_{\text{ow}} \mu\text{g} \cdot \text{g}^{-1} \cdot \text{sed} \cdot \text{OC}}{f_1 \cdot 2.38 [K_{\text{ow}}]^{0.82}}$$

Then K_{SBA} , the ratio of steady-state concentrations in sediment organic matter and clam lipid would be expressed

$$K_{\text{SBA}} = \frac{0.048 K_{\text{ow}} \mu\text{g} \cdot \text{g}^{-1} \cdot \text{sed} \cdot \text{OC}}{f_1 \cdot 2.38 [K_{\text{ow}}]^{0.82} / (\mu\text{g} \cdot \text{g}^{-1} \cdot \text{sed} \cdot \text{OC})} \\ = 0.42 [K_{\text{ow}}]^{0.18} \quad \text{assuming } f_1 = 0.048$$

An example of a study of the uptake from sediments is summarized in Table 5.14.²⁹ Surface sediments were derived from an estuary and sized giving a “bulk” fraction with particle size <1.0 mm and a “fine” fraction with particle size <0.125 mm. Note that the organic carbon content increased with decreasing particle size. Clams were maintained for 120 days on sediments that had been spiked with PCB congeners. Average congener levels in the sediments and clam tissue (4.7% fat) were reported. Values for K_{BA} were found to be consistently lower in clams on the fine sediments illustrating that the higher organic carbon affected the availability of the PCB (note that values listed for K_{BA} and K_{BSA} are the averages from individual clams and do not necessarily correspond to values derived from average tissue levels) and tended to increase and then decrease with increase in K_{ow} . Values of K_{BSA} tended to be higher in clams on the fine sediments.

TABLE 5.14 Accumulation of PCB Congeners in Clams from Sediments

PCB Congener No.	log K_{ow}	K_{SBA}^a	Bulk 0.80% OC				Fine 2.48% OC			
			C_{sed}^b	C_{org}^b	K_{BA}	K_{SBA}	C_{sed}^b	C_{org}^b	K_{BA}	K_{SBA}
18 (3 × Cl)	5.24	3.68	42.7	211	5.8	0.48	33.7	25	1.0	1.12
52 (4 × Cl)	5.84	4.72	55.8	1,027	21.8	1.47	54.4	244	5.8	3.13
118 (5 × Cl)	6.74	6.86	44.2	1,049	30.3	2.02	41.6	296	8.4	4.74
138 (6 × Cl)	6.83	7.12	56.5	979	19.9	1.39	52.9	297	6.3	3.70
180 (7 × Cl)	7.36	8.87	62.9	490	8.7	0.71	57.9	180	3.6	2.31
194 (8 × Cl)	7.80	10.6	44.7	160	4.0	0.35	39.8	67	1.9	1.12

^aCalculated from K_{ow} .

^b $\text{ng} \cdot \text{g}^{-1}$ dry weight basis.

Values for K_{BSA} observed in this study were consistently lower than those predicted although higher values have been reported in field studies of PCBs.³⁰ Predicted values are based on empirical relations between K_{ow} and K_{oc} and K_B , which would result in some uncertainty. For example, using different K_{ow}/K_{oc} and K_B relations a K_{BSA} of 1.9, has been reported, which is independent of K_{ow} .³¹ However, these projections do provide a basis for assessing the transfer of compounds from sediment to the biota but tend to overestimate the accumulation of compounds with $\log K_{ow} > 6$. This would parallel the relations observed with K_B and K_{ow} (Fig. 4.20) that illustrates the limited ability of these compounds with high K_{ow} to move across membranes. Variations among species and environmental conditions will also influence the distribution between sediments and biota and further studies are needed to develop a more comprehensive analysis of this process.

5.2.2.5 Bioaccumulation and Biomagnification With the introduction of the electron capture detector for GCs in the 1960s, detection limits for chlorinated hydrocarbons such as DDT were reduced to the 0.01 ppm range and investigators were able to detect these persistent compounds in environmental samples. Some of this early data³² from a study of biota associated with a river estuary on Long Island, N.Y. are compiled in Table 5.15. Concentrations in the organisms varied over three orders of magnitude from 0.040 mg · kg⁻¹ in plankton to 2.07 mg · kg⁻¹ in the carnivorous needlefish to as high as 75.5 mg · kg⁻¹ in a species of gull. Organisms higher in the food chain showed higher concentrations of DDT. Many other examples of this phenomenon have been reported.³¹ This “food chain magnification” or biomagnification was attributed to efficient transfer of the DDT from one level to the next with a reduced biomass at the higher level in the food chain. For example, assume organism A consumed 10 g of organism B that contained 10 μg of DDT (1 ppm) and 90% of the DDT was absorbed. If only 33% of this food was conserved as increased body weight in organism A containing 9 μg of DDT, the resultant concentration of DDT would be 9 μg in 3 g of tissue or 3 ppm. This simplistic example illustrates the basic idea.

In the aquatic environment, an organism can be exposed to a chemical through the water or the food and the change in concentration in the organism, C_f , involving

TABLE 5.15 DDT Levels in Biota from a Long Island Estuary

Sample	ΣDDT ^a (mg · kg ⁻¹)	Sample	ΣDDT (mg · kg ⁻¹)
Water	0.00005	Needlefish	2.07
Plankton	0.040	Green heron	3.57
Shrimp	0.16	Least tern	4.75
Mud snail	0.26	Common tern	5.17
Hard clam	0.42	Herring gull	7.53
Summer flounder	1.28	Cormorant	26.4
Pickrel	1.33	Ring-billed gull	75.5

^aSum of DDT and metabolites, DDE, and DDD.

both processes can be expressed

$$dC_f/dt = k_1C_w + \alpha FC_{fd} - k_2C_f - \gamma C_f$$

As noted before, k_1 would be the first-order rate constant defining the direct uptake from water, while the uptake from food would be expressed as a function of α , the absorption efficiency, the food intake, F (kg per kg body weight) and the concentration in the food, C_{fd} . A decrease in concentration would result from excretion, defined by k_2 and growth dilution expressed as a function of growth rate, γ , assuming exponential growth rate ($W_t = W_0e^{\gamma t}$). Note that loss constant k_2 could involve simple diffusion, metabolism, and physiological excretion. Uptake from water would be the only process involved for single-cell organisms, while, say, fish-eating birds would only be exposed through the food. Fish, on the other hand, may accumulate chemical both from the water and the food, with water being the predominant source.²¹ A steady-state bioaccumulation factor, K_{BA} , would thus be expressed

$$K_{BA} = \frac{[C_f]_{ss}}{C_w} = \frac{k_1 + \alpha F[K_B]_{fd}}{k_2 + \gamma}$$

where $C_{fd} = K_B C_w$ for the organism ingested.

It is of interest to compare the tendency of chemicals to accumulate in fish when exposed through the water or food. The change in concentration in a fish ingesting contaminated food can be expressed by a relation similar to that used to define uptake from water, taking into account uptake and excretion:

$$dC_f/dt = \alpha FC_{fd} - (k_2 + \gamma)C_f$$

and the concentration in the fish at time “ t ” would be expressed

$$[C_f]_t = \alpha F/(k_2 + \gamma)C_{fd}(1 - e^{-(k_2 + \gamma)t})$$

As with bioconcentration from water, at steady state, $dC_f/dt = 0$ and a bioaccumulation factor, K_{BA} can be expressed

$$K_{BA} = (\alpha F)/(k_2 + \gamma)$$

These relations have been used in the interpretation of observations with guppies in a study of the uptake of PCB congeners incorporated in food.³³ Tissue levels were monitored in guppies fed the contaminated diet for 30 weeks and during a 99-week depuration phase when they were fed control food. During the latter stage of the study, the concentration in the fish is defined

$$[C_f]_t = [C_f]_0 e^{-(k_2 + \gamma)t} \quad \text{or} \quad \ln[C_f]_t = \ln[C_f]_0 - (k_2 + \gamma)t$$

while the total amount in the fish, Q , would be defined

$$Q_t = Q_0 e^{-k_2 t} \quad \text{or} \quad \ln Q_t = \ln Q_0 - k_2 t$$

The slopes of the linear plots of $\ln C_f$ and $\ln Q$ versus time provide estimates of $(k_e + \gamma)$ and k_e , respectively. Data from the five of the PCB congeners studied are compiled in Table 5.16.

These PCB congeners (see Appendix) contain from 4 to 10 chloro substituents and as the $\log K_{ow}$ values indicate are quite hydrophobic. An exposure of 30 weeks was insufficient time to achieve steady state; $C_f/C_{fd} < K_{BA}$. Calculated K_B values for these congeners based on a fat content of 6.1% would be No. 52, 4.2×10^4 , No. 80, 1.8×10^5 , and No. 153, 5.1×10^5 , which are orders of magnitude higher than K_{BA} values observed for accumulation from food. This differential can be attributed to relative amounts of water and food processed by the fish and potential for the compounds to distribute into the more hydrophobic lipid compartment in the fish. For example, in this guppy study the lipid content of the food was 7.6% comparable to that of the fish and even if this decreases in the intestinal tract of the fish, the fat level in the fish would not be more than a factor of 2–3 higher. With the medaka used in the TCDD bioconcentration study (Table 4.9) it was observed that the fish cleared TCDD from a water volume equivalent to ~ 2000 times their body weight per day,¹⁹ while the guppies are only ingesting 25% of their body weight of food per week! Bioaccumulation and, hence, the potential for biomagnification appears to be a possibility with the more hydrophobic congeners assuming that one needs to achieve values of $K_{BA} > 2$. In this regard, it is of interest that a duplicate study with No. 209 gave a $K_{BA} = 5.94$.

There does not appear to be any systematic change in the efficiency with which these congeners are absorbed, however, the excretion rates, k_2 , illustrate the relation noted previously (Fig. 5.18) that compounds with higher K_{ow} values are not as readily excreted. Statistical analysis indicated that the k_2 value listed for No. 209 is not different from zero and, consequently, the change in concen-

TABLE 5.16 Accumulation of PCB Congeners from Food

Congener	$\log K_{ow}$	Conc. ($\text{mg} \cdot \text{kg}^{-1}$)		C_f/C_{fd}	$k_2 + \gamma$		γ (wk^{-1})	α (%)	K_{BA}^b
		Food	Fish ^a		(wk^{-1})	k_2 (wk^{-1})			
52	5.84	9.58	7.66	0.80	0.048	0.020	0.028	27	1.04
80	6.48	6.94	6.18	0.89	0.053	0.026	0.027	31	1.13
153	6.92	6.14	8.41	1.37	0.029	0.0019	0.027	37	2.84
194	7.80	8.09	10.4	1.29	0.031	0.0032	0.028	35	2.50
209	8.18	9.75	8.68	0.89	0.023	-0.041	0.027	24	2.28

^aAfter 30-week feeding period.

^b $K_{BA} = \alpha F / (k_2 + \gamma)$; $F = 0.25$ (kg food) \cdot (kg fish)⁻¹ \cdot week^{-1} .

hypothesis. These data were based on observations of the uptake of a series of chlorinated hydrocarbons and gives a regression equation

$$\log K_B(\text{triglyceride}) = 1.037 \log K_{\text{tg/w}} - 0.053 \text{ (correlation coefficient 0.95)}$$

with a slope of 1. Observations on marine zooplankton from estuaries in the eastern Pacific ocean also illustrated that lipid content was the overriding factor controlling the levels of PCBs detected in these samples.³⁶

High levels of contaminants observed in organisms at the top of a food chain such as seals, fish-eating birds, and so on may involve more efficient absorption in the digestive system. In addition, these organisms are exposed over a much longer period since they have longer life spans.

Biomagnification could occur in an aquatic system if the compound were taken up primarily from food and also showed a high K_{BA} . This could occur with PCB congener No. 209 (Table 4.14). With such a high K_{ow} , this compound would not bioconcentrate very efficiently, yet it is absorbed from the intestinal tract of the guppy as efficiently as congeners with lower K_{ow} values. Absorption of these hydrophobic compounds in the intestine may be facilitated by their being absorbed along with the lipid. So, uptake from food could predominate for this compound. This congener is not readily excreted, and thus if the same response was observed in successive levels in the food chain, biomagnification could occur.

REFERENCES

1. P. Yeagle, *The Structure of Biological Membranes*, CRC Press, Boca Raton, FL, 1992.
2. G. L. Flynn, S. H. Yalkowsky, and T. J. Roseman, *J. Pharm. Sci.* **63**, 479 (1974).
3. G. L. Flynn and S. H. Yalkowsky, *J. Pharm. Sci.* **61**, 838 (1972).
4. J. McKim, P. Schmieder, and G. Veith, *Toxicol. Appl. Pharmacol.* **77**, 1 (1985).
5. R. S. Hinz, C. R. Lorence, C. D. Hodson, C. Hansch, L. L. Hall, and R. H. Guy, *Fundam. Appl. Toxicol.* **17**, 575 (1991).
6. L. S. Shanker, D. J. Tocco, B. B. Brodie, and C. A. M. Hogben, *J. Pharmacol. Exp. Ther.* **123**, 81 (1958).
7. G. G. Briggs, R. H. Bromilow, and A. A. Evans, *Pestic. Sci.* **13**, 495 (1982).
8. G. G. Briggs, R. L. O. Rigitano, and R. H. Bromilow, *Pestic. Sci.* **19**, 101 (1987).
9. C. R. Harris, and W. W. Sans, *J. Agr. Food Chem.* **15**, 861 (1967).
10. M. J. I. Mattina, W. Iannucci-Berger, and L. Dykas, *J. Agr. Food Chem.* **48**, 1909 (2000).
11. A. Hulster, J. F. Müller, and H. Marschner, *Environ. Sci. Technol.* **28**, 1110 (1994).
12. C. Mc Farlane, T. Pfleeger, and J. Fletcher, *Environ. Toxicol. Chem.* **9**, 513 (1990).
13. C. E. Jeffree, "Structure and Ontogeny of Plant Cuticles," in *Plant Cuticles: an Integrated Functional Approach*, G. Kersteins, ed., Bios Scientific Publishers, Oxford, UK, 1996, p. 33.

14. J. C. Mc Farlane, "Anatomy and Physiology of Plant Conductive Systems," in *Plant Contamination, Modeling and Simulation of Organic Chemical Processes*, S. Trapp and J. C. Mc Farlane, eds., Lewis Publishers, Boca Raton, 1995, p. 13.
15. L. Schreiber and J. Schönherr, *Environ. Sci. Technol.* **26**, 153 (1992).
16. J. Schönherr and M. Riederer, *Rev. Environ. Contam. Toxicol.* **108**, 1 (1989).
17. L. A. Norris and V. H. Freed, *Weed Res.* **6**, 206 (1966).
18. S. Paterson, D. Mackay, D. Tam, and W. Y. Shiu, *Chemosphere* **21**, 297 (1990).
19. P. Schmeider, D. Lothenbach, J. Tietge, R. Erickson, and R. Johnson, *Environ. Toxicol. Chem.* **14**, 1735 (1995).
20. W. A. Bruggeman, L. B. J. M. Martron, D. Kooiman, and O. Hutzinger, *Chemosphere* **8**, 811 (1981).
21. D. W. Connell, *Rev. Environ. Contam. Toxicol.* **102**, 117 (1988).
22. C. T. Chiou, *Environ. Sci. Technol.* **19**, 57 (1985).
23. H. Könemann and K. van Leeuwen, *Chemosphere* **9**, 3 (1980).
24. D. W. Hawker and D. W. Connell, *Chemosphere* **14**, 1205 (1985).
25. A. Opperhuizen and D. T. H. M. Sijm, *Environ. Toxicol. Chem.* **9**, 175 (1990).
26. M. Haitzer, S. Hoss, W. Traunspurger, and C. Steinberg, *Aquat. Toxicol.* **45**, 147 (1999).
27. M. Haitzer, G. Abbt-Braun, W. Traunspurger, and C. E. W. Steinberg, *Environ. Toxicol. Chem.* **18**, 2782 (1999).
28. M. Haitzer, S. Hoss, W. Traunspurger, and C. Steinberg, *Chemosphere* **37**, 1335 (1998).
29. B. L. Boese, M. Winsor, H. Lee II, S. Echols, J. Pelletier, and R. Randall, *Environ. Toxicol. Chem.* **14**, 303 (1995).
30. J. L. Lake, N. I. Rubinstein, H. Lee II, C. A. Lake, J. Heltshe, and S. Pavignano, *Environ. Toxicol. Chem.* **9**, 1095 (1990).
31. L. H. Nowell, P. D. Capel, and P. D. Dileanis, *Pesticides in Stream Sediment and Aquatic Biota—Distribution, Trends and Governing Factors*, Lewis Publishers, Boca Raton, 1999, pp. 239–306.
32. G. M. Woodwell, C. F. Wurster, and P. A. Isaacson, *Science* **156**, 821 (1967).
33. D. T. H. M. Sijm, W. Seinen, and A. Opperhulzen, *Environ. Sci. Technol.* **26**, 2162 (1992).
34. G. A. Leblanc, *Environ. Sci. Technol.* **29**, 154 (1999).
35. J. A. Smith, P. J. Witkowski, and C. T. Chiou, *Rev. Environ. Contam. Toxicol.* **103**, 127 (1988).
36. J. R. Clayton, Jr., S. P. Pavlou, and N. F. Breiter, *Environ. Sci. Technol.* **11**, 676 (1977).

Photochemical Processes

It is common experience that sunlight can change materials, although we may not realize the chemical nature of these transformations. Colored objects will fade; some plastic materials, originally soft and pliable, can become brittle and most of us have experienced the discomfort of sunburn. The incidence of skin cancer is correlated with exposure to sunlight that induces changes in DNA. Thus in the context of this text it is important to develop a basis for assessing the extent to which compounds in the environment may be transformed by radiation. Consequently, it will be necessary to evaluate how radiation can interact with matter and what type of radiation induces chemical change. A discussion of how chemical change is produced will provide the perspective necessary for assessing which compounds might be susceptible, the rates at which these transformations occur, and the products that might be produced. This analysis must be relevant to those conditions that exist in the natural environment.

6.1 THE INTERACTION OF RADIATION WITH MATTER

6.1.1 Electromagnetic Radiation

The wavelength (λ) of the electromagnetic spectrum varies over 17 orders of magnitude (Table 6.1) and the frequency (ν) in cycles \cdot s⁻¹ is expressed as a function of wavelength and velocity, c (3.0×10^8 m \cdot s⁻¹).

$$\nu = c/\lambda$$

Radiation also acts as a particle, a photon, whose energy, E , is expressed as a function of frequency:

$$E = h \cdot \nu \quad \text{or} \quad E = h \cdot c/\lambda$$

where h is Planck's constant, 6.63×10^{-34} J \cdot s⁻¹. It is obvious that energy is inversely related to wavelength. It is possible to calculate energy in joules per Einstein

TABLE 6.1 Approximate Wavelength Ranges for Different Forms of Electromagnetic Radiation

Radiation Type	Wavelength (nm)
Radiowaves	$> 1 \times 10^9$
Microwaves	$3 \times 10^5 - 1 \times 10^9$
Infrared	$700 - 3 \times 10^5$
Visible	400–700
Ultraviolet	10–400
X-rays	0.1–10
Gamma rays	$1 \times 10^{-4} - 0.1$

(mole of photons) as a function of wavelength and compare these values with bond energies to determine what radiation might have sufficient energy to break a bond in an organic compound (Table 6.2).

Solar radiation at the surface of the earth (Fig. 6.1) is restricted to a narrower wavelength range and a lower intensity than that reaching the upper atmosphere. The cut-off at the lower wavelength (~ 290 nm) is due primarily to stratospheric ozone. It is clear, from Table 6.2, that the energy of solar radiation that reaches the earth's surface is sufficient to cleave bonds in organic compounds. X-rays and gamma rays, ionizing radiation, are more energetic but not as generally available in the environment.

6.1.2 Absorption Spectra

The ability of a compound to absorb radiation is readily determined using a spectrophotometer that compares the light absorbed by a solution with that of the solvent, and the absorbance, A , is expressed as a function of the wavelength of the incident light. Absorbance is defined by

$$A = \log \frac{I_0(\lambda)}{I(\lambda)}$$

TABLE 6.2 Comparison of Radiant and Bond Energies

λ (nm)	Radiant Energy (kJ · mol)	Bond Energy (kJ · mol)
200	597	C=C 590 C=F 490
300	398	C-H 414
400	298	C-C 331 C-O, C-Cl 326
500	239	C-S 289 C-N 285 C-Br 272

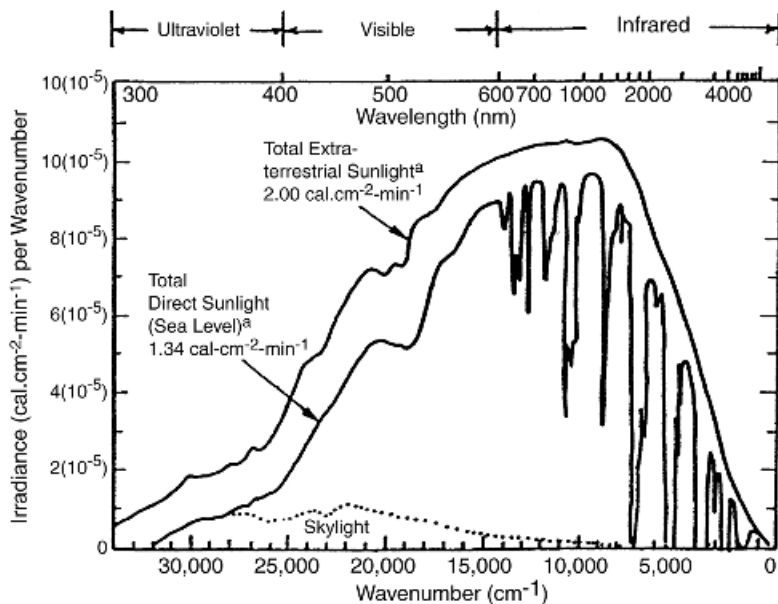


Figure 6.1 Spectral distribution of solar radiation.

where I_0 is the energy of the incident light at a specific wavelength and I is the energy of the emerging light at the same wavelength. The Beer–Lambert law relates absorbance to concentration, C in $\text{mol} \cdot \text{L}^{-1}$, length of the light path in cm, l , and the molar extinction coefficient $\varepsilon(\lambda)$, which would have units, $\text{L} \cdot \text{mol}^{-1} \cdot \text{cm}^{-1}$

$$A(\lambda) = \varepsilon(\lambda) \cdot C \cdot l$$

The molar extinction coefficient is an index of the efficiency with which a compound absorbs light at a given wavelength. It should also be noted that this relationship has been used extensively in analytical chemistry because concentration is directly related to absorbance that can be measured quite easily with a spectrophotometer.

In vapor-phase processes, it is conventional to express concentration, N , as $\text{molecules} \cdot \text{cm}^{-3}$ and absorption in terms of natural logarithms such that

$$\ln \frac{I_0}{I} = \sigma N l$$

With path length, l , in cm, the absorption cross section σ , will have units $\text{cm}^2 \cdot \text{molecule}^{-1}$. Taking into account the difference in concentration terms and logarithmic base, the relation between the molar extinction coefficient, $\varepsilon(\lambda)$ at a given wavelength and the equivalent absorption cross-section, $\sigma(\lambda)$ would be

$$\sigma(\lambda) = 3.82 \times 10^{-21} \varepsilon(\lambda)$$

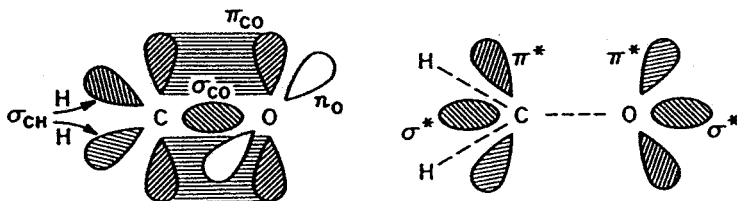


Figure 6.2 A schematic representation of bonding and anti-bonding orbitals in formaldehyde.

6.1.3 The Absorption Process—Molecular Orbitals

When atomic orbitals of atoms interact to form a covalent bond, the attraction between the two atoms is the result of the formation of a molecular orbital that concentrates electron density between the interacting atoms. Depending on the manner in which the atomic orbitals interact, sigma or pi bonding or antibonding orbitals may form. Antibonding orbitals are usually of a higher energy than the corresponding bonding orbital and as the term indicates do not result in any net bonding between atoms. Other valence electrons of the atoms involved would be classified as “nonbonding”, however, they can participate in excitation processes induced by electromagnetic radiation. Electrons in the inner shells of the atoms are not involved in these transitions.

These different molecular orbitals are illustrated schematically for a simple compound, formaldehyde (Fig. 6.2). The C—H bond is a sigma bond, while the C=O consists of a sigma and a pi bond, the latter resulting from the interaction of two-parallel atomic *p* orbitals. The additional two electron pairs associated with the oxygen would be in nonbonding orbitals. The antibonding orbitals between carbon and oxygen are also illustrated. Radiant energy will be absorbed at a wavelength where the energy of the photon corresponds to the energy change available to the electron. The absorption of radiant energy thus results in the movement of an electron from a lower to a higher energy orbital as illustrated in Figure 6.3 producing an

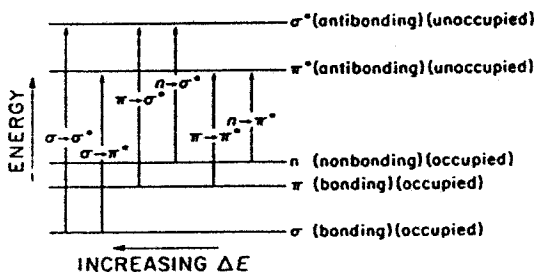


Figure 6.3 Representation of electron transitions indicating the relative magnitude of the energy change.

TABLE 6.3 Some Common Chromophores

Chromophore	Functional Group	Electron Transition	λ_{\max}	ϵ_{\max}
$-\ddot{\text{O}}-$	CH_3OH	$n \rightarrow \sigma^*$	1,830	500
$-\ddot{\text{S}}-$	$\text{C}_6\text{H}_{13}\text{SH}$	$n \rightarrow \sigma^*$	2,240	126
$-\ddot{\text{Cl}}:$	CH_3Cl	$n \rightarrow \sigma^*$	1,730	100
$-\ddot{\text{Br}}:$	CH_3Br	$n \rightarrow \sigma^*$	2,040	200
$-\ddot{\text{I}}:$	CH_3I	$n \rightarrow \sigma^*$	2,580	378
$-\ddot{\text{N}}-$	$(\text{CH}_3)_3\text{N}$	$n \rightarrow \sigma^*$	2,270	900
$> \text{C}=\text{C} <$	$\text{H}_2\text{C}=\text{CH}_2$	$\pi \rightarrow \pi^*$	1,710	15,500
$-\text{C}\equiv\text{C}-$	$\text{HC}\equiv\text{CH}$	$\pi \rightarrow \pi^*$	1,730	6,000
$> \text{C}=\ddot{\text{O}}:$	$(\text{CH}_3)_2\text{CO}$	$\pi \rightarrow \pi^*$	1,890	900
		$n \rightarrow \pi^*$	2,790	15

“excited” molecule. The most common transitions that correspond with radiant energy in the ultraviolet (UV) and visible range are $n \rightarrow \pi^*$, $\pi \rightarrow \pi^*$, and $n \rightarrow \sigma^*$. Some functional groups (chromophores) that provide these transitions are listed in Table 6.3 together with λ_{\max} and molar extinction coefficient. Absorption characteristics vary with the degree of unsaturation and the complexity of polynuclear aromatics (Tables 6.4 and 6.5). The organic chemist can thus predict the absorption tendencies of a compound. Ultraviolet–visible (UV–vis) spectra for some organic compounds have been compiled.¹

TABLE 6.4 Positions of First $\pi \rightarrow \pi^*$ Maxima in Compounds Containing Conjugated Double Bonds

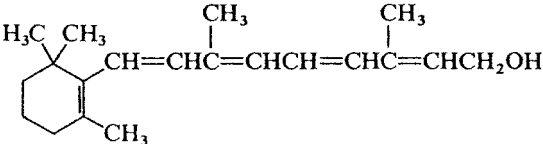
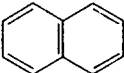
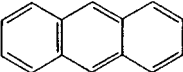
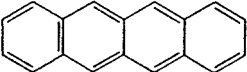
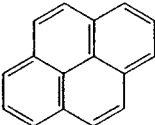
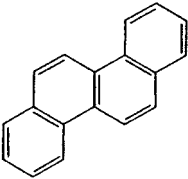
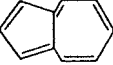
Compound	λ_{\max}	ϵ
$\text{CH}_2=\text{CHCH}=\text{CH}_2$	2,170	21,000
$\text{CH}_3\text{CH}=\text{CHCHO}$	2,170	16,000
$\text{CH}_2=\text{CHC}\equiv\text{CH}$	2,190	6,500
$\text{CH}_2=\text{CHC}\equiv\text{N}$	2,100	10,000
$\text{CH}_3\text{CH}=\text{CHNO}_2$	2,290	9,500
$\text{CH}_2=\text{CHCH}=\text{CHCH}=\text{CH}_2$	2,580	35,000
$\text{CH}_3\text{CH}=\text{CHCH}=\text{CHCH}=\text{CHCH}_2\text{OH}$	2,650	53,000
$\text{CH}_2=\text{CHCH}=\text{CHCHO}$	2,630	27,000
$\text{CH}_3(\text{CH}=\text{CH})_4\text{CH}_3$	2,960	52,000
	3,600	70,000
Vitamin A	3,280	51,000

TABLE 6.5 Absorption Spectra of Aromatic Hydrocarbons—Absorption Maxima of Highest Wavelength

	λ_{\max}	ϵ_{\max}
	2550	220
 Naphthalene	3120	250
 Anthracene	3750	7900
 Phenanthrene	3300	250
 Naphthacene	4730	11,000
 Pyrene	3520	630
 Chrysene	3600	630
 Azulene	6070	263

6.2 WHAT HAPPENS TO THE EXCITED SPECIES?

When molecules absorb radiant energy electrons are moved to higher energy levels creating a molecule that has more energy than its ground state; an “excited” species. A review of the behavior of the latter provides an understanding of how chemical

change can be produced. First, it will be useful to define some terminology that is used in photochemistry.

6.2.1 Singlets Triplets and Radicals

Most introductory chemistry texts will include the diagram in Figure 6.4 in the discussion of molecular orbitals. This schematic summarizes the allowed molecular orbitals for simple diatomic molecules and with the application of Hund's rule the distribution of the 16 electrons of O_2 result in two unpaired electrons in the π^* orbital. The paramagnetic response of oxygen is readily demonstrated by diverting the flow of liquid oxygen with a magnet. With magnetic properties influencing interaction with electromagnetic radiation, it is apparent that electron spin will be a factor in photochemical processes. The total spin, S , of all the electrons in a molecule is obtained by simply adding the spins ($\pm\frac{1}{2}$) of all the electrons. The spectroscopist studying excited species uses "spin multiplicity" given by $2S + 1$ to define response in a magnetic field. If all the electron spins are paired $S = 0$ and the spin multiplicity will be one and the species is referred to as a "singlet". The O_2 molecule has two unpaired electrons with parallel spins, $S = 1$ and spin multiplicity of 3 and is classified as a "triplet". Singlet-triplet transitions occur in transformations of excited species resulting in different deexcitation processes.²

A covalent bond represented by A:B may break to form either ions or radicals. Heterolytic cleavage, where the bonding electrons associate with either A or B

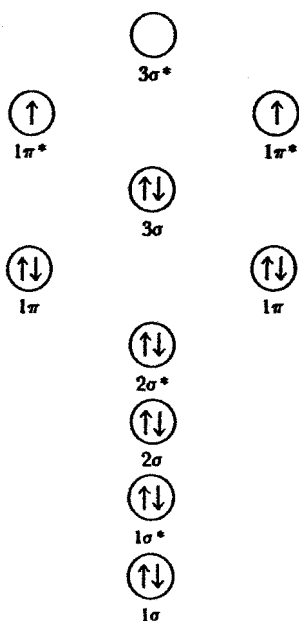
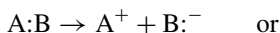
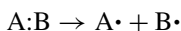


Figure 6.4 Electron distribution in the molecular orbitals of O_2 .

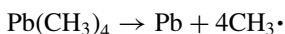
will yield ions;



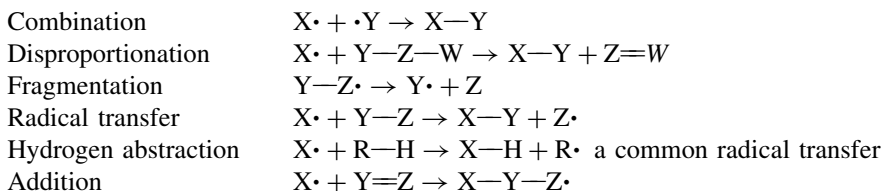
This process is facilitated in water since the energy generated by the water molecules or other polar solvents associating with the ions drives the process. Homolytic cleavage on the other hand, produces radicals



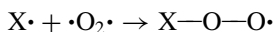
A free radical, then, has an unshared electron and has no charge. It is very reactive and not solvated and does not develop high concentrations in solution. It will be demonstrated that radicals can be produced photochemically and in some cases by thermal processes, for example,



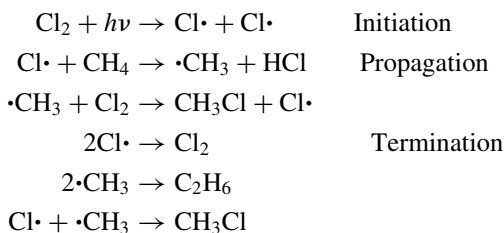
Radicals undergo a variety of reactions:



A common combination process involves reaction with molecular oxygen to form a reactive peroxide radical:



Many of the reactions listed above produce a radical and chain reaction results from a sequence of reactions illustrated by the photochemical chlorination of methane:



If propagation reactions compete favorably with termination reactions, the formation of two chlorine radicals could result in the reaction of many molecules of methane. It should be noted that this effect is important in the loss of stratospheric ozone resulting from the production of chlorine or bromine radicals from freons. Free radicals are very important in biological processes involving oxygen and their production is involved in some toxicological mechanism. In organic chemistry, free radicals are a major factor in polymerization processes.

6.2.2 Molecular Energy States and Jablonski Diagrams

Before discussing the possible transitions of the excited molecule, it will be useful to consider how a Jablonski diagram (Fig. 6.5) summarizes the energy states of a molecule. Both singlet and triplet energy levels are indicated along with vibration energy levels possible within the different S and T states. Note that the absorption of radiant energy that results in an electron moving from the ground state S_0 to the higher energy level, S_1 , does not involve a change in spin, however, the intersystem crossing (ISC) from S_1 to T_1 does. Internal conversion (IC), involves transition from an S_1 to an S_0 level (no change in spin) but at a much higher vibration energy status.

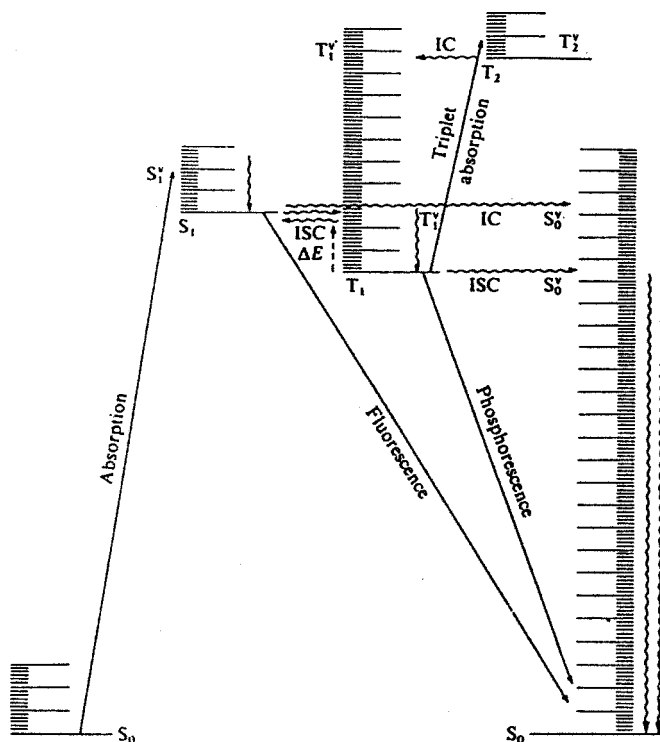


Figure 6.5 A Jablonski diagram illustrating transitions in a photoexcited molecule.

6.2.3 Transformations of the Excited Molecule

A variety of competing options are available to use the energy in the excited species, with only several resulting in chemical change. The processes involve



The species, M, can accept some energy from the excited molecule without undergoing any chemical change.



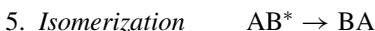
Light is emitted as fluorescence or phosphorescence depending on whether it originates from a singlet or triplet (Fig. 6.5). In the latter case, there is a time delay since the triplet state has a longer lifetime than the singlet. It can be seen from the Jablonski diagram that the energy of the fluorescence or phosphorescence radiation will define the energy levels of the singlet and triplet excited states.



This could involve either an internal conversion or intersystem crossing and the molecule remains in an excited state.



This transformation would be unlikely under environmental conditions since solar energy would not result in an excited state of sufficient energy.



An example of this transition is the conversion of trans retinol to cis retinol that occurs in the vision process.



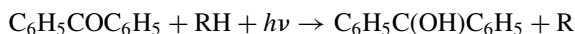
This process can result in the transformation of a molecule that does not absorb and the process is referred to as sensitization.



It can be seen that if a molecule at either an S_1 or T_1 excited state moves to a higher vibration level of the ground state that bond breaking could result.

8. *Direct reaction*

The reactivity of the excited species will be influenced by both its energy level and rearranged electron configuration. Excited species are usually both better electron donors and electron acceptors than their parent molecules. The excited electron would be more readily donated while the low-energy "vacancy" left by the excited electron would more readily accept an electron. The redistribution of electrons in molecular orbitals may influence shape and dipole moments. Hydrogen abstraction is a common reaction of excited species. For example, benzophenone in the presence of a suitable donor solvent such as ethanol is readily reduced to the alcohol.



6.2.4 Quantum Yield Φ

This quantity defines the efficiency of the photochemical process by expressing the amount of change induced by the light energy of a given wavelength. A distinction must be made, however, between a primary (φ) and overall or reaction (Φ) quantum yield. The former defines those processes directly involving the excited species.

$$\varphi_{\lambda} = \frac{\text{Molecules of AB}^* \text{ reacting by pathway } x}{\text{Photons of wavelength, } \lambda, \text{ absorbed}}$$

The Stark–Einstein law states that one molecule is excited for each quantum or photon of radiation absorbed, consequently, the sum of the primary quantum yields should equal one. This is illustrated by observations of φ for fluorescence ($S_1 \rightarrow S_0$) and intersystem crossing ($S_1 \rightarrow T_1$) for some aromatic hydrocarbons in ethanol solution (Table 6.6).³

For this series of compounds, with the exception of benzene, these two processes account for the response of the excited species.

The definition of environmental behavior, however, involves the overall quantum number, Φ :

$$\Phi_{\lambda} = \frac{\text{Molecules of AB reacted}}{\text{Photons of wavelength, } \lambda, \text{ absorbed}}$$

Figure 6.6 summarizes the reactions involved in the photolysis of *p*-chlorophenol⁴ at 254 or 296 nm in aqueous solution. Such a study involves the identification of products and postulation of the reaction sequence. Primary reactions involving the excited phenol, in this case produce the phenolic radical through dissociation and resorcinol by direct reaction with water. Subsequent secondary (sometimes referred to as “dark” reactions) reactions produce the products that can be detected. The major product was found to be the chloro-dihydroxy-biphenyl. The presence of oxygen resulted in an increase in the proportion of quinone formed. The derivation of a quantum yield requires a measurement of the intensity of the incident light along with the extinction coefficient and concentration of the compound in solution. The former is determined with an actinometer in which the amount of change induced in

TABLE 6.6 Primary Quantum Yields in Ethanol for some Aromatic Compounds

Compound	φ_f	φ_{ISC}	$\varphi_f + \varphi_{ISC}$
Benzene	0.04	0.15	0.19
Naphthalene	0.80	0.21	1.01
Anthracene	0.72	0.32	1.02
Phenanthrene	0.85	0.13	0.98
Pyrene	0.38	0.65	1.03

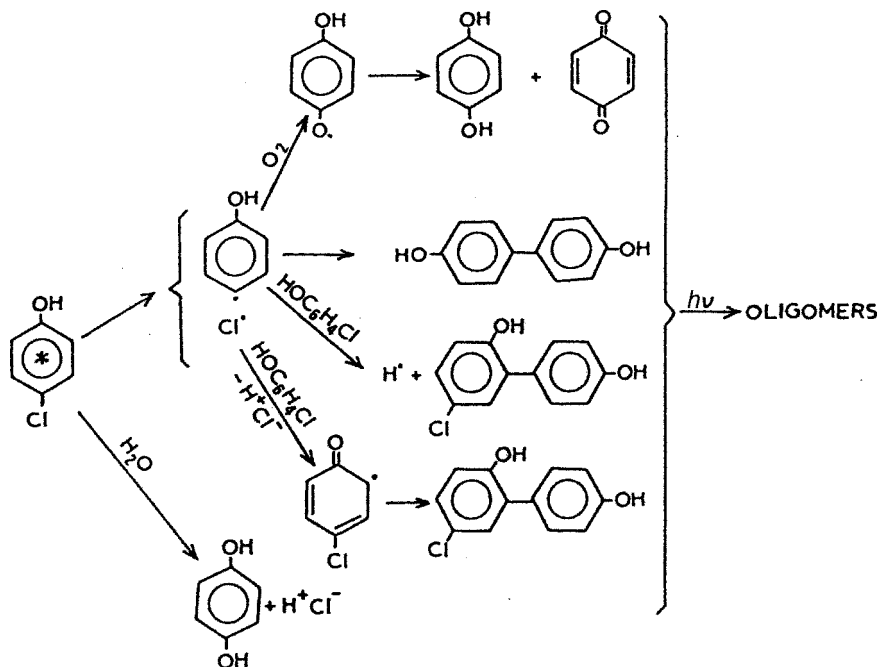


Figure 6.6 Reaction sequences for the photochemical degradation of *p*-chlorophenol. [Reproduced with permission from P. Boule, C. Guyon, A. Tissot, and J. Lemaire, "Specific Phototransformation of Xenobiotic Compounds: Chlorobenzenes and Halophenols", in R. G. Zika and W. J. Cooper, Eds, *Photochemistry of Environmental Aquatic Systems*, ACS Symposium Series No. 327, pp. 10–26. Copyright 1985, American Chemical Society.]

a compound of known Φ is monitored. Under the conditions of this study Φ was found to be 0.40. Quantum yields (Table 6.7)^{5–7} can change with change in wavelength of the incident light, but not to the same extent as with changes in solvent. Solvent also influences the secondary reactions and consequently the end products (Fig. 6.7).⁵

6.3 RATES OF DIRECT PHOTOLYSIS

When the compound absorbing radiation is transformed, the process is referred to as direct photolysis. Many studies in this area focus on the development of an understanding of the fundamentals of the process; defining energies of the excited states and reaction pathways. Such studies would be carried out under conditions where the incident radiation and reaction environment is carefully controlled. By contrast, investigations under environmental conditions must account for the fact that solar

TABLE 6.7 Overall Reaction Quantum Yields and Half-Lives in Sunlight⁵⁻⁷

Compound	Solvent	λ (nm)	Φ	Calc. $t_{1/2}$ ^b
Chlorobenzene	H ₂ O/1% Acetonitrile	250–300	0.37	170 year
1,2,4-Trichlorobenzene	H ₂ O/10% Acetonitrile	250–300	0.043	450 year
2-Chlorobiphenyl	H ₂ O/10% Acetonitrile	250–300	0.29	18 year
4-Chlorobiphenyl	H ₂ O/10% Acetonitrile	250–300	0.0020	8.2 year
2-Chlorobiphenylether	H ₂ O/10% Acetonitrile	250–300	0.19	3.6 day
2-Chlorobiphenylether	Hexane	250–300	0.97	
4-Chlorobiphenylether	H ₂ O/10% Acetonitrile	250–300	0.63	200 day
TCDD ^a	H ₂ O/10% Acetonitrile	313	0.0022	6 day
TCDD	H ₂ O/10% Acetonitrile	Sunlight	0.0007	
TCDD	Hexane	313	0.049	
PCDD ^a	H ₂ O/Acetonitrile	313	9.8×10^{-5}	15 day
	2:3,v/v			
HCDD ^a	H ₂ O/Acetonitrile	313	1.1×10^{-4}	6.3 day
	2:3,v/v			
Benz[a]anthracene	H ₂ O/1% Acetonitrile	313	3.2×10^{-3}	0.5 h
Benz[a]anthracene	H ₂ O/1% Acetonitrile	366	3.4×10^{-3}	
Benzo[a]pyrene	H ₂ O/1% Acetonitrile	313	8.9×10^{-4}	0.5 h
Benzo[a]pyrene	H ₂ O/1% Acetonitrile	366	5.4×10^{-4}	
Quinoline	H ₂ O/1% Acetonitrile	313	3.3×10^{-4}	20.9 day
Benzo[f]quinoline	H ₂ O/1% Acetonitrile	313	0.014	0.4 h

^aTCDD 2,3,7,8-tetrachlorodibenzodioxin.

PCDD 1,2,3,4,7-pentachlorodibenzodioxin.

HCDD 1,2,3,4,7,8-hexachlorodibenzodioxin.

^bCalculated at 40° latitude in summer.

radiation can be quite variable and the compound may be dispersed in the atmosphere or some surface water. However, through the development of computer programs to define the intensity of solar radiation and experimental observations of molar extinction coefficients and quantum yields it has become possible to predict the rates of degradation by direct photolysis.

6.3.1 Direct Photolysis in Water

Photolysis rates must be proportional to the total number of photons absorbed per unit time since only one molecule would be activated per photon absorbed according to the Stark–Einstein law. The reaction quantum yield would define the extent to which the activated molecules are transformed. The near-surface (≤ 50 cm) **specific rate of light absorption**, $k_a(\lambda)$ in water at a given wavelength is expressed in terms of the **solar irradiance**, $Z(\lambda)$ (photons \cdot cm⁻² \cdot s⁻¹, or meinsteins \cdot cm⁻² \cdot s⁻¹) and the molar extinction coefficient, $\epsilon(\lambda)$:

$$k_a(\lambda) = 2.3Z(\lambda)\epsilon(\lambda)$$

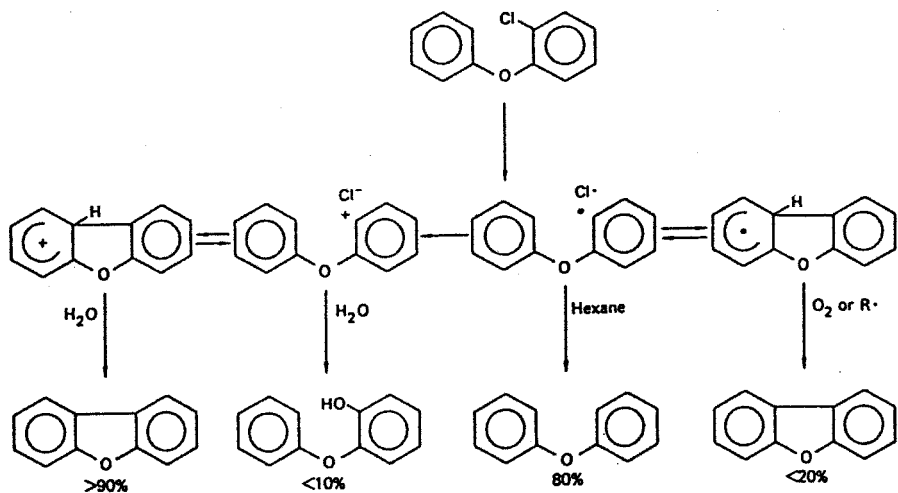


Figure 6.7 Effect of solvent on photochemical transformation of a chlorodiphenylether. [Reproduced with permission from D. Dulin, H. Drossman, and T. Mill, *Environ. Sci. Technol.* **20**, 72 (1986). Copyright © 1986, American Chemical Society.]

and the rate of absorption of light by the compound per unit volume would be $k_a(\lambda) \cdot C$, with C the molar concentration. The magnitude of Z will depend on the angular height of the sun and other atmospheric variables and will vary with time of day, season of the year and latitude. Computer programs have been developed to calculate Z and discussions of the concepts involved in defining this parameter are available.⁸⁻¹⁰ Values for Z are compiled in Table 6.8 for midday at 40° latitude over the four seasons. In addition, an averaged 24 h $Z(\lambda)$ is included that accounts for daily fluctuations and provides the basis for evaluating degradation rates of compounds that may take several days allowing comparison with degradation rates by other mechanisms. The units for $k_a(\lambda)$ would be

$$\begin{aligned} & (\text{einsteins} \cdot \text{cm}^{-2} \cdot \text{s}^{-1}) (\text{L} \cdot \text{mol}^{-1} \cdot \text{cm}^{-1}) \\ & \text{einsteins} \cdot \text{cm}^{-3} \cdot \text{s}^{-1} \cdot 1000 \text{ cm}^3 \cdot \text{mol}^{-1} \\ & 1000 \cdot \text{einsteins} \cdot \text{mol}^{-1} \cdot \text{s}^{-1} \end{aligned}$$

When $Z(\lambda)$ is expressed in meinsteins, $k_a(\lambda)$ has units of einsteins/mol/s.

The rate at which a compound is transformed by direct photolysis will be determined by the rate at which radiation is absorbed by that compound that will be determined, in turn, by the radiation available, Z , and the absorption of that radiation by the compound. The absorption of quinoline in the solar range is defined by the extinction coefficients (Table 6.9). Note that average molar extinction coefficients correspond to the wavelength range of Z and $k_a(\lambda)$ values can be calculated for

TABLE 6.8 Solar Irradiance in Water at Shallow Depth; Latitude 40°N

Wavelength (nm)	Z^a (meinstein · cm ⁻² · s ⁻¹)				Z_A^b (meinstein · cm ⁻² · day ⁻¹)			
	Spring	Summer	Fall	Winter	Spring	Summer	Fall	Winter
297.5	4.10 (-10)	1.19 (-9) ^c	1.57 (-10)	0.00	1.85 (-5)	6.17 (-5)	7.83 (-6)	5.49 (-7)
300.0	1.99 (-10)	3.98 (-9)	8.69 (-10)	1.21 (-10)	1.06 (-4)	2.69 (-4)	4.76 (-5)	5.13 (-6)
302.5	6.95 (-9)	1.20 (-8)	3.70 (-9)	6.10 (-10)	3.99 (-4)	8.30 (-4)	1.89 (-4)	3.02 (-5)
305.0	2.01 (-8)	3.00 (-8)	1.11 (-8)	2.82 (-9)	1.09 (-3)	1.95 (-3)	5.40 (-4)	1.19 (-4)
307.5	3.70 (-8)	5.06 (-8)	2.24 (-8)	7.46 (-9)	2.34 (-3)	3.74 (-3)	1.19 (-3)	3.38 (-4)
310	6.17 (-8)	8.21 (-8)	3.45 (-8)	1.42 (-8)	4.17 (-3)	6.17 (-3)	2.19 (-3)	7.53 (-4)
312.5	9.69 (-8)	1.19 (-7)	6.15 (-8)	2.94 (-8)	6.51 (-3)	9.07 (-3)	3.47 (-3)	1.39 (-3)
315	1.29 (-7)	1.55 (-7)	8.19 (-8)	4.49 (-8)	9.18 (-3)	1.22 (-2)	4.97 (-3)	2.22 (-3)
317.5	1.65 (-7)	1.91 (-7)	1.06 (-7)	6.00 (-8)	1.20 (-2)	1.55 (-2)	6.57 (-3)	3.19 (-3)
320	1.94 (-7)	2.24 (-7)	1.33 (-7)	8.26 (-8)	1.48 (-2)	1.87 (-2)	8.18 (-3)	4.23 (-3)
323.1	3.67 (-7)	4.18 (-7)	2.39 (-7)	1.50 (-7)	2.71 (-2)	3.35 (-2)	1.51 (-2)	8.25 (-3)
330	1.26 (-6)	1.40 (-6)	8.42 (-7)	5.67 (-7)	9.59 (-2)	1.16 (-1)	5.44 (-2)	3.16 (-2)
340	1.46 (-6)	1.60 (-6)	1.00 (-6)	6.97 (-7)	1.23 (-1)	1.46 (-1)	7.09 (-2)	4.31 (-2)
350	1.56 (-6)	1.71 (-6)	1.07 (-6)	7.45 (-7)	1.37 (-1)	1.62 (-1)	8.04 (-2)	4.98 (-2)
360	1.67 (-6)	1.82 (-6)	1.14 (-6)	7.94 (-7)	1.52 (-1)	1.79 (-1)	9.02 (-2)	5.68 (-2)
370	1.86 (-6)	2.02 (-6)	1.25 (-6)	8.62 (-7)	1.63 (-1)	1.91 (-1)	9.77 (-2)	6.22 (-2)
380	2.06 (-6)	2.24 (-6)	1.36 (-6)	9.32 (-7)	1.74 (-1)	2.04 (-1)	1.05 (-1)	6.78 (-2)
390	2.47 (-6)	2.67 (-6)	1.79 (-6)	1.33 (-6)	1.64 (-1)	1.93 (-1)	9.86 (-2)	6.33 (-2)
400	3.53 (-6)	3.83 (-6)	2.59 (-6)	1.92 (-6)	2.36 (-1)	2.76 (-1)	1.42 (-1)	9.11 (-2)
410	4.64 (-6)	5.01 (-6)	3.42 (-6)	2.55 (-6)	3.10 (-1)	3.64 (-1)	1.87 (-1)	1.20 (-1)
420	4.78 (-6)	5.14 (-6)	3.52 (-6)	2.64 (-6)	3.19 (-1)	3.74 (-1)	1.93 (-1)	1.24 (-1)
430	4.59 (-6)	4.94 (-6)	3.40 (-6)	2.55 (-6)	3.08 (-1)	3.61 (-1)	1.87 (-1)	1.20 (-1)
440	5.42 (-6)	5.82 (-6)	4.05 (-6)	3.05 (-6)	3.65 (-1)	4.26 (-1)	2.22 (-1)	1.43 (-1)

(continued)

TABLE 6.8 Continued

Wavelength (nm)	Z^a (meinstein \cdot cm $^{-2}$ \cdot s $^{-1}$)				Z_λ^b (meinstein \cdot cm $^{-2}$ \cdot day $^{-1}$)			
	Spring	Summer	Fall	Winter	Spring	Summer	Fall	Winter
450	6.10 (-6)	6.53 (-6)	4.56 (-6)	3.45 (-6)	4.11 (-1)	4.80 (-1)	2.51 (-1)	1.61 (-1)
460	6.15 (-6)	6.60 (-6)	4.63 (-6)	3.50 (-6)	4.16 (-1)	4.85 (-1)	2.54 (-1)	1.64 (-1)
470	6.37 (-6)	6.82 (-6)	4.79 (-6)	3.63 (-6)	4.30 (-1)	5.02 (-1)	2.63 (-1)	1.69 (-1)
480	6.50 (-6)	6.97 (-6)	4.91 (-6)	3.73 (-6)	4.40 (-1)	5.14 (-1)	2.70 (-1)	1.74 (-1)
490	6.15 (-6)	6.57 (-6)	4.66 (-6)	3.53 (-6)	4.16 (-1)	4.86 (-1)	2.56 (-1)	1.65 (-1)
500	6.27 (-6)	6.70 (-6)	4.76 (-6)	3.62 (-6)	4.25 (-1)	4.96 (-1)	2.62 (-1)	1.68 (-1)
525	6.60 (-6)	7.06 (-6)	5.06 (-6)	3.85 (-6)	1.12	1.31	6.93 (-1)	4.45 (-1)
550	6.85 (-6)	7.33 (-6)	5.27 (-6)	4.00 (-6)	1.16	1.36	7.21 (-1)	4.61 (-1)
575	6.92 (-6)	7.40 (-6)	5.34 (-6)	4.03 (-6)	1.17	1.37	7.22 (-1)	4.61 (-1)
600	6.98 (-6)	7.46 (-6)	5.41 (-6)	4.10 (-6)	1.18	1.38	7.39 (-1)	4.69 (-1)
625	7.00 (-6)	7.46 (-6)	5.46 (-6)	4.18 (-6)	1.20	1.40	7.50 (-1)	4.82 (-1)
650	7.03 (-6)	7.48 (-6)	5.51 (-6)	4.25 (-6)	1.21	1.41	7.62 (-1)	4.95 (-1)
675	7.01 (-6)	7.43 (-6)	5.52 (-6)	4.30 (-6)	1.22	1.41	7.68 (-1)	5.03 (-1)
700	6.95 (-6)	7.35 (-6)	5.47 (-6)	4.28 (-6)	1.21	1.40	7.66 (-1)	5.05 (-1)
750	6.65 (-6)	7.01 (-6)	5.27 (-6)	4.15 (-6)	2.33	2.69	1.48	9.84 (-1)
800	6.38 (-6)	6.72 (-6)	5.07 (-6)	4.01 (-6)	2.25	2.59	1.43	9.56 (-1)

^aAt shallow depth at midday.^bDay-averaged mid-season values. Sometimes designated by the symbol, L_λ .^cParentheses equal power of 10.

TABLE 6.9 Calculation of Near-Surface Specific Light Absorption Rate, k_a for Quinoline at 40° Latitude on a Clear Mid-summer Day

λ (center) (nm)	$\varepsilon(\lambda)$ (L · mol ⁻¹ · cm ⁻¹)	$Z(\lambda)$ 24 h (meinstein · cm ⁻² · day ⁻¹)	$k_a(\lambda)$ $k_a(\lambda) = 2.3 \cdot Z(\lambda) \cdot \varepsilon(\lambda)$
297.5	2910	2.68×10^{-5}	0.18
300.0	3050	1.17×10^{-4}	0.82
302.5	2740	3.60×10^{-4}	2.27
305.0	2480	8.47×10^{-4}	4.83
307.5	2050	1.62×10^{-3}	7.64
310.0	2440	2.68×10^{-3}	15.00
312.5	2920	3.94×10^{-3}	26.50
315.0	1680	5.30×10^{-3}	20.50
317.5	622	6.73×10^{-3}	9.63
320.0	269	8.12×10^{-3}	5.02
323.1	119	1.45×10^{-2}	3.97
330.0	26	5.03×10^{-2}	3.01
340.0	9	6.34×10^{-2}	1.31
$k_a = \Sigma k_a(\lambda) = 100.7$ einsteins (mol quinoline) ⁻¹ · day ⁻¹			

each $\Delta\lambda$. It can be seen in Figure 6.8 how Z and ε values interact in determining values of $k_a(\lambda)$. The specific rate of light absorption, k_a , for the compound is then represented by the integral of the $k_a(\lambda)/\lambda$ relation:

$$k_a = 2.303 \Sigma Z(\lambda) \cdot \varepsilon(\lambda)$$

which for quinoline under the conditions stipulated would be 100.7 einstein · mol⁻¹ · day⁻¹.

The rate at which a compound is transformed in a near-surface aquatic system is given by

$$-\left(\frac{dC}{dt}\right)_p = k_p C$$

where k_p is the first-order rate constant for direct photolysis. It is assumed that the reaction quantum yield is essentially constant over the absorption wavelength range and

$$k_p = \Phi k_a$$

Thus for the quinoline example with $\Phi = 3.3 \times 10^{-4}$ mol · einstein⁻¹

$$\begin{aligned} k_p &= 3.3 \times 10^{-4} (\text{mol} \cdot \text{einstein}^{-1}) \cdot 100.7 (\text{einstein} \cdot \text{mol}^{-1} \cdot \text{day}^{-1}) \\ &= 0.0332 \text{ day}^{-1} \end{aligned}$$

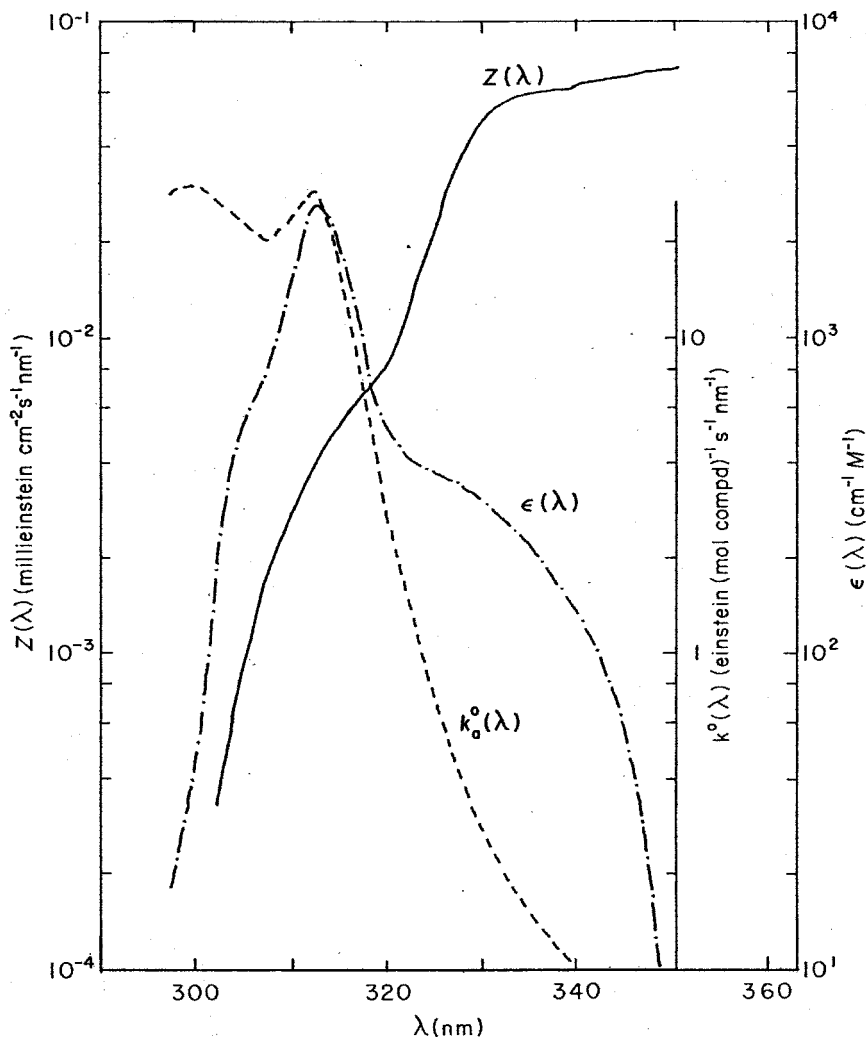


Figure 6.8 Graphical presentation of the data in Table 6.9 used to calculate the specific light absorption rate for quinoline at 40° latitude on a clear mid-summer day.

and the half-life would be given by

$$t_{1/2} = \frac{0.693}{0.0332} = 20.9 \text{ days}$$

Half-lives listed in Table 6.7 were calculated for summer at 40° latitude using either instantaneous noon, or 24-h integrated Z values depending on whether the half-life was substantially $<$ or $>$ 1 day. It is clear that direct photolysis will be an important

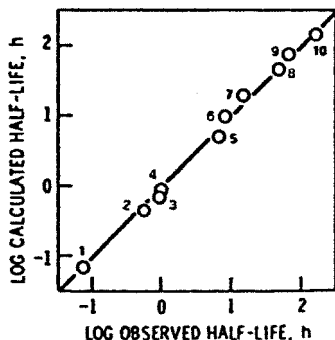


Figure 6.9 Comparison of calculated and observed half-lives for direct photolysis of several pesticides and pesticide derivatives; quantum yields given in parentheses. 1. *N*-Nitrosoatrazine in water ($\Phi = 0.30$); 2. trifluralin in water ($\Phi = 0.0020$); 3. DDE analogue of methoxychlor, DMDE, in water ($\Phi = 0.30$); 4. DMDE in hexadecane ($\Phi = 0.20$); 5. DDE in hexadecane ($\Phi = 0.26$); 6. diphenylmercury in water ($\Phi = 0.27$); 7. phenylmercuric acetate in water ($\Phi = 0.25$); 8. 2,4-D-butoxyethyl ester in hexadecane ($\Phi = 0.17$); 9. carbaryl in water ($\Phi = 0.0060$); 10. 2,4-D-butoxyethyl ester in water ($\Phi = 0.056$). [Reproduced with permission from R. G. Zepp and D. M. Cline, *Environ. Sci. Technol.* **11**, 359 (1977). Copyright © 1977, American Chemical Society.]

degradation process for some compounds such as polynuclear hydrocarbons. It is also of interest to note that low quantum yields may be compensated by high absorption efficiency to yield significant degradation rates. The utility of this approach is demonstrated by the correlation observed between experimental and calculated values (Fig. 6.9).

6.3.2 Direct Photolysis in Air

A similar approach can be used to estimate atmospheric degradation rates¹¹ with the first-order rate constant, k_p expressed as follows:

$$k_p = \Phi \sum \sigma_{\Delta\lambda} F_{\delta\lambda}$$

with Φ being the reaction quantum yield σ , the absorption cross-section in $\text{cm}^2 \text{molecule}^{-1}$ and F , the actinic flux in air in $\text{photons cm}^{-2} \cdot \text{s}^{-1}$. Radiation striking a volume of gas in the atmosphere includes direct solar radiation along with scattered and reflected radiation and varies with altitude, latitude, time of day, and season and values for F taking into account these variables have been compiled.¹¹

6.4 INDIRECT PHOTOLYSIS

A number of observations have demonstrated that compounds may be transformed more rapidly when irradiated in natural waters than in pure distilled water. Nitro-

aromatic compounds such as trinitrotoluene are common contaminants of military installations and from Figure 6.10 it is clear that this compound is more labile in samples of surface waters. Trinitrotoluene is transformed when irradiated in distilled water but at rates only 0.1–0.01 of those in natural waters.¹² Ethylene thiourea, dissolved in sterilized agricultural drainage water decomposes rapidly in sunlight, but is stable in pure water under comparable conditions.¹³ This compound has an absorption maximum at 240 nm and does not absorb in sunlight ($\lambda > 290$ nm). The reaction of the trinitrotoluene and the ethylene thiourea has been attributed to “sensitizing” action of dissolved organic matter in the natural water.

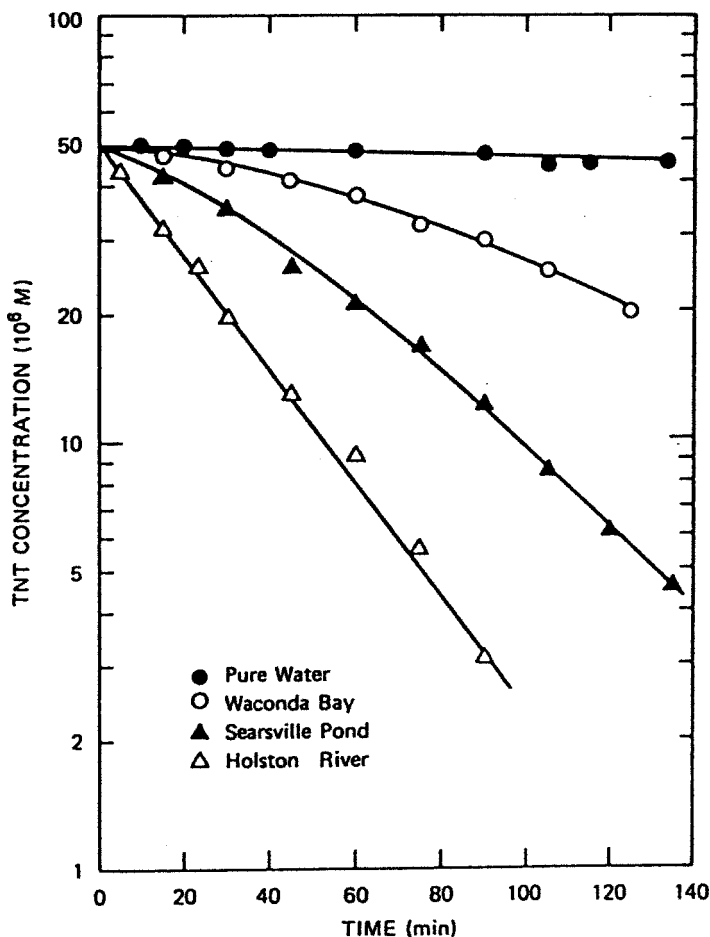
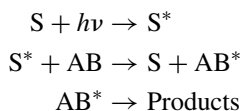


Figure 6.10 Photolysis at 313 nm of TNT ($4.9 \times 10^{-6} M$) in distilled and natural waters. [Reproduced from W. R. Mabey, D. Tse, A. Baraze, and T. Mill, “Photolysis of nitroaromatics in aquatic systems, 1. 2,4,6-Trinitrotoluene”, *Chemosphere* **12**, 3. Copyright 1983, with permission from Elsevier]

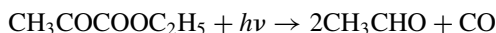
6.4.1 Processes Involved in Indirect Photolysis

When one compound absorbs radiant energy that is used in the transformation of another compound the photolysis process is said to be "indirect". Several mechanisms can be involved.

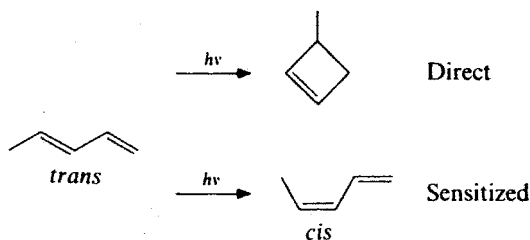
6.4.1.1 Energy Transfer from the Excited Molecule Although most indirect processes are considered to be sensitization effects, the transfer of energy from the excited molecule to some acceptor according to the strict definition of the term is "sensitization", which can be represented



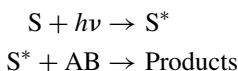
The energy transfer is a triplet-triplet process (p. 197) and because ketones provide high yields of the triplet state, compounds such as acetone, benzophenone, and diacetyl have been used in the study of these reactions. Sensitized reactions often result in a higher reaction quantum yield than observed in direct photolysis. The reaction quantum yield for the direct photolysis of ethyl pyruvate at 313 nm in benzene



increases from 0.17 to 0.32 when benzophenone is added to the system. It is postulated that the reaction is dependent on the formation of the triplet state that is enhanced in the presence of the ketone sensitizer. Direct photolysis of trans-penta-1,3-diene yields a cyclobutene while the sensitized process yields the cis isomer. This difference is attributed to different reactions of the singlet and triplet excited forms of the diene.



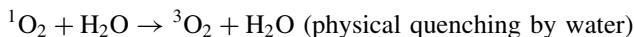
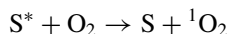
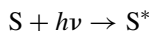
6.4.1.2 Reaction with the Excited Species This process can be represented as follows:



These reactions would involve either electron or proton transfer, however, there is only limited information describing such transformations.

6.4.1.3 Production of Active Oxidants The major oxidants generated in the atmosphere are ozone, O_3 , the hydroxyl radical $\cdot OH$, and the nitrate radical $\cdot ONO_2$, while in the aquatic environment singlet oxygen, 1O_2 , would appear to be the more significant. The importance of these components in environmental transformations is based on an understanding of the conditions needed for their generation, definition of environmental concentrations, and appropriate kinetics.

1. *Singlet Oxygen* Since the ground state of molecular oxygen is a triplet (p. 199) the excited molecule, following intersystem crossing, will be a singlet. The energy required to produce this excited species is quite low² (p. 150), $92 \text{ kJ} \cdot \text{mol}^{-1}$, and it can be produced by energy transfer from the triplet state of many dyes such as rose bengal and methylene blue as well as the DOM in natural waters. The steady-state concentrations of singlet oxygen in irradiated natural water samples were found to range from 6 to $28 \times 10^{-14} \text{ M}$.¹⁴ These data were obtained by monitoring the loss of a probe specific for 1O_2 , furfuryl alcohol. In the presence of this acceptor, A, steady-state levels of 1O_2 are determined by the following processes:



The rate expression for loss of the acceptor would be

$$-\left(\frac{dA}{dt}\right) = k_r[{}^1O_2]_{ss}[A]$$

where k_r is the second-order rate constant for the reaction of singlet oxygen with the acceptor. The absorption of the water samples are shown in Figure 6.11 and the rate of loss of furfuryl alcohol upon irradiation in solution with humic acid is given in Figure 6.12. Note that both humic acid and oxygen were required for the reaction with no reaction in distilled water and a reduced rate when the solution was purged with nitrogen. The presence of D_2O increased the rate of loss of the acceptor by increasing the steady-state concentration of 1O_2 , reducing the physical quenching by water. The reverse effect was observed with added azide, which reacts with the singlet oxygen. The

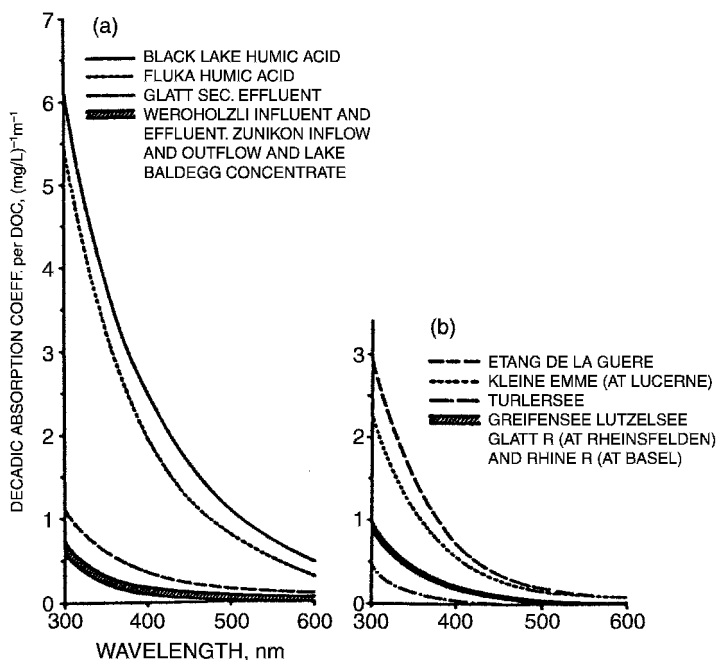


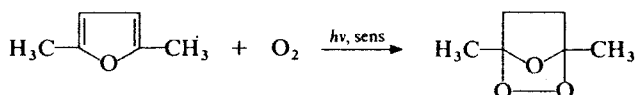
Figure 6.11 Absorption spectra of filtered waters used for singlet oxygen determinations: (a and b) waters at their natural pH, humics in pH 7 phosphate buffer. [Reproduced with permission from W. R. Haag and C. C. D. Yao, *Environ. Sci. Technol.* **26**, 1005 (1992). Copyright © 1992, American Chemical Society.]

first-order rate constant observed would then be expressed

$$k_{\text{obs}} = k_r[{}^1\text{O}_2]_{\text{ss}}$$

and $[{}^1\text{O}_2]_{\text{ss}}$ can be calculated since k_r has been determined to be $1.2 \times 10^8 \text{ M}^{-1} \cdot \text{s}^{-1}$. This study has also shown that the singlet oxygen concentration is proportional to the DOM concentration, and essentially independent of the molecular weight of the DOM components; that is, the sensitizing effect is not restricted to the higher molecular weight polymeric components.

Singlet oxygen reacts with furfuryl alcohol (a 1,3-diene) and 2,5-dimethyl furan (also used as a probe) in what is termed by the organic chemist as a *Diel's-Alder* reaction to produce an endoperoxide that reacts further to give the products illustrated.¹⁵ The reaction with an alkyl substituted alkene involves abstraction of the allylic hydrogen and recombination to form an



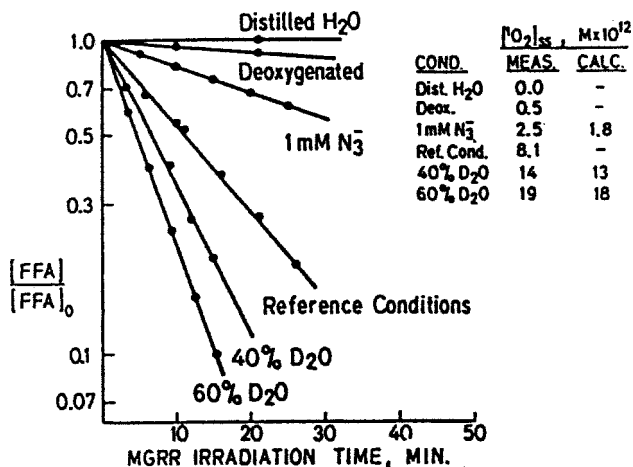
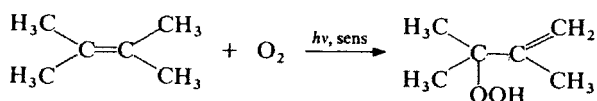


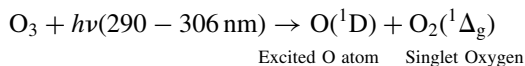
Figure 6.12 Loss of $10^{-4} M$ furfuryl alcohol, FFA, sensitized by Fluka humic acid ($\text{DOC} = 16 \text{ mg} \cdot \text{L}^{-1}$) at pH 7 irradiated using a high-pressure mercury lamp filtered through borosilicate glass. [Reproduced with permission from W. R. Haag and J. Hoigné, *Environ. Sci. Technol.* **20**, 341 (1986). Copyright © 1986, American Chemical Society.]

allylic hydroperoxide that reduce to the allylic alcohol.¹⁶ Singlet oxygen is a more active electron acceptor (oxidizing agent) than the ground state molecule and will oxidize sulfhydryl compounds, phenols, and aromatic amines.

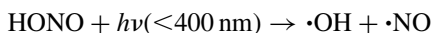


2. *Hydroxyl Radical* $\cdot\text{OH}$ This radical is produced in the atmosphere by several photochemical reactions:

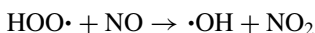
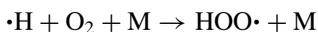
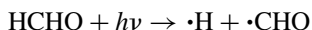
Reaction of an excited oxygen atom with water



Photolysis of nitrous acid, produced from the reaction of nitrogen oxides with water

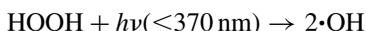


Photolysis of aldehydes and ketones



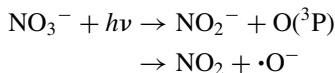
M represents some molecule that reduces the energy level of an excited molecule through collisions.

Cleavage of hydrogen peroxide



Levels of $\cdot\text{OH}$ in the atmosphere (Table 6.10) have been derived from trend and budget analyses of trace gases, CH_3CCl_3 , CO , and CHClF_2 that are oxidized primarily if not exclusively by this radical.¹⁷ It is of interest to observe how the distribution varies with latitude and season.

The hydroxyl radical may also be produced in aqueous systems through the photolytic reaction of nitrate ions that show a long-wavelength absorption maximum at 302 nm. Two primary reactions have been defined



The radical anion protonates rapidly to produce hydroxyl radicals;



This process has been studied in aqueous systems using probes (butyl chloride, nitrobenzene, and anisole) specific for hydroxyl radicals.¹⁸ The

TABLE 6.10 Atmospheric $\cdot\text{OH}$ Concentrations

Latitude	Jan.	July	Annual
90°–30°S	12.1 ^a	1.8	6.4
32°–0°S	12.8	12.3	15.4
0°–32°N	10.6	17.9	14.7
32°–90°N	1.5	16.5	7.3
Southern	15.3	8.0	11.6
Northern	7.0	17.3	11.6
Global	11.3	12.7	11.6

^a10⁵ molecules · cm⁻³.

steady-state concentration of hydroxyl radicals in irradiated samples can be derived in a fashion similar to that used for singlet oxygen:

$$k_{\text{obs}} = k_r[\cdot\text{OH}]_{\text{ss}}$$

where, in this case, k_r is the known rate constant for the probe with hydroxyl radical. The observed reaction rate increased with the concentration of nitrate ions and decreased with the addition of 1-octanol which, like DOM, competes for the radical. The rate at which hydroxyl radicals are generated in sunlight can be calculated as a function of the sunlight absorption rate, k_a , the reaction quantum yield, Φ , and the nitrate concentration:

$$d(\cdot\text{OH})/dt = k_a \cdot \Phi[\text{NO}_3^-] \text{ mol} \cdot \text{L}^{-1} \cdot \text{s}^{-1}$$

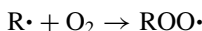
A value of $1.78 \times 10^{-5} \text{ s}^{-1}$ can be calculated for k_a for midday, mid-summer at 50°N with a nitrate concentration of 1 mM (1.4 mg of nitrate N/L; a common unit for environmental nitrate levels) and a quantum yield of 0.014,

$$\begin{aligned} d(\cdot\text{OH})/dt &= (1.78 \times 10^{-5})(0.014)(1 \times 10^{-4}) \\ &= 2.5 \times 10^{-11} \text{ M} \cdot \text{s}^{-1} \end{aligned}$$

This would be a maximum value for the near-surface production of hydroxyl radical at this location and nitrate level. With nitrate levels ranging from 1 to 10 mg of NO_3^-/L and DOC ranging from 1 to 16 mg/L steady-state levels of hydroxyl radical were calculated to vary from $1-10 \times 10^{-16} \text{ M}$.

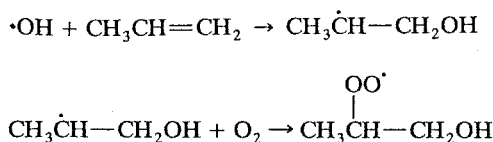
Hydroxyl radicals can also be produced by the photolysis of hydrogen peroxide,¹⁹ however, this process is not efficient since the absorption of $\text{H}_2\text{O}_2 > 300 \text{ nm}$ is very small. Thus nitrate photolysis would appear to be the major source of hydroxyl radicals in surface waters.

The two major reactions of hydroxyl radicals are hydrogen abstraction and addition²⁰ across a double bond. In fact, these radicals will react with any compound that has a C—H bond. The alkyl radical

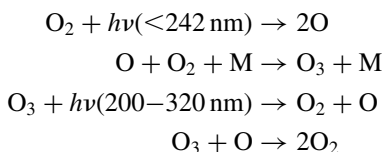


will react with molecular oxygen to form a peroxy radical that reacts further to give a range of oxidation products. The initial reaction of the hydroxy radical with an alkene yields a β hydroxy radical, which reacts further with molecular oxygen to give a (β -hydroxyalkyl)peroxy radical, a very reactive species that

produces a series of oxygenated products.



3. *Ozone* The generation of ozone in the stratosphere is beneficial since it protects from high-energy low-wave length UV radiation. By contrast, generation of ozone in the troposphere through the complex reactions of photochemical smog produces adverse environmental effects. Steady-state levels of ozone in the stratosphere depend on the balance between the photochemical reactions responsible for its production and degradation:

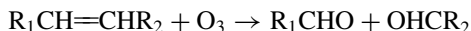


The generation of ozone in the troposphere depends on the photochemistry of nitrogen dioxide, NO_2 :

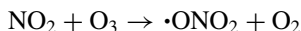


and the oxygen atom reacts with O_2 to form ozone in a reaction similar to that occurring in the stratosphere. Investigators in the field of atmospheric chemistry are concerned with the definition of the chemistry of this environmental compartment and many studies have focused on ozone dynamics. An “average” value of 30 ppb (7.5×10^{11} molecules $\cdot \text{cm}^{-3}$) is often cited, however, concentrations will vary with meteorological conditions, radiation intensity and levels of atmospheric pollutants and may exceed 100 ppb.

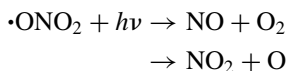
Under environmental conditions ozone can cleave alkenes to produce carbonyl derivatives.



4. *Nitrate Radical* $\cdot\text{ONO}_2$ Compared with ozone and the hydroxyl radical, an understanding of the role of this component in the atmosphere has developed more recently.²¹ It is formed by the reaction of ozone with nitrogen dioxide:

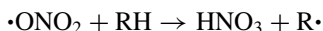


The nitrate radical is more significant at night since it is rapidly degraded in sunlight:

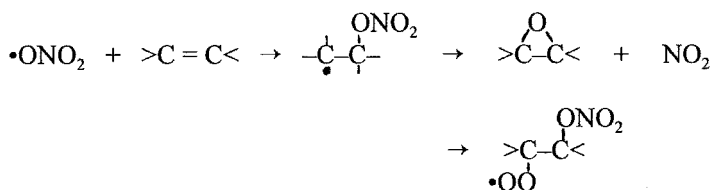


The hydroxyl radical is the main agent attacking organics during daylight hours while the nitrate radical would be more active at night. Ozone would show diurnal variation but is present throughout the day. With a concentration of ozone in the troposphere of 1.25×10^{12} molecules $\cdot \text{cm}^{-3}$ it has been shown that the concentration of nitrate radical would be 2.7×10^7 molecules $\cdot \text{cm}^{-3}$ (1 ppt).

Reactions of the nitrate and hydroxyl radical are similar. Hydrogen abstraction produces an alkyl radical that would react with oxygen to give the peroxy radical:



Addition to an alkene can result in the formation of nitrate derivatives, or an alkoxy biradical that can lead to the formation of an epoxide.



5. *Other Oxidants* Other reactive species may be generated as a consequence of photolytic activity. It has been shown above how peroxy radicals, $\text{ROO}\cdot$, alkoxy radicals, $\text{RO}\cdot$, and atomic oxygen may be formed. Hydrogen peroxide, H_2O_2 , superoxide, O_2^- would also be candidates, however, because of the complex series of reactions that can be involved, it is difficult to develop a systematic analysis of their involvement.

6.5 INDIRECT PHOTOLYSIS IN WATER

A variety of photolytic processes are possible and from the discussion above it is apparent that in surface waters, indirect effects depend primarily on the DOM. This component will reduce the rate of direct photolysis, but there are many examples where this reduction is compensated for by indirect reactions. However, under environmental conditions, it is not always possible to differentiate among the different options when

evaluating photolytic response. This section will provide examples of different indirect processes that have been demonstrated in "natural" water.

6.5.1 Energy Transfer

If 1,3-pentadiene, either the *cis* or the *trans* isomer, dissolved in a river water sample, is irradiated, isomerization occurs (p. 213) producing a photostationary state (Fig. 6.13).²² The same steady-state (60% *trans*) was achieved starting with either isomer and reflects a balance between the *cis* → *trans* and the *trans* → *cis* processes. The composition of the photostationary state observed with different water samples and humic acids are summarized in Table 6.11. Solutions were adjusted to be optically matched; each showing an absorbance of 0.20 at 366 nm. A small effect of wavelength is observed with smaller proportions of the *trans* isomer observed at 313 nm compared to 366 nm.

The first-order rate expression representing the sum of the rate constants for the two opposing processes is given by

$$\ln \left[\frac{(t_{\infty} - t_t)}{(t_{\infty} - t_0)} \right] = -k_s t$$

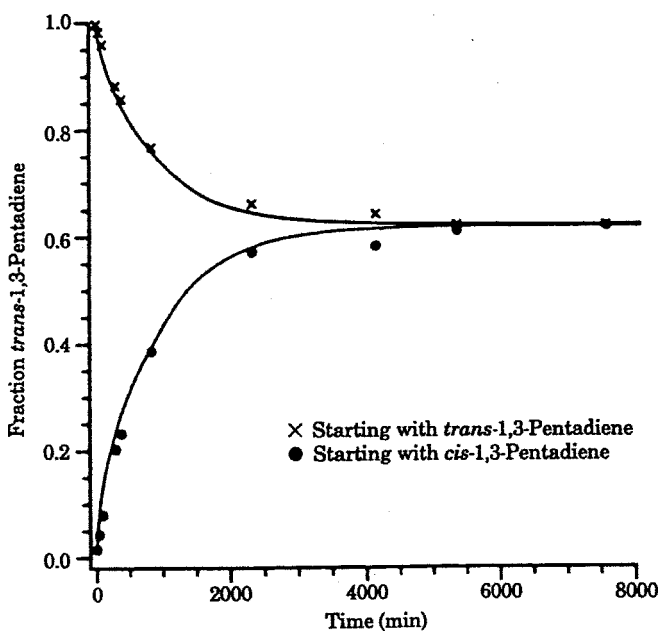


Figure 6.13 Photosensitized isomerization of *cis*- and *trans*-1,3-pentadiene in a natural water sample. [Reproduced with permission from R. G. Zepp, P. F. Schlotzhauer, and R. M. Sink, *Environ. Sci. Technol.* **19**, 74 (1985). Copyright © 1985, American Chemical Society.]

TABLE 6.11 Effect of Wavelength and DOM on Sensitized Isomerization of 1,3-Pentadiene

Pentadiene Dissolved in:	% trans Isomer at Steady State		
	Sunlight	313 nm	366 nm
Aucilla R., FL water	63.8	59.2	62.0
Suwanee R., FL water	64.5	58.8	61.6
Fluka humic ^a acid soln.	64.7	59.0	62.8
Aldrich humic ^a acid soln.	64.4	58.7	63.0
Contech humic ^a acid soln.	63.4	61.1	62.0

^aCommercial products.

with t_∞ , t_0 , and t_t the fraction of the trans isomer present at the photostationary state, at time zero and at time t . Irradiation of the cis isomer in Athens Georgia on an overcast July day provided the kinetic information in Figure 6.14.²³ Under these conditions, t_∞ was 56% and since t_0 was 1% the denominator is a constant and a plot of $\ln(t_\infty - t_t)$ gives a linear relation. Sensitized isomerization first-order rate constants under these conditions were found to be 0.17, 0.12, and 0.091 h⁻¹ for the river water, Aldrich humic acid, and Fluka humic acid, respectively. Note that no isomerization was observed in distilled water and the reaction is attributed to energy transferred from the excited humic acid.

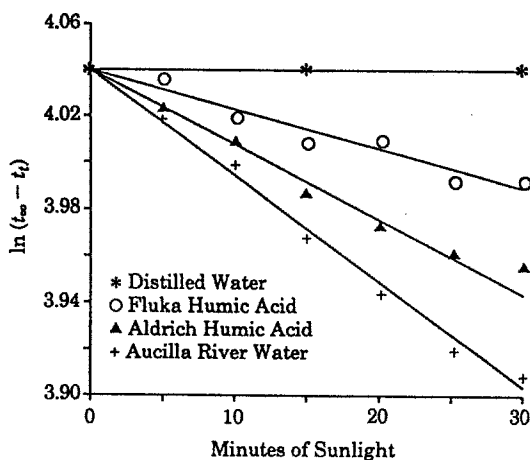


Figure 6.14 Rate of photoisomerization, in sunlight of *cis*-1,3-pentadiene in the presence of DOM. The fraction of the diene in the trans form at equilibrium, t_∞ , expressed in relation to that at time, t . [Reproduced from R. G. Zepp, G. L. Baughman, and P. F. Schlotzhauer, "Comparison of photochemical behavior of various humic substances in water: 1. Sunlight induced reactions of aquatic pollutants photosensitized by humic substances", *Chemosphere* 10, 109. Copyright 1981, with permission from Elsevier.]

Since the photostationary state contains a higher proportion of the trans isomer one would conclude that it is less efficient than the cis isomer in the energy-transfer process. By using solutions of pure sensitizers (Table 6.11) with known triplet state energies²² it was demonstrated that the proportion of trans isomer in the steady state decreased with increasing triplet-state energy. From these data, one would conclude that the energy of the excited triplet of the DOM complex would be $\sim 250 \text{ kJ} \cdot \text{mol}^{-1}$ corresponding with proportion of trans isomer observed at the photostationary state (Table 6.12).

This example illustrates that DOM in natural waters can be excited in sunlight and produce change by energy transfer. At this point, there is no systematic method for predicting what reactions might be induced, however, the energy of the triplet states produced in the DOM will limit the nature of the transformation.

6.5.2 Singlet Oxygen $^1\text{O}_2$

By using either dimethylfuran or furfuraldehyde as probes, it has been established that irradiation of natural waters can generate singlet oxygen through a sensitization process involving the DOM.¹⁴ An average concentration of $4 \times 10^{-14} \text{ M}$ was reported in the top meter of 18 waters evaluated. The question arises as to whether this level would be sufficient to oxidize contaminants that could be present in these waters at low concentrations.

The transformation of several compounds (Table 6.13) were monitored in aqueous solution containing the dye, rose bengal ($5 \text{ mg} \cdot \text{L}^{-1}$), as a sensitizer. That these reactions were indeed due to $^1\text{O}_2$ was established by the fact that azide, an $^1\text{O}_2$ scavenger, reduced oxidation rates by a factor of 9, and the use of 90 : 10 $\text{D}_2\text{O}/\text{H}_2\text{O}$ enhanced rates by a factor of 5. The D_2O reduces the quenching of $^1\text{O}_2$ by water. The rate at which compounds are oxidized would be given by

$$dP/dt = k_2[\text{P}][^1\text{O}_2]_{\text{ss}}$$

which gives a pseudo-first-order relation where

$$k_1 = k_2[^1\text{O}_2]_{\text{ss}}$$

TABLE 6.12 Effect of Sensitizer on the Photostationary State of 1,3-Pentadiene

Sensitizer	T_1 ($\text{kJ} \cdot \text{mol}^{-1}$)	% trans Isomer
Acetophenone	305	56
<i>p</i> -(Trimethylammonium)- benzophenone chloride	293	56
Naphthalene	254	60
Naphthalene-2,6-disulfonic acid, sodium salt	251	60
2-Acetophenone	248	66
1-Acetophenone	236	71

TABLE 6.13 Rate Constants for Reaction with Singlet Oxygen at 19°C

Compound	k_2 ($M^{-1} s^{-1}$)	$t_{1/2}^a$ (h)	Reaction Type
2,3-Dimethyl-2-butene	1.1×10^8	44	-ene reaction
Diethyl sulfide	1.8×10^7	270	Sulfide oxidation
Dimethyl furan	8.2×10^8	5.7	Endoperoxide formation
Furfuryl alcohol	1.2×10^8	40	Endoperoxide formation
2,4-Dichlorophenolate (pK_a 7.8)	1.2×10^8	62	Electron transfer
2,4,6-Trichlorophenolate (pK_a 6.1)	1.2×10^8	62	Endoperoxide formation

^aCalculated for $[^1O_2]_{ss} = 4 \times 10^{-14} M$, at pH 8.

The first-order rate constants are derived from experimental observations and the steady-state concentration of singlet oxygen that is calculated from the rate of transformation of the furfuraldehyde whose k_2 is known. Rate constants observed are tabulated in Table 6.13. The effect of pH on the rate of transformation of phenols (Fig. 6.15) demonstrates that the phenolate anion reacts more rapidly (~ 100 -fold) than the undissociated neutral compound.

A more extensive evaluation of the reaction of singlet oxygen with substituted phenols has been reported²⁴ and some of the data are compiled in Table 6.14. At a given pH, the overall constant would be a composite of both the neutral and charged forms:

$$d(\text{total phenol})/dt = (k_{ArOH}[ArOH] + k_{ArO^-}[ArO^-])[^1O_2]_{ss}$$

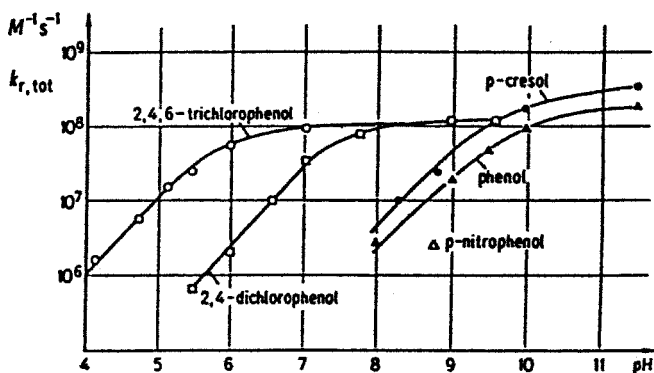


Figure 6.15 Influence of pH on the rate of oxidation of aqueous solutions of phenols by singlet oxygen. [Reproduced from F. E. Scully and J. Hoigné, "Rate constants for reactions of singlet oxygen with phenols and other compounds", *Chemosphere* **16**, 681. Copyright © 1987, with permission from Elsevier.]

TABLE 6.14 Reaction of Singlet Oxygen with Phenols—Rate Constants

Phenol	pK _a	Σσ ⁻ (m, p)	k _{ArOH₁} (M ⁻¹ s ⁻¹)	k _{ArO⁻} (M ⁻¹ s ⁻¹)	k _{tot} ^a (M ⁻¹ s ⁻¹)	t _{1/2} ^b (h)
Unsubstituted (1)	10.00	0.00	2.6 × 10 ⁶	1.55 × 10 ⁸	4.1 × 10 ⁶	1174
4-Acetyl (2)	8.05	0.87	1.5 × 10 ⁶	2.36 × 10 ⁷	1.2 × 10 ⁷	401
4-(<i>tert</i> -Butyl) (3)	10.39	-0.13	1.2 × 10 ⁷	3.55 × 10 ⁸	1.3 × 10 ⁷	370
3-Chloro (5)	9.12	0.37	5.4 × 10 ⁶	1.60 × 10 ⁸	1.6 × 10 ⁷	301
4-Chloro (6)	9.41	0.27	6.0 × 10 ⁶	1.93 × 10 ⁸	1.3 × 10 ⁷	370
4-Cyano (10)	7.97	1.00	2.4 × 10 ⁵	6.14 × 10 ⁶	2.8 × 10 ⁶	1719
4-Hydroxy (11)	9.85	-0.16	3.8 × 10 ⁷		3.7 × 10 ⁷	130
3-Methoxy (13)	9.65	0.12	1.3 × 10 ⁷	2.85 × 10 ⁸	1.90 × 10 ⁷	267
4-Methoxy (14)	10.21	-0.16	2.2 × 10 ⁷	6.67 × 10 ⁸	2.2 × 10 ⁷	219
4-Methyl (16)	10.28	-0.15	9.6 × 10 ⁶	3.5 × 10 ⁸	9.6 × 10 ⁶	501
3-Nitro (18)	8.35	0.71	2.7 × 10 ⁶	6.05 × 10 ⁷	2.06 × 10 ⁷	234
4-Nitro (19)	7.16	1.24	2.6 × 10 ⁵	5.12 × 10 ⁶	4.48 × 10 ⁶	1074

^aCalculated for pH 8.0.^bCalculated for [¹O₂] = 4 × 10⁻¹⁴ M.

and the overall rate constant k_{tot} would be given by

$$k_{\text{tot}} = (1 - \alpha)k_{\text{ArOH}} + \alpha k_{\text{ArO}^-}$$

where α is the fraction of the phenol that is dissociated which can be expressed

$$\alpha = 1/(1 + 10^{(\text{pK}_a - \text{pH})})$$

From these data, one can conclude that under environmental conditions, phenols are not oxidized rapidly by singlet oxygen in natural waters, but on the other hand, one would not anticipate that phenols would be persistent contaminants like PCBs. It is also of interest to note that the rate constants for both the neutral and anionic (Fig. 6.16) forms correlate well with substituent σ^- constants.

6.5.3 Hydroxyl Radical

Rate constants in aqueous solution for the reaction of hydroxyl radicals with organic compounds (Table 6.15) have been selected from comprehensive literature summaries.^{25,26}

It is difficult to control and define the levels of hydroxyl radicals in a reaction system and rate constants are often derived using competition kinetics sometimes referred to as relative rate techniques.²⁷ In this experimental approach, a compound, U , whose reaction rate is not known is allowed to react with hydroxyl radical in the presence of a reference compound, R , whose reaction rate is known. Assuming the compounds are only reacting with $\cdot\text{OH}$, the proportionate loss of the reference

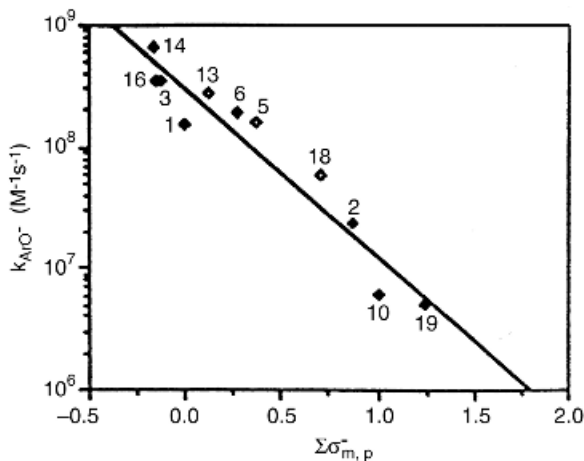


Figure 6.16 Correlation of sigma values with rate of oxidation of phenolate anions by singlet oxygen. Open symbols indicate phenols with meta substituents and filled symbols, phenols with para substituents. Numbers indicate phenols listed in Table 6.13. [Reproduced with permission from P. G. Tratnyek and J. Hoigné, *Environ. Sci. Technol.* **25**, 1596 (1991). Copyright © 1991, American Chemical Society.]

compound over time t , in terms of the concentration of hydroxyl radical is given by

$$\ln(R_0/R_t) = k_r t$$

since the reaction is first order with respect to hydroxyl radical. In the usual kinetic terminology, R_0 would be the concentration of the reference compound at $t = 0$, and R_t the concentration after time t . The rate constant for the reference compound is k_r . In a similar fashion, the proportionate loss of the compound whose rate constant is to

TABLE 6.15 Hydroxyl Radical Reactions Rate Constants in Aqueous Solution

Compound	$k_2 (M^{-1} s^{-1})$	Compound	$k_2 (M^{-1} s^{-1})$
Butane	4.6×10^9	Dichloromethane	9.9×10^7
Octane	9.1×10^9	Chloroform	5.4×10^7
Cyclohexane	6.1×10^9	1,1,2-Trichloroethane	1.3×10^8
Benzene	7.8×10^9	1,2-Dibromo-3-chloropropane	4.2×10^8
Naphthalene	5×10^9	2-Bromoethanol	3.5×10^8
Phenol	1.4×10^{10}	Chlorobenzene	7.8×10^9
Aniline	1.4×10^{10}	<i>m</i> -Dichlorobenzene	5.0×10^9
Diethyl sulfide	1.4×10^{10}	Lindane	5.8×10^8

be determined is

$$\ln(U_0/U_t) = k_u t$$

The ratio of the loss of U relative to R would be

$$\frac{\ln(U_0/U_t)}{\ln(R_0/R_t)} = \frac{k_u}{k_r} \quad \text{and thus}$$

$$\ln(U_0/U_t) = (k_u/k_r) \ln(R_0/R_t)$$

The extent of oxidation is varied by changing the initial concentration of the oxidant generating the radical and $\ln(U_0/U_t)$ is plotted as a function of $\ln(R_0/R_t)$ giving a straight line, which passes through zero, with slope, k_u/k_r (Fig. 6.17). This experimental approach is used both in vapor phase and solution. It is also of interest to note that in light of the extensive data set for vapor phase reactions of hydroxyl radicals that they correlate well with reaction rates in aqueous solution (Fig. 6.18).

Hydroxyl radical levels in natural waters (near-surface) mid-summer at 50° latitude have been estimated to range from 1×10^{-16} to $1 \times 10^{-15} M$. If k_2 is of the order of $10^9 M^{-1} s^{-1}$, half-lives would range from 1925 to 192.5 h. Compounds with k_2 values of 10^{10} under the same conditions would give half-lives ranging from 192.5 to 19.25 h. Higher levels of hydroxyl radical would be generated with more intensive solar radiation, so with some compounds, and adequate intensity

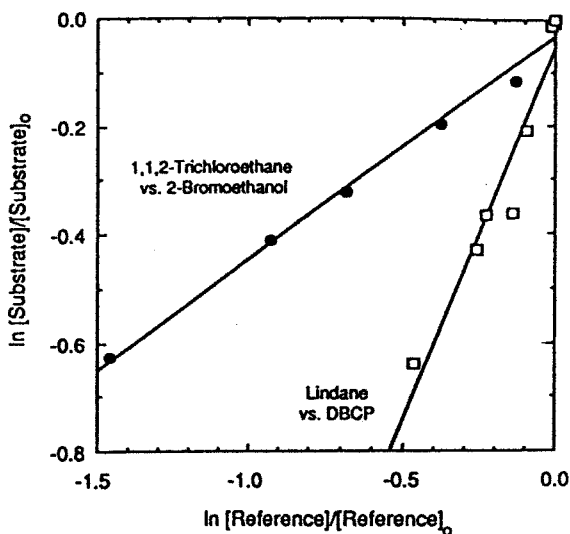


Figure 6.17 Illustration of relative rate data used for determining hydroxyl radical reaction rates. [Reproduced with permission from W. R. Haag and C. C. D. Yao, *Environ. Sci. Technol.* **26**, 1005 (1992). Copyright © 1992, American Chemical Society.]

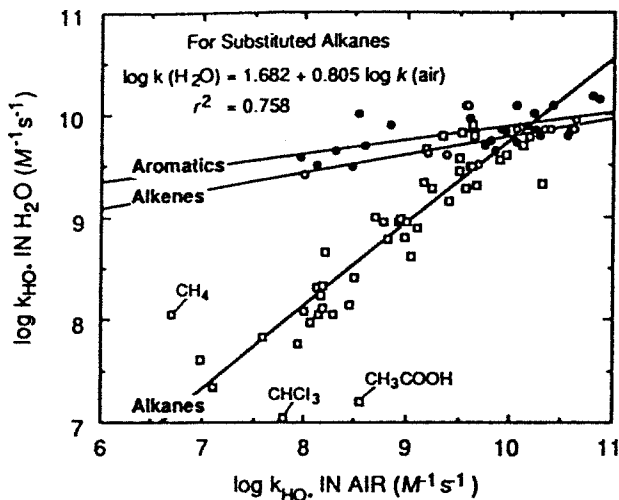


Figure 6.18 Correlation of hydroxyl radical rate constants for un-ionized forms of compounds in water versus those in air. Substituted alkanes, open squares; alkenes, open circles; aromatics, filled circles. [Reproduced with permission from W. R. Haag and C. C. D. Yao, *Environ. Sci. Technol.* **26**, 1005 (1992). Copyright © 1992, American Chemical Society.]

of solar radiation, this process could result in significant degradation rates. It has been proposed that flooded rice fields could provide a suitable environment for hydroxyl radical reactions.¹⁹ These fields to which large amounts of nitrogenous fertilizers are applied provide clear shallow (10 cm) water and nitrate levels ranging from 2 to 12 mg · L⁻¹. It has been demonstrated that the pesticides that are applied to these systems degrade in samples of irradiated field water at rates consistent with those observed in an experimental system evaluating reaction with hydroxyl radical. Hydroxyl radicals may also be involved with oxidation processes in waters treated with ozone. Under basic conditions, ozone decomposes to produce hydroxyl radicals.²⁸



6.5.4 Direct Reaction with Sensitizer Triplet State

Energy transfer, discussed above, is one example of the direct reaction of the excited triplet state. It is also possible that the excited triplet could react directly through electron or hydrogen-atom transfer. The photochemical reactivity of a series of phenols (methyl and methoxy substituents) in the presence of natural DOM and ketone sensitizers can be best explained by the latter processes.²⁹ Reactions were carried out at pH 8 where phenols existed primarily (>98%) in the undissociated form, which were shown (p. 225) not to be particularly reactive with singlet oxygen.

However, at 25°C, solutions of 2,4,6-trimethylphenol were transformed rapidly (Fig. 6.19) when irradiated in the presence of natural DOM (Fluka humic acid) or 3-methoxy-acetophenone, a known ketone sensitizer selected to provide a reference for the keto functional groups present in the fulvic and humic acids (Fig. 2.3).

The reaction of the phenol cannot be attributed to direct energy transfer since the triplet energies of the phenols studied ranged from 321 to 346 kJ · mol⁻¹, higher than the triplet energies of the sensitizers (249–303 kJ · mol⁻¹). Only ~10% of the reaction could be attributed to ¹O₂ since the reaction rate was affected to only a small extent by D₂O or azide. The former would increase the rate of reaction with ¹O₂ by reducing the scavenging obtained with H₂O, while the latter would decrease the rate by competing for the ¹O₂. Consequently, it has been proposed that the reaction involves electron and proton transfer (Fig. 6.20) with the excited triplet to produce a phenol radical that is further oxidized. The response observed with a series of substituted phenols using different samples of dissolved organic matter was within the response range observed with several ketone sensitizers. It was concluded that the activity of the dissolved organic matter mimicked a mixture of excited aromatic ketones.

6.5.5 Semiconductor Photocatalysis

Irradiation (320–440 nm) of an aqueous solution of chloroform in the presence of a 0.1% suspension of titanium dioxide resulted in a rapid loss of the chloroform with a concomitant stoichiometric release of chloride ion (Fig. 6.21). Note that no reaction

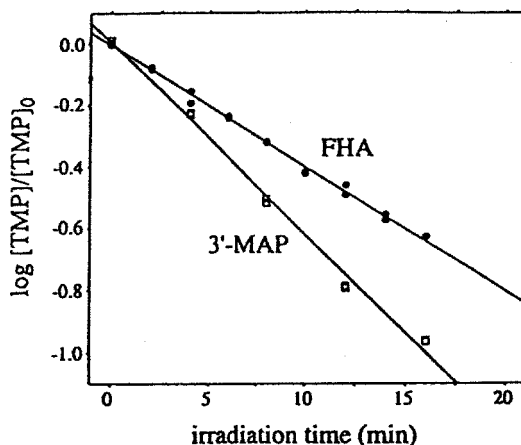


Figure 6.19 Photosensitized transformation of 10 μM 2,4,6-trimethylphenol, TMP, in the presence of humic acid, FHA (15 mg C/L), or a ketone sensitizer, 3'-methoxyacetophenone, 3'-MAP (100 μM). Irradiated with a 320-nm cutoff. [Reproduced with permission from S. Canonica, U. Jans, K. Stemmler, and J. Hoigné, *Environ. Sci. Technol.* **29**, 1822 (1995). Copyright © 1995, American Chemical Society.]

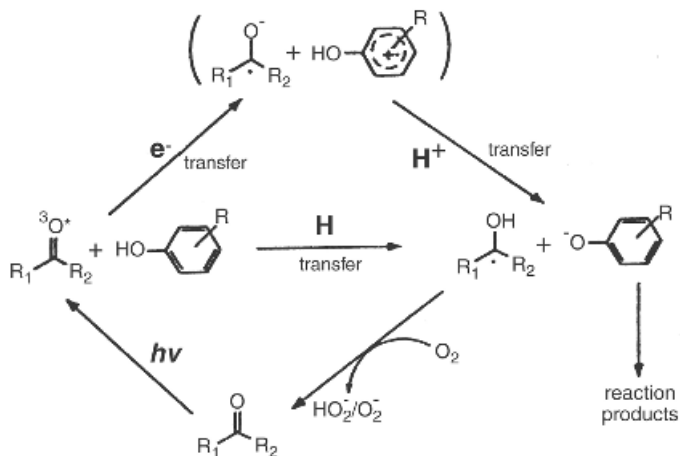


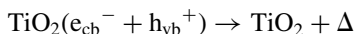
Figure 6.20 Proposed reaction sequence involving the reduction of the triplet excited ketone to its ketyl radical with subsequent oxidation of the latter to the ground-state ketone. [Reproduced with permission from S. Canonica, U. Jans, K. Stemmler, and J. Hoigné, *Environ. Sci. Technol.* **29**, 1822 (1995). Copyright © 1995, American Chemical Society.]

was observed in the presence of TiO_2 without radiation and the radiation alone also was without effect. It was further established that the chloroform was completely “mineralized” to CO_2 and HCl . Since concentration is expressed on a logarithmic scale, the linear relation indicates a first-order process. This system is of particular interest to those concerned with reducing contaminant levels in waste streams, and so on,³⁰ providing a relatively benign procedure, adding the oxide and irradiation, for achieving their objective. Consequently, there has been a considerable effort to understand the mechanisms of these reactions and it has been demonstrated that many classes of organics would react,³¹ including; chlorinated aromatics and aliphatics, nitrogenous compounds, hydrocarbons, carboxylic acids, and alcohols with many of the compounds completely oxidized. This process may be of limited significance in natural environments, however, consideration of the process expands one’s understanding of photosensitized reactions.

The electronic structure of a semiconductor (note TiO_2 and ZnO are the compounds most commonly used) is characterized by a filled valence band and an empty conduction band. A photon with energy that matches or exceeds the bandgap energy can promote an electron from the valence band to the delocalized state of the conduction band (e_{cb}^-) leaving a hole (h_{vb}^+) behind:



In the absence of reactive electron donors or acceptors on the surface, relaxation of the excited state occurs rapidly with release of heat



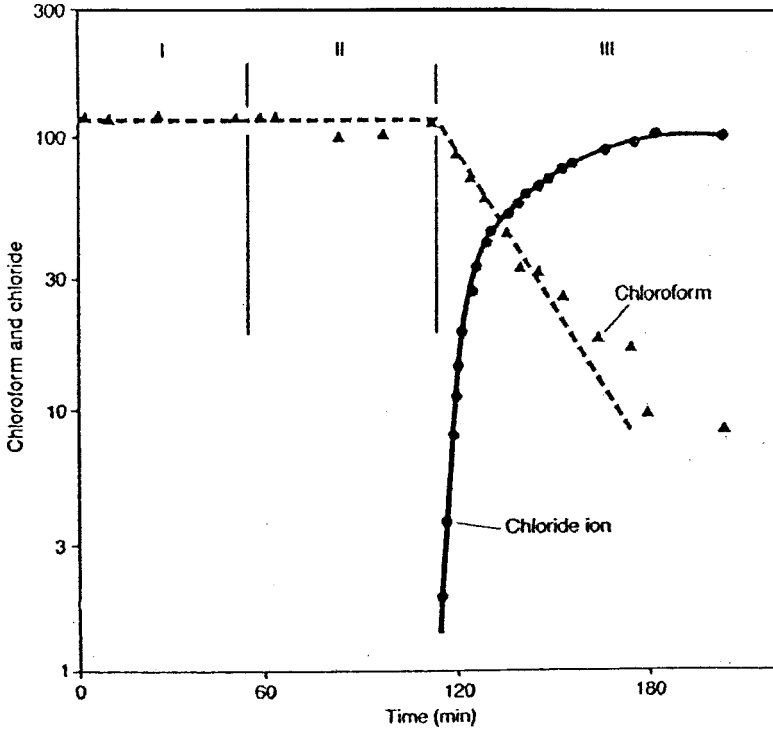
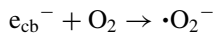


Figure 6.21 Photocatalyzed degradation of chloroform (initial concentration 122 ppm) in the presence of titanium oxide. I, illumination only; II, catalyst only; illumination plus catalyst. [Reproduced with permission from D. F. Ollis, *Environ. Sci. Technol.*, **19**, 480 (1985). Copyright © 1985, American Chemical Society.]

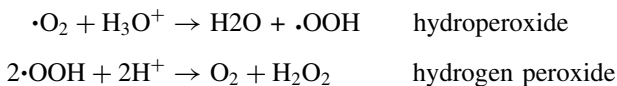
The conduction band electrons are good reductants—electron donors—(+0.5 to -1.5 V versus the hydrogen electrode) and react with an acceptor:



while the valence band holes are strong oxidants—electron acceptors—(+1.0 to +3.5 V versus the hydrogen electrode). The conduction band electrons often react with surface O_2 to form the superoxide radical anion



which in turn can react to produce other active oxygen species as follows:



Most organic photodegradation reactions utilize the oxidizing power of the valence band holes, primarily mediated by the production of hydroxyl radical

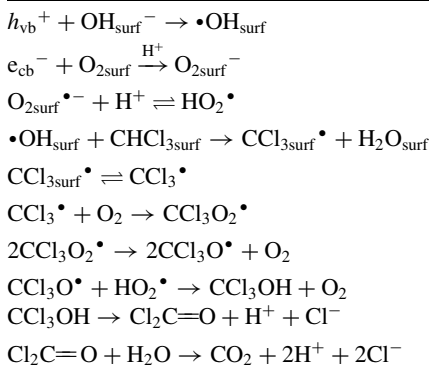


although direct electron transfer from the adsorbed organic substrate may occur. It is necessary, however, to provide a reducible species (e.g., O_2) to react with the conduction band electrons, to prevent a build up of charge. Reaction of these electrons with an acceptor also reduces the tendency of the electron to fill the hole providing a longer interval for reaction at the hole.

A reaction sequence has been proposed (Table 6.16) to account for the complete oxidation of chloroform.³² Note that an hydroxyl radical, produced at the valence band hole, abstracts a hydrogen from chloroform at the surface. The $\cdot\text{CCl}_3$ radical produced then reacts in solution with elemental oxygen and other active oxygen species generated through the conduction band electrons resulting in the production of CO_2 and Cl^- .

It is of interest to contrast the response of chloroform and carbon tetrachloride since the latter would not undergo hydrogen abstraction at the valence band hole. However, CCl_4 is readily degraded (Fig. 6.22) when irradiated (1.46×10^{-3} einstein $\cdot \text{L}^{-1} \cdot \text{min}^{-1}$ at 310–400 nm) in the presence of a suspension of TiO_2 ($0.5 \text{ g} \cdot \text{L}^{-1}$)³³ and an electron donor, 2-propanol. It can be seen (Table 6.17) that the presence of an electron donor, that reacts at the valence band hole, results in a significant increase in rate as reflected by the rate of chloride production. Reaction rate is also influenced by pH as is the production of intermediates. At the lower pH chloroform, tetrachloroethene, and hexachloroethane are detected. The initial reaction of CCl_4 would involve conduction band electrons and the following steps

TABLE 6.16 Proposed Mechanism for Chloroform Degradation^a



^aReproduced with permission from C. Kormann, D. W. Bahnemann, and M. R. Hoffmann, *Environ. Sci. Technol.*, **25**, 494 (1991). Copyright © 1991, American Chemical Society.

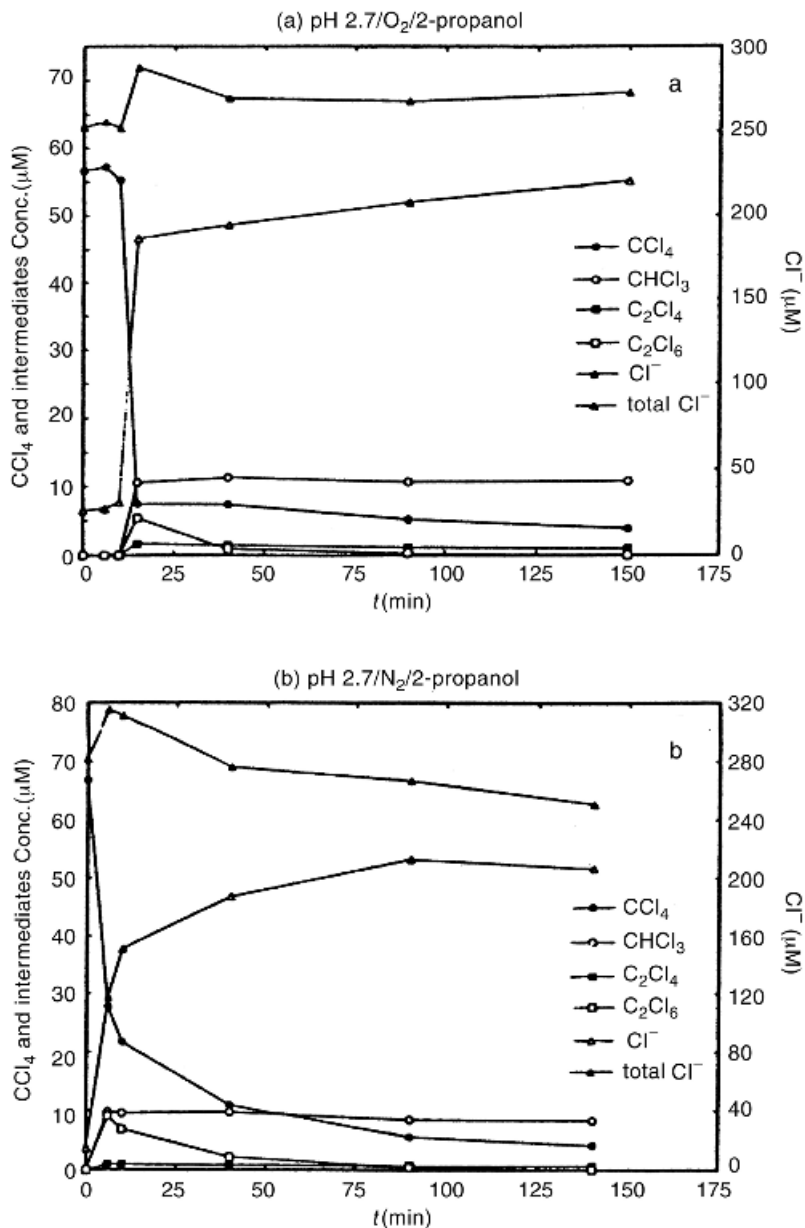
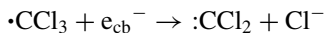
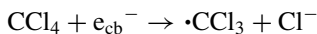


Figure 6.22 Photocatalyzed degradation of carbon tetrachloride at pH 2.7 illustrating the role of propanol as an electron donor. (a), oxygenated; (b), deoxygenated. $0.5 \text{ g} \cdot \text{L}^{-1}$, TiO_2 . [Reproduced with permission from W. Choi and M. R. Hoffmann, *Environ. Sci. Technol.* **29**, 1646 (1995). Copyright © 1995, American Chemical Society.]

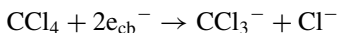
TABLE 6.17 Electron Donors, pH, and Degradation of CCl₄

e ⁻ Donor	$d[\text{Cl}^-]/dt$ ($\mu\text{M min}^{-1}$)	
	pH 2.8	pH 11.0
None, H ₂ O	0.6	0.8
Methanol	5.9	64.1
Ethanol	24.5	43.3
1-Propanol	18.5	31.7
2-Propanol	46.0	38.0

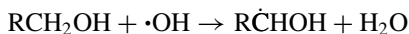
have been postulated



or alternatively, a two-electron transfer could occur



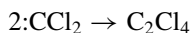
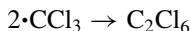
The alcohol would react at the valence band hole, enhancing the availability of conduction band electrons and also producing a radical through abstraction of an α H by the hydroxyl radical:



These radical intermediates are strong one-electron reductants which can react directly with CCl₄



The intermediates observed would result from the following reactions:



In the presence of O_2 , production of CO_2 would involve a series of reactions of $\bullet CCl_3$ comparable to that outlined in Table 6.16 for chloroform. Conversion of CCl_4 is also observed in the absence of O_2 involving the following hydrolysis and subsequent oxidation at the valence band hole.



To account for the fact that intermediates were not observed at pH 12.4, it was suggested that a two-electron transfer was favored and that the resultant $:CCl_2$ hydrolyzed rapidly precluding the formation of C_2Cl_4 .

The initial rate of these reactions has been expressed in terms of the proportion of the catalytic surface covered by the substrate, θ , and the maximum rate, k , observed at saturation. The adsorption is expressed by a Langmuir isotherm in terms of the concentration in solution, C , and a binding constant K :

$$\theta_x = \frac{K \cdot C}{1 + KC}$$

The rate of reaction would then be expressed

$$\text{Rate} = \frac{kKC}{1 + KC}$$

This relation, often referred to as Langmuir–Hinshelwood kinetics, is similar to Michaelis–Menten kinetics used to define enzyme-catalyzed processes (p. 303), and a comparable linear form

$$1/(\text{rate}) = 1/k + 1/(kK) \cdot (1/C)$$

of the expression (known as a Lineweaver–Burke plot in enzyme kinetics) can provide estimates of the binding constant, K , and max rate constant, k . Plotting $1/(\text{rate})$ as a function of $1/C$ gives a straight line with intercept, $1/k$, and slope $1/(kK)$ as illustrated in Figure 6.23.³⁴ Values derived for some halogenated aliphatic compounds using this analysis are summarized in Table 6.18. The reaction system contained 0.1% TiO_2 and irradiated at 320–440 nm.

This empirical approach does not provide a systematic basis for defining kinetics for it is not possible to draw any conclusions regarding mechanism. The catalyzed oxidation of chloroform according to the following stoichiometry:



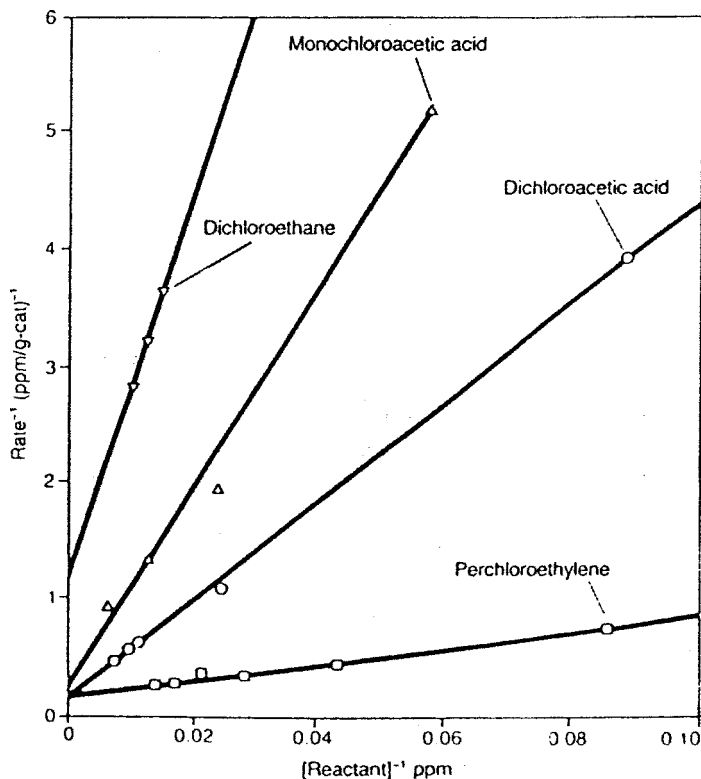


Figure 6.23 Reciprocal plots of rate as a function of concentration suggesting a Langmuir surface interaction for the catalyzed reaction. [Reproduced with permission from D. H. Ollis et al., *J. Catal.* **88**, 89 (1984). Copyright © 1984, American Chemical Society.]

would suggest the following rate expression:

$$-d[\text{CHCl}_3]/dt = k[\text{CHCl}_3]_{\text{surf}}[\text{O}_2]_{\text{surf}}$$

The concentrations of chloroform and oxygen on the TiO_2 catalyst can be derived from Langmuir adsorption isotherms and it is of interest to note that with chloro-

TABLE 6.18 Binding Constants and Max. Rates for Halogenated Compounds

Compound	k^a	K^b	Compound	k^a	K^b
CH_2Cl_2	1.6	0.02	$\text{ClCH}_2\text{CH}_2\text{Cl}$	1.1	0.01
CHCl_3	4.4	0.003	CHBr_2CH_3	3.9	0.02
CCl_4	0.18	0.005	$\text{BrCH}_2\text{CH}_2\text{Br}$	2.2	0.02
CH_2Br_2	4.1	0.02	ClCH_2COOH	5.5	0.002
CHBr_3	6.2	0.01	Cl_2CHCOOH	8.5	0.003

^a $\text{ppm} \cdot \text{min}^{-1} \cdot \text{g catalyst}^{-1}$.

^b ppm^{-1} .

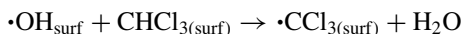
form, a two-site model is needed (note discussion of Langmuir isotherms in sorption discussion) to define the fraction $\theta(\text{CHCl}_3)$ of sites occupied:

$$\theta(\text{CHCl}_3) = \frac{X_1 K_1 [\text{CHCl}_3]}{1 + K_1 [\text{CHCl}_3]} + \frac{X_2 K_2 [\text{CHCl}_3]}{1 + K_2 [\text{CHCl}_3]}$$

and with the P(25) TiO_2 used, X_1 and X_2 were found to be 0.02 and 0.98 and K_1 and K_2 10^4M^{-1} and 1M^{-1} , respectively. The surface concentration of chloroform would thus be expressed as

$$[\text{CHCl}_3]_{\text{surf}} = \theta(\text{CHCl}_3)[\text{CHCl}_3]$$

We would not expect that O_2 would be limiting (Table 6.15) providing it is effective in scavenging e_{cb}^- . The rate-limiting step most likely would be



The steady-state concentration of $\cdot\text{OH}_{\text{surf}}$ would be a function of light intensity (I) and the efficiency with which these radicals are generated ($\Phi_{\cdot\text{OH}}$) at the valence band hole and other competing reactions.

$$\cdot\text{OH}_{\text{surf}}(\text{steady state}) = I\Phi_{\cdot\text{OH}} - k[\cdot\text{OH}_{\text{surf}}][\text{CHCl}_3(\text{surf})] - k_2[\cdot\text{OH}_{\text{surf}}]^2$$

such as the combination of two $\cdot\text{OH}$ to produce H_2O_2 . It can be seen that the definition of the kinetic relations is quite complex and there is no obvious connection to the reaction parameters derived from Langmuir–Hinshelwood approach. From this discussion, it is apparent that any interference with adsorption on TiO_2 could affect reaction rate. Anions such as Cl^- and HCO_3^- inhibit by adsorbing to positive surface sites and pH modulates this response by determining surface charge.

6.6 INDIRECT PHOTOLYSIS IN THE ATMOSPHERE, VAPOR PHASE

Indirect processes in the atmosphere are concerned almost exclusively with the action of photochemically produced active oxidants. By far, the most significant species would be the hydroxyl radical because of the wide range of compounds that will react and the rates at which these transformations occur. The nitrate radical, being active at night, would also be of significance and ozone can react with some compounds at rates comparable with those observed with the hydroxyl radical. Other oxidants would include the hydroperoxy radical, $\text{HO}_2\cdot$, that is generated in some oxidation sequences and atomic chlorine, which can be generated in the marine boundary layer but it would not be significant in a global context (p. 180).¹¹ An extensive database has developed in this area from research in atmospheric chemistry. Investigators in this field are concerned with the chemistry of the atmosphere,

the nature of the various inputs, and the reactions that these compounds undergo and the overall effect on air quality. This monograph focuses on the chemical and asks the question, What can happen to a compound that may distribute into this environmental compartment? The connection between the two fields is obvious.

6.6.1 Lifetimes

In most cases, the reaction of an organic compound with atmospheric oxidants would be expected to comply with second order kinetics:

$$\text{Reaction rate} = k_2[\text{compound}][\text{oxidant}]$$

If a steady-state concentration is assumed for the oxidant the reaction would show first-order kinetics with

$$k_1 = k_2[\text{oxidant}]$$

For a first-order reaction, the concentration, C_t , at time t , is expressed as a function of the initial concentration, C_0

$$C_t = C_0 e^{-kt} \quad \text{or logarithmically as} \quad \ln C_t = \ln C_0 - k_1 t$$

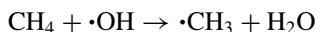
When $C_t = C_0/2$:

$$\ln C_0 - \ln 2 = \ln C_0 - k_1 t_{1/2} \quad \text{and the half-life} \quad t_{1/2} = \ln 2/k_1$$

In the field of atmospheric chemistry, it has become convention to define lifetime, τ , as the time when $C_t = C_0/e$, and in this case

$$\tau = 1/k_1$$

For example, the second-order rate constant for the reaction of methane with hydroxyl radical



at 25°C is $6.3 \times 10^{-15} \text{ cm}^3 \cdot \text{molecule}^{-1} \cdot \text{s}^{-1}$ (note that $\text{cm}^3 \cdot \text{molecule}^{-1} \cdot \text{s}^{-1} \times 6.02 \times 10^{20} = \text{M}^{-1} \cdot \text{s}^{-1}$). Using a daytime average $\cdot\text{OH}$ concentration of

$$1 \times 10^6 \text{ radicals cm}^{-3}$$

$$\begin{aligned} t_{1/2} &= 0.693/[1 \times 10^6][6.3 \times 10^{-15}] \\ &= 3.5 \text{ years} \end{aligned}$$

$$\begin{aligned} \tau &= 1/[1 \times 10^6][6.3 \times 10^{-15}] \\ &= 5.0 \text{ years} \end{aligned}$$

It is important to understand that these values provide a conceptual base for evaluating the environmental behavior of compounds that one does not gather from simply comparing rate constants. However, it must be recognized that assuming a steady-state concentration for the hydroxyl radical is somewhat artificial, since it has been noted that this parameter varies with time and latitude, and so on. In addition, the calculation applies only for the oxidant in question. If other reactions occur, a lifetime calculated for just the hydroxyl radical would overestimate persistence. On the other hand, for a compound such as methane where the reaction with hydroxyl radical is the major reaction, the calculated lifetime would be a realistic estimate of persistence.

6.6.2 Oxidative Reactions: Rates and Mechanisms

Detailed reviews of the reactions of hydroxyl radicals,²⁰ ozone,³⁵ and nitrate radicals²¹ with different classes of organic compounds are available. In addition, IUPAC sponsors a continuing program to evaluate and compile kinetic information on these reactions and these reports are published in the *Journal of Physical Chemical reference Data*. The analysis lists among other data the preferred rate constants and where possible, information on temperature effects. A recent analysis³⁶ focuses primarily on reactions of hydroxyl and nitrate radicals. This extensive database provides an opportunity for developing systematic approaches to predicting reaction rates.

6.6.2.1 Alkanes Kinetic data have been compiled for reactions with hydroxyl radicals^{37,38} and nitrate radicals,³⁹ both of which react by abstracting a hydrogen atom making alkanes obvious targets. From the examples listed in Table 6.19, it is apparent that the hydroxyl radical is the more active oxidant by four orders of magnitude. Consequently, the nitrate radical reaction would only assume significance relative to the hydroxyl radical if an appropriate concentration differential occurred. Rate constants increase with larger and more complex molecules and with hydroxyl radicals, k_2 can exceed $10^{-11} \text{ cm}^3 \cdot \text{molecule}^{-1} \cdot \text{s}^{-1}$.

From the kinetic theory of gases, it is possible to calculate the frequency that molecules collide as a function of velocity, which depends on molecular weight and temperature, and molecular diameter. If every collision at 25°C resulted in a reaction, a rate constant of the order of $3\text{--}5 \times 10^{-10} \text{ cm}^3 \cdot \text{molecule}^{-1} \cdot \text{s}^{-1}$

TABLE 6.19 Rate Constants at 25°C for Reactions of Hydroxyl and Nitrate Radicals with Alkanes

Alkane	k_{OH} ($10^{-12} \text{ cm}^3 \cdot \text{molecule}^{-1} \cdot \text{s}^{-1}$)	k_{NO_3} ($10^{-17} \text{ cm}^3 \cdot \text{molecule}^{-1} \cdot \text{s}^{-1}$)
Methane	0.00618	<0.1
Ethane	0.254	0.14
Propane	1.12	1.7
<i>n</i> -Butane	2.44	4.59
2-Methylpropane	2.19	10.6
<i>n</i> -Pentane	4.0	8.7
2-Methylbutane	3.7	16
2,2-Dimethylpropane	0.85	
<i>n</i> -Hexane	5.45	11
Cyclohexane	7.21	14
<i>n</i> -Heptane	7.0	15
2,2-Dimethylpentane	3.4	
<i>n</i> -Octane	8.7	19
2,2,4-Trimethylpentane	3.6	
<i>n</i> -Decane	11.2	
<i>n</i> -Hexadecane	23	

would be achieved. Thus these hydroxyl radical reactions can be very efficient with 1 in 10 collisions resulting in a reaction.

The C—H bond energies vary from ~423 kJ for a primary C—H; ~410 kJ for a secondary bond and ~402 kJ mol⁻¹ for a tertiary bond. Thus for a reaction involving hydrogen abstraction one would predict that tertiary C—H bonds would be most susceptible and that the overall reaction rate would depend on both the number and type of C—H bonds. An empirical structure–activity relation for predicting rates of hydroxyl radical reactions has been developed based on this assumption.²⁰ The rate constant for a given compound is expressed as a function of the number of each type of bond and the adjacent functional groups as follows:

$$\text{Primary C—H} \quad k'_p(\text{CH}_3\text{X}) = k_p\text{F}(\text{X})$$

$$\text{Secondary C—H} \quad k'_s(\text{CH}_2\text{XY}) = k_s\text{F}(\text{X})\text{F}(\text{Y})$$

$$\text{Tertiary C—H} \quad k'_t(\text{CHXYZ}) = k_t\text{F}(\text{X})\text{F}(\text{Y})\text{F}(\text{Z})$$

where k_p , k_s , and k_t represent the rate constants for the different C—H bonds and F factors indicate the influence of adjacent groups X, Y, and Z (Table 6.20). Substituent factors (Table 6.20) have been derived through statistical analysis of rate constants from >500 compounds.⁴⁰

TABLE 6.20 Substituent Factors at 25°C

X	F(X)	X	F(X)
-CH ₃	1.00	=O	8.7
-CH ₂ , >CH, >C <	1.23	-CHO	0.75
-F	0.094	-OH	3.5
-Cl	0.38	-OR (alkyl)	8.4
-Br	0.28	-COOH	0.74
-I	0.53	-COOR (alkyl)	0.74
-CHCl ₂ , CH ₂ Cl, -CHCl-	0.36	-CH ₂ CO-	3.9
-CH ₂ Br	0.46	-CCl ₃	0.069

By using the recommended group rate constants at 25°C⁴⁰:

$$\begin{aligned} \text{CH}_3\text{—}, k_p &= 1.36 \times 10^{-13} \text{ cm}^3 \cdot \text{molecule}^{-1} \cdot \text{s}^{-1} \\ \text{—CH}_2\text{—}, k_s &= 9.34 \times 10^{-13} \text{ cm}^3 \cdot \text{molecule}^{-1} \cdot \text{s}^{-1} \\ >\text{CH—}, k_t &= 1.94 \times 10^{-12} \text{ cm}^3 \cdot \text{molecule}^{-1} \cdot \text{s}^{-1} \end{aligned}$$

the rate constants for the reaction of hydroxyl radical with (a) *n*-pentane and (b) 2,2-dimethyl pentane would be derived as follows:

(a) *n*-Pentane $\text{CH}_3\text{CH}_2\text{CH}_2\text{CH}_2\text{CH}_3$ Exptl k_{OH} $4.0 \times 10^{-12} \text{ cm}^3 \cdot \text{molecule}^{-1} \cdot \text{s}^{-1}$

primary 2(C*H ₃ CH ₂ —)	$2(1.36 \times 10^{-13} \times 1.23)$	3.35×10^{-13}
secondary 2(—CH ₂ C*H ₂ CH ₃)	$2(9.34 \times 10^{-13} \times 1.00 \times 1.23)$	2.30×10^{-12}
secondary —CH ₂ C*H ₂ CH ₂	$9.34 \times 10^{-13} \times 1.23 \times 1.23$	1.41×10^{-12}

Predicted $k_{\text{OH}} = \Sigma_{p,s} = 4.04 \times 10^{-12} \text{ cm}^3 \cdot \text{molecule}^{-1} \cdot \text{s}^{-1}$

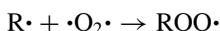
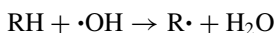
(b) 2,2-Dimethyl pentane (CH₃)₃CCH₂CH₂CH₃ Exptl k_{OH} $3.4 \times 10^{-12} \text{ cm}^3 \cdot \text{molecule}^{-1} \cdot \text{s}^{-1}$

primary 3(C*H ₃ —C—)	$3(1.36 \times 10^{-13} \times 1.23)$	5.02×10^{-13}
primary C*H ₃ CH ₂ —	$1.36 \times 10^{-13} \times 1.23$	1.67×10^{-13}
secondary —C—C*H ₂ CH ₂	$9.34 \times 10^{-13} \times 1.23 \times 1.23$	1.41×10^{-12}
secondary CH ₂ C*H ₂ CH ₃	$9.34 \times 10^{-13} \times 1.23 \times 1.00$	1.14×10^{-12}

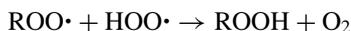
Predicted $k_{\text{OH}} = \Sigma_{p,s} = 3.23 \times 10^{-12} \text{ cm}^3 \cdot \text{molecule}^{-1} \cdot \text{s}^{-1}$

This approach can be adapted for both cyclic and unsaturated aliphatic compounds⁴⁰ with predicted rate constants usually being within a factor of 2 of the experimental values. Other approaches to the prediction of k_{OH} are based on molecular properties such as ionization potential, bond dissociation energies, infrared (IR) absorption frequencies, and so on, however, these methods are not as generally applicable because of the limited availability of the molecular parameters.⁴⁰

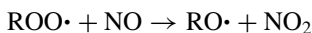
Thus a comprehensive base is available for assessing the rates at which alkanes will react with hydroxyl radicals. It is also useful to be able to define the product(s) of these reactions. Hydrogen abstraction produces an alkyl radical that in air reacts with oxygen to produce an alkyl peroxide radical:



The alkyl peroxide can react with a hydroperoxide radical to produce an acid:

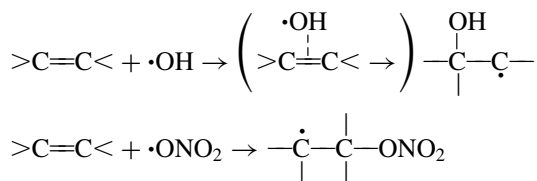


In addition, this radical can react with nitric oxide, a common atmospheric contaminant to produce an alkoxy radical that may either decompose, isomerize, or react with oxygen to produce an aldehyde:



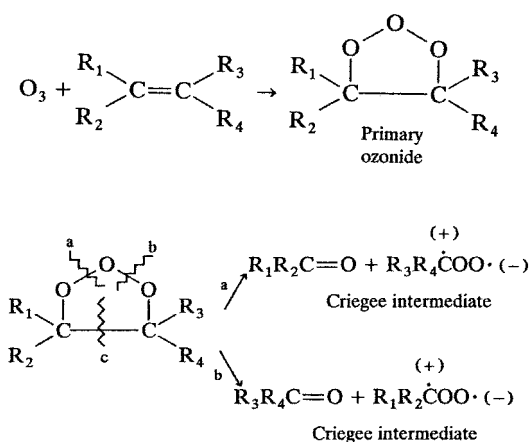
Further reactions with hydroxyl radicals could ensue with the net effect that a complex mixture of oxygenated compounds will result.

6.6.2.2 Alkenes Hydroxyl and nitrate radicals as well as ozone can react with alkenes. Although hydrogen abstraction is possible with the two radicals, addition to the double bond is the preferred reaction:



The radicals produced undergo a similar reaction sequence to that of the alkanes. Ozone adds across the double bond forming an unstable ozonide that breaks

down to form an aldehyde or ketone and a “Criegee” intermediate, which exists

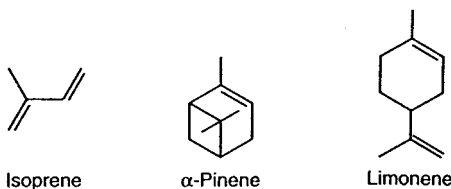


as a biradical in the vapor phase. This intermediate may react with a number of components in the atmosphere, however, the most likely reaction is with water to produce an aldehyde or carboxylic acid. From the rate constants compiled in Table 6.21 it can be seen that reactions with the hydroxyl radical are the most rapid, approaching the diffusion controlled limit of $3\text{--}5 \times 10^{-10} \text{ cm}^3 \cdot \text{molecule}^{-1} \cdot \text{s}^{-1}$. It is also of interest to note that all three oxidants, at typical atmospheric concentrations, can play a significant role in the degradation of alkenes (Table 6.22).

TABLE 6.21 Rate Constants for the Reaction of Hydroxyl and Nitrate Radicals and Ozone with Alkenes

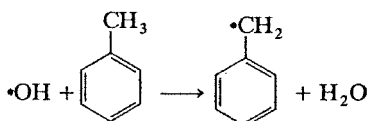
Alkene	$k_{\text{OH}} \times 10^{-12}$ ($\text{cm}^3 \cdot \text{molecule}^{-1} \cdot \text{s}^{-1}$)	$k_{\text{NO}_3} \times 10^{-13}$ ($\text{cm}^3 \cdot \text{molecule}^{-1} \cdot \text{s}^{-1}$)	$k_{\text{O}_3} \times 10^{-18}$ ($\text{cm}^3 \cdot \text{molecule}^{-1} \cdot \text{s}^{-1}$)
Ethene	8.52	0.0021	1.6
1-Butene	31.4	0.014	9.64
<i>cis</i> -2-Butene	56.4	3.5	125
<i>trans</i> -2-Butene	64.0	3.9	190
2-Methylpropene	51.4	3.3	11.3
1-Hexene	37		11.0
Cyclohexene	67.7	5.9	81.4
1,3-Butadiene	66.6	1.0	6.3
Isoprene	101	6.8	12.8
Limonene	171	120	200
α -Pinene	53.7	59	86.6
Methyl vinyl ketone	18.8	<0.006	5.6

Isoprene, α -pinene, and limonene are representative of a series of compounds,



isoprenoids and terpenoids, that are based on the five-carbon isoprene unit and emitted in large amounts by plants. Isoprene is released from hardwood species such as oaks and is the major volatile compound, excluding methane, emitted by plants (p. 226).¹¹ Conifers tend to release the C_{10} monoterpenes. These compounds are released by many plant species and because of the amounts emitted and their reactivity they can have a significant impact on atmospheric chemistry. These observations also serve as a reminder that chemicals of biogenic origin can be as significant in the environment as those of anthropogenic origin.

6.6.2.3 Aromatic Hydrocarbons Rate constants for the reaction of hydroxyl and nitrate radicals with some aromatic hydrocarbons are compiled in Table 6.23, and it is clear that with a few exceptions, that the hydroxyl radical is the more



important oxidant. The reaction of hydroxyl radical with toluene can involve hydrogen abstraction from the methyl side chain, with the generation of benzaldehyde or

TABLE 6.22 Lifetimes of Alkenes

Compound	$\cdot\text{OH}^a$	$\cdot\text{ONO}_2^b$	O_3^c
Ethene	32.6 h	220 day	9.64 day
<i>trans</i> -2-Butene	4.34 h	2.85 h	1.95 h
Cyclohexene	4.10 h	1.88 h	44.55 h
Isoprene	2.75 h	1.63 h	28.9 h
α -Pinene	5.17 h	11 min	4.28 h

^aCalculated using a 12-h average conc. of 1×10^6 molecules $\cdot \text{cm}^3$.

^bCalculated using a 12-h nighttime average conc. of 2.5×10^8 molecules $\cdot \text{cm}^3$.

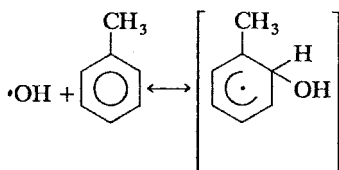
^cCalculated using a 24-h average conc. of 7.5×10^{11} molecules $\cdot \text{cm}^3$.

TABLE 6.23 Rate Constants for the Reaction of Hydroxyl and Nitrate Radicals with Aromatic Hydrocarbons at Ambient Temperatures^a

Compound	k ($\text{cm}^3 \cdot \text{molecule}^{-1} \cdot \text{s}^{-1}$)	
	$\cdot\text{OH}$	$\cdot\text{ONO}_2$
Benzene	1.2×10^{-12}	3.2×10^{-17}
Toluene	6.0×10^{-12}	6.9×10^{-17}
<i>o</i> -Xylene	1.37×10^{-11}	3.7×10^{-16}
<i>p</i> -Xylene	1.43×10^{-11}	2.4×10^{-16}
1,2,3-Trimethyl benzene	3.27×10^{-11}	2.2×10^{-15}
Ethylbenzene	7.1×10^{-12}	7×10^{-16}
Biphenyl	7.2×10^{-12}	
Naphthalene	2.16×10^{-11}	3.6×10^{-28} ^b
Acenaphthene	1.1×10^{-10}	5.5×10^{-12}
Phenanthrene	1.3×10^{-11}	1.2×10^{-13}
Pyrene	5×10^{-11}	1.6×10^{-27} ^b
Anthracene	1.7×10^{-11}	

^aTaken from Refs. 21 and 11.^bMeasured in the presence of NO_2 .

addition to the aromatic ring:



The latter reaction gives rise to a complex series of reactions with >50 oxygenated products being identified.⁴² Over 20% of the product was contributed by methyl glyoxal, glyoxal, and methylbutenedial and benzaldehyde.

The reaction of hydroxyl radical with toluene provides a most unusual Arrhenius plot (Fig. 6.24).

This relation expresses the rate constant as a function of the activation energy and temperature

$$k = Ae^{-E_a/RT}$$

and a linear relation is observed between $\ln k$ and $1/T$. The biphasic relation shows a conventional increase of k with increased temperature at higher temperatures and the reverse relation at lower temperatures. At higher temperatures the hydrogen-abstraction process is favored while the addition to the aromatic ring predominates at lower

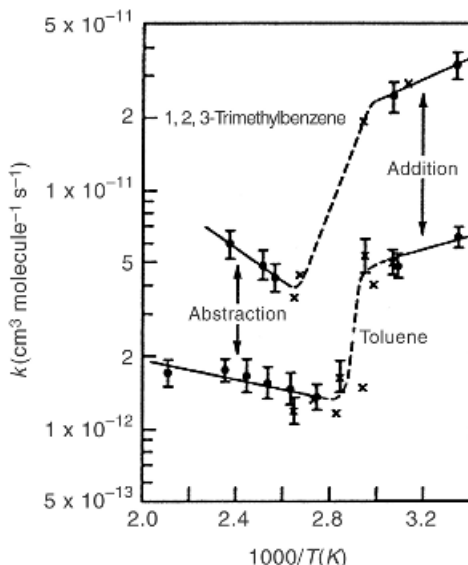


Figure 6.24 Arrhenius plots of $\log k$ versus $1000/T$ for the reaction of hydroxyl radical with toluene and 1,2,3-trimethylbenzene illustrating the response associated with the mechanisms of hydrogen abstraction and addition to the aromatic ring. [Reproduced with permission from R. A. Perry, R. Atkinson, and J. N. Pitts, *J. Phys. Chem.* **81**, 296 (1977). Copyright © 1977, American Chemical Society.]

temperatures. The inverse relation between rate and temperature is explained by the fact that, at higher temperatures, the hydroxyl–toluene adduct decomposes back to toluene limiting further reaction. At ambient temperatures it is noted that hydrogen abstraction contributes only $\sim 5\%$ to the overall reaction.

The nature of the reactions of hydroxyl radicals with polynuclear aromatic hydrocarbons is illustrated by studies of products observed with naphthalene (Fig. 6.25).⁴³ Addition of the hydroxyl radical to the aromatic ring produces ring opening with the 2-formylcinnamaldehyde being the major product. Reaction of the radical adduct with atmospheric nitrogen dioxide produces phenols and nitro derivatives. Formation of the latter from polynuclear aromatic hydrogens is of significance in that these derivatives tend to be mutagenic.

The rate constants for addition of hydroxyl radicals to the benzene ring correlate with the electrophilic substituent constants, σ^{+44} (Fig. 6.26).²⁰ This relation can be used to predict reaction rates of hydroxyl radicals with substituted benzene compounds using the relation⁴⁵

$$\log k_{\text{OH}} = -11.71 - 1.34 \sum \sigma^{+}$$

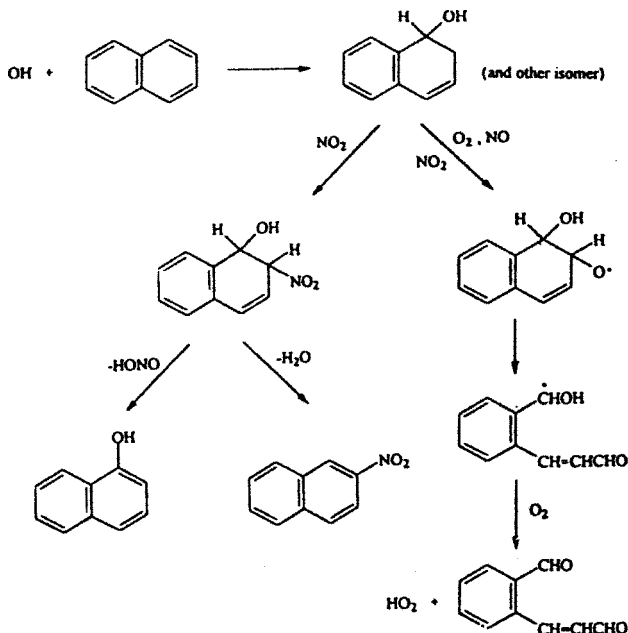


Figure 6.25 Reaction scheme for the reaction of hydroxyl radical with naphthalene. [Reproduced with permission from J. Sasaki, S. M. Aschmann, E. S. C. Kwok, R. Atkinson, and J. Arey, *Environ. Sci. Technol.* **31**, 3173 (1997). Copyright © 1997, American Chemical Society.]

Values for $\Sigma\sigma^+$ listed in Table 6.24, are derived from values for σ^+ (Table 6.24) assuming

1. Steric hindrance is not a factor and $\sigma^+(\text{o-}) = \sigma^+(\text{p-})$.
2. $\Sigma\sigma^+$ is the sum of all substituent σ^+ in the ring.
3. The OH radical adds to the position yielding the most negative value for $\Sigma\sigma^+$, preferably a free position.

For example, $\Sigma\sigma^+$ for 1,2,3-trimethyl benzene is derived by considering the influence of the three methyl groups on the 4,5,6-positions as follows:

Position-4	<i>o</i> -CH ₃ , <i>m</i> -CH ₃ , <i>p</i> -CH ₃	$\Sigma\sigma^+ = -0.066 + 2(-0.311) = -0.688$
Position-5	2(<i>m</i> -CH ₃), <i>p</i> -CH ₃	$\Sigma\sigma^+ = 2(-0.066) + -0.311 = -0.443$
Position-6	<i>o</i> -CH ₃ , <i>m</i> -CH ₃ , <i>p</i> -CH ₃	$\Sigma\sigma^+ = -0.688$

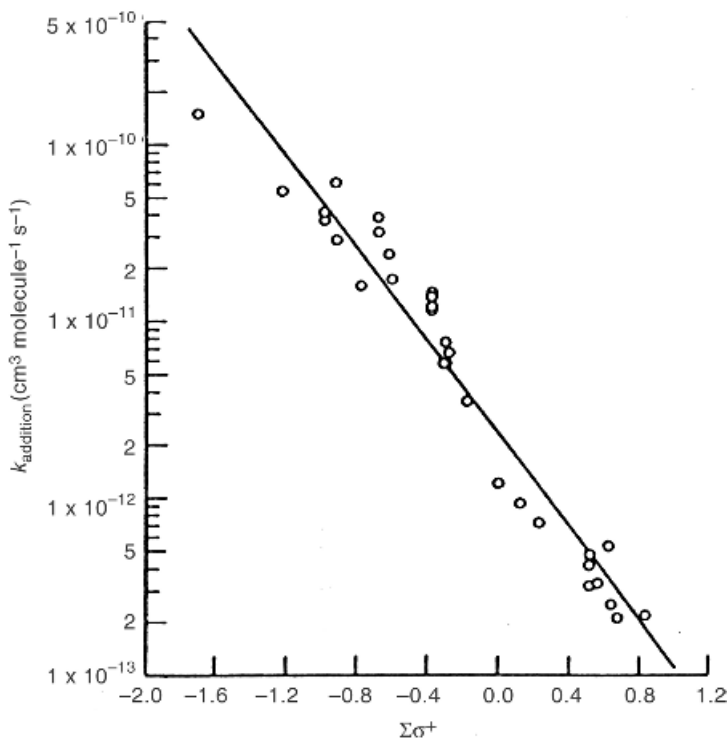


Figure 6.26 Correlation between rate constants for the addition of hydroxyl radicals to the benzene ring and electrophylic sigma substituent constants. [Reproduced with permission from R. Atkinson, *Chem. Rev.* **85**, 69 (1985). Copyright © 1985, American Chemical Society.]

TABLE 6.24 Electrophilic Substituent Constants^a

Substituent	m	o,p	Substituent	m	o,p
HO—	0.121	-0.92	C ₂ H ₅ OOC—	0.366	0.482
CH ₃ O—	0.047	-0.778	ClCH ₂ —	0.14	-0.01
C ₆ H ₅ O—	0.252	-0.500	Cl—	0.399	0.114
CH ₃ —	-0.066	-0.311	Br—	0.405	0.150
C ₂ H ₅ —	-0.064	-0.295	I—	0.359	0.135
<i>i</i> -C ₃ H ₇ —	-0.060	-0.280	HOOC—	0.322	0.421
C ₆ H ₅ —	0.109	-0.179	NO ₂ —	0.674	0.778

^aSee Ref. 44.

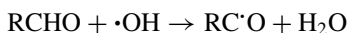
The OH radical would thus react at positions 4 and 6 with a calculated rate constant of

$$\begin{aligned}\log k_{\text{OH}} &= -11.71 - 1.34\Sigma\sigma^+ \\ &= -11.71 - 1.34 \times (-0.688) \\ &= -10.7\end{aligned}$$

The calculated value of 1.63×10^{-11} compares favorably with an experimental value²⁰ of $3.16 \times 10^{-11} \text{ cm}^3 \cdot \text{molecule}^{-1} \cdot \text{s}^{-1}$. These estimates of rate constants are usually within a factor of 2 (Table 6.25), however this approach cannot be used with benzaldehyde or anilines since the radical reacts at the substituent; i.e., hydrogen abstraction from the aldehyde CHO.

6.6.2.4 Oxygen Containing Compounds Although nitrate radicals may react with many oxygen-containing compounds, the hydroxyl radical again is the more effective oxidant and rate constants are compiled in Table 6.26 for reference.

With aldehydes the preferred reaction is hydrogen abstraction from the —CHO group.



The resulting radical reacts with O₂ to form an unstable acyl radical that decomposes to an alkyl radical and the reaction of this species has been reviewed above. In this

TABLE 6.25 Comparison of Calculated and Experimental Rate Constants^a for the Reactions of ·OH with Substituted Benzene Compounds^a

Compound	$\Sigma\sigma^+$	$k_{\text{OH}} (\text{cm}^3 \cdot \text{molecule}^{-1} \cdot \text{s}^{-1})$	
		Exptl.	Calc.
Toluene	-0.311	5.7×10^{-12}	5.1×10^{-12}
<i>o</i> -Xylene	-0.377	1.34×10^{-11}	6.24×10^{-12}
Ethylbenzene	-0.295	7.5×10^{-12}	4.85×10^{-12}
Phenol	-0.92	2.83×10^{-11}	3.33×10^{-11}
Methoxybenzene	-0.778	1.57×10^{-11}	2.15×10^{-11}
<i>o</i> -Cresol	-0.986	3.7×10^{-11}	4.08×10^{-11}
Chlorobenzene	0.114	9.4×10^{-13}	1.37×10^{-12}
1,2-Dichlorobenzene	0.513	4.2×10^{-13}	4.00×10^{-13}
1,2,4-Trichlorobenzene	0.627	5.32×10^{-13}	2.82×10^{-13}
Nitrobenzene	0.674	2.1×10^{-13}	2.44×10^{-13}

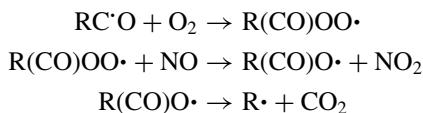
^aFrom Ref. 20.

TABLE 6.26 Rate Constants for the Reaction of Hydroxyl Radicals with Oxygen-Containing Compounds at Ambient Temperatures^a

Compound		cm ³ · molecule ⁻¹ · s ⁻¹
Aldehydes	Formaldehyde	9.2 × 10 ⁻¹²
	Acetaldehyde	1.6 × 10 ⁻¹¹
	Benzaldehyde	1.4 × 10 ⁻¹¹
Ketones	Acetone	6.2 × 10 ⁻¹³
	2-Pentanone	4.64 × 10 ⁻¹²
Alcohols	Methanol	1 × 10 ⁻¹²
	Ethanol	3.0 × 10 ⁻¹²
	1-Propanol	5.3 × 10 ⁻¹²
	Phenol	2.83 × 10 ⁻¹¹
Acids	<i>o</i> -Cresol	3.41 × 10 ⁻¹¹
	Formic	4.5 × 10 ⁻¹³
	Acetic	6 × 10 ⁻¹³
Ethers	Dimethyl ether	3.5 × 10 ⁻¹²
	Diethyl ether	1.3 × 10 ⁻¹¹
Acids	Formic acid	4.5 × 10 ⁻¹³
	Acetic acid	1.6 × 10 ⁻¹²
	Butyric acid	2.4 × 10 ⁻¹²
Esters	Ethyl acetate	1.7 × 10 ⁻¹²
	<i>n</i> -Propyl acetate	4.2 × 10 ⁻¹²

^aTaken from Ref. 20.

reaction sequence,



With the other oxygen functional groups it can be seen that rate constants reflect primarily the availability of secondary and tertiary C—H bonds as one might expect for hydrogen abstraction reactions. The reaction of the hydroxyl radical will reflect primarily the characteristics of the hydrocarbon component of the molecule.

6.6.2.5 Halogenated Compounds Many halogenated compounds, either because of their extensive use or their persistence are of environmental interest. The smaller, halogenated aliphatics have been used extensively and are common ground water contaminants,⁴⁶ while the persistence of the PCBs and chlorinated dibenzo dioxins is well documented. Hydroxyl radicals are the more important oxidants in the vapor phase and the hydrocarbon structure determines the nature of the reaction. Second-order rate constants for some of these compounds are summarized in Table 6.27.

TABLE 6.27 Rate Constants for the Reaction of Hydroxyl Radicals with Halogenated Compounds at Ambient Temperatures^a

Compound	k_{OH} ($\text{cm}^3 \cdot \text{molecule}^{-1} \cdot \text{s}^{-1}$)	Compound	k_{OH} ($\text{cm}^3 \cdot \text{molecule}^{-1} \cdot \text{s}^{-1}$)
CH ₃ Cl	4.4×10^{-14}	2-Chlorobiphenyl	2.8×10^{-12}
CH ₃ Br	3.5×10^{-14}	3-Chlorobiphenyl	5.2×10^{-12}
CH ₂ Cl ₂	1.5×10^{-13}	4-Chlorobiphenyl	3.8×10^{-12}
CHCl ₃	1.1×10^{-13}	2,2'-Dichlorobiphenyl	2.0×10^{-12}
CH ₃ CCl ₃	1.1×10^{-14}	3,3'-Dichlorobiphenyl	4.1×10^{-12}
CH ₂ ClCHCl ₂	3.2×10^{-13}	2,4',5- Trichlorobiphenyl	1.2×10^{-12}
CHCl=CCl ₂	2.35×10^{-12}	2,2',3,5'- Tetrachlorobiphenyl	8.0×10^{-13}
CCl ₂ =CCl ₂	1.69×10^{-13}	2,2',3,5',6- Pentachlorobiphenyl	4.0×10^{-13}
C ₆ H ₅ Cl	4.2×10^{-13}	2,3,4,5,6- Pentachlorobiphenyl	9.0×10^{-13}
C ₆ H ₅ Br	7.0×10^{-13}	1-Chlorodibenzo- <i>p</i> - dioxin	4.7×10^{-12}
<i>o</i> -C ₆ H ₄ Cl ₂	4.2×10^{-13}	Trichlorodibenzo- <i>p</i> - dioxin ^b	$4.5\text{--}5.9 \times 10^{-12}$
<i>m</i> -C ₆ H ₄ Cl ₂	7.2×10^{-13}	Tetrachlorodibenzo- <i>p</i> - dioxin ^b	$2.0\text{--}5.1 \times 10^{-12}$

^aFrom Refs. 20; 45; 47.^bCalculated values from Ref. 45.

Hydroxyl radicals can react with halogenated compounds at rates that are significant in determining the persistence of these compounds in the atmosphere, however, it is apparent that the electronegative character of the chlorine substituents does reduce the rate of the reactions. On the other hand, hydroxyl radicals do not react appreciably with freons, CF₂Cl₂ or CFCI₃ with rate constants of the order of $10^{-16} \text{ cm}^3 \cdot \text{molecule}^{-1} \cdot \text{s}^{-1}$.²⁰

6.6.3 Atmospheric Sinks

Compounds released to the environment distribute among the major environmental compartments, air, water, soil, and biota as a function of their physical chemical properties and models can provide a basis to predict how different compounds behave. Adverse effects will depend on persistence in a compartment. In this context, it is readily apparent that the hydroxyl radical serves as a very efficient atmospheric scavenger. Other oxidants may show activity with a limited series of compounds, but the hydroxyl radical is unique in the broad range of organic compounds with which it reacts and the rates at which these reactions proceed. Lifetimes for selected compounds based on reactions with the hydroxyl radical are compiled in Table 6.28.

TABLE 6.28 Atmospheric Lifetimes Based on Reaction with Hydroxyl Radical

Compound	τ	Compound	τ
Propane	10.3 day	Toluene	46.3 h
<i>n</i> -Hexane	2.1 day	Phenol	9.82 h
Methyl bromide	330 day	Naphthalene	12.9 h
Chloroform	105 day	Phenanthrene	24.4 h
Cyclohexane	38.5 h	2,4',5'-Trichlorobiphenyl	9.64 day
1,3-Butadiene	4.17 h	2,2',3,5'-Tetrachlorobiphenyl	14.5 day
α -Pinene	5.17 h	Tetrachlordibenzodioxin	2.3–5.8 day

The environmental role of the hydroxyl radical is underscored by the significance of compounds that react only slowly or not at all with it. Methane, ($\tau = 5$ years) generated by biological activity, is considered a “green-house” gas while the freons (chlorofluoro- methanes and ethanes) with no hydrogen atoms to abstract are key contributors to stratospheric ozone loss. Methyl bromide has found extensive use for treating agricultural produce for international distribution and as a soil sterilant, is also considered of significance in ozone depletion.

6.7 INDIRECT PHOTOLYSIS IN THE ATMOSPHERE: PARTICULATE PHASE

Compounds that evaporate may remain in the gas phase but can also distribute onto particles in the atmosphere. Other compounds may be released on particles such as the polynuclear aromatic hydrocarbons produced in the combustion of diesel fuel or in wood smoke. It is of interest to explore how compounds distribute between the particle and the vapor phase since this will influence their environmental behavior. Distribution onto a particle will enhance the potential for wet or dry deposition, major transport processes for moving compounds to surface water or onto vegetation. Compounds in the vapor phase will be subject to a range of photoinduced transformation processes, but how susceptible are compounds sorbed on particles?

6.7.1 Vapor-Particle Distribution

Suspended atmospheric particles vary in size and composition.^{11,48} Smaller particles ($<0.08 \mu\text{m}$) arise from condensation from the vapor phase while the larger particles ($>2.5 \mu\text{m}$) are produced by processes such as the weathering of soils, volcanic activity, and so on. Composition of the particles will vary with location and total carbon comprises 10–20% of the total suspended particles (TSP).⁴⁸ The average urban TSP load has been reported to be $98 \mu\text{g} \cdot \text{m}^{-3}$ of air.⁴⁸ The vapor–particle distribution under field conditions is evaluated using a device⁴⁸ in which air is drawn through the sampler such that particles will be trapped first on a filter while compounds in the vapor phase will be absorbed on the absorbent plug. Each phase

can then be analyzed and the distribution of individual compounds established. It is recognized that molecules in the vapor phase may sorb to the particle filter while molecules sorbed on particles may evaporate during sampling and be trapped on the absorbent and techniques have been introduced to minimize these complications.⁴⁹ The distribution of a semivolatile organic compound (SOC) is defined by K_p , which is essentially the ratio of the SOC in the two phases and is expressed

$$K_p = C_p/C_g = (F/TSP)/A$$

where F (filter-associated material), is the conc of SOC in the air ($\text{ng} \cdot \text{m}^{-3}$) associated with particles; TSP is the concentration of total suspended particles ($\mu\text{g} \cdot \text{m}^{-3}$) giving C_p in $\text{ng} \cdot \mu\text{g}^{-1}$ and A (from the absorbent) = C_g , the concentration in the vapor phase ($\text{ng} \cdot \text{m}^{-3}$). The parameter K_p thus has units $\text{m}^3 \cdot \mu\text{g}^{-1}$.

Air was sampled in the southeast of Chicago, a heavily industrialized area with steel mills, incinerators, landfills, coke ovens, and so on. Eleven samples ranging, in volume, from 261 to 329 m^3 were collected.⁵⁰ TSP levels ranged from 30 to 169 $\mu\text{g} \cdot \text{m}^{-3}$ with total carbon content varying from 17 to 31%. The total PCB levels in these samples ranged from 0.32 to 9.9 $\text{ng} \cdot \text{m}^3$ while PAH levels were considerably higher; 75–1410 $\text{ng} \cdot \text{m}^3$. The distribution of individual PCBs and PAH components indicated by K_p correlated with vapor pressure (p_L) of the supercooled liquid (for solids at ambient temperatures) as shown in Figure 6.27. This relation between K_p and p_L is consistent with the Junge–Pankow model⁵¹ based on Langmuir-type adsorption that would predict a slope of -1 . Deviation from this value is attributed to the fact that equilibrium may not have been achieved during sampling and to the possibility that, in the case of PAHs, some components may be incorporated in the particle and are not available to distribute into the vapor phase. The model would also predict that the intercept would depend on the surface area of the particle and the number of sorption sites per unit area. This adsorption

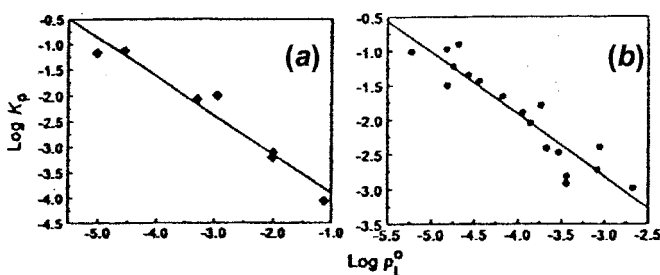


Figure 6.27 Distribution of polynuclear aromatic hydrocarbons, (a), and PCB congeners, (b), between vapor and particle phases from an air sample taken in Chicago related to vapor pressure of the super cooled liquid. [Reproduced with permission from W. E. Cotham and T. F. Bidleman, *Environ. Sci. Technol.* **29**, 2782 (1995). Copyright © 1995, American Chemical Society.]

model may also be expressed by the relation

$$\varphi = c\theta/(p_L + c\theta)$$

where φ is the fraction of chemical sorbed to the particles, θ , the particle surface area per unit volume of air (assumed to be $1.1 \times 10^{-5} \text{ cm}^2 \cdot \text{cm}^{-3}$ of air), and c ($\text{Pa} \cdot \text{cm}$), a factor related to the heats of desorption and evaporation. A value of $17.2 \text{ Pa} \cdot \text{cm}$ is often used. The fraction, φ , can be expressed as a function of K_p .

$$\varphi = C_p(\text{TSP})/[C_g + C_p(\text{TSP})] = K_p(\text{TSP})/[1 + K_p(\text{TSP})]$$

The relation between K_p and p_L can also be explained by a partitioning model,⁵² a process comparable to that discussed for the distribution into SOM (see Sorption, Chapter 3). At equilibrium, the chemical potential in the vapor phase would be equal to that in organic phase of the particle; that is, the compound would have the same tendency to leave each compartment and with units of $\text{m}^3 \cdot \mu\text{g}^{-1}$ for K_p , it was shown that

$$K_p = (10^{-6}RTf_{\text{om}})/(M_{\text{om}}\gamma_{\text{om}}p_L)$$

where f_{om} is the fraction of the particle mass that is absorbing organic matter with molecular weight M_{om} ($\text{g} \cdot \text{mol}^{-1}$) and γ_{om} the activity of the compound in question in the organic complex. This relation would also predict a linear relation of $\log K_p$ as a function of $\log p_L$ with a slope of -1 :

$$\log K_p = -\log p_L + \log[(10^{-6}RTf_{\text{om}})/(MW_{\text{om}}\gamma_{\text{om}})]$$

Another study in a less polluted area of Chicago,⁵³ reported that the average level of PCBs of 15 samples was $350 \text{ pg} \cdot \text{m}^{-3}$ with a mass percent distribution shown in Figure 6.28. Tri- (Nos. 18–37) and tetra-chlorobiphenyls (Nos. 42–74) were the predominant congeners identified (see Appendix for PCB congener numbering) distributed onto particles as a function of the degree of chlorination (Table 6.29).

These data also showed that the distribution between the vapor and particulate phase, K_p , correlated well with the liquid-phase vapor pressure p_L :

$$\log K_p = -0.715 - 5.14 \log p_L \quad (r^2 = 0.886)$$

By using this expression, it is possible to calculate K_p (Table 6.30) for a series of PCB congeners detected in these samples using values for p_L .⁵⁴

It is also apparent (Fig. 6.29) that K_p correlates with the octanol–air partition coefficient, K_{oa} , and this would follow from the fact that p_L can be expressed as a linear function of K_{oa} .⁵⁵ In the equilibrium distribution of a compound between the vapor phase and octanol, the fugacity or partial pressure of the compound in

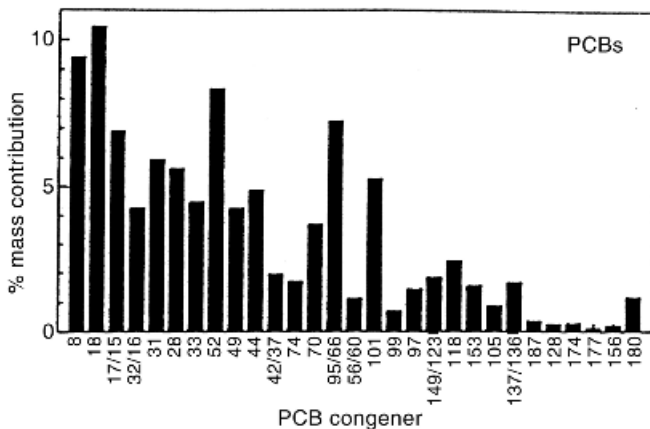


Figure 6.28 Mass percent contribution of PCB congeners in Chicago air. [Reproduced with permission from T. Harner and T. F. Bidleman, *Environ. Sci. Technol.* **32**, 1494 (1998). Copyright © 1998, American Chemical Society.]

the vapor phase is given by

$$P_g = (n/V)RT = C_g RT$$

where C_g is the concentration in the vapor phase. The fugacity of the compound in octanol solution, P_o , is defined by Raoult’s law.

$$P_o = X_o \gamma_o p_L$$

where X_o and γ_o are the mole fraction and activity coefficient of the compound in octanol. Converting mole fraction to a concentration term

$$P_o = C_o MW_o \gamma_o p_L / (10^3 \rho_o)$$

TABLE 6.29 Particulate Distribution of PCBs in Chicago Air Samples

PCB	% Particulate
3-CL	7.3
4-CL	16.7
5-CL	34.7
6-CL	58.3
7-CL	66.2
8-CL	79.5

TABLE 6.30 Values at 25°C of K_p , p_L , and K_{oa} for PCB Congeners Detected in Chicago Air Samples

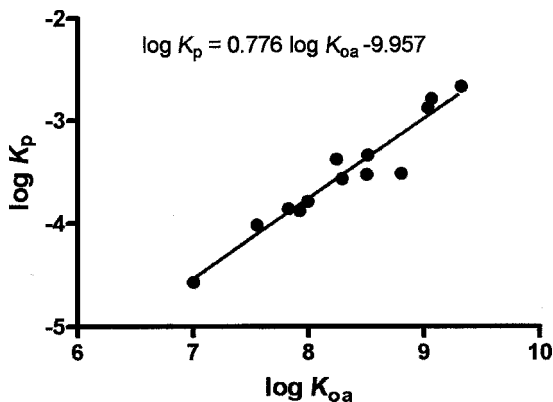
Congener No.	$\log p_L$ (P)	K_p ($\mu\text{g} \cdot \text{m}^{-3}$)	$\log K_{oa}^a$
8	-0.81	-4.56	7.00
33	-1.58	-4.01	7.55
44	-1.90	-3.78	7.99
49	-1.78	-3.87	7.92
52	-1.80	-3.85	7.82
66	-2.21	-3.56	8.29
70	-2.27	-3.52	8.50
95	-2.28	-3.51	8.80
99	-2.53	-3.33	8.51
101	-2.48	-3.37	8.24
128	-3.47	-2.66	9.32
138	-3.30	-2.78	9.06
153	-3.17	-2.87	9.03

^aFrom Ref. 56.

where C_o is the concentration in octanol and MW_o and ρ_o are the molecular weight and density of octanol. At equilibrium the fugacities (see Synthesis, Chapter 10) in the two phases must be equal and so

$$C_g RT = C_o MW_o \gamma_o p_L / (10^3 \rho_o) \quad \text{and}$$

$$p_L = 10^3 \rho_o RT / (MW_o K_{oa} \gamma_o)$$

**Figure 6.29** Correlation between the particle/vapor phase constant, K_p and K_{oa} . Data taken from Table 6.30.

Substituting for p_L in the partitioning relation for K_p

$$K_p = 10^{-9} K_{oa} f_{om} MW_o \gamma_o / (MW_{om} \gamma_{om} \rho_o)$$

Since the density of octanol at 20°C is 820 kg · m³

$$K_p = 1.22 \times 10^{-12} K_{oa} f_{om} (MW_o / MW_{om}) (\gamma_o / \gamma_{om}) \quad \text{and}$$

$$\log K_p = \log K_{oa} + [\log f_{om} + \log (MW_o / MW_{om}) (\gamma_o / \gamma_{om}) - 11.91]$$

The fraction of the particle mass consisting of absorbing organic matter (MW_{om} and γ_{om}) is defined by f_{om} and has been found to be ~20% in an urban environment. Thus for a given series of compounds, providing γ_o / γ_{om} is reasonably constant, there would be a linear relation between $\log K_p$ and $\log K_{oa}$ with a slope of +1, which has been reported for PAHs as well as chlorinated hydrocarbons similar to the PCBs.^{53,55} This relation would be consistent with a partitioning process with octanol being a reasonable surrogate for the absorbing organic matter of the particles. It is often difficult to measure p_L for the less volatile compounds, and thus K_{oa} would be a more practical predictor of vapor–particle distribution. As a first approximation one can assume that MW_o / MW_{om} and $\gamma_o / \gamma_{om} = 1$ and

$$\log K_p = \log K_{oa} + \log f_{om} - 11.91$$

providing a crude approximation of the distribution of a compound between these two compartments.

6.7.2 Photochemical Processes on Particles

Most of the investigations in this area have focused on PAHs because of their wide distribution in the particulates and because of the mutagenic properties of oxidative products. From the data summarized in Table 6.31, it can be seen that the response of

TABLE 6.31 Photolytic Degradation of PAHs on Particulates

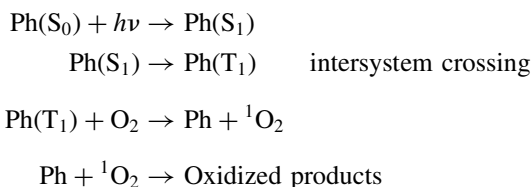
PAH	Half-life (h)				
	Silica Gel	Alumina	Fly Ash	Carbon Black	•OH vap. phase ^a
Acenaphthene	2.0	2.2	44		1.75
Phenanthrene	150	45	49	>1000	14.8
Anthracene	2.9	0.5	48	310	11.3
Pyrene	21	31	46	>1000	3.85
Fluorene	110	62	37	>1000	12.

^aCalculated using k_{OH} from Table 6.24 and assuming [$\bullet OH$] is 1×10^6 molecules · cm⁻³.

these compounds varies dramatically with the composition of the particle.⁵⁶ The surface areas of the silica gel, alumina, fly ash (recovered from a coal fired power plant) and carbon black were found to be 637, 224, 5.10, and 11.6 m² · g⁻¹ and the concentration of PAH on the particles (25 μg · g⁻¹) resulted in less than a monolayer. The carbon black was known to contain PAHs. Concentrations of the PAHs were monitored when subjected to radiation of 300–410 nm.

On silica gel and alumina, the PAHs show a wide range of photolytic activity suggesting a relationship between structure and activity. On the fly ash, similar half-lives were observed that would indicate, in this instance, that the process is independent of the PAH structure and dependent on the physical and chemical properties of the substrate. The PAHs are more stable on the carbon black and there is little variation among the different compounds. For comparison, the vapor-phase half-lives have been calculated and in most instances are shorter than those observed on the particles. Pyrene is a noted exception showing more rapid degradation on silica gel and alumina than by the hydroxyl radical process in the vapor phase.

Silica gel and alumina are white, whereas the fly ash and carbon black are black and it has been proposed that the latter may absorb more of the incident light reducing the rate of reaction of the adsorbed PAHs. It has been demonstrated⁵⁷ that the photolytic reaction phenanthrene on silica gel involves the addition of singlet oxygen and subsequent thermal and/or photochemical steps to produce a series of oxygenated derivatives. The reaction scheme proposed is as follows:



The phenanthrene acts as a sensitizer generating the singlet oxygen that in turn reacts with the ground-state molecule resulting in the oxidative transformations. This type of reaction has also been demonstrated in the photooxidation of anthracene associated with particulate organic matter. At this point, however, it is not clear why the reaction rates vary between silica gel and alumina.

In summary, if organic compounds can “see” solar radiation either in surface water or in the atmosphere, there are many mechanisms that can result in their transformation. The hydroxyl radical is extremely versatile and any compound with a C—H bond may react by this process. In a sense, these processes are a mixed blessing in that on the one hand compounds emitted in significant amounts react to produce a major impact on air quality. By contrast, these processes are probably the most efficient in the degradation of compounds released into the environment. Those compounds that react slowly or not at all, such as the freons and methane, can contribute to global impacts. The significance of these transformation processes is obvious.

REFERENCES

1. E. Pretsch, J. T. Clerc, J. Seibl, and W. Simon, *Spectral Data for Structure Determination of Organic Compounds*. Springer-Verlag, Berlin, 1989.
2. R. P. Wayne, *Principles and Applications of Photochemistry*. Oxford University Press, Oxford, 1988, 268 pp.
3. R. P. Wayne, *Principles and Applications of Photochemistry*. Oxford University Press, Oxford, 1988, p. 80.
4. P. Boule, C. Guyon, A. Tissot, and J. Lemaire, "Specific Phototransformation of Xenobiotic Compounds: Chlorobenzenes and Halophenols", in R. G. Zika and W. J. Cooper, Eds, *Photochemistry of Environmental Aquatic Systems*, ACS Symposium Series No. 327, American Chemical Society, Washington D.C., 1985, pp. 10–26.
5. D. Dulin, H. Drossman, and T. Mill, *Environ. Sci. Technol.* **20**, 72 (1986).
6. T. Mill, W. R. Mabey, B. Y. Lan, and A. Baraze, *Chemosphere* **10**, 1281 (1981).
7. G. G. Choudry and G. R. B. Webster, "Quantum Yields of Polychlorodibenzo-*p*-dioxins", in R. G. Zika and W. J. Cooper, Eds, *Photochemistry of Environmental Aquatic Systems*, ACS Symposium Series No. 327, American Chemical Society, Washington D.C. 1985, pp. 60–74.
8. R. G. Zepp and D. M. Cline, *Environ. Sci. Technol.* **11**, 359 (1977).
9. A. Leifer, *The Kinetics of Environmental Aquatic Photochemistry*, ACS Professional Reference Book, American Chemical Society, Washington, D.C. 1988.
10. R. P. Schwarzenbach, P. M. Gschwend, and D. M. Imboden, *Environmental Organic Chemistry*, John Wiley Sons, Inc., New York, 1993, p. 436.
11. B. J. Finlayson-Pitts and J. N. Pitts, Jr., *Chemistry of the Upper and Lower Atmosphere. Theory, Experiments and Applications*, Academic Press, San Diego, 2000, pp. 61–83.
12. W. R. Mabey, D. Tse, A. Baraze, and T. Mill, *Chemosphere* **12**, 3 (1983).
13. R. D. Ross and D. G. Crosby, *J. Agric. Food Chem.* **21**, 335 (1973).
14. W. R. Haag and J. Hoigné, *Environ. Sci. Technol.* **20**, 341 (1986).
15. W. R. Haag, J. Hoigné, E. Gassmann, and A. M. Braun, *Chemosphere* **13**, 631 (1984).
16. W. Horspool and D. Arместо, *Organic Photochemistry: a Comprehensive Treatment*, Ellis Horwood PTR Prentice Hall, New York, 1992, p. 119.
17. C. M. Spivakovsky et al., *J. Geophys. Res.* **105**, 8931 (2000).
18. R. G. Zepp, J. Hoigné, and H. Bader, *Environ. Sci. Technol.* **21**, 443 (1987).
19. R. P. Schwarzenbach, P. M. Gschwend, and D. M. Imboden, *Environmental Organic Chemistry*, John Wiley Sons, Inc., New York, 1993, p. 471.
20. R. Atkinson, *Chem. Rev.* **86**, 69 (1986).
21. R. P. Wayne et al. *Atmospheric Environ.* **25A**, 1 (1991).
22. R. G. Zepp, P. F. Schlotzhauer, and R. M. Sink, *Environ. Sci. Technol.* **19**, 74 (1985).
23. R. G. Zepp, G. L. Baughman, and P. F. Schlotzhauer, *Chemosphere* **10**, 109 (1981).
24. P. G. Tratnyek and J. Hoigné, *Environ. Sci. Technol.* **25**, 1596 (1991).
25. G. V. Buxton, C. L. Greenstock, W. P. Helman, and A. B. Ross, *J. Phys. Chem. Ref. Data* **17**, 513 (1988).
26. W. R. Haag and C. C. D. Yao, *Environ. Sci. Technol.* **26**, 1005 (1992).
27. J. Hoigné and H. Bader, *Water Res.* **10**, 377 (1976).

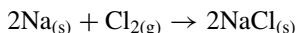
28. R. Atkinson, *Chem. Rev.* **85**, 69 (1985).
29. S. Canonica, U. Jans, K. Stemmler, and J. Hoigné, *Environ. Sci. Technol.* **29**, 1822 (1995).
30. D. Bahemann, J. Cunningham, M. A. Fox, E. Pelizzetti, P. Pichat, and N. Serpone, "Photocatalytic Treatment of Waters", in G. R. Helz, R. G. Zepp, and D. G. Crosby, Eds., *Aquatic and Surface Photochemistry*, Lewis Publishers, Boca Raton, 1994, pp. 261–316.
31. M. R. Hoffmann, S. T. Martin, W. Choi, and D. Bahnemann, *Chem. Rev.* **95**, 69 (1995).
32. C. Kormann, D. W. Bahnemann, and M. R. Hoffmann, *Environ. Sci. Technol.* **25**, 494 (1991).
33. W. Choi and M. R. Hoffmann, *Environ. Sci. Technol.* **29**, 1646 (1995).
34. D. F. Ollis, *Environ. Sci. Technol.* **19**, 480 (1985).
35. R. Atkinson and W. P. L. Carter, *Chem. Rev.* **84**, 437 (1984).
36. R. Atkinson et al., *J. Phys. Chem. Ref. Data* **28** 191 (1999).
37. R. Atkinson, *J. Phys. Chem. Ref. Data* **26**, 215 (1997).
38. R. Atkinson et al., *J. Phys. Chem. Ref. Data* **26**, 521 (1997).
39. R. Atkinson, *J. Phys. Chem. Ref. Data* **20**, 459 (1991).
40. E. S. C. Kwok and R. Atkinson, *Atmos. Environ.* **29**, 1685 (1995).
41. R. Criegee, "Mechanisms of Ozonolysis" *Angew. Chem., Int. Ed. Engl.* **14**, 745 (1975).
42. J. Yu and H. E. Jeffries, *Atmos. Environ.* **31**, 2261 (1997).
43. J. Sasaki, S. M. Aschmann, E. S. C. Kwok, R. Atkinson, and J. Arey, *Environ. Sci. Technol.* **31**, 3173 (1997).
44. H. C. Brown and Y. Okamoto, *J. Am Chem. Soc.* **80**, 4979 (1958).
45. E. S. C. Kwok, R. Atkinson, and J. Arey, *Environ. Sci. Technol.* **29**, 1591 (1995).
46. T. M. Vogel, C. S. Criddle, and P. L. McCarty, *Environ. Sci. Technol.* **21**, 722 (1987).
47. P. N. Anderson and R. A. Hites, *Environ. Sci. Technol.* **30**, 1756 (1996).
48. T. F. Bidleman, *Environ. Sci. Technol.* **22**, 361 (1988).
49. T. Harner and T. F. Bidleman, *Environ. Sci. Technol.* **32**, 1494 (1998).
50. W. E. Cotham and T. F. Bidleman, *Environ. Sci. Technol.* **29**, 2782 (1995).
51. J. F. Pankow, *Atmos. Environ.* **21**, 2275 (1987).
52. J. F. Pankow, *Atmos. Environ.* **28**, 185 (1994).
53. T. Harner and T. F. Bidleman, *Environ. Sci. Technol.* **32**, 1494 (1998).
54. R. L. Falconer and T. F. Bidleman, *Atmos. Environ.* **28**, 547 (1994).
55. A. Finizio, D. Mackay, T. Bidleman, and T. Harner, *Atmos. Environ.* **31**, 2289 (1997).
56. T. D. Behymer and R. A. Hites, *Environ. Sci. Technol.* **19**, 1004 (1985).
57. J. T. Barbas, M. E. Sigman, and R. Dabestani, *Environ. Sci. Technol.* **30**, 1776 (1996).

Redox Processes

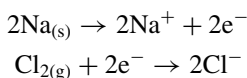
To what extent can compounds be transformed by reactions involving electron transfer—redox processes? First, it would need to be established that “electron-rich” or “electron-poor” environments exist that could induce compounds to either accept or donate electrons producing either reductions or oxidations. Second, it would be necessary to define the potential for compounds to participate in such processes. Aerobic environments are common. The atmosphere contains 20% elemental oxygen, an important electron acceptor or oxidizing agent. However, the direct reaction of oxygen with organic compounds is slow, but we have seen that oxidations occur through the involvement of solar energy in the production of active intermediates and in biota through enzyme catalysis. Anaerobic environments are also quite common. Many aquatic sediments and muds would be so classified along with deep groundwater and environments of waste treatment processes. Agricultural systems such as rice paddies can also be anaerobic. Although the term “anaerobic” implies an environment low in oxygen, the reducing potential of such environments depends on the presence of reducing agents. The significance of these processes can be assessed by first defining the range of redox conditions that can exist and summarizing those characteristics that determine which compounds could react. This will entail a review of oxidation numbers and reduction potentials. Factors that affect the rate of these reactions will then be considered.

7.1 CHARACTERISTICS OF REDOX REACTIONS

Some of the features of these processes are illustrated by considering the following simple reaction:

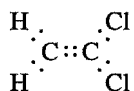


The reaction can be divided into its component parts,



The sodium atoms (the reducing agent) give up electrons and the oxidation number of the sodium increases from 0 (free element) to +1 (charge on the simple ion). The chlorine acts as an oxidizing agent and accepts electrons with its oxidation number decreasing from 0 to -1 . Keep in mind that an oxidation results in an increase in oxidation number, while a reduction results in a decrease in oxidation number. These two “half-reactions” define the oxidation and reduction steps upon which the overall reaction depends.

Electron movement in a redox reaction are tracked by determining change in oxidation number. Most introductory chemistry texts will provide rules that can be applied to establish the oxidation number of elements in simple inorganic species. However, assigning oxidation numbers becomes more complex when dealing with organic compounds. By using an electron dot representation of the molecule, bonding electrons are counted with the more electronegative element and the resulting “net charge” on an atom is its oxidation number. Consider 1,1-dichloroethene



given that the electronegativities for Cl, C, and H are 3.0, 2.5, and 2.1, respectively. With carbon “2” we would count $6 e^-$ and with a charge of $+4$ associated with “C” (nucleus plus inner-shell electrons), this carbon would have an oxidation number of -2 . By contrast, you would count only $2 e^-$ with carbon 1 and this carbon would have an oxidation number of $+2$. Some simple alkyl halides are tabulated in Table 7.1, along with oxidation numbers. When carbon shows a high oxidation number it has the potential to accept electrons and be reduced (e.g., carbon tetrachloride) and conversely a low oxidation number (e.g., methane) or reduced form indicates a potential to donate electrons and be oxidized.

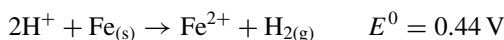
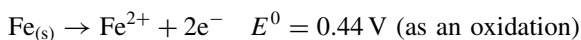
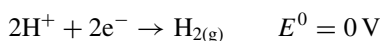
7.1.1 Reduction Potentials—Energetics

In redox processes, thermodynamic changes are defined by reduction potentials. It is possible to set a redox system up so that the electron transfer occurs in an external circuit and the tendency for the reaction to proceed is reflected by the electric potential that drives the electron flux. A standard reduction potential (E^0) is assigned to

TABLE 7.1 Variation in Oxidation Number of Carbon

Compound	Formula	Carbon Oxidation No.
Methane	CH ₄	-4
Carbon tetrachloride	CCl ₄	$+4$
Hexachloroethane	Cl ₃ C · CCl ₃	$+3$
Methylchloroform	H ₃ C · CCl ₃	$-3, +3$
Carbon dioxide	CO ₂	$+4$
Dichloromethane	CH ₂ Cl ₂	0
Chloroform	CHCl ₃	$+2$

half-reactions written as reduction processes, Table 7.2. These standard reduction potentials assume that reactants are in their standard states (unit activity) and relate to the standard hydrogen electrode that is arbitrarily given an E^0 of 0 V. The more positive the electrode potential, the more likely the reaction will proceed as a reduction. Consequently, elemental chlorine would show a high potential to accept electrons and act as an oxidizing agent and be reduced to chloride ion. Elemental sodium, by contrast, will readily donate electrons forming sodium ions acting as a reducing agent. Considering the iron and hydrogen half-reactions, the hydrogen half-reaction, showing the higher reduction potential, will proceed as written. Iron will be oxidized, so the half-reaction is reversed and the sign of E^0 becomes positive. The overall E^0 for the reaction is the sum of the E^0 values. Hydrogen ions will then oxidize elemental iron to Fe^{2+} .



The standard free energy change ΔG^0 is expressed

$$\Delta G^0 = -nFE^0$$

where n is the number of electrons transferred (in this case; 2) and F is the charge of a mole of electrons (96,490 C) giving in this case a value of $-84.9 \text{ kJ} \cdot \text{mol}^{-1}$, indicating that this process would be classified as spontaneous.

TABLE 7.2 Some E^0 Values for Reduction Half-Reactions

Half-Reaction		E^0 (V)	$E^0(\text{W})$ (V)
Oxidized	Reduced		
$\text{Cl}_{2(\text{g})} + 2\text{e}^-$	$\rightleftharpoons 2\text{Cl}^-$	+1.36	
$\text{O}_{2(\text{g})} + 4\text{H}^+ + 4\text{e}^-$	$\rightleftharpoons 2\text{H}_2\text{O}$	+1.22	+0.81
$\text{NO}_3^- + 2\text{H}^+ + 2\text{e}^-$	$\rightleftharpoons \text{NO}_2^- + \text{H}_2\text{O}$	+0.83	+0.42
$\text{NO}_3^- + 10\text{H}^+ + 8\text{e}^-$	$\rightleftharpoons \text{NH}_4 + 3\text{H}_2\text{O}$	+0.88	+0.36
$\text{SO}_4^{2-} + 9\text{H}^+ + 8\text{e}^-$	$\rightleftharpoons \text{HS}^- + 4\text{H}_2\text{O}$	+0.25	-0.22
$\text{S}_{(\text{s})} + 2\text{H}^+ + 2\text{e}^-$	$\rightleftharpoons \text{H}_2\text{S}_{(\text{g})}$	+0.17	-0.24
$\text{CO}_2 + 8\text{H}^+ + 8\text{e}^-$	$\rightleftharpoons \text{CH}_{4(\text{g})} + 2\text{H}_2\text{O}$	+0.17	-0.25
$2\text{H}^+ + 2\text{e}^-$	$\rightleftharpoons \text{H}_{2(\text{g})}$	0.00	-0.41
$6\text{CO}_{2(\text{g})} + 24\text{H}^+ + 24\text{e}^-$	$\rightleftharpoons (\text{C}_6\text{H}_{12})_6 + 6\text{H}_2\text{O}$	-0.01	-0.43
$\text{Fe}^{2+} + 2\text{e}^-$	$\rightleftharpoons \text{Fe}_{(\text{s})}$	-0.44	
$\text{Na}^+ + \text{e}^-$	$\rightleftharpoons \text{Na}_{(\text{s})}$	-2.71	

7.1.2 Nernst Equation

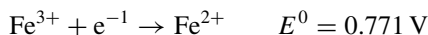
In equilibrium systems, the law of mass action tells us that one can influence the tendency of the reaction to proceed by varying the concentrations of the reactants and products. Consequently, one can anticipate that the reduction potential for a given half-reaction will likewise vary with concentrations of the constituents. This relation is defined by the Nernst equation:

$$E_H = E^0 - \frac{2.303RT}{nF} \log \frac{[\text{products}]}{[\text{reactants}]}$$

$$= E^0 - \frac{0.059}{n} \log \frac{[\text{products}]}{[\text{reactants}]}$$

when $T = 298 \text{ K}$, $F = 96,490 \text{ C} \cdot \text{mol}^{-1}$, and $R = 8.314 \text{ J} \cdot \text{mol}^{-1} \cdot \text{K}^{-1}$.

By applying this relation to the $\text{Fe}^{3+}/\text{Fe}^{2+}$ half-reaction,



$$E = E^0 - 0.059 \log [\text{Fe}^{2+}]/[\text{Fe}^{3+}]$$

When $[\text{Fe}^{3+}] = [\text{Fe}^{2+}] = 1$ (standard conditions) the logarithmic component is zero and $E = E^0$. However, when the system is at equilibrium and $\Delta G = 0$ and $E = 0$, then $E^0 = RT \ln K_{\text{eq}}$. Thus it is important to understand that in a given system $[\text{Fe}^{2+}]/[\text{Fe}^{3+}]$ will modulate the value of E , while if the redox potential of the environment is established by external factors, it will determine $[\text{Fe}^{2+}]/[\text{Fe}^{3+}]$. The behavior of acids and bases in relation to the environmental pH provides a comparable effect (p. 56). For example, when $[\text{Fe}^{2+}] = 1 \times 10^{-3} \text{ M}$ and $[\text{Fe}^{3+}] = 1 \times 10^{-5} \text{ M}$

$$E = 0.771 - 0.059 \log (1 \times 10^{-3})/(1 \times 10^{-5}) = 0.771 - 0.118 = 0.653$$

and, conversely, if $E = 0.81 \text{ V}$, a value observed in aerated water;

$$\log [\text{Fe}^{2+}]/[\text{Fe}^{3+}] = (0.81 - 0.771)/-0.059 = -0.696, \quad \text{and}$$

$$[\text{Fe}^{2+}]/[\text{Fe}^{3+}] = 0.20$$

Systems that show high values of E^0 such as Cl_2/Cl^- and $\text{O}_2/\text{H}_2\text{O}$ would provide an electron-poor environment since the oxygen and chlorine are readily reduced (accept electrons). The converse would apply in systems with low E^0 values such as $\text{Fe}^{2+}/\text{Fe}_{(s)}$.

7.1.3 E(W) Redox Potential in Natural Water

It is useful to calculate $E(W)$, a redox potential that would apply in ambient waters. This can be done by setting the pH at 7 and keeping standard activities for other

components. In some instances, it may be appropriate to also adjust the activity of a component such as chloride ion which is a common constituent of natural waters. For the nitrate/nitrite system, then

$$E_H(W) = 0.83 - 0.059/2 \log \frac{[\text{NO}_2^-]}{[\text{NO}_3^-][\text{H}^+]^2} = 0.83 - 0.0592/2 \log 1 \times 10^{14} \\ = 0.42 \text{ V}$$

When adjusting for pH effect on E_H , it should be noted that the hydrogen ion concentration, in addition to being a component of the mass action expression, can affect the acid/base ratio. For example, in the following H_2S system:



and the Nernst equations would be

$$E_H = +0.14 - \frac{0.059}{2} \log \frac{[\text{H}_2\text{S}]}{[\text{H}^+]^2}$$

However, $\text{p}K_{a1}$ for H_2S is 7 and it has been shown that the concentration of the neutral species can be defined (Phys. Properties, Chapter 1):

$$[\text{H}_2\text{S}] = \frac{[\text{H}_2\text{S}]_{\text{tot}}[\text{H}^+]}{K_a + [\text{H}^+]}$$

By substituting for $[\text{H}_2\text{S}]$ in the Nernst equation, E_H is now defined

$$E_H = +0.14 - \frac{0.059}{2} \log \frac{[\text{H}_2\text{S}]_{\text{tot}}}{(K_a + [\text{H}^+])[\text{H}^+]}$$

For example, in a 5-mM solution of H_2S at pH 6.5 ($[\text{H}^+] = 3.16 \times 10^{-7} \text{ M}$) and $K_{a1} = 1 \times 10^{-7}$:

$$E_H = +0.14 - 0.0295 \log \frac{5 \times 10^{-3}}{(1 \times 10^{-7} + 3.16 \times 10^{-7})(3.16 \times 10^{-7})} = -0.172 \text{ V}$$

7.2 REDOX STATUS OF NATURAL SYSTEMS

It is useful to evaluate the redox levels that could develop in natural waters and sediments. One might expect to find a more oxidative environment (higher E_H) in systems in equilibrium with the atmosphere. Reducing environments often result from microbial activity in anaerobic systems. It is also useful to consider how the redox status of any system might be measured.

7.2.1 Redox Levels in Natural Waters

The E_H of water in equilibrium with the atmosphere can be calculated from the O_2/H_2O system assuming that P_{O_2} is 0.20 atm and a pH of 7

$$\begin{aligned} E_H &= 1.22 - 0.059/4 \log \frac{[H_2O]}{P_{O_2}[H^+]^4} \\ &= 1.22 - 0.059/4 \log \frac{1}{0.2[10^{-7}]^4} \\ &= 1.22 - 0.059/4 \log 5 \times 10^{28} = 0.80 \end{aligned}$$

Changing the pH from 6 to 8 would result in E_H decreasing from 0.86 to 0.74.

Reducing environments often result from microbial activity. For example, if oxygen is limiting, some organisms may use sulfate (usually available in natural waters) as an electron acceptor to oxidize organic matter. The redox status would then be a function of the SO_4^{2-}/HS^- balance. If the $[SO_4^{2-}] = 10^{-2} M$ and $[HS^-] = 10^{-4} M$ and pH 7:

$$\begin{aligned} E_H &= 0.25 - 0.059/8 \log \frac{[HS^-][H_2O]^4}{[SO_4^{2-}][H^+]^9} \\ &= 0.25 - 0.059/8 \log 10^{61} \\ &= 0.25 - 0.45 = -0.20 V \end{aligned}$$

which would indicate a reducing environment. Other redox couples may provide lower values of E_H , however, these examples give some indication of the range that might be observed.

7.2.2 Determining Redox Status

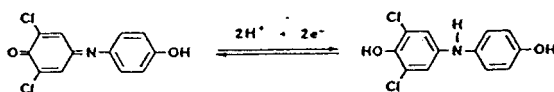
Platinum electrodes in conjunction with a reference electrode can be used to measure E_H values in environmental samples. However, these values cannot be considered definitive since they may represent a composite response of several redox couples and the actual response of the electrode can be limiting. A more direct approach is to measure the proportion of the oxidized and reduced components in a system and calculate E_H using the Nernst equation. Redox indicators [listed below with $E^0(W)$] may also be used as probes to assess redox status.¹ Comparable to acid-base indicators, the color of these compounds changes when oxidized or reduced. With the exception of resorufin which is pink, the oxidized form of these compounds is blue while the reduced counterpart is yellow or colorless.

These compounds have also been used to assess the reducing capacity of sediments. Those with high reduction potentials are reduced very rapidly in anaerobic sediment slurries while indicators such as indigo trisulfonate are reduced much more slowly. It is suggested that anaerobic sediments contain a reservoir of mild

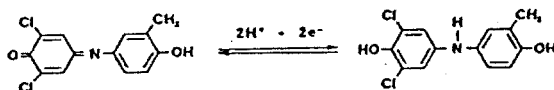
reducing agents that react rapidly with substances with higher reduction potentials. Compounds with lower reduction potentials are reduced more slowly by stronger reducing agents which may be produced more slowly, perhaps by microbial activity.

2,6-Dichlorophenol

$$E^0(W) = 0.217 \text{ V}$$

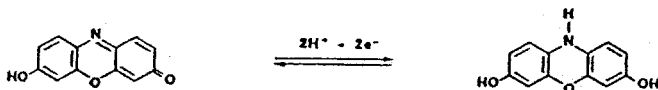
2,6-Dichloroindo-*o*-cresol

$$E^0(W) = 0.181 \text{ V}$$



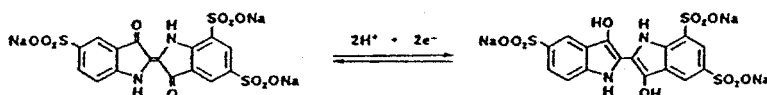
Resorufin

$$E^0(W) = -0.051 \text{ V}$$



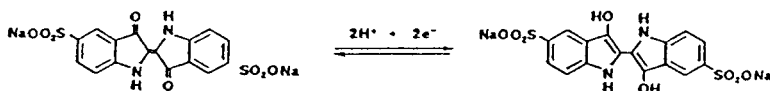
Indigo-5,5',7-trisulfonate

$$E^0(W) = -0.081 \text{ V}$$



Indigo-5,5'-disulfonate

$$E^0(W) = -0.125 \text{ V}$$

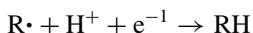
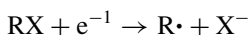


7.3 REDOX BEHAVIOR OF ENVIRONMENTAL CONTAMINANTS

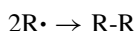
Oxidative transformations, as noted above, are more likely to be induced by enzyme-catalyzed processes in biota or photoinduced reactions in the atmosphere or in water. Consequently, this analysis will focus on reductions. The carbon of halogenated aliphatic compounds shows a high positive oxidation state (Table 7.1) and thus these compounds would be candidates for reduction. Since these compounds have been used extensively and may be released into the environment,² it is useful to assess the significance of these transformation processes.

Three reactions can result from the reduction of halogenated aliphatics, examples of which are given in Table 7.3. A **hydrogenolysis** reaction results in the replace-

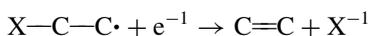
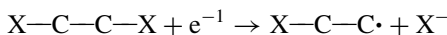
ment of a halogen by hydrogen involving two steps:



Free radical (see Chapter 6 for a discussion of radicals) produced in the first step may combine to give a **coupling** reaction



Compounds with halogens on neighboring carbons can produce an unsaturated derivative through a **dihalo-elimination** reaction:



It is also of interest that aromatic nitro substituents may be reduced to the corresponding amine since aromatic nitro compounds find use as explosives and are common contaminants around military installations.³

7.3.1 Reduction Potentials for Halogenated Compounds

The potential for a compound to be reduced can be evaluated from the reduction potential of the appropriate half-reaction in relation to that of an environment in which it might exist. This can be accomplished using standard free energies of formation (ΔG_f^0):

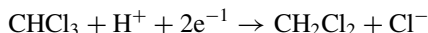
$$\Delta G^0 = \Sigma(\Delta G^0 \text{ formation})_{\text{prod.}} - \Sigma(\Delta G^0 \text{ formation})_{\text{react}}$$

and using the relation $\Delta G^0 = -nFE^0$ to derive the reduction potential.

TABLE 7.3 Reduction Potentials of Environmental Contaminants

Half Reaction		$E^0(\text{W})$ (V)
Oxidized	Reduced	
$\text{Cl}_3\text{C}-\text{CCl}_3 + 2\text{e}^{-}$	$\rightleftharpoons \text{Cl}_2\text{C}=\text{CCl}_2 + 2\text{Cl}^{-}$	+1.13
$\text{Cl}_3\text{C}-\text{CCl}_2 + 2\text{e}^{-}$	$\rightleftharpoons \text{Cl}_2\text{C}=\text{CHCl} + 2\text{Cl}^{-}$	+1.05
$\text{Cl}_2\text{HC}-\text{CHCl}_2 + 2\text{e}^{-}$	$\rightleftharpoons \text{ClHC}=\text{CHCl} + 2\text{Cl}^{-}$	+0.93
$\text{Cl}_2\text{HC}-\text{CH}_2\text{Cl} + 2\text{e}^{-}$	$\rightleftharpoons \text{ClHC}=\text{CH}_2 + 2\text{Cl}^{-}$	+0.79
$\text{CCl}_4 + \text{H}^{+} + 2\text{e}^{-}$	$\rightleftharpoons \text{CHCl}_3 + \text{Cl}^{-}$	+0.67
$\text{CBr}_4 + \text{H}^{+} + 2\text{e}^{-}$	$\rightleftharpoons \text{CHBr}_3 + \text{Br}^{-}$	+0.83
$\text{Cl}_2\text{HC}-\text{CHCl}_2 + \text{H}^{+} + 2\text{e}^{-}$	$\rightleftharpoons \text{ClH}_2\text{C}-\text{CHCl}_2 + \text{Cl}^{-}$	+0.51
$\text{ClH}_2\text{C}-\text{CHCl}_2 + \text{H}^{+} + 2\text{e}^{-}$	$\rightleftharpoons \text{ClH}_2\text{C}-\text{CH}_2\text{Cl} + \text{Cl}^{-}$	+0.54
$\text{CHCl}_3 + \text{H}^{+} + 2\text{e}^{-}$	$\rightleftharpoons \text{CH}_2\text{Cl}_2 + \text{Cl}^{-}$	+0.52
$\text{C}_6\text{H}_5\text{NO}_2 + 6\text{H}^{+} + 6\text{e}^{-}$	$\rightleftharpoons \text{C}_6\text{H}_5\text{NH}_2 + 2\text{H}_2\text{O}$	+0.42

This approach can be illustrated using the following hydrogenolysis half-reaction:



Aqueous phase values for ΔG_f^0 are required and can be calculated from the following:

$$\Delta G_f^0(\text{aq}) = \Delta G_f^0(\text{g}) + RT \ln H$$

where the Henry's law constant adjusts for the movement from vapor phase into solution. The values required are listed in Table 7.4 and ΔG_f^0 would be expressed

$$\begin{aligned} \Delta G_f^0 &= \Delta G_f^0[\text{CH}_2\text{Cl}_2(\text{aq})] + \Delta G_f^0[\text{Cl}^{-}(\text{aq})] \\ &\quad - \Delta G_f^0[\text{CHCl}_3(\text{aq})] - \Delta G_f^0[\text{H}^+(\text{aq})] \\ &= (-56.8 - 131.3) - (-64.3 + 0) \\ &= -123.8 \text{ kJ} \cdot \text{mol}^{-1} \end{aligned}$$

$$E^0 = -\Delta G^0/nF = -(-123,800/2 \times 96,500) = 0.64 \text{ V}$$

To calculate an $E(W)$ one uses the Nernst equation assuming pH 7 and 1×10^{-3} chloride ion since it is a common constituent in natural waters and $[\text{CH}_2\text{Cl}_2] = [\text{CHCl}_3] = 1$.

$$\begin{aligned} E_H &= 0.64 - 0.059/2 \log \frac{[\text{CH}_2\text{Cl}_2][\text{Cl}^{-}]}{[\text{CHCl}_3][\text{H}^+]} \\ &= 0.64 - 0.059/2 \log (1 \times 10^{-3})(1 \times 10^{-7}) = 0.52 \text{ V} \end{aligned}$$

Errors, say in H^+ , could result in some variation in estimates of E_H , however, the values derived will provide a basis to assess the potential for compounds to be reduced. Values of $E^0(W)$ for other compounds are listed in Table 7.3.²

For comparison, a value for a nitrobenzene is included. This approach has been extended to other chlorinated compounds^{4,5} and some illustrative values for

TABLE 7.4 Free Energies of Formation

Component	$\Delta G_f^0(\text{g})$ (kJ · mol ⁻¹)	H (L · atm · mol ⁻¹)	$\Delta G_f^0(\text{aq})$
CHCl ₃	-66.9	2.88	-64.3
CH ₂ Cl ₂	-58.5	2.03	-56.8
H ⁺			0
Cl ⁻			-131.3

hydrogenolysis reactions are listed in Table 7.5. These values have been calculated for pH 7 and a chloride ion concentration of $1 \times 10^{-3} M$. The error associated with these calculations is estimated to be in the range of 40 mV.

By considering the reducing potential of some anaerobic environments, the positive $E^0(W)$ values indicate that the energetics would favor the reduction of these compounds. With the polychlorinated compounds it is of interest to note how the $E(W)$ varies with the location of the chlorine involved.

7.4 KINETICS OF REDUCTION REACTIONS

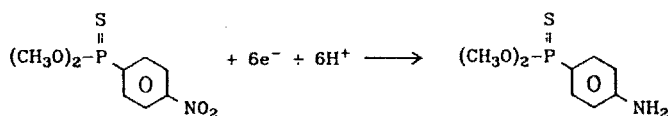
To this point, from an analysis of E^0 values it has been established that a number of environmentally significant compounds would be susceptible to reduction and the reducing capability is present. Do these processes proceed at significant rates under environmental conditions? It had been observed 25 years ago that highly chlorinated compounds such as DDT and toxaphene were degraded more rapidly in anaerobic soil systems.^{6,7} The degradation rate decreased with a decrease in the reduction potential and both microbial and abiotic processes were involved.

TABLE 7.5 Reduction Potentials for Hydrogenolysis of Halogenated Aromatics

Reactant	Product	$E^0(W)$ (V)
Hexachlorobenzene	Pentachlorobenzene	+0.567
1,2,3,4-Tetrachlorobenzene	1,2,3-Trichlorobenzene	+0.479
	1,2,4-Trichlorobenzene	+0.538
3,4-Dichlorobenzoate	3-Chlorobenzoate	+0.561
	4-Chlorobenzoate	+0.439
3-Chlorobenzoate	Benzoate	+0.386
3-Bromobenzoate	Benzoate	+0.468
2,3,4-Trichlorophenol	2,3-Dichlorophenol	+0.495
	2,4-Dichlorophenol	+0.537
	3,4-Dichlorophenol	+0.468
4-Chlorophenol	Phenol	+0.527
1,2,3,6,7,8-Hexachlorodioxin	1,2,3,7,8-Pentachlorodioxin	+0.483
	1,2,3,6,8-Pentachlorodioxin	+0.542
	1,2,3,6,7-Pentachlorodioxin	+0.479
1,2,3,7,8-Pentachlorodioxin	2,3,7,8-Tetrachlorodioxin	+0.474
	1,3,7,8-Tetrachlorodioxin	+0.538
	1,2,7,8-Tetrachlorodioxin	+0.474
2,3,7,8-Tetrachlorodioxin	2,3,7-Trichlorodioxin	+0.418
1,2,3,4-Tetrachlorodioxin	1,2,4-Trichlorodioxin	+0.581
	1,2,3-Trichlorodioxin	+0.518
2-Chlorodioxin	dibenzo- <i>p</i> -dioxin	+0.544
1-Chlorodioxin	dibenzo- <i>p</i> -dioxin	+0.539

The degradation of several alkyl halides was monitored in sediment water dispersions that were taken from the bottom of ponds and maintained under nitrogen.⁸ The rate at which these compounds were degraded at 25°C is summarized in Table 7.6. The E_H of the reaction dispersion was -0.140 V and the sediment/water ratio was 0.075 ($\text{g} \cdot \text{g}^{-1}$). Initial concentrations of the alkyl halides were in the 0.1 – 10 μM range. Dihalo elimination to produce the alkene was the preferred reaction rather than hydrogenolysis and the reaction was first order with respect to the concentration of the alkyl halide. These data do not resolve whether the process is abiotic, microbial, or both. However, activity was still observed after the sediments had been sterilized either by autoclaving or treatment with biocides indicating that the abiotic process was of significance.

In a related study,⁹ it has been demonstrated that the nitro group in methyl parathion is rapidly reduced to the corresponding amine in samples of anaerobic sediments. With sediment suspension



(~ 0.1 $\text{g} \cdot \text{g}^{-1}$ water) a first-order degradation was observed at 22°C. With initial concentrations varying from 2×10^{-8} to 3×10^{-7} M a rate constant of 2.8×10^{-2} min^{-1} was obtained. This was equivalent to a half-life of 25 min. The kinetic data and the observation that sterilization did not eliminate the reductive activity, indicated that the abiotic process was of significance.

7.4.1 Electron-Transport Mediators

Nitrobenzene is reduced to the corresponding aniline in several steps and it has been shown that

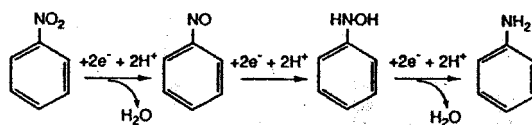
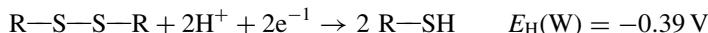


TABLE 7.6 Degradation of Alkyl Halides in Anaerobic Sediments

Compound	k (min^{-1})	Half-Life
Hexachloroethane	1.9×10^{-2}	36 min
1,2-Diodoethane	2.9×10^{-2}	24 min
1,2-Dibromoethane	2.1×10^{-4}	55 h
1,1,2,2-Tetrachloroethane	7.3×10^{-5}	6.6 day
1,2-Dichloroethane	$< 1.4 \times 10^{-5}$	> 35 day

the rate of this process is enhanced by the presence of natural (dissolved) organic matter (Fig. 7.1).¹⁰ This response differs from previous observations of the effect of dissolved organic matter where a contaminant can be protected from degradation and distribution into other compartments by distributing into this compartment (Chapters 5 & 8). This reaction was carried out at 25°C in the presence of 5 mM H₂S at pH 7.2, which would give an E_H of -0.207 V. The hydroxylamine intermediate is observed, however, the nitroso derivative is not because it reacts very rapidly. The rate of reaction is directly proportional to the amount of organic carbon and varies with the source of the natural organic matter (Fig. 7.2). The observed first-order rate constant can then be adjusted by the amount of organic carbon giving the second-order constants tabulated for the different systems evaluated (Table 7.7). It is suggested that the natural organic matter influences the reduction rate by providing a “mediator”, which facilitates electron transfer (Fig. 7.3). Earlier studies^{11,12} had demonstrated that the rate of reduction of organochlorine compounds was enhanced by iron porphyrin compounds such as hematin, which mimic related compounds such as the cytochromes, which are involved in electron transfer in biological systems. The effect of the natural organic matter may not be due to this type of compound, but it is known to contain quinones that would have a counterpart in biological electron transfer in coenzyme Q10. In fact, the higher activity of the walnut extract might be explained by its high content of quinones such as juglone.

This hypothesis finds support from observations of the effect of the naturally occurring quinones, juglone and lawsone, and an iron porphyrin (Table 7.8) on the reduction of nitrobenzenes¹³ (Fig. 7.4). Note that the electron carriers are present in micromolar (juglone, 10–150 μM ; lawsone, 3–250 μM , and porphyrin, 2–40 μM) rather than the 5-mM concentrations of the reducing compounds. A cysteine–cystine system was used with the iron porphyrin that was precipitated by H₂S. In the presence of H₂S, the $E_H(W)$ in the H₂S system was -0.192 V and < -0.380 V in the cysteine system. Reactions were carried out in the pH range of 6–8 at 25°C. All three



compounds increased the rate of reduction with the iron porphyrin the most active. Negligible reduction was observed in the absence of the electron carriers. It can be calculated from $E_H(W)$ values that at pH 7 both juglone and the iron porphyrin are completely reduced in the presence of the H₂S and cysteine, however, with lawsone this parameter is more sensitive to pH.

An interesting response to pH changes is observed with juglone (Fig. 7.5), where the rate constant is plotted as a function of the concentration of the reduced anion [HJUG]⁻. The linear relation observed to pH 7 indicates that the anion is more effective in transferring electrons than the neutral species and the rate constant could be expressed

$$k_{\text{obs}} = k^{\text{HQ}^-} [\text{HJUG}^-]$$

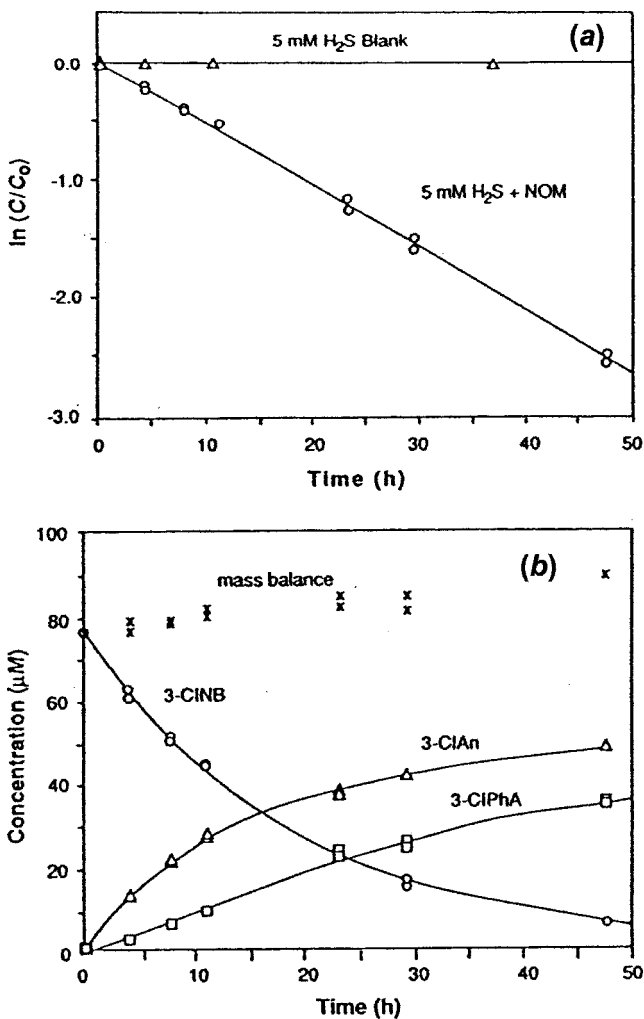


Figure 7.1 Reduction of 3-chloronitrobenzene in 5-mM aqueous hydrogen sulfide containing Hyde County natural organic matter ($66 \text{ mg c} \cdot \text{L}^{-1}$) at pH 7.2 and 25°C . (a) Plot of concentration at time t , C , in relation to initial concentration, C_0 , indicating pseudo-first-order kinetics. The blank indicates no reaction in the absence of the organic matter. (b) Disappearance of the chloronitrobenzene, and appearance of reaction products, 3-chlorophenylhydroxylamine, and 3-chloroaniline. [Reproduced with permission from F. M. Dunnivant, R. P. Schwarzenbach, and D. L. Macalady, *Environ. Sci. Technol.* **26**, 2133 (1992). Copyright © 1992, American Chemical Society.]

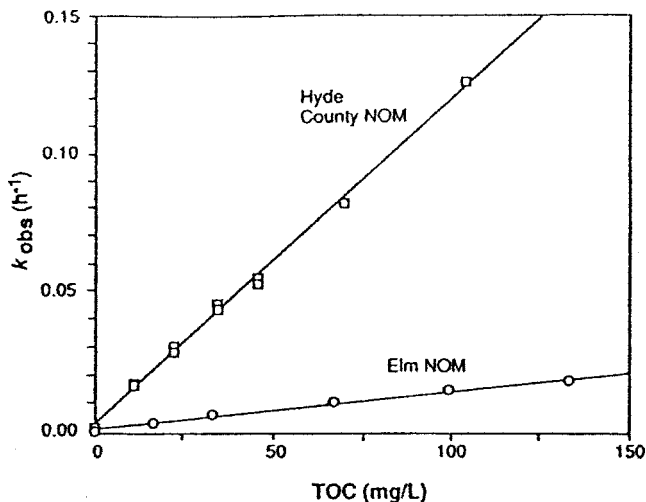


Figure 7.2 Effect of the concentration of natural organic matter ($mg\ C \cdot L^{-1}$) from two water sources on pseudo-first-order rate constants for the reduction of 3-chloronitrobenzene in 5-mM hydrogen sulfide and at 25°C. Hyde County water, pH 7.50; elm extract, pH 7.00. [Reproduced with permission from F. M. Dunnivant, R. P. Schwarzenbach, and D. L. Macalady, *Environ. Sci. Technol.* **26**, 2133 (1992). Copyright © 1992, American Chemical Society.]

The discontinuity above pH 7 is explained by the much greater activity of the dianion, JUG^{-2} , which would be present in very low proportions from pH 7–8. The reason why these compounds transfer electrons more efficiently than the cysteine or the H_2S is not understood.

TABLE 7.7 Normalized Reduction Rate Constants for 3-Chloronitrobenzene^a

Source	TOC ($mg \cdot L^{-1}$)	$k, h^{-1} \cdot (mg \cdot oc \cdot L^{-1})^{-1}$
MW-6 (ground water)	62	2.0×10^{-4}
MW-10 (ground water)	15	4.3×10^{-4}
Georgetown (stream draining a bog)	59	6.3×10^{-4}
Great Dismal Swamp (stream draining a bog)	38	8.4×10^{-4}
Suwanee (stream draining a bog)	111	1.3×10^{-4}
Hyde County (stream draining a bog)	132	6.5×10^{-4}
Kölliken (landfill leachate)	202	1.2×10^{-3}
Bayreuth (landfill leachate)	126	4.1×10^{-4}
Elm (tree extract)	200	2.7×10^{-4}
Walnut (tree extract)	80	6.2×10^{-3}

^aReaction at 25°C and pH 7 in the presence of 5 mM H_2S .

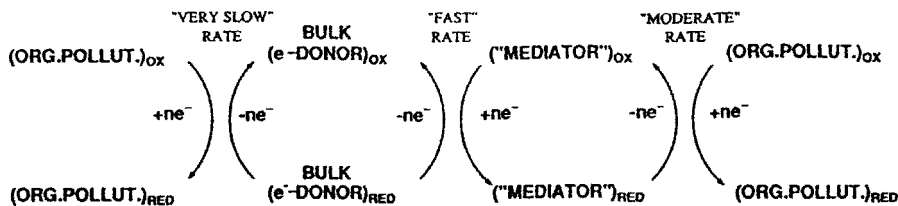


Figure 7.3 Schematic electron carrier mechanism to account for action of natural organic matter. [Reproduced with permission from F. M. Dunnivant, R. P. Schwarzenbach, and D. L. Macalady, *Environ. Sci. Technol.*, **26**, 2133 (1992). Copyright © 1992, American Chemical Society.]

Polyhalogenated methanes and ethanes are also reduced in both H_2S (1 mM)/juglone (200 μM) and the iron porphyrin (2–50 μM) cysteine (5 mM) systems.¹⁴ The reduction for some alkyl halides in the presence of the iron porphyrin is indicated by a second-order rate constant, since the rate is proportional to the concentration of both the alkyl halide and the porphyrin (Table 7.9). A half-life at a concentration of 10 μM iron porphyrin is included.

These compounds were also reduced in the presence of the quinone electron carrier, juglone, and it is postulated that the actual electron carrier is a mercaptojuglone formed by the reaction of H_2S with the quinone. This introduces an additional complicating factor in that these HS compounds can act as nucleophiles undergoing a nucleophilic substitution reaction with alkyl halides (see Hydrolysis, Chapter 8) and the data suggest that both reactions are occurring.

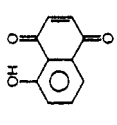
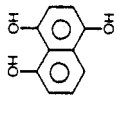
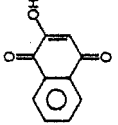
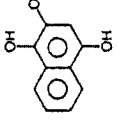
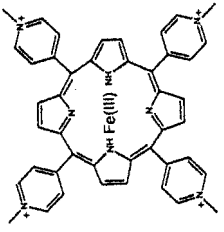
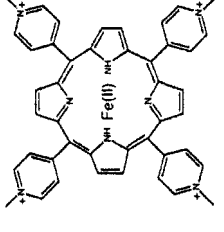
7.4.2 Reaction with Zero-Valent Metals

The $E_{\text{H}}(\text{W})$ values for the hydrogenolysis reaction of many chlorinated hydrocarbons range from around +0.4 to as high as +1.0 V (Tables 7.3 and 7.5) and the energetics would favor this reduction by elemental (zero-valent) iron with a E_{H}^0 of -0.44 V. This type of reaction would not be expected to be significant in the natural environment, however, it is receiving attention because of potential use in reducing the levels of alkyl halides in water.

The reduction of 1,1,1-trichloroethane (TCA) by elemental iron or zinc is summarized in Figures 7.6 and 7.7.¹⁵ These reactions were carried out in solutions buffered at pH 7.5 at room temperature.

The initial concentration of TCA was 200 μM and 0.5 g of zinc (30 mesh) and 1.0 g of iron (100 mesh) was used in 150 mL of solution. First-order rate constants were derived for the loss of TCA (Table 7.10) giving half-lives under these conditions of 0.60 and 1.44 h for zinc and iron, respectively. The metals appear to be involved in the degradation process beyond the simple contribution of electrons since the product patterns are quite distinct. For example, in the presence of zinc the yield of ethane is higher and 1,1-dichloroethane (DCA) lower than observed with iron. The DCA reacted only slowly and accumulated during the reaction. A

TABLE 7.8 Structural Formulas, Reduction Potentials (E_h), and Acidity Constants for the Two Quinones and the Iron Porphyrin Used as Electron Carriers^a

Oxidized Form	Oxidized Form	Reduced Form	E_h^0 (V)	E_h^{Or} (pH 7) (V)	$pK_a^{(ok)}$	$pK_{a,1}^{(red)}$	$pK_{a,2}^{(red)}$
8-Hydroxy-1,4-naphthoquinone (juglone)		$+2e^- + 2H^+ \rightleftharpoons$ 	0.428	0.033	8.00	6.60	10.60
2-Hydroxy-1,4-naphthoquinone (lawsone)	JUG 	$+2e^- + 2H^+ \rightleftharpoons$ 	0.351	-0.152	3.98	8.68	10.71
<i>meso</i> -Tetrakis (<i>N</i> -methylpyridyl)iron porphyrin	LAW 	$+e^- \rightleftharpoons$ 	0.171	0.065	5.21	(> 10)	

^aReproduced with permission from R. P. Schwarzenbach, R. Stierli, K. Lanz, and J. Zeyer, *Environ. Sci. Technol.* **24**, 1566 (1990). Copyright © 1990, American Chemical Society.

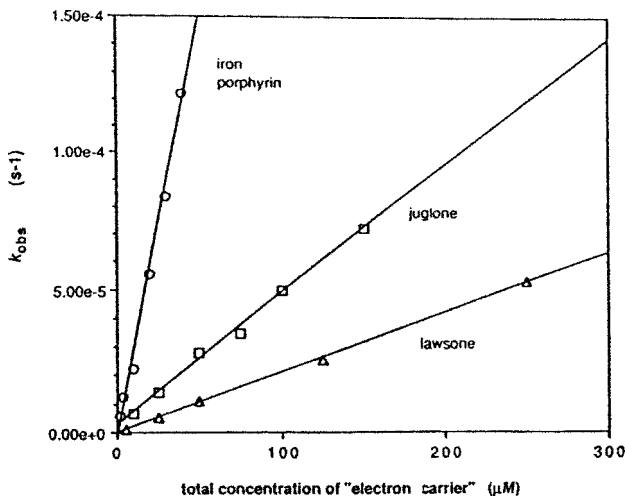


Figure 7.4 Pseudo-first-order rate constants for the reduction of 4-chloronitrobenzene as a function of the concentration of electron carrier in the presence of 5 mM H₂S or 5-mM cysteine (porphyrin) at 25°C and pH 7.18 (juglone); 7.24 (lawsone), and 7.03 (porphyrin). [Reproduced with permission from R. P. Schwarzenbach, R. Stierli, K. Lanz, and J. Zeyer, *Environ. Sci. Technol.* **24**, 1566 (1990). Copyright © 1990, American Chemical Society.]

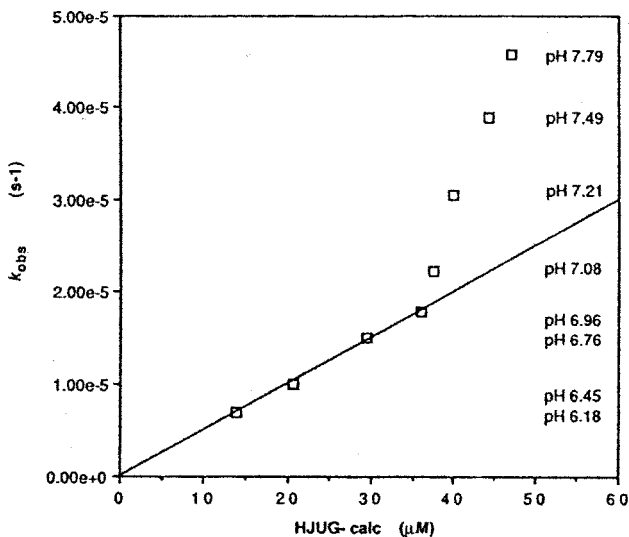


Figure 7.5 Effect of pH on the pseudo-first-order rate constants for the reduction of 4-chloronitrobenzene in the presence of 5 mM H₂S and 50 μM total juglone. Rate constant plotted as a function of the concentration of reduced juglone. [Reproduced with permission from R. P. Schwarzenbach, R. Stierli, K. Lanz, and J. Zeyer, *Environ. Sci. Technol.* **24**, 1566 (1990). Copyright © 1990, American Chemical Society.]

TABLE 7.9 Rate of Reduction of Alkyl Halides in the Presence of Cysteine and an Iron Porphyrin at pH 7

Methanes (20°C)			Ethanes (25°C)		
Compound	k_2 ($M^{-1} \cdot s^{-1}$)	$t_{1/2}^a$	Compound	k_2 ($M^{-1} \cdot s^{-1}$)	$t_{1/2}^a$
CHCl ₃	NMR ^b		CHCl ₂ —CHCl ₂	0.010	80 day
CFCl ₃	0.10	193 h	CCl ₃ —CH ₃	0.032	25 day
CHBrCl ₂	5.8	3.3 h	CCl ₂ F—CClF ₂	0.038	21 day
CCl ₄	5.9	3.3 h	CCl ₃ C—CH ₂	1.2	16 h
CHBr ₃	8.9	2.2 h	CCl ₃ —CF ₃	8.6	2.2 h
CHBr ₂ Cl	12	1.6 h	CHCl ₂ —CCl ₃	9.5	2.0 h
CFBr ₃	69	17 min	CF ₂ Cl—CCl ₃	13	1.5 h
CBrCl ₃	250	4.6 min	CCl ₃ —CCl ₃	48	24 min
CBr ₂ Cl ₂	610	1.9 min			

^aCalculated for 1×10^{-5} M iron porphyrin.

^bNo detectable reaction over 8 h.

reaction sequence (Fig. 7.8) has been proposed to account for the products produced. Both hydrogenolysis and coupling reactions are implicated in the sequence of reactions.

A small amount of 1,1-dichloroethene (DCE) was detected when a copper–iron system was used and its formation was attributed to a **dehydrochlorination** reac-

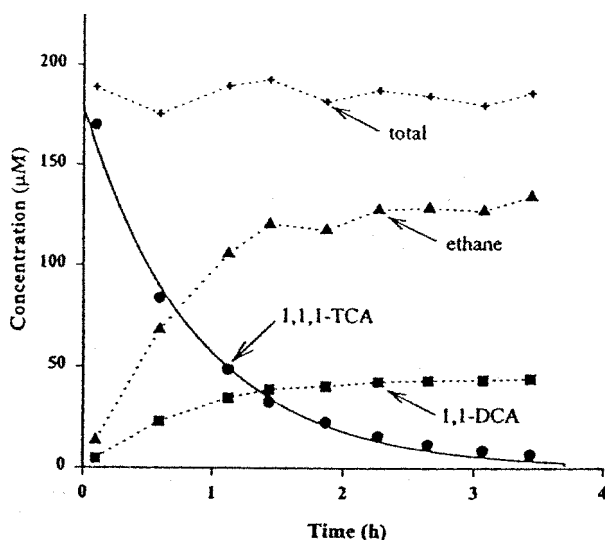


Figure 7.6 Reduction of 1,1,1-trichloroethane (TCA) by metallic zinc in tris buffer at pH 7.5. Solid line denotes exponential decay. [Reproduced with permission from J. P. Fennelly and A. L. Roberts, *Environ. Sci. Technol.* **32**, 1980 (1998). Copyright © 1998, American Chemical Society.]

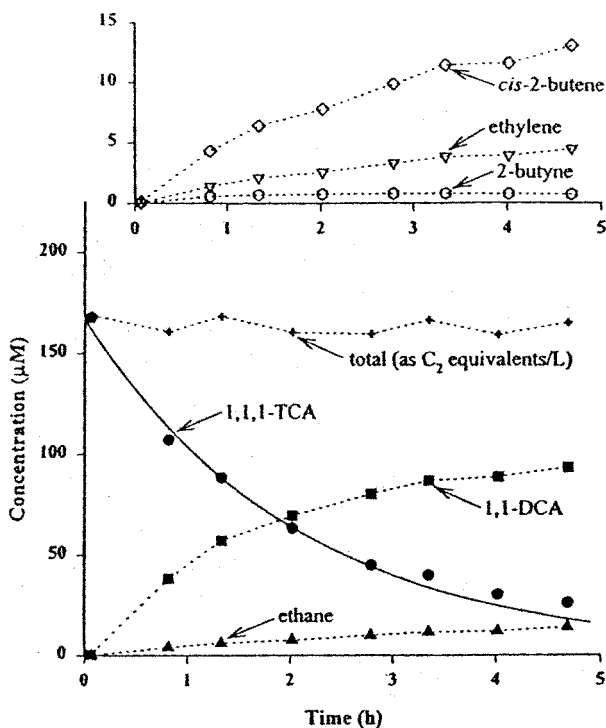


Figure 7.7 Reduction of 1,1,1-trichloroethane (TCA) by metallic iron at pH 7.5. Solid line denotes exponential decay and inset shows minor products not observed in the zinc reaction. [Reproduced with permission from J. P. Fennelly and A. L. Roberts, *Environ. Sci. Technol.* **32**, 1980 (1998). Copyright © 1998, American Chemical Society.]

tion, where a double bond is produced by splitting out HCl. In another study¹⁶ using 1,1,1-trichloroethene (TCE) it was demonstrated that the reaction rate is directly proportional to the metal surface area (Fig. 7.9) and, consequently, rate constants observed (k_{obs}) are normalized to account for this effect as follows:

$$k_{\text{sa}} = k_{\text{obs}} / (\text{surf. area}) \text{h}^{-1} \cdot \text{L} \cdot \text{m}^{-2}$$

TABLE 7.10 Reaction Kinetics for the Reduction of TCA by Metals

Metal	g 150 mL ⁻¹	k_{obs} (h ⁻¹)	$t_{1/2}$ (h)	k_{sa} (L · m ⁻² · h ⁻¹)
Zinc ^a	0.5	1.15	0.60	10.0
Iron ^a	1.0	0.48	1.44	0.46
Iron–nickel	1.0	1.86	0.37	1.77
Iron–copper	1.0	1.35	0.51	1.29

^aSurface area: iron, 0.16 m² · g⁻¹; zinc, 0.035 m² · g⁻¹.

The kinetics for the reduction of TCA in the presence of zinc or iron in addition to iron treated with catalytic amounts of nickel or copper are summarized in Table 7.10. Small amounts of nickel or copper (0.035 mol%) on the iron enhance the reaction rate. The reduction of other alkyl halides at ambient temperatures has been reported (Table 7.11).¹⁷ Iron (10 g; surf. area $0.287 \text{ m}^2 \cdot \text{g}^{-1}$) was added to 40 mL of an aqueous solution of the compound giving a surface area-to-volume ratio of $0.072 \text{ m}^2 \cdot \text{mL}^{-1}$. The products formed were not monitored in this study, however, it is of interest to note that most of the compounds tested reacted quite rapidly.

It has been reported that DDT and its derivatives, DDD and DDE, are dechlorinated by zero-valent iron.¹⁸ Note that the reaction rate with DDT and DDE was independent of the amount of iron and dependent on the rate at which the solid material moved into solution. Keep in mind that the solubility of DDT is only 3–5 ppb. Reaction rate is enhanced by surfactants.

There has been considerable interest in these zero-valent iron reactions because of their potential for use in reducing the level of alkyl halides in ground water. Compounds such as 1,2-dichloroethane, 1,1,1-trichloroethane, trichloroethene, and tetrachloroethene have been used widely as degreasing agents, in dry cleaning processes and in the manufacture of semiconductors. Related compounds, dichloropropene and dibromochloropropane, have been used as soil fumigants. Since these alkyl halides are quite water soluble it is not surprising that they are often detected in ground water. The current clean-up practice is to “pump and purge”. The contaminated water is pumped out, and aerated to remove the volatile contaminants and returned to the aquifer. This process is expensive and not efficient. An alternative

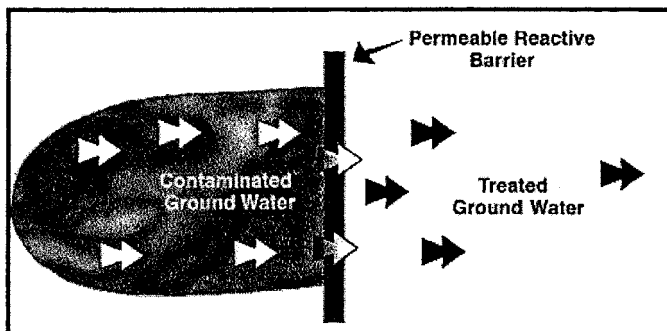
TABLE 7.11 Reduction of Alkyl Halides in the Presence of Iron

Compound	S_w (ppm)	Conc (ppm ^a)	k_{obs} (h ⁻¹)	$t_{1/2}$ (h)	k_{sa} (L · m ² · h ⁻¹)
CCl ₄	757	1.63	2.77	0.25	38.5
CHCl ₃	8200	2.01	0.021	33	0.292
CHBr ₃	3010	2.12	2.89	0.24	40.1
CH ₂ Cl ₂	20,000	2.75	^b		
CCl ₃ —CCl ₃	50	3.62	5.33	0.13	74.0
CHCl ₂ —CHCl ₂	2900	2.51	0.0361	19.2	0.501
CCl ₃ —CH ₂ Cl	2900	2.33	0.157	4.4	2.18
CCl ₃ —CH ₃	1500	0.68	0.131	5.3	1.82
CCl ₂ —CCl ₂	150	2.25	0.0387	17.9	0.538
CCl ₂ —CHCl	1100	1.56	0.0510	13.6	0.708
CCl ₂ —CH ₂	2250	2.33	0.0173	40.0	0.240
<i>trans</i> CHCl=CHCl	6300	1.77	0.0126	55	1.75
<i>cis</i> CHCl=CHCl	3500	1.95	1.60×10^{-3}	433	0.022
CH ₂ =CHCl	2670	3.66	1.85×10^{-3}	374	0.025

^aConcentration in the reaction system.

^bNo reaction observed.

approach involves the use of a permeable reactive barrier with the contaminant



being degraded as it passes through. An instillation at a semiconductor plant consisted of a 4-ft barrier of granular iron filings that was 40-ft wide and 20-ft deep. As the groundwater passed through, levels of TCE were reduced from 30–68 ppb to <0.5 ppb and *cis* 1,2-dichloroethene were reduced from 393–1916 to 0.5 ppb.¹⁹ The advantages of this approach are obvious providing the hydrology is understood, and studies are in progress to further test its efficacy. Other factors, such as the most effective reducing system (iron or iron/nickel, etc.) and the actual structure of the barrier are under investigation. The US Environmental Protection Agency (USEPA) co-ordinates a “Permeable Reactive Barriers Action Team” and their web site: (http://www.rtdf.org/public/permbarr/pbar_qa.htm) compiles profiles of over 30 ongoing and completed pilot and full-scale operations in the United States and Canada.

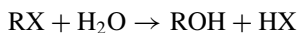
REFERENCES

1. P. G. Tratnyek and N. L. Wolfe, *Environ. Toxicol. Chem.* **9**, 289 (1990).
2. T. M. Vogel, C. S. Criddle and P. L. McCarty, *Environ. Sci. Technol.* **21**, 722 (1987).
3. S. S. Talmage, D. M. Opresko, C. J. Maxwell, C. J. E. Welsh, F. M. Cretella, P. H. Reno and F. B. Daniel, *Rev. Environ. Contam. Toxicol.* **161**, 1 (1999).
4. J. Dolfig and B. K. Harrison, *Environ. Sci. Technol.* **26**, 2213 (1992).
5. C. Huang, B. K. Harrison, J. Madura and J. Dolfig, *Environ. Toxicol. Chem.* **15**, 824 (1996).
6. J. F. Parr and S. Smith, *Soil Sci.* **118**, 45 (1974).
7. J. F. Parr and S. Smith, *Soil Sci.* **121**, 52 (1976).
8. C. T. Jafvert and N. L. Wolfe, *Environ. Toxicol. Chem.* **6**, 827 (1987).
9. N. L. Wolfe, B. E. Kitchens, D. L. Macalady and T. J. Grundl, *Environ. Toxicol. Chem.* **5**, 1019 (1986).
10. F. M. Dunnivant, R. P. Schwarzenbach and D. L. Macalady, *Environ. Sci. Technol.* **26**, 2133 (1992).

11. G. M. Klečka and S. J. Gonsior, *Chemosphere* **13**, 391 (1984).
12. J. A. Zoro, J. M. Hunter, G. Eglinton and G. C. Ware, *Nature (London)* **247**, 237 (1974).
13. R. P. Schwarzenbach, R. Stierli, K. Lanz and J. Zeyer, *Environ. Sci. Technol.* **24**, 1566 (1990).
14. J. A. Perlinger, J. Buschmann, W. Angst and R. P. Schwarzenbach, *Environ. Sci. Technol.* **32**, 2431 (1998).
15. J. P. Fennelly and A. L. Roberts, *Environ. Sci. Technol.* **32**, 1980 (1998).
16. C. Su and R. W. Puls, *Environ. Sci. Technol.* **33**, 163 (1999).
17. R. W. Gillham and S. F. O'Hannesin, *Ground Water* **32**, 958 (1994).
18. G. D. Sayles, G. You, M. Wang and M. J. Kupferle, *Environ. Sci. Technol.* **31**, 3448 (1997).
19. E. L. Appleton, *Environ. Sci. Technol.* **30**, 536A (1996).

Hydrolysis

Perhaps the most ubiquitous compound in the environment is water. A large proportion of the earth's surface is covered by the oceans, and in the terrestrial environment there are large fresh water lakes, rivers, and streams. The soil retains water because of the hydrophylic nature of clay surfaces. Water is a major constituent of all cells. Even though a small molecule like water has an unusually high boiling point, it does have appreciable vapor pressure at ambient conditions and thus the atmosphere also contains substantial amounts of water. Any compound introduced into the environment, therefore, will encounter water and the question that needs to be addressed is the extent to which and the conditions under which they might react. Such a process is usually classified as a hydrolysis reaction and the net effect is the exchange of some group "X" with OH



which may involve a variety of intermediates depending on the compound and conditions.

8.1 HYDROLYSIS KINETICS

The overall rate law for a hydrolysis process is given by

$$-\frac{d(\text{RX})}{dt} = k_h[\text{RX}] = k_b[\text{RX}][\text{OH}^-] + k_a[\text{RX}][\text{H}^+] + k_w[\text{RX}]$$

where k_a and k_b are the second-order rate constants for the acid- and base-catalyzed reactions and k_w is a pseudo-first-order rate constant for the direct reaction with water, a solvolysis reaction. Strictly speaking, $k_w = k'_w[\text{H}_2\text{O}]$, which would simplify to first order since $[\text{H}_2\text{O}]$ is a constant. Note that in most discussions of this reaction the direct solvolysis reaction is termed the "neutral" reaction, however, students consistently interpret this terminology as the rate constant for pH 7. To minimize

this confusion, the “neutral” reaction will be referred to as the “direct” using the less ambiguous k_w to represent the rate constant.

The pseudo-first-order rate constant, k_h , is the observed or estimated rate constant for a specific pH, assuming that in all three reactions the rate is first order in [RX] and would be expressed

$$k_h = k_a[\text{H}^+] + k_b[\text{OH}^-] + k_w$$

Since the ion product for water is given by

$$K_w = [\text{H}^+][\text{OH}^-] = 1 \times 10^{-14}$$

it is possible to express the overall rate constant as a function of $[\text{H}^+]$ by rewriting the base-catalyzed expression as $k_b \cdot K_w/[\text{H}^+]$.

8.1.1 pH Effects

The effect of pH on hydrolysis rates is illustrated by expressing $\log k_h$ as a function of pH (Fig. 8.1).

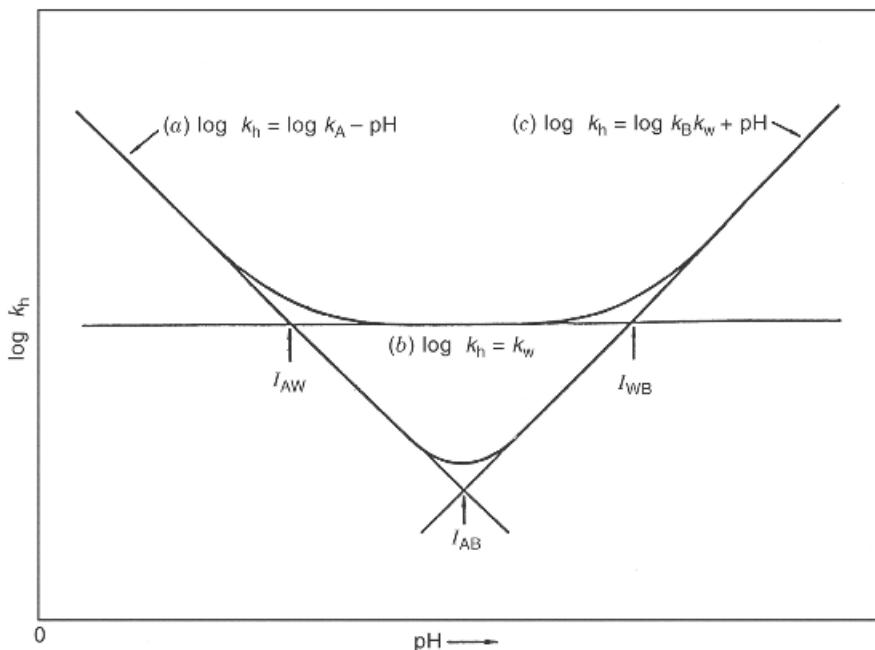


Figure 8.1 The pH dependence of k_h in acid- and base-catalyzed reactions along with the direct reaction with water.

At low pH, one would anticipate that the acid-catalyzed reaction would predominate and

$$\log k_h = \log k_a - \text{pH}$$

the logarithm of the reaction rate constant would decrease with an increase in pH with a slope of -1 . Conversely, at high pH the base-catalyzed process would predominate and

$$\log k_h = \log k_b + (\text{pH} - 14)$$

$\log k_h$ increasing with pH with a slope of $+1$. The direct reaction would be independent of pH. The configuration of $\log k_h/\text{pH}$ curves will vary with the relative magnitude of the rates of the three different reactions (Fig. 8.2). At the inflection point I_{aw} , the rate of the acid-catalyzed reaction would equal the rate of the direct solvolysis reaction and the pH at this point would be

$$\log k_a - \text{pH} = \log k_w$$

$$\text{pH}(I_{aw}) = \log \frac{k_a}{k_w}$$

In a similar fashion, it can be demonstrated that

$$\text{pH}(I_{bw}) = \log \frac{k_w}{k_b} + 14$$

$$\text{pH}(I_{ab}) = \frac{1}{2} \left(\log \frac{k_a}{k_b} + 14 \right)$$

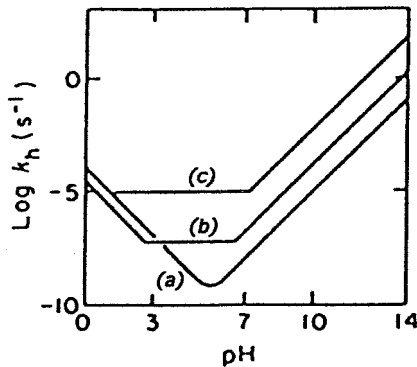


Figure 8.2 The pH rate profiles for (a) ethylacetate, (b) phenyl acetate, and (c) 2,4-dinitrophenylacetate.

TABLE 8.1 Hydrolysis Rates of Esters of Carboxylic Acids^a

R ₁ COOR ₂		At pH 7					Inflection pH		
R ₁	R ₂	k_a (M ⁻¹ · s ⁻¹)	k_w (s ⁻¹)	k_b (M ⁻¹ · s ⁻¹)	k_h (s ⁻¹)	t _{1/2}	I _{aw}	I _{ab}	I _{bw}
H-	C ₂ H ₅			25.7	2.57 × 10 ⁻⁶	3.12 day			
CH ₃	CH ₃	1.13 × 10 ⁻⁴		0.18	1.8 × 10 ⁻⁸	1.2 year		5.4	
CH ₃ -	C ₂ H ₅	1.1 × 10 ⁻⁴	1.5 × 10 ⁻¹⁰	0.108	1.1 × 10 ⁻⁸	2.0 year	(5.9)	5.5	(5.2)
CH ₃ -	C(CH ₃) ₃	1.3 × 10 ⁻⁴		1.5 × 10 ⁻³	1.6 × 10 ⁻¹⁰	140 year		6.5	
CH ₃ -	C ₆ H ₅	7.8 × 10 ⁻⁵	6.6 × 10 ⁻⁸	1.4	2.1 × 10 ⁻⁷	38 day	3.1	(4.6)	6.0
CH ₃	2,4(NO ₂) ₂ C ₆ H ₃		1.1 × 10 ⁻⁵	94	2.9 × 10 ⁻⁵	9.4 h			7.1
ClCH ₂	CH ₃	8.5 × 10 ⁻⁵	2.1 × 10 ⁻⁷	140	1.4 × 10 ⁻⁵	14 h		(3.9)	5.2
Cl ₂ CH	CH ₃	2.33 × 10 ⁻⁴	1.53 × 10 ⁻⁵	2.8 × 10 ³	3.0 × 10 ⁻⁴	38 min	2.6	(3.5)	5.7
Cl ₂ CH	C ₆ H ₅		1.76 × 10 ⁻³	1.28 × 10 ⁴	3.1 × 10 ⁻³	3.7 min	1.2		7.1
Cl ₃ C	CH ₃		7.33 × 10 ⁻⁴		7.33 × 10 ⁻⁴	<15 min			
C ₆ H ₅	CH ₃ ^b	4.0 × 10 ⁻⁷		1.9 × 10 ⁻³	1.9 × 10 ⁻¹⁰	118		5.2	
C ₆ H ₅	C ₂ H ₅ ^c			0.030	3.0 × 10 ⁻⁹	7.3 year			
C ₆ H ₅	C ₂ H ₅ ^d	9.9 × 10 ⁻⁸		2.8 × 10 ⁻³	2.8 × 10 ⁻¹⁰	79 year		4.8	
p(NO ₂)C ₆ H ₄	CH ₃ ^e	4.3 × 10 ⁻⁷		0.074	7.4 × 10 ⁻⁹	3.0 year		4.38	

^aData taken from Ref. 2.^bMethanol (55%)^cWater^dAcetone (60%)^eMethanol (60%)

The pH of these inflection points can be useful in defining environmental behavior. For example, if the pH for the I_{wb} inflection is say, 10, then one can conclude that the base-catalyzed reaction would not be of significance in the soil environment.

8.1.2 Temperature Effects

The effect of temperature on the reaction rate is defined by the Arrhenius equation

$$k = A \cdot e^{-E_a/RT}$$

where A accounts for the frequency and orientation of collisions that could result in a reaction and the exponential term defines the frequency of these collisions that would have sufficient energy to result in a reaction. The parameter E_a is referred to as the Activation energy. These two parameters can be derived from a plot of $\ln k$ as a function of $1/T$ since

$$\ln k = \ln A - E_a/RT$$

and can be used to predict changes in reaction rate with temperature. This relation can also be evaluated using the more sophisticated transition state theory that is outlined elsewhere.^{1,2} Activation energies range from 50 to 100 kJ · mol⁻¹ and based on a value of 70–75 kJ · mol⁻⁴:

A 1° change in temperature causes a 10% change in k .

A 10° change in temperature changes k by a factor of 2.5.

A 25° change in temperature changes k by a factor of 10.

For first-order processes, the half-life is independent of the concentration and for hydrolysis reactions at a specific pH can be expressed

$$t_{1/2} = \ln 2/k_h$$

8.2 ESTERS OF CARBOXYLIC ACIDS

The hydrolysis of these compounds have been studied extensively and illustrative kinetic information is summarized in Table 8.1.

Esters of carboxylic acids vary dramatically in their susceptibility to hydrolysis. The half-lives of esters listed above vary from minutes to years. Much of the older data in the literature was derived in studies designed to establish reaction mechanisms rather than define environmental behavior and mixed solvents were often used because of solubility and analytical limitations. There is no systematic approach for extrapolating to an aqueous system, however, the rate of hydrolysis is usually higher in water as the one example of ethyl benzoate (water vs. 60% acetone) illustrates.³ It

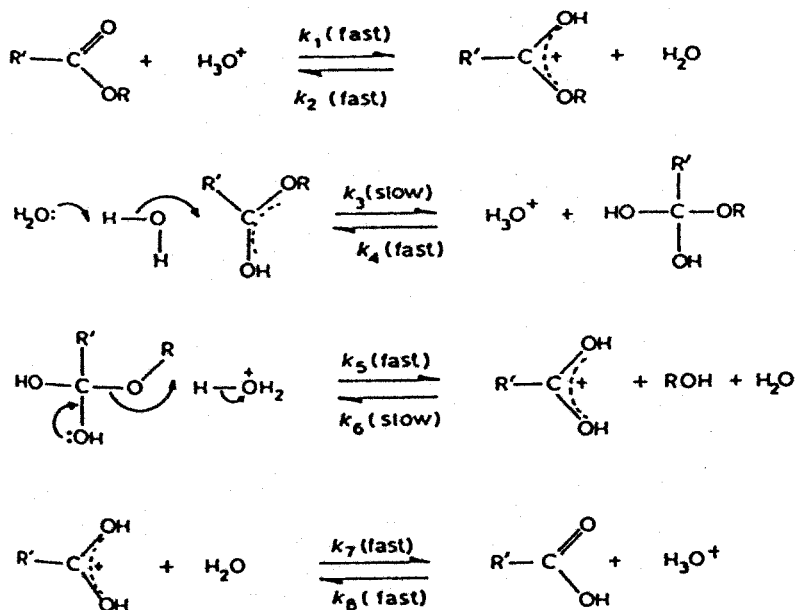


Figure 8.3 Mechanism of the acid-catalyzed hydrolysis of an ester of a carboxylic acid.

is also of interest to note that the contribution of the acid-catalyzed process is more significant with those compounds less susceptible to hydrolysis.

The mechanisms of the three hydrolysis reactions given in Figures 8.3–8.5 provide a basis for interpreting the variation in rates and the development of predictive relations. In all cases, and particularly with the direct and base-catalyzed reactions, the limiting step appears to be the rate of nucleophilic attack at the carbonyl carbon. The hydroxyl ion and oxygen of water would be classified as nucleophiles, since they would carry a small negative charge due to the excess of nonbonded electrons and would consequently be attracted to an electrophilic site, the carbon of the carbonyl, which would carry a slight positive charge. The successive substitution of chlorine in methyl acetate results in the half-life at pH 7 decreasing from 1.2 years with methyl acetate to <15 min for methyl trichloroacetate. The chlorine atoms are electronegative and induce an increase in the positive charge associated with the carbonyl carbon facilitating the nucleophilic attack. Note that this inductive effect is very pronounced in the direct and base-catalyzed reactions but has little effect on the rate of the acid-catalyzed reaction.

8.2.1 Hammett Relations and Inductive Effects of Substituents

Hammett relations used to define inductive effects of substituents in a benzene ring on dissociation constants of acids (see p. 60) can provide a systematic approach to evaluate the inductive effects of substituents on the hydrolysis of esters. The induc-

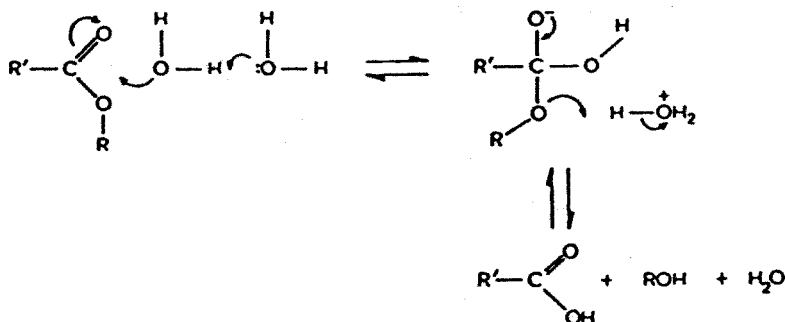


Figure 8.4 Mechanism for the direct reaction of an ester of a carboxylic acid with water.

tive effect of the substituents on the distribution of charge affects the ease with which a hydrogen ion is lost in the former while in the latter it affects the ease with which a nucleophile attacks the carbonyl carbon. The Hammett relation can be expressed

$$\log k_X / \log k_H = \rho\sigma \quad \text{or} \quad \log k_X = \rho\sigma + \log k_H$$

where ρ indicates the sensitivity of the system to inductive effects and σ provides an estimate of the inductive effect of the substituent group and k_X and k_H represent the rate constants for the substituted and unsubstituted compound, respectively. The effect of substituents on the base-catalyzed hydrolysis of ethyl benzoate esters in 85% ethanol is illustrated in Figure 8.6. This series of esters gives a ρ value of +2.56 and with a k_H of $5.5 \times 10^{-4} \text{ M}^{-1} \text{ s}^{-1}$ and a Hammett equation:

$$\log k_X = 2.56\sigma - 3.26$$

Thus it is possible to use this expression to predict the rate of hydrolysis of other substituted ethyl benzoates in 85% ethanol and it can be assumed the rate of hydrolysis in water would be higher by a factor of 2–3. Relations for other series of esters have been compiled.⁴

Inductive effects of substituents in the alcohol moiety of the ester do not influence hydrolysis rates to the same extent. Note that the rates of hydrolysis vary over almost

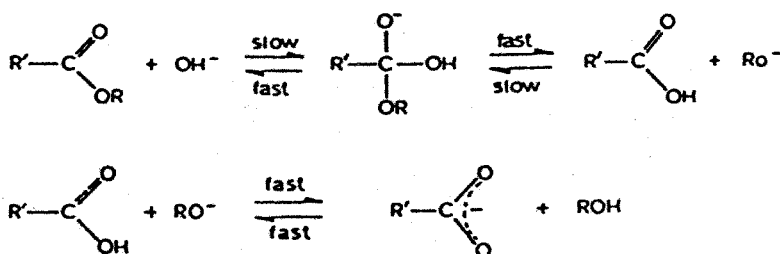


Figure 8.5 Mechanism for the base-catalyzed hydrolysis of an ester of a carboxylic acid.

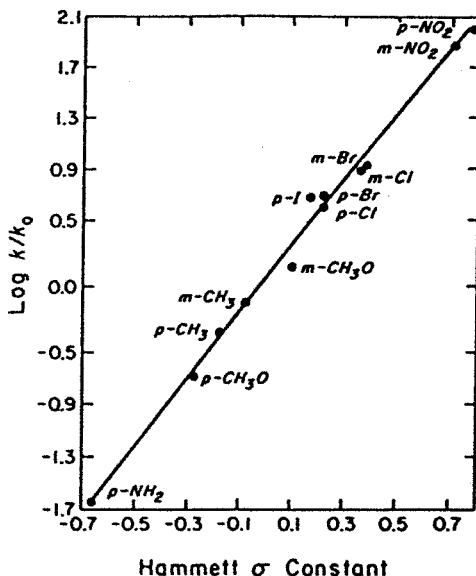


Figure 8.6 Inductive effects of substituents in the phenyl ring on the hydrolysis of ethyl benzoates.

four orders of magnitude with variation in the acid moiety of the ester (Fig. 8.6) while substituents in the alcohol moiety of phenyl benzoate result in only a tenfold change in rate. It has been observed, however, that the rate of the base-catalyzed reaction is inversely correlated with the pK_a of the leaving group, that is, the alcohol (Fig. 8.7). The reason for this relation can be explained by the fact that after the hydroxide ion reacts at the carbonyl carbon (Fig. 8.5) the intermediate can either lose the RO^- and the reaction proceeds or lose the OH^- in a reversible step. The tendency for the reaction to proceed will be influenced by the extent to which the alcohol (leaving group) can exist as the anion that will clearly be related to its pK_a . Thus substituents in the acid moiety of the ester influence the partial charge on the carbonyl carbon and affect the first step of the reaction while substituents in the alcohol moiety influence the second step.

8.2.2 Steric Effects

It has been observed that the rate of the base-catalyzed hydrolysis of esters of phthalic acid decrease with the size of the alcohol moiety,⁵ Table 8.2. A Taft–Hancock relation relates rate constant, k , to the inductive effect of these substituents σ^* , the steric effect E_s , and the rate constant k_0 of the dimethyl ester. The coefficient 4.59 corresponds to the ρ of the Hammett equation and reflects the sensitivity to

$$\log k = 4.59\sigma^* + 1.52E_s + \log k_0$$

Phenyl Sub.	σ	pK_a^a	$k_w (M^{-1}s^{-1})$
C_6H_5-		9.92	0.051
C_6H_4 <i>m</i> CH_3	-0.07	10.07	0.028
<i>m</i> Cl	0.37	9.09	0.149
<i>m</i> $COCH_3$	0.38	9.07	0.179
<i>m</i> CN	0.61	8.56	0.520
<i>m</i> NO_2	0.71	8.34	0.700
<i>p</i> $COOC_2H_5$	0.45	8.92	0.261
<i>p</i> NO_2	1.24	7.15	1.61
<i>p</i> CN	0.88	7.96	0.850
<i>p</i> $COCH_3$	0.50	8.81	0.377

^a Hammett Equn. $pK_a = 9.92 - 2.23\sigma$

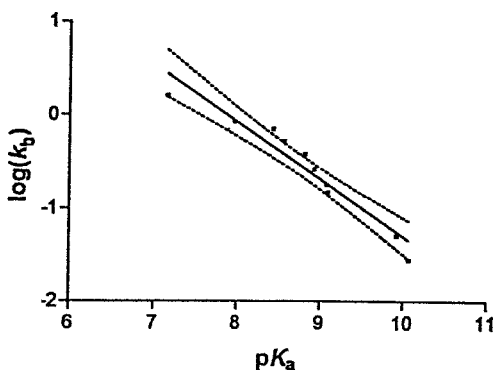


Figure 8.7 Correlation between the base-catalyzed rate of hydrolysis of phenyl benzoates and the pK_a of the phenolic leaving group. The pK_a values derived from the Hammett equation for phenols.

inductive effects while the sensitivity to steric effects is indicated by the coefficient 1.52. It should be noted that these compounds are widely distributed in the environment, particularly the ethylhexyl ester, commonly referred to as DEHP. They find use as plasticizers which modify the properties of polymers and can slowly leach into solutions with which they come into contact. Thus, the widespread use of these products and the stability of the DEHP accounts for its frequent detection. It is clear from these data that the persistence of DEHP is due, in part, to its resistance to hydrolysis. Low-water solubility also would result in DEHP distributing, say into environmental compartments where hydrolysis reactions would not occur.

The esters of the common herbicide 2,4-D (2,4-dichlorophenoxyacetic acid) also illustrate how the rate of hydrolysis is influenced by the size of the alcohol moiety,^{6,7} Table 8.3. It is clear that the steric effect is amplified by the number of substituents located near the reaction site; compare methyl and 2-propyl and 1- and 2-octyl esters. The inductive effect of an oxygen substituent is also apparent. A discussion

TABLE 8.2 Base-Catalyzed Hydrolysis of Esters of Phthalic Acid at 30°C

Ester	S_w (ppm) (25°C)	k_b ($M^{-1} \cdot s^{-1}$)	$t_{1/2}$ pH 8	σ^*	E_s
Dimethyl-	4320	6.9×10^{-2}	116 day	0.00	0.00
Diethyl-	896	2.5×10^{-2}	320 day	-0.100	-0.07
Di- <i>n</i> -butyl	13	1.0×10^{-2}	2.20 year	-0.130	-0.39
Di- <i>n</i> -octyl	3.0	1.4×10^{-3}	15.7 year	-0.125	-0.93
Di(2-ethylhexyl)	0.40	1.1×10^{-4}	200 year	-0.225	-1.13

TABLE 8.3 Hydrolysis of 2,4-D Esters in Water at 28°C

Ester	k_b ($M^{-1} \cdot s^{-1}$)	$t_{1/2}$ pH 8 (h)
Methyl	17.3	11.1
2-Propyl	1.1	175
1-Butyl	3.7	52
1-Octyl	3.7	52
2-Octyl	0.52	37
2-Butoxyethyl	30.2	6.4
2-Butoxymethylethyl	4.3	45

of these mechanistic aspects illustrates how substituents influence reaction rates. Although there is not an extensive database, it is also possible to predict the rate at which esters will hydrolyze within an order of magnitude to allow some assessment of the environmental significance of this process.

8.2.3 Effect of Dissolved Organic Matter

It has been demonstrated that DOM can enhance aqueous solubility (Phys. Chem. Properties, Chapter 2) as compounds of low-solubility partition into the hydrophobic

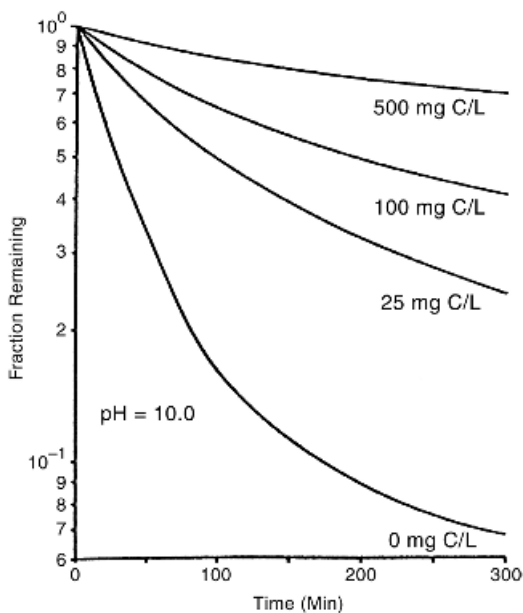


Figure 8.8 Partitioning of the 1-octyl ester of 2,4-D into dissolved humic substances and the effect on the rate of the base-catalyzed catalysis of the ester. [Reproduced with permission from E. M. Perdue and N. L. Wolfe, *Environ. Sci. Technol.* **16**, 847 (1982). Copyright © 1982, American Chemical Society.]

regions of the DOM. Since natural waters will usually contain DOM it is of interest to assess the extent to which it might influence hydrolysis rates. The addition of humic acid clearly reduces the rate at which the octyl ester of 2,4-D hydrolyzes at pH 10⁷ (Fig. 8.8). The tendency of this compound to distribute from water into the DOM is indicated by log K_{DOM} of 4.5. One would also expect a comparable effect on the hydrolysis of DEHP because of its low water solubility but not, say, with the dimethyl phthalate.

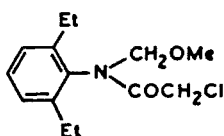
8.3 NITROGEN DERIVATIVES OF CARBOXYLIC ACIDS

Although the hydrolysis of acid halides and acid anhydrides could be reviewed, at the present the following nitrogen-containing derivatives would be more significant in the environmental context:

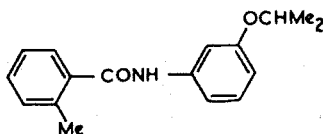


8.3.1 Amides

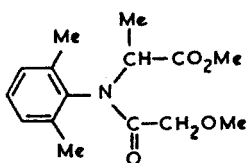
The amide bond is the key linkage as amino acids combine to form proteins and in the production of the polymer nylon. The herbicides and fungicides listed below also contain amide bonds.



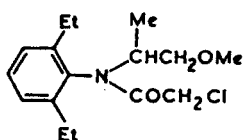
Alachlor



Mepronil



Metalaxyl



Metolachlor

Hydrolysis of amides will yield the acid and amine and the mechanisms are comparable to those reviewed for esters and comparable structure–activity patterns are observed. However, amides hydrolyze at rates a thousand-fold slower (Table 8.4)

TABLE 8.4 Rates of Hydrolysis of Amides at 25°C

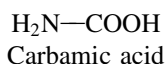
R ₁ CONR ₂ R ₃			At pH 7				
R ₁	R ₂	R ₃	k_a (M ⁻¹ · s ⁻¹)	k_b (M ⁻¹ · s ⁻¹)	k_h (s ⁻¹)	$t_{1/2}$	I_{ab}
CH ₃	H	H	8.3×10^{-6}	4.71×10^{-5}	5.55×10^{-12}	3,950 year	6.62
<i>i</i> C ₄ H ₁₁	H	H	4.63×10^{-6}	2.40×10^{-5}	2.86×10^{-12}	7,700 year	6.64
ClCH ₂	H	H	1.1×10^{-5}	0.15	1.5×10^{-8}	533 day	4.93
Cl ₂ H	H	H		0.30	3.0×10^{-8}	266 day	
CH ₃	CH ₃	H	3.2×10^{-7}	5.46×10^{-6}	5.76×10^{-13}	38,000 year	6.38
CH ₃	C ₂ H ₅	H	9.36×10^{-8}	3.10×10^{-6}	3.10×10^{-13}	70,000 year	6.23
CH ₃	C ₂ H ₅	CH ₃	5.16×10^{-7}	1.14×10^{-5}	1.19×10^{-12}	18,500 year	6.33

than those observed in comparable esters (Table 8.1). Rate constants for the acid-catalyzed process are comparable to those observed with esters, but the base-catalyzed reaction is much slower. The —NR₁R₂ group is not as strong an electron-withdrawing group as the —OR of an ester and the p*K*_a values of the amine leaving groups would be much higher than corresponding alcohols (R₁R₂NH ⇌ R₁R₂N⁻ + H⁺). No data is available for the direct reaction with water probably because the rate constants are so low.

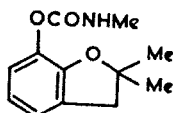
It is clear from these data that it is unlikely that the hydrolysis of an amide bond will be of significance under ambient conditions.

8.3.2 Carbamates

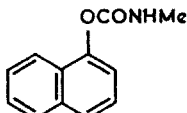
These compounds are derivatives of carbamic acid and exhibit the characteristics of



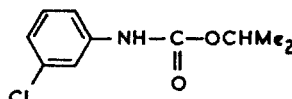
both an ester and an amide, and include a number of widely used insecticides and herbicides. Carbofuran and Carbaryl are used extensively as insecticides and Chlorpropham as a herbicide.



Carbofuran



Carbaryl



Chlorpropham

The acid-catalyzed process is of little significance and most of the attention has focused on the base-catalyzed reaction. If the mechanism corresponds to that of the base-catalyzed hydrolysis of an ester (Fig. 8.5), one would predict that RO⁻ leaving

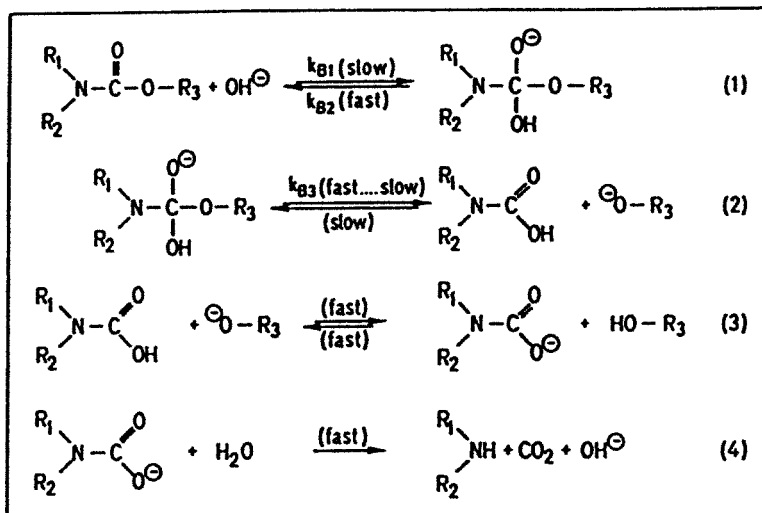


Figure 8.9 Reaction scheme for the base-catalyzed hydrolysis of carbamates.

group would be preferred over the $\text{R}_1\text{R}_2\text{N}^-$ with subsequent release of CO_2 and the amine (Fig. 8.9). Kinetic data are given for several carbamates in Table 8.5. Note that k_b values vary dramatically depending on whether the nitrogen has an H substituent or not. It has been demonstrated⁸ that the rate of hydrolysis of *N*-methyl and *N*-phenyl carbamates is influenced by the $\text{p}K_a$ of the alcohol leaving group (Fig. 8.10) and the structure/activity correlation can be expressed

$$\log k_b = -\rho \cdot \text{p}K_a + C$$

where ρ indicates the influence of the leaving group and C is the intercept. For the *N*-methyl and *N*-phenyl carbamates, ρ was found to be 0.91 and 1.1, respectively. By

TABLE 8.5 Hydrolysis of Carbamates at 25°C

$\text{R}_1\text{OCONR}_2\text{R}_3$						
R_1	R_2	R_3	$k_b \text{ (M}^{-1} \cdot \text{s}^{-1}\text{)}$	$k_h \text{ (s}^{-1}\text{) at pH 7}$	$t_{1/2}$	
C_6H_5	C_6H_5	H	54.2	5.42×10^{-6}	1.5 day	
C_6H_5	C_6H_5	CH_3	4.2×10^{-5}	4.2×10^{-12}	5,200 year	
<i>p</i> - $\text{NO}_2\text{C}_6\text{H}_5$	C_6H_5	H	2.7×10^5	0.027	26 s	
<i>p</i> - $\text{NO}_2\text{C}_6\text{H}_5$	C_6H_5	CH_3	8.0×10^{-4}	8.0×10^{-11}	275 year	
C_2H_5	CH_3	CH_3	4.5×10^{-6}	4.5×10^{-13}	49,000 year	
C_2H_5	CH_3	H	5.5×10^{-6}	5.5×10^{-13}	40,000 year	

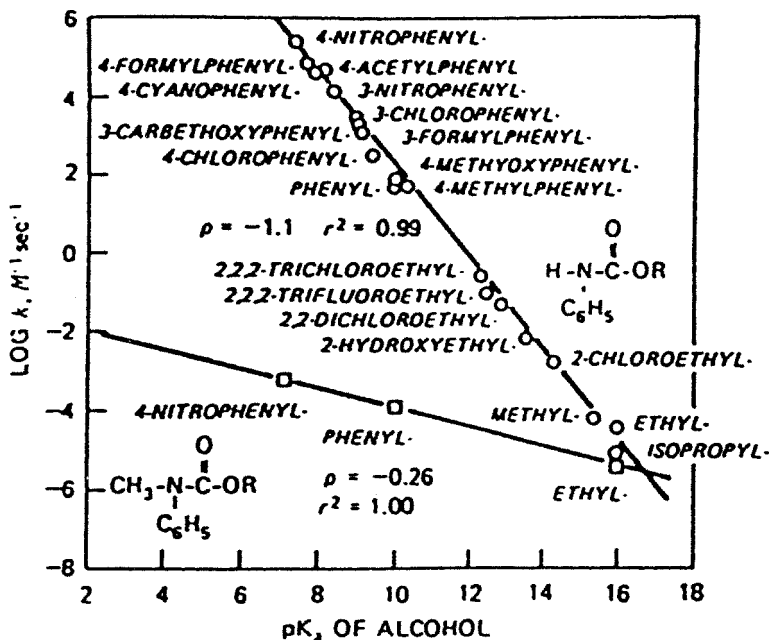


Figure 8.10 Base-catalyzed second-order rate constants for the hydrolysis of *N*-phenyl- and *N*-phenyl-methyl carbamates illustrating the effect of the substitution on the carbamate nitrogen. [Reproduce from N. L. Wolfe, R. G. Zepp and D. F. Paris, "Carbaryl, propham, and chlopropham: a comparison of the rates of hydrolysis and photolysis with the rate of biolysis", *Water Res.* **12**, 561. Copyright © 1978, with permission from Elsevier.

contrast, for the disubstituted counterparts, *N,N*-dimethyl and *N*-methyl-*N*-phenyl, ρ values of 0.17 and 0.26 were observed. It is proposed that a different mechanism involving the nitrogen "H" is active with the RHN— carbamates.

A number of carbamates have been used as insecticides and a few as herbicides. Kinetic parameters for several of these compounds are summarized in Table 8.6. Note that the base-catalyzed reaction is the more important, however, some reports indicate that for some compounds, the direct reaction with water can be significant with I_{wb} values of 6–7. Unfortunately, there is only limited information in this area. Note that these data also illustrate how the substituents on the N influence hydrolysis. The k_b values for the dimethyl compounds are orders of magnitude lower than the methyl counterparts. Aldicarb represents a variation in that the ester component of the molecule is derived from an oxime ($\text{RCH}=\text{NOH}$) rather than an alcohol. It also illustrates the significance of hydrolysis in understanding its environmental behavior. Aldicarb has been very effective in controlling insect pests in potatoes, but because of its high water solubility (6000 ppm) has been detected as a contaminant in groundwater.⁹ This effect has been observed only in acid (pH 5.5) but not in basic (pH 8.0) soils.

Aldicarb is rapidly oxidized to the sulfone and the hydrolysis half-life, at 15°C, decreases from 412 to 16 day at pH 8, consequently, the compound would be degraded before there was time for it to move through the soil profile to ground water.

8.4 ESTERS OF PHOSPHORIC ACID AND RELATED COMPOUNDS

Esters of orthophosphoric acid have been used extensively as plasticizers and lubricant additives. Others have been used as flame retardants. Many sulfur analogues find use as insecticides, while the introduction of P—C bonds give phosphonic and phosphinic acids. Esters of pyrophosphoric acid ($H_4P_2O_7$) are also of interest as are amide derivatives.

The characteristics of the hydrolysis process are illustrated by observations with the insecticide fenitrothion.¹⁰ From Figure 8.11 it is seen that there is no significant acid-catalyzed reaction and that the base-catalyzed reaction is more active than the direct solvolysis reaction. At 23°C, a k_w of $5.55 \times 10^{-6} \cdot \text{min}^{-1}$ and a k_b of $0.15 \text{ M}^{-1} \cdot \text{min}^{-1}$ was reported. At pH values of 9 and above, only the phenol and the dimethylphosphorothioic acid were formed. This would result from hydroxide ion attacking the phosphorus. A mixture of the phenol and demethylfenitrothion is obtained at pH values of 7 and below. The demethylation results from water reacting at the C of the C—O—P. It was also reported that the proportion of the demethylation increased with an increase in temperature. This complex mechanism

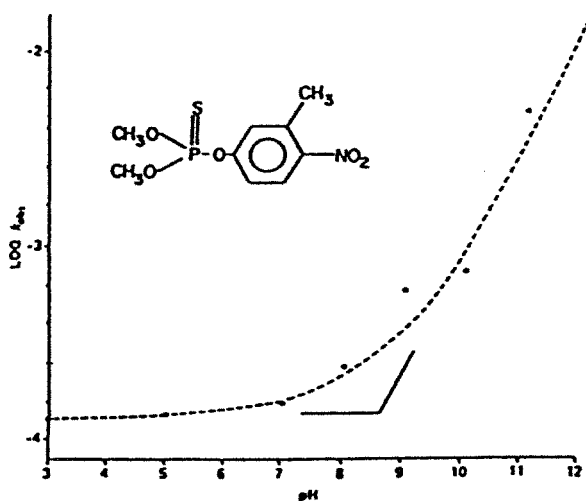
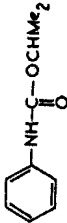
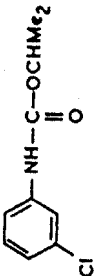
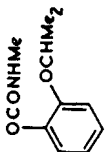
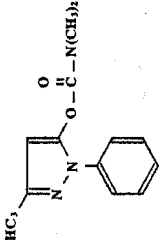
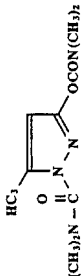
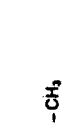


Figure 8.11 Observed rate of hydrolysis of the organothiophosphate at 49.5°C as a function of pH. [Reproduced with permission from R. Greenhalgh, K. L. Dhawan, and P. Weinberger, *J. Agric. Food Chem.* **28**, 102 (1980). Copyright © 1980, American Chemical Society.]

TABLE 8.6 Hydrolysis of Carbamate Herbicides and Insecticides

Compound	Structure	Temperature (°C)	k_w (s ⁻¹)	k_b (M ⁻¹ · s ⁻¹)	I_{wb}
Herbicides					
Propham		27		7.6×10^{-6}	
Chlorpropham		27		2.0×10^{-5}	
Insecticides					
Propoxur		20		0.51	
Pyrolan		20		0.0116	
Dimetilan		20		5.7×10^{-5}	

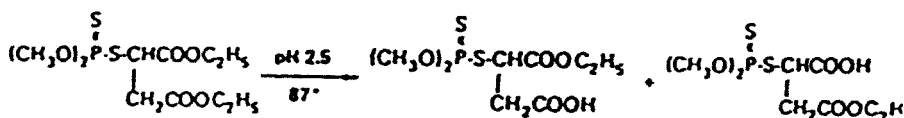
Sevin		25	9×10^{-7}	50	6.3
Aldicarb		15	1.75×10^{-9}	0.0149	7.1
Aldicarb sulfoxide		15	1.83×10^{-8}	0.231	6.9
Aldicarb sulfone		15	1.79×10^{-8}	0.490	6.6

and range of products is representative of what is observed with this class of compounds.¹¹

Note that the rates of the base-catalyzed reactions of the oxon derivatives of parathion and diazinon are higher than their thio counterparts (Table 8.7). This result might be expected with hydroxyl attack on the phosphorus with oxygen being considerably more electronegative than sulfur. The water would react at the carbon of the C—O and this reaction would not be influenced to the same extent. The rates of base-catalyzed reactions can be correlated with the pK_a of the leaving groups¹² as was observed with esters of carboxylic acids (Fig. 8.7). Sequential reactions will ultimately produce phosphoric acid or its sulfur analogue. It has been reported, however, that the anion of the phosphate diester is resistant to hydrolysis in basic solution but reacts more readily as the neutral species in acid solution.¹³ The mono-ester, by contrast hydrolyses readily in basic solution.

Malathion has low mammalian toxicity and is widely used as an insecticide. It is informative to review the hydrolysis of this compound since both the thiophosphate and carboxylic ester components of the molecule would be susceptible.¹⁴ The major product under acid conditions is the monoacid (two isomers are possible) with little involvement of the thiophosphate moiety (Reaction 1, Fig. 8.12). At pH 4, malathion would have a half-life of 4.5 years at 27°C. Since environmental pH values rarely are this low, the base-catalyzed process would be more relevant. Under these conditions, the carboxylic ester would hydrolyze (k_{mh}), while an elimination reaction (k_{me}) occurs with the thiophosphate ester splitting out H_2S from the thiolsuccinate to

Reaction 1.



Reaction 2.

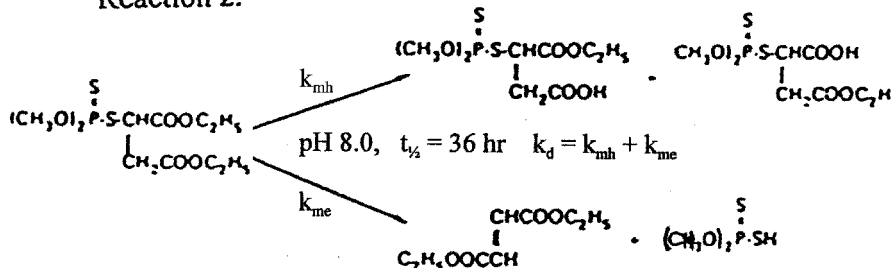


Figure 8.12 Interplay between esters of carboxylic and thiophosphoric acids in the hydrolysis of malathion. [Reproduced with permission from N. L. Wolfe, R. G. Zepp, J. A. Gordon, G. L. Baughman, and D. M. Cline, *Environ. Sci. and Technol.* **11**, 88 (1977). Copyright © 1977, American Chemical Society.]

generate fumaric acid (Reaction 2). The overall degradation of the malathion then reflects the combined effect of these two processes, and rate constants would indicate that the elimination reaction would constitute 74% of the reaction, with ester hydrolysis 26%. The mono-ester and diacid derivatives are considerably more stable than the parent compound. It is important to be able to make such an analysis to define both the products produced and their stability because they could be as significant in the environment as the parent from which they were derived.

8.5 HALOGENATED COMPOUNDS

Carbon atoms will be susceptible to nucleophilic attack by water or hydroxide ions when bonded to the electronegative halogens that induce a small positive charge in the carbon. Two distinct mechanisms (Fig. 8.13) can be involved. A bimolecular nucleophilic substitution (S_N2) reaction involves the reaction of the nucleophile to form a pentavalent intermediate and the loss of the halide leaving group results in the production of the alcohol. Reaction rate is a function of the concentration of the nucleophile and the substrate molecule. In fact, most of the direct solvolysis and base-catalyzed reactions already discussed would be so classified. By contrast, an S_N1 reaction is a first-order reaction with rate being a function of the substrate and the rate-limiting step being the dissociation of the leaving group prior to reacting with the nucleophile. The S_N1 process is observed with reactions of a tertiary carbon and a benzylic carbon and usually results in a rapid reaction.

Some illustrative kinetic data for halogenated compounds are summarized in Table 8.9.

There is no acid-catalyzed reaction for these compounds and halogenated aromatics (e.g., chlorobenzene) and vinyl halides are not susceptible to hydrolysis. This would account, in part, for the persistence of the PCBs and DDT related compounds. The rates of these reactions are influenced by bond strength, that is,

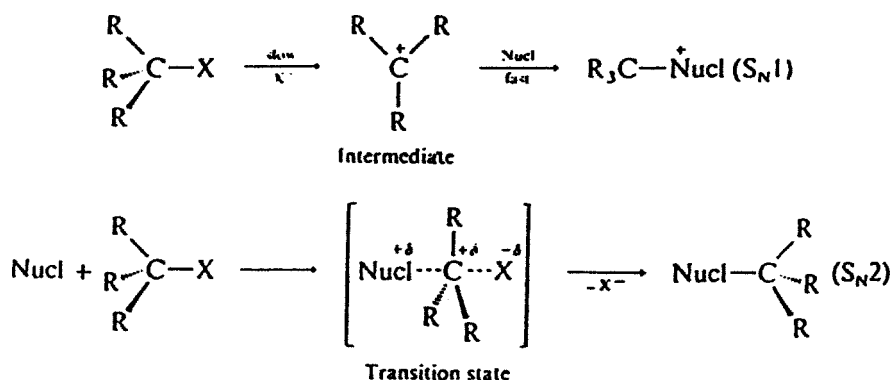
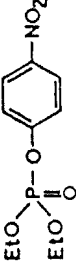
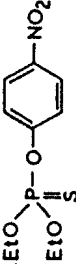
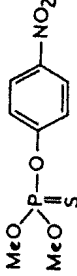
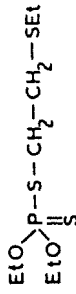
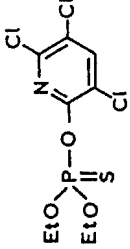
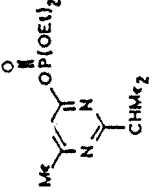
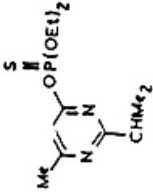


Figure 8.13 Substitution reactions with alkyl halides that result in a hydrolysis reaction when water acts as a nucleophile.

TABLE 8.7 Hydrolysis Kinetics for Organophosphates at 25°C^a

Compound	Structure	k_w (s ⁻¹)	k_b (M ⁻¹ · s ⁻¹)	$t_{1/2}$ pH 7	I_{wb}
Trimethylphosphate	(CH ₃ O) ₃ -P=O	1.9×10^{-8}	1.6×10^{-4}	1.2 year	10.0
Triphenylphosphate	(C ₆ H ₅ O) ₃ -P=O	$<3 \times 10^{-9}$	0.25	5.5 year	10.7
Paraoxon		7.3×10^{-8}	0.39	72 day	<6
Parathion		8.3×10^{-8}	0.057	89 day	8.2
Methyl parathion		1.2×10^{-7}	0.011	67 day	9.0
Disulfoton		1.4×10^{-7}	2.0×10^{-3}	57 day	10.0
Chlorpyrifos ^b		1.0×10^{-7}	0.019	79 day	8.7

Diazoxon ^c		2.8×10^{-7}	0.076	23 day	8.6
Diazinon ^{d,e}		4.3×10^{-8}	5.3×10^{-3}	178 day	8.9

^aSelected values from Ref. 1, P. 396.

^bBase-catalyzed process not strictly second order¹¹; k_b estimated from observations at pH 9.8–10.7.

^cN-contg. ring gives a k_a of $0.65 \text{ M}^{-1} \cdot \text{s}^{-1}$ and I_{aw} of 6.4.

^dN-contg. ring gives a k_a of $0.021 \text{ M}^{-1} \cdot \text{s}^{-1}$ and I_{aw} of 5.7.

^eRate constants given for 20°C.

TABLE 8.8 Kinetic Parameters for the Hydrolysis of Malathion at 27°C

Compound/pH	k_a, k_b ($M^{-1} \cdot s^{-1}$)	k_h (s^{-1})	$t_{1/2}$	Product(s)
Malathion, pH 4	4.8×10^{-5}	4.8×10^{-9}	4.5 year	Mono-acids
Malathion pH 8	5.5	5.5×10^{-6}	35 h	
Malathion elimination	3.9			Diethyl and ethyl hydrogen fumarates, dimethylphosphorodithioic acid
Malathion ester	1.4			Mono acid
Mono-ester pH 8	0.31	3.1×10^{-7}	26 day	Ethyl hydrogen fumarate, diacid, dimethyl phosphorodithioic acid
Diacid pH 8	0.018	1.8×10^{-8}	445 day	Thio succinic acid, dimethyl phosphorodithioic acid

C—F versus C—Cl, steric factors, nature of the leaving group and mechanism; S_N1 reactions clearly result in higher reaction rate. A systematic treatment of these variables has not been developed at this point.

Methyl bromide has been used extensively as a soil sterilant and in the treatment of fruit and vegetables in international commerce to minimize the introduction of pests. When applied to soil, a large proportion of the methyl bromide evaporates. Significant amounts of this compound are found in the marine environment. Recently, there has been concern that methyl bromide could be contributing to ozone loss in the stratosphere and there has been an effort to find substitutes. Methyl

TABLE 8.9 Rates of Hydrolysis of Halogenated Compounds at 25°C^a

Compound	k_w (s^{-1})	k_b ($M^{-1} \cdot s^{-1}$)	k_h (s^{-1}) pH 7	$t_{1/2}$ pH 7	I_{wb}
CH ₃ F	7.44×10^{-10}	5.82×10^{-7}	7.44×10^{-7}	29.5 year	11.1
CH ₃ Cl	2.37×10^{-8}	6.18×10^{-6}	2.37×10^{-8}	338 day	11.6
CH ₃ Br	4.09×10^{-7}	1.41×10^{-4}	4.09×10^{-7}	20 day	11.5
CH ₃ I	7.28×10^{-8}	6.47×10^{-5}	7.28×10^{-8}	110 day	11.0
C ₂ H ₅ Cl	2.10×10^{-7}		2.10×10^{-7}	38 day	>12
C ₂ H ₅ Br	2.64×10^{-7}		2.64×10^{-7}	30 day	>12
CH ₃ CH ₂ CH ₂ Br	3.04×10^{-7}		3.04×10^{-7}	26 day	>12
CH ₃ CHBrCH ₃	3.86×10^{-6}		3.86×10^{-6}	2.1 day	>12
CH ₂ CHCH ₂ Br	1.64×10^{-5}		1.64×10^{-5}	12 h	>12
(CH ₃) ₃ CF ^b	3.87×10^{-5}		3.87×10^{-5}	5.0 h	>13
(CH ₃)CCl ^b	3.02×10^{-2}		3.02×10^{-2}	23 s	>13
C ₆ H ₅ CH ₂ Cl ^b	1.28×10^{-5}		1.28×10^{-5}	15 h	>13
C ₆ H ₅ CH ₂ Br ^b	1.45×10^{-4}		1.45×10^{-4}	1.3 h	>13

^aData from Ref. 2.

^bReaction proceeds by S_N1 process.

TABLE 8.10 Rates of Hydrolysis of Polyhalogenated Alkanes at 25°C^a

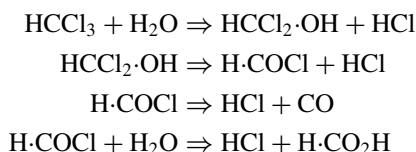
Compound	k_w (s ⁻¹)	k_b (M ⁻¹ · s ⁻¹)	k_h (s ⁻¹) pH 7	$t_{1/2}$ pH 7
CH ₂ Cl ₂	3.1×10^{-11}	2.2×10^{-8}	3.1×10^{-11}	700 year
CHCl ₃	7×10^{-13}	6.5×10^{-5}	7.2×10^{-12}	≈3000 year
CHBr ₃ ²		3.2×10^{-4}	3.2×10^{-11}	≈3000 year
CHBrCl ₂ ²		1.60×10^{-3}	1.60×10^{-10}	140 year
CHBr ₂ Cl ²		8.01×10^{-4}	8.01×10^{-11}	275 year
CHBrClF ²		0.215	2.15×10^{-8}	370 day
CH ₂ BrCH ₂ Br	6.0×10^{-9}		6.0×10^{-9}	3.7 year
Cl ₃ CCH ₃	2.3×10^{-8}		2.3×10^{-8}	350 day
Cl ₂ CHCHCl ₂		1.8	1.8×10^{-7}	45 day
BrCH ₂ CHBrCH ₃	2.5×10^{-8}		2.5×10^{-8}	320 day
BrCH ₂ CHBrCH ₂ Cl	≈ 1×10^{-10}	5.7×10^{-3}	5.7×10^{-10}	38 year

^aData taken from Refs. 1 and 2.^bObservations made in 662:3 dioxane/water.

bromide hydrolyses rapidly (Table 8.9), so the question arises as to how it might survive to induce an effect in the stratosphere. Although water vapor exists in the atmosphere the concentration is much less than the $55.5 \text{ mol} \cdot \text{L}^{-1}$ in aqueous solution. It can be calculated that at 75% humidity and 25°C the concentration of water in the air is only $9.6 \times 10^{-4} \text{ mol} \cdot \text{L}^{-1}$, which difference will result in a longer atmospheric lifetime.

The hydrolysis of polyhalogenated alkanes is quite complex resulting in slower reaction rates, varying products and with some substitution patterns, elimination reactions in addition to the substitution reactions that are usually observed. Kinetic data for some compounds is summarized in Table 8.10.

One might predict from previous analysis that additional chlorine substituents would enhance the positive charge on carbon and produce an increase in the rate of hydrolysis. Clearly, this is not so for the halomethanes and it has been suggested that steric effects may override any inductive effect. Under ambient conditions, hydrolysis would not be a significant degradation process for these compounds. A range of products is observed. While hydrolysis of methyl chloride yields methanol, dichloromethane gives formaldehyde. Trihalomethanes react to form carbon monoxide and formic acid with the former being the major product. The following sequence for the reaction with water has been suggested.¹⁵ The bromochloromethanes are of interest in that they can be formed in the chlorination of drinking



for the hydrolysis reaction, it is concluded that the former reactions may be more important at lower temperatures. It was also noted that the polysulfide ion (S_n^{2-}), detected at higher pH values, may be more effective nucleophiles than HS^- . Thus under anoxic conditions in the presence of sulfur, reactions of alkyl halides can be more complex than simple hydrolysis.

REFERENCES

1. R. P. Schwarzenbach, P. M. Gschwend, and D. M. Imboden, *Environmental Organic Chemistry*, John Wiley & Sons, Inc., New York, 1993, p. 274.
2. W. Mabey and T. Mill, *J. Phys. Chem. Ref. Data* **7**, 383 (1978).
3. A. J. Kirby, "Hydrolysis and Formation of Esters of Organic Acids", in C. H. Bamford and C. F. H. Tipper, Eds, *Comprehensive Chemical Kinetics*, Vol. 10, Elsevier, Amsterdam, The Netherlands, 1972, pp. 57–208.
4. W. J. Lyman, W. F. Reehl, and D. H. Rosenblatt, *Handbook of Chemical Property Estimation Methods*, McGraw-Hill Book Co. New York, 1981, pp. 7–1, 7–48.
5. N. L. Wolfe, W. C. Steen, and L. A. Burns, *Chemosphere* **9**, 403 (1980).
6. R. G. Zepp, N. L. Wolfe, J. A. Gordon, and G. L. Baughman, *Environ. Sci. Technol.* **9**, 1144 (1975).
7. E. M. Perdue and N. L. Wolfe, *Environ. Sci. Technol.* **16**, 847 (1982).
8. N. L. Wolfe, R. G. Zepp, and D. F. Paris, *Water Res.* **12**, 561 (1978).
9. H. A. Moore and C. J. Miles, *Rev Environ. Contam. Toxicol.* **105**, 99 (1988).
10. R. Greenhalgh, K. L. Dhawan, and P. Weinberger, *J. Agric. Food Chem.* **28**, 102 (1980).
11. D. Macalady and N. L. Wolfe, *J. Agric. Food Chem.* **31**, 1139 (1983).
12. N. L. Wolfe, *Chemosphere*, **9**, 571 (1980).
13. C. A. Bunton, M. M. Mhala, K. G. Oldham, and C. A. Vernon, *J. Chem. Soc.* 3293 (1960).
14. N. L. Wolfe, R. G. Zepp, J. A. Gordon, G. L. Baughman, and D. M. Cline, *Environ. Sci. Technol.* **11**, 88 (1977).
15. I. Fells and E. A. Moelwyn-Hughes, *J. Chem. Soc.* 398 (1959).
16. W. R. Haag and T. Mill, *Environ. Sci. Technol.* **22**, 658 (1988).
17. R. P. Schwarzenbach, W. Giger, C. Schaffner, and O. Wanner, *Env. Sci. Technol.* **19**, 322 (1985).
18. A. L. Roberts, P. N. Sanborn, and P. M. Gschwend, *Env. Sci. Technol.* **26**, 2263 (1992).

Metabolic Transformation

Organic compounds can be absorbed, and in some cases, concentrated in organisms (see Absorption and Bioconcentration, Chapter 5). The toxicological question is What does the chemical do to the organism? The converse, What does the organism do to the chemical? is of concern to the environmental chemist. The most important process in this regard concerns the potential for compounds to be degraded in soil by the action of soil microorganisms. Transformation occurring in plants is significant in relation to herbicide action and potential use in bioremediation of contaminated sites. Metabolic transformations in higher organisms can result in the production of more toxic derivatives but also results in the production of polar derivatives that are more readily excreted. The latter process is an important variable in determining the tendency to bioaccumulate.

Biological transformations are unique in that the reactions are catalyzed by enzymes and the cell can generate the energy to drive a reaction. For example, in the latter case, conjugation (Phase II) reactions often involve the participation of a “high-energy” cofactor. The catalytic action of an enzyme reduces the activation energy to give significant reaction rates at ambient temperatures. What becomes apparent is the versatility of these processes, in that biological systems are able to modify almost any organic compound. For example, many organisms are able to metabolize DDT, a compound that was first synthesized in 1873 and introduced as an insecticide in the 1940s. Where and how does such a capability develop? The answer to this question doubtless involves the fact that there are numerous naturally occurring halogenated counterparts¹ and it has been recently been reported that the chloride ion in fresh plant material is converted to chlorinated hydrocarbons as the material weathers.² It should be noted that the enzymes that can metabolize exogenous compounds are also responsible for transformations of endogenous cellular constituents.

The kinetics of enzyme-catalyzed reactions will be discussed followed by a listing of the different systems of importance in the metabolism of exogenous organic compounds. The objective will be to develop a background sufficient to project the metabolites one might expect to form from an organic compound. Some unique aspects of plant systems will be discussed followed by an analysis of degradation processes in soil.

9.1 ENZYME KINETICS

Compounds or substrates that react with an enzyme are bound at an active site that defines specificity and provides orientation required for the reaction (Fig. 9.1). In many cases coenzymes (e.g., A, B, and C) are bound in close proximity, participate in the reaction and are regenerated.

Molecules that do not fit the active site precisely do not react and can inhibit the catalytic process. The suffix -ase denotes an enzyme, while the prefix indicates the type of reaction being catalyzed. For example, a dehydrogenase denotes an enzyme that catalyzes the removal of hydrogen atoms while a methyltransferase is an enzyme that transfers methyl groups. A systematic nomenclature has been developed for classifying enzymes, which is usually described in biochemistry texts.

Coenzymes are small molecules (in comparison to proteins) present in cells that “cooperate” with the protein in carrying out a reaction. For example, nicotinamide

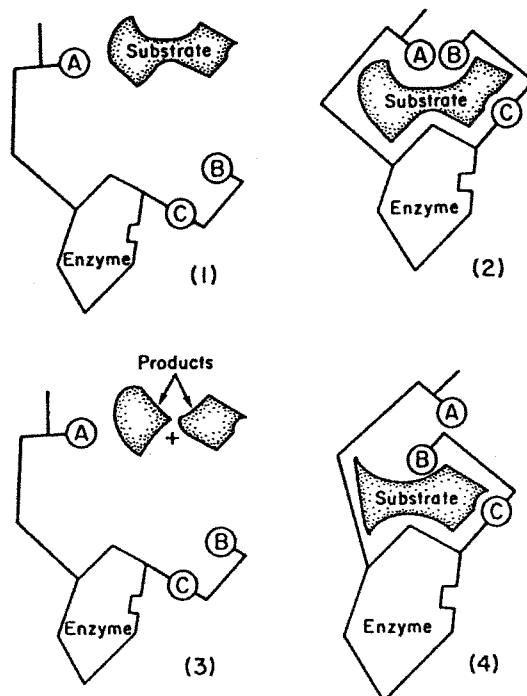
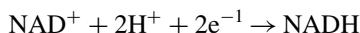


Figure 9.1 Schematic representation of enzymatic action 1. Substrate and enzyme. 2. Substrate binds to enzyme at group C inducing proper alignment of catalytic groups A and B. 3. Reaction results in release of products and regeneration of free enzyme. 4. Potential substrates which are either too large or too small do not align correctly and a reaction does not occur.

adenine dinucleotide (NAD^+), adenosine diphosphate linked through ribose to niacinamide, participates in redox processes:



as does its phosphorylated relative, NADP^+ . Flavin adenine dinucleotide (FAD) is also involved in redox processes. Note that these two coenzymes are based on the micronutrients, niacin, and riboflavin. Other coenzymes assist in group transfer and carboxylation.

An enzyme-catalyzed reaction can be represented schematically



The substrate, S, combines with enzyme, E, to form the enzyme–substrate complex, ES, which then reacts to form product, P, and regenerate enzyme. Assuming that the reverse reaction of product with the enzyme is negligible, the rate at which product is formed, v , would be given by

$$v = k_2\text{ES}$$

where k_2 would be the first-order reaction constant for catalytic reaction. If it is also assumed that k_2 is small compared with the k_1 and k_{-1} , the rates of formation and dissociation of ES, it can be demonstrated that the rate of the enzyme-catalyzed reaction can be expressed:³

$$v = \frac{k_2[\text{E}]_t[\text{S}]}{[\text{S}] + K_m}$$

This is referred to as the Michaelis–Menten relation and $K_m = k_{-1}/k_1$ the Michaelis constant, an estimate of the affinity of the substrate for the enzyme. When $[\text{S}] \gg K_m$, all the active sites on the enzyme are filled and $v = k_2 [\text{E}]_t = V_{\max}$, and thus,

$$v = \frac{V_{\max}[\text{S}]}{[\text{S}] + K_m}$$

The reaction rate increases with substrate concentration to the point where the available enzyme is saturated and $v = V_{\max}$ the reaction becoming zero order (Fig. 9.2). When $[\text{S}] \ll K_m$ the reaction becomes first order, $v = V_{\max}/K_m[\text{S}]$ assuming $[\text{E}]_t$ is constant. When $[\text{S}] = K_m$, $v = V_{\max}/2$. The parameter K_m is also an index of the slope of the $v/[\text{S}]$ relation.

This kinetic model for enzyme catalysis is equivalent with the Langmuir isotherm (see Sorption, Chapter 3) the only difference being that adsorption on the surface leads to a reaction. And in a similar fashion a double reciprocal plot can be used

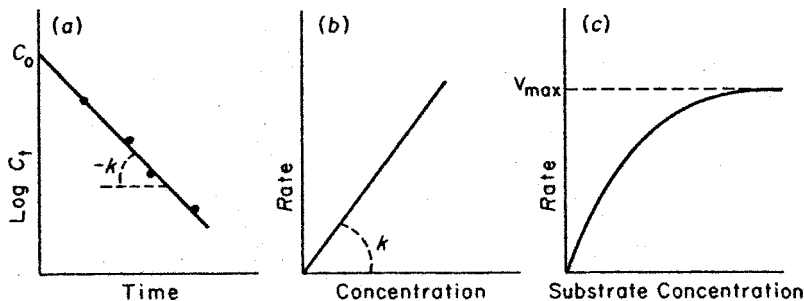


Figure 9.2 (a) Linear relation between logarithm of reactant concentration and time for a first-order reaction. (b) Influence of reactant concentration on rate for a first-order reaction. (c) Rate of an enzyme-catalyzed reaction as a function of substrate concentration.

to determine both K_m and V_{max} :

$$\frac{1}{v} = \frac{1}{V_{max}} + (K_m/V_{max})1/[S]$$

Plotting $1/v$ as a function of $1/[S]$ gives a straight line with a slope of K_m/V_{max} and an intercept of $1/V_{max}$.

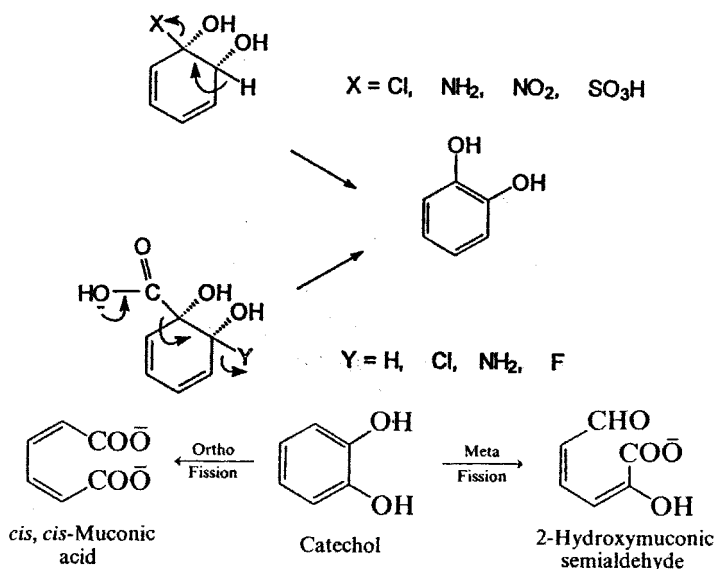
In an environmental context it should be emphasized that, in contrast to homogeneous reactions, enzyme-catalyzed processes will saturate because of the limited capacity that is available. These systems are also more efficient at lower concentrations. For example, at a higher concentration, it will take longer for 25% conversion of the substrate than at a lower concentration.

9.2 ENZYME-CATALYZED TRANSFORMATIONS

This has been a very active field of investigation in recent years and a very extensive literature has developed. It is beyond the scope of this text to provide a comprehensive discussion of these processes, however, examples will be given of different reactions catalyzed by enzymes to provide some reference for predicting metabolites that could arise from a given organic compound. It is useful to distinguish between biodegradation or mineralization, which implies complete conversion to CO_2 , Cl^- , NH_3 , observed in some microbial systems and biotransformation, the conversion by one or more enzymes to some metabolite. It has been the convention to classify biotransformations as either Phase I or Phase II reactions. The former involve small changes such as the introduction of an hydroxyl or epoxide, or a hydrolysis of an ester or amide, while the latter produce a conjugate by the reaction of the compound in question with some cellular constituent such as glutathione or glucuronic acid.

9.2.1 Phase I Reactions

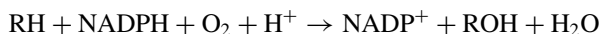
9.2.1.1 Dioxygenase Reactions These enzymes are more commonly observed in microorganisms and introduce both atoms of elemental oxygen into the aromatic ring to form a *cis*-1,2-dihydrodiol accompanied by the release of a



ring substituent while catechol oxygenases cleave the aromatic ring.⁴ Some dioxygenases can react with long-chain aliphatic compounds. Dioxygenases have been shown to be important in the microbial degradation of PCBs and it has been reported that these systems are more active in the ring containing fewer chlorine substituents. Congeners substituted in the 2- or 6- positions are also less reactive.

The aromatic ring may be cleaved either by an ortho (1,2-cleavage) or meta (2,3-cleavage) reaction with catechol. Note that, with benzene, simple fragments are produced that could be utilized in normal cellular processes.

9.2.1.2 Cytochrome P450 Monooxygenase Reactions The cytochrome P450 mediated reaction introduces one atom of elemental oxygen into a compound according to the overall reaction



Cytochrome P450 is a heme containing protein and the "P450" designator refers to its spectral characteristics. The >400 cytochrome P450s characterized,⁵ are widely distributed among animals, plants,⁶ and microorganisms.⁴ Genetic variants responsible for this family of enzymes have been studied extensively to establish the amino acid sequence relations among the different isoforms, their distribution and cata-

logue variations in substrate specificity. Cytochrome P450 systems are unusual in metabolizing a wide range of substrates in contrast to the specificity usually attributed to enzymes. This is often attributed to the fact that any tissue or organism may have several isoforms of differing substrate activity, but it has been noted that individual isoforms also may be active with a wide range of molecules. The actual mechanism of the P450 system involves a complex reaction cycle.⁵

The versatility of the P450 oxygenases is summarized in Figure 9.3. Epoxides can be introduced into aromatic rings or across double bonds. The former reaction leads to a hydroxy or dihydrodiol. It is most unlikely to observe aldrin in environmental samples since it is rapidly converted to dieldrin, a common environmental contaminant that is very stable. Aliphatic chains can be hydroxylated and ethers, thioethers, and substituted amines dealkylated. The conversion of parathion to the more reactive paraoxon is a factor in the mechanism of toxic action, as well as its environmental stability (see Hydrolysis, Chapter 8). The situation can be complicated by the fact that a substrate can often undergo more than one reaction.

9.2.1.3 Flavin Monooxygenases A flavin-containing enzyme requiring NADPH and O₂ from animal systems can convert amines (secondary and tertiary) and sulfur-containing compounds to the oxides (Fig. 9.3). Related flavin-containing monooxygenases have also been identified in microorganisms, however, these systems catalyze the hydroxylation of phenols.

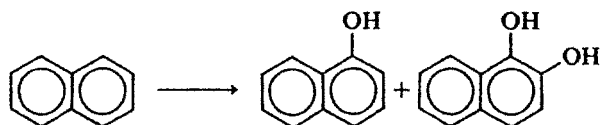
9.2.1.4 Dehydrogenases and Oxidases An alcohol dehydrogenase oxidizes alcohols to aldehydes, which in turn are oxidized to carboxylic acids by an aldehyde dehydrogenase. Amine oxidases catalyze the oxidation of primary amines to alcohols.

9.2.1.5 Reductions Microbial and mammalian nitroreductase reduces nitro compounds to amines. Chlorinated alkanes and alkenes are common contaminants in ground water and chlorinated aromatics, PCBs, organochlorine pesticides, are often detected in soils and sediments and it has been of interest to evaluate the potential for these compounds to be metabolized. A number of microorganisms are able to dechlorinate both halogenated aliphatic and aromatic compounds in a reduction reaction.⁴ It has been observed that the more highly chlorinated congeners are more reactive in these systems in contrast to the response in oxidative dechlorinations.

9.2.1.6 Hydrolases Enzymes that catalyze the hydrolysis of esters of carboxylic acids, phosphoric acids as well as amides are widely distributed in many species. It has been demonstrated with purified enzymes that these hydrolases often are active with both esters and amides of carboxylic acids.

This brief analysis of the capability of Phase I enzymes shows that enzymes can modify organic compounds by attacking different functional groups as well as the carbon skeletons of both aliphatic and aromatic compounds.

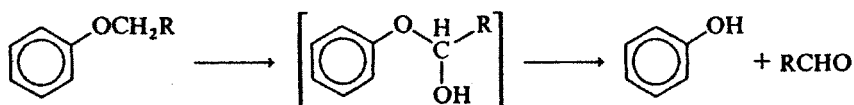
Aromatic hydroxylation



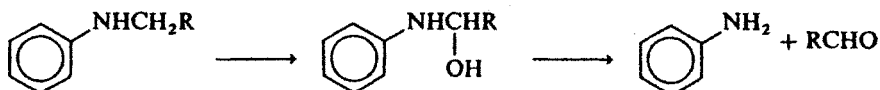
Aliphatic hydroxylation



O-Dealkylation of aromatic ethers



N-Dealkylation of secondary amines



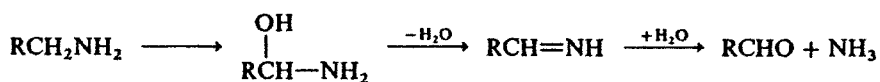
N-Hydroxylation of aromatic amines



N-Oxide formation from alkyl and aryl tertiary amines



Oxidative deamination



Epoxidation



Desulfuration

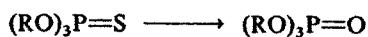
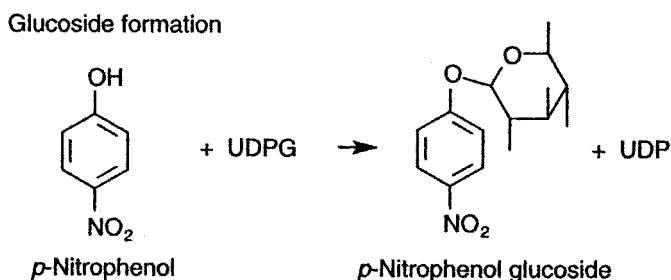


Figure 9.3 P450 Monooxygenase reactions.

9.2.2 Phase II Reactions

These conjugation reactions usually result in the formation of more polar derivatives which, in higher organisms, facilitate excretion. These processes do not appear to be prevalent in microorganisms, however, plants use them to inactivate exogenous compounds.

9.2.2.1 Glycoside Conjugation A glycoside is formed when a monosaccharide such as glucose reacts with, say CH_3OH , splitting out water to form methyl glucoside.



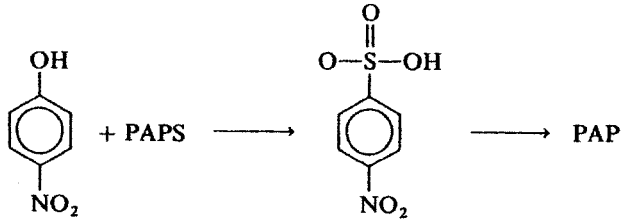
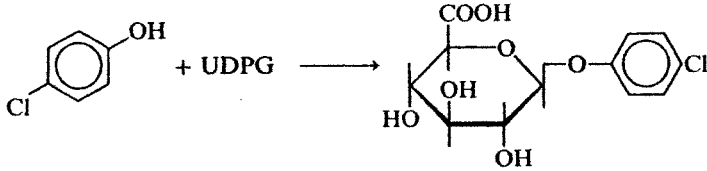
The conjugation of glucuronic acid to form a glucuronide is more common in higher animals, while in plants it is more likely to observe the formation of a glucoside, through the reaction with glucose (Fig. 9.4). These reactions are effected through the formation of a “high energy” conjugating intermediate, uridinediphosphate glucuronic acid (UDPGA) or uridinediphosphate glucose (UDPG) and the action of transferase enzymes:



The uridine triphosphate would be generated in the cell through the action of adenosine triphosphate (ATP) the compound responsible for energy transduction. In passing, it should be noted that the cell uses UDPG in the synthesis of polysaccharides such as glycogen. The conjugation reaction may involve $-\text{OH}$, $-\text{NH}$, and $-\text{SH}$ functional groups. It is obvious how this conjugation reaction produces a more hydrophylic derivative.

9.2.2.2 Glutathione Transferase Reactions Glutathione (GSH), a tripeptide, comprised of glutamic acid, cysteine and glycine, is a common constituent of most cells. Note that the peptide bond of the glutamic involves the γ - rather

Sulphation

Formation of β -D-glucuronides

Mercapturic acid formation from glutathione conjugation

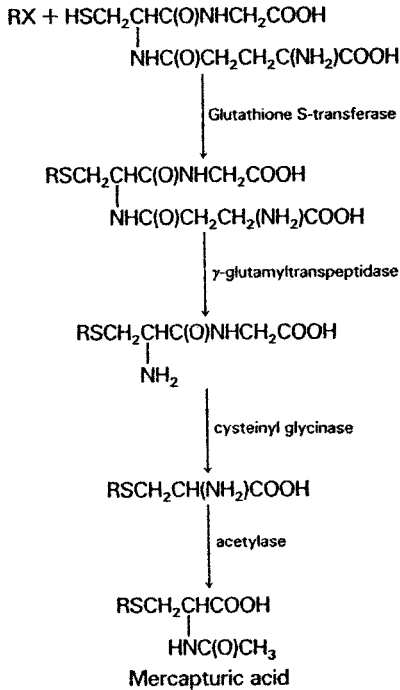
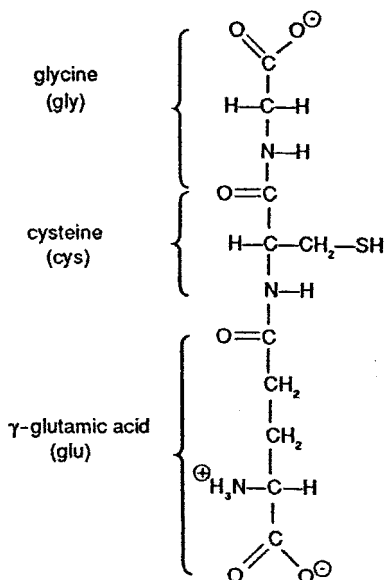


Figure 9.4 Some Phase II reactions.

than the α -carboxyl.



Homoglutathione, where β -alanine replaces glycine, is found in plants and is the major free —SH component in soybeans and mung bean. The sulfur of glutathione provides a negative site on the molecule that facilitates interaction with molecules with electrophilic sites such as a carbon in which a chlorine induces a small positive charge. Other reactive functional groups would include, epoxides, carbon-carbon double bonds (Fig. 9.4). Parenthetically, it can be noted that these electrophilic sites can produce toxic damage by reacting with nucleic acids or proteins and GSH can serve a protective role in cells. The reactions can proceed nonenzymatically with some very reactive compounds but usually are catalyzed by glutathione-*S*-transferases. Numerous isozymes have been characterized, and these enzymes are widely distributed in animals and plants. They are very specific in their requirement for GSH but individual isozymes can catalyze the transferase reaction with a range of substrates. In animals, the glutamic acid and glycine are removed by hydrolytic enzymes to produce the cysteine conjugate that is N-acetylated to produce a mercapturic acid. These derivatives are often excreted in urine. In plants, glutathione conjugates undergo a variety of reactions including conversion to the cysteine derivative along with oxidation of the sulfur and acylation, in this case with malonic acid (Fig. 9.5).⁷ These reactions have been of interest in elucidating the selective response and the development of resistance to herbicides.

9.2.2.3 Esters and Amides Hydroxyl and amino substituents can react with “energy-rich” forms of sulfate and acyl groups to form esters and amides. The active form of sulfate is 3'-phospho-adenosine-5'-phosphosulfate (PAPS) while the

acyl-groups react as coenzyme A derivatives, primarily as acetyl-S-CoA and malonyl-S-CoA in plants.

9.2.2.4 Metabolic Maps Other metabolic transformations, both Phase I and II have been reported⁵ but this discussion has provided an overview of the more common processes. More detailed analyses of the molecular biology and modes of action of these different enzyme systems are provided in biochemical and toxicology texts. Different organisms and for that matter, different tissues from the same organism, will show characteristic metabolic patterns for a given exogenous organic molecule that will be limited to specific Phase I and Phase II transformations. Metabolic maps have been developed that summarize all the different transformations that have been reported for a given compound (Fig. 9.6). This information can be useful for the analytical chemist given the task of determining the levels of some compound in an environmental sample. The nature of the derivative or conjugate will determine the efficacy of extraction steps and in the case of say a glucuronide, necessitate hydrolysis prior to extraction with an organic solvent.

9.3 METABOLISM IN PLANTS

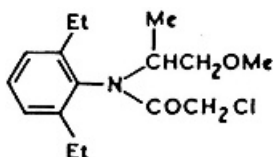
Phase I enzymes of plants such as the P450 monooxygenases are very versatile reflecting their involvement in the production of a wide range of endogenous constituents such as sterols, lignin intermediates, terpenes, flavanoid pigments, and other secondary products. Plants, however, are unique in the production of insoluble conjugates (Phase III processes) and the transport of soluble conjugates into the vacuole.

9.3.1 Insoluble Conjugates and Compartmentation

In the study of herbicide metabolism, it has been observed that the parent compound and its metabolites can be incorporated into lignin, cellulose, and some proteins. These products are insoluble, resistant to hydrolytic enzymes, immobile, and consequently nontoxic. Rigorous procedures may be needed to release the metabolite for analysis.⁸

The vacuole, enclosed by the tonoplast membrane, may constitute as much as 90% of the volume of the mature plant cell and can provide a temporary storage site for intermediary metabolites such as organic acids. Substances such as tannins and calcium oxalate appear to be permanently deposited in the vacuole. It also seems to serve as a repository for metabolites that could be toxic to the plant cell. It has been demonstrated that the glutathione conjugate of metolachlor, a herbicide

based on chloroacetanilide, accumulates in the vacuole against a concentration



Metolachlor

gradient. This energy-dependent transport system seems to accommodate a range of GSH conjugates, however, the requirement for GSH is specific. Similar “GSH pumps” have been described in mammalian systems. Further metabolism of the conjugate may occur in the vacuole (Fig. 9.7). There is also evidence that a similar, but independent, energy-dependent transport system exists for glucoside conjugates.

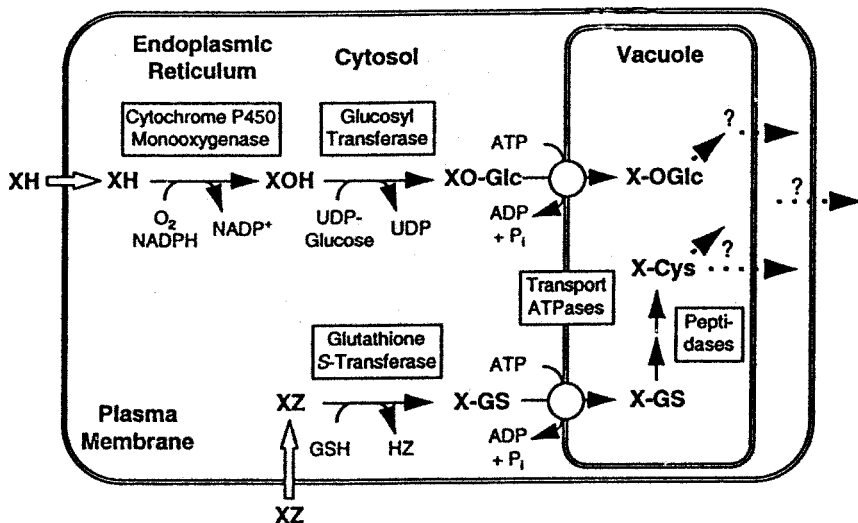


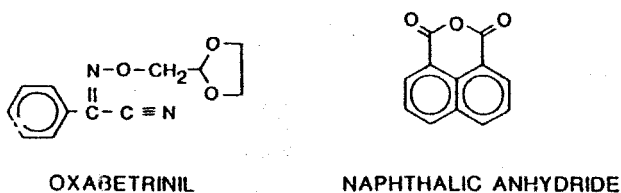
Figure 9.7 Schematic representation of herbicide detoxification in a plant cell. Both XH and XZ are herbicides entering the oxidation–glucose conjugation pathway and the glutathione-dependent pathway, respectively. XOH is the hydroxylated herbicide; XO-Glc, XGS and Xcys are the glucose, GSH and Cysteine conjugates respectively. [Reproduced with permission of the authors from K. Kreuz and E. Martinoia, “Herbicide Metabolism in Plants: Integrated Pathways of Detoxication,” in G. T. Brooks and T. R. Roberts, Eds., *Pesticide Chemistry and Bioscience, The Food-Environment Challenge*, Serial Pub. No. 233, The Royal Society of Chemistry, Cambridge, 1999, pp. 277–287.]

9.3.2 Influencing Plant Metabolism

The activity of the P450 monooxygenases of plants can be influenced by a variety of environmental factors such as, light, fungal attack, and wounding. As with mammalian systems, chemicals can also induce the P450 monooxygenase activity in plants. This response is illustrated (Table 9.1) by the aromatic hydroxylation of three herbicides by microsomes from wheat seedlings. (Note that P450 monooxygenases are associated with the smooth endoplasmic reticulum a cellular membrane that is recovered in the microsomal fraction upon differential centrifugation of the homogenized tissue.) Naphthalic anhydride (NA) and phenobarbital (PB) were applied as a seed dressing, while ethanol was applied to the shoots 24 h prior to harvesting.

The activity increased by factors ranging from $\times 5$ to $\times 20$ with ethanol being the most active compound in this system. It is of interest to note that the increase in activity occurred without any change in the level of cytochrome P450. Comparable K_m values observed with triasulfuron would indicate that the induced and noninduced or constitutive isozymes are similar. Increased K_m values observed with the induced isozymes acting on dicofop and chlorsulfuron are different than the constitutive isozyme. It is concluded that wheat seedlings can show several P450 monooxygenase isozymes with differing substrate activity.

Naphthalic anhydride, oxabetrinil, and three other "herbicide antidotes" induce the activity of glutathione-*S*-transferase (GST) in sorghum seedlings.⁹ The response in the seedlings (Table 9.2) was induced in the seedlings by treatment of the seeds at the rate of 1.25 or 2.5-g \cdot kg⁻¹ seed respectively, for the oxabetrinil and naphthalic



anhydride. Note that the oxabetrinil induced an increase in GST activity relative to metalochlor but not to 1-chloro-2,4-dinitrobenzene (CDNB). When a soluble protein preparation was fractionated on an anion exchange column (Fig. 9.8) and GST activity monitored, the untreated showed one fraction active to CDNB and one active to metalochlor. Treatment with the oxabetrinil produced an increase in the amount of the CDNB fraction and induced the expression of four additional proteins active toward metalochlor. These data illustrate how different isozymes can be isolated and demonstrate the characteristics of the inducing activity of the oxabetrinil.

Naphthalic anhydride and oxabetrinil would be examples of compounds that are called "safeners" in the herbicide field.¹⁰ They are a diverse group of compounds that enhance the tolerance of crops to herbicides. It has been illustrated above that the protective activity of these compounds can be attributed to their ability to enhance the metabolism of a herbicide. Note that naphthalic anhydride can induce

TABLE 9.1 Induction of Microsomal Hydroxylase Activity in Wheat Seedlings

Inducer	P450 (pmol · mg prot ⁻¹)	Hydroxylase (pmol · min ⁻¹ · mg prot ⁻¹)				Apparent K_m (μM)		
		Diclofop	Triasulfuron	Chlorsulfuron	Diclofop	Triasulfuron	Chlorsulfuron	
None	224 ± 19	11 ± 2	13 ± 3	9 ± 3	45 ± 15	13 ± 4	13 ± 3	
NA	228 ± 28	60 ± 16	77 ± 12	66 ± 7	117 ± 6	13 ± 1	14 ± 4	
PB	253 ± 22	176 ± 20	254 ± 41	126 ± 3	127 ± 17	14 ± 0	32 ± 5	
Ethanol	231 ± 42	83 ± 7	126 ± 14	115 ± 32	103 ± 28	14 ± 1	25 ± 8	

TABLE 9.2 Effect of Oxabetranil on GST Activity in Sorghum

Treatment	GST Activity	
	CDNB ($\mu\text{mol} \cdot \text{mg}^{-1} \cdot \text{min}^{-1}$)	Metolachlor ($\text{nmol} \cdot \text{mg}^{-1} \cdot \text{h}^{-1}$)
Untreated	0.275 ± 0.021	0.061 ± 0.020
Oxabetranil	0.376 ± 0.024	0.404 ± 0.052

both P450 monooxygenase and GST activity. Other safeners may enhance vacuolar transport of GSH and glucoside conjugates.

Metabolic activity of plants is also being modulated by genetic engineering to produce herbicide-tolerant species. A variety of hydrolases, monooxygenases, GSTs and acetyl, and glucose transferases and their corresponding genes have been used to produce tolerance in plants. For example, “Roundup-ready” soy

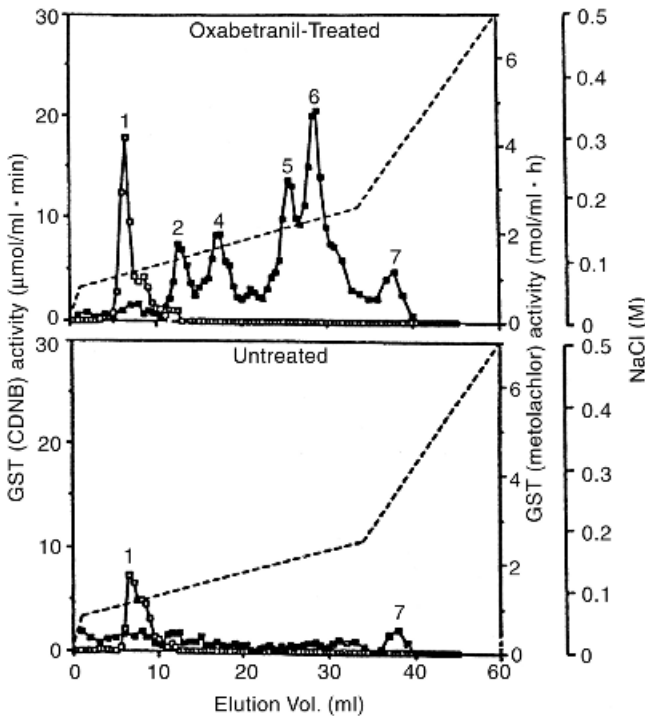


Figure 9.8 Glutathione transferase profiles from etiolated shoots from untreated and oxabetranil-treated sorghum seed. [Reproduced with permission from J. V. Dean, J. W. Gronwald, and C. V. Eberlein, *Plant Physiol.* **92**, 467. Copyright 1990, American Society of Plant Biologists.]

beans have been engineered to metabolize glyphosate, a herbicide with desirable environmental properties, that is active when applied to foliage.

9.4 DEGRADATION RATES IN SOIL: SOIL MICROORGANISMS

Many organic compounds are applied directly to soil while others end up in soil or sediments either as they are disposed in landfills or move by erosion into sediments. Consequently, it is important to know how rapidly a compound breaks down in this environmental compartment. This information is particularly important in the use of pesticides. A herbicide that breaks down slower than anticipated may carry over from one season to the next and produce damage in the newly planted crop. By contrast if a soil-applied insecticide or herbicide breaks down too quickly it will not produce the desired level of control. The compounds that break down rapidly do not present a threat to groundwater since they do not persist long enough to leach through the soil profile. This information will also be critical in assessing super fund sites and managing hazardous landfills.

Under field conditions, organic compounds may be lost through evaporation, leaching through the soil profile or physical degradation processes. However, it has been established that microflora are primarily responsible for the degradation of organic compounds in soil. Unless a physical process predominates, sterilization of the soil almost completely eliminates degradation. Soil should be perceived as a complex ecosystem. It is estimated that every acre of soil contains two tons of living things: algae, amoeba, fungi, actinomycetes, and bacteria.¹¹ These organisms play critical roles in nutrient cycling and the degradation of recalcitrant plant polymers such as cellulose and lignin. Organic carbon provides the energy for microbiological growth and development and is limiting in most soils; the system being considered oligotrophic. Because of this limitation soil microbial populations tend to be dormant and different species flourish when presented with an acceptable form of carbon. It has been reported that only 15–30% of the bacterial population in soil is active under favorable conditions.¹²

Most organic compounds will ultimately be mineralized in soil. While some species of microorganisms can grow on say, toluene, as a sole carbon source producing CO₂ and water, the breakdown of organic compounds is often the result of a cooperative action of several organisms. The natural soil environment of course would contain a complex mix of both substrates and microorganisms. Soil microbiology is an important focus in the field of soil science and workers in this area adopt a taxonomic approach to the degradation of organic compounds by isolating, identifying, and characterizing the metabolic capabilities of soil microorganisms.⁴

9.4.1 Soil Half-Lives

A variety of approaches can be used to observe the rate at which organic compounds degrade in soil. Laboratory studies may involve a perfusion approach where the concentration in solution is monitored as it is recycled through a soil column.¹³ In an

TABLE 9.3 Soil Half-Lives at 20–25°C

Compound	Class	Half-Life (day)
1,2-dichloropropane	Chloroaliphatic	700
Atrazine	Triazine	60
Simazine	Triazine	60
Parathion	Organophosphate	14
Malathion	Organophosphate	1
Chlorpyrifos	Organophosphate	30
Carbaryl	Carbamate	10
Diuron	Urea	90
2,4-D acid	Phenoxy acetic acid	10
Dicamba	Benzoic acid	14
Lindane	Organochlorine	400
Dieldrin	Organochlorine	1000
DDE	Organochlorine	1000
DDT	Organochlorine	1000

alternative approach, chemical is incorporated in samples of soil and the concentration monitored while maintaining appropriate temperature and water levels.¹⁴ When ¹⁴C-labeled compound is used, the rate of mineralization can be determined by monitoring the production of ¹⁴CO₂. This type of information is required by regulatory agencies for pesticides and other contaminants and USEPA has provided experimental protocols.¹⁵ Observations under field conditions become more complex, in that the losses measured can involve evaporation and leaching as well as physical and metabolic processes. Laboratory observations often show first-order kinetics and rate constants and half-lives ($\ln 2/k_1$) are cited. Other studies may cite a time for 50% loss (DT₅₀), which is interpolated from a graphical presentation of the data without defining the kinetic order.

Comprehensive summaries of biodegradation rates have been compiled for pesticides,¹⁶ and other organic compounds of environmental significance.^{11,17} Half-lives at 20–25°C for some pesticides are compiled in Table 9.3. Persistence in soil varies over several orders of magnitude with the nature of the compound. These values only provide a relative indication of the persistence of these compounds in soil because degradation rates vary considerably with location and environmental conditions. For example, field half-lives for parathion range from 2–150 days and for DDE from 2–15.6 years!

9.4.2 Factors Influencing Soil Degradation

The variation in soil degradation rates depend on factors influencing biological activity including temperature, moisture, and oxygen tension along with those factors that control the availability of the substrate.

9.4.2.1 Biological Adaptation It had been noted that some pesticides lose their ability to control a pest after multiple applications and this effect did not involve the development of resistance in the pest, but was associated with an increased rate of degradation. The degradation of two fungicides, iprodione and vinclozolin after three applications (May 23, July 3, and August 5) at a rate of $4 \text{ kg} \cdot \text{hectare}^{-1}$ is summarized in Figure 9.9.¹⁸ The degradation rates increased with the number of applications and the concentration applied. It is of interest to note that after 3 years use vinclozolin was not effective in controlling white rot infection in onions. Another example of this inductive or adaptive effect has been provided by the study of the effect of aromatic hydrocarbons on the ability of aerobic marine sediments to mineralize polynuclear aromatic hydrocarbons.¹⁹ These compounds are commonly found in petroleum and with the occurrence of oil spills the ability of microorganisms to respond to a spill is an important consideration. Sediment slurries were incubated with the hydrocarbons for 7 or 14 days after which a ^{14}C -labeled compound was added and the rate of $^{14}\text{CO}_2$ monitored. From Table 9.4 it can be seen after 14-day preincubation that benzene and anthracene induced the degradation of anthracene and anthracene, benzene, naphthalene, and phenanthrene all induced the degradation of naphthalene. Glucose, an energy source that could stimulate microbial growth, was without effect. This study illustrates the complexity of the inductive-adaptive process in that cross-induction can occur but it is not clear what factors influence the process.

This increase in metabolic activity could involve a number of processes. Given the fact that carbon is often a limiting factor for the growth and development of soil microbes, the introduction of a new source of carbon would theoretically select for any organism that could utilize that source. This response is difficult to prove since it would be necessary to demonstrate an increase in the number of the selected

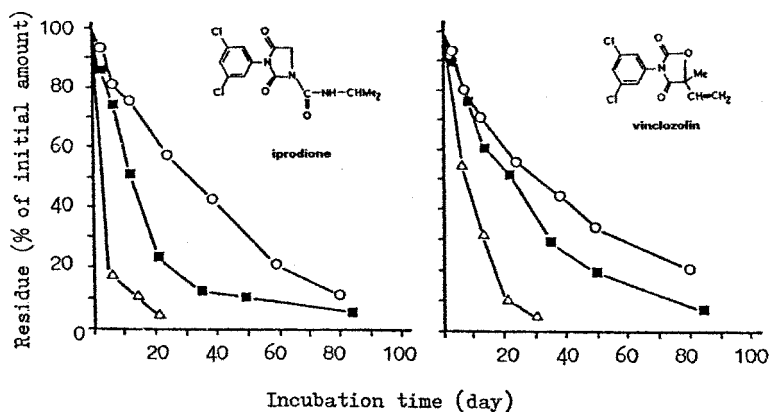


Figure 9.9 Degradation of sequential applications of iprodione and vinclozolin in soil (pH 6.5) ○, first treatment; ■ second treatment; △ third treatment. [Reproduced with permission from A. Walker, *Pesticide Sci.* **21**, 219, 1987. Copyright, Society of Chemical Industry with permission granted by John Wiley & Sons, Ltd. on behalf of the SCI.]

TABLE 9.4 Induction of Hydrocarbon Mineralization after 14-Day Incubation

Treatment	Substrate	Rate (%/day)	Amount (%14 day)	Substrate	Rate (%/day)	Amount (%14 day)
Control	A	0.07	1.32	N	0.70	8.29
Glucose	A	0.05	0.42	N	0.13	9.74
Anthracene	A	1.60	9.62	N	8.99	48.71
Benzene	A	0.66	7.56	N	10.63	54.48
Naphthalene	A	0.04	0.24	N	8.46	47.71
Phenanthrene	A	0.07	0.71	N	6.70	40.16

species and soil microbes are not always the easiest to handle under laboratory conditions. Note that polynuclear hydrocarbons can induce the activity of a dioxygenase that hydroxylates and cleaves aromatic rings.¹⁹ So the enhanced activity observed in marine sediments could be explained by such a response. The chemical acts by influencing the expression of the gene coding for the enzyme so that more is produced. The complicated interactions observed could result from differences in inducing activity and the substrate activities of the enzymes induced.

Genetic changes could also result in modulation of metabolic activity. This could result from mutations, but the transfer of genes on plasmids among microbial communities also appears to be a factor. Plasmids are autonomous circular DNA molecules that can self-replicate in cells, and can carry genes that can impart antibiotic resistance and other qualities to the cell as well as genes involved in degradative processes. In addition, there are specific mechanisms whereby plasmids can move between cells.²⁰ Consequently, if a plasmid carrying a gene coding for an enzyme specific for the degradation of a given compound, transfers into the cell of a different species and replicates, that species would acquire an enhanced ability to degrade that compound. An illustration of this phenomenon is the study of the gene coding for naphthalene dioxygenase in bacterial strains isolated from a site contaminated with coal tar waste.²¹ The gene for this enzyme was identical in six of the eight strains investigated and carried by the plasmid. It was thus postulated that the ability of these strains to metabolize naphthalene was enhanced by the presence of the naphthalene dioxygenase that resulted from plasmid transfer.

The rate of soil degradation is a major factor in defining the environmental behavior of an organic compound. Unfortunately, there is no systematic basis for assessing the potential for microbial degradation in a given environment. Even if the microbial classes of a given soil could be identified, there is still no systematic basis for correlating degradative activity in soil with the species.²⁰ There is no other recourse than experimental observations of degradation rates either in the laboratory or the field, which can require extended incubation time. The application of techniques in molecular biology are now beginning to provide a basis for assessing biodegradation capability by detecting the genes that code for the enzymes involved. First, the DNA is extracted from a soil sample and using the property of DNA/DNA hybridization a DNA probe for the gene in question can be used to detect the level

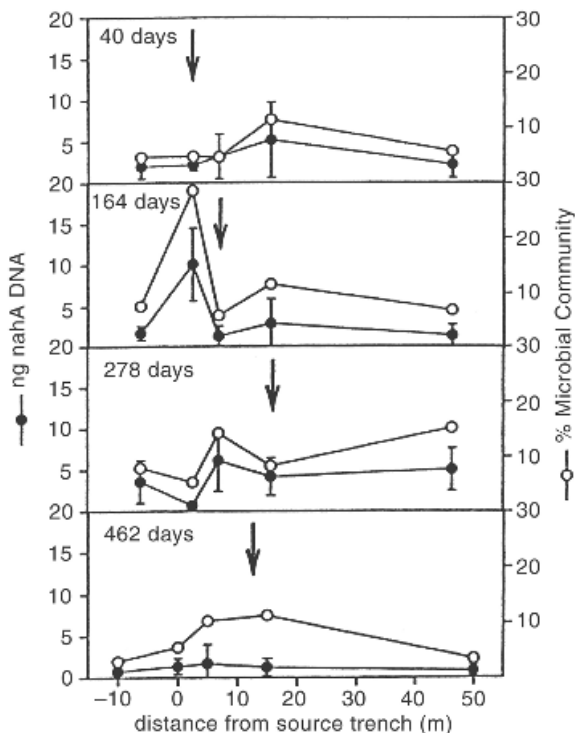


Figure 9.10 Distribution of naphthalene-degrading genotypes, as judged by the concentration of *nahA* gene sequence per gram of soil, in subsurface aquifer sediments. Bold arrows represent the distance the front edge of the plume has traveled. [Reprinted with permission from R. D. Stapleton, G. S. Saylor, J. M. Boggs, E. L. Libelo, T. Stauffer, and W. G. Macintyre, *Environ. Sci. Technol.* **34**, 1991 (2000). Copyright © 2000, American Chemical Society.]

of that gene in the soil DNA. This technique would not necessarily predict the actual level of the corresponding activity, since this would be determined by the manner in which the gene is expressed. An example of this approach is provided by a study of the microbial response to a petroleum plume moving in a groundwater study.²² The study used probes for five different enzymes that would be involved in the different hydrocarbons present in the petroleum sample. The response to a probe for naphthalene dioxygenase is given in Figure 9.10 and it shows that the distribution of the gene corresponded to the movement of the petroleum plume. There was a correlation between the actual degradation of naphthalene and the incidence of the gene. This technology shows promise of providing definitive information on the metabolic potential of a given soil sample.

9.4.2.2 Temperature One can anticipate that degradation rates in soil will vary with temperature for two reasons. Enzyme-catalyzed reactions usually increase

with temperature to a point where heat may denature the enzyme and limit activity, and temperature can provide a selection pressure for microorganisms. Some species are favored by low and others by higher temperatures. The effect of temperature on the degradation of the herbicide, alachlor, in soils has been studied in the laboratory²³ and observations from two of the soils studied are compiled in Table 9.5. First-order rate constants are listed along with soil properties. Increasing the temperature from 5 to 25°C increased the degradation rate and over this range no adverse effect was noted. The rate constants fit the Arrhenius equation ($\ln k_1 = -E_a/(R/T + \ln A)$) giving an estimate of the activation energy, E_a . The difference observed between the two soils reflected the difference in biomass. A seasonal effect has been demonstrated in the field, where, in eastern Canada, the disappearance half-life of the triazine herbicide Atrazine was 37 days when applied in May or June and 198 days when applied in September.²⁴ The average monthly temperature for 4 months following the applications were 13.1–21.8°C and –0.2 to –9.6°C.

Much of the data compiled for soil degradation rates under field conditions has been taken from studies in the temperate zone. A useful comparison of soil degradation rates in the tropics has been provided by a study in Brazil²⁵ carried out in the central western region, latitude 15°53'S where the mean annual temperature is 23°C. The dissipation of 10 different pesticides was monitored for 80 days under field conditions. The data was found to fit a biexponential decay model ($r^2 > 0.97$):

$$C_t = C_1 e^{-k_1 t} + C_2 e^{-k_2 t} + C_3 \quad \text{where } C_0 = C_1 + C_2 + C_3$$

and C_1 and C_2 are the fractions of C_0 , the initial concentration, subject to the two dissipation rates. This model assumes that the chemical partitions instantaneously into two noninteracting compartments, possibly a soil solution and a sorbed phase, which show differing degradation rates.²⁶ Although these data fit this model, the assumption of instantaneous partitioning would not be supported by the current concepts defining distribution in soil. The data for six pesticides compiled in Table 9.6 are taken from observations in a Haplustox soil with 1.6–3.1% OC and a pH of 4.8–5.6. Field half-lives are higher in the temperate zone by factors of 2.5–37.5 with the pesticides listed. One might expect that the more rapid dissipation under tropical conditions could reflect involvement of evaporation and perhaps photochemical losses in addition to microbial degradation. Evaporation is more likely from wet soil and the relative tendency is related to HLC/K_d , (see evaporation chapter) and it is of interest to note that the three compounds that show the largest difference in persistence, chlorpyrifos, endosulfan α , and trifluralin, also have the highest HLC/K_d ratios. More comprehensive investigations would be necessary to establish the extent to which the different processes contribute to the overall differentials in persistence. Tropical conditions would also influence the rate of microbial degradation. In this regard, it is of interest to note that the field half-life of alachlor observed in Brazil is comparable to that observed at 25°C in the laboratory (Table 9.5) when losses from evaporation would be minimal. The values for k_2 do

TABLE 9.5 Effect of Temperature on the Degradation of Alachlor in Soil

Soil	Depth (cm)	OM (%)	pH	Moisture (%)	Biomass (mg · C · kg ⁻¹)	Temp (°C)	k ₁ (day ⁻¹)	t _{1/2} (day)	E _a (kJ · mol ⁻¹)
Cottage field	0–20	3.74	5.36	15.2	286.4	5	0.0072	95.9	75.4
						10	0.0116	60.0	
						15	0.0224	31.0	
						20	0.0399	17.4	
						25	0.0601	11.5	
Little cherry	40–60	2.20	6.16	14.6	123.9	5	0.0025	279.6	71.8
						15	0.0076	91.6	
						25	0.0199	34.0	

TABLE 9.6 Pesticide Degradation Rates under Tropical Conditions

Pesticide	$t_{1/2}$ days		Temperature ^b	C_0			k_1			K_d (mL · g ⁻¹)	HLC ^a (Pa · m ³ · mol ⁻¹)
	Brazil	Temperature ^b		C ₀	C ₁	C ₂	(day ⁻¹)	k_2			
Alachlor	5.9	15	3288	3219	69	0.122	0.014	5.2	0.0062		
Atrazine	7.4	60	1659	833	826	0.526	0.026	4.4	0.00029		
Chlorpyrifos	0.8	30	1573	1277	288	1.443	0.073	170	1.75		
Endosulfan α	1.7	50	642	378	256	1.228	0.058	134	2.98		
Simazine	16.9	60	1448	1341	107	0.046		6.3	0.00034		
Trifluralin	4.0	60	1471	719	660	0.539	0.053	188	4.02		
Metolachlor	20.0	90	3395	3191	204	0.038		2.9	0.00091		

^aTaken from Ref. 27.

^bTemperate zone estimates; see Ref. 16.

not differ to the same degree as those for k_1 and it is possible that the rate of dissipation defined by this quantity reflects the rate at which the compounds are released from a “bound compartment”.

Studies of the anaerobic metabolism of 2,3,4,6-tetrachlorobiphenyl by freshwater sediments have demonstrated that temperature not only influences rate but may also influence metabolic pathways.²⁸ The metabolism of this PCB congener was monitored for 1 year in sediments (exposed or not exposed to PCBs) under anaerobic conditions at temperatures ranging from 4 to 66°C. Dechlorination steps are summarized in Figure 9.11 with the black arrows indicating reactions observed in the nonexposed sediment. All reactions were observed with the exposed sediment. Little if any reaction was detected at 4°C and at the higher temperatures (37°C and above in the nonexposed sediment and 37–45°C with the exposed sediment). However, from 50–60°C almost 90% conversion to the 2,4,6-CB was observed. An example of the differences reported is provided in Figure 9.12. At 15 and 20°C, the first step was the loss of *m*-chlorine to produce the 2,4,6-CB. However, at 15°C the production of the 2,4-CB is favored along with the 4-CB in contrast

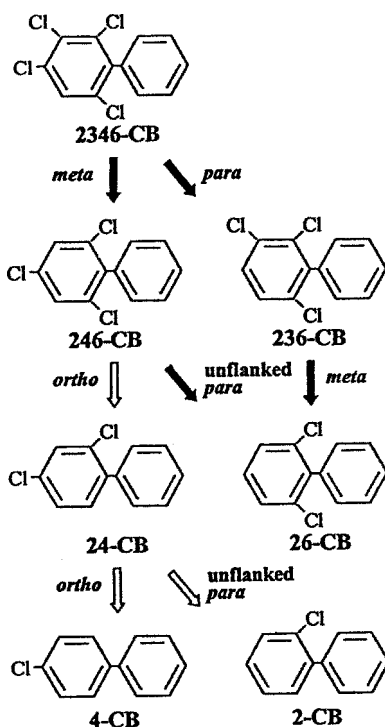


Figure 9.11 Dechlorination pathways of 2,3,4,6-tetrachlorobiphenyl in Sandy Creek Nature Center Pond sediment samples (black arrows) and Woods Pond sediments (all arrows). [Reproduced with permission from Q. Wu, D. L. Bedard, and J. Wiegel, *Appl. Environ. Microbiol.* **63**, 2836. Copyright 1997, American Society for Microbiology.]

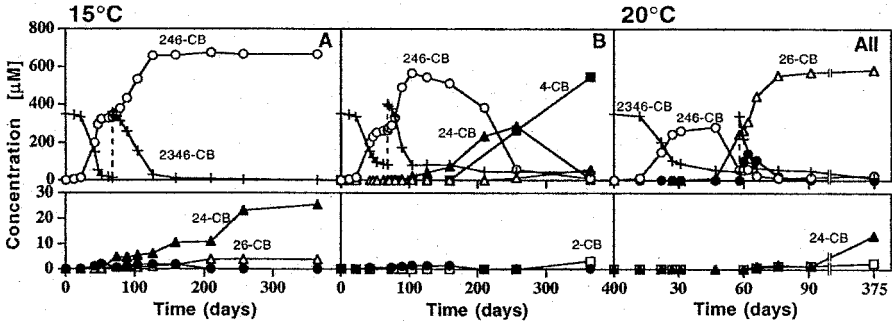


Figure 9.12 Time course of dechlorination of 2,3,4,6-tetrachlorobiphenyl in Woods Pond sediments at 15 and 20°C. At 15°C 6 samples followed “A” and six, “B”. At 20°C, all six samples followed pattern indicated. [Reproduced with permission from Q. Wu, D. L. Bedard, and J. Wiegel, *Appl. Environ. Microbiol.* **63**, 2836. Copyright 1997, American Society for Microbiology.]

to 20°C where the production of the 2,6-CB is favored. The temperature effects observed in this study are quite complex and it is not possible to develop any systematic relations because of the variation among replicates that would reflect the heterogeneous distribution of microorganisms in the soil.

9.4.2.3 Soil Moisture This parameter varies with atmospheric conditions and although microorganisms may survive through dry cycles moisture is required for optimum activity. An example of the effect of soil moisture on the rate of dissipation of alachlor is summarized in Table 9.7.²³ As expected the rate of metabolism of alachlor at 15°C decreased with a decrease in moisture level. The half-life could be expressed as a function of the moisture content:

$$t_{1/2} = A M^{-B}$$

TABLE 9.7 Effect of Moisture on the Degradation of Alachlor at 15°C

Soil	Depth (cm)	Moisture		k_1 (day ⁻¹)	$t_{1/2}$ (day)	A	B
		(%)					
Cottage field	0–20	16.0		0.0442	15.7	4290	2.07
		13.52		0.0386	18.0		
		9.94		0.0214	32.3		
		7.44		0.0097	71.2		
		6.90		0.0084	82.8		
Little cherry	49–60	11.08		0.0083	83.1	1864	1.33
		10.19		0.0085	82.0		
		6.58		0.0051	135.4		
		5.45		0.0035	196.6		
		4.34		0.0025	281.4		

with A and B being constants and B reflecting the sensitivity of the system to moisture. Given these degradation data for alachlor it is possible to use models to predict the patterns of field degradation (Fig. 9.13) using atmospheric data to estimate soil temperatures and moisture levels.²³

9.4.2.4 Anaerobic Effects Many of the Phase I transformation processes require elemental oxygen and proceed under aerobic conditions. By contrast, anaerobic environments can occur in soils and particularly in aquatic sediments. The contribution of organisms that function under these conditions was illustrated by observations on sediments from the Hudson river in New York that had been contaminated with PCBs. Considerable quantities of PCBs had been released to the river

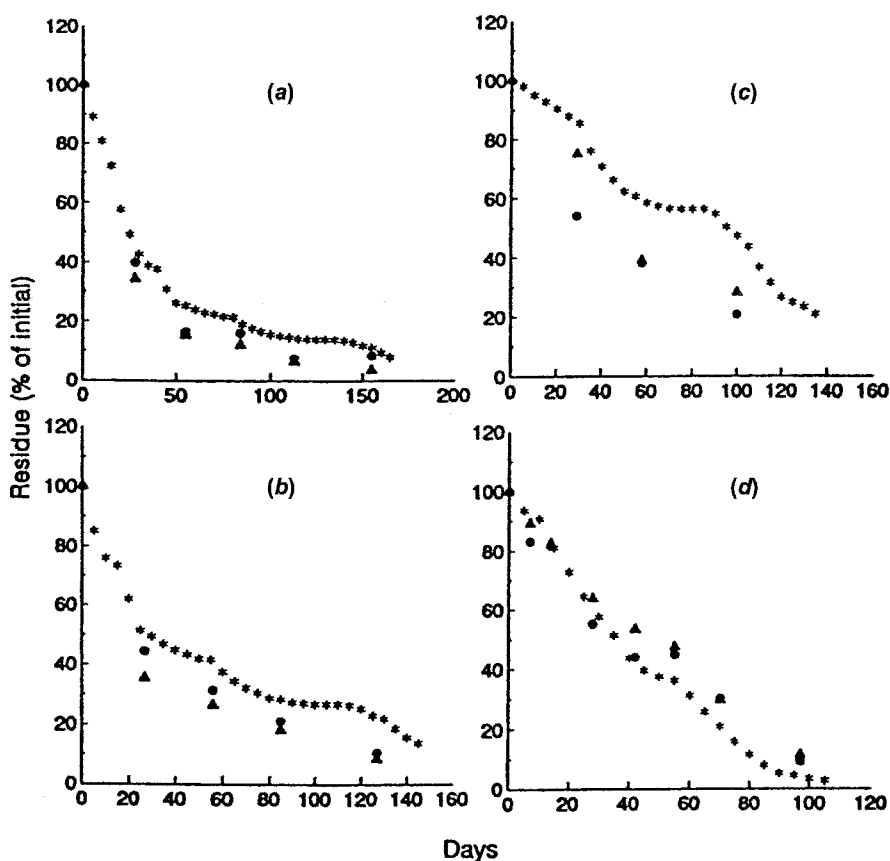


Figure 9.13 Residues of alachlor recovered from Little Cherry soil following applications in the field on (a) 27 September 1990, (b) October 1990, (c) 21 November 1990, and (d) 11 April 1991. ●, experimental replicates; *, predicted. [Reproduced with permission from A. Walker, Y. Moon, and S. J. Welch, *Pest. Sci.* 35, 109, 1992. Copyright, Society of Chemical Industry with permission granted by John Wiley & Sons, Ltd. on behalf of the SCI.]

between 1952 and 1971 by plants manufacturing capacitors. Two PCB chromatograms from sediment samples (Fig. 9.14) show widely diverse patterns.²⁹ Pattern A, which was comparable to Aroclor 1242 (see Appendix), originally used in the plants was observed in surface sediments whereas Pattern C, which had lost large proportions of the more highly chlorinated congeners was observed in deep sediments. This differential was surprising since the more highly chlorinated congeners were considered the more recalcitrant, being strongly sorbed and certainly more resistant to degradation under aerobic conditions. As noted (Reduction), however, the more highly chlorinated congeners are in a more oxidized form and thus more susceptible to reduction and it was established that the loss of these congeners was due to microbial reductive dechlorination.

The extensive use of PCBs was predicated on their chemical stability, which was also manifest in their persistence in the environment. The management of contaminated sites has often involved the removal of the soil or sediment and transfer to some secured landfill that is really not a solution. It has been proposed that the degradation of PCBs might be accomplished by taking advantage of microbial activity under anaerobic conditions to transform the more highly chlorinated congeners to those that could be mineralized under aerobic conditions. This concept has been evaluated in laboratory studies using a weathered (aged) PCB-contaminated soil and observing the changes in PCB composition following incubation with a mixed anaerobic culture derived from a contaminated site, followed by incubation under aerobic conditions with a microbial strain known to metabolize PCBs.³⁰ The soil was contaminated with Aroclor 1260, which contains significant proportions of hexa-, hepta-, and octochloro congeners. The incubations were carried out at 21 °C for 3–4 months under anaerobic conditions and up to 28 days under aerobic conditions.

Incubation of the contaminated soil under anaerobic conditions with the mixed culture resulted in significant reductions of the highly chlorinated congeners (Fig. 9.15). This change was due to dechlorination since the actual molar concentration of PCB congeners was unchanged but the number of chloro- substituents per molecule decreased (Table 9.8). The major products were tri- and tetrachloro congeners. These transformations should have resulted in a 11% reduction in mass but this was not detected. The products of the anaerobic dechlorination were degraded, but not completely during the aerobic incubation and an overall decrease in both molar concentration and mass resulted. It was of interest to note that some of the more chlorinated congeners were also lost during the aerobic treatment, although aerobic incubation without prior anaerobic treatment only resulted in the loss of 10% of the PCB, which was not statistically significant. These results would suggest that this approach could have some potential under field conditions.

9.4.2.5 Concentration It is possible that, say, in the case of a spill, that a toxic concentration could be achieved and microbial activity lost. This response would be unusual and would not be expected under the usual environmental conditions. When a solution of the herbicide atrazine is continuously recycled through a soil column the concentration declines consistent with a first-order process,¹³ that is, a linear

Publisher's Note:
Permission to reproduce this image
online was not granted by the
copyright holder. Readers are kindly
requested to refer to the printed version
of this article.

Figure 9.14 Gas chromatograms of upper Hudson River sediments that show a surface pattern (top) that corresponds to largely unchanged Aroclor 1242 and a subsurface pattern that indicates loss of the more highly chlorinated congeners with a concomitant increase in mono- and dichloro- derivatives. [Reprinted with permission from J. F. Brown, Jr., D. L. Bedard, M. J. Brennan, J. Carnahan, H. Feng, and R. E. Wagner, *Science* **236**, 709. Copyright 1987, American Association for the Advancement of Science.]

relation is observed between the logarithm of the concentration and time (Fig. 9.16). However, for a true first-order process variations in the initial concentration should change the intercept but not the slope ($-k_1$). In this case, it is observed that the slope increases with decreasing concentration and the half-life decreases from 250 to 108 days. This response is consistent with what one might expect from an enzyme-catalyzed process. Change in concentration with time can approximate first-order processes, but the process becomes less efficient as concentration increases. Many observations under field conditions are consistent with this laboratory study. Other observations, however, have shown just the opposite response; organic compounds are not metabolized as efficiently at very low concentrations. For example, the formation of $^{14}\text{CO}_2$ from 2,4-dichlorophenoxy[2- ^{14}C]-acetate by a natural microbial community in a sample of stream water was more efficient at high than low concentrations (Fig. 9.17).³¹ A similar response was observed with the carbamate insecticide, Sevin. By contrast, in the same system, chloroacetic and *p*-chlorobenzoic acids produced CO_2 more efficiently at lower concentrations. It has been suggested that, for some compounds, a metabolic threshold may exist,³² and this limitation could account for their persistence at low concentrations. Explanations for such a response are tentative, and it is not clear why 2,4-D should respond differently from *p*-chlorobenzoic acid. These observations do emphasize the need to be cautious in extrapolating from laboratory observations at higher concentrations to the lower concentrations that could occur in the field.

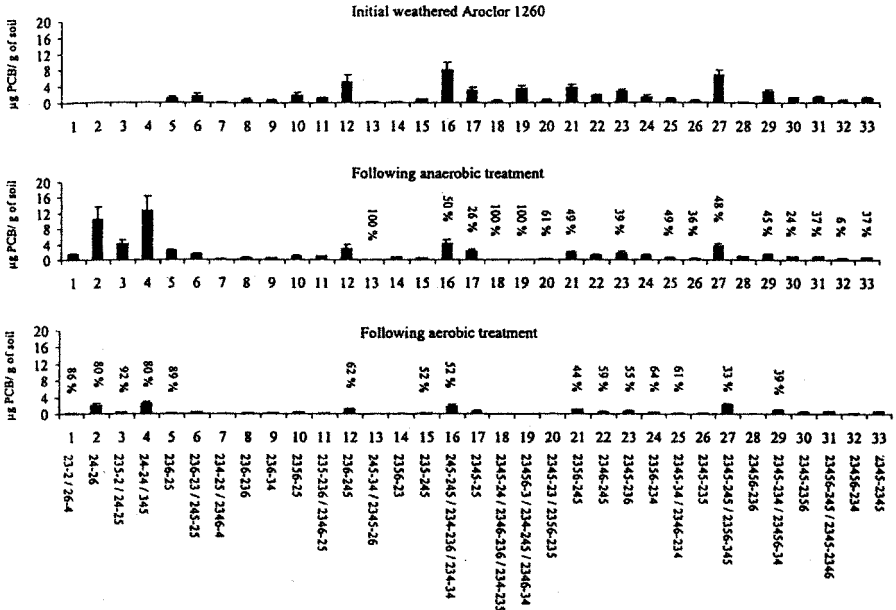


Figure 9.15 Sequential treatment of PCB contaminated soil. Histograms indicate major congeners of weathered Arochlor 1260 with percent removal in each treatment phase given for those that were significantly degraded. Note that anaerobic treatment resulted in losses of the more highly chlorinated congeners to give increases in the less chlorinated species that were in turn lost during aerobic treatment. [Reproduced with permission from E. R. Master, V. W.-M. Lai, B. Kuipers, W. R. Cullen, and W. W. Mohn, *Environ. Sci. Technol.* 36, 100 (2002). Copyright © 2002 American Chemical Society.]

9.4.2.6 Soil Organic Matter This variable can influence the rate of microbial degradation by controlling the availability in soil because the available concentration will decrease with increased sorption in soils of high organic matter content. However, high organic matter can enhance the proliferation of microbial communities and thus increase the rate of degradation. It has been suggested that soil organic matter could also decrease the metabolism of some organic compounds simply by competing in the microbial metabolic pathways. These complex interactions make it difficult to predict how this variable might affect degradation rates.

The rate of degradation of the herbicide triclopyr at 35°C, has been evaluated in laboratory studies using soils that differed in organic carbon content (Table 9.9)³³ and the data fitted to a two-compartment model:

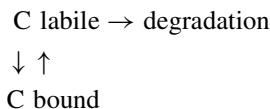


TABLE 9.8 PCB Concentrations in Treated Soil

Treatment	PCBs · g ⁻¹ soil		
	(nmol)	(μg)	Cl/PCB Molecule
Initial soil	157.4 ± 15.7 ^a	58.7 ± 5.7	6.4 ± 0.031
After anaerobic incubation	162.1 ± 45.4	58.3 ± 14.4	5.2 ± 0.068
After aerobic incubation	55.5 ± 10.5	19.6 ± 3.6	5.5 ± 0.12

^aMean and standard error.

The compound is only available for degradation in the labile compartment that would include the amount in solution and possibly some that might be sorbed but readily available. The compound in the bound compartment is only degraded as it desorbs. This model does represent, perhaps simplistically, what could occur in soil and the concentrations in the two compartments can be expressed

$$\frac{dC_L}{dt} = -(k + k_1)C_L + k_{-1}C_B$$

$$\frac{dC_B}{dt} = k_1C_L - k_{-1}C_B$$

The degradation patterns observed in the two soils are quite distinct (Fig. 9.18) and show differences in the derived rate constants (Table 9.9). Degradation in the Illinois soil compared with the California soil is characterized by higher degradation and binding rates and lower desorbing rate. This results in a higher proportion of the compound being bound, such that the desorbing rate controls the rate of degradation after the first 100 days. This effect is not as pronounced with the California soil since the desorption and degradation rates are comparable. The difference in the organic carbon content of the two soils may well explain the differing responses since higher organic carbon level could lead to higher biomass (see Table 9.5) and a consequent higher degradation rate as well as an increased tendency to bind in soil reducing the concentration for degradation.

Another example of the effect of soil organic matter is provided by investigations of the breakdown of pesticides in surface (0–25 cm) and subsurface soils (25–50 cm) (Table 9.10).³⁴ The surface and subsurface soils contained 0.53 and 0.15% organic carbon and 21 and 15-μg microbial carbon per gram of soil, respectively. Degradation rates approximated first-order kinetics and half-lives are tabulated for comparison. One might anticipate longer half-lives in the subsurface soils because of reduced microbial activity, but the response was inconsistent; some compounds being degraded more rapidly in these soils. Compounds with higher K_{OC} values (chlorpyrifos, chlorthal dimethyl, and propyzamide) were degraded more rapidly in the subsurface soil while the reverse was true for those compounds with low K_{OC} values (fenamiphos, metalaxyl, metribuzin). With the two compounds with

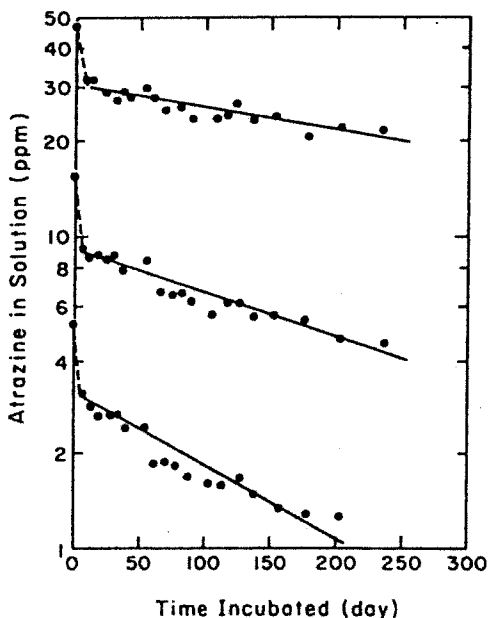


Figure 9.16 Atrazine degradation in a silt loam soil. The atrazine solution is continuously recycled through the soil column and sampled at specified time intervals. [Reproduced from D. E. Armstrong, G. Chesters, and R. F. Harris, *Proc. Soil Sci. Soc. Am.* **31**, 61 (1967) with permission from the Soil Science Society of America.]

$K_{OC} = 400$, linuron was more rapidly degraded in the subsurface soil while prometryne was more rapidly degraded in the surface soil. This response could be explained by the interaction of availability, determined by sorption, and degradation rate that would be a function of the level of microbial activity. The rate of degradation of compounds with higher K_{OC} values is influenced more by sorption as determined by the level of soil OC, while with compounds that are not sorbed extensively degradation reflects the level of microbial activity also related to the level of soil OC.

9.4.2.7 Aged Residues The longer organic compounds remain in soil the more difficult they are to remove. The actual mechanism(s) by which these “aged residues” develop is not understood (see Sorption, Chapter 3). Since this process would influence the availability of soil residues it would be expected to affect the rate of microbial degradation. This has been demonstrated in a laboratory study of the mineralization of 4-nitrophenol and phenanthrene.³⁵ Different soils were sterilized, ^{14}C -labeled compounds added and allowed to age for periods up to 305 days before inoculation with specific strains that mineralized either the phenanthrene or phenol. Mineralization was measured by monitoring the generation of $^{14}\text{CO}_2$. The effect of aging on the mineralization of the phenol in a Lima loam (4.0% OM) and an Edwards muck (19.3% OM) is illustrated in Figure 9.19.

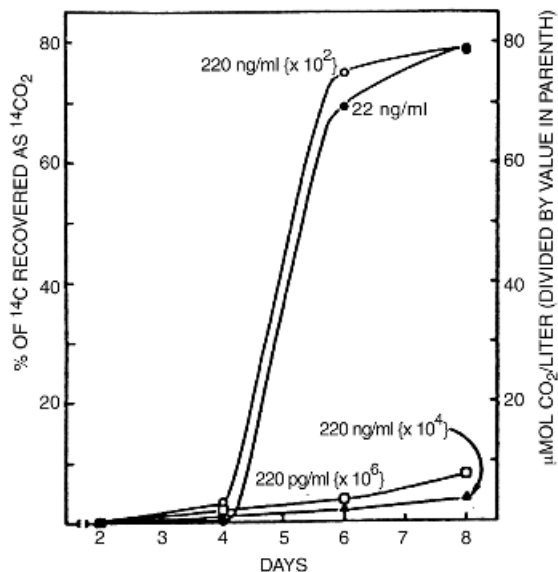


Figure 9.17 Formation of $^{14}\text{CO}_2$ from 2,4-dichlorophenoxy[2- ^{14}C]acetic acid added to stream water at four initial concentrations. [Reproduced with permission from R. S. Boethling and M. Alexander, *Appl. Environ. Microbiol.* **37**, 1211. Copyright 1979, American Society for Microbiology.]

The maximum rates of mineralization of the two compounds decreased with aging (Table 9.11) and it is of interest to note that the phenol was metabolized at higher rate than the phenanthrene. This could involve differences in the sizes of the inoculum used or differing mineralizing efficiencies of the two strains. The large difference in K_{OM} between the phenol (64.6) and phenanthrene (6310) calculated from $\log K_{ow}$ values of 2.04 and 4.46 (see Sorption, Chapter 3) would result in a large difference in C_e for equivalent levels of x/m . The proportion of the 4-nitrophenol (pK_a 7.08) in solution would be enhanced by the fact that mineralization reaction were carried out around pH 7.

The mechanism of the “aging” process has not been established, consequently, it is not yet possible to predict how the properties of the soil and the chemical interact with time in determining the availability of a compound for metabolism.

9.4.2.8 Soil pH With the exception of some extreme cases, soils will show pH in the range of 4–8.5. The soil pH can affect distribution of species in a soil

TABLE 9.9 Rate Constants for Triclopyr Degradation

Soil	pH	%OC	k_1 (day $^{-1}$) Binding	k_{-1} (day $^{-1}$) Desorbing	k (day $^{-1}$) Degrading
Flanagan silty clay loam, IL.	5.8	4.2	0.01426	0.00498	0.0767
Yolo county loam, CA	6.5	0.8	0.005488	0.01266	0.01714

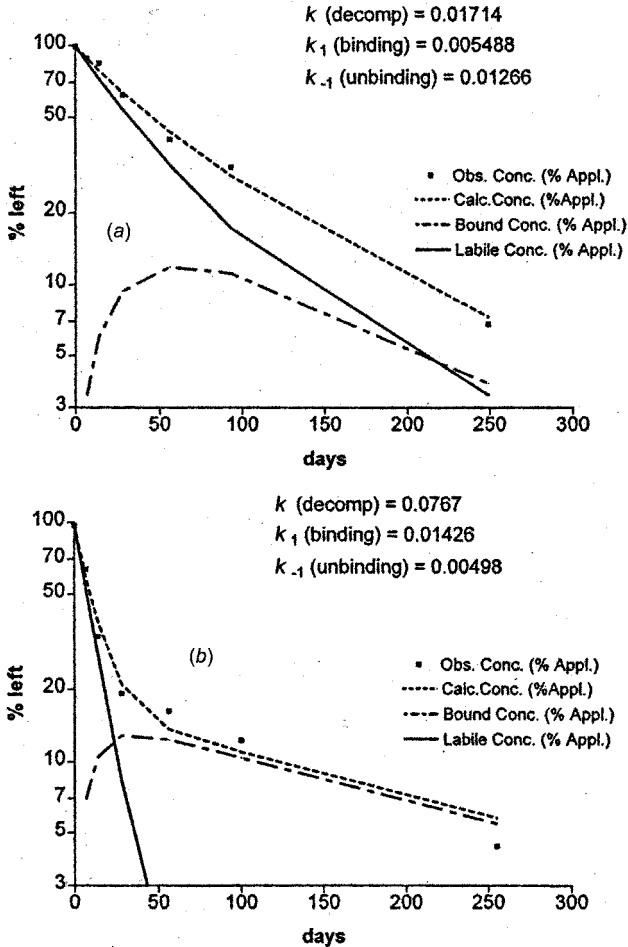


Figure 9.18 Degradation of trichlopyr at 35°C in A, a California soil (0.8% organic carbon, pH 6.5) and B, an Illinois soil (4.2% organic matter, pH 5.8) giving experimental values (■) and values calculated from the two-compartment model for the kinetic constants (day^{-1}) and the proportion found in the bound and labile compartments. [From J. W. Hamaker and C. A. I. Goring, "Turnover of Pesticide Residues in Soil," in R. F. Gould, Ed., *Bound and Conjugated Pesticide Residues*, A. C. S. Symposium Series, No. 29, American Chemical Society, Washington, D.C., 1976, pp. 219–243.]

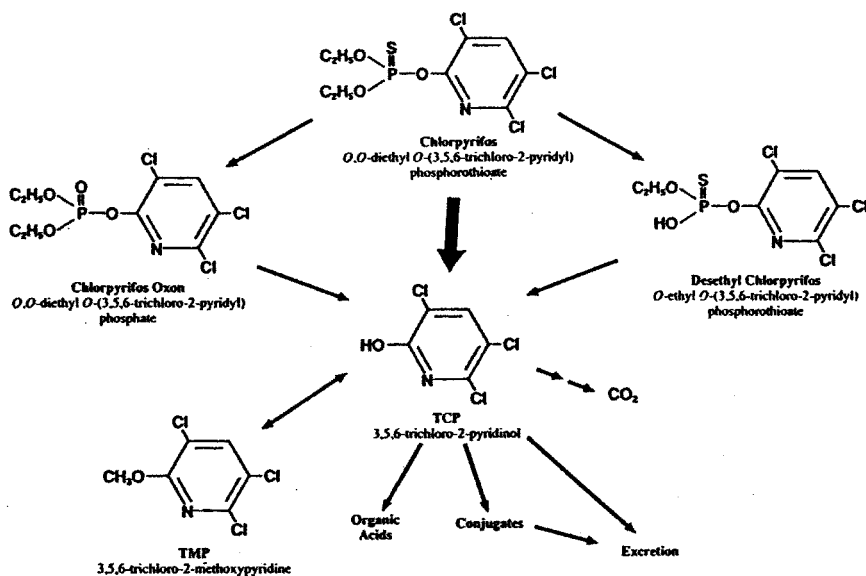
community since, for example, fungi are more tolerant of acid while actinomycetes tend to be more tolerant of alkaline conditions. However, it would be very difficult to interpret the effect of soil pH on degradation rate in terms of changes in composition of the microbial community. Soil microorganisms are not amenable to this type of microbiological analysis. Consequently, the effects of varying soil pH are readily observed in abiotic reactions such as hydrolysis.

TABLE 9.10 Degradation of Pesticides in Surface and Subsurface Soils

Compound	K_{OC} (mL · g ⁻¹) ^a	Half-Life (day)	
		Surface	Subsurface
Chlorpyrifos	6070	93	23
Chlorthal dimethyl	5000	40	24
Fenamiphos	100	24	72
Linuron	400	142	88
Metalaxyl	61	48	117
Metribuzin	268	46	77
Prometryne	400	64	141
Propyzamide	775	92	64

^aFrom Ref. 16.

The persistence of the common organophosphate insecticide, chlorpyrifos in soils of varying pH, provide an interesting illustration of this effect.³⁶ It was shown that “problem” soils (those in which the insecticide did not control the pest) were characterized by short chlorpyrifos half-lives (3.8–8.9 days) associated with a soil pH of 8. In soils where this insecticide was effective, half-lives of ~30 days were observed along with soil pH values from 5–7. This effect of pH would be consistent with what might be expected with organophosphates (see Hydrolysis, Chapter 8), however, it is not certain to what extent the reaction is mediated by microorganisms. The degradation of chlorpyrifos in soil involves the following sequence of reactions: with the major intermediate being trichloropyridinol (TCP). The degradation of ¹⁴C ring-labeled chlorpyrifos in the “problem” soils



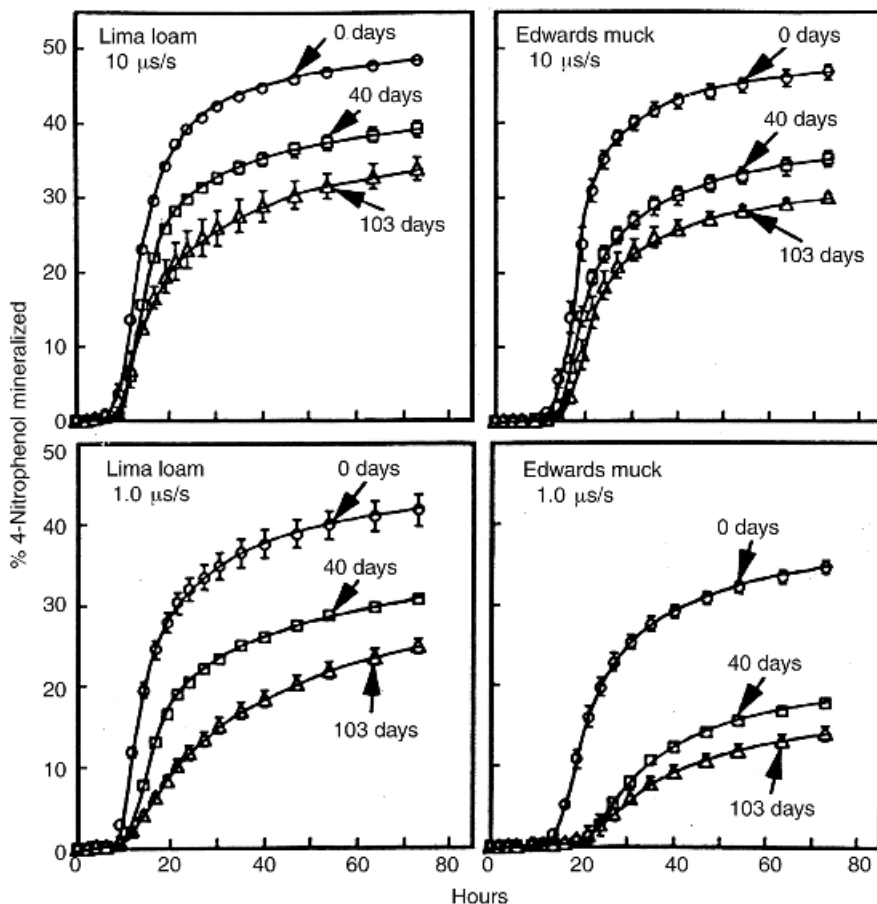


Figure 9.19 Mineralization of two concentrations of 4-nitrophenol by bacterium, WS-5, aged in Lima loam (4.0% organic matter, pH 7.2) and Edwards muck (19.3% organic matter, pH 6.9). [Reproduced with permission from P. B. Hatzinger and M. Alexander, *Environ. Sci. Technol.* **29**, 537 (1995). Copyright © 1995, American Chemical Society.]

was observed in natural and sterilized (irradiated) soil (Table 9.12). It is significant that after 14 days, the loss of the parent compound in the sterilized soil is almost the same as that observed in its sterilized counterpart. It does not necessarily follow that this step is abiotic in the natural soil, however, it could explain the observation that, unlike some other organophosphates, multiple applications of chlorpyrifos does not enhance its degradation rate. On the other hand, mineralization of the TCP is clearly dependent on soil microorganisms and this capability is quite limited in two of the soils studied.

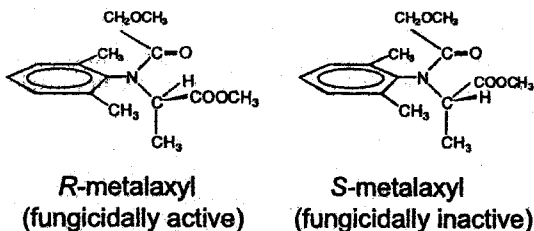
Chlorpyrifos has been used extensively and many studies have focused on soil behavior with the results of these studies emphasizing the variability in persistence

TABLE 9.11 Effect of "Aging" on Maximum Mineralization Rates for 4-Nitrophenol and Phenanthrene

4-Nitrophenol			Phenanthrene		
Aging (day)	Mineralization Rate %/h ⁻¹		Aging (day)	Mineralization Rate %/h ⁻¹	
	Loam	Muck		Loam	Muck
0	3.92	3.60	0	0.733	0.479
40	3.18	2.58	13	0.600	0.345
103	2.11	2.26	27	0.554	0.300
			84	0.466	0.270

that can occur. The DT₅₀ values ranging from 1.9 to 1576 days have been reported with application rates varying from 0.1 to 1000 ppm, soil pH from 5.2 to 9.1, organic carbon from 0.48 to 28.3, and temperature from 18 to 35°C.³⁷

9.4.2.9 Chiral Effects Traditional methodology in synthetic organic chemistry led to racemic mixtures of chiral compounds. Recent developments, however, have made it possible to both synthesize the pure enantiomers and resolve them analytically. The fungicide, metalaxyl, contains a chiral carbon and the two enantiomers

**TABLE 9.12** Degradation of Chlorpyrifos in Soil

Soil	Pembina	St. Thomas	Dewitt	Medina				
pH	8.0	8.1	8.0	8.1				
% OC	2.7	3.0	1.9	2.1				
Half-life (day)	8.9	5.6	3.8	4.9				
% ¹⁴ C Recovered after 14 Days								
	Natural	Sterile	Natural	Sterile	Natural	Sterile	Natural	Sterile
Chlorpyrifos	34.6	43.9	26.2	36.8	12.8	20.3	19.0	24.8
TCP	20.1	51.2	44.5	61.2	77.0	77.8	71.5	70.3
¹⁴ CO ₂	34.1	0.2	23.8	0.3	4.7	0.3	4.5	0.4

have been produced. It has been established that the *R*-form is responsible for the fungicidal activity and is currently replacing the conventional racemic mixture that had been used. The application rate can be reduced by almost one-half; an obvious environmental advantage. Since it is not unusual for biological systems to show stereospecific responses, the question arises as to the environmental behavior of the different enantiomers.

R-Metalaxyl was lost more rapidly in soil at 23°C than the *S*-counterpart (Fig. 9.20).³⁸ The acid produced by hydrolysis of the ester, was the primary metabolite detected with the chiral configuration being retained. By using the racemic mixture, first-order rate constants for the *R*- and *S*-enantiomers were found to be 0.060 and 0.015 day⁻¹, respectively. The degradation of the acid derivatives was also shown to be stereoselective, however, the *S*-enantiomer was lost more rapidly than the *R*-form (0.030 vs. 0.014 day⁻¹). Starting with a racemic mixture the enantiomer ratio (ER = [S]/[R]) can be expressed as a function of the degradation rate constants of each enantiomer:

$$R_t = R_0 e^{-k_R t} \quad \text{and} \quad S_t = S_0 e^{-k_S t}$$

$$ER_t = [S]_t/[R]_t = [S_0]/[R_0] e^{-(k_R - k_S)t}$$

and since, in a racemic mixture $R_0 = S_0$

$$\ln ER_t = \Delta k t \quad \text{where} \quad \Delta k = k_R - k_S$$

Plotting $\ln ER$ as a function of t gives a straight line with the slope, $\Delta k = 0.038$ day⁻¹, which corresponds with a value of 0.045 day⁻¹ derived from rate constants calculated directly. The linear relation is lost when most of the *R*-enantiomer is lost. This stereospecific process clearly indicates the involvement of a biologically mediated process.

The investigation of the behavior of enantiomeric forms is an emerging field of study. One might expect to observe the kind of selectivity illustrated in this study, but at this point there is no basis for predicting how different enantiomeric isomers will respond.

9.5 DEGRADATION IN SOIL AND IMPACT ON GROUNDWATER

Groundwater is an important resource worldwide. Monitoring programs have found many examples of aquifers contaminated with low levels of organic compounds. Because water temperatures are usually low as is the level of any microbial activity, there is little potential for degradation processes to affect the levels of pollutants in an aquifer. Remediation processes are complex and expensive, so prevention of contamination becomes the best strategy for maintaining water quality. Contamination results from organic compounds leaching through the soil profile in the water, finally reaching the saturated zone. In many cases, soil characteristics are the overriding

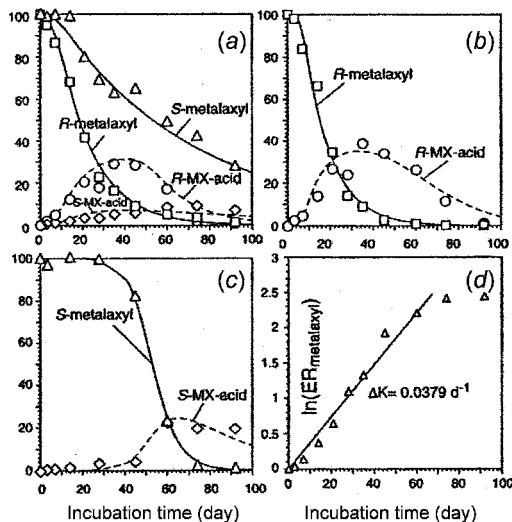


Figure 9.20 Degradation of *rac*-, (*R*)- and (*S*)-, metalaxyl in soil. (a) Degradation of *rac*-metalaxyl showing faster loss of the (*R*)-enantiomer. (b) Degradation of (*R*)-metalaxyl. (c) Degradation of (*S*)-metalaxyl showing a pronounced lag phase. (d) Plot of $\ln ER$ ($ER = [S]/[R]$) with time giving a rate difference of 0.038 day^{-1} and a linear relation showing that the enantioselectivity was maintained until $t > 60$ day. [Reproduced with permission from H. Buser, M. D. Müller, T. Poiger, and M. E. Balmer, *Environ. Sci. Technol.* **36**, 221 (2002). Copyright © 2002, American Chemical Society.]

factors in determining the potential for contamination. When a shallow aquifer is overlaid by a very porous soil with low sorbing capacity almost any organic compound will result in contamination given adequate movement of water through the system. By contrast, with a deep aquifer and a nonporous highly sorbing soil overlayer, organic compounds would be unlikely to reach the saturated zone. Between these two extremes the properties of the compound will be a factor in determining the potential for contamination.

Trichlorethylene, a solvent used extensively as a degreasing agent is often detected in groundwater as a result of inappropriate disposal practices or spills. Pesticides, by contrast, can be intentionally incorporated or applied to the soil and the detection of ethylene dibromide and aldicarb in groundwater prompted extensive surveys in the United States. After sampling thousands of wells particularly in agricultural areas, and analyzing for many pesticides, it was found that certain compounds were detected more frequently (Table 9.13).³⁹ By contrast, organophosphates and their sulfur analogues that have been used extensively are rarely detected. The different response must reflect differences in those properties influencing the tendency to leach. Sorption would restrict the movement through soil and the K_{OC} of the compound would thus provide a useful reference. Leaching through the soil profile is a relatively slow process since it depends on the water flux. Irrigation and precipitation would provide an excess and would result in downward move-

ment while surface evaporation would result in upward capillary movement through the soil. Consequently, compounds that persist in soil would have a better chance of being leached. Volatility could be a factor in some situations, but is not usually regarded as one of the major determining factors.

A number of mathematical models have been developed to simulate leaching.³⁹ These models would incorporate properties of the chemical and the soil along with application rates and hydrological factors. The objective of this analysis, however, is to focus on the chemical to determine what approach could be used to rank chemicals according to their potential to leach. This could provide what is termed a “First Tier” approach to identify potential “leachers” should they be present in favorable soil environments.

9.5.1 Groundwater Ubiquity Score (GUS)

An empirical approach has been used to classify pesticides based on their sorption and persistence.⁴⁰ When “leachers” and “nonleachers” are plotted as a function of the logarithm of their K_{OC} ($\text{mL} \cdot \text{g}^{-1}$) and soil $t_{1/2}$ (day), the former plot toward the left and upper region (Fig. 9.21). Hyperbolic functions were used to differentiate between the two classes:

$$\text{GUS} = \log_{10}(t_{1/2}) \times (4 - \log_{10} K_{OC})$$

With $\text{GUS} > 2.8$, pesticides were classified as leachers and $\text{GUS} < 1.8$, nonleachers. $\text{GUS} = 1.8\text{--}2.8$ was considered to be a transition zone that would indicate further analysis to predict their response in a given situation. From Table 9.14, it can be seen that pesticides that are often detected in groundwater are characterized by high GUS values. Also note that organophosphates, chlorpyrifos, and malathion

TABLE 9.13 Frequency with Which Some Pesticides Have Been Detected in U.S. Groundwater Samples

Compound and Class	MRL ^a ($\mu\text{g} \cdot \text{L}^{-1}$)	Detects	Wells Sampled
Atrazine, Triazine	0.12	1512	26,909
Metolachlor, acetanilide	0.75	213	22,255
2,4-D, phenoxy acetic acid	0.25	141	6,142
Diuron, substituted urea	0.32	160	17,865
Aldicarb sulfone, carbamate	0.62	5,070	37,652
Carbofuran, carbamate	1.2	4,107	27,881
DDT	0.15	108	3,115
Chlorpyrifos, organophosphate		32	5,398
Parathion, organophosphate		3	3,529
Ethylene dibromide	0.010	2,918	20,221

^aMinimum reporting level.

give low GUS values, primarily because of their short half-lives, which, of course, was the reason for selecting this class of compounds to replace the chlorinated organics such as DDT that were causing problems because of their persistence.

9.5.2 Degradation Rate and Groundwater Impact

The variation in K_{OC} values for a given compound would involve experimental uncertainties and some variation with the type of organic matter but would be expected to be less than an order of magnitude (see Sorption, Chapter 3). Degradation rates in soil can vary dramatically and, consequently, can influence the tendency to leach through soil to groundwater. Aldicarb, a carbamate, is very toxic and its detection in groundwater in a potato growing area of Long Island, N.Y., prompted a widespread effort to assess this type of impact from pesticides. Soil organisms oxidize aldicarb quite rapidly to the sulfoxide and sulfone (Fig. 9.22) with the parent and metabolites all being subject to simple physical hydrolysis.⁴¹ The sulfoxide and sulfone usually predominate in environmental samples.

An extensive monitoring study (8404 wells) in the Long Island region found that 13% of the wells contained aldicarb residues at concentrations above the 7 ppb health guideline, with the highest sample being 515 ppb. The contamination resulted from extensive use of aldicarb on sandy (porous, low SOC) acidic soils (pH ~5) subject to heavy rainfall and/or irrigation after application. By contrast, despite exten-

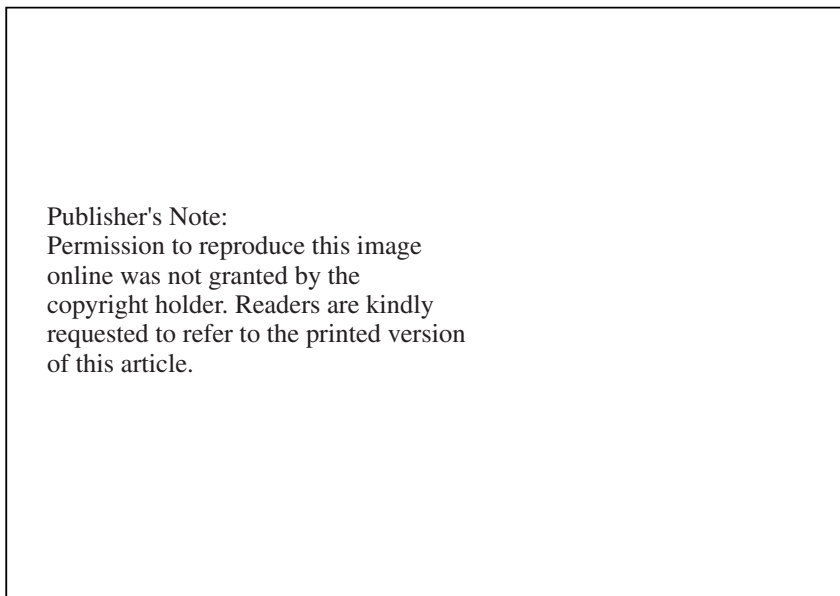


Figure 9.21 Distribution of pesticides that leach (●) and that do not leach (○) to groundwater and the GUS relation. [Reprinted with permission from D. I. Gustafson, *Environ. Toxicol. Chem.* **8**, 339. Copyright 1989, SETAC, Pensacola, FL, USA.]

TABLE 9.14 GUS Values for Selected Pesticides

Compound	K_{oc}^a	$t_{1/2}^a$	GUS	Compound	K_{oc}	$t_{1/2}$	GUS
Alachlor	170	15	2.1	1,2-Dichloropropane	50	700	6.6
Aldicarb	30	30	3.7	DDT	2×10^6	2000	-7.6
Aldicarb sulfone	10	20	3.9	Ethylene dibromide	34	100	4.9
Atrazine	100	60	3.6	Lindane	1100	100	1.9
Bromacil	32	60	4.4	Malathion	1800	2	0.22
Carbofuran	22	50	4.5	Methomyl	72	30	4.0
Chlorpyrifos	6070	30	0.32	Metolachlor	200	90	3.3
Dacthal	5000	100	0.60	Metribuzin	60	40	4.0
DBCP ^b	70	180	4.9	Simazine	130	60	3.4

^a From Ref. 16.

^b Dibromochloropropane.

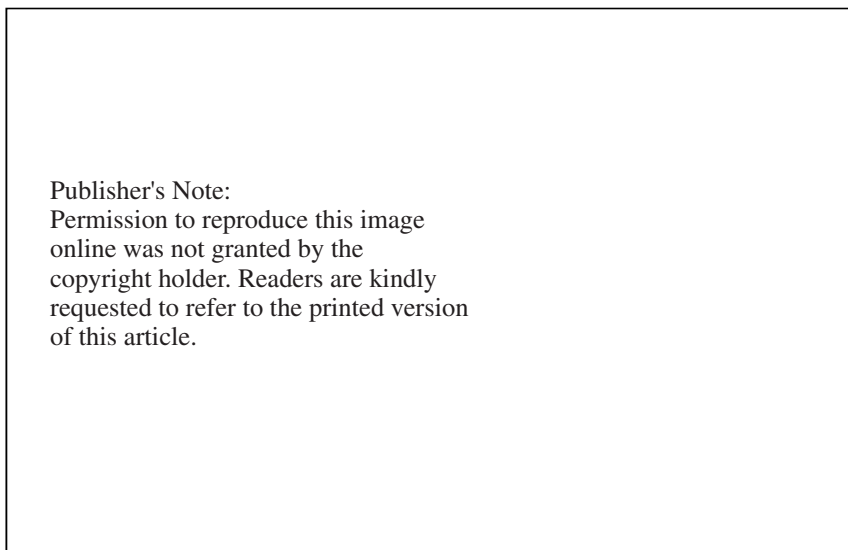


Figure 9.22 Degradation pathways for aldicarb.

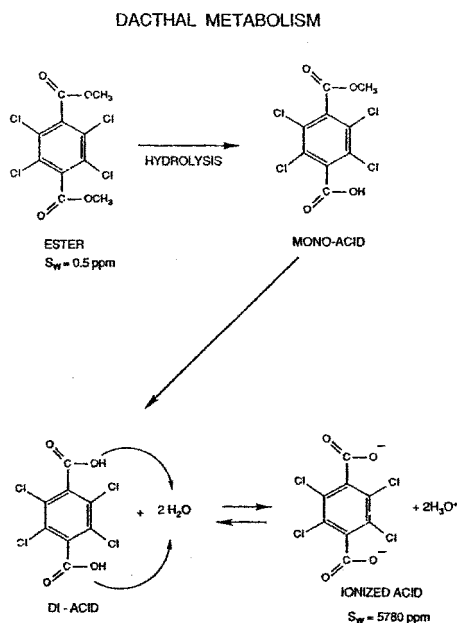
sive use, aldicarb residues could not be detected in a vulnerable aquifer (contained high nitrate and herbicide metabolite levels) associated with an agricultural region in eastern Oregon. Flood irrigation was used in this region on alkaline soils (pH 8–8.5) with low organic matter.⁴² The different response reflects the effect of soil pH on the rate of hydrolysis (Table 9.15) of aldicarb and its metabolites. Observations in dis-

TABLE 9.15 Rates of Hydrolysis of Aldicarb Sulfoxide and Sulfone at 23°C

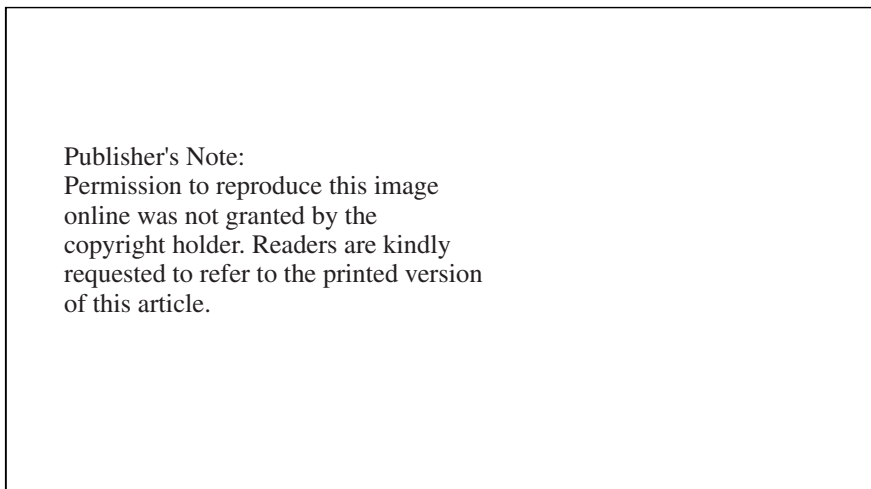
pH	k_h (day ⁻¹)		$t_{1/2}$ (days)	
	Sulfoxide	Sulfone	Sulfoxide	Sulfone
4.0	2.01×10^{-3}	5.31×10^{-4}	345	1304
5.0	2.05×10^{-4}	2.07×10^{-4}	3378	3345
6.0	2.80×10^{-4}	8.44×10^{-4}	2477	821
7.0	3.70×10^{-3}	8.35×10^{-3}	186	83
8.0	2.77×10^{-2}	7.22×10^{-2}	25	9.6
9.0	0.315	0.77	2.2	0.9
k_a (day ⁻¹)	20.1	5.71		
k_b (day ⁻¹)	2.77×10^4	7.22×10^4		
pH (I_{ab})	5.43	4.94		

tilled water provide a useful reference for reaction occurring in the soil water matrix.⁴³ The kinetic information does not indicate that the pH-independent pathway is of significance, hence estimates of k_a and k_b can be derived and the minimum rate of hydrolysis for both derivatives occurs around pH 5. The sulfoxide and sulfone are quite persistent at this pH with half-lives of the order of 3000 days at 23°C. Hydrolysis rates increase with temperature and the half-lives decrease to 340 and 485 days for the sulfoxide and sulfone. This analysis illustrates how soil pH can have a dramatic effect on the persistence of aldicarb and its derivatives and determine the extent to which it might leach through soil and contaminate groundwater.

With aldicarb, soil degradation can convert a "leacher" into a "nonleacher". The herbicide, Dacthal provides an example of the reverse effect, a "nonleacher" converted into a "leacher". Because of its low solubility, high K_{OC} , and relatively short half-life this compound shows a low GUS value (Table 9.14) and would not be expected to leach. The methyl esters of this molecule hydrolyze to generate the diacid and the kinetics of this process have been studied in the alkaline soils



from eastern Oregon.⁴⁴ These soils have a pH of 8.1 and 1.59% OM and the sample used was taken from a field in which onions had been raised and contained residual diacid. At 25°C, added dacthal degraded rapidly ($t_{1/2} = 16$ day) (Fig. 9.23). The initial reaction was due to soil microflora since the half-life increased ($t_{1/2} = 88.6$ day) at 38°C. Little of the mono-acid was detected since it was observed that it hydrolyzed more rapidly than the parent. The diacid metabolite was very stable with virtually no degradation observed over the experimental period. This compound would exist primarily as the anion at the soil pH with a solubility of



Publisher's Note:
Permission to reproduce this image
online was not granted by the
copyright holder. Readers are kindly
requested to refer to the printed version
of this article.

Figure 9.23 Degradation of dacthal in soil that contained residues of the diacid metabolite. Concentration of dacthal (□), the diacid produced (◆), and control soil (■). [Reproduced with permission from A. Wettasinghe and I. J. Tinsley, "Degradation of dacthal and its metabolites in soil", *Bull. Environ. Contam. Toxicol.* **50**, 226. Copyright 1993 Springer-Verlag, New York.]

>5000 ppm and would have little tendency to sorb, consequently it is not surprising that significant levels of this metabolite have been detected in groundwater.

REFERENCES

1. S. A. Tittlemier, M. Simon, W. M. Jarman, J. E. Elliot, and R. J. Norstrom, *Environ Sci. Technol.* **33**, 26 (1999).
2. W. H. Casey, *Science* **295**, 985 (Feb. 8, 2002).
3. C. K. Matthews and K. E. van Holde, *Biochemistry*, Benjamin/Cummings Publishing Co., Redwood City, CA, 1990.
4. A. H. Neilson, *Organic Chemicals, an Environmental Perspective*, Lewis Publishers, Boca Raton, FL, 2000.
5. E. Hodgson and P. E. Levi, *Modern Toxicology*, Appleton and Lange, Stamford CN, 1997.
6. M. A. Schuler, *Crit. Rev. Plant Sci.* **15**, 235 (1996).
7. G. L. Lamoreux, R. H. Shimabukuro, and D. S. Frear, "Glutathione and Glucoside Conjugation in Herbicide Selectivity", in J. C. Caseley, G. W. Cussans, and R. K. Atkin, Eds., *Herbicide Resistance in Weeds and Crops*, Butterworth-Heinemann Ltd., Oxford, 1991, pp. 227–262.

8. D. Coupland, "The Role of Compartmentation of Herbicides and their Metabolites in Resistance Mechanisms", in J. C. Caseley, G. W. Cussans, and R. K. Atkin, Eds., *Herbicide Resistance in Weeds and Crops*, Butterworth-Heinemann Ltd., Oxford, 1991, pp. 263–278.
9. J. V. Dean, J. W. Gronwald, and C. V. Eberlein, *Plant Physiol.* **92**, 467 (1990).
10. K. Kreuz and E. Martinoia, "Herbicide Metabolism in Plants: Integrated Pathways of Detoxication", in G. T. Brooks and T. R. Roberts, Eds., *Pesticide Chemistry and Bioscience, The Food-Environment Challenge*, Serial Pub. No 233, The Royal Society of Chemistry, Cambridge, U.K., 1999, pp. 277–287.
11. K. M. Scow, "Rate of Biodegradation", in W. J. Lyman, W. F. Reehl, and D. H. Rosenblatt, Eds., *Handbook of Chemical Properties Estimation Methods*, McGraw Hill, New York, 1982, pp. 9-1-85.
12. K. D. Racke, "Pesticides in the Soil Microbial Ecosystem", in K. D. Racke and J. R. Coats, Eds., *Enhanced Biodegradation of Pesticides in the Environment*, ACS Symposium Series No. 426, American Chemical Society, Washington, D.C. 1990, pp. 1–13.
13. D. E. Armstrong, G. Chesters, and R. F. Harris, *Proc. Soil Sci. Soc. Am.* **31**, 61 (1967).
14. A. Walker, Y. Moon, and S. J. Welch, *Pest. Sci.* **35**, 109 (1992).
15. USEPA, "Fate, Transport and Transformation Guidelines", Soil Biodegradation, OPPTS 835.3300, Jan. 1998.
16. A. G. Hornsby, R. D. Wauchope, and A. E. Herner, *Pesticide Properties in the Environment*, Springer, New York, 1996.
17. D. Mackay, W. Y. Shiu, and K. C. Ma, *Illustrated Handbook of Physical-Chemical Properties and Environmental Fate for Organic Chemicals*, Vols. I, II, and III, Lewis Publishers, Boca Raton, FL, 1992.
18. A. Walker, *Pesticide Sci.* **21**, 219, 1987.
19. J. E. Bauer and D. G. Capone, *Appl. Environ. Microbiol.* **54**, 1649 (1988).
20. J. S. Karns, "Molecular Genetics of Pesticide Degradation by Soil Bacteria", in K. D. Racke and J. R. Coats, Eds., *Enhanced Biodegradation of Pesticides in the Environment*, ACS Symposium Series No. 426, American Chemical Society, Washington, D.C. 1990, pp. 141–152.
21. J. B. Herrick, K. G. Stuart-Keil, W. C. Ghiorse, and E. L. Madsen, *Appl. Environ. Microbiol.* **63**, 2330 (1997).
22. R. D. Stapleton, G. S. Sayler, J. M. Boggs, E. L. Libelo, T. Stauffer, and W. G. Macintyre, *Environ. Sci. Technol.* **34**, 1991 (2000).
23. A. Walker, Y. Moon, and S. J. Welch, *Pesticid. Sci.* **35**, 109 (1992).
24. R. Frank, B. S. Clegg, and N. K. Patni, *Arch. Environ. Contam. Toxicol.* **21**, 41 (1991).
25. V. Laabs, W. Amelung, A. Pinto, and W. Zech, *J. Environ. Qual.* **31**, 256 (2002).
26. J. D. Wolt, H. P. Nelson, Jr., C. B. Cleveland, and I. J. van Wesenbeeck, *Rev. Environ. Contam. Toxicol.* **169**, 123 (2001).
27. L. R. Suntion, W. Y. Shiu, D. Mackay, J. N. Seiber, and D. Glotfelty, *Rev. Environ. Contam. Toxicol.* **103**, 1 (1988).
28. Q. Wu, D. L. Bedard, and J. Wiegel, *Appl. Environ. Microbiol.* **63**, 2836 (1997).
29. J. F. Brown, Jr., D. L. Bedard, M. J. Brennan, J. Carnahan, H. Feng, and R. E. Wagner, *Science* **236**, 709 (1987).

30. E. R. Master, V. W.-M. Lai, B. Kuipers, W. R. Cullen, and W. W. Mohn, *Environ. Sci. Technol.* **36**, 100 (2002).
31. R. S. Boethling and M. Alexander, *Appl. Environ. Microbiol.* **37**, 1211 (1979).
32. M. Alexander, *Env. Sci. Technol.* **19**, 106 (1985).
33. J. W. Hamaker and C. A. I. Goring, "Turnover of Pesticide Residues in Soil", in R. F. Gould, Ed., *Bound and Conjugated Pesticide Residues*, A.C.S. Symposium Series, No. 29, American Chemical Society, Washington, D.C., 1976, pp. 219–243.
34. H. J. Di, L. A. G. Aylmore, and R. S. Kookana, *Soil Sci.* **163**, 404 (1998).
35. P. B. Hatzinger and M. Alexander, *Environ. Sci. Technol.* **29**, 537 (1995).
36. K. D. Racke, D. A. Laskowski, and M. R. Schultz, *J. Agr. Food Chem.* **38**, 1430 (1990).
37. K. D. Racke, *Rev. Environ. Contam. Toxicol.* **131**, 2 (1993).
38. H. Buser, M. D. Müller, T. Poiger, and M. E. Balmer, *Environ. Sci. Technol.* **36**, 221 (2002).
39. J. E. Barbash and E. A. Resek, *Pesticides in Ground Water Distribution, Trends and Governing Factors*, Ann Arbor Press Inc., Chelsea, MI, 1996, 588 pp.
40. D. I. Gustafson, *Environ. Toxicol. Chem.* **8**, 339 (1989).
41. H. A. Moyer and C. J. Miles, *Rev. Env. Contam. Toxicol.* **105**, 99 (1988).
42. C. C. Shock, M. Seddigh, J. H. Hobson, I. J. Tinsley, B. M. Shock, and L. R. Durand, *Agron. J.* **90**, 399 (1988).
43. E. N. Lightfoot, P. S. Thorne, R. L. Jones, J. L. Hansen, and R. R. Romine, *Environ. Toxicol. Chem.* **6**, 377 (1987).
44. A. Wettasinghe and I. J. Tinsley, *Bull. Environ. Contam. Toxicol.* **50**, 226 (1993).

Synthesis

The major objective of environmental chemistry is to interpret and predict the behavior of chemicals, for example, as they might leach from a landfill, are released into the air, or water from some industrial facility or applied for the control of pests of agricultural or public health significance. An understanding of how the compound distributes and persists is critical in controlling these situations to minimize adverse effects. To this point, the discussion has focused on specific processes controlling distribution and transformation and it is necessary to outline approaches that are being used to define how they interact. For example, the transformation of any compound will depend on how it distributes, while the distribution, in turn, will be influenced by the manner in which the compound is released; is it released into the atmosphere or incorporated into the soil?

Two basic approaches are being used in this overall analysis. In one approach, experimental systems are developed to represent some part of the environment and the behavior of the chemical is monitored in these systems. Alternatively, mathematical models can be constructed using those quantities defining distribution, and transformation along with appropriate environmental parameters. Examples will be provided to illustrate these approaches, but this discussion will not be comprehensive given the extensive developments in these areas. The primary objective will be to develop a sense for how the individual processes contribute to the overall behavior of a compound.

10.1 MICROCOSMS AND MESOCOSMS

Microcosms can be defined as “controlled, reproducible laboratory systems that attempt to simulate the situation in a portion of the real world”,¹ while mesocosms are “manmade, surrogate ecosystems that can be used to assess the fate and effects of chemicals at many different levels of biological organization”.² Mesocosms are “bounded, and partially enclosed outdoor experimental systems that fall, in complexity, between laboratory microcosms and the real world macrocosm”.² The definition of a mesocosm has been refined further as a “physically confined multitrophic

and self-maintaining system that has a duration time exceeding the penultimate trophic level present and whose size is sufficient to enable pertinent sampling and measurements without seriously influencing the structure and dynamics of the system".³ Thus mesocosms are larger, more biologically complex outdoor experimental units in contrast to the smaller laboratory microcosm. Useful information on chemical dynamics is derived from mesocosms, however, the major use of these systems is in the definition of ecological effects of chemicals. Generally speaking, microcosms are more contained and provide a more comprehensive analysis of the environmental distribution of a chemical.

10.1.1 Microcosms

Many simple laboratory microcosms have been constructed primarily to assess the behavior of the chemical in both terrestrial and aquatic systems.³⁻⁵ Another approach has been to bring a "piece" of the environment into the laboratory. Soil cores have been used to monitor the fate of both inorganic and organic contaminants.¹ A complex terrestrial microcosm will be described to illustrate what is involved in the design and operation of such a unit and the nature of the data generated.

10.1.1.1 Terrestrial Laboratory Microcosm⁶⁻⁸ The microcosm (Fig. 10.1) consists of a glass box (1.0 × 0.75 × 0.61-m deep) with a Plexiglass lid that is fitted with an access port (20 × 30 cm). Lighting is provided by white fluorescent tubes and pink incandescent fixtures providing 2500 foot candles at the soil surface with a 16-h daily photoperiod. Dawn and dusk were simulated by varying the power from 0 to 100% and vice versa over a 30-min period. The day–night temperature varied from 30.25 to 18.25°C. Filtered air flowed through the chamber at 50 L · m⁻¹ and was sampled for particulates, condensate and gases at the exhaust port. Soil was comprised of potting mix (10% by weight), sea sand (45%) and illite clay (45%) and was added as three 6–8-cm layers with each layer compacted overnight. Earthworms (75) and nematodes (40,000) were incorporated in the last layer of soil. Water is supplied as "rain" through nozzles suspended in the lid or in some instances through a "spring" system.

The chemicals (Table 10.1) used in this study were fungicides and were added by treating the alfalfa (30 g) and rye grass (20 g) seed with the ¹⁴C-labeled compounds at levels consistent with normal agricultural practice. After the seeds were scattered on the soil surface, they were covered with 1–2 cm of soil mixture and sea sand.

Organisms were selected based on their tendency to influence the distribution of the chemical between soil, plant, and other organisms, the ease with which they can be maintained in the laboratory and their compatibility. Inputs into the microcosm are summarized in Table 10.2. The development, construction and operation of such a system is quite complex and very expensive. It thus becomes important to review the data generated and to evaluate the extent to which it provides a reasonable representation of the natural environment and whether this information justifies the expense.

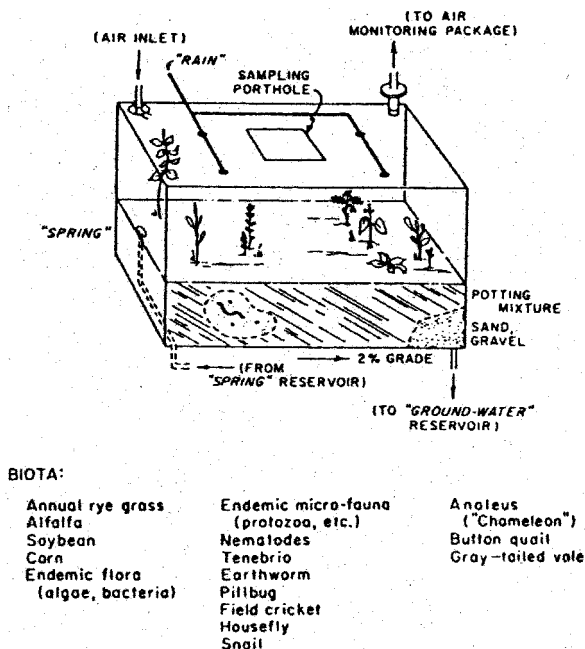


Figure 10.1 Schematic representation of a terrestrial microcosm chamber. [Reproduced with permission from J. W. Gillett and J. D. Gile, *Intern. J. Environmental Studies* **10**, 15. Copyright 1976, Taylor and Francis.]

At termination, the distribution of the compounds, among the compartments of the microcosm is summarized in Figure 10.2, while the profile through the soil is given in Figure 10.3. It is a useful exercise to interpret these data in terms of the properties of the compounds (Table 10.1).

10.1.1.2 Dieldrin Retention of this compound in soil and its limited movement through soil would be consistent with the slow degradation rate and the high K_{ow}

TABLE 10.1 Properties at 25°C of Fungicides Used in Microcosm Studies

Compound	S_w ($\text{mg} \cdot \text{L}^{-1}$)	P^o (Pa)	$\log K_{ow}$	$t_{1/2}^b$ (day)	H'
Pentachloronitrobenzene (PCNB)	0.071	0.015	5.28	150–300	0.025
Pentachlorophenol (PCP) ^a	15	0.115	5.12	40	3.19×10^{-5}
Hexachlorobenzene (HCB)	0.005	0.0023	5.50	>1000	0.056
Captan	5.10	1.1×10^{-5}	2.35	3–5	2.42×10^{-4}
Dieldrin (HEOD)	0.20	4.00×10^{-4}	5.20	>1000	0.0013

^a PCP, $pK_a = 4.90$.

^b Approximate half-life in soil.

TABLE 10.2 Inputs to the Terrestrial Microcosm

Day	Input
0	← 3 layers of soil ← earthworms, nematodes ← rye grass seed (30 g), alfalfa seed (20 g)
10	
19	← 100 crickets ← 100 pill bugs ← 100 meal worm larvae ← 6 snails
20	
30	← vole ← 50 crickets
34	← crickets and/or meal worm larvae
36	← crickets and/or meal worm larvae
39	Termination HCB
41	Termination PCP and Dieldrin
44	Termination Captan
47	Termination PCNB

(= high K_{oc}). A value for the organic matter content of the soil is not listed, however, it would be expected to be relatively high (possibly 2–5%) given the amount of potting mix used. Loss to air would be related to the Henry's law constant, since the moisture level in the system would need to be maintained and the low value for dieldrin would be consistent with this assumption. The proportion associated with plants is of interest but could be accounted for by the tendency to distribute into the roots (Fig. 10.4).

10.1.1.3 HCB One might expect this compound to show a distribution comparable to dieldrin, however, the distribution into air might appear to be unusually high, but not inconsistent with the fact that the Henry's law constant for HCB is 40 times higher than that for dieldrin.

10.1.1.4 PCNB The distribution of this compound into air can also be related to its Henry's law constant, while uptake and retention in plants could be associated with the fact that it is more readily metabolized. The most likely metabolite is the amine, which would be more water soluble than the parent, and more readily move through the plant.

10.1.1.5 PCP Although a soil pH is not provided, it is reasonable to assume that it would be >5 and this compound would exist primarily as the more water soluble anion. This would account for its movement through the soil. However, the proportion detected in the air is unexpected. One possibility to account for this anomaly

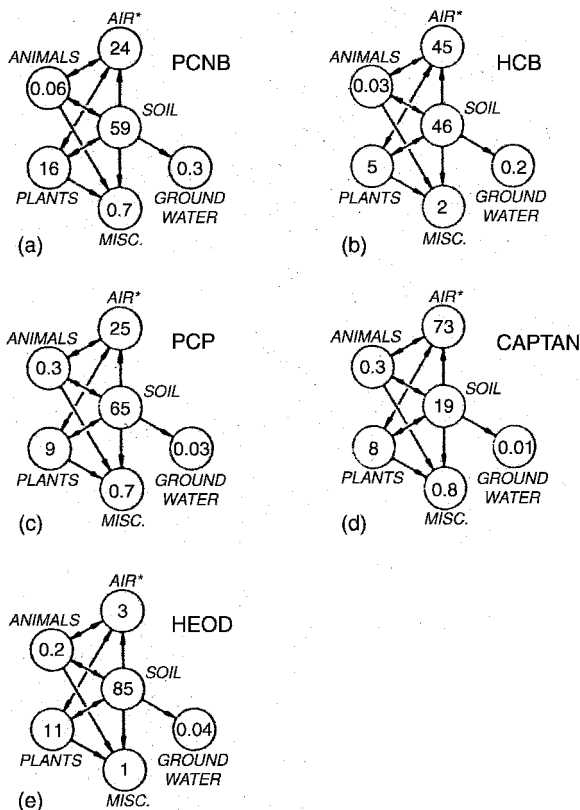


Figure 10.2 The ^{14}C mass balance in the microcosm after seed treatment with (a), pentachloronitrobenzene, (b), hexachlorobenzene, (c) pentachlorophenol, (d), captan, (e), dieldrin (HEOD). [Reproduced with permission from J. D. Gile and J. W. Gillett, *J. Agr. Food Chem.* 27, 1159 (1979). Copyright © 1979, American Chemical Society.]

is metabolism to $^{14}\text{CO}_2$. The trapping system would not differentiate between labeled parent compound as a gas and CO_2 .

10.1.1.6 Captan Loss of this compound from soil can be explained by its low persistence in this compartment. But the high proportion detected in the air is inconsistent with its low Henry's law constant. This response is due to the fact that unlike the other compounds tested that have the ^{14}C incorporated in a stable ring, the ^{14}C label is in a $-\text{SCCl}_3$ fragment that is readily metabolized to CO_2 . Movement through soil would also be limited by the rapid metabolism of this compound.

This analysis demonstrates that the microcosm provides distribution data that is consistent with what might be predicted on the basis of the relevant properties of the compounds, although the data do demonstrate that even the location of the label can have a significant effect. More definitive information could be generated by chemical

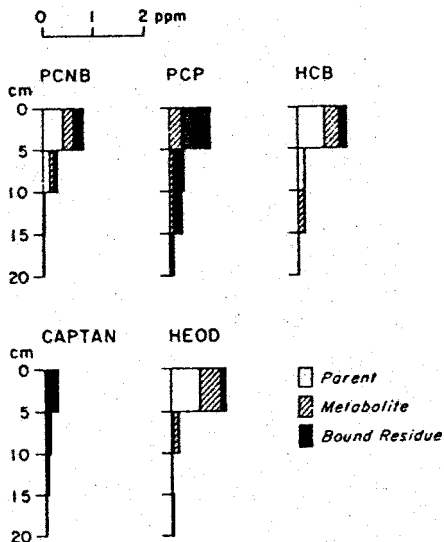


Figure 10.3 Vertical profile of ^{14}C distribution in soil at the completion of the experiment. Chemicals applied as a seed treatment. [Reproduced with permission from J. D. Gile and J. W. Gillett, *J. Agr. Food Chem.* **27**, 1159 (1979). Copyright © 1979, American Chemical Society.]

analysis of the compound and its metabolites, however, this would increase the cost of the study dramatically. Additional information was generated regarding the levels and disposition of the compounds in the alfalfa and rye grass. Differentiation between the parent compound and metabolites was accomplished by chromatography on silica gel plates (Fig. 10.4). Although the data are inconsistent, the differences in metabolism among the compounds is evident and the decrease with time is probably due to dilution as the plant mass increases with time. Levels of the compounds in the biota were also reported but will not be included here.

10.1.2 Mesocosms

Mesocosms have been developed to represent a variety of aquatic systems² including model streams, experimental ponds, flow-through wetlands, and enclosures. The primary focus of this approach is to assess ecotoxicological effects with the complementary data on chemical behavior a necessary adjunct to develop dose–response relations.

10.1.2.1 Limnocorral Study A “limnocorral” is an enclosed water column in a lake, pond, or marine environment that may or may not be in contact with the bottom sediments. Such a system has been used to study the effects of a wood preservative, tetrachlorophenol (Fig. 10.5).^{10,11} The water column (5 m × 5 m and ~4.5 m deep) is enclosed by vinyl walls and a polyethylene liner was installed

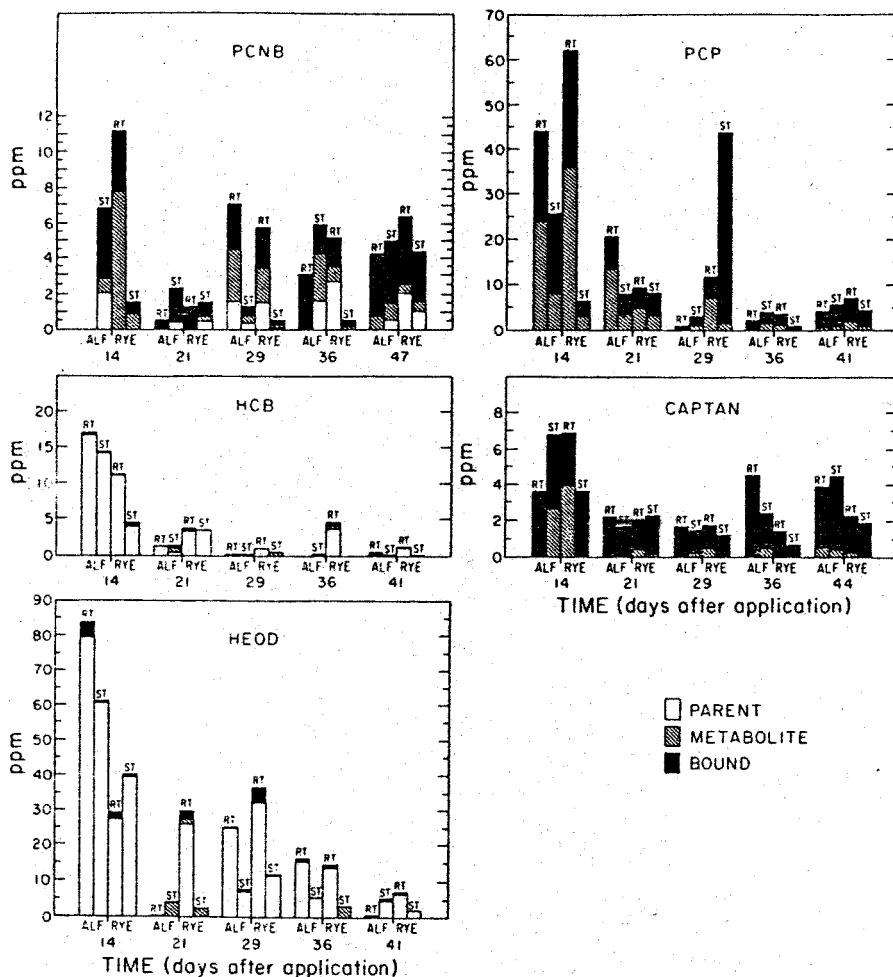


Figure 10.4 Residue patterns in alfalfa and rye grass shoots and roots from the microcosm after chemical applied as a seed treatment. [Reproduced with permission from J. D. Gile and J. W. Gillett, *J. Agr. Food Chem.* **27**, 1159 (1979). Copyright © 1979, American Chemical Society.]

prior to each study to minimize the effect of biota accumulating on the vinyl walls. The enclosure is in contact with an unconsolidated organic sediment layer that is up to several meters deep. The DOC content was $6.7 \text{ mg} \cdot \text{L}^{-1}$ and the pH 8.1–8.4. Surface temperatures ranged from 22.5 to 25.0°C. Specified amounts of a commercial product containing 2,3,4,6-tetrachlorophenol (15.7%) and pentachlorophenol (2.4%) as the sodium salts were dissolved in a liter of the lake water in a sprayer and applied as a single uniform surface treatment. Since the pK_a values of the tetrachlorophenol and the PCP contaminant were 5.5 and 4.9, respectively, they would

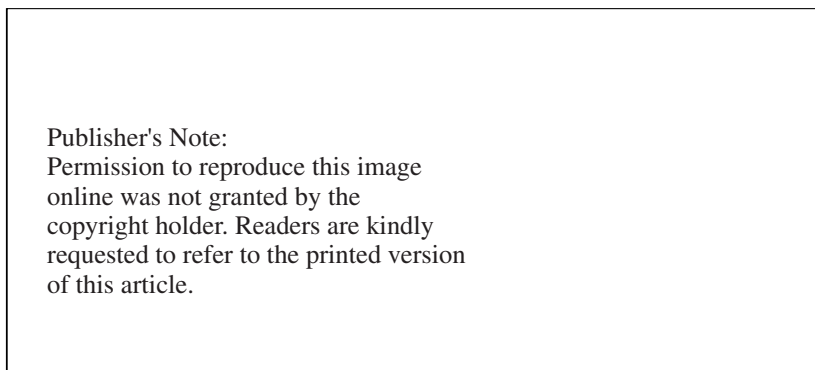


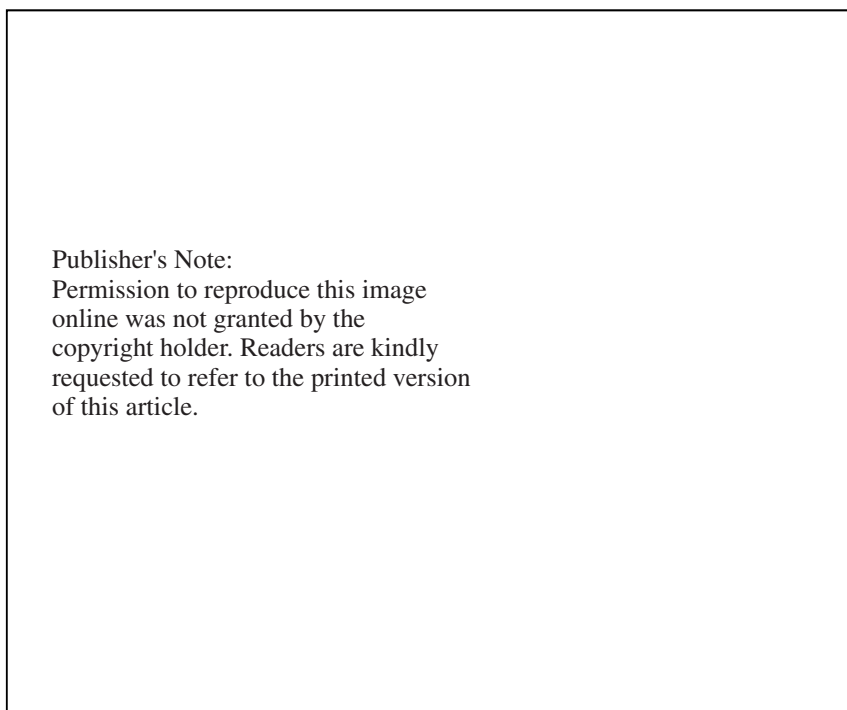
Figure 10.5 Schematic representation of a limnocorral. [Reproduced with permission from K. Liber, K. R. Solomon, and J. H. Carey, *Environ. Toxicol. Chem.* **16**, 293. Copyright 1997, SETAC, Pensacola, FL, USA.]

exist as the anion at the pH of the limnocorrals. The change in concentration of the phenols in the water was monitored as a function of application time and depth. A depth-integrating sampler was used to give an overall estimate of the amount of phenol in the system. In addition, the concentration was monitored in the sediments and on a sample of the polyethylene to assess the extent that sorption on the liner could be a factor.

The change in concentration of the two phenols is shown in Figure 10.6. The rate of loss approximates a first-order process and the times for 50% loss, DT_{50} , are summarized in Table 10.3. In Experiment 1, the phenols were applied between 10:25 and 11:45 AM, and in Experiment 2, at dusk, between 7:30 and 8:45 PM with sunrise occurring ~ 10 h later. It was proposed that photochemical degradation was primarily responsible for the loss of the phenols and the evening application delayed the degradation and also allowed more time for the chemicals to move into deeper water. Since both compounds existed as anions, evaporation would not contribute to the loss. Biological transformation would also be limited since the phenols did not

TABLE 10.3 Tetra- and Pentachlorophenol Degradation in a Limnocorral

Experiment	Treatment Level ($\text{mg} \cdot \text{L}^{-1}$)	DT_{50} (day)
Morning application	TeCP 0.065	0.44
	TeCP 0.65	0.99
	PCP 0.010	0.55
	PCP 0.10	1.08
Evening application	TeCP 0.65	3.75
	TeCP 1.30	5.18
	PCP 0.10	3.44
	PCP 0.20	4.77



Publisher's Note:
 Permission to reproduce this image
 online was not granted by the
 copyright holder. Readers are kindly
 requested to refer to the printed version
 of this article.

Figure 10.6 Dissipation of 2,3,4,6-tetrachlorophenol (TeCP) and pentachlorophenol (PCP) using integrated water samples from a limnocorral (a) following a morning application and (b) an evening application. [Reproduced with permission from K. Liber, K. R. Solomon, and J. H. Carey, *Environ. Toxicol. Chem.* **16**, 293. Copyright 1997, SETAC, Pensacola, FL USA.]

accumulate to any extent in the biota. These two compounds did not prove to be particularly persistent in this system with >99% loss occurring over the 43-day experimental period for the morning application and the 63-day period for the evening application. That photodegradation was primarily responsible for the loss was supported by the observation that the phenols persisted for longer periods in deeper water (Table 10.4), the radiant energy being attenuated by the water column.

The distribution of the phenols into sediment and a polyethylene liner sample is given in Figure 10.7. So little compound was associated with the liner that it was not considered a significant factor in accounting for their overall fate. Pentachlorophenol accumulated in sediments to a greater extent than the tetrachlorophenol. This tendency is illustrated by the fact that at 15 days the concentration of the former in the wet sediment was $8.8 \mu\text{g} \cdot \text{kg}^{-1}$ with a water column concentration of $1.8 \mu\text{g} \cdot \text{L}^{-1}$ while the corresponding values for the tetra phenol were $2.0 \mu\text{g} \cdot \text{kg}^{-1}$ and $28.6 \mu\text{g} \cdot \text{L}^{-1}$. The sediments contained >90% water and the amount of tetrachlorophenol in sediment can be accounted for by what is dissolved

TABLE 10.4 Chlorophenol Persistence with Depth

Compound	Depth (cm)	DT ₅₀ (h)
Tetrachlorophenol	5	8.8
	50	12.1
	100	55.0
Pentachlorophenol	5	8.8
	50	12.0
	100	58.2

in the water. Sorption of the pentachlorophenol could perhaps be due to the formation of ion pairs (see Section 3.5.2.1, Sorption) since one would not expect the anion to sorb to any extent.

This mesocosm study provides useful information on the behavior of these phenols in an aquatic system, but to obtain an overall assessment of the utility of this approach it is necessary to illustrate the ecological information that is generated.¹³ The response was associated with the levels of phenol since little if any change was observed when the product was applied in the morning and photochemical degradation reduced the levels present. However, at the higher concentrations resulting from the evening application, decreases were observed in abundance in two major classes of organisms (Fig. 10.8). Rotifers were more susceptible as a class than the macrozooplankton, however, both had recovered by the end of the experimental period. Variations in response were observed within the rotifer class with one species (*Polyarthra*) exhibiting a concentration-dependent response and another

Publisher's Note:
 Permission to reproduce this image
 online was not granted by the
 copyright holder. Readers are kindly
 requested to refer to the printed version
 of this article.

Figure 10.7 Fate of TeCP and PCP in water, sediment, and adsorbed to the plastic liner of the limnocorral treated with $0.75 \text{ mg} \cdot \text{L}^{-1}$ of DIATOX[®] (0.65 mg TeCP and 0.10 mg PCP). [Reproduced with permission from K. Liber, K. R. Solomon and J. H. Carey, *Environ. Toxicol. Chem.* **16**, 293. Copyright 1997, SETAC, Pensacola, FL, USA.]

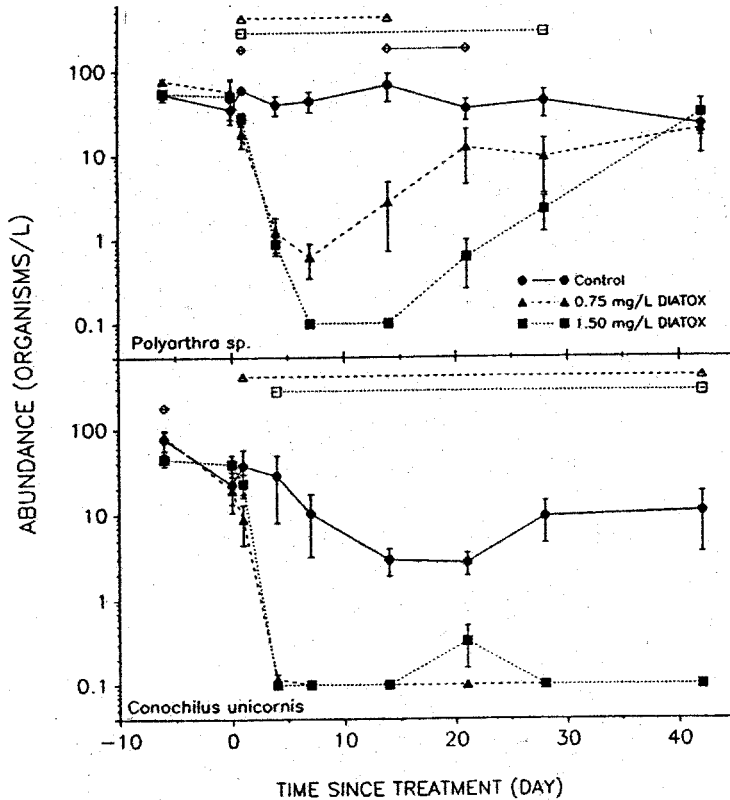


Figure 10.8 Changes in abundance of two rotifer taxa in control, 0.75 and 1.50 mg · L⁻¹ DIATOX treated limnocorrals. Open symbols and horizontal lines at the top of each figure indicate when treatments were significantly different. [Reproduced with permission from K. Liber, K. R. Solomon, N. K. Kaushik, and J. H. Carey, "Impact of 2,3,4,6-Tetrachlorophenol (DIATOX[®]) on Plankton Communities in Limnocorrals", in R. L. Graney, J. H. Kennedy, and J. H. Rodger's, Eds., *Aquatic Mesocosm Studies in Ecological Risk Assessment*, Copyright 1993, Lewis Publishers, Boca Raton, pp. 257–294.]

(*Conochilus*) not recovering within the experimental period. Much more information is reported but it can be seen that the mesocosm units are of sufficient size to support populations of organisms that are large enough to assess response to the chemical but not so large as to preclude replication. Note that each observation represents the mean from three units.

10.2 MATHEMATICAL MODELS

A mathematical expression that defines a given process provides an index of the level of understanding of that process. This expression is based on an understanding

of mechanism—how does the system work? Quite often, experimental information provides the basis for a mechanistic hypothesis (model) which, in turn, provides the stimulus for additional studies that either validates, or leads to further refinement of the model. Simple models are used, for example, to define the rates of chemical reactions in solution while more complex models, represented by Michaelis–Menten kinetics, can be used to represent the rate of an enzyme-catalyzed reaction. Mathematical representations or models are an integral part of the scientific process.

It has been demonstrated that it is possible to develop simple mathematical models to define many of those processes that are involved in determining environmental behavior. A logical extension of this approach is to explore the possibility that a mathematical integration of these simple models can provide a more complex model that will represent the overall behavior of compounds in the environment. This has been an active area of research in the field of environmental chemistry and models have been developed to simulate many systems ranging from the relatively confined situation of the movement through soil to groundwater, to the behavior of a compound in a large geographic region. Note that even the former model becomes very complex when all the contributing variables are considered. It has been said (attributed to a statistician, George Box) that “all models are wrong, but some are useful!”

The implication is that for even a relatively simple system it is difficult to develop a model that truly represents the natural environment. It is found that the more precise the objective the greater the data requirements and the more restrictive the model becomes. So, all models, to some extent, involve a compromise. Consequently, it is necessary to define the objective of a modeling study that will then determine the interpretation of the output and how it can be “useful”. Unfortunately, there are numerous illustrations of how the output of a model can be misinterpreted and misused.

In this respect, then, an important distinction is that between a research and an evaluative model. The latter will consist of a more simplified representation of a natural system and not require large data input. Although the model may provide a numerical solution, it should only be considered a rough estimate. Such models cannot be validated in the strict sense of the word although environmental observations can provide some indication as to whether solutions are “in the ball park”! This level of precision is useful for comparative purposes and can provide an overall assessment of the environmental behavior of a chemical within the constraints defined. Such a model is a useful educational tool and the level of precision can be adequate for management decisions.

By contrast, a research model is designed to test a hypothesis and will have a clear mechanistic base and a comprehensive data requirement. Validation becomes an integral part of the process in suggesting further refinements in the model and/or the hypothesis. The model can also suggest possible research directions. A research model will be more restricted in scope than an evaluative model. Consequently extrapolations from a restricted research model or expecting evaluative models to provide precise quantitative assessments would be examples of misuse.

10.2.1 Multimedia, Mackay-Type Fugacity Models

These evaluative models divide the environment into homogeneous compartments, air, soil, water, and sediment and define the distribution among, and loss from these compartments. The models are based on the properties of the compound that define its distribution and transformation as well as characteristics of the environment under study, such as size of, and advective rates through compartments.¹³⁻¹⁶ Three levels, of increasing complexity, have been defined (Fig. 10.9):

Level I outlines how a given quantity of chemical would equilibrate among environmental compartments.

Level II builds on this distribution by introducing factors determining loss from the system both by advective flow out of, or chemical transformations that could occur in a compartment. With a constant chemical input, a steady state is defined.

Level III adds an additional degree of complexity by defining the rates of transfer between compartments. A constant input will generate a steady state, but the chemical will not be at equilibrium among the compartments.

10.2.1.1 Fugacity and Fugacity Capacity The fugacity, f , of a compound in a given phase is defined as its “escaping tendency” from that phase and will have units of pressure. Thus the fugacity of a gas will be its partial pressure while the fugacity of a pure liquid or solid will be given by its equilibrium vapor pressure at the specified temperature. When a compound is at equilibrium between two phases, its fugacity will be the same in each phase and there will be no net movement between phases. The fugacity would be represented by the level of the fluid in each tank (Fig. 10.9), will indicate the direction of mass flow, and is compared to temperature that will determine the direction of the flow of heat energy.

Concentration ($\text{mol} \cdot \text{m}^{-3}$) is a linear function of fugacity (Pa) and is defined

$$C = f \cdot Z$$

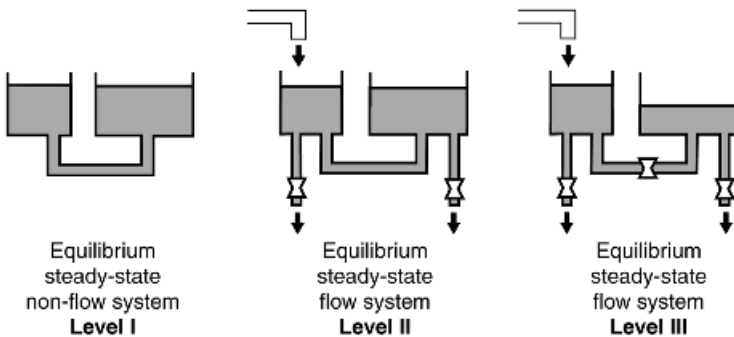


Figure 10.9 Tank analogies for the levels I, II, and III fugacity models. [Reproduced from D. Mackay and S. Paterson, *Environ. Sci. Technol.* **16**, 654A (1982) with permission of the author.]

with Z , the fugacity capacity having units of $\text{mol} \cdot \text{Pa}^{-1} \cdot \text{m}^{-3}$ and is represented by the size of the tank (Fig. 10.9). Consequently, if a compound is at equilibrium between two phases

$$f_1 = f_2 \quad \text{and} \quad C_1/Z_1 = C_2/Z_2 \quad \text{and so} \\ C_1/C_2 = Z_1/Z_2 = K_e$$

The equilibrium constant is then the ratio of the fugacity capacities. The magnitude of Z will depend on temperature and the properties of the compound as they relate to the characteristics of a given phase. Compounds will accumulate in compartments with a high value of Z . The next step is to define Z for environmental compartments; air, water, soil, sediments, and biota.

Z_{air} . The fugacity is the partial pressure, P_a . From the equation of state, the concentration of the compound in the vapor phase will be given by

$$C_{\text{air}} = f_{\text{air}} Z_{\text{air}} = \frac{n}{V} = \frac{P}{RT} = \frac{f_{\text{air}}}{RT}$$

and so, $Z_{\text{air}} = 1/RT = 4.04 \times 10^{-4} \text{ mol} \cdot \text{m}^{-3} \cdot \text{Pa}^{-1}$ at 298°C and $R = 8.31 \text{ Pa} \cdot \text{m}^3 \cdot \text{mol}^{-1} \cdot \text{K}^{-1}$.

Z_w . The fugacity of a compound in water, f_w , would be given by the pressure of that compound in the vapor phase that would be defined by the Henry's law constant, and so

$$Z_w = C_w/f_w = C_w/P = 1/H$$

The fugacity capacity in water is thus the reciprocal of the Henry's law constant. It should be emphasized that the concentration of the compound in water refers only to the amount in solution and does not include compound that could be associated with suspended sediment, for example.

Z_s . This analysis would apply to soils or sediments. At equilibrium the fugacities in soil and water would be equal, and so

$$f_s = f_w \quad \text{and thus} \quad C_s/Z_s = H \cdot C_w,$$

remembering that the fugacity of a compound in aqueous solution would be its vapor pressure as defined by H . Also note that the concentration in the sorbed phase would be $\text{mol} \cdot \text{m}^{-3}$. The soil/water distribution ratio, K_d has units $\text{mL} \cdot \text{g}^{-1}$ and would be defined:

$$K_d = X/C_w$$

The amount sorbed, X , is defined as mass per unit mass of sorbent and thus:

$$C_s = X \cdot \rho_s$$

where ρ_s , the density of the soil or sediment, would be expressed as $\text{g} \cdot \text{mL}^{-1}$ or $10^6 \text{ g} \cdot \text{m}^{-3}$. So,

$$Z_s = C_s/H \cdot C_w = \frac{X\rho_s K_d}{X \cdot H} = K_d \rho_s / H \text{ or sometimes referred to as } Z_w(K_d \rho_s)$$

In the event density is cited as $\text{kg} \cdot \text{m}^{-3}$, $Z_s = K_d \rho_s^* / 1000H$. The sorption potential of a neutral compound is defined by the soil–organic carbon distribution ratio K_{oc} and, consequently, for a specific soil or sediment $K_d = \varphi_{oc} K_{oc}$, where φ_{oc} is the mass fraction of organic carbon in the soil. Experimental values of K_{oc} may be available in the literature but can also be derived from K_{ow} or S_w as has been discussed previously (Sorption, Chapter 3).

An analysis comparable to that developed for soil gives Z value for biota

$$Z_{bi} = (K_B \rho_{bi}) / H \approx K_B / H$$

since the density would be close to one.

Experimental values for the bioconcentration factor K_B may be available or can be derived from K_{ow} as discussed (Absorption & Bioconcentration Chapter 5).

10.2.1.2 Level I Model The components of a multimedia model are illustrated in the schematic (Fig. 10.10) with the four major compartments being, air, water, sediment, and soil. The equilibrium distribution of a fixed quantity of chemical among these compartments is defined by the Level I model, and by definition, the fugacities in each compartment would be equal

$$f_1 = f_2 = f_3 = \dots f_i$$

The number of moles in a compartment, M_i , would be determined by its volume and concentration

$$M_i = C_i V_i = f_i Z_i V_i$$

The total amount of compound added to the system, M_{tot} , would be the sum of the amounts in each compartment, since in this model it is assumed that there is no loss from a compartment by degradation or advection, and thus

$$M_{tot} = \sum M_i = \sum f_i Z_i V_i = f_i \sum z_i V_i$$

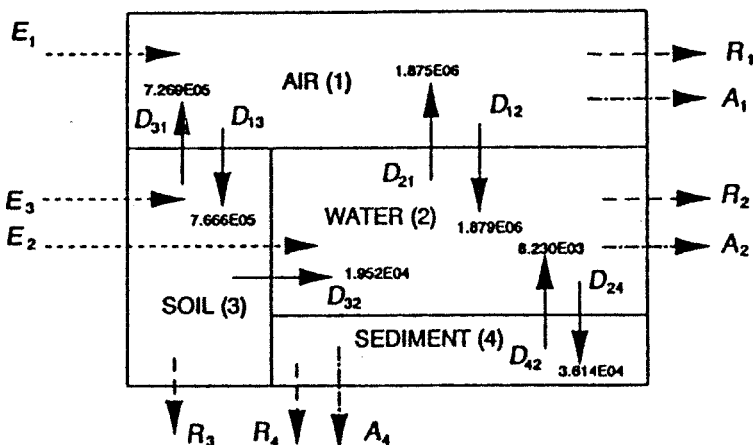


Figure 10.10 Representation of the four major compartments of a fugacity model along with D values for intercompartment transfer in a level III model. Input, E , reaction, R , and advection, A , options are indicated. [Reprinted from D. Mackay, S. Paterson, and W. Y. Shiu, "Generic models for evaluating the regional fate of chemicals", *Chemosphere* **24**, 695. Copyright 1992, with permission from Elsevier.]

the fugacity can be calculated

$$f = M_{\text{tot}} / (\sum Z_i V_i)$$

and the concentration ($C_i = f \cdot Z_i$) total amount in each compartment ($M_i = C_i V_i$) at equilibrium can be calculated.

The use of this model is illustrated by the distribution of 1,2,3-trichlorobenzene in a regional system¹⁷ whose characteristics are summarized in Table 10.5. This system has also been used in the analysis of the environmental behavior of many compounds.¹⁸ An area of 100,000 km² (1×10^{11} m²), which would correspond roughly to the area of the state of Ohio, and a 1000 m atmospheric height have been selected. It is also assumed that 10% of the area is water with an average depth of 20 m that would give this compartment a volume of 2×10^{11} m³. The soil is considered to be mixed uniformly to a depth of 10 cm giving a volume of

TABLE 10.5 Model Dimensions

Property	Air	Water	Soil	Sediment	Susp. Sed.	Biota
Area (m ²)	1×10^{11}	1×10^{10}	9×10^{10}	1×10^{10}		
Depth (m)	1000	20	0.1	0.01		
Volume (m ³)	1×10^{14}	2×10^{11}	9×10^9	1×10^8	1×10^6	2×10^5
φ_{oc}			0.02	0.04	0.20	
ρ g · mL ⁻¹		1.0	2.4	2.4	1.5	

$9 \times 10^9 \text{ m}^3$. The bottom sediment would have the same area as the water and assuming a depth of 1 cm would occupy a volume of $1 \times 10^8 \text{ m}^3$. The suspended sediments and biota are also included. The properties of 1,2,3-trichlorobenzene that are required to calculate fugacity capacity, Z , values are listed in Table 10.6. Assuming that an arbitrary amount of the chlorobenzene, $M_{\text{tot}} = 100,000 \text{ kg}$ (551.0 mol), is released in this region, the distribution can be calculated by determining Z values, summing $Z_i V_i$, and calculating the fugacity at equilibrium as summarized in Table 10.7.

This analysis would thus predict that the chlorobenzene would distribute primarily into the air. Higher concentrations are associated with higher values of the fugacity capacity factor, Z . It is understood, however, that this Level I model is hypothetical and at best would represent how a persistent chemical could distribute given sufficient time to approach an equilibrium situation. On the other hand, the model does not require a lot of data and is simple to calculate.

10.2.1.3 Level II Model The added refinement involves accounting for losses from compartments either by advection or reaction. A steady state is achieved where input is balanced by the loss from the system, but the compartments remain at equilibrium as indicated by the fluid height in the tank analogy (Fig. 10.9). Quantities defining the loss of 1,2,3-trichlorobenzene from the system by advection and reaction are compiled in Table 10.8. Photochemical reactions would be the most likely processes involved in air and water, while microbial degradation would be active in soil and bottom sediments, and the use of first-order rate constants (h^{-1}) is an appropriate approximation.

Assuming that there are several processes involved in the transformation of the trichlorobenzene in the atmosphere, the overall rate of loss would be the sum of the individual processes:

$$\begin{aligned} \text{Rate of reaction in air (mol} \cdot \text{h}^{-1} \cdot \text{m}^{-3}\text{)} &= k_1 C_{\text{air}} + k_2 C_{\text{air}} + k_3 C_{\text{air}} \cdots \\ &= C_{\text{air}} \sum k_i = C_{\text{air}} K \end{aligned}$$

The total loss from the atmosphere would be expressed

$$\text{Total reaction in air (mol} \cdot \text{h}^{-1}\text{)} = C_{\text{air}} \cdot K \cdot V$$

TABLE 10.6 Properties of 1,2,3-Trichlorobenzene at 25°C

Molecular Weight	181.5 g · mol ⁻¹
Equilibrium vapor pressure	28 Pa
Aqueous solubility	0.116 mol · m ³
log K_{ow}	4.10
$K_{\text{oc}} = 0.41 K_{\text{ow}}$	5,162
$K_{\text{B}} = 0.05 K_{\text{ow}}$ (assuming 5% fat)	629

TABLE 10.7 Level I Model for 1,2,3-Trichlorobenzene

Compartment	V (m ³)	Z (mol · m ⁻³ · Pa ⁻¹)	$V_i Z_i$	$C_i = f Z_i$ (mol · m ⁻³)	C_i (mg · L ⁻¹)	Total (kg %)
Air	1×10^{14}	4.034×10^{-4}	4.034×10^{10}	4.394×10^{-9}	7.973×10^{-7}	79,732 (79.732)
Water	2×10^{11}	4.133×10^{-3}	8.266×10^8	4.502×10^{-8}	8.169×10^{-6}	1,634 (1.634)
Soil	9×10^9	1.024	9.216×10^9	1.115×10^{-5}	2.024×10^{-3}	18,216 (18.216)
Biota	2×10^5	2.602	4.604×10^5	2.834×10^{-5}	5.142×10^{-3}	1,0284 (0.00103)
Susp. Sed.	1×10^6	6.400	6.400×10^6	6.972×10^{-5}	1.265×10^{-2}	12,650 (0.0126)
Bottom Sed.	1×10^8	2.048	2.048×10^8	2.316×10^{-5}	4.048×10^{-3}	404.80 (0.4048)
$\Sigma V_i Z_i = 5.0594 \times 10^{10}$ mol · Pa ⁻¹ ; $f = 5.5096 \times 10^5$ mol/5.0594 × 10 ¹⁰ = 1.089 × 10 ⁻⁵ Pa						100,000 (100)

TABLE 10.8 Reaction and Advection Loss for 1,2,3-Trichlorobenzene

Compart.	Reaction					Advection			
	$V_i Z_i$ (mol · Pa ⁻¹)	$t_{1/2}$ (h)	K (h ⁻¹)	D_r (mol · Pa ⁻¹ · h ⁻¹)	Res time (h)	Rate (m ³ · h ⁻¹)	K (h ⁻¹)	D_a (mol · Pa ⁻¹ · h ⁻¹)	
Air	4.034×10^{10}	550	0.00126	5.0828×10^7	100	1×10^{12}	0.010	4.034×10^8	
Water	8.266×10^8	1,700	4.077×10^{-4}	3.3700×10^5	1000	1×10^8	0.00050	4.133×10^5	
Soil	9.216×10^9	5,500	1.26×10^{-4}	1.1612×10^6					
Sediment	2.048×10^8	17,000	4.076×10^{-5}	8.3476×10^3	50,000	2×10^3	2.00×10^{-5}	4.096×10^3	
				$\Sigma D_r = 5.23345 \times 10^7$			$\Sigma D_a = 4.03817 \times 10^8$		
								$f = 5.5096 \times 10^3 \text{ mol} \cdot \text{h}^{-1} / (\Sigma D_r + D_a) = 5.5096 \times 10^3 / (4.561515 \times 10^8) = 1.208 \times 10^{-5} \text{ Pa}$	

The total loss from the system by reaction would be the sum of the reactions in each compartment;

$$\begin{aligned} \text{Total loss (mol} \cdot \text{h}^{-1}) &= C_{\text{air}} \cdot K_{\text{air}} V_{\text{air}} + C_{\text{water}} K_{\text{water}} V_{\text{water}} \\ &\quad + C_{\text{soil}} K_{\text{soil}} V_{\text{soil}} + C_{\text{sed}} K_{\text{sed}} V_{\text{sed}} \\ &= \sum C_i K_i V_i \\ &= \sum f_i Z_i K_i V_i \quad \text{and since the system is at equilibrium} \\ &= f(\sum Z_i K_i V_i) \end{aligned}$$

A reaction “*D*” value is defined for each compartment: $D_r(\text{mol} \cdot \text{h}^{-1} \cdot \text{Pa}^{-1}) = ZKV$ and are listed in Table 10.8. The magnitude of this parameter reflects the size of the compartment, the tendency of the compound to distribute into the compartment, and the overall reaction rate in that compartment. In this case, it would be predicted that the transformation of the chlorobenzene in air would be the most significant. The actual loss by reaction from each compartment would be, $D_r f$.

A first-order rate constant, K_a , can also be defined for advective movement through a compartment as the flow rate, in $\text{m}^3 \cdot \text{h}^{-1}$, divided by the total volume of the compartment. A residence time would then be $1/K_a$. A residence time of 100 h is given for the atmospheric compartment (Table 8.8) giving a K_a for this compartment of 0.01 h^{-1} or $10^{12} \text{ m}^3 \cdot \text{h}^{-1}$. And an advection “*D*” value can be calculated for each compartment in a similar fashion to that for reactions. Note advective flow is also defined for the water and sediment compartments with the latter reflecting permanent burial of sediment. Advective values are somewhat arbitrary but are needed to assess the overall behavior of the compound.

At steady-state, loss from the system would balance the amount being introduced (I), and so,

$$\begin{aligned} I(\text{mol} \cdot \text{h}^{-1}) &= f(\sum D_r + \sum D_a) \quad \text{and thus} \\ f &= I/(\sum D_r + \sum D_a) \end{aligned}$$

For an input rate of $1000 \text{ kg} \cdot \text{h}^{-1}$ ($5.5096 \times 10^3 \text{ mol} \cdot \text{h}^{-1}$) a fugacity of $1.208 \times 10^{-5} \text{ Pa}$ can be calculated. Equilibrium concentrations in each compartment will thus be given by $Z_i f$ and the total amount in a compartment by $V_i Z_i f$ and it is seen (Table 10.9) that the distribution among compartments is the same as that given by the Level I model. The rate of loss ($\text{mol} \cdot \text{h}^{-1}$) by reaction or advection from a compartment will be given by $D_i f$. This analysis projects that air movement is responsible for the major loss from this system. Most of the reactive loss occurs in the atmosphere that is consistent with the fact that the compound distributes into this compartment and the most active degradation reactions occur there also. The residence time provides an index of persistence in that it estimates how long it takes for the 1000 kg to move through the system. It also indicates the time required for the concentrations to build up to the point where the rate of loss balances the input rate.

TABLE 10.9 Level II Model for 1,2,3-Trichlorobenzene

Compartment	$C = fZ$ (mol · m ⁻³)	Total (kg %)	Loss (kg · h ⁻¹)		
			Reaction	Advection	Total (%)
Air	4.87×10^{-9}	88,391 (79.6)	111.4	884.5	995.9 (99.6)
Water	4.99×10^{-8}	1,811.4 (1.63)	0.739	0.906	1.645 (0.165)
Soil	1.24×10^{-5}	20,255 (18.26)	2.546		2.546 (0.255)
Biota	3.14×10^{-5}	1.140 (0.00103)			
Susp. Sed.	7.73×10^{-5}	14.03 (0.0126)			
Sediment	2.47×10^{-5}	448.3 (0.404)	0.0183	0.00898	0.0273 (0.0003)
Totals		110,921 kg	114.7	885.4	1000.1
Residence times total kg/(kg · h ⁻¹)			967.1 h	125.3 h	110.9 h

10.2.1.4 Level III Model The two simple models require minimum input, the mathematical solution is not complex, and they provide some useful perspective. It is obvious, however, that these models are simplistic and do not provide a realistic representation of the natural environment. The Level III model (Fig. 10.9) introduces an added level of complexity by considering the rates at which a compound moves between compartments that results in a steady state where the distribution among compartments is not at equilibrium. More data is required and the mathematical solution becomes more complex. The amount of information generated increases and a more comprehensive analysis of the behavior of the compound is provided. While this model can in no way be considered exact in the way it represents chemical behavior, the level of complexity achieved is such that it has become an acceptable evaluative tool.

In this approach,^{15,16} four heterogeneous compartments are considered with the volume fractions given in Table 10.10. The fugacity capacity, Z , of each compartment is a composite value based on the Z values of each constituent. The rates of transformation in and advection from compartments are defined by the same D values outlined in the Level II model. Transfer between compartments involves a number of different processes (Table 10.11), which also are defined by D values with the same units, $\text{mol} \cdot \text{h}^{-1} \cdot \text{Pa}^{-1}$. An overall D value for transfer between two compartment will be the sum of the D values for the individual processes involved. Transfer mechanism involves either a diffusion process similar to that responsible for the evaporation of a compound from water (see Evaporation, Chapter 4) or carrier process such as washing the chemical out of the vapor phase in the rain or deposition of chemical carrying aerosol particles on soil or water.

The derivation of diffusion D values¹⁹ for intermedia transport can be illustrated by considering evaporation from water as represented by the two-film model (see

TABLE 10.10 Level III Compartment Dimensions and Fugacity

Compartment		V (m^3)	Volume Fraction	Z ($\text{mol} \cdot \text{m}^{-3} \cdot \text{Pa}^{-1}$)		
				Constituent	Compartment	
Air	Air	1×10^{14}	~ 1	4.034×10^{-4}	4.034×10^{-4}	
	Aerosol		2×10^{-11}			
Water	Water	2×10^{11}	~ 1	4.133×10^{-3}	4.1676×10^{-3}	
	Susp. Sed.		5×10^{-6}			6.400
	Biota		1×10^{-6}			2.602
Soil		1.8×10^9			0.5134	
	Air		0.2	4.034×10^{-4}		
	Water		0.3	4.133×10^{-3}		
	Solid		0.5	1.024		
Sediment		5×10^8			0.4129	
	Water		0.8	4.133×10^{-3}		
	Solid		0.2	2.048		

TABLE 10.11 Intercompartment Transfer Processes

Compartment	Process	Compartment	Process
Air (1) → Water (2)	Diffusion	Water (2) → Air (1)	Diffusion
	Rain dissolution	Soil (3) → Air (1)	Diffusion
	Wet deposition	Soil (3) → Water (2)	Water run-off
	Dry Deposition		Soil erosion
Air (1) → Soil (3)	Diffusion	Water (2) → Sediment (4)	Diffusion
	Rain Dissolution		Deposition
	Wet Deposition	Sediment (4) → Water (2)	Diffusion
	Dry Deposition		Resuspension

Evaporation, Chapter 4). The flux through the water film is defined by the mass transfer coefficient k_w ($\text{m} \cdot \text{h}^{-1}$), the interface area (m^2), and the concentration differential between the bulk liquid phase (C_w) and the liquid interface (C_{wi}):

$$\text{Flux } N \text{ (mol} \cdot \text{m}^{-2} \cdot \text{h}^{-1}\text{)} = k_w A (C_w - C_{wi}) = k_w A Z_w (f_w - f_i)$$

At steady state, the corresponding flux through the air film will be given by

$$\text{Flux} = k_a A (C_{ai} - C_a) = k_a A Z_a (f_i - f_a)$$

with f_i being the fugacity at the interface. Thus,

$$\begin{aligned} N/D_w &= f_w - f_i & \text{and,} \\ N/D_a &= f_i - f_a \end{aligned}$$

Adding

$$\begin{aligned} N/D_w + N/D_a &= N(1/D_w + 1/D_a) = f_w - f_a = N/D_{wa} & \text{and} \\ N &= D_{wa}(f_w - f_a) \end{aligned}$$

where

$$1/D_{wa} = 1/D_w + 1/D_a = 1/(k_w A Z_w) + 1/(k_a A Z_a)$$

The net evaporative loss can then be viewed as the balance between an evaporation rate $D_{wa} f_w$ and a condensation rate, $D_{wa} f_a$. The D values for other diffusion processes can be derived in a comparable manner.

The nondiffusive, irreversible intermedia transport, such as wet or dry particle deposition from the atmosphere or erosion from soil can be defined by a D value where the flux N ($\text{mol} \cdot \text{h}^{-1}$) is

$$N = GC = GZf = Df$$

TABLE 10.12 Compartment Fugacities (Pa); Level III 1,2,3-Trichlorobenzene Model

Compartment	1000 kg · h ⁻¹ (5509.6 mol) Emitted into		
	Air	Water	Soil
Air (1)	1.210×10^{-5}	7.389×10^{-6}	4.679×10^{-6}
Water (2)	7.437×10^{-6}	1.800×10^{-3}	2.111×10^{-5}
Soil (3)	4.885×10^{-6}	2.965×10^{-6}	2.886×10^{-3}
Sediment (4)	1.294×10^{-5}	3.130×10^{-3}	3.672×10^{-5}

where G is the volumetric flow rate ($\text{m}^3 \cdot \text{h}^{-1}$) and D will again have units of $\text{mol} \cdot \text{h}^{-1} \cdot \text{Pa}^{-1}$. Representative mass transfer coefficients and volumetric flow rates have been defined¹⁷ and D values for the different intermedia-transfer processes for the 1,2,3-trichlorobenzene have been calculated (Fig. 10.10). This diagram also indicates input options (E) as well as reaction (R) and advection (A) processes that have been defined in the Level II model.

Mass balance relations can be derived for each of the four compartments where the input processes are balanced by intermedia transfer, advection, and degradation processes. These four equations provide an algebraic approach to the calculation of the four unknown fugacities¹⁷ that are compiled (Table 10.12) for emission at the rate of $1000 \text{ kg} \cdot \text{h}^{-1}$ into either the air, water, or soil compartment.

The differences in fugacity among compartments demonstrate that the system is not at equilibrium. Having determined fugacities, one can calculate the steady-state concentration, $f_i Z_i$, and the total amount in each compartment, $f_i Z_i V_i$ (Table 10.13). The rates of transfer between compartments and loss by advection and reaction are calculated from D values ($D_i f_i$). This analysis emphasizes that the manner in which a compound is released has a dramatic effect on the overall distribution and persistence as indicated by residence time. It is obvious why the compound will be more persistent in soil because the opportunity for the compound to move out of this compartment is much less than water or air and the degradation rate in this compartment

TABLE 10.13 Steady-State Amounts (mol) of 1,2,3-Trichlorobenzene in Compartments Level III Model

Compartment	5509.6 mol · h ⁻¹ Emitted into		
	Air	Water	Soil
Air	4.8804×10^5 (90.1)	2.9802×10^5 (12.1)	1.8870×10^5 (0.70)
Water	6.1983×10^3 (1.14)	1.4997×10^6 (60.6)	1.7592×10^4 (0.07)
Soil	4.4848×10^4 (8.28)	2.7388×10^4 (1.11)	2.6661×10^7 (99.2)
Sediment	2.6700×10^3 (0.49)	6.4628×10^5 (26.2)	7.5813×10^3 (0/03)
Total	5.4176×10^5	2.4714×10^6	2.6875×10^7
Residence time	98.33 h	448.6 h	4,877.8 h

is much slower than that in air. Noted that the model can be used to assess the response when the compound is released into all three compartments.

The concentration in each compartment in $\text{mol} \cdot \text{m}^{-3}$ is given by $Z_i f_i$ and the concentration in soil and sediment on a dry-weight basis can be derived by taking into account that soil is 50% and sediment 20% by volume solids of density $2.4 \text{ g} \cdot \text{mL}^{-1}$. One can estimate concentration in the biota assuming the chemical in this compartment is at equilibrium with that in water and sufficient time has elapsed to achieve this condition. It is of interest to observe (Table 10.14) that the concentration of the trichlorobenzene in air varies at most by a factor of 3 among the three release scenarios in contrast to concentrations in water that vary by a factor of >200 . This observation is of interest in that one normally assumes that atmospheric levels are controlled by managing emissions into this compartment, however, with compounds such as this trichlorobenzene, providing there is a sufficient water-air interface, release into water can result in levels in the atmosphere comparable to that predicted by atmospheric release.

The Level III model uses ~ 40 quantities¹⁶ that are specific to the environment. These would include the dimensions of the compartments as well as the values used to define the movement between compartments. The latter are not chemical specific in contrast to the Z values. In some instances, the environmental parameters such as sediment resuspension are not well defined. The rates of degradation are specific to the chemical and the environmental compartment. Emission rates may be reasonably precise if the model is applied to a specific source, that is, some facility operating with discharge permits, however, these values are more difficult to define on a regional basis. Despite these uncertainties it has been shown that with some compounds, output from such models can be in reasonable agreement with environmental data.²⁰

An evaluation of the utility of these multimedia models²¹ has noted that they provide an effective mechanism of ranking chemicals, both new and existing. The environmental data derived from the models can provide a basis for developing a "first-cut" risk assessment and baselines for assessing the risk from hazardous waste sites. Since the data input is not overwhelming and the numerical manipulations straightforward, the models provide a cheap and rapid way to evaluate the

TABLE 10.14 Steady-State Concentrations of 1,2,3-Trichlorobenzene Predicted by the Level III Model

Compartment Concentration	5509.6 $\text{mol} \cdot \text{h}^{-1}$ Emitted into		
	Air	Water	Soil
Air $\mu\text{g} \cdot \text{m}^{-3}$	0.886	0.541	0.343
Water $\text{ng} \cdot \text{L}^{-1}$	5.63	1,360	16.0
Soil $\mu\text{g} \cdot \text{kg}^{-1}$ dry wt.	0.38	0.23	224
Sediment $\mu\text{g} \cdot \text{kg}^{-1}$ dry wt.	2.02	489	5.73
Biota $\mu\text{g} \cdot \text{kg}^{-1}$ wet wt.	3.51	850	9.97

influence of both environmental and chemical variables. The fugacity approach is also quite versatile. The concept has been illustrated using regional models, but it can also be used to model chemical uptake in a plant.²²

The fugacity model has been introduced as one example of how a mathematical approach can provide a more holistic assessment of the environmental behavior of a chemical. It must be emphasized that numerous mathematical models have been developed to simulate chemical behavior. Many of these focus on a mechanistic approach taking into account the different components that might be involved. The mathematics can become considerably more sophisticated and the models may apply to a more restricted area; for example, the movement of a chemical through soil to groundwater. It is beyond the scope of this treatise to develop a more comprehensive analysis of models. However, it is important for the student to be aware of the versatility and utility of this technology.

REFERENCES

1. J. K. Frederickson and H. Bolton, Jr., "Terrestrial Microcosms for risk Assessment of Soil-Applied Microorganisms and Pesticides", in J. T. Selikoff's, Ed., *Ecotoxicology: Responses, Biomarkers and Risk Assessment*, Organization for Economic Co-operation and Development, Paris, 1997, pp. 459–488.
2. T. Caquet, L. Lagadic, and S. R. Sheffield, *Rev. Env. Contam. Toxicol.* **165**, 1 (2000).
3. L. K. Cole, R. L. Metcalf, and J. R. Sanborn, *Intern. J. Environ. Studies* **10**, 7 (1976).
4. R. G. Nash and M. L. Beall, *J. Agr. Food Chem.* **28**, 614 (1980).
5. J. N. Huckins, J. D. Petty, and M. A. Heitkamp, *Chemosphere* **13**, 1329 (1984).
6. J. W. Gillett and J. D. Gile, *Intern. J. Environmental Studies* **10**, 15 (1976).
7. J. D. Gile and J. W. Gillett, *J. Agr. Food Chem.* **27**, 1159 (1979).
8. J. D. Gile, J. C. Collins, and J. W. Gillett, *Environ. Sci. Technol.* **14**, (1980).
9. J. D. Gile and J. W. Gillett, *Arch. Environ. Contam. Toxicol.* **8**, 107 (1979).
10. K. Liber, N. K. Kaushik, K. R. Solomon, and J. H. Carey, *Environ. Toxicol. Chem.* **11**, 61 (1992).
11. K. Liber, K. R. Solomon, and J. H. Carey, *Environ. Toxicol. Chem.* **16**, 293 (1997).
12. K. Liber, K. R. Solomon, N. K. Kaushik, and J. H. Carey, "Impact of 2,3,4,6-Tetrachlorophenol (DIATOX[®]) on Plankton Communities in Limnocorrals", in R. L. Graney, J. H. Kennedy, and J. H. Rodger's, Eds., *Aquatic Mesocosm Studies in Ecological Risk Assessment*, Lewis Publishers, Boca Raton, FL, 1993, pp. 257–294.
13. D. Mackay, *Environ. Sci. Technol.* **13**, 1218, (1979).
14. D. Mackay and S. Paterson, *Environ. Sci. Technol.* **15**, 1006 (1981).
15. D. Mackay and S. Paterson, *Environ. Sci. Technol.* **16**, 654A (1982).
16. D. Mackay and S. Paterson, *Environ. Sci. Technol.* **25**, 427 (1991).
17. D. Mackay, S. Paterson, and W. Y. Shiu, *Chemosphere* **24**, 695 (1992).
18. D. Mackay, W. Y. Shiu, and K. C. Ma, *Illustrated Handbook of Physical-Chemical Properties and Environmental Fate for Chemicals*, Lewis Publishers, Boca Raton, FL. Vol. I, Monoaromatic Hydrocarbons, Chlorobenzenes and PCBs, 1992. Vol. II, Polynuclear

- Aromatic Hydrocarbons, Polychlorinated Dioxins, Bibenzofurans, 1993. Vol. III, Volatile Organic Chemicals. Vol. IV, Oxygen, Nitrogen and Sulfur Containing Compounds. Vol. V, Pesticide Chemicals, 1997.
19. D. Mackay, *Multimedia Environmental Models*, Lewis Publishers, Inc. Chelsea, MI, 1991, pp. 143–183.
 20. C. E. Cowan, D. Mackay, T. C. J. Feijtel, D. van de Meent, A. Di Guardo, J. Davies, and N. Mackay, *The Multi-Media fate model: A Vital tool for Predicting the fate of Chemicals*, SETAC Press, Pensacola FL, 1994.
 21. D. Mackay, A. DiGuardo, S. Paterson, G. Kicsi, and C. E. Cowan, *Environ. Toxicol. Chem.* **15**, 1618, 1996.
 22. S. Paterson and D. Mackay, “Interpreting Chemical Partitioning in Soil-Plant-Air Systems with a Fugacity Model”, in S. Trapp and J. C. Mc Farlane’s, Eds., *Plant Contamination, Modeling and Simulation of Organic Chemical Processes*, Lewis Publishers, Boca Raton, FL, 1995, pp. 191–214.

APPENDIX

Information on PCBs is summarized in Tables 1 and 2.

TABLE A.1 Approximate Percentages (w/v) of Aroclors with Different Degrees of Chlorination^a

Number of Chlorine Atoms in Molecule	Chlorine weight (%)	Aroclor						
		1221	1232	1016	1242	1248	1254	1260
0	0	10	—	—				
1	18.8	50	26	2	3			
2	31.8	35	29	19	13	2		
3	41.3	4	24	57	28	18		
4	48.6	1	15	22	30	40	11	
5	54.4				22	36	49	12
6	59.9				4	4	34	38
7	62.8						6	41
8	66.0							8
9	68.8							1

^a From WHO/EURO (1987).

TABLE A.2 PCB Compositions of Aroclors in mol%

IUPAC No.	Chlorine Substitution Pattern	Aroclor				
		1242	1016	1248	1254	1260
	BP	0.01	0.50			
1	2	0.68	0.80			
2	3	0.04	0.10			
3	4	0.22	1.00			
4	2,2'	3.99	4.36	0.25		
6	2,3'	1.24	1.37	0.69	0.07	

(continued)

TABLE A.2 *Continued*

IUPAC No.	Chlorine Substitution Pattern	Aroclor				
		1242	1016	1248	1254	1260
7	2.4	1.04	1.16			
8	2.4'	8.97	10.30	0.18		
9	2.5	0.31	0.34	Trace		
10	2.6T 0.13	0.20				
12	3.4	0.09	0.11			
13	3.4'	0.12	0.12			
14	3.5	0.35	0.37			
15	4.4'	0.99	1.07			
16	2.3.2'	3.25	3.50	0.84		
17	2.4.2'	2.92	3.14	0.19		
18	2.5.2'	9.36	10.87	9.95	0.07	
19	2.6.2'	0.97	1.08			
20	2.3.3'	3.64	3.99			
22	2.3.4'	2.64	2.80	1.24	Trace	Trace
25	2.4.3'	1.68	1.79			
26	2.5.3'	0.55	0.62	0.75		
27	2.6.3'	0.54	0.58			
28	2.4.4'	13.30	14.48	Trace		
31	2.5.4'	4.53	4.72	9.31	0.72	
32	2.6.4'	2.15	2.31	1.46		
33	3.4.2'	2.83	3.08			
35	3.4.3'	0.66	0.38			
37	3.4.4'	1.62	1.89	1.28	0.20	0.09
39	3.5.4'	1.03	1.08			
40	2.3.2'.3'	0.15	0.18	1.12	0.26	0.04
41	2.3.4.2'	1.67	2.00			
42	2.3.2'.4'			7.05	2.18	0.66
43	2.3.5.2'	0.44	0.47			
44	2.3.2'.5'	1.06	1.14			
45	2.3.6.2'	0.90	1.00	5.73	0.15	
46	2.3.2'.6'	0.31	0.33			
47	2.4.2'.4'	1.65	1.8	3.18	0.52	0.88
48	2.4.5.2'	1.33	1.41			
?	2.5.2'.4'			3.81	1.63	0.44
49	2.4.2'.5'	3.28	3.48			
52	2.5.2'.5'	4.08	4.35	8.36	4.36	1.91
53	2.5.2'.6'	0.97	1.07	6.30	0.13	
54	2.6.2'.6'	0.17	0.19			
55	2.3.4.3'			0.11	0.43	0.12
56	2.3.3'.4'	0.60	Trace	0.18	0.03	
60	2.3.4.4'	0.21				

(continued)

TABLE A.2 *Continued*

IUPAC No.	Chlorine Substitution Pattern	Aroclor				
		1242	1016	1248	1254	1260
66	2.4.3'.4'	0.81	0.14	4.95	2.24	0.22
70	2.5.3'.4'	1.11		6.38	4.75	0.85
71	2.6.3'.4'			0.65		
72	2.5.3'.5'	0.33		2.10	1.01	0.28
74	2.4.5.4'	2.02	1.35	0.25	0.30	0.09
75	2.4.6.4'	2.18	2.40			
76	3.4.5.2'	Trace		Trace	0.18	0.01
77	3.4.3'.4'	0.34		0.47	0.12T0.04	
78	3.4.5.3'	0.52				
79	3.4.3'.5'	0.24	Trace	0.23	0.04	
80	3.5.3'.5'T		Trace	Trace	Trace	
81	3.4.5.4'	0.28				
83	2.3.5.2'.3'			Trace	0.32	0.09
84	2.3.6.2'.3'	0.38	0.01	0.71	1.72	0.69
85	2.3.4.2'.4'	0.40		0.55	2.15	0.31
?	2.3.4.3'.5'			0.02	0.55	0.14
87	2.3.4.2'.5'	0.09		1.05	3.81	1.10
91	2.3.6.2'.4'	Trace		1.78	5.00	3.22
92	2.3.5.2'.5'	0.12	0.20	0.63	0.21	
95	2.3.6.2'.5'	0.53	0.18			
97	2.4.5.2'.3'			0.78	2.59	0.63
98	2.4.6.2'.3'	0.13	0.04			
99	2.4.5.2'.4'	0.55		2.52	6.10	0.82
101	2.4.5.2'.5'	0.27		1.50	6.98	5.04
102	2.4.5.2'.6'			Trace	Trace	Trace
105	2.3.4.3'.4'	0.25				
106	2.3.4.5.3'				0.40	0.06
108	2.3.4.3'.5'	0.46	0.16			
110	2.3.6.3'.4'			1.69	8.51	3.57
113	2.3.6.3'.5'	0.39	0.01	3.10	Trace	0.01
114	2.3.4.5.4'				0.25	0.03
118	2.4.5.3'.4'				8.09	2.00
120	2.4.5.3'.5'	0.31		Trace	0.15	3.01
121	2.4.6.3'.5'	0.92		4.32	3.51	0.57
123	3.4.5.2'.4'	0.36				
?	3.4.5.2'.3'			Trace	0.76	1.88
126	3.4.5.3'.4'	0.03			0.16	1.59
127	3.4.5.3'.5'	0.05				
128	2.3.4.2'.3'.4'				1.31	0.47
131	2.3.4.6.2'.3'				0.14	0.01
132	2.3.4.2'.3'.6'			Trace	2.00	2.77

(continued)

TABLE A.2 *Continued*

IUPAC No.	Chlorine Substitution Pattern	Aroclor				
		1242	1016	1248	1254	1260
133	2.3.5.2'.3'.5'			1.13	0.03	0.06
134	2.3.5.6.2'.3'			0.11	0.38	1.01
135	2.3.5.2'.3'.6'		T	0.20	0.29	
136	2.3.6.2'.3'.6'			0.20	0.34	1.12
138	2.3.4.2'.4'5'	0.08		0.19	4.17	5.01
143	2.3.4.5.2'.6'	0.07				
148	2.3.5.2'.4'.6'			0.12	0.07	0.06R
149	2.4.5.2'.3'.6'			0.77	3.59	9.52
151	2.3.5.6.2'.5'			Trace	0.33	0.06
153	2.4.5.2'.4'.5'	0.02		0.13	3.32	8.22
154	2.4.5.4'.6'				0.14	
156	2.3.4.5.3'.4'					0.41
157	2.3.4.3'.4'.5'				0.18	0.03
158	2.3.4.6.3'.4'				0.46	0.18
159	2.4.5.2'.3'.5'				0.75	1.48
163	2.3.5.6.3'.4'					Trace
167	2.4.5.3'.4'5'				0.21	0.17
168	2.4.6.3'.4'.5'			0.56	4.23	0.59
170	2.3.4.5.2'.3'.4'				0.43	0.62
171	2.3.4.6.2'.3'.4'		T	0.30	4.31	
174	2.3.4.5.2'.3'.6'				Trace	0.09
176	2.3.4.6.2'.3'.6'			0.09	Trace	0.57
177	2.3.5.6.2'.3'.4'					Trace
179	2.3.5.6.2'.3'.6'				0.56	0.83
180	2.3.4.5.2'.4'.5'				0.76	7.20
181	2.3.4.5.6.2'.4'				0.28	2.72
182	2.3.4.5.2'.4'6'				Trace	0.47
183	2.3.4.6.2'.4'.5'				1.16	2.58
185	2.3.4.5.6.2'.5'				1.11	5.65
186	2.3.4.5.6.2'.6'			Trace	Trace	0.37
187	2.3.5.6.2'.4'.5'				0.48	1.12
189	2.3.4.5.3'.4'.5'					0.13
190	2.3.4.5.6.3'.4'					0.02
192	2.3.4.5.6.3'.5'				0.20	0.97
193	2.3.5.6.3'.4'.5'				2.30	
194	2.3.4.5.2'.3'.4'.5'					2.21
195	2.3.4.5.6.2'.3'.4'					Trace
196	2.3.4.5.2'.3'.4'.6'					0.79
197	2.3.4.6.2'.3'.4'.6'					0.30
198	2.3.4.5.6.2'.3'.5'				1.00	0.15
199	2.3.4.5.6.2'.3'.6'					0.38

(continued)

TABLE A.2 Continued

IUPAC No.	Chlorine Substitution Pattern	Aroclor				
		1242	1016	1248	1254	1260
200	2.3.4.6.2'.3'.5'.6'				Trace	0.15
202	2.3.5.6.2'.3'.5'.6'				Trace	0.31
203	2.3.4.5.6.2'.4'.5'					0.08
204	2.3.4.5.6.2'.4'.6'				Trace	0.13
205	2.3.4.5.6.3'.4'.5'					0.01
206	2.3.4.5.6.2'.3'.4'.5'					0.51
207	2.3.4.5.6.2'.3'.4'.6'					1.15
208T	2.3.4.5.6.2'.3'.5'.6'					1.64
?	2.3.4.5.6.2'.3'.5'.6'					0.18

ACKNOWLEDGMENT

Table A.1: Reproduced with permission from International Programme on Chemical Safety, Environmental Health Criteria 140, Polychlorinated Biphenyls and Terphenyls (Second Edition). Copyright, World Health Organization, 1993.

Table A.2: Reproduced from EHC 140, Polychlorinated Biphenyls and Terphenyls being compiled from *J. Chromatography* **169**, P. Albro and C.E. Parker, "Comparison of the compositions of Aroclor[®] 1242 and Aroclor 1016[®]" p. 161 and *J. Chromatography* **205**, P. Albro, J.J. Corbett and J.L. Schroeder, "Quantitative characteristics of PCB mixtures Aroclors[®] 1248, 1254, 1260 by GC using capillary columns" p. 103. Copyright 1979 and 1981, with permission from Elsevier.

Index

- Absorption spectrum:
 absorbance, 194
 Beer-Lambert law, 195
 extinction coefficient, 195
- Absorption through:
 fish gills, 156
 K_{ow} and uptake, 157, Fig. 5.4
 membrane and barrier layer control, 153
 gastrointestinal system, 158
 weak acids and bases, 159
 ion trap effect, weak acids, 159
 plant roots, 160
 skin, 157
 dermal flux and K_{ow} , 158, Fig. 5.5
- Acid/base:
 Brönsted-Lowry definition, 51
 neutral/charged ratio and pH, 56
- Acid:
 dissociation constants, pK_a , 51
 organic acids, pK_a , 53, Table 2.19
- Actinometer:
 measurement of light intensity, 203
- Activity coefficient:
 octanol/water part. coeff. relations, 40
 organic compds. in aqueous soln., 15
 relation to solubility, 19
- Adsorbate:
 definition, 80
- Adsorbent:
 definition, 80
- Adsorption:
 definition, 80
 onto charcoal from water, 89, Fig. 3.8
- Aged residues in soil:
 differential extraction, 107, Fig. 3.21
 environmental significance, 110
 irreversible compartment, 107, Table 3.12
 Langmuir isotherm, 107
 soil degradation and, 343, Fig. 9.19
 sorption/desorption studies, 106
- Aldicarb:
 groundwater contaminant, 352
 soil pH and degradation, 354, Table 9.15
- Alkanes:
 oxidation by hydroxyl radicals
 predictive structure/activity system, 241
 rate constants, 240, Table 6.19
 reaction products, 242
 oxidation rates, nitrate radicals, 240, Table 6.19
- Alkenes:
 oxidation by:
 hydroxyl radicals, 242, Table 6.21
 nitrate radicals, 243, Table 6.21
 oxidation by ozone,
 reaction rates, 243, Table 6.21
 reaction mechanisms, 243
- Alkyl halides:
 hydrolysis reactions, 203
 iron porphyrin catalyzed reduction, 278, Table 7.9
 reactions with sulfur, 308
 reduction potentials, 269, Table 7.4
 reduction in sediments, 271, Table 7.6
 zero valent metal reduction, 281
- Antoine equation: 11, Table 2.2
- Aqueous solubility: see solubility in water
- Aromatic hydrocarbons: including polynuclear hydrocarbons, PAH
 Henry's law constants, 35, Table 2.12
 metabolism in marine sediments, 331, Table 9.4

- Aromatic hydrocarbons *cont.*
- molecular surface area and solubility, 65, Table 2.25
 - oxidation rates with:
 - hydroxyl radicals, 245, Table 6.23
 - nitrate radicals, 245, Table 6.23
 - particle deposition onto leaves, 116
 - particle/vapor distribution, 253
 - K_p /vap. pressure relation, 253, Fig. 6.27
 - photolysis half-lives, 205, Table 6.7
 - photolytic degradation on particles, 257, Table 6.31
 - solubility in water, 24, Table 2.7
 - vapor phase partitioning onto leaves, 115
 - vapor pressures, 7, Table 2.2
 - vapor pressure/temp. relations, 7, Table 2.2
- Atmospheric particulates:
- characteristics, 252
 - particle/vapor distribution:
 - correlation of K_p with vap pressure, 254
 - correlation of K_p with K_{oa} , 256, Fig. 6.29
 - distribution constant, K_p , 253
 - Langmuir adsorption model, 253
 - partitioning model, 254
 - PCB distribution, 253, Fig. 6.27
 - PAH distribution, 253, Fig. 6.27
- Bases:
- conjugate acid, dissociation constants, 51
 - organic bases, pK_a values, 55, Table 2.21
- Beer-Lambert law:
- absorbance and concentration, 195
- Bioaccumulation:
- clam study, uptake from sediments, 184
 - K_{oc} involvement, 185
 - PCB bioaccumulation, 185, Table 5.14
 - definition, 174
- Bioconcentration:
- bioconcentration factor, K_B , 174
 - correlation with K_{ow} , 177, 179
 - definition, 174
 - DOM effect on K_B , 182, Fig. 5.21
 - experimental determination, 175
 - exposure time and, 181
 - growth dilution in exptl. exposure, 176
 - normalized for lipid content, 177
 - PCB congeners, 178, Table 5.12
 - TCDD study, 176
 - single compartment model, 174
 - steady state relation, 175
 - uptake/excretion balance, 175
 - excretion rate and K_{ow} , 179, Fig. 5.18
- Biomagnification:
- definition, 174
 - food chain distribution and fat content, 189
 - food versus water uptake, 187
 - species K_B/K_{tg} correlations, 189, Fig. 5.22
 - PCB uptake from food, 188, Table 5.16
- Biomembrane:
- composition, 150
 - liquid crystal configuration, 150
 - structure, phospholipid bilayer, 150
 - transport kinetics, 151
 - Fick's laws, 151
 - permeability, 152
 - transport kinetics, barrier model, 152
 - lag time, 153
 - membrane and water barrier control, 152
 - membrane flux and K_{ow} , 154, Fig. 5.3
 - model validation with polymer membrane, 154
 - uptake across fish gills, 157, Fig. 5.4
 - transport processes, 150
 - active transport, 150
 - facilitated transport, 150
 - passive diffusion, 150
- Brunauer Emmet Teller, BET, isotherm:
- adsorption from solution onto fir needles, 171, Fig. 5.14
 - characteristics, 83
 - linear form, 83
 - sorption on dry soil from vapor phase, 100, Fig. 3.16
- Carbamates:
- hydrolysis reactions, 296, Table 8.5
 - pesticide hydrolysis, 300, Table 8.6
- Carbon tetrachloride:
- oxidation by semi-conductor catalyzed photolysis, 232, Fig. 6.22
- Cation exchange:
- sorption of weak bases in soil, 96
- Chemical potential:
- definition, 19
 - in the solution process, 19
- Chemisorption:
- definition, 80
- Chlordane:
- plant uptake, species variation, 166, Table 5.7
- Chloroform:
- semi-conductor catalyzed photolysis, 231, Fig. 6.21
- Chlorinated benzenes:
- Henry's law constants, 36, Table 2.12
 - reduction potentials, 270, Table 7.5

- solubility in water, 24, Table 2.7
 1,2,3-trichlorobenzene, fugacity models, 373
 vapor pressures, 7, Table 2.2
 vapor pressure/temp. relations, 7, Table 2.2
- Chlorinated-dibenzodioxins:
 Henry's law constants, 36, Table 2.12
 molar volume and solubility, 65
 molar volume and vapor pressure, 64
 particle deposition onto leaves, 117
 plant uptake from soil, species variation, 167,
 Fig. 5.11
 reduction potentials, 270, Table 7.5
 solubility in water, 24, Table 2.7
- TCDD, 2,3,7,8-tetrachloro-, bioconcentration, 176
 vapor phase partitioning into leaves, 117
 vapor pressures, 7, Table 2.2
 vapor pressure/temp. relations, 7, Table 2.2
- Chlorinated-dibenzofurans:
 particle deposition onto leaves, 119
 solubility in water, 24, Table 2.7
 vapor phase partitioning into leaves, 119
 vapor pressures, 7, Table 2.2
 vapor pressure/temp. relations, 7, Table 2.2
- Clausius-Clapeyron equation:
 temp/vap. press reation, 10, Fig. 2.3
- Clays:
 properties, 76, Fig. 3.1
- Competition kinetics:
 detn. of hydroxyl radical reaction rates, 225
- Concentration units:
 interconversion, 23
 molarity, 22
 mole fraction, 22
 mass fraction, 22
 ppm, ppb, 23
- Cutan:
 leaf cuticle component, 110
- Cutin:
 leaf cuticle component, 110
 distribution from air into, 111
- DDE:
 vapor/spruce needle distribution, 115, Fig. 3.25
- DDT:
 evaporative loss from water, 129, Fig. 4.3
- Dacthal, DCPA:
 evaporative loss from soil, 143
 groundwater contamination, 355
- Dieldrin:
 evaporation from soil surface, 137, Fig. 4.7
 terrestrial microcosm study, 361, Fig. 10.2
 uptake by carrots, effect of SOM, 165, Table 5.6
- Diffusivity, D:
 Fick's laws, 151
- Dihaloelimination:
 reduction reaction, 268
- Dioxygenase reaction:
 cleavage of aromatic ring, 315
- Dissolved organic matter, DOM:
 analysis of water samples, 32
 effect on:
 K_B , 182, Fig. 5.21
 water solubility, 31, Fig. 2.8
 Henry's law constant, 37
 hydrolysis reactions, 294, Fig. 8.8
 reduction rate enhancement, 271 Fig. 7.1
 solute availability, 31
 distribution ratio, K_{dom} , 31, 37
- Electromagnetic radiation:
 absorption,
 electron transitions, 197
 excited species, 198
 functional groups and electron transitions,
 197
 maxima, 197, Tables 6.3, 4, 5
 spectrum, 194
 bond energy vs radiant energy, 194, Table 6.2
 molecular orbitals and absorption, 196
 radiant energy, 194
 solar radiation, 195, Fig. 6.1
- Enzyme kinetics:
 Michaelis-Menten relation, 312
- Enzymatic reactions:
 phase I reactions, 315,
 phase II reactions, 318, Fig. 9.4
- Esters of carboxylic acids:
 hydrolysis reactions, 289, Table 8.1
- Esters of phosphoric acid:
 hydrolysis, reactions, 299, Table 8.7
- Evaporation process:
 mechanism, 123
- Evaporation and atmospheric movement:
 global distribution of chlorinated organics, 146
 global fractionation, 146
 pesticide movement, 144
 PCB, Great Lakes flux, 146
- Evaporation from soil:
 evaporation from soil column, 139
 H' and depletion at surface, 141
 humidity and transport to surface, 140
 K_d , and transport to surface, 141
 evaporation from soil surface, 136
 evap. of dieldrin from moist soil, 137, Fig. 4.7

- Evaporation from soil *cont.*
 field study of Dacthal, 143, Table 4.19
 moisture effect, 143
 vapor density over soil, 135
 effect of concentration, 135, Fig. 4.5
 effect of soil composition, 136, Table 4.7
 effect of soil water, 136, Fig. 4.6
- Evaporation of pure compound:
 vap. pressure and mol. weight, 124, Table 4.1
 Knudsen equation, 125
 evaporation coefficient, β , 125
 rates at ambient conditions, 126, Table 4.2
- Evaporation of miscible solutes from water:
 Raoult's law, 126
- Evaporation of sl. soluble solutes from water:
 surface depletion model, 126
 depletion constant, α , 126
 evaporation half-life, 127
 evaporation half-lives, 128, Table 4.3
 Knudsen equation, 126
 relation between α and H , 129, Fig. 4.2
 vapor and liquid phase control, 127
- two-film model, 131
 control, liquid and vapor phase, 132
 half-life, calculation, 132, Table 4.6
 overall mass transfer coefficient, 132
 water and air transfer coeffs, calculation, 133
- Fick's laws:
 evaporation from water, 131
 biomembrane transport, 151
- Fish:
 uptake through gills, 156
- Fluorescence:
 emission of radiant energy, 202
- Foliar absorption from solution:
 absorption flux:
 K_{ow} , correlation with, 172, Fig. 5.16
 needle surface area, 172, Fig. 5.15
 adsorption versus absorption, two phase process,
 171
 BET isotherm, 171, Fig. 5.14
- Foliar sorption:
 cuticle matrix, distribution from vapor, 111
 plant/air distribution ratio, K_{pa} , 112
 relation to K_{oa} , 112
 variation in K_{pa}/K_{oa} with species, 113, Fig.
 3.24
 two compartment process, 114
 vapor phase partitioning and particle deposition,
 115
 mathematical treatment, 116, Fig. 3.26
 uptake of environmental residues, 118, Fig.
 3.27
 uptake from the atmosphere, 110
- Free radicals:
 chain reactions, 200
 definition, 200
 reactions, 200
- Freundlich isotherm:
 characteristics, 84
 linear form, 84
 two-site form, 102
- Fugacity, f : 371
- Fugacity capacity, Z : 372
- Fulvic acid:
 characterization, 77
 structure, 78, Fig. 3.3
- Global distribution:
 of chlorinated organics, 146
- Glutathione:
 structure, 320
- Glutathione conjugates:
 distribution in plants, 324, Fig. 9.7
 plant processes, 321, Fig. 9.5
 reaction to form mercapturic acid, 319
- Glutathione transferases:
 reactions, 318
 induction in plants, 327, Fig. 9.8
- Glyphosate:
 pK_a values, 58, Fig. 2.15
 env. pH and species present, 56, Fig. 2.15
- Groundwater contamination:
 aldicarb degradation rate and, 354, Table 9.15
 Dacthal degradation and, 355, Fig. 9.23
 GUS values, 351
 K_{om} and, 350
 soil degradation rate and, 352
- Groundwater ubiquity score: 351
- Hammett equation:
 linear free energy relation for pK_a , 60
- Henry's law constant, H :
 definition, 33
 derivation from sol. and vap. press., 33
 dimensionless constant, H' , 33
 (DOM) effect, 37, Fig. 2.10
 evaporation from water, 127
 experimental values, 36, Table s 2.11–12
 exptl. values vs P/S_w , 36, Table 2.11
 experimental determination,
 head space analysis, 34

- gas purging, 34
- salinity effect, 37, Table 2.13
- temperature effect, 37, Fig 2.13
- units and interconversion, 33
- Hexachlorobenzene, HCB:
 - global distribution, 146, Fig. 4.13
 - terrestrial microcosm study, 362, Fig. 10.2
- Humic acid: 77
- Humins: 77
- Humus: soil organic matter, 77
- Hydrogenolysis:
 - reduction reaction, 268
- Hydrolysis kinetics:
 - rate law, 281
 - acid, k_a , base catalysis, k_b , 285
 - direct reaction with water, k_w , 285
 - DOM and rate, 294, Fig. 8.8
 - pH effects, 286
 - log k_h /pH relations, 286, Fig. 8.1
 - inflection points, I_{aw} , I_{ab} , I_{bw} , 287
 - temperature effects, 289
 - half lives, 289
- Hydrolysis reactions:
 - alkyl halides, 303
 - nucleophilic substitution reactions, 303
 - kinetic parameters, 306, Table 8.9
 - reaction with H_2S and HS^- , 308
 - amides, 295, Table 8.4
 - carbamates, 296, Table 8.5
 - substituent effects, 298
 - esters of carboxylic acids, 289
 - Hammett equations, 290
 - inductive effects, 290
 - kinetic parameters, 288, Table 8.1
 - leaving group pK_a and rate, 292, Fig. 8.7
 - reaction mechanisms, 291
 - steric effects, 292
 - organophosphate esters, 299
 - kinetic parameters, 304, Table 8.7
 - malathion hydrolysis, 302, Table 8.8
- Hydroxyl radical:
 - atmospheric levels, 217, Table 6.10
 - atmospheric lifetimes, 252, Table 6.28
 - oxidation of aromatic hydrocarbons;
 - addition to the aromatic ring, 245
 - correlation of rates with σ constants, 248, Fig. 6.26
 - naphthalene, reaction, products, 247
 - reaction rates, 245, Table 6.23
 - toluene, H abstraction, addition to ring, 244
 - toluene temperature effect, 246, Fig. 6.24
 - oxidation rates for:
 - alkenes, 243, Table 6.21
 - chlorinated compounds, 250, Table 6.27
 - oxygen-contg. compds., 250, Table 6.26
 - production in the atmosphere, 217
 - rate of generation, 218
 - reaction rates in aq. soln., 227, Table 6.15
 - competition kinetics, 226
 - correlation with rates in vapor phase, 228, Fig. 6.18
 - reactions, 218
 - semi-conductor catalyzed production, 232
- Ion pairs:
 - weak acid and K_{ow} , 57
 - pentachlorophenol sorption in soil, 95
- Ion trap effect:
 - intestinal uptake of weak acids, 159
 - uptake through roots, 164, Fig. 5.9
- Isotherm:
 - Brunauer Emmet Teller (BET), 83
 - definition, 81
 - Freundlich, 84
 - Langmuir, 82
- Jablonski diagram:
 - transition of excited molecule, 201
- K_B : bioconcentration factor, 174
- K_d : soil/water distribution const., 89
- K_{om} , K_{oc} :
 - aqueous solubility, S_w , and K_{om} , 93
 - co-solvent exptl. determination, 88, Fig. 3.7
 - definition, 86
 - K_{om} values, 88, Table 3.5
 - K_{om}/K_{oc} relation, 86
 - K_{ow} and K_{om} relations, 94, Table 3.9
 - sediment K_{oc} and bioaccumulation in clams, 184
 - variation among soils, 89, Table 3.6
 - variation with time, 105, Fig. 3.19
- K_{ow} : octanol/water partition coeff., 39
- K_p : particle vapor distribution ratio, 254
- K^s : salting out constant, 27
- Knudsen effusion method:
 - determination of vap. pressure, 8
- Langmuir isotherm:
 - atmospheric particle/vapor distribution, 253
 - cation sorption in soil, 97

- Langmuir isotherm *cont.*
 characteristics, 82
 irreversible sorption in soil, 107
 linear form, 82
 semi-conductor photo-catalysis, 235
- Leaf surface:
 cuticle composition, 110
- Lifetimes:
 atmospheric degradation, 238, Table 6.28
- Limnocorral: 366, Fig. 10.5
- Lindane:
 evaporation from soil column, 139, Fig. 4.9–10
 sorption on soil from water, 90, Fig. 3.9
 sorption on soil from hexane, 99, Fig. 3.15
- Linear free energy relations:
 definition, 44
 Hammett equations, 60, Table 2.24
 sigma values, 61, Table 2.23
 π values and fragment constants
 to calculate K_{ow} , 43
- Malathion:
 hydrolysis reactions, 302
- Mathematical models:
 classification, 370
 multimedia fugacity models, 371
- Mesocosm:
 definition, 359
 limnocorral:
 chlorophenol dynamics in, 367, Figs. 10.6–7
 construction, 366, Fig. 10.5
 ecotoxicological effects, 368, Fig. 10.8
- Metabolic maps: 322, Fig. 9.6
- Microcosm:
 definition, 359
 terrestrial microcosm:
 design, 360, Fig. 10.1
 environmental distribution, 363, Fig. 10.2
 metabolism, 365, Fig. 10.4
 movement through soil, 364, Fig. 10.3
- Molar volume:
 aqueous solubility and, 64
 determination, 63
 octanol/water coeff. and, 41
 vapor pressure and, 64
- Molecular orbitals:
 absorption of radiant energy, 196
 singlets, 199
 triplets, 199
- Molecular surface area:
 aqueous solubility and, 65
 determination, 63
- Monoxygenases:
 cyt. P450 reactions, 315, Fig. 9.3
 distribution, 315
 flavin-containing enzymes, 316
- Multimedia fugacity models:
 applications, 383
 advection and degradation inputs, 378
 intercompartment transfer, 381, Table 10.11
 levels, schematic, 371, Fig. 10.9
 solutions for 1,2,3-trichlorobenzene:
 level I, 373
 level II, 375
 level III, 380
 regional system, Table 10.5, Fig. 10.10
- Natural waters:
 organic matter content, 30, Fig. 2.7
 reduction potential, $E(W)$, 266
- Nernst equation:
 reduction potentials and conc., 264
- Nitrate radical:
 oxidation rates for:
 alkanes, 240, Table 6.19
 alkenes, 243, Table 6.21
 aromatic hydrocarbons, 245, Table 6.23
 production reaction, 220
 reactions, 220
- Nucleophilic substitution reactions:
 alkyl halide hydrolysis, 303
 H_2S and HS^- reaction with alkyl halides, 308
- Octanol/air partition coefficient:
 derivation from H' and K_{ow} 50
 experimental determination, 50
 experimental vs calculated values, 50, Table 2.19
- Octanol/water partition coeff., K_{ow} :
 bioconcentration factor correlation, 177
 triglyceride/water part. coeff. reln., 178
 definition, 39
 calculation,
 using fragment constants, 45
 using π values, 43
 experimental determination,
 generator column, 41
 liquid chromatography, indirect method, 42
 shake flask, 41
 experimental values, 45, 46, Tables 2.17–18
 relation to uptake:
 across skin, 158, Fig. 5.5
 by plant roots, RCF and, 161, Fig. 5.7

- by roots and distribution through plant, TSCF and, 162, Fig. 5.8
- from solution into fir needles, 173, Fig. 5.16
- through fish gills, 157, Fig. 5.4
- temperature effect, 47
- thermodynamics, 40
- water solubility relation, 47, Figs. 2.12–13
- On-line data sources: 67
- Organic matter:
 - in natural waters, 30, Fig. 2.7
- Oxidation number: 262
- Ozone:
 - oxidation rates for alkenes, 243
 - lifetimes, 244, Table 6.22
 - reaction mechanism, 242
 - production in the troposphere, 219
 - reactions, 219
- pH:
 - effect on octanol/water partitioning, 57, Figs. 2.16, 17
 - env. pH and neutral/charged ratio of acids and bases, 56
 - salt effects, ion pairs, 57
- pK_a,
 - see acid dissociation constant, 51
 - effect on,
 - intestinal absorption, 159
 - plant uptake from soil, 164
 - experimental determination, 59
 - env. pH and neutral charged ratio of acid and bases, 56
 - Hammett equations, 61, Table 2.24
 - organic acid values, 53, Table 2.20
 - organic bases, values, 55, Table 2.21
- Parathion:
 - sorption on soil from water, 90, Fig. 3.9
 - sorption on soil from hexane, 99, Fig. 3.14
- Partitioning:
 - soil/water, 81, 89
- Paraquat:
 - solubility and sorption in soil, 99
- Partition coefficient, definition, 39
- Passive diffusion:
 - membrane transport, 150
- Pentachlorophenol:
 - uptake from solution by fir needles, 170
 - sorption in soil, pH effect, 94, Fig. 3.11
 - terrestrial microcosm study, 362, Fig. 10.2
- Permeability:
 - membrane transport, D.K_{m,w}, 152
- Phase I reactions:
 - dehydrogenases, 316
 - dioxygenase, 315
 - hydrolases, 316
 - monooxygenase, 315
 - oxygenases, 315
 - reductases, 316
- Phase II reactions:
 - amide formation, 320
 - ester formation, 320
 - glucoside conjugation, 318
 - glucuronides, 318
 - glutathione conjugates, 318
- Phase diagram, 9, Fig. 2.1
- Phenanthrene:
 - aged residues, sorption/desorption, 106, Fig. 3.20
- Phenoxyacetic acids, 2,4-D, 2,4,5,T:
 - absorption and translocation in maple, 173, Table 5.10
 - concentration and degradation, 340, Fig. 9.17
 - hydrolysis of esters, 294, Table 8.3
 - pH and uptake and distribution in plants, 164
- Phloem:
 - plant vascular system, 160
- Photo-induced excited molecule:
 - electron transitions,
 - intersystem crossing, 201
 - internal conversion, 201
 - transformation processes,
 - dissociation, 202
 - quenching, 202
 - fluorescence, 202
 - intra-molecular transfer, 202
 - ionization, 202
 - intermolecular transfer, sensitization, 202
 - isomerization, 202
 - Jablonski diagram, 201
- Phosphorescence:
 - emission of radiant energy, 202
- Photolysis:
 - direct photolysis in air, 211
 - direct photolysis in water, 205
 - calc. versus exptl. rates, 211, Fig. 6.9
 - first order rate constant, k_p, 209
 - half-life calculation, 210, Table 6.7
 - rate calculation, 205
 - specific rate of light absorption, k_a(γ), 205
 - quinoline photolysis rate, 209, Table 6.9
 - indirect photolysis, 211
 - atmospheric lifetimes, 238
 - production of active oxidants, 214
 - sensitization, 213
 - water reactions, 221

- Phthalic acid esters:
hydrolysis rates, 293, Table 8.2
- Pi, π , values:
calculating K_{ow} , 46
substituent values, 44, Tables 2.15 & 16
- Plant metabolism:
genetic engineering, 327
glutathione conjugate distribution, 324, Fig. 9.7
insoluble conjugates, 322
induction of GSH-transferases, 325, Fig. 9.8
- Plant vascular system:
phloem, 160
xylem, 160
- Polarity, 18
- Polychlorinated biphenyls (PCBs):
bioconc. in goldfish, 177, Table 5.12.
bioaccum. from food, 188, Table 5.12
distribution onto leaf surface, 112
Great Lakes flux, 146
Henry's law constants, 36, Table 2.11
molecular surface area and solubility, 65
 K_{ow} values, 45, Table 2.17
particle deposition onto leaves, 117
particle/vapor distribution, 253
 K_p /vap. pressure relation, 253, Fig. 6.27
reduction in anaerobic sediment, 338, Fig. 9.14
sediment PCBs and bioaccum. in clams, 185, Table 5.14
soil sorption experiment, 82
soil degradation, temp. effect, 336, Fig. 9.12
solubility in water, 24, Table 2.7
super-critical fluid extraction of aged residues, 107, Fig. 3.21
vapor phase partitioning into leaves, 117
vapor pressures, 7, Table 2.2
vapor pressure/temp. relations, 7, Table 2.2
- Polynuclear aromatic hydrocarbon, PAH: see aromatic hydrocarbons
- Prometone:
evaporation from soil column, 142, Fig. 4.10
- Pyrene:
soil K_d values, 87, Table 3.4
 K_{oc} variation among soils, 87
- Quantum yield:
overall quantum yield, 203, Table 6.7
solvent effect, 205
wavelength effect, 205
primary quantum yield, 203, Table 6.6
- Quenching:
energy loss from excited species, 202
- Raoult's law, 15
- Redox reactions:
electron transfer process, 261
indicators, 267
reduction reactions,
hydrogenolysis, 268
dihaloelimination, 268
- Reduction potentials:
alkyl halides, 268, Table 7.4
chlorinated benzenes and dioxins, 270, Table 7.5
definition, 263
determination, 266
free energy change and, 263
natural waters, E(W), 265
Nernst equation, 269
- Reduction reaction kinetics:
alkyl halides,
in sediments, 271
catalyzed by iron porphyrin, 278, Table 7.9
electron transport mediators
dissolved (natural) organic matter, 272, Fig. 7.1
quinones, juglone 272
iron porphyrins, 272
zero-valent metal reduction, 275
remediation application, 282
- Root uptake:
distribution through plant,
relation of TSCF to soil pH, 164
transpiration stream conc. factor, TSCF, 162
TSCF and K_{ow} relation, 163, Fig. 5.8
root concentration factor, RCF, 161
relation to K_{ow} , 162, Fig. 5.7
relation to pH, 165, Fig. 5.9
pH effect, ion trap mechanism, 165
root structure, 160
SOM and uptake, 165, Table 5.6
transfer to atmosphere, 169
variation among plant species,
chlordane and zucchini, 166
chlorinated dioxins and furans, 167, Fig. 5.11
- Safeners:
induction of plant GSH-transferases, 327
- Salting out constant, K^s , 27, Table 2.9
- Semi-conductor photocatalysis:
carbon tetrachloride oxidation, 232
electron donor effects, 234
pH effects, 234
chloroform oxidation, 231, Fig. 6.21
reaction sequence, 232, Table 6.16
reaction rates, 236, Table 6.18

- Langmuir isotherm and, 235
- semiconductor electronic structure:
 - valence band, 230
 - conduction band, 230
 - photo-induced electron transition, 230
 - valence band hole oxidation, 232
 - production of hydroxyl radical, 232
- Sensitization reactions:
 - excited species intermolecular transfer, 202
 - indirect photolysis, 212
 - isomerization reaction in water, 221
 - DOM effect, 222
 - energy considerations, 223
 - ketone sensitizers, 213
- Singlet oxygen:
 - detn. in natural waters, 214
 - DOM sensitizers, 215
 - furfuryl alcohol probe, 215
 - indirect photolysis, 214
 - phenol oxidation, 224, Table 6.14
 - anion reaction, 225
 - pH effect, 224, Fig. 6.15
 - reaction rate and σ constants, 226, Fig. 6.16
 - production by sensitization, 214
 - reactions, 215
- Singlets:
 - electron spin, 199
- Soil constituents:
 - clays, 76
 - sand, 75
 - silt, 75
- Soil degradation:
 - aged residues, 343, Fig. 9.19
 - anaerobic sediments:
 - reduction of PCBs, 338, Fig. 9.14
 - remediation strategy, 339, Fig. 9.15
 - biological adaptation, 330
 - fungicide serial applications, 330, Fig. 9.9
 - gene probes for enzymes, 331, Fig. 9.10
 - PAH metabolism in marine sediments, 331, Table 9.4
 - plasmid transfer, 331
 - chiral differences, 348, Fig. 9.20
 - groundwater impact and, 352
 - mineralization, 329
 - moisture effect, 337, Table 9.7
 - half-lives, 328
 - microorganisms, 328
 - soil pH:
 - degradation of aldicarb, 354, Table 9.15
 - persistence of chlorpyrifos, Table 9.12
 - SOM effect, 342, Fig. 9.18
 - substrate concentration, 340, Fig. 9.16–17
 - temperature:
 - effect on metabolic pathways, 336, Fig. 9.12
 - laboratory study, 334, Table 9.5
 - regional variation, 335, Table 9.6
- Soil organic carbon, SOC:
 - K_{oc} , SOC/water distribution ratio, 86
- Soil organic matter, SOM:
 - components, 77
 - degradation rates in soil and, 341, Fig. 9.18
 - K_{om} , 86
 - (OM)/(OC) relation, 79
 - plant root uptake and, 165
 - surface area, 79
- Soil pH:
 - degradation of:
 - aldicarb, 354, Table 9.15
 - chlorpyrifos, 346, Table 9.12
 - sorption of pentachlorophenol, 94
 - sorption of weak bases, 95
- Soil sorption from hexane:
 - non-linear isotherm, 99, Figs. 3.14–15
 - water, competitive effect, 100
- Soil sorption from vapor phase:
 - BET isotherms, 100, Fig. 3.16
 - humidity competitive effect, 100, Fig. 3.17
 - on peat soil, 100, Fig. 3.18
- Soil sorption from water:
 - aged residues, 104
 - kinetics, 101
 - non-linear isotherms, 90, Fig. 3.10
 - competitive effect, 90
 - carbonaceous material, 92
 - non-polar organics, mechanism, 89
 - temperature effect, 90
 - partitioning, 89
 - sorbate properties, 92
 - two-site process, 101
 - weak acids, pentachlorophenol, 94, Fig. 3.11
 - ion pair involvement, 95
 - weak bases, 95
 - cation exchange, 96
 - competitive effects, heats of sorption, 98
 - sorption isotherms, 97, Fig. 3.12, 13
- Soil/water distribution ratio, K_d :
 - clay content and K_d , 86, Fig. 3.6
 - definition, 89
 - SOC and K_d , 86, Fig. 3.6
- Solar radiation:
 - surface spectrum, 195
 - solar irradiance, $Z(\gamma)$, 207, Table 6.8
- Solubility:
 - definition, 17
 - solution process, 17
 - solution thermodynamics, 18

- Solubility in water, S_w :
 - concentration units, 21
 - criteria for experimental data, 21
 - DOM enhancement, 27, Fig. 2.7
 - experimental determination:
 - shake flask method, 20
 - generator column, 20
 - salinity effects, 27, Table 2.9
 - solubility data, 24, Table 2.7
 - solubility in sea water, 27, Table 2.9
 - super-cooled liquids, 25, Table 2.8
 - temperature effects, 25, Table 2.7
- Solutions:
 - vapor pressure, Raoult's law, 15
- Sorption:
 - definition, 81
- Sorption isotherms:
 - batch experiment, soil/water, 81
- Super-cooled liquid:
 - definition, phase diagram, 10, Fig. 2.1
 - relation between S_w and K_{om} , 93
 - relation between S_w and K_{ow} , 49, Fig. 2.13
 - solubility in water, 26, Table 2.8
 - vapor pressure of, 11
- Super-critical fluid extraction:
 - aged PCB residues, 107, Fig. 3.21
- Surface depletion model:
 - evaporation from water, 126

- Titanium dioxide:
 - semi-conductor catalyzed photolysis, 229
- Transpiration stream concentration factor, TSCF:
 - index of distribution in plant, 162

- relation to K_{ow} , 163, Fig. 5.8
- 2,4,5-Trimethylamine:
 - pH and octanol/water partitioning, 59, Fig. 2.16
- Triplets:
 - electron spin, 199
- Two-film model:
 - evaporation from water, 131
- Vapor density:
 - calculation from vap. press., 6
 - concentration units, ppm, 8
- Vapor pressure:
 - definition, 5
 - determination:
 - gas saturation method, 8
 - headspace analysis, 8
 - Knudson effusion method, 8
 - experimental values, 7, Table 2.2
 - estimating v boiling point, 14
 - estimated v experimental, 16, Table 2.4
 - solutions, Raoult's law, 15
 - super-cooled liquid, calculation, 13
 - temperature effects, 10
 - temperature relations, 7, Table 2.2
 - units, 6, Table 2.1

- Xylem:
 - plant vascular system, 160

- Zero-valent metal:
 - reduction of alkyl halides, 281, Table 7.10
 - groundwater remediation, 282